XXIX Danube Conference

XXIX Conference of the Danubian Countries
on Hydrological Forecasting and Hydrological
Bases of Water Management

Conference proceedings
Full papers

September 6–8, 2021
Brno

# XXIX Conference of the Danubian Countries

on Hydrological Forecasting and Hydrological Bases
of Water Management

Conference proceedings
Full papers

September 6–8, 2021
Brno, Czech Republic
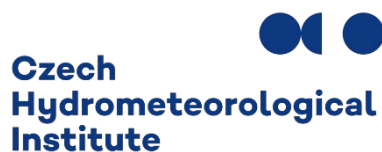
Organized by

Under the auspices of

Czech National Committee for UNESCO
Intergovernmental Hydrological Programme Danube

Co-organizers

Czech National Committee for Hydrology
CREA Hydro & Energy
Povodí Moravy
Czech Scientific and Technical Water Management Company
Technical University of Vienna
University of Ljubljana, Faculty of Civil and Geodetic Engineering

Obsah

Introductory word

Conference of Danubian countries has become traditional platform for sharing outcomes of research and science among experts in the field of hydrology and water management in the most „shared" basin of the World. Czech Republic agreed to host XXIX Conference after the last Conference in Kiev took place. But, as you all know, the World has changed since. Preparation of the XXIX Conference was not easy under the uncertainty of the pandemic development and at a certain time, a decision has been made to hold it virtually.

Virtual format is limiting due to lack of coffee break and evening discussions, which result in establishing of new professional connections and friendships. But, we feel that having a conference is important to preserve and stimulate existing connections in these difficult times.

All the more so, we highly appreciated number of papers submitted that proved the interest of the community in scientific gathering and knowledge sharing. You can find collection of contributions in these Proceedings.

I urge you to read papers, and if interested in some, contact its authors, as you would during the nearest coffee break while in the in-person conference. Let's try to stimulate dialog and cooperation despite the unpleasant current conditions. Keep in mind, that while there were periods of interrupted travelling among countries in Europe during last two years, the water of Danube and its tributaries never stopped running and connecting all countries that share its basin.

Jan Daňhelka

Topic 1

Data: traditional & emerging, measurement, management & analysis

Estimation of design discharges in terms of seasonality and length of time series

Veronika Bačová MITKOVÁ

Institute of Hydrology, Slovak Academy of Sciences, Dúbravska cesta 9, 841 04 Bratislava, Slovakia),
email: mitkova@uh.savba.sk

Abstract

The paper deals with the effect of two factors on the accuracy of T-year discharge estimation resp. fluctuations in the estimation of these discharges. The AM method was used to analyze the effect of the time series length and seasonality (winter, summer) on the accuracy of T-year maximum discharges estimation. The series of daily discharges and peak discharges on the Topľa River at Hanušovce nad Topľou for the period of 1931–2015 were used as input data. The maximum annual discharges (AM) method was used with theoretical probability distributions Log-Pearson III, Gamma and Log-Normal.

Introduction

Floods occur in Europe very often and flood frequency analysis plays a major role in the design of hydraulic structures and flood control management. The flood frequency analysis deals with solution of the relationship between peak discharges of the flood waves and probability of their return period (T). Determining the specific values from a 100- to 1 000-year flood for engineering practice is extremely complex.

All statistical methods which are used to estimate the floods with a very long return period are associated with great uncertainties. Such uncertainty is associated with several factors e.g. time series length, inclusion/non-inclusion of the historical floods into the time series, river regime or type of theoretical probability distribution. The estimation of the uncertainty at the design discharges was investigated for example by Coxon et al. (2015). The inclusion of historic pre-instrumental data to statistically analyzed data series was investigated in Elleder et al. (2013); Kjeldsen et al., (2014) or Pekárová (2019). Brazdil et al. (2006) studied historic hydrological materials in order to estimate floods threat in Europe. Estimation of the uncertainty at the design discharges was investigated for example by Merz and Thieken (2009) or Rogger et al. (2012). In addition to this factor, the type of theoretical probability distribution that is used to estimate maximum (extreme) values has an impact on the estimation of T-year discharges. Bačová (2019) compared the two most commonly used methods in estimating T-year maximum discharges, AM method and POT method. The author analysed effect of the threshold level value and various data set (peaks, mean daily discharges) on estimated values of QT. Malamud and Turcotte (2006) showed that, the most commonly used distributions in hydrology can be divided into four groups: the normal family (normal, Lognormal), the general extreme value family (GEV, Gumbel, Fréchet, reverse Weibull), the Pearson type III family (Gamma, Pearson type III, Log-Pearson type III), and the Generalized Pareto distribution.

An important outcome of this study is how setting of time series at a gauging station can determine the magnitude of designed discharges. In this approach Log-Pearson theoretical probability distribution type III. was used. Subsequently, estimated T-year maximum discharges were compared with other two theoretical distribution types used in Slovakia: Log-normal and Gamma probability distribution. The set of daily discharges and peak discharges on the Topľa River at Hanušovce nad Topľou for the period of 1931–2015 was used as input data for our case study.

Methodology

In our analysis we use one type of the theoretical probability distribution the Log-Pearson distribution type III (LP III). The advantage of this particular technique is that extrapolation can be made of the values for events with return periods well beyond the observed flood events. To estimate the distribution parameters, the method described in Bulletin17B was used (IACWD, 1982). The cumulative distribution function and probability distribution function according Hosking and Wallis (1997) are defined as:

If $\gamma \neq 0$ let $\alpha = 4/\gamma^2$ and $\xi = \mu - 2\sigma/\gamma$

If $\gamma > 0$ then:

$$F(x) = G(\alpha, \frac{x-\xi}{\beta})/\Gamma(\alpha), \tag{1}$$

$$f(x) = \frac{(x-\xi)^{\alpha-1}e^{-(x-\xi)/\beta}}{\beta^\alpha \Gamma(\alpha)} \tag{2}$$

If $\gamma < 0$ then

$$F(x) = 1 - G(\alpha, \frac{\xi-x}{\beta})/\Gamma(\alpha) \tag{3}$$

$$F(x) = 1 - G(\alpha, \frac{\xi-x}{\beta})/\Gamma(\alpha), \tag{4}$$

where

μ – location parameter;

σ – scale parameter;

γ – shape parameter;

Γ – Gamma function.

Subsequently, the LP III probability distribution was compared with other recommended probability distributions (Gamma and Log-normal) according to OTN ŽTP 3112-1: 03. To verify the accuracy of theoretical distributions, we used a non-parametric Kolmogorov-Smirnov goodness of fit test for the significance level $\alpha = 0.05$.

Topľa River basin and input data

The Topľa is upland/lowland type of river in eastern Slovakia. The catchment drainage area is 1 506 km² with length of 129.8 km (Figure 1). The long-term mean daily discharge amounts at station Hanušovce nad Topľou was 8.1 m³s⁻¹ during period 1931–2015 and the maximum discharge during the analyzed period was 449 m³s⁻¹ (date: 06.04.1932). Figure 1 also shows the exceeding probabilities of the maximum annual discharges according to Log-Pearson Type III. probability distribution (LPIII). Peak annual discharges (points), linear trend (red line), and 4-years moving averages for the Topľa River at Hanušovce nad Topľou during the period 1931–2015 are shown in Figure 2. In the analysed period, two dry periods of 1954–1964 and 1990–1999 were occurred. While wet periods can be described only as years with extreme flood events (e.g. 1932, 1948, 1952, or 1980), a relatively prolonged wet period was in 2004–2010. Annual maximum discharges show a decreasing trend for the period of 1931–2015.

Comparison of the LPIII distribution with the theoretical probability distributions that were (and still are) most widely used hydrological practice in Slovakia: Gamma distribution and Log-normal distribution are listed in Table 1. We can see relatively small differences in the values of estimated T-year maximum discharge values in comparison with other two types of theoretical probability distributions used in hydrological analyses of extremes in the Slovakia. The lowest values of estimated T-year maximum discharges, achieved Gamma theoretical probability distribution, especially for discharges with high return periods.
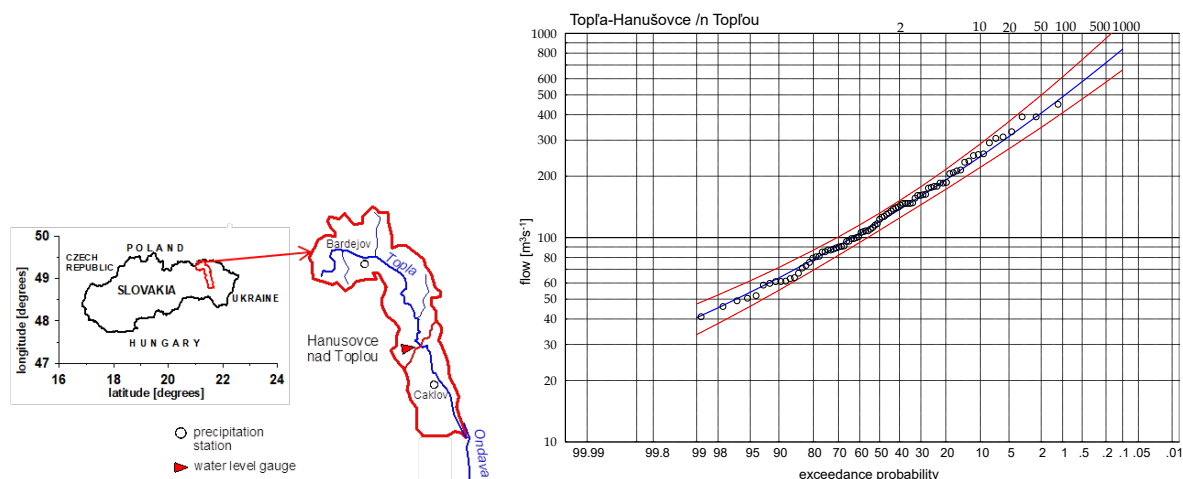
Fig. 1 A scheme of the Topľa River basin (left) and exceedance probability of the annual peak discharges of the Topľa River: Hanušovce nad Topľou within 1931–2015 period (right).
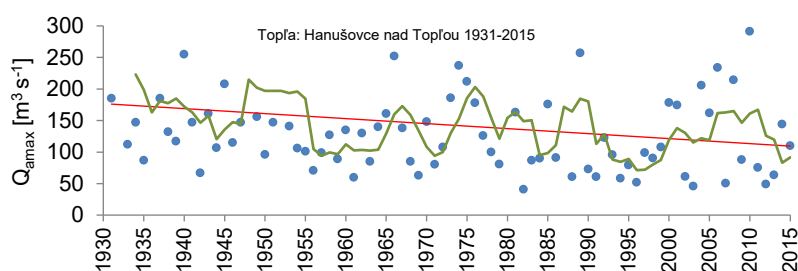
Fig. 2 Peak annual discharges (points), linear trend (red line), and 4-years moving averages for the Topľa River at Hanušovce nad Topľa during the period 1931–2015.

Table 1 T-year maximum discharges Q_{Tmax} [m^3s^{-1}] on the Topľa River: Hanušovce nad Topľou (1931–2015) estimated from maximum annual discharges Qamax

N [year]	2	5	10	50	100	200	500	1 000
P [%]	39	18	9.5	2	1	0.5	0.2	0.1
Log-Pearson III								
QTmax [m^3s^{-1}]	139	193	249	398	473	556	679	783
Pvalue K-S	0.999							
Log-normal								
QTmax [m^3s^{-1}]	146	199	252	380	439	502	589	660
Pvalue K-S	0.987							
Gamma								
QTmax [m^3s^{-1}]	148	204	255	360	404	446	506	541
P_{value} K-S	0.744							

Results

The effect of time series length on the T-year discharge estimation

For analysing the effect of the length of the data series on the estimation of T-year discharges, the period 1931–2015 was divided into two shorter periods: 1931–1973 and 1974–2015.

We had chosen this approach because for the frequency analysis is recommended the length of the observation series 5T (FEH, 1999). If T = 50 years, then a 250-member observation series is required for a reliable estimate of Q50. Such a length of data series (AM) is practically absent. Therefore, the probability of a reliable estimate of T-year maximum discharge for short-range river basins is relatively low. In the case of the 50-year observation series, the probability of Q100 is 39% and in the case of the 100-year series is 63% (Viessman et al. 1977). The estimated values of the QTmax for shorter periods of the data series are listed in Table 2. There is compared the LPIII distribution with other frequently used and recommended hydrological distributions in

10

hydrological practice in Slovakia: Log-normal distribution and Gamma distribution. The exceedance probabilities of the annual peak discharges for two shorter periods of the Topľa River at Hanušovce nad Topľou according the LPIII distribution are presented in Figure 3a–b.

Table 2 Comparison of the estimated QTmax for shorter periods on the Topľa River: Hanušovce nad Topľou

1931–1973								
N [year]	2	5	10	50	100	200	500	1 000
P [%]	39	18	9.5	2	1	0.5	0.2	0.1
Log-Pearson III								
QTmax [m³s⁻¹]	143	198	257	427	519	627	797	949
Pvalue K-S	0.813							
Log-normal								
QTmax [m³s⁻¹]	161	202	249	357	408	457	527	583
Pvalue K-S	0.787							
Gamma								
QTmax [m³s⁻¹]	169	219	272	321	428	472	529	571
Pvalue K-S	0.44							
1974–2015								
N [roky]	2	5	10	50	100	200	500	1 000
P [%]	39	18	9.5	2	1	0.5	0.2	0.1
Log-Pearson III								
QTmax [m³s⁻¹]	125	180	239	408	499	602	760	899
Pvalue K-S	0.74							
Log-normal								
Qamax [m³s⁻¹]	137	181	233	362	423	488	580	654
Pvalue K-S	0.74							
Gamma								
QTmax [m³s⁻¹]	144	189	236	336	376	416	467	505
Pvalue K-S	0.55							
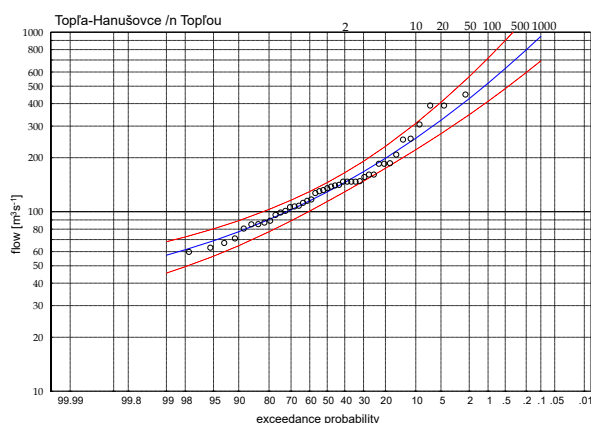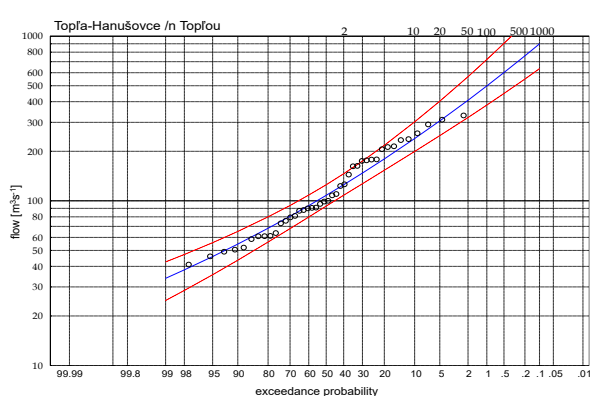
a)   b)

Fig. 3 The exceedance probabilities of the annual maximum discharges according to Log-Pearson Type III. probability distribution (LPIII) a) period 1931–1973 and b) period 1974–2015 on the Topľa River: Hanušovce nad Topľou.

The effect of the seasonality on the T-year discharge estimation

For dividing the year into seasons, we proceeded from the analysis of the occurrence of floods and from the evaluation of the Topľa runoff regime during the year. In terms of the type of runoff regime, Topľa belongs to the highland-lowland area with rain-snow runoff with the culmination of river runoffs in the month of March, respectively April. The measured data were divided into two seasons:

• Summer season is from May to October, when peak discharges occur only from heavy rainfall (Figure 6a).
• Winter season is from November to April, when peak discharges occur by combining heavy rainfall in the form of snow and rain as well as snow melting in the area (Figure 6b).

The distributions of the mean monthly discharges in 10-year periods of the Topľa River: Hanušovce nad Topľou are illustrated in Figure 4. Figure 5 illustrates month of the annual maximum discharges occurrence (period of 1931–2015) on the Topľa River at Hanušovce nad Topľou. The statistical data series were supplemented with maximum discharges in the given season, so that there are 85 measurements per season.
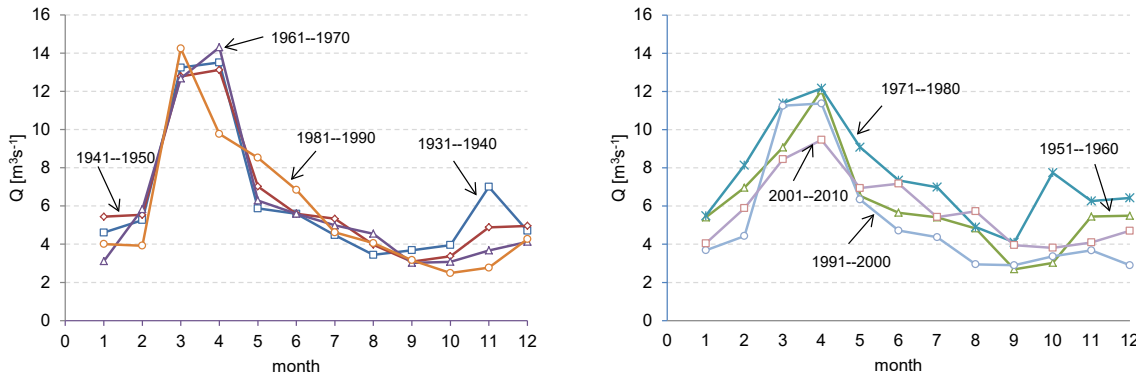
Fig. 4 The distributions of the mean monthly discharges in 10-year periods of the Topľa River: Hanušovce nad Topľou.
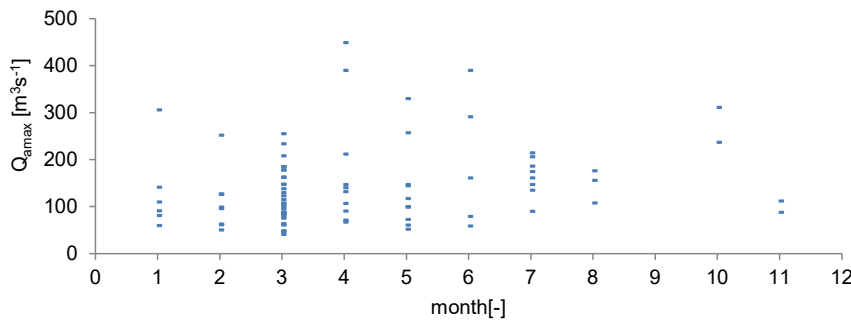
Fig. 5 Month of the annual maximum discharges occurrence (period of 1931–2015) on the Topľa River at Hanušovce nad Topľou.
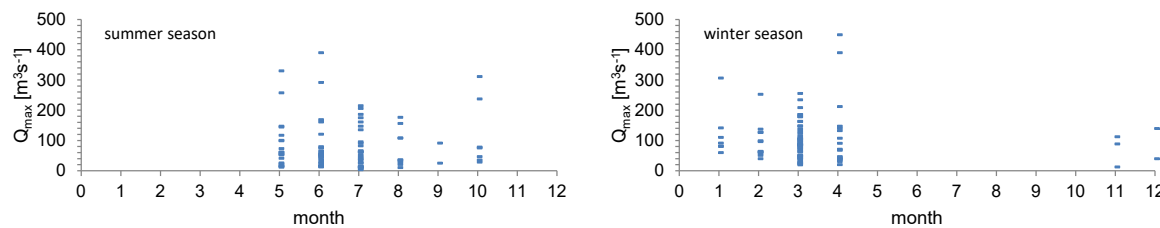
Fig. 6 Occurrence of extreme discharges in month of the summer season (left) and winter season (right), with supplemented maximum discharges in a given season (number of measurements is still 85 per season).

The estimated values of the Q_{Tmax} for summer season and winter season are listed in Table 3. There is compared the LPIII distribution with other frequently used and recommended hydrological distributions in hydrological practice in Slovakia: Log-normal distribution and Gamma distribution. The exceedance probabilities of the maximum seasonal discharges of the Topľa River at Hanušovce nad Topľou according the LPIII distribution are presented in Figure 7a–b.

Table 3 Comparison of the estimated QTmax in selected two season a) summer and b) winter on the Topľa River: Hanušovce nad Topľou

Summer season								
N [year]	2	5	10	50	100	200	500	1 000
P [%]	39	18	9.5	2	1	0.5	0.2	0.1
Log-Pearson III								
QTmax [m^{3}s^{-1}]	68	124	194	423	558	718	975	1209
Pvalue K-S	0.953							
Log-normal								
QTmax [m^{3}s^{-1}]	75	124	193	422	555	714	971	1202
Pvalue K-S	0.922							
Gamma								
QTmax [m^{3}s^{-1}1]	86	134	189	318	373	428	501	556
Pvalue K-S	0.79							
Winter season								
N [roky]	2	5	10	50	100	200	500	1 000
P [%]	39	18	9.5	2	1	0.5	0.2	0.1
Log-Pearson III								
QTmax [m^{3}s^{-1}]	117	172	228	372	443	518	626	715
Pvalue K-S	0.94							
Log-normal								
QTmax [m^{3}s^{-1}]	108	151	204	347	419	498	613	710
Pvalue K-S	0.73							
Gamma								
QTmax [m^{3}s^{-1}]	115	159	208	315	360	404	462	504
Pvalue K-S	0.78							
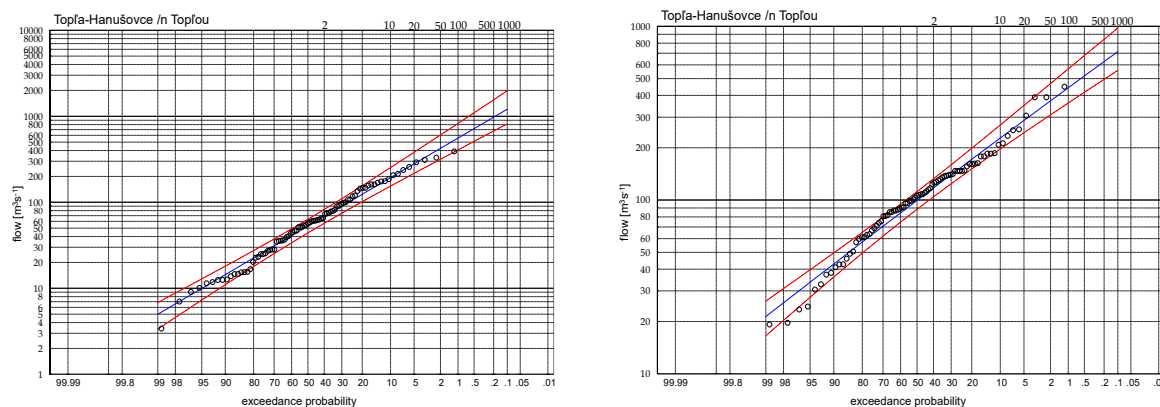
Fig. 7 Exceedance probabilities of the maximum discharges according to Log-Pearson Type III. probability distribution (LPIII) a) summer season and b) winter season on the Topľa River: Hanušovce nad Topľou.

Comparisons of the estimated maximum discharges with a return period of 100 and 1000 years according to the selected procedures are shown in Figure 8. The highest estimated values of Q_T were achieved according the LPIII distribution.
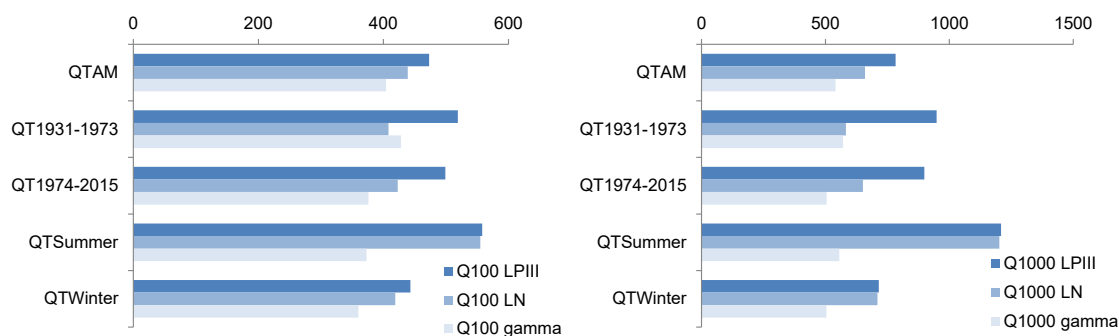
Fig. 8 Comparisons of the estimated maximum discharges with a return period of 100 and 1000 years according to the selected procedures.

Conclusion

The first part of the paper deals with the estimation of the QT from annual peak discharges on the Topľa River at Hanušovce nad Topľou (1931–2015). Results of this part showed relatively small differences in the values of estimated T-year maximum discharge values in comparison with other two types of theoretical probability distributions used in hydrological analyses of extremes in the Slovakia. The lowest values of estimated T-year maximum discharges, achieved Gamma theoretical probability distribution, especially for discharges with high return periods. Phien and Jivajirajah (1984) dealt with the use of the Log-Person III distribution to estimate the maximum annual rainfall and discharges. They concluded that this distribution is more suitable for discharges with a higher return period, but for the annual floods the existence of an upper bound of the distribution, in some cases may cause some higher uncertainties. Comparing the suitability of several types of probability distributions (GEV, LPIII and Gumbel) for estimating T-year discharges was discussed in Millington et al. (2011). Authors do not prefer any of the selected distributions as better and recommend further research. Results of our analysis indicate that the LPIII distribution is suitable distribution for T-year discharge estimation with a higher return period.

Estimation of flood magnitudes to be used as a basis to design the hydraulic structures and flood control management is therefore of crucial importance. Therefore, the paper also presented an estimation of the T-year maximum discharges by the AM method and analysed the effect of the time series length and seasonality (winter, summer) on the accuracy of T-year maximum discharges estimation. Results showed that not only the selection of the distribution function to estimate T-year discharges but also the processing of the statistical series affect the results of the estimation. The shorter periods showed higher estimations of the T-year discharges. The highest estimated values according the LPIII distribution was achieved for summer season. The lowest estimated value according the LPIII distribution was achieved for winter season. When interpreting the results, it should be borne in mind that the T-year maximum discharges are related to the length of the analysed series and therefore estimated values with very high return periods are extrapolated and that each statistical method is burdened with some uncertainty that may be caused by alone method, but also the data, which may be burdened by a certain measurement error.

Acknowledgements

References

Bačová Mitková, V. (2019): The peak over threshold method and its uncertainty in determining of T-year maximum discharges: Case study at the Topľa River. In Acta Hydrologica Slovaca, 2019, Vol. 20, No. 1, 32–43, ISSN 1335-6291. (In Slovak)

Brazdil, R., Kundzewicz Z., W. and Benito, G. (2006): Historical hydrology for studying flood risk in Europe. *Hydrological Science Journal*, **51** (5), 739–764, DOI:10.1623/hysj.51.5.739.

Coxon, G., Freer J., Westerberg I. K., Wagener T., Woods R., and Smith P. J., 2015. A novel framework for discharge uncer-tainty quantification applied to 500 UK gauging stations, *Water Resour. Res.*, **51**, 5531–5546, doi:10.1002/2014WR016532.

Elleder, L., Herget, J., Roggenkamp, T., and Nießen, A. (2013): Historic floods in the city of Prague – a reconstruction of peak discharges for 1481–1825 based on documentary sources, *Hydrology Research*, **44** (2), 202–214.

FEH (1999): Flood estimation handbook. Wallingford (Institute of Hydrology), ISBN 0 948540 94 X.

Hosking J.R.M., Wallis J.R. (1997): Regional Frequency Analysis. Cambridge University Press. Cambridge. 244 p. ISBN 0521019400, 9780521019408.

IACWD (1982): Guidelines for determining flood flow frequency, Bulletin 17-B. Technical report, Interagency Committee on Water Data, Hydrology Subcommittee. 194 pp.

Kjeldsen, T. R., Macdonald, N., Lang, M., Mediero, et al. (2014): Documentary evidence of past floods in Europe and their utility in flood frequency estimation, *Journal of Hydrology*, **517**, 963–973. ISSN 0022-1694.

Malamud, B.D., Turcotte, D.L., (2006): The applicability of power-law frequency statistics to floods. Journal of Hydrology 322,168–180. https://doi.org/10.1016/j.jhydrol.2005.02.032.

Merz B., Thieken A.H. (2009): Flood risk curves and uncertainty bounds. *Natural Hazards*, vol. **51**, issue, 3, 437–458, DOI: 10.1007/s11069-009-9452-6.

Millington N., Das S., Simonovic S. P., (2011): The Comparison of GEV, Log-Pearson Type 3 and Gumbel Distributions in the Upper Thames River Watershed under Global Climate Models. Water Resources Research Report. Department of Civil and Environmental Engineering The University of Western Ontario London, Ontario, Canada, September 2011, 1–54.

OTN ŽP 3112–1: 03 ME SR (2003): Quantities of surface and groundwater. Hydrological data of surface waters. Quantification of the flood regime. Part 1: Determination of T-year flow rates and T-year flow waves at larger flows Branch technical standard OTN ŽP 3112–1: 03, Ministry of Environment SR, Bratislava, 31 p. (in Slovak)

Phien, H.N. a Jivajirajah, T. (1984): Applications of the log Pearson type-3 distribution in hydrology. *J. Hydrol.*, **73**, 359–372.

Pekárová, P., Miklánek, P. (eds.), 2019. Flood regime of rivers in the Danube River basin. Follow-up IX of Regional Cooperation of the Danube Countries in IHP UNESCO. IH SAS, Bratislava, 215 p. +527 p. app., DOI: 10.31577/2019.9788089139460.

Rogger M., Kohl B., Pirkl H., Viglione A., Komma J., Kirnbauer R., Merz R. and Blöschl G. (2012): Runoff models and flood frequency statistics for design flood estimation in Austria – Do they tell a consistent story? *Journal of Hydrology*, 456–457, 16 August 2012, 30–43.

Viessman, J. R. W., Knapp, J. W., Lewis, G. L, Harbaugh, T. E. (1977): Introduction to hydrology. New York (Harper and Row), 704 p., ISBN0700224971.

Interactions of water chemistry in headwaters with wetlands: Comparative study for selected Czech mountains

Kateřina FRAINDOVÁ, Milada MATOUŠKOVÁ, Zdeněk KLIMENT, Lukáš VLČEK, Vojtěch VLACH, Pavla ŠPRINGEROVÁ

Charles University, Faculty of Science, Department of Physical Geography and Geoecology, Czech Republic, email: katerina.fraindova@natur.cuni.cz, email: milada.matouskova@natur.cuni.cz, email: zdenek.kliment@natur.cuni.cz, email: lukas.vlcek@natur.cuni.cz, email: vojtech.vlach@natur.cuni.cz, email: pavla.springer@gmail.com

Abstract

River headwaters have a high environmental value. Unfortunately, the biogeochemical process in headwaters in context of regional climate change have not been fully examined. This study focuses on changes in correlations of 16 biogeochemical parameters related to different types of rainfall-runoff events and land cover conditions for eight headwater catchments in Central Europe. Multiple methods as linear regression, Spearman rank correlation, Principal Components Analysis and C/Q hysteresis loops revealed main relationships. Presence of peatlands and waterlogged spruce forests had decisive influence on the biogeochemistry (mainly for COD_{Mn}, humins, Fe, $P–PO_4^{3-}$ TP, and $N–NO_3^-$). The strongest positive correlation of organic matter (COD_{Mn}) and Fe is represented in a catchment with the largest area of damaged forest (70 %), but with asmaller proportion of wetlands (8 %). High flow rates influence the release of greater amounts of organic matter and $N–NO_3^-$.

Introduction

Water quality belongs to the most important key factors for human life and whole ecosystem. As the quality of potable surface waters declines (Delpla et al. 2009), importance of headwater streams, as usually the least polluted water bodies, is increasing. Nevertheless, headwater streams are also very sensitive to any input of pollutants or climatic changes and can be thus assumed as an initial indicator to these variations (Ockenden et al. 2016). A typical example is strong acidification in Central European headwaters in the early 1990s. Currently, the ongoing climate change can be observed, manifested mainly by an increase in average annual air and water temperatures (European Environment Agency 2017) and by the increased risk of extreme rainfall-runoff events (Easterling et al. 2000). These anomalies have led to changes in the biogeochemistry of surface waters as well. The greatest changes in the chemistry of montane streams occur in two periods: during the spring snowmelt and during the dry summer period (Soulsby et al. 2001). In recent years, researchers have observed the release of a greater amount of natural organic matter (Evans et al. 2005, Lepistö et al. 2014, Porcal et al. 2009, Ritson et al. 2014), which has been linked to rising average annual temperatures (Fenner et al. 2013, Worrall et al. 2003), changes in atmospheric depositions, and the increased pH of surface waters (Hruška et al. 2009, Löfgren et al. 2010). Greater amounts of organic matter may also be released into upland streams as a result of presence of different types of wetlands within a catchment (Austnes et al. 2010, Laudon et al. 2011) or the peatbogs drainage (Marttila et al. 2018). High water treatment costs and the formation of mutagenic and carcinogenic chlorinated organic by-products are direct consequences of elevated organic matter levels (Bull et al. 2011, Zheng et al. 2016). Therefore, it is important to monitor current and potential sources of drinking water continuously.

Water quality can be monitored using complex indicators, such as electrical conductivity. Conductivity is not only a comprehensive indicator, but it is also relatively inexpensive and simple to measure continuously. Therefore, continual monitoring can be used to note changes in the context of rainfall-runoff events (Cano-Paoli et al. 2019). A disadvantage of this method is the difficulty of assessing the impact of factors such as rock type and water age (Evans et al. 2014), the previous water table, and catchment saturation (Burns et al. 2001). The seasons have a major impact on values of conductivity, especially spring, when snow melts (Evans and Davies 1998). Specific conductance is linearly correlated to ionic strength (Orndorff et al. 2015) and to total dissolved solids (Timpano et al. 2010), therefore, it is used as a proxy for total dissolved solids (Orndorff

et al. 2015). While conductivity values are influenced not only by discharge levels but also by catchment conditions, it is possible to determine changes occurring at the onset and the end of a rainfall-runoff event and classify the hysteresis (Su et al. 2017, Zuecco et al. 2016).

Another comprehensive indicator of water quality is CODMn (chemical oxygen demand using permanganate method), which characterizes total organic water pollution. It is commonly used as a proxy for DOM (dissolved organic matter), whether its source is organic or inorganic matter (Oulehle and Hruška 2009). Main nutrients include N and P, which are limiting factors in plant growth. Increased concentrations of these compounds may indicate organic pollution or rapid decomposition and mineralization of the peat layer (Haapalehto et al. 2011). Even though a significant decrease in sulphur emissions has been recorded since the 1990s in Central Europe, the decrease in nitrogen emissions has not been as marked; it is also assumed that greater amounts of nitrates will be released into streams from the soil in the future (Oulehle et al. 2012). Changes in the amount of various forms of nitrogen can be observed not only as a result of human impact (Broussard and Turner 2009, Lassaletta et al. 2010), but also as the result of differing land cover (Jones et al. 2008, Von Schiller et al. 2009) or disturbances in a catchment (Aber et al. 2002). Increased concentrations of phosphorous compounds occur not only as a result of human activities, but also due to larger area of peatbogs in a catchment (Rupp et al. 2004).

Base cations, which include calcium (Ca), magnesium (Mg), potassium (K), and sodium (Na), represent other important indicators of water quality; with the exception of sodium, all of them are basic plant nutrients that help maintain soil fertility and play an important role in soil and groundwater acid levels. Even though their main source is mineral weathering, the composition of atmospheric deposition has a major influence on their release (Ledesma et al. 2013). Another indicator of water quality is iron (Fe), whose concentration has increased in some places over the last 10 to 20 years and which has been connected to "water brownification" (Knorr 2013, Sarkkola et al. 2013, Selle et al. 2019), but the driver/s behind the trends are not sufficiently explained (Björnerås et al. 2019). Higher concentration of Fe is related to presence of peatbogs due to the higher concentrations of organic matter and humic substances, which cause iron mobilization (Kida et al. 2018). Other factors affecting the Fe concentration are the proportion of coniferous forest on the total catchment area (Björnerås et al. 2017) or high sulphate concentration in organic soils (Björnerås et al. 2019).

All water quality indicators are particularly dependent on the season (Lepistö et al. 2008, Lassaletta et al. 2010, Penna et al. 2015) and on the rainfall-runoff process (Erlandsson et al. 2008, Köhler et al. 2008, Fučík et al. 2017). Runoff water is diluted after long-lasting rains (Noskovič et al. 2013, Penna et al. 2015). Nevertheless, the concentrations of organic matter can increase during rainfall-runoff events at the end of long dry periods (Worrall et al. 2004, Ockenden et al. 2016, Broder et al. 2017). Groundwater (Šanda et al. 2014, Zajíček et al. 2016), land cover and the presence of peatbogs (Muller et al. 2015) play also an important role in runoff formation during rainfall-runoff events.

Eight catchments in similar natural conditions headwater areas of Šumava Mts. and Krušné hory Mts. were selected for investigation. The main objective of our study is to analyse changes of headwaters biogeochemistry focused on diverse rainfall-runoff conditions in catchments with different proportion of wetland (especially peatbogs) cover and forest with different amounts of disturbance. We hypothesized that (1) the presence of wetlands (peatbogs) in catchments affects the surface water quality in context of increased organic matter and higher release of humic substances, Fe and CODMn during higher discharges; (2) iron mobilization is controlled more by organic matter (humic substances, CODMn) concentration than pH or discharge; (3) the type of rainfall-runoff event has a larger impact on specific conductivity (SC) and pH changes than the catchment preconditions.

Methodology

Study sites

The study was carried out in two headwater localities of the Elbe River basin in south and west part of Czechia –Šumava Mts. and Krušné hory Mts. (see Fig. 1). They are characterized by natural conditions with some degree of land protection and with no influence of large human settlements and industry. The catchments in the central parts of the Šumava National park are located in the headwater areas of the Vydra River – Ptačí Brook (PTA), Javoří Brook (JAV), Cikánský Brook (CIK), Březnický Brook (BRE), Rokytka Brook (ROK) and Rokytka left tributary (ROK2). The altitudes are ranging from 1,000 to 1,350 m a. s. l. with a long-term average annual precipitation of about 1,300 mm and an average annual air temperature of 3.6°C (1961–2000, Tolasz and Baštýřová 2007). The catchments of the western part of the Krušné hory Mts. – Rolava (ROL) and

Slatinný Brook (SLA) are located at altitudes ranging from 744 to 965 m a. s. l. with long-term mean annual precipitation of about 900 mm and a mean annual air temperature of 5.1°C (1961–2000, Tolasz and Baštýřová 2007). While no significant trends were found in precipitation totals, there were significant increases in air temperatures, especially since the late 1980s, by about 1.5°C (Kliment et al. 2011, Langhammer et al. 2015, Langhammer and Bernsteinová 2020), which conditioned changes in the seasonal distribution of runoff – earlier melting of snow cover, higher frequencies of high flow discharge and more pronounced summer dry periods with earlier onset (Blahušiaková et al. 2020, Vlach et al. 2020). The area of study catchments ranged from 0.14 km2 (ROK^2) to 22.4 km^2 (SLA). Long-term specific discharges (2008–2013) ranges from 29.3 l.s^{-1}.km^{-2} (BRE) to 41.2 l.s^{-1}.km^{-2} (ROK2) in Šumava Mts. (Vlček et al. 2016) and about 14–15 l.s^{-1}.km^{-2} (ROL, SLA) in Krušné hory Mts. Due to the occurrence of dry years, the values of flows in the monitored period 2014–2020 were lower. More details can be found in Table 1.
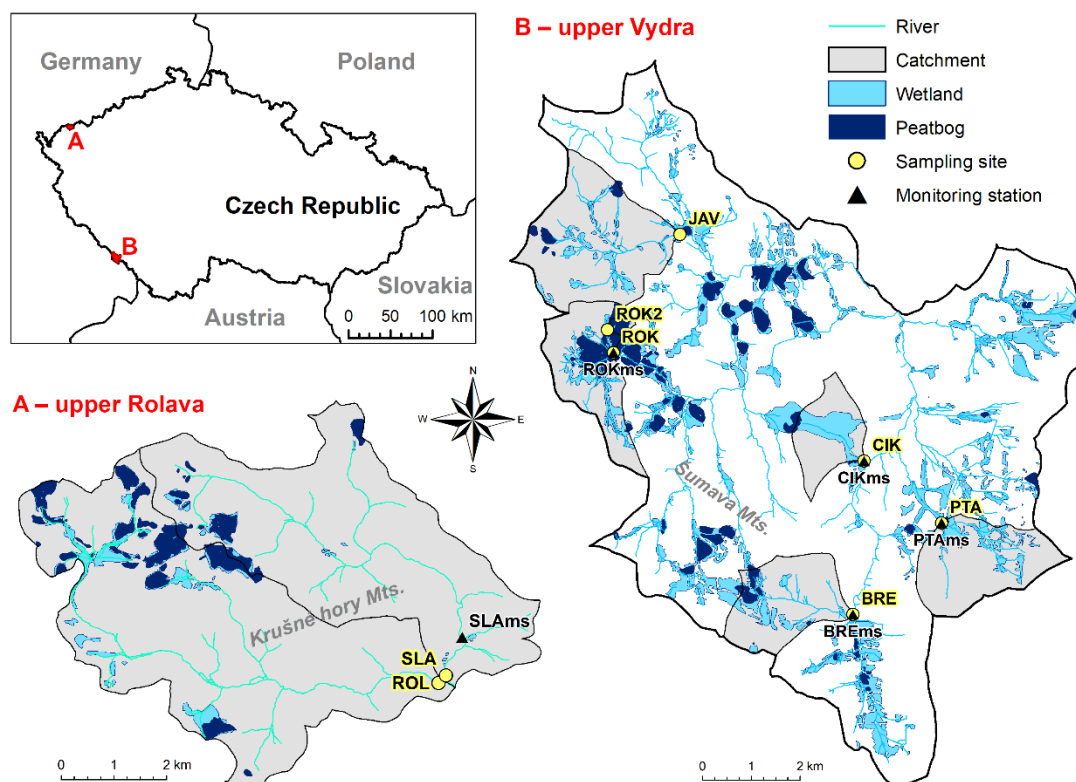
Fig. 1 Locations of the studied catchments. Source: ARCČR 500, DIBAVOD, WMS – Orthophoto.

Bedrock of study catchments is created mainly by metamorphic rocks and granite. Dominating soils are Podzols and Histosols. Histosols were formed on the flat uplands and are in prevalence in three catchments in upper Vydra (ROK2, ROK, CIK). Large parts occupy wetland areas with ratio from 83 % (ROK2) to 3% (SLA) of catchment area (Base map of the Czech Republic 1:10 000, Czech Office for Surveying and Cadastre).

Five land cover categories (as possible drivers of water quality changes) were derived for the study catchments – healthy spruce forest (HSF), damaged forest (DF), decayed forest with partly regeneration (DFR), meadow (M) and peatbog (PB). Damaged forest by the bark beetle induced forest disturbance and decayed forest with partly regeneration were determined by Su et al. (2017). In the central part Šumava Mts., the infestation accelerated after the most recent windstorms in 2007 and 2008. As a result, large-scale bark beetle-induced tree mortality was present, and it affected gradually all study catchments. Disturbed area was left to natural processes without substantial human intervention. Catchments are also characterized by the presence of peatbogs and waterlogged spruce forests. Typical peatbog cover ranges from 79.9 % (ROK2) to 0.1 % (PTA). CIK catchment was partially drained using open ditches in the past. Since 2004, drainage ditches were dammed during revitalization process, which results in water retaining for a longer period. A larger proportion of healthy spruce forest / meadows is in the Krušné hory Mts. catchments – 90 % (SLA), 70 % (ROL)/ 15 % (ROL), 8 % (SLA).

Table 1 Basic characteristics of the studied catchments. Notes: HSF= Healthy spruce forest, DFR= Decayed forest with partly regeneration, DF= Damaged forest, M=Meadow, WL=Wetland area, PB= Peat bogs; Specific discharge (q) is calculated from 10-minutes data in 2014–2020 period.

Site	Long	Lat	Area	Average Slope	q_a	Vegetation						Geology	Soils	Anthropogenic influence
	[°]	[°]	[km²]	[°]	[l.s⁻¹.km⁻²]	[%]								
						HSF	DFR	DF	M	WL	PB			
PTA	13°30'38"	48°59'12"	4.09	5.59	28.06	40		20[a]		11	0.1	Metamorphic rocks	Podzols	No (some old drains with a very small influence)
JAV	13°26'08"	49°02'20"	6.34	5.67	35.49	10		70		8	2.3	Metamorphic rocks, Granite	Podzols	No
CIK	13°29'18"	48°59'52"	2.17	4.2	24.88	80		10		29	0.8	Metamorphic rocks, Quaternary sediments	Podzols / Histosols	Drainage system with revitalizing measures
BRE	13°29'10"	48°58'10"	3.5	6	31.50		80[a]			14	3.9	Metamorphic rocks	Podzols	No (some old drains with a very small influence)
ROK	13°25'03"	49°01'01"	3.82	3.58	32.40	30		30		22	16.8	Quaternary sediments	Podzols / Histosols	No (some old drains with a very small influence)
ROK2	13°24'57"	49°01'16"	0.14	3.5	33.57	10	30	15		83	79.9	Quaternary sediments	Histosols / Podzols	No (some old drains with a very small influence)
ROL	12°41'49"	50°22'33"	22.4	4.67	18.17	70			15	10	6.6	Granite	Podzols	Forest management
SLA	12°41'55"	50°22'38"	17.7	6.28	18.39	90			8	3	2.8	Granite	Podzols	Forest management

Chemical and physical parameters

Two main data sources were used to analyse changes in surface water quality in headwater areas. The first data source included seasonal field measurements and water samples for laboratory analyses at selected sites in headwater areas collected between October 2013 and November 2019[1] – six sampling sites in the upper Vydra (PTA, JAV, CIK, BRE, ROK, ROK2) and two sampling sites in the upper Rolava (ROL, SLA; Fig. 1). In total, 25 samples were collected from the upper Vydra (24 samples at JAV and ROK and 20 at ROK2) and 22 from the upper Rolava. Water samples were taken from the middle of streams at a medium depth using a 1.5 l plastic bottles. All samples were kept in the cool (<10°C) and dark containers upon sampling and until analysis in the laboratory. Laboratory analyses were undertaken in Charles University's Institute for Environmental Studies immediately, usually within 24 hours after sampling. Analysis focused specifically on pH, specific conductivity (SC), total hardness (TH), Ca^{2+}, $N–NO_2^-$, $N–NO_3^-$, $N–NH_4^+$, $P–PO_4^{3-}$, total phosphorus (TP), Fe, Cl^-, COD_{Mn}, humins, $ANC_{4.5}$, and $BNC_{8.5}$. The degree of pollution based on COD_{Mn} was determined by the so-called Kubel method based on the oxidation of organic substances by potassium permanganate in an acidic environment. Nitrites, nitrates, ammonium ions and TP were analysed spectrophotometrically using a UNICAM SP 1800 Ultraviolet spectrophotometer. During water sampling, the discharge in each catchment was also measured using hydrometric propellers (Ott C2 and C31) and the Flow Tracker (SONTEK) device. Water temperature (t), pH, SC and dissolved O_2 (DO) concentration were measured in situ using the Hach-Lange HQ40-D Multimeter.

The second data source was collected between 2013 and 2019 using a network of automatic water quality monitoring stations of the Department of Physical Geography and Geoecology, Charles University. These stations, located in the upper Vydra catchment (four monitoring sites) and the upper Rolava catchment (one monitoring site), provided a continuous dataset of water levels, SC (measured in $\mu S.cm^{-1}$) and pH in a ten-minute step (CUNI 2018).

Applied methods and data analyses

The normal distribution of all variables was checked with the Shapiro-Wilk test (Shapiro and Wilk 1965). While the data were non-normally distributed, the non-parametric tests were used further.

As the observations were dependent (same date of sampling), Friedman test (Friedman 1937) at the 0.05% level of significance with a Nemenyi post-hoc test was performed for evaluating significant differences between stations for all water quality variables. All tests were conducted in XLSTAT Software (Addinsoft 2018). Linear regressions were performed to relate runoff conditions to water quality parameters. Further, the dependency of 15 physicochemical parameters and specific runoff in every catchment were analysed through correlation analysis with Spearman r coefficients (Spearman 1904). Missing data were deleted pairwise.

In order to extract linear relationship among a set of variables, Principal component analysis (PCA) was performed in Excel using the XLSTAT on normalized data series for 16 physicochemical parameters (pH, SC, t, DO, TH, Ca^{2+}, $N–NO_2^-$, $N–NO_3^-$, $N–NH_4^+$, $P–PO_4^{3-}$, TP, Fe, COD_{Mn}, humins, $ANC_{4.5}$, and $BNC_{8.5}$), 8 catchment characteristics (HSF = Healthy spruce forest, DFR = Decayed forest with partly regeneration, DF = Damaged forest, M = Meadow, WL = Wetland area, PB = Peat bogs, Slope, Area) and discharge. The PCA defines the association of individual compounds' concentration and properties of each profile (Wackernagel 1995, Shrestha and Kazama 2007).

The second data source of ten-minute continuous data (discharge, SC, pH) from a network of automatic monitoring stations was used in order to analyse extreme hydrological events. Seven rainfall-runoff events defined by: (1) the sudden increase of discharge from the baseline; (2) the peak; and (3) the end of the wave was selected regard to the occurrence at the monitoring sites. The ends of the events were defined by the discharge drop to the initial level or the discharge sharply increases again as the result of another rainfall event.

---

[1] $N–NO_2^-$, TP (total phosphorus), $ANC_{4.5}$ (acid neutralization capacity) and $BNC_{8.5}$ (base neutralization capacity) values were only measured from October 2013 to May 2016.

These events were divided into three different groups: (1) consecutive summer rainfall-runoff events (9 July 2014, 12 July 2014, 14 July 2014, 22 July 2014) as "summer"; (2) events that occurred after long-lasting dry periods (8 October 2015, 16 October 2015) as "drought"; (3) events associated with spring snowmelt (18 April 2016) as "snowmelt".

To analyse the behaviour of SC and pH, simple C/Q hysteresis loops (Williams 1989) were examined for each event. At first, values of SC, pH and discharge were normalized as:

$$u(t) = \frac{x(t) - x_{min}}{x_{max} - x_{min}} \tag{1}$$

$$v(t) = \frac{y(t) - y_{min}}{y_{max} - y_{min}} \tag{2}$$

where $x(t)$ and $y(t)$ are two variables of time t; x_{min}, x_{max}, y_{min} and y_{max} are minimum and maximum values of independent and dependent variables; and $u(t)$ and $v(t)$ are normalized variables $x(t)$ and $y(t)$. The two normalized variables range between 0 and 1, which were converted to a range from 0 to 100 in order to express these values as percentages. C/Q hysteresis loops were categorized into 4 classes and 6 types according to its shape (class I: clockwise – 1 type, class II: counter-clockwise – 2 types, class III: eight shaped – 2 types, class IV: mixed – 1 type).

Results

Regression between physicochemical parameters and discharge

Using PCA, it is possible to see the main relationships between each profiles, individual parameters and catchment characteristics (Fig. 2). The first two factors explain together 66.02 % of the variance among the 16 physicochemical parameters, 8 catchment characteristics and discharge. The 21 variables are well represented on the plane under consideration, either by the first component (SC, DO, Ca^{2+}, COD_{Mn}, $N–NO_2^-$, $N–NO_3^-$, $P–PO_4^{3-}$, Fe, TP, humins, TH, WL, M, Area, Slope, Discharge) or by the second (water temperature, pH, $ANC_{4.5}$, $BNC_{8.3}$, DF). The sampling sites can be roughly divided in two groups. Group A includes sampling sites with < 20 % wetland cover and comprises two subgroups. The first subgroup - the upper Rolava catchment (ROL and SLA) is defined mainly by higher concentrations of DO and slightly higher values of SC, but lower values of other parameters, that corresponds with the box-plots and is related to lower mean temperatures and larger catchment area, steeper slopes and larger area of meadows and healthy spruce forest. The second subgroup comprises profiles in upper Vydra catchment (PTA, JAV, BRE), which exhibit higher pH possibly due to less wetland cover (< 15 %) than other profiles in upper Vydra. Group B includes sampling sites with > 20 % wetland cover and higher concentration of organic compounds. Profiles ROK2 and CIK are represented by the slightest catchment slope with lowest pH, higher COD_{Mn}, humins, Fe and $P–PO_4^{3-}$, which corresponds with the results that mean slope has been considered as the strongest (negative) determinant of organic matter (Parry et al. 2015).
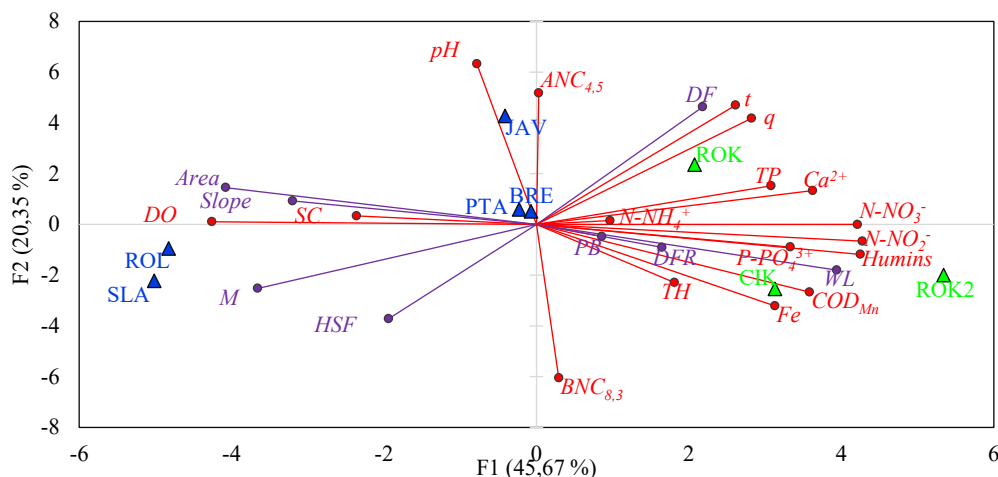
Fig. 2   *Principal component analyses (PCA) of measured parameters, catchment characteristics and discharge in 8 catchments (2013–2019). Individual profiles: Filled blue triangles (< 20 % wetlands), filled green triangles (>20 % wetlands). SC = specific conductivity, t = water temperature, DO = dissolved O2, TH = total hardness, TP = total phosphorus, Fe, CODMn = chemical oxygen demand, ANC4.5 = acid neutralization capacity, BNC8.5 = base neutralization capacity, HSF = healthy spruce forest, DF = damaged forest, DFR = decayed forest with partly regeneration, M = meadow, WL = wetlands, PB = peatbog, q = discharge.*
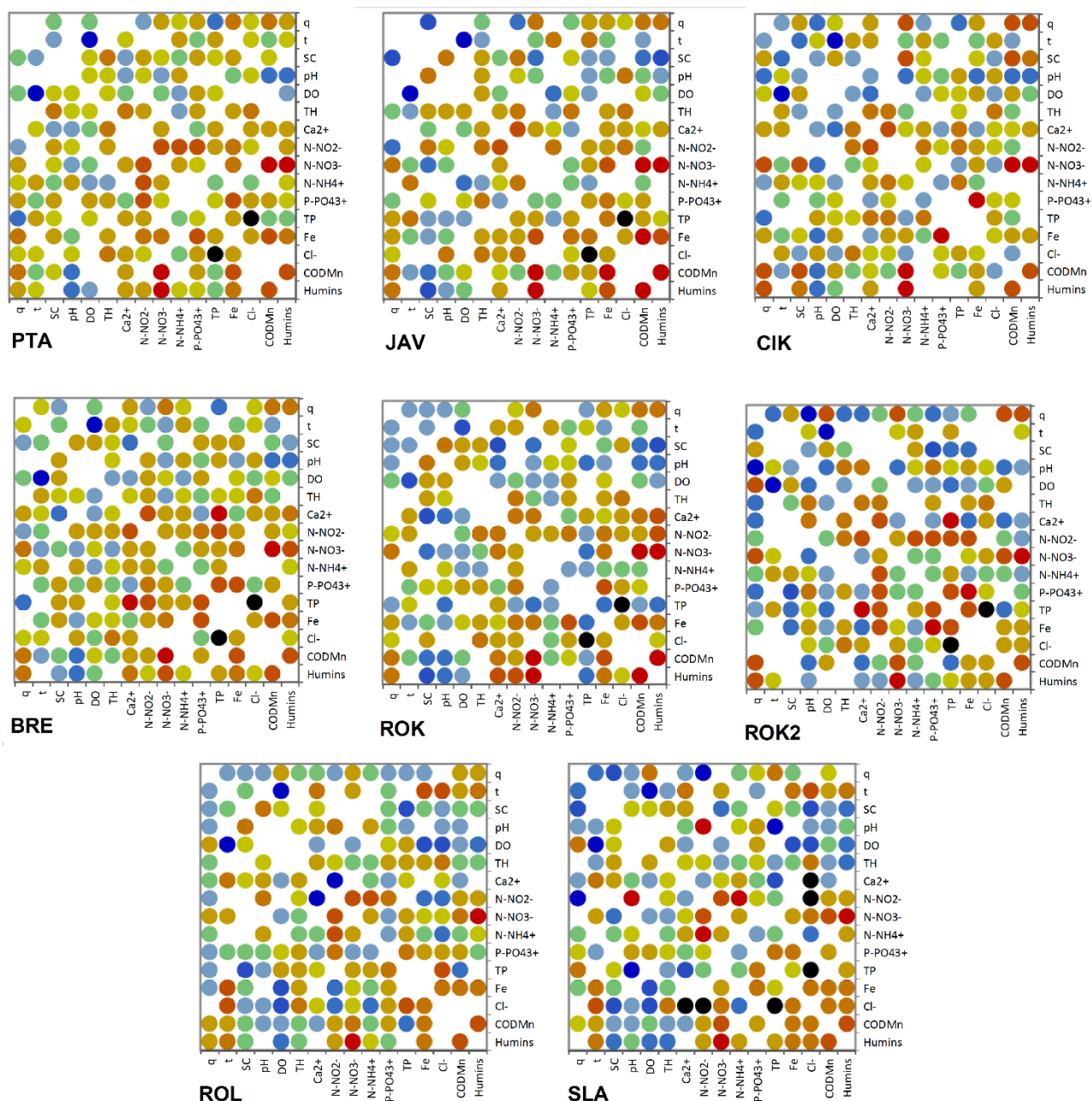
Fig. 3   *Correlation maps of Spearman's rank correlation; The blue colour corresponds to a correlation close to −1 and the red colour corresponds to a correlation close to 1. Green corresponds to a correlation close to 0.*

Discharge and catchment conditions before rainfall-runoff events have a fundamental impact on the behaviour of water quality parameters (Erlandsson *et al.* 2008, Köhler *et al.* 2008, Fučík *et al.* 2017). Even the rainwater is relatively low in dissolved minerals (Holko *et al.* 2006, Cano-Paoli *et al.*2019), decrease of SC with increasing discharge was registered only at SLA profile in upper Rolava and JAV in upper Vydra in our study. Both catchments have ≤ 10 % wetland cover. Positive linear correlation was observed at other profiles (CIK, ROK2) or there was no relationship. Positive relationship of

discharge and SC may be related to revitalization measures at the CIK monitoring site in the Šumava Mts. Increased SC values have been recorded in the outflow in revitalized water-logged forests in the Šumava Mts. which is consistent with the study Bufková *et al.* (2010). The most marked negative impact of discharge on pH can be observed in catchments with greatest wetland cover at CIK and ROK2 sites (p<0.05; Fig. 2, 3), corresponding to Kocum *et al.* (2016).

Discharge is considered as one of the most important factors contributing to changes in organic matter concentrations. For example, Erlandsson *et al.* (2008) note a strong positive correlation between COD_{Mn} and changes in discharge. Our results show that COD_{Mn} increases with increasing discharge. The changes of humins concentration with increasing discharge are similarly to COD_{Mn} (Fig. 2, 3). The greatest linear increase in humins was observed at the BRE and CIK sampling sites (slope > 0.9), the coefficient of determination indicates a medium relationship ($R^2 > 0.5$). Using Spearman's rank correlation coefficient, a significant relationship (p < 0.05) between humins and discharge was determined at JAV, CIK, BRE, ROK, ROK2 sites with the strongest relationship (p < 0.01) at CIK and ROK2 sites with the greatest wetland cover. The greatest release of organic matter is also related to iron reduction/oxidation cycles (Grybos *et al.* 2009, Knorr 2013). Coefficient of determination indicated positive correlation between COD_{Mn} and Fe in all catchments with the strongest correlation at JAV ($R^2 > 0.7$). This was also confirmed by Spearman's correlation coefficient (p < 0.05) at all sites with an exception of CIK and ROK2 (Fig. 3).

At most of the monitoring sites, there was also an increase in $N–NO_3^-$ during higher rates of discharge. This relationship was observed in particular at sites in the upper Vydra catchment (Fig. 2, 3) with significant correlation (p < 0.05) at JAV, CIK, BRE, ROK, ROK2 sites. In the upper Rolava catchment and the JAV profile, the increase of $N–NO_3^-$ was not significant (p > 0.05). Increased concentrations of $N-NO_3^-$ in small montane streams after rainfall events may also be caused by increased organic matter in study areas or atmospheric deposition and soil microbial response to N deposition, resulting in greater export of humic material (Peterson *et al.* 2001, Findlay 2005). A strong positive correlation between the concentration of $N–NO_3^-$ and humins was found at all monitoring sites (p < 0.01).

Linear regression or Spearman's rank correlation coefficient did not confirm any relationship between $N–NH_4^+$ and discharge. In case of $N–NO_2^-$, the change is not clear as well, because it is a highly reactive compound; under aerobic conditions it oxidizes quite easily into nitrates (Pitter 2009).

Slight positive correlations (p < 0.1) of iron concentrations and discharge have been observed only at the PTA and JAV sampling sites (Fig. 3). At SLA and ROL sites, higher concentrations of Fe were not positively correlated with higher discharge, but rather with higher temperatures, corresponding to Sarkkola *et al.* (2013).

Increased phosphorous concentrations have been associated with higher discharge, although in summer after long dry periods, significant increases in phosphorous concentrations in streams have also been observed as in studies of Jennings *et al.* (2009), Ockenden *et al.* (2016). At our study sites, the $P–PO_4^{3-}$ concentrations are generally very low, especially during spring and autumn. At the ROK2 site, the highest concentrations of this compound were found during the lowest discharge (0.06 mg.l^{-1}). Values of TP are the highest mainly in winter and during low discharge (PTA, CIK, ROL).

Even though the release of iron from peat soils could be related to acidic conditions, only a slight negative correlations between pH values and iron concentrations ($R^2 > 0.25$) were observed at PTA, CIK, BRE and JAV using linear regression. This correlation was confirmed by the Spearman's correlation coefficient only at CIK profile. Sarkkola *et al.* (2013) also found that water pH was not a significant factor explaining Fe concentrations, but rather the water temperature. A significant positive correlation of temperature and Fe was confirmed only at upper Rolava (Fig. 3).

An analysis of specific conductivity and pH during rainfall-runoff events
SC behaviour and the shape of hysteresis loops during rainfall-runoff events often differ greatly (Evans and Davies, 1998), while pH hysteresis loops are more often similar. However, many factors influence the final shape of hysteresis loops (Whitfield and Schreier, 1981). Based on an analysis of events at each sampling site, six different C/Q hysteresis loop types were identified. These types can be classified as belonging to one of four basic loop shapes (clockwise, counter-clockwise, eight-shaped, and mixed).

The dominant type of hysteresis loop of SC in the upper Vydra catchment was type 2 (counter-clockwise); in the upper Rolava catchment, the dominant type was type 1 (clockwise; Table 2) which also corresponds with the results of linear regression. Similar types of hysteresis loop of SC were identified at sampling sites in the upper Vydra catchment especially during consecutive summer rainfall-runoff events (particularly type 2 counter-clockwise loops). These findings correspond with those of an earlier study (Su *et al.* 2017) investigating rainfall-runoff events at PTAms, BREms, and ROKms in 2011–2014. During individual events, dissolved ionic compounds were released from the soil into streams; once baseflow conditions returned, SC values decreased to their initial values. This behaviour was primarily caused by the effect of peatbogs. The situation was slightly different in BRE catchment, where 80 % of forest cover has been decayed with only small part of regenerated area. During the onset of each rainfall-runoff event, an initial decrease in SC values occurred (resulting in an eight-shaped loop), but then SC values developed following the same pattern observed at other sampling sites. The same behaviour was also observed in study Su *et al.* (2017). The study site in the upper Rolava catchment (SLAms) behaved differently during consecutive summer rainfall-runoff events (resulting in type 1 clockwise loops for SC). During these events, stream water was diluted with water poor in dissolved ionic compounds. Catchment in the upper Rolava behaved similarly during snowmelt (resulting in type 1 clockwise loops), when water poor in dissolved ionic compounds diluted stream water. In the upper Vydra catchment, SC also decreased at the onset of events; hysteresis loop shape was type 3 – counter-clockwise. The CIKms sampling site demonstrated completely different behaviour during a snowmelt event (type 2), during which ion-rich water was released from the soil. After long dry periods, the findings from the upper Vydra catchment were like those made during other rainfall-runoff events (ROKms and BREms, eight-shaped; CIKms and PTAms counter-clockwise), whereas findings from the upper Rolava catchment differed. The first rainfall event after a long dry period led to increased SC with increased discharge and decreased SC after the end of the event (type 2). During the subsequent rainfall event, SC figures remained constant at first, but as the event subsided and discharge decreased, SC values began to increase and remained higher (type 6 – mixed).

In contrast, SC mainly increased during rainfall events after long dry periods at most of the sampling sites, which is primarily related to greater mineralization when groundwater levels drop, as well as the subsequent washing out of these materials after rain. Considering the ongoing effects of climate change, increasing air and water temperatures, and increased occurrence of extreme meteorological events (longer dry periods, flash flooding), this behaviour may have a fundamental impact on ecosystems (Worrall *et al.* 2004, Jennings *et al.* 2009, Broder *et al.* 2017).

The pH changes during rainfall-runoff events were represented mainly by type 1 (clockwise) C/Q hysteresis loop with its highest concentration on the rising limb. This was an expected outcome, because the pH of groundwater is more neutral than the event water components (Carrol *et al.*2007), but the velocity of decreasing of pH were different. The decrease of pH was much more rapid during consecutive summer rainfall-runoff events than during a snowmelt event and after a long dry period.

Table 2 Classification of C/Q hysteresis loops at each sampling site during rainfall-runoff events, 2014–2016; SC = specific conductivity, Q = discharge. pink background = clockwise, blue background = counter-clockwise, green background = eight-shaped, yellow background = mixed loop class, NE = Not evaluated.

	Consecutive summer rainfall-runoff events				After long-lasting dry periods		Spring snowmelt
Profile	9th July 2014	12th July 2014	14th July 2014	22nd July 2014	8th October 2015	16th October 2015	18th April 2016
	SC/Q hysteresis loop						
PTAms	2	2	2	2	2	2	*-NE-*
CIKms	2	2	2	2	2	2	2
BREms	5	2	*-NE-*	5	5	5	3
ROKms	5	2	2	2	2	5	3
SLAms	1	1	3	1	6	6	1
	pH/Q hysteresis loop						
PTAms	1	1	1	1	3	1	*-NE-*
CIKms	1	1	1	1	1	1	1
BREms	1	4	*-NE-*	4	3	1	3
ROKms	1	1	1	1	1	1	1
SLAms	*-NE-*	*-NE-*	*-NE-*	*-NE-*	*-NE-*	*-NE-*	*-NE-*

Conclusion

This study shows results of an analysis of 16 physicochemical parameters in 8 headwater catchments with presence of wetlands and peatbogs.

As we hypothesized:

(1) Increased concentrations of organic matter (represented mainly by COD_{Mn} and humins) and their higher release during greater discharges were observed in catchments with > 20 % of wetlands dominated by peat. Catchments with higher wetland cover were represented by higher TP, $N–NO_3^-$ and a significant decrease in pH during high streamflow rates. Higher mean concentrations of Fe were also detected, but discharge was not the main driver of higher release of Fe in catchments with > 20 % of wetlands.

(2) Concentration of Fe was correlated with COD_{Mn} concentration more than with pH or discharge. Iron and organic matter (more COD_{Mn}, less humic substances) mobilization in catchments was influenced by wetland area, but the strongest correlation of Fe and COD_{Mn} was noticed in the catchment with a relatively small proportion of wetlands (8 %) and peatbogs (2.3 %), but with 70 % of damaged forest cover in the catchment.

(3) The analysis of SC and pH changes during rainfall-runoff events showed that the type of rainfall-runoff event affects the velocity of pH changes. The decrease of pH was much more rapid during consecutive summer rainfall-runoff events than during a snowmelt event and after a long dry period. The changes of SC were controlled not only by the type of rainfall-runoff event, but also by the hydrological preconditions of the catchment.

Overall, considered as a drinking water source, higher concentration of natural organic matter is the main issue in Šumava and Krušné hory headwaters, because of the possible formation of disinfection by-products after water treatment. Not only wetlands and peatbog areas affect the concentration of organic substances, but also the total area, mean slope and hydrological precondition of the catchment. In contrast, values of pH, $BNC_{8.3}$ or $ANC_{4.5}$ did not have any connection to natural organic matter in our study. Restoration of drained peatland in one catchment appeared considerably problematic from the geochemical point of view, especially when associated with extreme rainfall-runoff events.

Acknowledgements

References

Aber JD, et al. (2002) *Inorganic Nitrogen Losses from a Forested Ecosystem in Response to Physical, Chemical, Biotic, and Climatic Perturbations, Ecosystems*, **60** (5), 648–658.

Addinsoft (2018) XLStat reference manual. Paris, Addinsoft.

Austnes K, et al. (2010) Effects of storm events on mobilisation and in-stream processing of dissolved organic matter (dom) in a welsh peatland catchment, *Biogeochemistry*, **99**, 157–173.

Björnerås C, et al. (2017) Widespread Increases in Iron Concentration in European and North American Freshwaters, *Global Biogeochemical Cycles*, **31** (10), 1488–1500.

Björnerås C, et al. (2019) High sulfate concentration enhances iron mobilization from organic soil to water, *Biogeochemistry*, **144**, 245–259.

Blahušiaková A, et al. (2020) Snow and climate trends and their impact on seasonal runoff and hydrological drought types in selected mountain catchments in Central Europe, *Hydrological Sciences Journal*, **65** (12), 2083–2096.

Broder T, Knorr KH and Biester H (2017) Changes in dissolved organic matter quality in a peatland and forest headwater stream as a function of seasonality and hydrologic conditions, *Hydrology and Earth System Sciences*, **21** (4), 2035–2051.

Broussard W and Turner RE (2009) A century of changing land-use and water-quality relationships in the continental US, *Frontiers in Ecology and the Environment*, **7** (6), 302–307.

Bufková I, Stíbal F and Mikulášková E (2010) Restoration of Drained Mires in the Šumava National Park, Czech Republic. In: M. Eiseltová, ed. Restoration of Lakes, Streams, Floodplains, and Bogs in Europe, Wetlands: Ecology, Conservation and Management, Dordrecht: Springer, 331–354.

Bull RJ et al. (2011) Potential carcinogenic hazards of non-regulated disinfection by-products: Haloquinones, halo-cyclopentene and cyclohexene derivatives, N-halamines, halonitriles, and heterocyclic amines, *Toxicology*, **286** (1–3), 1–19.

Burns DA, et al. (2001) Quantifying contributions to storm runoff through end-member mixing analysis and hydrologic measurements at the Panola Mountain research watershed (Georgia, USA), *Hydrological Processes*, **15** (10), 1903–1924.

Cano-Paoli K, Chiogna G, and Bellin A (2019) Convenient use of electrical conductivity measurements to investigate hydrological processes in Alpine headwaters, *Science of the Total Environment*, **685**, 37–49.

Carroll KP, Rose S, and Peters NE (2007) Concentration/discharge hysteresis analysis of storm events at the Panola mountain research watershed, Georgia, USA. Proceedings of the Georgia Water Resources Conference, March 27–29, 2007. University of Georgia, Athens, GA, USA.

CENIA (2012) Data from: CORINE Land Cover 2012 [dataset]. Available from: http://geoportal.gov.cz/php/wmc/data/54624695-29f0-4f98-be9d-635ac0a80137.wmc [Accesed 20 March 2019].

CUNI (2018) Data from: Hydro-Meteorological Monitoring Network [dataset]. Prague: Charles University.

Delpla I, et al. (2009) Impacts of climate change on surface water quality in relation to drinking water production, *Environment International*, **35** (8), 1225–1233.

Easterling DR, et al. (2000) Climate extremes: Observations, modeling, and impacts, *Science*, **289** (5487), 2068–2074.

Erlandsson M, et al. (2008) Thirty-five years of synchrony in the organic matter concentrations of Swedish rivers explained by variation in flow and sulphate, *Global Change Biology*, **14** (5), 1191–1198.

European Environment Agency (2017) Climate change impacts and vulnerabilities 2016 – EEA Report No 1/2017 [online]. Available from: https://www.eea.europa.eu/publications/climate-change-impacts-and-vulnerability-2016 [Accessed 3 September 2019].

Evans CD, Monteith DT, and Cooper DM (2005) Long-term increases in surface water dissolved organic carbon: Observations, possible causes and environmental impacts, *Environmental Pollution*, **137** (1), 55–71.

Evans C and Davies TD (1998) Causes of concentration/discharge hysteresis and its potential as a tool for analysis of episode hydrochemistry, *Water Resources Research*, **34** (1), 129–137.

Evans DM, et al. (2014) Long-Term Trends of Specific Conductance in Waters Discharged by Coal-Mine Valley Fills in Central Appalachia, USA, *Journal of the American Water Resources Association,* **50** (6), 1449–1460.

Fenner N, Freeman C, and Worrall F (2013) Hydrological Controls on Dissolved Organic Carbon Production and Release from UK Peatlands. In: A.J. Baird, et al., eds. Carbon Cycling in Northern Peatlands, Geophysical Monograph Series 184, Washington, D.C., American Geophysical Union, 237–249.

Findlay SE (2005) Increased carbon transport in the Hudson River: unexpected consequence of nitrogen deposition?, Frontiers in Ecology and the Environment, 3: 133–137. doi: 10.1890/1540-9295(2005)003[0133:ICTITH]2.0.CO;2

Friedman M (1937) The use of ranks to avoid the assumption of normality implicit in the analysis of variance, *Journal of the American Statistical Association*, **32**, 675–701.

Fučík P, et al. (2017) Incorporating rainfall-runoff events into nitrate-nitrogen and phosphorus load assessments for small tile-drained catchments, *Water*, **9** (9), 712.

Grybos M, et al. (2007) Is trace metal release in wetland soils controlled by organic matter mobility mobility or Fe-oxyhydroxides reduction?, *Journal of Colloid and Interface Science*, **314**, 490–501.

Haapalehto TO, et al. (2011) The Effects of Peatland Restoration on Water-Table Depth, Elemental Concentrations, and Vegetation: 10 Years of Changes, *Restoration Ecology*, **19** (5), 587–598.

Holko L, et al. (2006) Variation of nitrates in runoff from mountain and rural areas, *Biologia*, **61** (19), S270–S274.

Hruška J, et al. (2009) Increased Dissolved Organic Carbon (DOC) in central European streams is driven by reductions in ionic strength rather than climate change or decreasing acidity, *Environmental Science and Technology*, **43** (12), 4320–4326.

Jennings E, et al. (2009) Impacts of climate change on phosphorus loading from a grassland catchment: Implications for future management, *Water Research*, **43** (17), 4316–4326.

Jones DL, et al. (2008) Dissolved organic carbon and nitrogen dynamics in temperate coniferous forest plantations, *European Journal of Soil Science*, **59** (6), 1038–1048.

Kida M, et al. (2018) Contribution of humic substances to dissolved organic matter optical properties and iron mobilization, *Aquatic Sciences*, **80** (26).

Kliment Z, et al. (2011) Evaluation of trends in hydro-climatic long-term data series for selected mountains catchments. In: H. Středová, , J. Rožnovský, T. Litschmann, eds., Mikroklima a mezoklima krajinných struktur a antropogenních prostředí, 2–4 February 2011 Skalní mlýn. Prague: Česká bioklimatická společnost v nakl. Český hydrometeorologický ústav. 52 pp.

Knorr KH (2013) DOC-dynamics in a small headwater catchment as driven by redox fluctuations and hydrological flow paths – are DOC exports mediated by iron reduction/oxidation cycles?, *Biogeosciences*, **10** (2), 891–904.

Kocum J, et al. (2016) Geochemical evidence for peat bog contribution to the streamflow generation process: case study of the Vltava River headwaters, Czech Republic, *Hydrological Sciences Journal*, **61** (14), 2579–2589.

Köhler SJ, et al. (2008) Climate's control of intra-annual and interannual variability of total organic carbon concentration and flux in two contrasting boreal landscape elements, Journal of Geophysical Research: *Biogeosciences*, **113** (3), G03012.

Langhammer J, Su Y, and Bernsteinová J (2015) Runoff response to climate warming and forest disturbance in a mid-mountain basin, *Water*, **7** (7), 3320–3342.

Langhammer J, and Bernsteinová J (2020) Which Aspects of Hydrological Regime in Mid-Latitude Montane Basins Are Affected by Climate Change?, *Water*, **12** (8), 2279.

Lassaletta L, et al. (2010) Headwater streams: Neglected ecosystems in the EU Water Framework Directive. Implications for nitrogen pollution control, *Environmental Science and Policy*, **13** (5), 423–433.

Laudon H, et al. (2011) Patterns and dynamics of dissolved organic carbon (doc) in boreal streams: The role of processes, connectivity, and scaling, *Ecosystems*, **14**, 880–893.

Ledesma JLJ, et al. (2013) Riparian zone control on base cation concentration in boreal streams, *Biogeosciences*, **10** (6), 3849–3868.

Lepistö, A., Futter, M.N., and Kortelainen, P., 2014. Almost 50 years of monitoring shows that climate, not forestry, controls long-term organic carbon fluxes in a large boreal watershed, *Global Change Biology*, **20** (4), 1225–1237.

Lepistö A, Kortelainen P, and Mattsson T (2008) Increased organic C and N leaching in a northern boreal river basin in Finland, *Global Biogeochemical Cycles*, **22** (3), GB3029.

Löfgren S, Gustafsson JP, and Bringmark L (2010) Decreasing DOC trends in soil solution along the hillslopes at two IM sites in southern Sweden - Geochemical modeling of organic matter solubility during acidification recovery, *Science of the Total Environment*, **409** (1), 201–210.

Muller FLL, et al. (2015) Effects of temperature, rainfall and conifer felling practices on the surface water chemistry of northern peatlands, *Biogeochemistry*, **126**, 343–362.

Noskovič J, et al. (2013) Time and Place Changes in pH And Conductivity in the Water of Čaradice Stream, *Acta Horticulturae et Regiotectuare*, **16** (1), 24–28.

Ockenden MC, et al. (2016) Changing climate and nutrient transfers: Evidence from high temporal resolution concentration-flow dynamics in headwater catchments, *Science of the Total Environment*, 548–549, 325–339.

Orndorff ZW, et al. (2015) A column evaluation of Appalachian coal mine spoils' temporal leaching behavior, *Environmental Pollution*, **204**, 39–47.

Oulehle F, et al. (2012) Modelling soil nitrogen: The MAGIC model with nitrogen retention linked to carbon turnover using decomposer dynamics, *Environmental Pollution*, **165**, 158–166.

Oulehle F, and Hruška J (2009) Rising trends of dissolved organic matter in drinking-water reservoirs as a result of recovery from acidification in the Ore Mts., Czech Republic, *Environmental Pollution*, **157** (12), 3433–3439.

Parry LE, et al. (2015) The influence ofslope and peatland vegetation type on riverine dissolved organic carbon and water colour at different scales, *Science of the Total Environment*, 527–528, 530–539.

Penna D, et al. (2015) Seasonal changes in runoff generation in a small forested mountain catchment, *Hydrological Processes*, **29** (8), 2027–2042.

Peterson BJ, et al. (2001) Control of nitrogen export from watersheds by headwater streams. *Science*, **292** (5514), 86–90.

Pitter P (2009) Hydrochemie, Prague, Publishing VŠCHT.

Porcal P, et al. (2009) Humic substances-part 7: The biogeochemistry of dissolved organic carbon and its interactions with climate change, *Environmental Science and Pollution Research*, **16** (6), 714–726.

Ritson JP, et al. (2014) The impact of climate change on the treatability of dissolved organic matter (DOM) in upland water supplies: A UK perspective, *Science of the Total Environment*, 473–474, 714–730.

Rupp H, Meissner R, and Leinweber P (2004) Effects of extensive land use and re-wetting on diffuse phosphorus pollution in fen areas - Results from a case study in the Drömling catchment, Germany, *Journal of Plant Nutrition and Soil Science*, **167** (4), 408–416.

Šanda M, et al. (2014) Run-off formation in a humid, temperate headwater catchment using a combined hydrological, hydrochemical and isotopic approach (Jizera Mountains, Czech Republic), *Hydrological Processes*, **28** (8), 3217–3229.

Sarkkola S, et al. (2013) Iron concentrations are increasing in surface waters from forested headwater catchments in eastern Finland, *Science of the Total Environment*, 463–464, 683–689.

Selle B, Knorr KH, and Lischeid G (2019) Mobilisation and transport of dissolved organic carbon and iron in peat catchments—Insights from the Lehstenbach stream in Germany using generalised additive models, *Hydrological Processes*, 1–13.

Shapiro SS, and Wilk MB (1965) An analysis of variance test for normality (complete samples), *Biometrika*, **52**, 591–611.

Shrestha S, and Kazama F (2007) Assessment of surface water quality using multivariate statistical techniques: a case study of the Fuji river basin, Japan, *Environmental Modelling & Software*, **22** (4), 464–475.

Soulsby C, et al. (2001) Seasonality, water quality trends and biological responses in four streams in the Cairngorm Mountains, Scotland, *European Surgical Research,* **5** (3), 433–450.

Spearman C (1904) The proof and measurement of association between two things, *American journal of psychology*, **15** (1), 72–101.

Su Y, Langhammer J, and Jarsjö J (2017) Geochemical responses of forested catchments to bark beetle infestation: Evidence from high frequency in-stream electrical conductivity monitoring, *Journal of Hydrology*, **550**, 635–649.

Timpano AJ, et al. (2010) Isolating Effects of Total Dissolved Solids on Aquatic Life in Central Appalachian Coalfield Streams. In: RI Barnhisel, ed. National Meeting of the American Society of Mining and Reclamation June 5–10 Pittsburgh. Lexington: ASMR, 1284–1302.

Tolasz R, and Baštýřová H (2007) Climate atlas of Czechia, Prague, Czech Hydrometeorological Institute.

Vlach V, Ledvinka O, and Matouskova M (2020) Changing Low Flow and Streamflow Drought Seasonality in Central European Headwaters, *Water*, **12** (12), 3575.

Vlček L, et al. (2016) Influence of peat soils on runoff process: case study of Vydra River headwaters, Czechia, *Geografie*, **121** (2), 235–253.

von Schiller D, Martí E, and Riera JL (2009) Nitrate retention and removal in Mediterranean streams bordered by contrasting land uses: a ^{15}N tracer study, *Biogeosciences*, **6** (2), 181–196.

Wackernagel H (1995) Multivariate Geostatistics, Berlin, Springer-Verlag.

Whitfield PH, and Schreier H (1981) Hysteresis in relationships between discharge and water chemistry in the Fraser River basin, British Columbia, *Limnology and Oceanography*, **26** (6), 1179–1182.

Williams GP (1989) Sediment concentration versus water discharge during single hydrologic events in rivers, *Journal of Hydrology*, **111** (1–4), 89–106.

Worrall F, Burt T, and Adamson J (2004) Can climate change explain increases in DOC flux from upland peat catchments?, *Science of the Total Environment*, **326** (1–3), 95–112.

Worrall F, Burt T, and Shedden R (2003) Long term records of riverine dissolved organic matter, *Biogeochemistry*, **64** (2), 165–178.

Zajíček A, Pomije T, and Kvítek T (2016) Event water detection in tile drainage runoff using stable isotopes and a water temperature in small agricultural catchment in Bohemian-Moravian Highlands, Czech Republic, *Environmental Earth Sciences*, **75**, 838.

Zheng Q, et al. (2016) Characterization of natural organic matter in water for optimizing water treatment and minimizing disinfection by-product formation, *Journal of Environmental Sciences*, **42**, 1–5.

Zuecco G, et al. (2016) A versatile index to characterize hysteresis between hydrological variables at the runoff event timescale, *Hydrological Processes*, **30** (9), 1449–1466.

Qualitative analysis of surface waters of danube river (within borders of Ukraine)

Igor GOPCHAK[1], Tetiana BASIUK[2], Artem YATSYK[3]

[1, 3] National University of Water and Environmental Engineering, Ukraine, email: [1] i.v.hopchaknuwm.edu.ua, [3] yatsyk_vg19@nuwm.edu.ua[3, 2] International University of Economics and Humanities Academician Stepan Demianchuk, Ukraine, email: [3] email: [2] tanya_basyuk@ukr.net

Introduction

Today, in the times of exacerbation of many environmental problems associated with pollution of natural waters, the issues of water quality research are of particular importance. The problem of assessing the quality of surface waters is extremely relevant and requires constant attention due to the growing anthropogenic pressure on water bodies. The main causes of their pollution are: discharges of untreated and insufficiently treated municipal and industrial wastewater directly into water bodies, and through the municipal sewerage system; inflow of pollutants into water bodies in the process of surface runoff from built-up areas and agricultural lands; soil erosion in the water intake area (Snizhko, 2001).

Virtually all major rivers of Ukraine are integrated into a single hydrological system that operates both in our country and abroad. The issues of assessing the quality of surface waters are especially relevant in the transboundary movement of pollutants by rivers from one state to another, creating potential threats to the environmental and human welfare. Migration of pollutants with watercourses from one state to another underlines to its international character, the need to combine efforts and resources of states to protect and restore transboundary rivers, in particular, convergence and harmonization of national and international law, international environmental cooperation. To improve transboundary monitoring of surface water quality, it is necessary to coordinate management decisions in the field of water management with other countries that have common transboundary watercourses, disseminate environmental and water management information, develop common criteria for assessing the ecological status of river basins, etc. (Directive 2000; Yatsyk et al. 2006, 2017; Bielski A. 2012; Anpilova, 2013; Gopchak et al., 2019).

Study of both practical and theoretical aspects of the ecological status of natural waters is important, as it allows for the rational use of water bodies and ensures their protection from pollution. Therefore, timely monitoring of the quality of surface waters of river basins is a necessary step before analysis and summarization of information on the state of water bodies, forecast of its changes and development of scientifically sound recommendations for appropriate management decisions in the use, protection and reproduction of water bodies and resources.

The water resources of the Danube River are used not only by Ukraine, but also by a number of other European countries. There are 17 countries within the Danube River Basin, and environmental pollution is a serious problem both for the Danube Basin as a whole and for the section of the Danube River located in Ukraine. (World Wide Fund for Nature, 2002). The state of surface waters of the Danube River largely depends on the negative side effects from the process of water usage and economic activity in the catchment area. The ecological condition of the river's surface waters is influenced by various factors. The main source of pollution of the Danube River within Ukraine is wastewater from enterprises and housing & communal services. In light of this, there exists a need for scientific substantiation of rational water usage and development of measures to protect the waters of the Danube River from pollution. And the first step in this journey is assessment of the quality of surface water.

The purpose of the study was to assess the quality of surface waters of the Danube River within its Ukrainian part.

Methodology

Ecological assessment of surface water quality of the Danube River was carried out using the system of classification of standards for assessment of surface water quality of Ukraine in accordance with the «Methodology of ecological assessment of surface water quality by relevant categories»

The ecological assessment of the surface water quality of the Western Bug River was carried out using the data from systematic observations, on the basis of the ecological classification of the surface water quality of the land and estuaries of Ukraine. It includes a set of hydrophysical, hydrochemical, hydrobiological and other indicators that reflect the characteristics of the aquatic ecosystems (Metodyka …, 1998). According to the «Methodology of ecological assessment of surface water quality by relevant categories», the initial data were grouped into three blocks of indicators: the index of the content of salt components in fresh water (I_1); index of tropho-saprobic (ecological and sanitary) indicators (I_2); index of indicators of content of specific toxic and radioactive substances (I_3). Based on block index values (I_1, I_2, I_3), in accordance with standards of surface running waters quality, the integrated (ecological) index was calculated (I_E). Based on the obtained ecological assessment indices, the class and category of water quality were determined (Fig. 1). For efficiency of calculations, the table 1 was developed with selected subcategories of water quality within seven categories and five classes and verbal characteristics of decimal values of block indices according to the degree of purity (pollution) of water. According to (Metodyka…, 1998) 5 classes of water quality were established, with every class having corresponding category and grade.
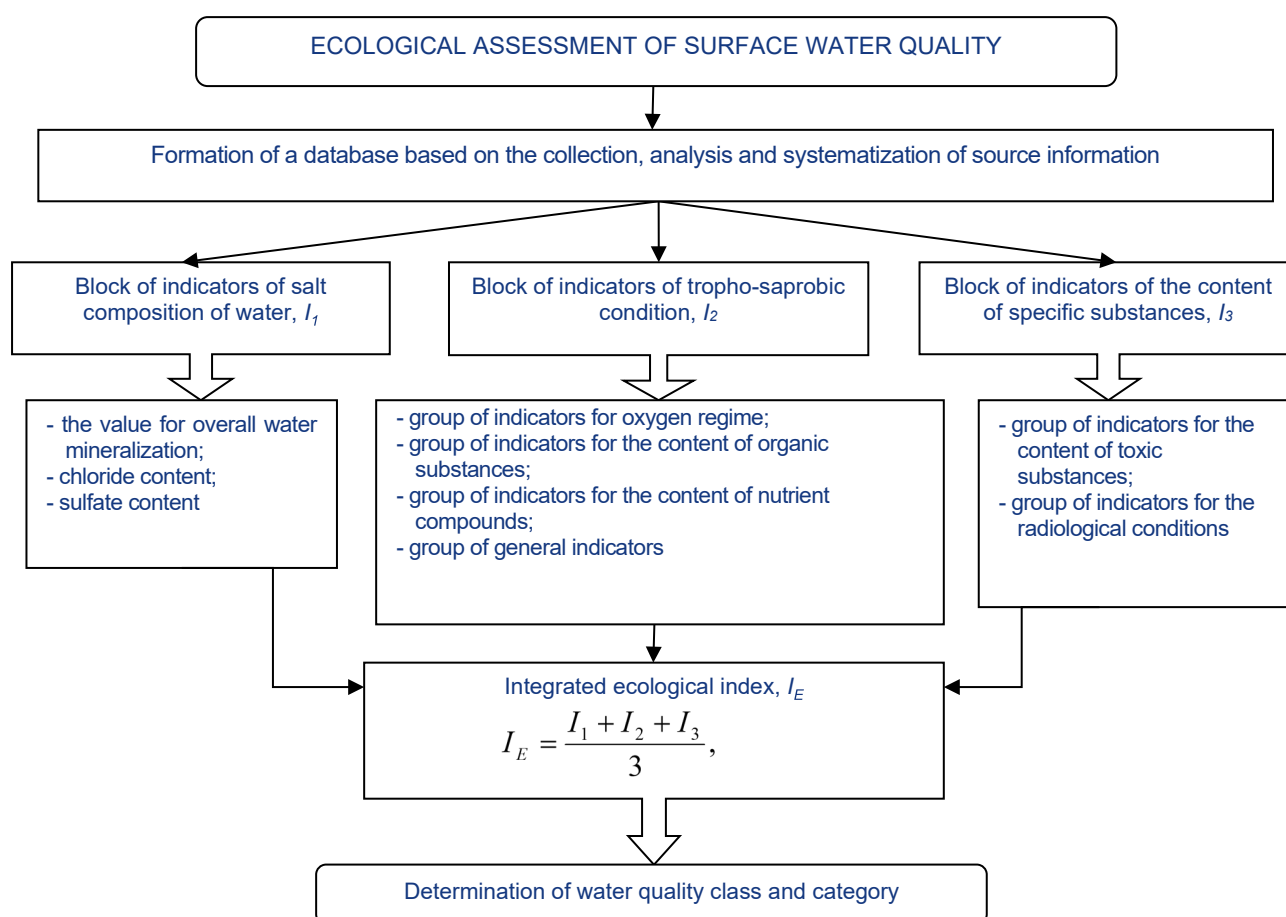

Fig. 1 Block diagram of ecological assessment of surface water quality of the Danube river

Table 1 Classes and categories of surface quality according to ecological classification (Methods…, 1998)

Names of classes and categories of water quality according to their natural state	class	I	II		III		IV	V
		excellent	good		satisfactory		bad	very bad
	category	1	2	3	4	5	6	7
		excellent	very good	good	satisfactory	mediocre	bad	very bad
Names of classes and categories of water by degree of its purity (contamination)	class	I	II		III		IV	V
		very pure	pure		polluted		dirty	very dirty
	category	1	2	3	4	5	6	7
		very pure	pure	quite pure	slightly polluted	moderately polluted	dirty	very dirty

Results

The Danube River is the second longest and largest river (by catchment area) in Europe, being 2860 km long, with 175 km stretch situated within the Odessa region, functioning as the main waterway in southern Ukraine, supplying water to local population and industries (irrigation, drinking needs, shipping, etc.) . The Danube is a transboundary river. The total area of the Danube River basin is 817 thousand km^2 (8% of the total territory of Europe). The largest tributaries of the Danube, which originate in Ukraine – the rivers Tisza, Prut, Seret supply about 15 km^3 of water per year. This is only 7.3% of the annual runoff of the Danube. Only small section of the lower Danube (170 km) is situated on the territory of Ukraine, from the city of Reni to its mouth (Polishchuk, Shega, 1998).

Danube basin has one medium river in its basin – Yalpug (total length of the river 142 km, in Ukraine – 8 km). Its annual runoff is 24.6 million m^3. Among all the small rivers in the Lower Danube sub-basin, Kyrhyzh-Kytai, Aliyaha, Nerushai, Velykyi Kotlabukh, and Drakulya stand out. Due to the climate change and anthropogenic activity, there is a decrease in amount of water in small rivers. The group of Danube reservoirs includes freshwater reservoirs located on the left side of the Kili branch of the Danube in the area from Reni: Kahul, Kartal, Kuhurluy, Katlabukh, Sof'ya, Kytai.

The climate of the Ukrainian part of the Danube river basin is moderately warm. It is characterized as moderately continental, with short mild winters and frequent thaws, long hot dry summers, insufficient rainfall. Such climatic conditions exist due to complex interaction of many physical and geographical factors, of which the most important are: the radiological conditions, specifics of local atmospheric circulation, local terrain and influence of the sea.

Black Sea lowland stands on the territories of the Danube river basin, the surface of which has an absolute height of 150–130 m. In this area, exists a variety of different forms of terrain: by genesis – accumulative, erosive, denudation, subsidence, artificial. Wide watersheds (primary-accumulative plains) are typical for the northern and north-eastern parts of the basin. In the southeast – Upper Pliocene marine terraces. Along the sea there is a variety of coastal accumulative landforms – beaches, spits, shoals. Parts of the sea shores, estuaries and lakes are abrasive, landsliding, and sometimes landsliping.

Tectonically, lowland is part of the Black Sea basin, filled with almost horizontal thick layers of sedimentary rocks, mainly marine Paleogene and Neogene sediments (clays, sands, sandy-clayey and sandy-limestone rocks, limestones), on which lie the continental deposits of the brown clays, loesses, loess loams.

Area is dominated by steppe landscapes with dark chestnut soils. Most of the steppes are plowed and are used as agricultural land. In general, the flatter terrain contributes to the intensive economic development of the region.

Precambrian, Paleozoic, Mesozoic and Cenozoic sediments are observed in the geological structure of the Danube river basin.

The territory of the Danube River Basin is part of the Black Sea Artesian Basin and is characterized by quite complex hydrogeological conditions. Groundwaters are observed in almost all sediments. Groundwater is found in Quaternary and Neogene rocks and is characterized by varying depth, methods and ease of its extraction, distribution and quality. The direction of movement in Quaternary and Neogene sediments (groundwater) in natural conditions coincide mainly with the slope of the earth's surface, the feeding area coincides with the area of distribution, unloading takes place in the valleys. There are nine aquifers in the region. Within the basin, the depth to the aquifers is usually from 20 to 30 m. The total groundwater reserves in the Danube River Basin are limited and require strict control over their use.

The Danube basin is dominated by steppe landscapes. Main soils of the region are common chernozems and southern chernozems, and within the Danube terrace plain and in the south-west of the watershed plain – micellar-carbonate soil are predominant.

The hydrological regime of the Ukrainian part of the Danube basin mainly depends on climatic conditions. Water regime has three main phases – spring floods, summer and autumn floods, autumn and winter lows.

In general, the ecological status of the surface waters of the Danube basin is influenced by various factors, which are also closely interrelated. For the most part, the greatest impact on the surface water resources of the Danube River in this area is caused by wastewater discharges into surface water bodies without proper treatment, which cause surface water pollution.

To assess the surface water quality of the Danube, four state monitoring points were selected, which allowed to characterize the hydroecological condition of the river within the territory of Ukraine from Reni (163 km from the mouth of the river) to Vilkove (20 km). Measurement of water quality indicators at state monitoring points is carried out periodically (quarterly) according to certain parameters, the obtained results are provided to the management for generalization.

The worst data for hydroecological observations of water quality on the Danube River, which were conducted in 2019 by laboratories of the State Agency of Water Resources of Ukraine, were used as initial data for calculations.

Block of indicators for salt composition (I_1). Based on studies of surface waters of the Danube River in terms of salt composition of water (Table 2), it was found that the mineralization, which reflects the physical and geographical conditions of river runoff formation, ranged from 512.92 mg/dm^3 (Reni) to 605.99 mg/dm^3 (Kiliya). Therefore, river waters by the criterion of mineralization are defined as fresh oligohaline waters and correspond to the 2 category of II class water quality («good» by class, «pure» by degree of purity).

Table 2 Ecological assessment of the surface water quality of the Danube River according to the indicators of salt composition, I_1

#	Indicator	Danube, Reni (163 km)		Danube, Izmail (94 km)		Danube, Kiliya (48 km)		Danube, Vilkove (20 km)	
		value	category	value	category	value	category	value	category
1	Sum of ions, mg/dm^3	512.92	2	573.07	2	605.99	2	509.78	2
2	Chlorides, mg/dm^3	35.50	3	35.50	3	177.30	5	35.45	3
3	Sulfates, mg/dm^3	225.10	6	273.10	6	253.92	6	213.12	6
Value I_1		3.7	4	3.7	4	3.7	4	4.3	4
Water quality class		III		III		III		III	

The value of chloride content in the surface waters of the Danube River ranged from 35.45 mg/dm^3 (Izmail) to 177.30 mg/dm^3 (Norin River), which is within normal limits (350 mg/dm^3). The water quality corresponded to the II (Reni, Izmail, Vilkove – «good» in class, «pure» in the degree of purity) and III class (Kiliya – «satisfactory» in class, «polluted» in degree of purity).

The value of sulfate content ranged from 213.12 mg/dm^3 (Vilkove) to 273.10 mg/dm^3 (Izmail) at the ecological optimum – 500 mg/dm^3. According to this indicator, water quality at all observation points corresponded to class IV quality («bad» in class, «dirty» in degree of purity).

In general, the indicators of the salt block *(I_1)* are within the maximum allowable concentration for fishery reservoirs. The surface waters of the Danube River in this block belong to the third class of water quality («satisfactory» in class, «polluted» in the degree of purity).

Block of tropho-saprobic (ecological and sanitary) indicators (I_2). According to the indicators of this block (Table 3), the surface waters of the rivers under study belong to the 5th category of the III class of water quality («satisfactory» in terms of class, «polluted» in terms of purity).

Table 3 Ecological assessment of the surface water quality of the Danube River according to the indicators of the tropho-saprobic block (ecological and sanitary) indicators, I_2

#	Indicator	Danube, Reni (163 km)		Danube, Izmail (94 km)		Danube, Kiliya (48 km)		Danube, Vilkove (20 km)	
		value	category	value	category	value	category	value	category
1	Suspended substances, mg / dm^3	54.00	6	72.00	6	67.00	6	113.00	7
2	pH	7.74	2	8.15	3	7.83	2	8.12	3
3	Ammoniacal nitrogen, mg / dm^3	0.5	4	0.43	4	1.5	6	0.31	4
4	Nitrite-nitrogen, mg / dm^3	0.05	5	0.05	5	0.12	7	0.05	5
5	Nitrate-nitrogen, mg / dm^3	6.20	7	5.00	7	8.00	7	4.42	7

6	Phosphorus phosphates, mg / dm^3	0.3	6	0.47	7	0.3	6	0.24	6
7	Dissolved oxygen, mg / dm^3	8.50	1	8.10	1	9.00	1	8.20	1
8	Chemical oxygen demand, COD	59.00	6	56.00	6	52.63	6	66.00	7
9	BOD$_5$, mg / dm^3	5.00	5	3.60	4	4.30	5	4.00	4
Value I_2		4.7	5	4.8	5	5.1	5	4.9	5
Water quality class		III		III		III		III	

It should be noted that the following indicators had the greatest influence on the value of the block index of tropho-saprobic (ecological-sanitary) indicators *(I₂)*: content of ammonium, nitrite and nitrate nitrogen; phosphorus content and chemical oxygen demand. Surface waters according to these indicators belonged to 6–7 categories of IV–V quality class («bad» – «very bad» by class; «dirty» – «very dirty» by degree of purity).

Block of specific toxic substances (I₃). Regarding the block of specific toxic substances (Table 4), the quality of surface waters of the Danube River corresponded to the II class of quality in the areas of Reni and Vilkove («good» by class, «pure» by degree of purity), and in areas Ishmael and Kiliya – class III («satisfactory» by class, «polluted» by degree of purity).

Table 4 Ecological assessment of the surface water quality of the Danube river according to the indicators of the block for specific toxic substances , I₃

#	Indicator	Danube, Reni (163 km)		Danube, Izmail (94 km)		Danube, Kiliya (48 km)		Danube, Vilkove (20 km)	
		value	category	value	category	value	category	value	category
1	Total iron, mg/dm^3	0.20	4	0.20	4	0.20	4	0.20	4
2	Petroleum products, mg/dm^3	0.01	2	0.01	2	0.02	2	0.03	3
3	SPAR, mg/dm^3	0.23	4	0.20	3	0.33	4	0.17	3
Value I_2		3.3	3	3.5	4	4.00	4.0	3.3	3
Water quality class		II		III		III		II	

The results of the ecological assessment of the surface water quality of the Danube river by block indices *(I₁, I₂, I₃)* are presented in the table. 5.

Table 5 Ecological assessment of the surface water quality of the Danube River according to block indices (I_1, I_2, I_3)

№ з/п	Station (distance from the mouth of the river)	Index value											
		I_1				I_2				I_3			
		value	category	sub category	class	value	category	sub category	class	value	category	sub category	class
1	Danube, Reni (163 km)	3,7	4	3–4	III	4.7	5	4–5	III	3.3	3	3(4)	II
2	Danube, Izmail (94 km)	3.7	4	3–4	III	4.8	5	5(4)	III	3.5	4	3–4	III
3	Danube, Kiliya (48 km)	3.7	4	3–4	III	5.1	5	5	III	4.0	4	4	III
4	Danube, Vilkove (20 km)	4.3	4	4(5)	III	4.9	5	5(4)	III	3.3	3	3(4)	II

Integrated Environmental Assessment (IE). According to the final integrated ecological index *(I_E)*, the surface waters of the Danube River at all observation points belong to the III class, 4 category of water quality and are characterized as «satisfactory» by condition and «polluted» by the degree of purity (Table 6).

Table 6 Integrated environmental assessment of the surface water quality of the Danube River (I_E)

#	Station (distance from the mouth of the river)	I_E	Category	Subcategory	Class	Condition by class, category	Degree of purity by class, category	Condition, by subcategory	Degree of purity, by subcategory
1	Danube, Reni (163 km)	3.9	4	4(3)	III	satisfactory, quite good	polluted, slightly polluted	satisfactory, with tendency towards good	slightly polluted, with tendency towards fairly clean
2	Danube, Izmail (94 km)	4.0	4	4	III	satisfactory, quite good	polluted, slightly polluted	satisfactory	slightly polluted
3	Danube, Kiliya (48 km)	4.3	4	4(5)	III	satisfactory, quite good	polluted, slightly polluted	satisfactory, with a tendency to approach mediocre	slightly polluted with a tendency to approach moderately polluted
4	Danube, Vilkove (20 km)	4.2	4	4	III	satisfactory, quite good	polluted, slightly polluted	satisfactory	slightly polluted

The priority measures that will improve the ecological status of the surface waters of the Danube are:

1) reconstruction of existing and construction of new water treatment facilities;

2) cessation of discharge of untreated effluents into the river;

3) strict implementation of current water protection legislation by water users.

Conclusion

Thus, the results of observations of the quality of surface waters of the Danube River within Ukraine in 2019 indicate their satisfactory condition. The quality of water according to the Integrated Ecological Index (I_E) corresponds to the III class of quality, which indicates the need for targeted measures to improve the ecological situation and protect the ecosystem of the Danube River.

To improve transboundary monitoring of surface water quality, it is necessary to coordinate water management decisions with other countries that have common transboundary watercourses, disseminate environmental and water management information, develop common criteria for assessing the ecological status of river basins. That is why it is necessary to do timely monitoring of the quality of surface waters of the basin and analyze & summarize information on the state of water bodies, forecast its changes and develop scientifically sound recommendations for appropriate management decisions in the use, protection and recreation of water resources.

Determining the quality of water in the Danube is important for assessing the ecological situation of its basin in order to further substantiate the main areas of water protection activities to improve the ecological condition of the river and establish environmental standards for water quality. All this outlines the prospects for further research.

References

Anpilova Y. 2013. Informatsiini tekhnolohii dlia upravlinnia ekolohichnoiu bezpekoiu poverkhnevykh vod: monohrafiia [Information technologies for the management of surface water ecological safety: monograph]. Kiev. Azymut-Ukraina. ISBN 978-966-1541-49-7. pp. 104.

Bielski A. 2012. *Inżynieria i Ochrona Środowiska*. T.15. Nr **2**, p. 119–142.

Directive 2000/60/EC of the European Parliament and of the Council of 23 October 2000 establishing a framework for Community action in the field of water policy. OJ L 327 p. 1–73.

Gopchak I., Basiuk T., Bialyk I., Pinchuk O., Gerasimov I. 2019. Dynamics of changes in surface water quality indicators of the Western Bug River basin within Ukraine using GIS technologies. *Journal of Water and Land Development*. No. **42** (VII–IX) p. 67–75. DOI: 10.2478/jwld-2019-0046.

Metodyka ekolohichnoi otsinky yakosti poverkhnevykh vod za vidpovidnymy katehoriiamy [Methods of environmental assessment of surface water quality in the relevant categories]. 1998. Kyiv. pp. 28.

Polishchuk V., Sheha V. 1998. Istorychna biohrafiia Dunaiu abo nahalni problemy sohodennia u svitli osoblyvostei velykoi yevropeiskoi richky [Historical biography of the Danube or urgent problems of today in the light of the peculiarities of the great European river]. Kyiv. pp. 680 s.

Snizhko S. 2001. Otsinka ta prohnozuvannia yakosti pryrodnykh vod [Assessment and forecasting of natural water quality]. Kyiv. Nika-Tsentr. ISBN 966-521-078-5. pp. 264.

World Wide Fund for Nature, 2002. A vision for the Danube Delta, Vienna / Odessa.

Yatsyk A. Zhukynskyi V., Cherniavska A., Yezlovetska I. 2006. Dosvid vykorystannia «Metodyky ekolohichnoi otsinky yakosti poverkhnevykh vod za vidpovidnymy katehoriiamy» (poiasnennia, zasterezhennia, pryklady) [Experience of using "Methods of environmental assessment of surface water quality in the relevant categories" (explanation, reservations, examples)]. Kyiv. Oriiany. ISBN 966-8305-55-8 pp. 44.

Yatsyk A., Pasheniuk I., Gopchak I., Basiuk T. 2017. Vodo-hospodarsko-ekolohichne raionuvannia yak osnova zbere-zhennia i vidnovlennia vodnykh resursiv [Water-ecological zoning as a basis for conservation and restoration of water re-sources]. Zbirka dopovidei Mizhnarodnoho Konhresu «ETEVK-2017». Kyiv, TOV "PRAIM-PRINT" p. 167–171

Influence of 30-year reference periods on characteristic periodic discharges

Mira KOBOLD, Florjana ULAGA

Slovenian Environment Agency, Vojkova 1b, Ljubljana, Slovenia, mira.kobold@gov.si, florjana.ulaga@gov.si

Abstract

Data from the 125-year series of discharges at the Litija gauging station on the Sava River show great temporal variability of river flows in Slovenia. The annual river balance indicator for the period 1961–2019 shows that the decline in Slovenia's net runoff is 2.2% per decade. Therefore, the choice of a 30-year comparative period strongly influences the values of the period averages. The analysis was performed for the reference periods recommended by the World Meteorological Organization in history, namely 1931–1960, 1961–1990 and 1981–2010, and currently the last 30-year period of available discharges in Slovenia 1990–2019. The averages of the mean annual discharges in the considered 30-year periods decrease from the earliest period 1931–1960 to the last 1990–2019 for the four analysed stations with the longest data sets in Slovenia. Similar results are obtained for minimum annual discharges with the highest averages for the period 1961–1990. On the contrary, the 30-year averages of maximum annual discharges show a positive trend. The highest values of the 30-year averages are mainly for the period 1961–1990. The results show that the values of characteristic period discharges are highly dependent on the length of the data sets and the choice of the reference period.

Introduction

River discharges are constantly changing over time. The temporal variability of river discharges in Slovenia is very high. Climate is the main factor affecting the flow regime. River flows mainly depend on the height of precipitation, its temporal and spatial distribution, air temperature and the height and duration of the snow cover. Analyses show that flow regimes of Slovenian rivers are becoming more and more similar (Kobold et al., 2012). Due to the shorter duration of the snow cover, the spring peak decreases, while the autumn peak rises due to an increase in the autumn rainfall. In addition to the annual, the inter-annual variability of flows is also high in Slovenia. The data of national hydrological monitoring show a decreasing trend of discharges for Slovenian rivers (Kobold et al., 2012). The indicator of the annual river balance (ARSO, 2021) shows a declining trend in water quantities in Slovenia (Fig. 1). According to the linear trend in the period 1961–2019, the decline in Slovenia's net runoff is 2.2% per decade.

The fluctuation of the mean annual flow is clearly seen on the Sava River in Litija, where a continuous set of data is available from 1895 (Fig. 2). A comparison of the mean annual discharges with the average of the whole period (1895–2019) shows that at the end of the 19th and in the first half of the 20th century the years were predominantly wet, with the exception of individual drought years. In the second half of the 20th century, the mean annual discharges gradually decreased towards the end of the century and were mostly below the period average. The increase in mean annual discharges is seen again at the beginning of the 21st century, with dry years being no exception.
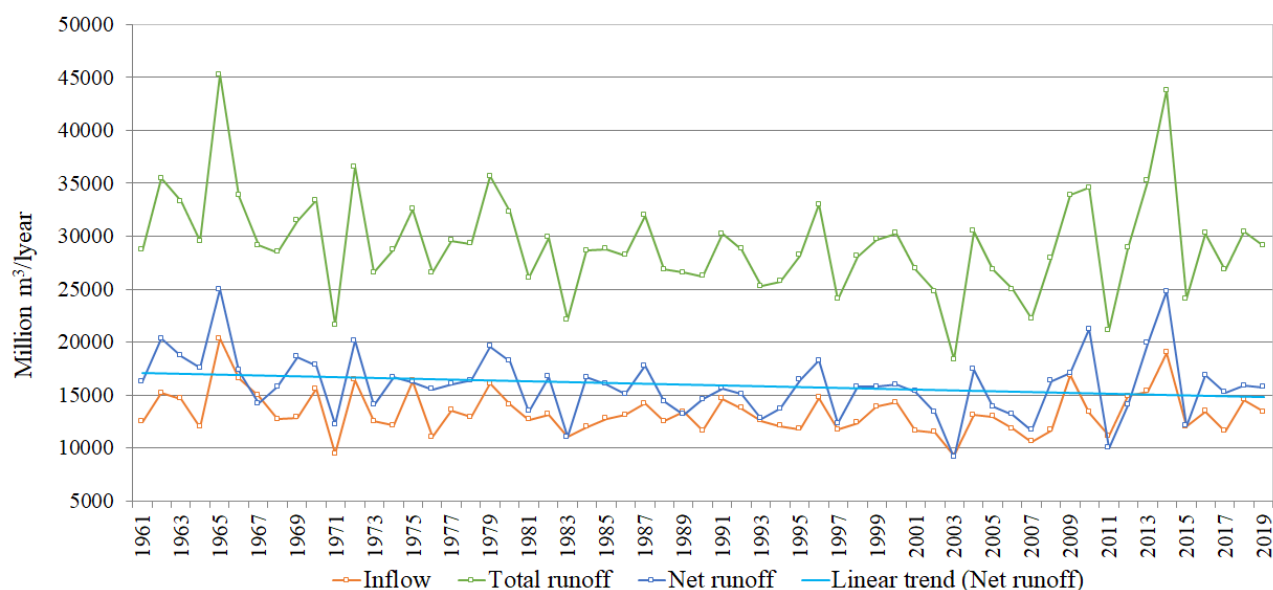
Fig. 1 Annual river balance of Slovenia (net runoff is the difference between total runoff and inflow).
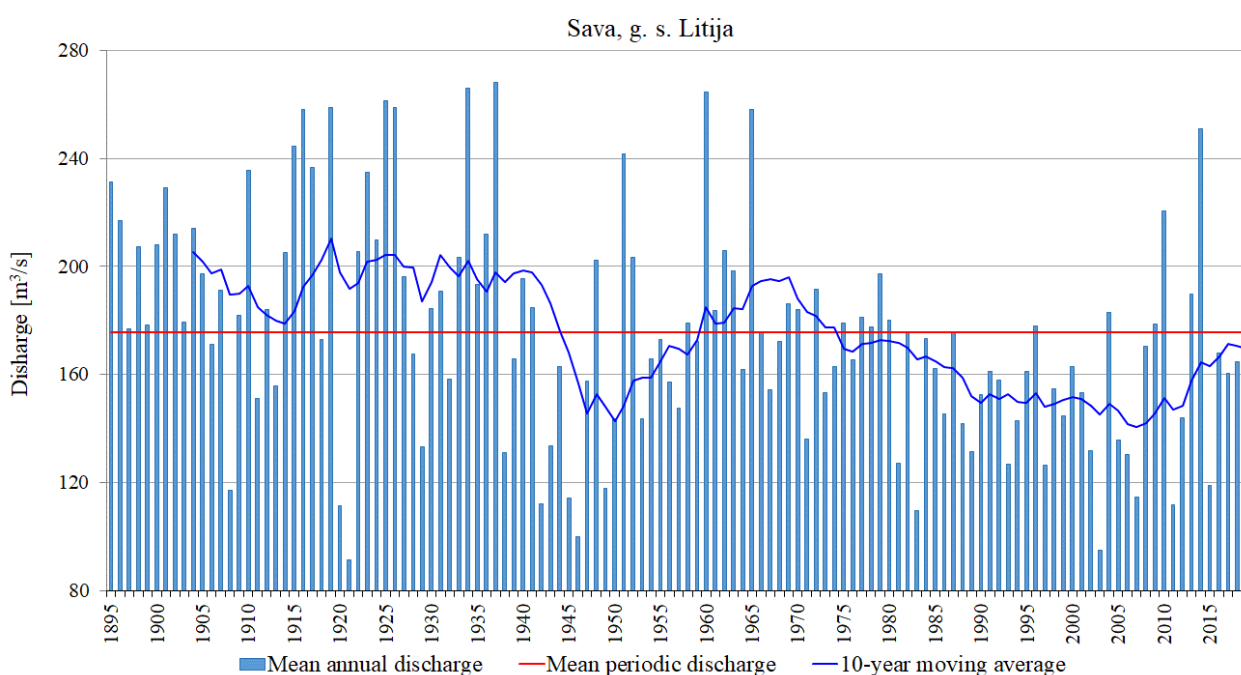
Fig. 2 Mean annual and periodic discharges and 10-year moving average of the Sava River at the Litija gauging station.

It is common practice to compare current observational data with long-term averages. Period averages of climatological and hydrological data serve as a reference against which recent or current observations can be compared. The World Meteorological Organization recommends the use of standard normal climate period for comparison among different data sets on a consistent basis (WMO, 2017). The general recommendation is to use 30-year reference period. The 30-year reference period was set as the standard mainly because only 30 years of data were available when the recommendation was first published (WMO, 2011). The current reference period is 1981–2010, which is already moving to 1991–2020 to compare variations especially in temperature and precipitation to the new 30-year average (WMO, 2020).

The Decree on criteria for determination and on the mode of monitoring and reporting of ecologically acceptable flow (Official Gazette of the Republic of Slovenia, No. 97/09) recommends the data from the last 30 years for the calculation of mean and mean low periodic discharges in Slovenia. According to officially available data of the Slovenian Environment Agency, this period is currently 1990–2019.

Methodology and data

Using different 30-year periods, an analysis of 30-year characteristic discharges was performed. The historical practice of climate averages, described in the manuals and technical regulations of the World Meteorological Organization (WMO, 2011; WMO, 2019), dates back to the first half of the 20th century. The general recommendation is to use 30-year reference periods. At the 17th World Meteorological Congress in 2015, the definition of the standard climatological average changed and now refers to the last 30-year period ending with 0 at the end of the year (currently this period is 1981–2010) instead of 30-year periods, which do not overlap (1901–1930, 1931–1960, 1961–1990, and in the future 1991–2020) as it was before (WMO, 2017). However, a period of 30 years is not enough to calculate extreme statistics and return periods. In these cases, the entire available data period is usually taken.

In analyses of trends and periodic averages, the results are strongly depend on the considered period and the length of time series. For four water gauging stations on the Slovenian rivers in the Danube River Basin with the longest data sets (Table 1), the common period of data since 1926 was taken. Period averages of the most commonly used characteristic discharges in hydrology (mean, minimum and maximum annual discharges) were calculated for different 30-year periods according to WMO recommendations (WMO, 2017) and internal state regulation (Official Gazette of the Republic of Slovenia, 2009).

Tab. 1 Basic data of analysed gauging stations

Gauging station	River	Longitude	Latitude	Catchment area [km²]	Zero point [m a.s.l.]	Data from the year
Litija	Sava	14.83357	46.05704	4849.67	230.55	1895
Metlika	Kolpa	15.32775	45.63506	1966.27	126.96	1926
Moste	Ljubljanica	14.54917	46.05572	1777.96	281.32	1924
Nazarje	Savinja	14.95727	46.32160	457.11	337.03	1926

Results

Mean annual discharges

For the gauging stations Litija on the Sava River, Metlika on the Kolpa River, Moste on the Ljubljanica River and Nazarje on the Savinja River, the results of mean annual discharges (Qs) for the 30-year periods 1931–1960, 1961–1990, 1981–2010 and 1989–2018 are shown in Fig. 3. With the exception of the Ljubljanica River, the highest values of average periodic discharges were reached for the period 1931–1960. For all stations, the trend of discharges is negative. The lowest values are for the period 1981–2010. For the last 30-year period (1990–2019), a slightly positive trend has already been detected compared to 1981–2010.
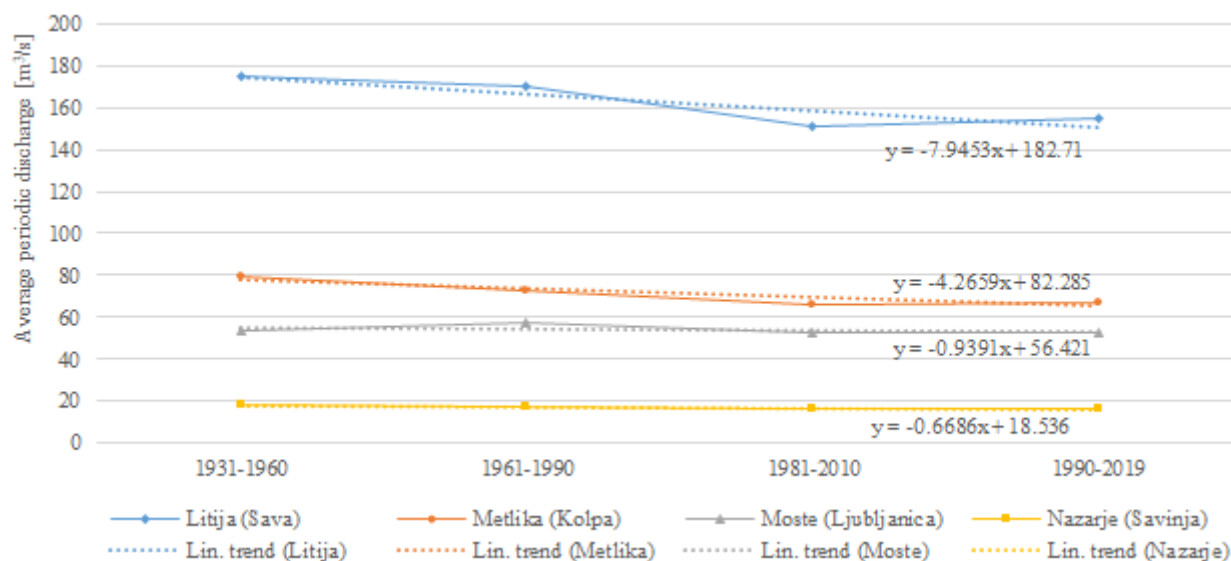
Fig. 3 Average discharges of mean annual flows for four 30-year periods and trends for the gauging stations with the longest data sets in Slovenia.

Figure 4 shows the 30-year averages of mean annual discharges for the Sava River at Litija gauging station for the entire data set. The value of the 30-year average discharges is the highest for the period 1901–1930. In the following 30-year periods, the values decrease and the lowest value is reached for the period 1981–2010. The last shown 30-year period (1990–2019) gives a slightly higher value of the average discharge than the period 1981–2010.
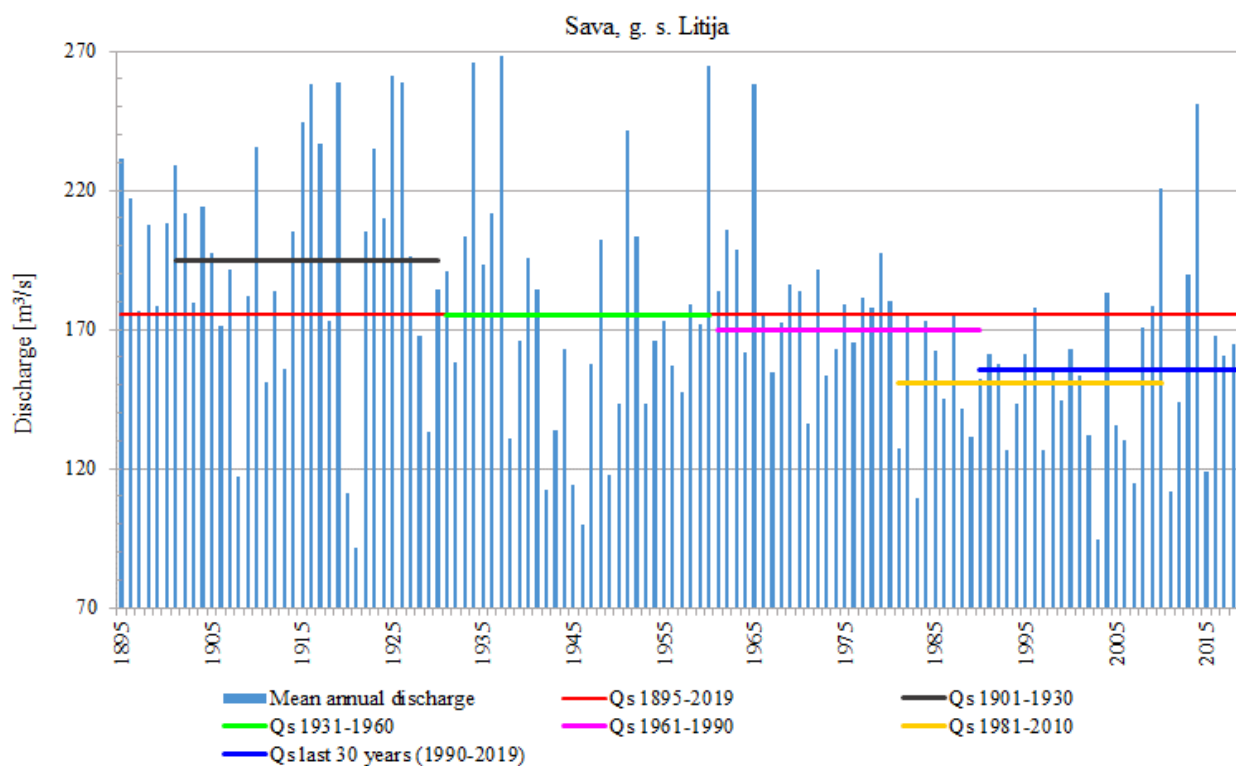
Fig. 4 Mean annual discharges, average of the entire period and 30-year averages of discharges for the Sava River at Litija.

For all four analysed stations, the deviations of the 30-year averages from the average of the period 1926–2019 are shown in Fig. 5. The largest deviations in the negative direction are for the period 1981–2010,

42

followed by the period 1990–2019. The deviations are the largest for the stations Litija on the Sava River and Metlika on the Kolpa River. The karst river Ljubljanica has the smallest deviation.
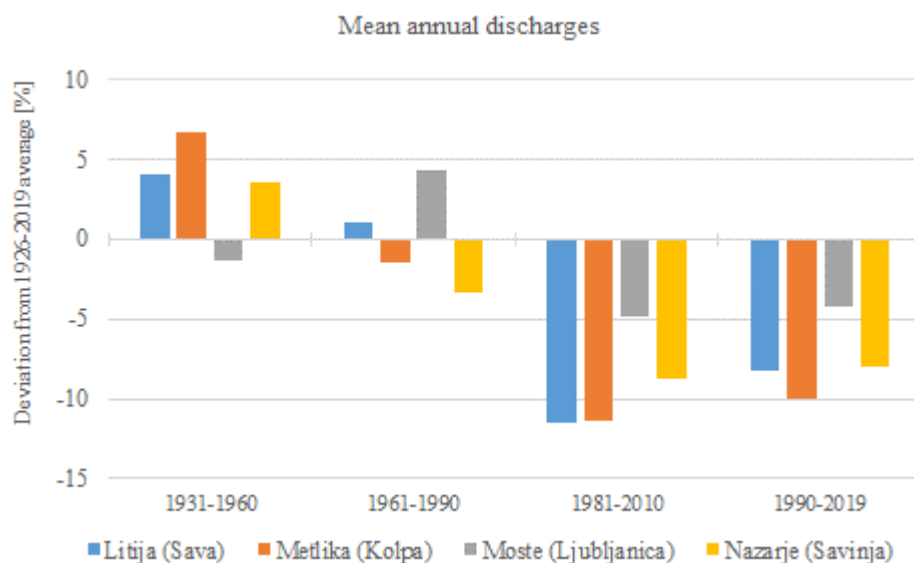
Fig. 5 Deviation of average periodic mean discharges from the average of the period 1926–2019.

Minimum annual discharges

Similar results as for mean annual discharges are for minimum annual discharges (Qnp). The trend is negative for all four analysed stations (Litija on the Sava, Metlika on the Kolpa, Moste on the Ljubljanica and Nazarje on the Savinja) for the 30-year averages 1931–1960, 1961–1990, 1981–2010 and 1990–2019 of minimum annual discharges (Fig. 6). The highest values are for the period 1961–1990, and the lowest for the last period 1990–2019, only Metlika (Kolpa) has the lowest average for the period 1981–2010. The analysis of the whole period for the Sava River at Litija gives the highest value for the period 1901–1930 and the lowest for the last period (Fig. 7). The lowest values for the last period are the result of long periods of drought, which are becoming more frequent in Slovenia (Sušnik et al., 2013). The deviations of the 30-year averages from the average of the period 1926–2019 show that low flows remain below the period average by about 5% (Fig. 8).
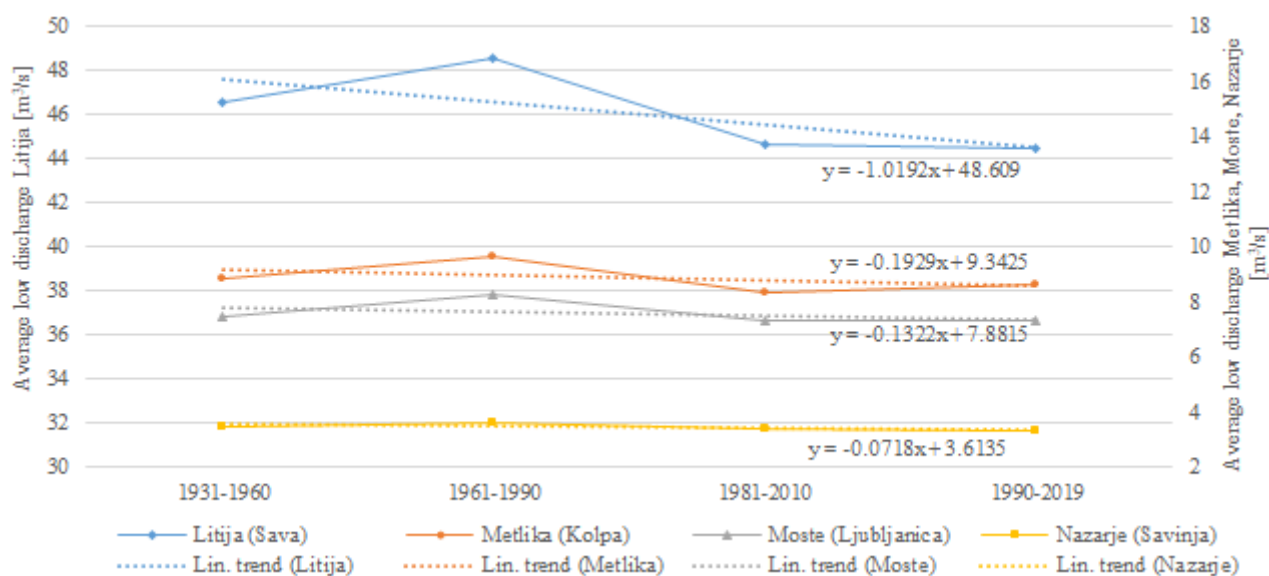

Fig. 6 Average discharges of minimum annual discharges for four 30-year periods and trends for four gauging stations.
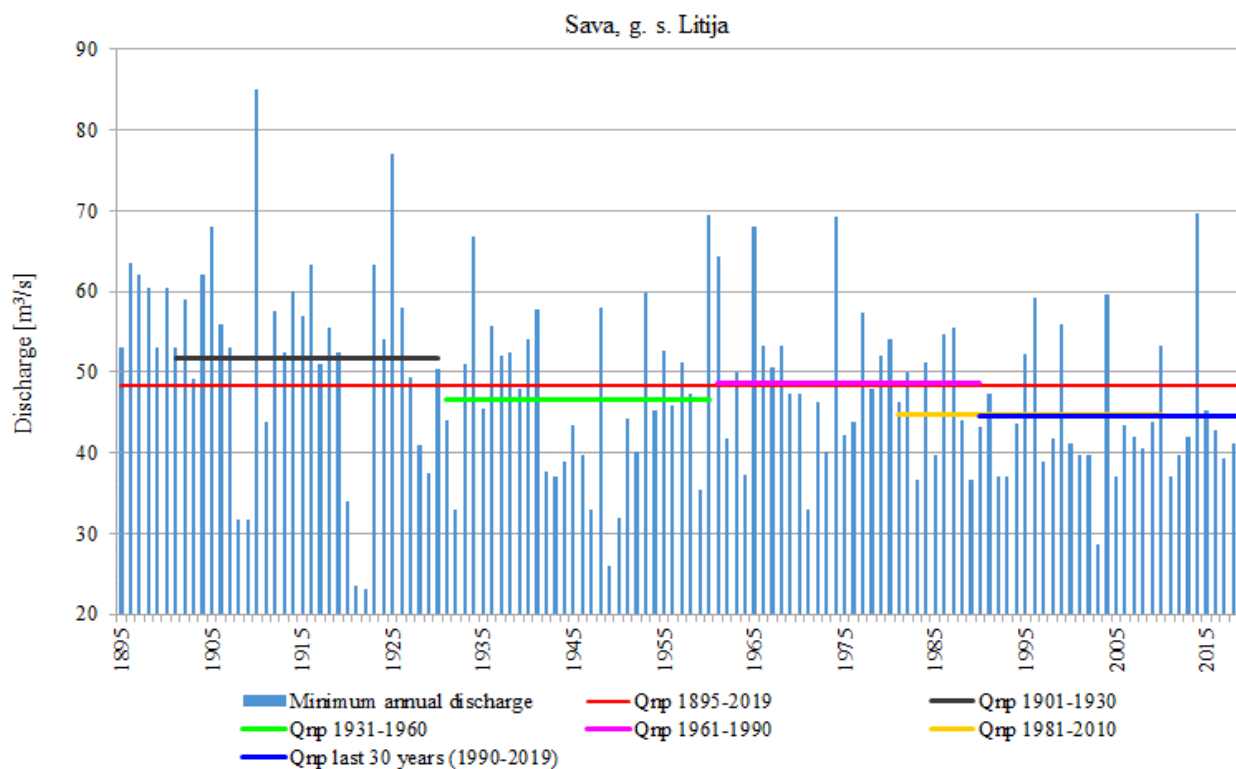
Fig. 7 Minimum annual discharges, average of the entire period and 30-year averages of minimum annual discharges for the Sava River at Litija.
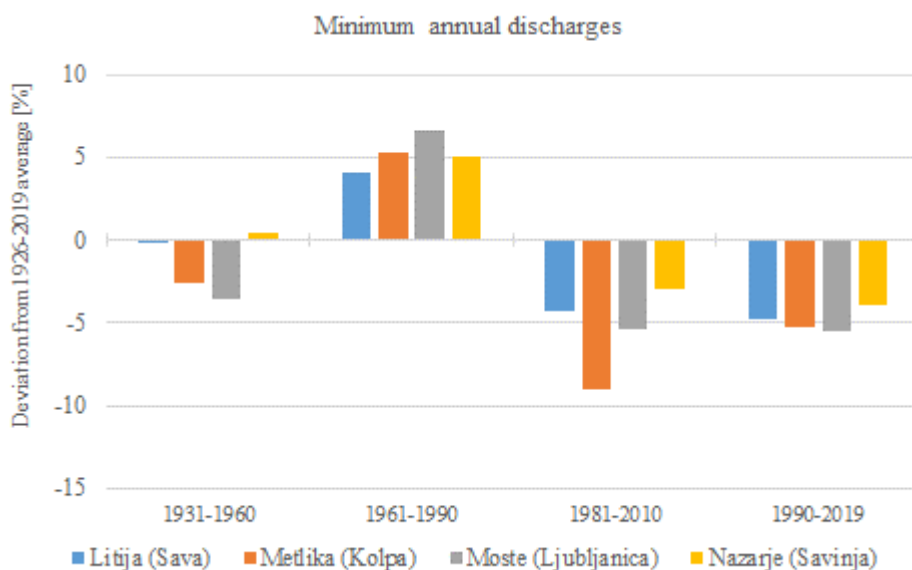
Fig. 8 Deviation of average periodic minimum discharges from the average of the period 1926–2019.

Maximum annual discharges

At high flows, the maximum annual peak discharges (Qvk) were analysed. In contrast to mean and low flows, the 30-year averages of maximum annual discharges show a positive trend for all four analysed stations (Fig. 9). The highest values of the 30-year averages are for the period 1961–1990, only the Savinja River has the highest average in the last 30-year period 1990–2019. The analysis of the entire period for the Sava in Litija is shown in Fig. 10. For the period 1931–1960, the average value of

maximum annual discharges is by far the lowest and the only one below the average of the entire period (Figs. 10 and 11).
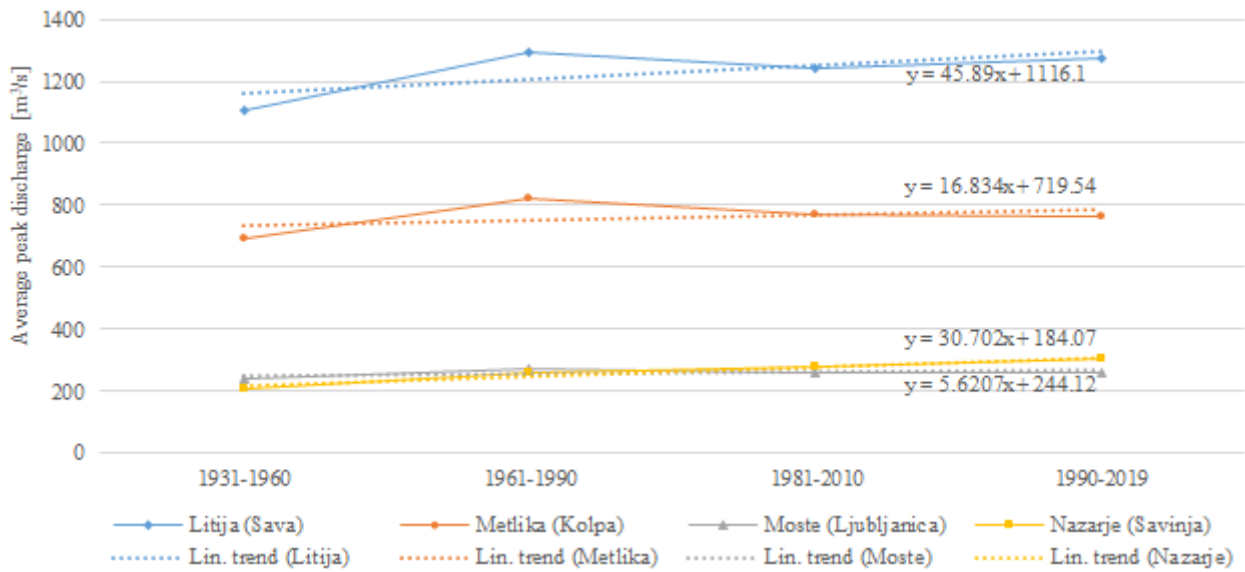

Fig. 9 Averages of maximum annual discharges for four 30-year periods and trends for four gauging stations.
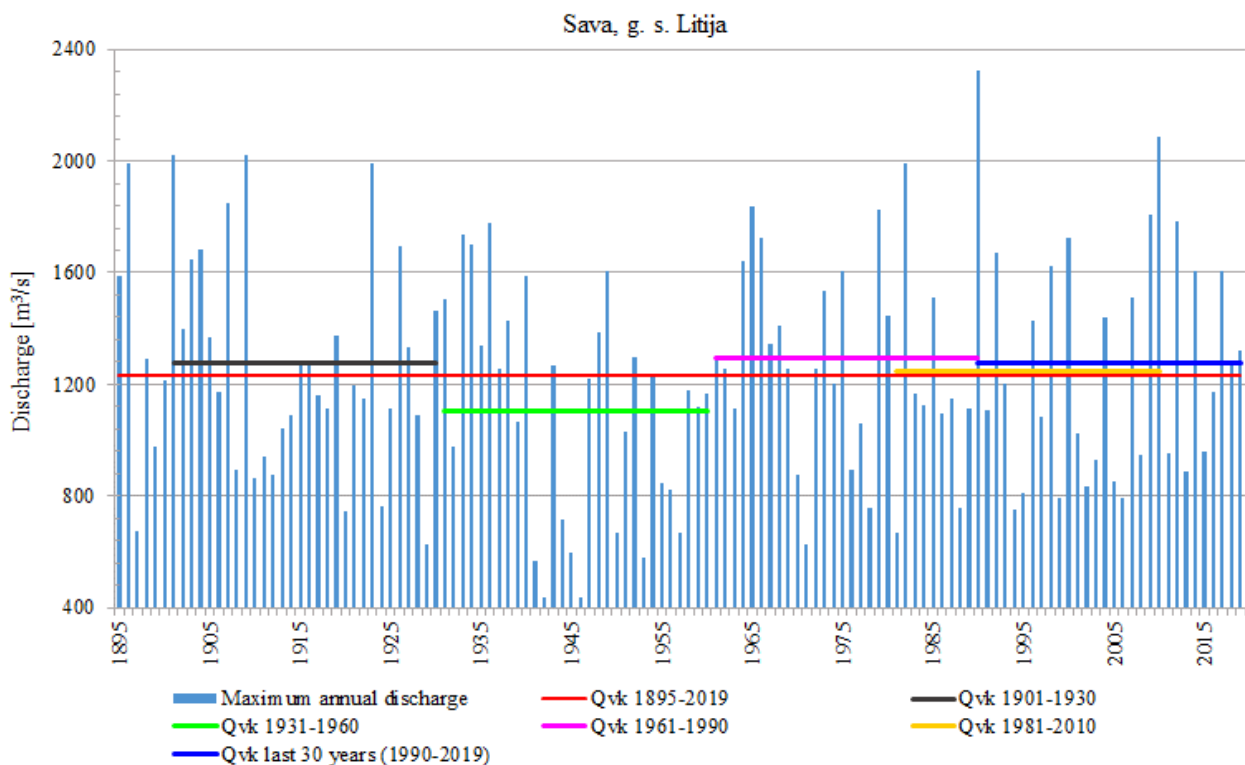

Fig. 10 Maximum annual discharges, average of the entire period and 30-year averages of the maximum annual discharges for the Sava River at Litija.

45
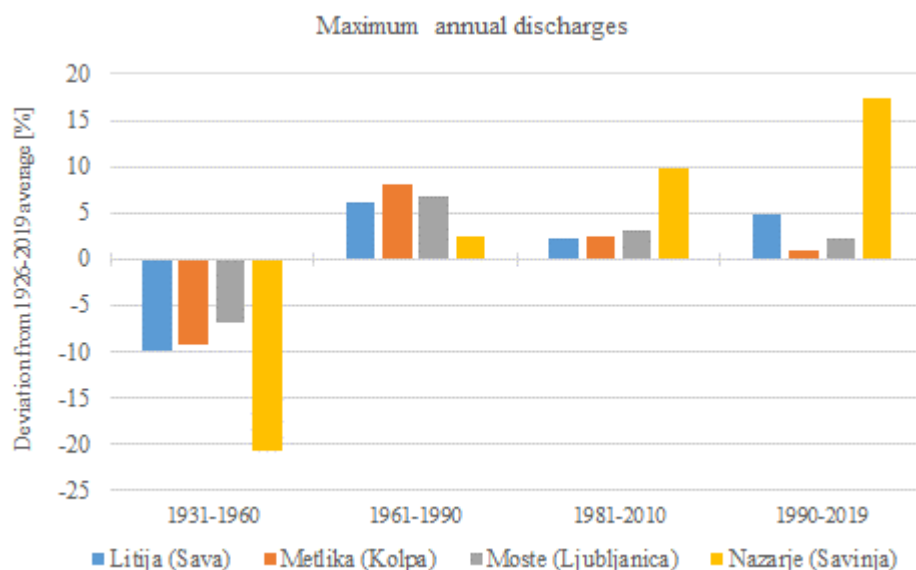
Fig. 11 Deviation of average periodic maximum discharges from the average of the period 1926–2019.

Conclusions

The values of the characteristic period discharges depend very much on the length of the time series and on the choice of the reference period. The example of the Sava River at the Litija gauging station, which has more than 120 years of data, shows that the characteristic discharges of 30-year periods can differ greatly from the average of the entire period of data. 30-year averages are also strongly influenced by the choice of a 30-year period. For mean and low periodic discharges, the values of 30-year averages were the highest at the beginning of the last century and gradually decreased until the last 30-year period for all four analysed gauging stations. In the case of high waters, the trend is mainly increasing.

The choice of the long-term reference period influences the results of the analyses, so it is necessary to indicate the reference period when publishing the results of analyses. At the Slovenian Environment Agency, the current monthly and annual data of river flows, which are published in the agency monthly bulletins and annual reports, are compared with the period 1981–2010, according to WMO recommendations (WMO, 2017). The reference period 1981–2010 was also used to assess climate change in Slovenia until the end of the 21st century (Bertalanič et al.). In the case of extraordinary events, such as floods and droughts, the entire available data sets are included in the analysis, as this is the only way to obtain actual information on the intensity and magnitude of the event compared to historical events.

The average discharges for different 30-year periods can vary greatly. Ecologically acceptable flow in Slovenia is usually determined from the value of average low flow for the last 30 years (Official Gazette of the Republic of Slovenia, No. 97/09). Depending on the 30-year period used to estimate the average low discharge, different estimates can be obtained for the same watercourse or even the same location, and consequently the values of the ecologically acceptable flow when water rights are granted.

References

ARSO (2021) Pregled hidroloških razmer površinskih voda v Sloveniji. Poročilo o monitoringu za leto 2019. Ljubljana, Ministrstvo za okolje in prostor, Agencija Republike Slovenije za okolje. 47–48. http://www.arso.gov.si/vode/publikacije in poročila/Poročilo o hidrološkem monitoringu površinskih voda za leto 2018.pdf (last access: 18 May 2021).

Bertalanič R, Dolinar M, Draksler A, Honzak L, Kobold M, Kozjek K, Lokpošek N, Medevd A, Vertačnik G, Vlahović Ž, Žust A (2018) Ocena podnebnih sprememb v Sloveniji do konca 21. stoletja. Sintezno poročilo – prvi del. Ljubljana: Ministrstvo za okolje in prostor, Agencija Republike Slovenije za okolje.

Kobold M, Dolinar M, Frantar P (2012) Sprememba vodnega režima zaradi podnebnih sprememb in drugih antropogenih vplivov, Zbornik prispevkov, I. kongres o vodah Slovenije 2012, Ljubljana, Slovenija, Fakulteta za gradbeništvo in geodezijo, 7–22.

Official Gazette of the Republic of Slovenia (No. 97/09) The Decree on criteria for determination and on the mode of monitoring and reporting of ecologically acceptable flow.

Sušnik A, Gregorič G, Uhan J, Kobold M, Andjelov M, Petan S, Pavlič U, Valher A (2013) Spremenljivost suš v slovenskem prostoru in analiza suše 2013. Zbornik 24. Mišičev vodarski dan, Maribor, *Vodnogospodarski biro*, 102–109.

WMO (2011) Guide to Climatological Practices, WMO-No. 100, Geneva.

WMO (2017) WMO Guidelines on the Calculation of Climate Normals, WMO-No. 1203, Geneva.

WMO (2019) Technical Regulations, WMO-No. 49, Geneva.

WMO (2020) Updated 30-year reference period reflects changing climate. https://public.wmo.int/en/media/news/updated-30-year-reference-period-reflects-changing-climate. Published 5 May 2021 (last access: 24 May 2021).

Low Flow Analysis of the Drava River

Valentina SEKELJ[1], Lidija TADIĆ[2], Tamara BRLEKOVIĆ[2]

[1] Pipelife Hrvatska d.o.o., email: valentina.sekelj@gmail.com, [2,3] Faculty of Civil Engineering and Architecture, email: ltadic@gfos.hr, email: tamaradadic@gfos.hr

Abstract

Low-flow periods are considered equally critical from both water management and ecological perspectives. According to catchments' hydrological and physical features, levels of resilience to both extremes – floods and low-flow periods (or hydrological droughts) can be different. Low-flow episodes are very difficult to recognize owing to the ambiguous definition of 'low flow'. Several indices have been recommended; the most frequently used ones include those obtained from low-flow statistics and the standardized streamflow index (SSI). Level of catchment resilience also depends on anthropogenic impacts over a longer time period. Also, it usually has seasonal character. According to (Soto, 2020), studies on streamflow trends (on an annual or seasonal basis) have become a fundamental question in hydrological research in recent years. In addition, a pan-European study on a dataset of more than 600 daily streamflow records was analyzed to detect spatial and temporal changes in streamflow droughts. In most catchments, there were no significant changes, but distinct regional differences were found in all time periods (Hisdal, 2001). Hydrological analysis of hydrological regime of the Danube River and its tributaries projected considerable changes of seasonal streamflow in the next 30 years (Stagl, 2020). The Drava River water regime also has been studied and results showed increasing of upstream mean annual discharge variabilities due to significant precipitation variability and decreasing of downstream mean annual discharge variabilities (Gajić-Čapka, 2010).

Introduction

Some of climate change effects are extreme hydrological events: precipitation events have smaller frequencies, but their intensities are higher and drought periods are longer and more frequent. Drought is one of the most frequent natural hazards related to climate change. It is often defined from climatological point of view (e.g. Herring et al., 2015; Heim, 2015) and its severity is usually defined by severity of anomaly (precipitation, air temperature, water temperature etc.). Dry and warm weather with precipitation deficit usually generates meteorological drought. Water deficiency and high evapotranspiration decrease water budget in the soil what in vegetation period causes agricultural drought. Precipitation deficit decreases run off and reduces it to base flow (Stahl, 2001). Figure 1 explains occurrence of meteorological, agricultural and hydrological drought and their relationship.

Damages caused by drought are enormous, in agricultural production, public water supply, production of hydropower energy, environment, etc. So, analysis of low flows, and occurrence of hydrological drought has great importance in water management.
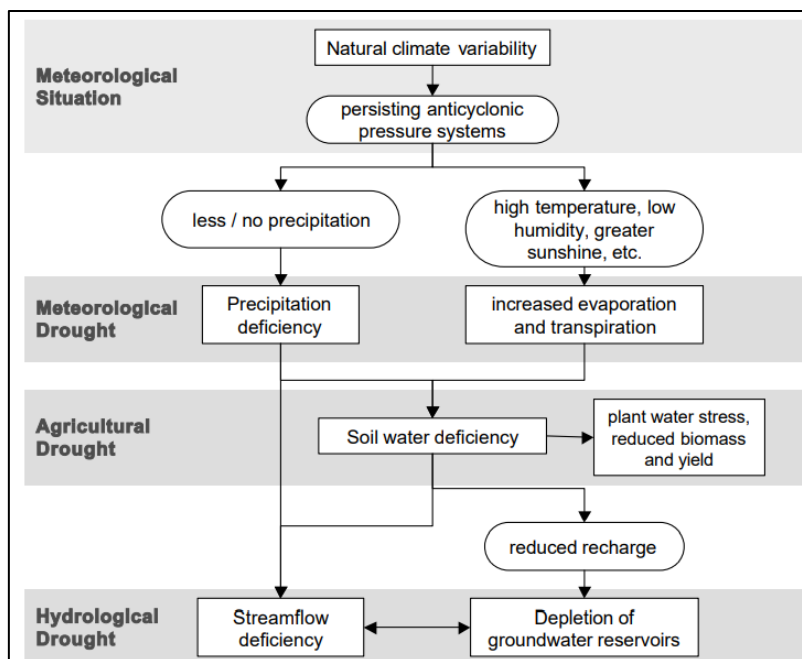
Fig. 1 The sequence of drought impacts associated with meteorological, agricultural and hydrological drought (Source: National Drought Mitigation Centre, http://enso.unl.edu/ndmc/enigma/def2.htm)

Study area

This paper is going to analyze changes in low flow regime of the Drava River in the last sixty years. Analyzed area belongs to lower Drava catchment which has suffers from upstream climate change impacts and anthropogenic activities (hydro-power plants), too (Bonacci et al., 2009).

The Drava River origin is in Italy (1 192 m a.s.l.). It flows through Austria, Hungary and Croatia with catchment area of 38 500 km^2 (16.5 % of it belong to Croatia). Its length is 739 km, and its mouth is 19 km downstream Osijek into the Danube River (Fig. 3) (source: https://frisco-project.eu/hr/slivna-podrucja-rijeka/drava/).

The Drava River has basically glacial water regime characterized by low discharges in the winter (January) and maximum discharges in May or June. The analyzed area has a typical lowland catchment characterized by a mild slope, pronounced river meandering, and alluvial soil with dominant agricultural fields, lately very often facing water deficit during vegetation period. The water regime of the Drava River is pluvial-glacial, characterized by low water content in winter, and high in late spring and in the first half of summer. The mean flow of the analyzed fifty-seven-year period for the hydrological station Terezino Polje is 517,13 m^3/s, while for Donji Miholjac it is slightly higher 531.18 m3/s. Figure 2 presents minimum annual and seasonal discharges of both hydrological stations.
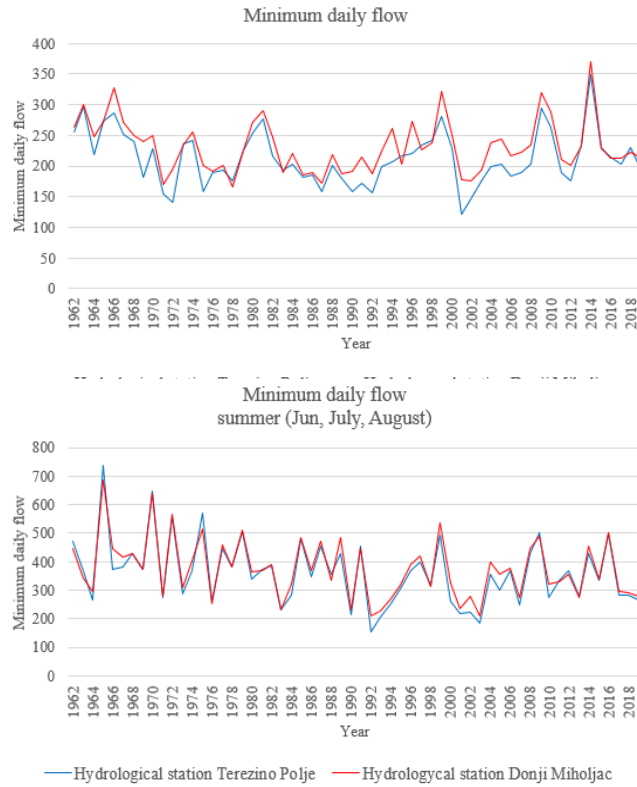
Fig. 2 Minimum daily flows of the hydrological station Donji Miholjac and Terezino polje from 1962 to 2019
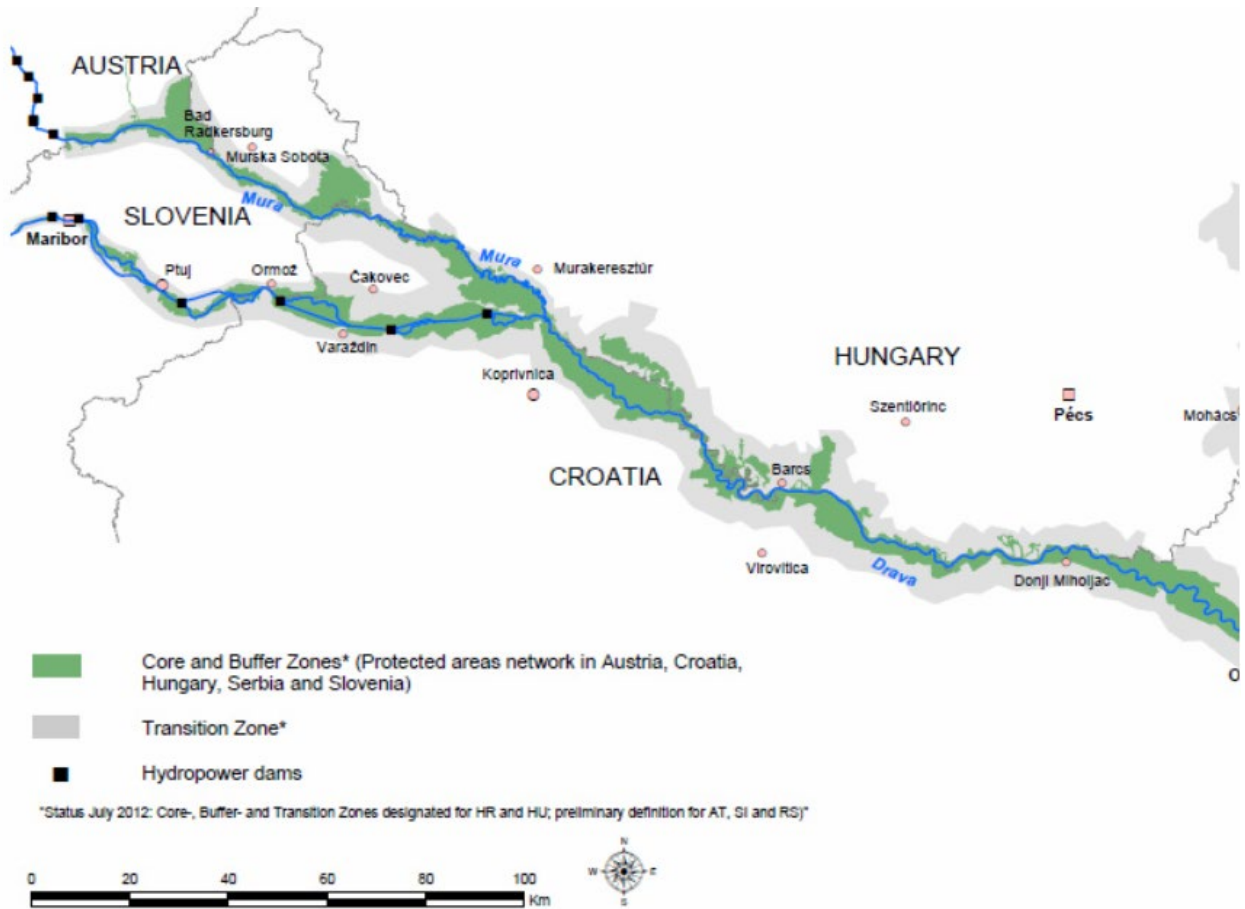
Fig. 3 The flow of the Drava river (source: http://www.olddrava.com/international-cooperation)

Methodology

The most common low-flow indices are the mean flow, coefficient of variation in the annual mean flow, flow-duration curve, annual minimum flows, streamflow deficit durations, streamflow deficit volumes, recession indices. In this paper, an analysis of proposed low-flow indices is presented, based on daily discharges from 1962 to 2019 measured on two hydrological stations of the Drava River in Croatia (Table 1). The section between these two hydrological stations is the most endangered by hydrological drought (Tadić, 2019).

Tab. 1 Basic hydrological data of analyzed sub-catchments

Hydrological station	Distance from the confluence (rkm)	Catchment area (x100 km²)	Available date series of water level	Available date series of daily discharges
Terezino Polje	152.3	33.9	1925–2019	1962–2019
Donji Miholjac	80.6	37.1	1926–2019	1962–2019

Results

Mean flow

Mean flow is one of the most used parameters in hydrology and water resources planning. It can be determined based on a time series of data or daily flows by summing all values and dividing by the number of records or days (WMO manual, 2008). Mean flow is usually calculated for the calendar year or hydrological data series, and also can be calculated for certain months or seasons.

Based on the daily flows of the Drava River from the hydrological stations Donji Miholjac and Terezino Polje, the average flow of the entire period (from 1962 to 2019) was determined. The average flow of the fifty-seven-year period for Terezino Polje is 517.13 m³/s, while for Donji Miholjac it is slightly higher at 531.18 m³/s. Also, the analyzed period is divided into four seasons: spring (March, April and May), summer (June, July and August), autumn (September, October and November) and winter (December, January and February). Mean seasonal flows are shown in Table 2.

Tab. 2 Mean seasonal flows

Hydrological stations	SPRING (MAM)	SUMMER (JJA)	AUTUMN (SON)	WINTER (DJF)
Terezino Polje	554.56 m³/s	632.38 m³/s	498.81 m³/s	379.43 m³/s
Donji Miholjac	568.41 m³/s	637.11 m³/s	505.83 m³/s	406.79 m³/s

Coefficient of variation in the annual mean flow

The coefficient of variation (CV) is a parameter that indicates dispersion of data points around the mean in a series (μ) or the expected value of X, E {X}. It is obtained as a ratio of the standard deviation (σ) and the mean value, or $CV = \sigma / \mu$ (WMO Manual, 2008). The coefficient of variation was calculated for the mean annual flow rates from 1962 to 2019. The calculation indicates a slightly higher dispersion of data points for the upstream hydrological station Terezino Polje (CV = 0.17157), while for Donji Miholjac is CV = 0.17137.

Trend analysis in the annual mean and minimum flow, and mean and minimum seasonal flow

In order to reach conclusions about changes in the occurrence of low flows, a trend analysis was performed based on data on daily flows of the Drava River measured at the hydrological stations Donji Miholjac and Terezino Polje. For analysis and drawing conclusions it is necessary to have a sufficiently long data set. In this case, the fifty-seven-year period from 1962 to 2019 was analyzed. Trends in low-flow series can be caused by anthropogenic impacts, for example by the regulation structures, or using water for irrigation purposes. Another reason for the increasing low flows frequencies is climate change. In particular, changes in the quantity and temporal distribution of rainfall and increasing evapotranspiration (Stahl, 2001). With the predicted increase in global temperatures, scientists generally

agree that the global hydrological cycle will change, suggesting that extreme events, droughts, and floods will become more frequent (Watson et al., 1998).

For the purpose of statistical assessment of the presence of the trend of the observed variable or daily flow, in this case the Mann-Kendall test was used. This test is non-parametric and is based on ranking members in a time series. The trend may be ascending or descending; the observed variable is constantly decreasing or increasing over time. Trends were considered significant for $p < 0.05$.

Trend analysis was performed on a) mean and minimum annual flows and b) mean and minimum monthly flows from 1962 to 2019 (Fig. 4 and Fig. 5). Finally, a seasonal trend analysis was conducted. Each year is divided into four seasons: winter (December, January, February), spring (March, April, May), summer (June, July, August) and autumn (September, October, November).
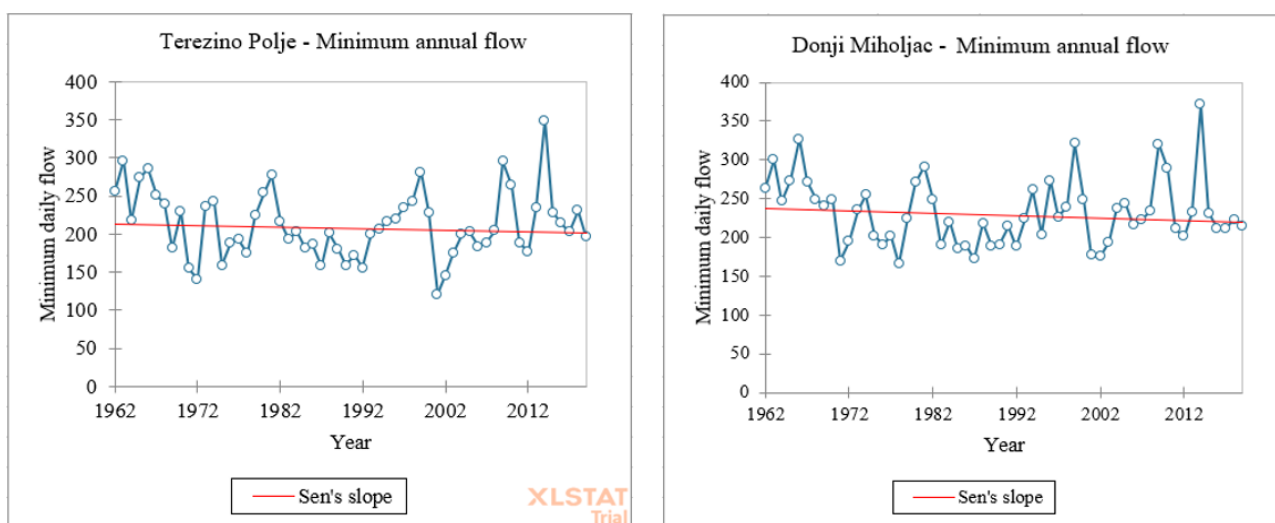
Fig. 4 Movement of minimum annual flows
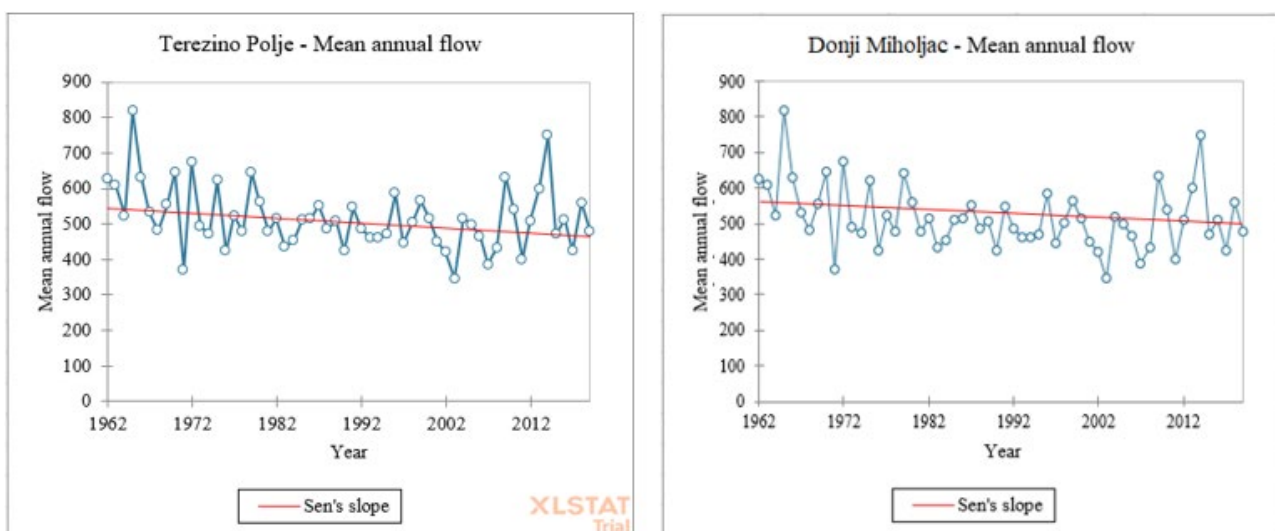
Fig. 5 Movement of mean annual flows

By analyzing the trend of minimum annual flow on the two hydrological stations we can observe a descending trend, but it is not statistically significant, while the descending trend of average annual flows is statistically significant. Test results and trends in minimum and mean monthly flows of the analyzed fifty-seven-year period is shown in Table 3. The magnitude of the trend was obtained using the Thiel–Sen Slope.

Tab. 3 Significance of the minimum and mean monthly flows

Hydrological station	Terezino Polje		Donji Miholjac	
MONTH	Minimum annual discharges	Mean monthly discharges	Minimum annual discharges	Mean monthly discharges
January (J)	$p > 0,05$	$p > 0,05$	$p > 0,05$	$p > 0,05$
February (F)	$p > 0,05$	$p > 0,05$	$p > 0,05$	$p > 0,05$
March (M)	$p > 0,05$ increasing trend	$p > 0,05$	$p > 0,05$ increasing trend	$p > 0,05$
April (A)	$p > 0,05$	$p > 0,05$	$p > 0,05$	$p > 0,05$
May (M)	$p > 0,05$	$p > 0,05$	$p > 0,05$	$p > 0,05$
June (J)	$p < 0,05$ statistically significant decreasing trend	$p < 0,05$ statistically significant decreasing trend	$p < 0,05$ statistically significant decreasing trend	$p < 0,05$ statistically significant decreasing trend
July (J)	$p < 0,05$ statistically significant decreasing trend	$p < 0,05$ statistically significant decreasing trend	$p < 0,05$ statistically significant decreasing trend	$p < 0,05$ statistically significant decreasing trend
August (A)	$p > 0,05$	$p > 0,05$	$p > 0,05$	$p > 0,05$
September (S)	$p > 0,05$	$p > 0,05$	$p > 0,05$	$p > 0,05$
October (O)	$p > 0,05$	$p > 0,05$	$p > 0,05$	$p > 0,05$
November (N)	$p > 0,05$ increasing trend	$p > 0,05$	$p > 0,05$ increasing trend	$p > 0,05$
December (D)	$p > 0,05$ increasing trend	$p > 0,05$	$p > 0,05$ increasing trend	$p > 0,05$

Seasonal analysis and application of the Man Kendall trend test to minimum flows distributed over four seasons (spring, summer, fall, and winter) identified a statistically significant declining trend during the summer months at both hydrological stations.
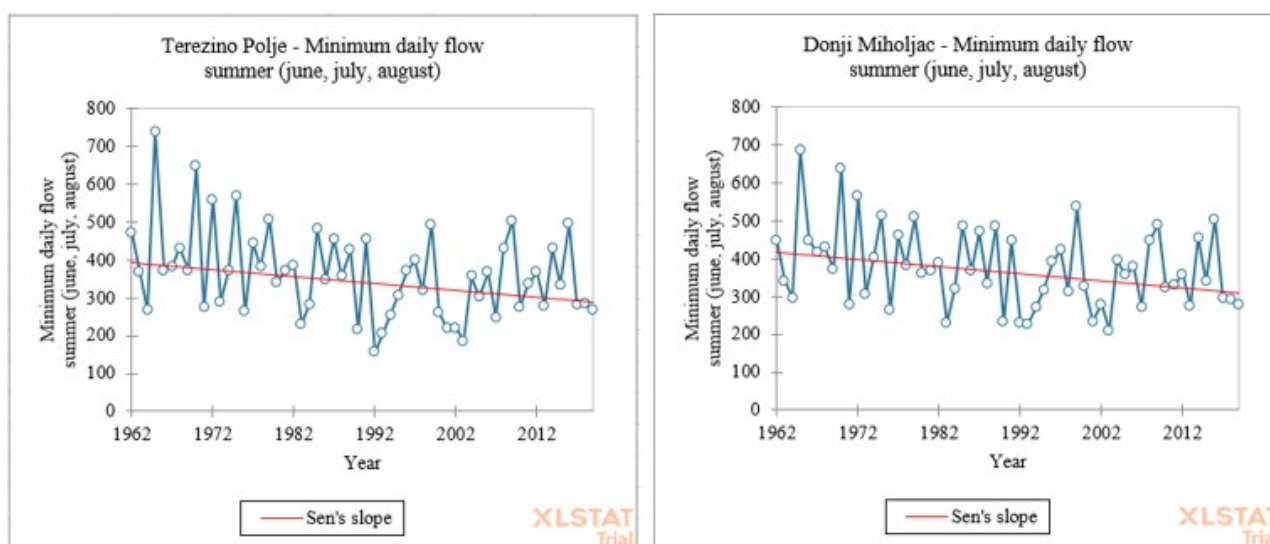
Fig. 6 Statistically significant decreasing trend during the summer months

Homogeneity tests

Hydroclimatic homogeneity tests allow detecting a change along with a time series data (Kang et al., 2012). In general, by examining the homogeneity of a data set, we determine whether the series is homogeneous throughout the observed period or at a certain point in time. Homogeneity test analysis depends on the chosen significance level, test algorithm, and test variable (Yozgatligil et al., 2016).

The standard normal homogeneity test (SNHT) was applied in this paper. The homogeneity of minimum and mean annual flows and the homogeneity of minimum and mean monthly flows were examined. The

tests were performed based on the flow from both hydrological stations, and the results of flow homogeneity testing of Terezino Polje hydrological station are shown in Table 4. Due to the small mutual distance of hydrological stations and very small differences in flow rates the results of homogeneity testing for the Donji Miholjac station coincide with the station Terezino Polje.

Tab. 4 Homogeneity test analysis – Terezino Polje

Mean annual flow											
Statistically significant decreasing trend	Yes										
Homogeneous series	Yes										
Minimum annual flow											
Statistically significant decreasing trend	Yes										
Homogeneous series	No										
Minimum monthly flow											
Homogeneous series											
January	February	March	April	May	June	July	August	September	October	November	December
Yes	Yes	Yes	Yes	Yes	No	No	Yes	Yes	Yes	Yes	Yes
Mean monthly flow											
Homogeneous series											
January	February	March	April	May	June	July	August	September	October	November	December
Yes	Yes	Yes	Yes	Yes	Yes	Yes	Yes	Yes	Yes	Yes	Yes
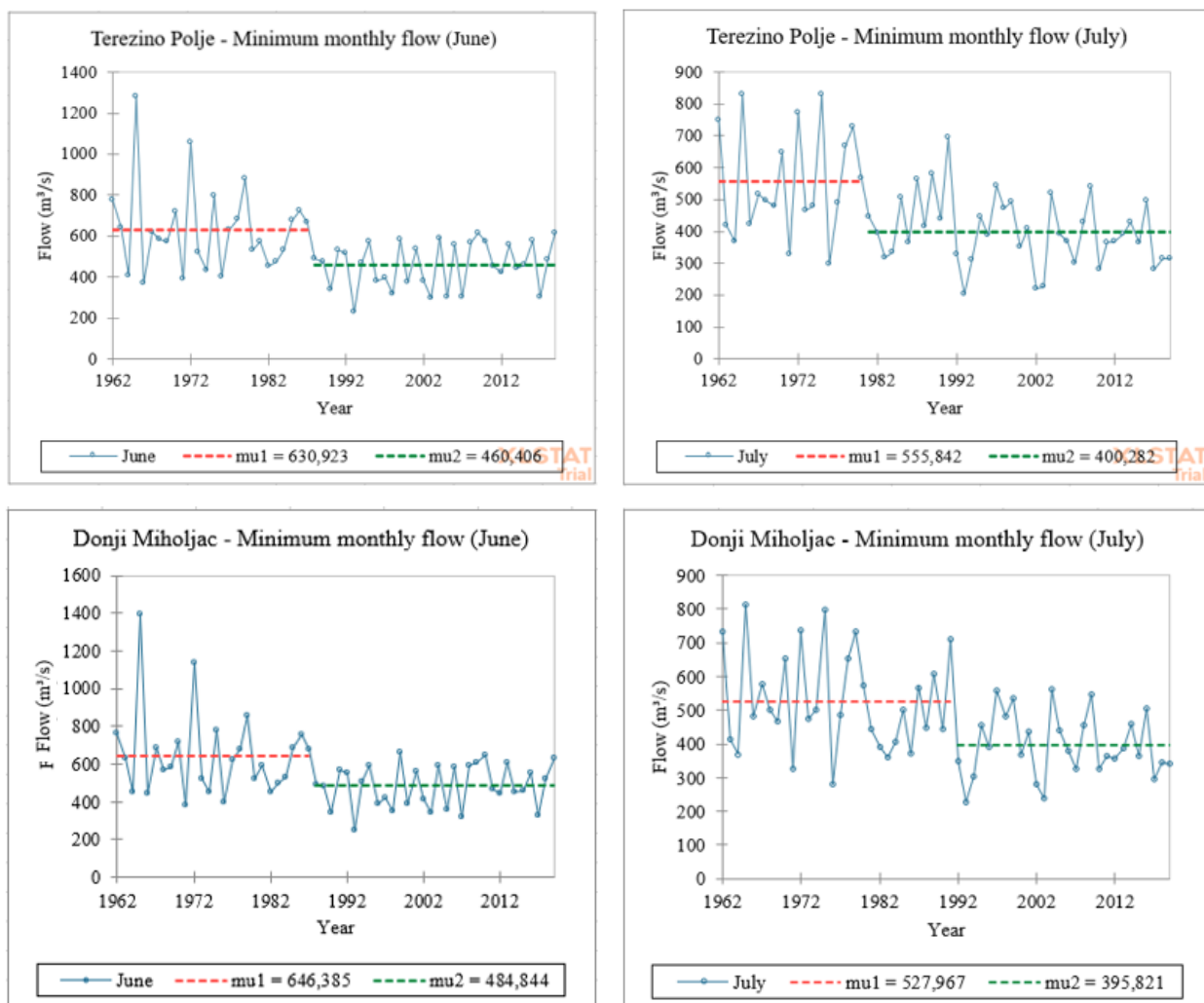
Fig. 7 Homogeneity test analysis

In the analyzed fifty-seven-year period, the largest deviations occur during the summer months. By analyzing trends based on minimum flows in June and July, we concluded that the declining trend is statistically significant. The average value of minimum flows in June at station Terezino Polje was 630.92 m³/s, and since 1987 there has been a significant decrease and the average value has dropped to 460.41 m³/s. The declining trend continues in July with a slightly smaller difference in flow reduction. The downstream station Donji Miholjac also has a statistically significant declining trend, and the series is inhomogeneous. Up tov1987, the mean value of the minimum flows in June was 646.38, and then decreased to 161.54 m³/s. The turning point in July was 1991, when the average flow value decreased by 132.15 m³/s.

Flow-duration curve

A flow-duration curve (FDC) represents the relationship between the magnitude and frequency of daily, weekly, monthly (or some other time interval of) streamflow for a particular river basin, providing an estimate of the percentage of time a given streamflow was equaled or exceeded over a historical period (Vogel and Fennessey, 1994). In general, a flow duration curve is a curve that shows the percentage of time or number of days in a year, during which the flow is equal to or greater than given quantities regardless of the chronological sequence (Žugaj et al. 2011). The flow duration curve for Terezino Polje and Donji Miholjac is shown in Figure 8, and the frequency analysis is shown in Table 5.

Tab. 5 Flow frequency analysis

Donji Miholjac			Terezino Polje		
Flow Q(m³/s)	Frequency (days)	Frequency (%)	Flow Q(m³/s)	Frequency (days)	Frequency (%)
166–589	14 519	68,538			
589–800	3 963	18,708	121–515	12 716	60,026
800–1012	1 645	7,765	515–910	6 970	32,902
1 012–1 223	651	3,073	910–1 304	1 226	5,787
1 223–1 435	249	1,175	1 304–1 699	216	1,020
1 435–1 646	99	0,467	1 699–2 094	34	0,160
1 646–1 858	33	0,156	2 094–2 488	15	0,071
1 858–2 069	16	0,076	2 488–2 882	7	0,033
2 069–2 282	9	0,042			
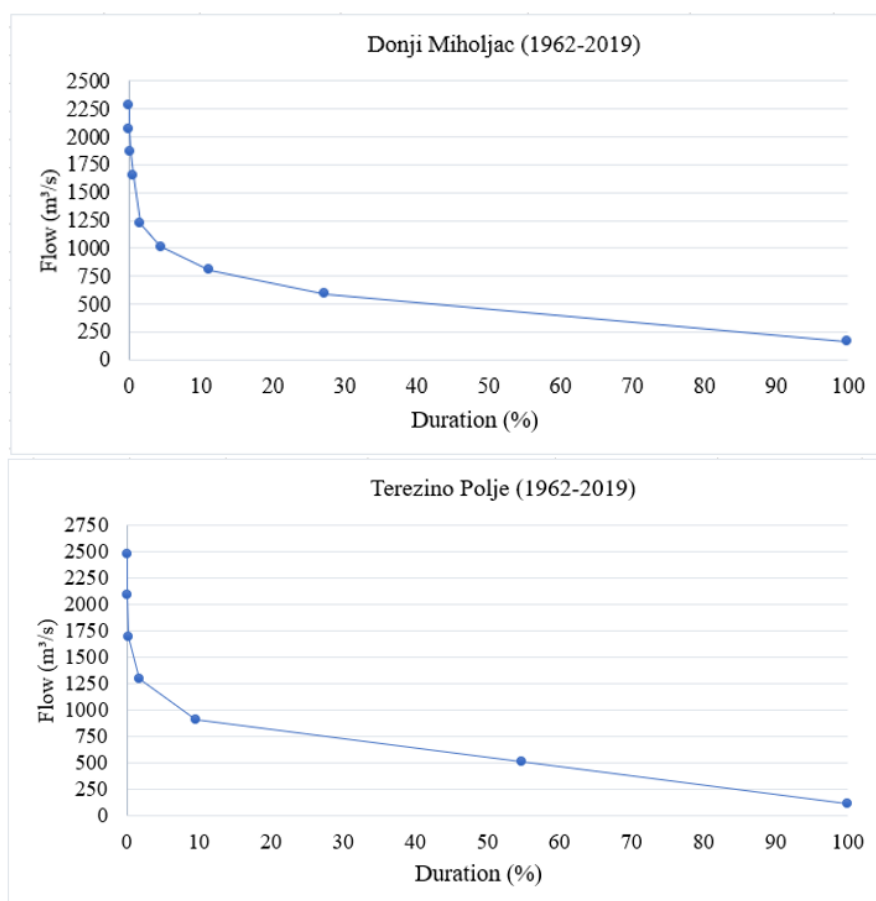
Fig. 8 Flow duration curve

Streamflow deficit, deficit duration and deficit volume

Flow deficits are periods when river flow is below a certain threshold that defines drought or critical deficit (Hisdal et al. 2004). There are two main methods for defining and characterizing deficits: the threshold level method and the algorithm of sequential peaks. In this paper, hydrological drought is defined using the threshold method, according to which drought occurs when the observed variable, the flow falls below a predetermined threshold, and the event continues until the threshold is exceeded again. On the threshold selection affects research purpose, region or area, and available data. Relatively low thresholds are used for multi-year river flow data, in the range Q70–Q95 (Kjeldsten et al., 2000). As a fixed limit or level that defines drought, in this paper was selected an 80 percent value (Q80) based on the flow duration curve. For the station Terezino Polje, according to the Flow duration curve, Q80 is 292 m³/s, and for Donji Miholjac 282 m³/s. After defining a threshold, it is possible to determine the other parameter hydrological drought: the beginning of the deficit, the duration of the deficit and its volume (Fig. 9).
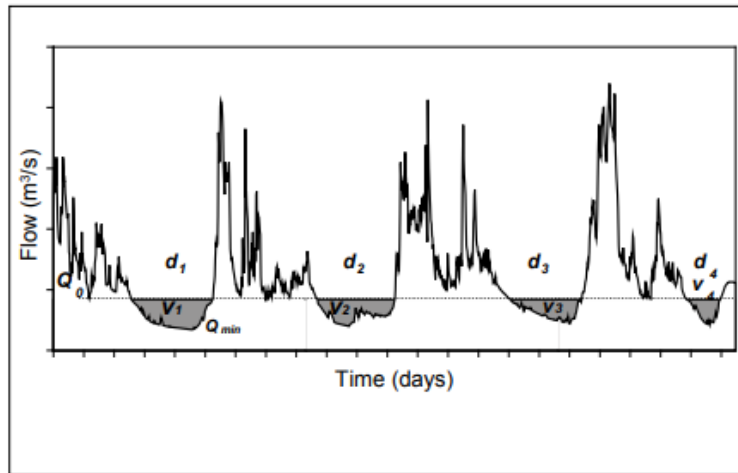
Fig. 9 Definition of deficit characteristics (Hisdal at al., 2004)

Based on the daily flows of the fifty-seven-year period and the defined limit values, the total duration of the deficit during each year is defined (Figure 9). Finally, picture no. 11 shows the movement of the total deficit volume over the observed period.
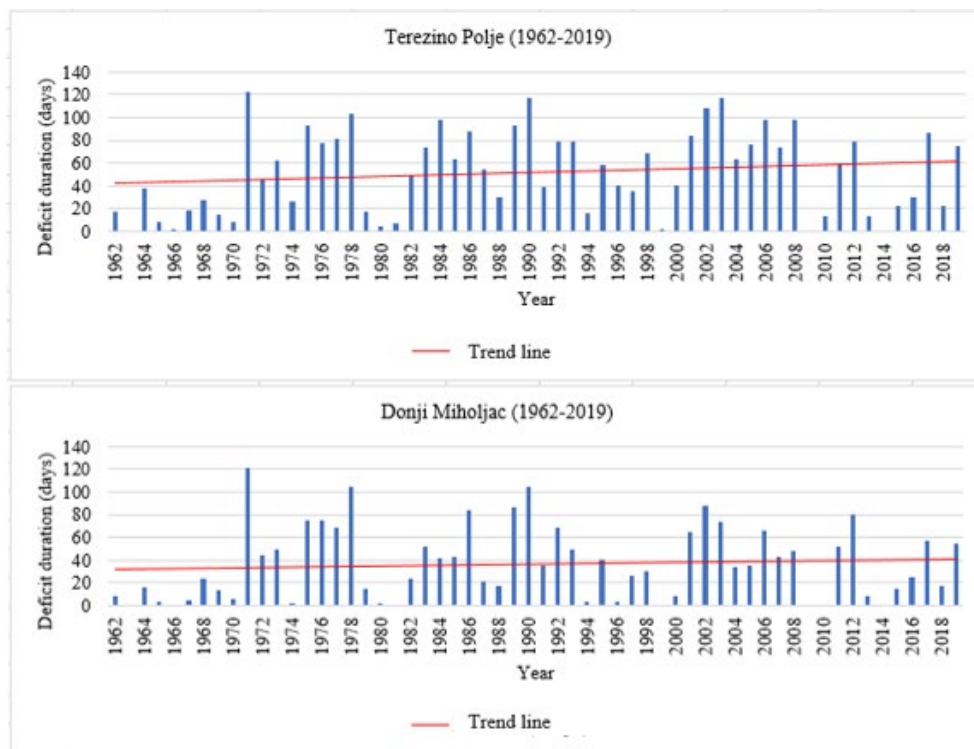
Fig. 10 Deficit duration analysis (days)
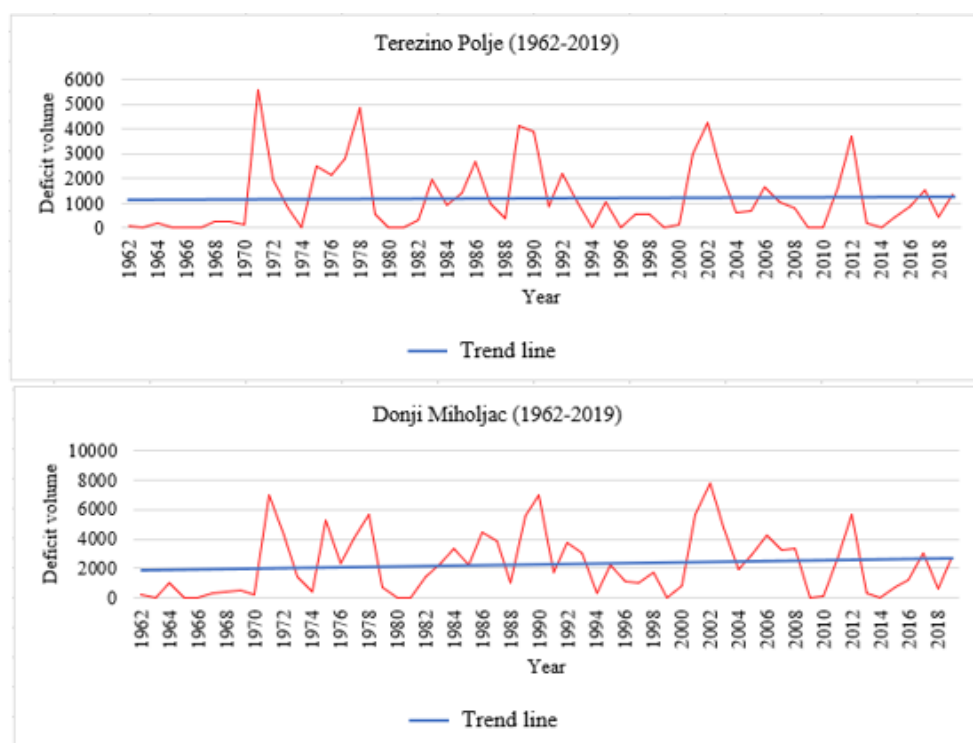
Fig. 11 Deficit volume analysis

To analyze the graphical representation of volume movements and deficit durations during fifty-seven-year period, a trend line was inserted. The duration of the deficit at both hydrological stations shows a slight upward trend, the flow deficits are becoming longer, while the volume of the deficit is slightly increasing. Based on the data on the volume and duration of the deficit, the Man Kendall trend test was performed, and the homogeneity of the series was examined using the Standard normal homogeneity test (SNHT). At both stations, data series are homogeneous, and the trend is ascending, but the growth is not statistically significant.

Recession analysis

Based on the deficit duration data during the analyzed fifty-seven-year period, the histogram in Figure 12 shows the frequency of recession periods or low flows. As a fixed limit or level that defines the drought in this case was also selected 80 percent value (Q80) based on the flow duration curve. In the histogram, the durations were divided into groups of 10 days. The average value of the recession duration is 52.13 days for the hydrological station Terezino Polje, while for the downstream station Donji Miholjac it is smaller, 36.77 days. The driest year, or the year with the longest recession duration (more than 120 days) is 1970 for both measuring stations.
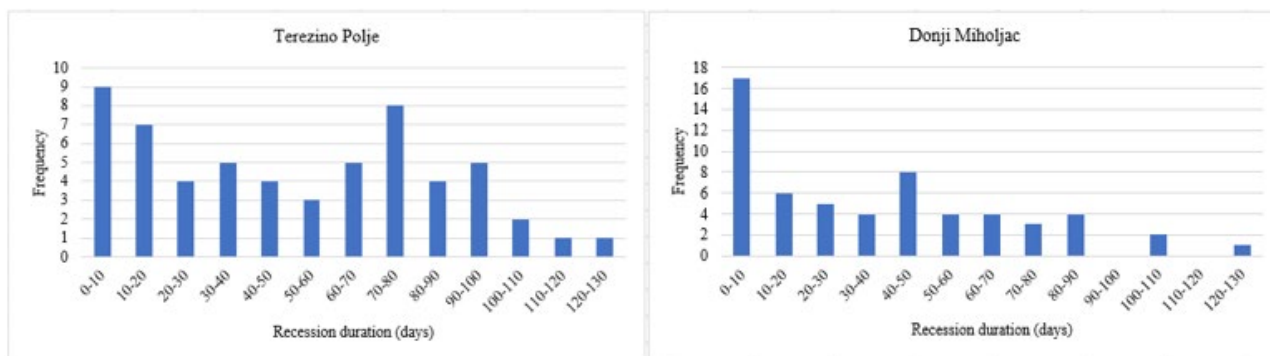
Fig. 12 Histogram of recession lenght (duration)

Conclusion

Drought is a phenomenon that is not easy to define nowadays. It is caused by meteorological conditions, and it appears all over the world with significant impacts and harmful consequences. Numerous indicators and indices have been developed that serve to determine and analyze drought and are based on a series of hydrometeorological variables. In this paper, low flow indicators are analyzed, using the daily flows of the Drava River from the hydrological station Terezino Polje and Donji Miholjac. The World Meteorological Organization (WMO) defines low flow as the „flow of water in a stream during prolonged dry weather". This indicates an inherent relation between the occurrence of low flows and droughts.

By analyzing the daily flows of the fifty-seven-year period, we notice great similarities in the behavior of the index at the Terezino Polje and Donji Miholjac stations. The mean flow of the analyzed period for Terezino polje is 517.13 m³/s, while for the downstream station it is 531.18 m³/s. The lowest flow in Donji Miholjac (166 m³/s) was measured on 12 December 1978, and in Terezino Polje on 31 December 2001 (121 m³/s). Trend testing was conducted at minimum mean annual flows and seasonal flows using the nonparametric Man Kendall trend test. The trend analysis points to significant decreasing, negative flow trend in the summer months (June and July), which may cause harmful consequences for ecosystem development as well as for agricultural production. In addition, it was found that the series of minimum flows in the summer months are not homogeneous. In the late 1980s, a significant reduction in flow began.

The flow duration curves are very similar for both stations and have a slight decline. Flows higher than 750 m³/s last 10% of the total time. Based on the duration curve, a fixed limit or level defining drought was selected (Q80). At least, this value was used to analyze the duration and volume of the deficit. Graphs and trend lines indicate an increasing duration of low flows and an increase in the volume of deficits. The analyzed and determined changes in low flow trends are in accordance with the often-mentioned scenarios of climate change, which predict an increase in the frequency of droughts and more intense and frequent extremes (Climate Change 2014).

References

Bonacci, O., Oskoruš, D. (2010) The changes in the lower Drava River water level, discharge and suspended sediment regime, *Environmental Earth Sciences*, Volume **59**, Issue 8, pp. 1661–1670

Bonacci, O., Oskoruš, D. (2008.) The influence of three Croatian hydroelectric power plants operation on the river Drava hydrological and sediment regime. U: XXIVth Conference of the Danubian countries on the hydrological forecasting and hydrological bases of water management (ur. M. Brilly i M. Šraj), Slovenian National Committee for the IHP UNESCO (ISBN: 978-961-91091-2-1), Ljubljana, Slovenija.

Climate Change 2014: Impacts, Adaptation, and Vulnerability, Volume II: Regional Aspects, Europe, IPPC Working Group II Contribution to the IPCC 5th Assessment Report, Accepted Unedited Final Draft Report, 201

C. Yozgatligil, Yazici C (2016) Comparison of homogeneity tests for temperature using a simulation study, *International Journal of Climatology*, vol. **36**, no. 1, pp. 62–81

Gajić-Čapka M, Cesarec K (2010) Trend i varijabilnost protoka i klimatskih veličina u slivu rijeke Drave, *Hrvatske vode*, **18** (71); 19–30

H. M. Kang, F. Yusof (2012) Homogeneity tests on daily rainfall series, *International Journal of Contemporary Mathematical Sciences*, vol. **7**, no. 1, pp. 9–22

Hisdal, H., B. Clausen, A. Gustard, E. Peters,L.M.Tallaksen(2004) Event definitions and indices. ln: llydrol ogi cal Drought Processes and Estimation Methodsfor Stream.flow and Ground water (L.M . Tallaksen and H.A.J . van Lanen, eds). *Developments in Water Science*, **48**, Elsevier Science B.V., Amsterdam: 139-198.-198.

Hisdal H, Stahl K, Tallaksen LM, Demuth S (2001) Have streamflow droughts in Europe become more sever or frequent? *International Journal of Climatology*, **21**, 317–333.

Ridolfi, E., Kumar, H., Bárdossy, A (2020) A methodology to estimate flow duration curves at partially ungauged basins, *Hydrol. Earth Syst. Sci.*, **24**, 2043–2060

Soto B (2020) Trends of hydrograph components in rivers of North of Iberian Peninsula during 1972–2012, *Environmental Earth Sciences*, **79**: 16

Stagl JC, Hattermann FF (2020) Impacts of Climate Change on the Hydrological Regime of the Danube River and Its Tributaries Using an Ensemble of Climate Scenarios, *Water 2015*, **7** (11), 6139–6172.

Tadić L, Brleković T (2019) Hydrological Characteristics of the Drava River in Croatia, In: Lóczy D. (eds) The Drava River. Springer Geography. Springer, Cham. https://doi.org/10.1007/978-3-319-92816-6_6

Voge l, R. M. & Fene ssey, N. M. (1994) Flow duration curves. I: New interpretation and confid ence interval s. .I. *Water Resour. Plan. Manage*. **120** (4), 485–504.

Watson, R. T., Zinyowera, M. C., & Moss, R. H. (1997) The Regional Impacts of Climate Change: An Assessment of Vulnerability (517 p.). A Special Report of IPCC Working Group II, Cambridge: Cambridge University Press.

World Meteorological Organization (2008) Manual on low-flow estimation and prediction / World Meteorological Organization WMO Geneva

Žugaj, R., Andreić, Ž., Pavlić, K., Fuštar, L. (2011) Krivulje trajanja protoka. Građevinar: časopis *Hrvatskog saveza građevinskih inženjera*, **63** (12), 1061–1068.

Comparison of one- and two-dimensional models for flood mapping in urban environments

Snezhanka BALABANOVA, Vesela STOYANOVA

National Institute of Meteorology and Hydrology at the Bulgarian Academy of Science, Bulgaria, Tzarigradsko chaussee 66, 1784 Sofia, Bulgaria, e-mails: Snezana.Balabanova@meteo.bg, Vesela.Popova@meteo.bg

Introduction

Floods are natural phenomena as a result of a combination of natural, geological and anthropogenic factors. Every year, floods cause loss of life, economic losses, adverse effects on the environment and cultural heritage all over the world. Floods are complex processes that have to be properly analyzed in order to know the exact spatial and temporal changes during a flood as well as the causes of these changes. Hydraulic modeling is used to model river flows, delineate floodplains, analyze flood characteristics, to identify the causes of flood and flood consequences.

The 'Floods Directive' 2007/60/CE by the European Parliament requires all Member States shall prepare flood hazard maps according to the three scenarios: (a) floods with a low probability; (b) floods with a medium probability; (c) floods with a high probability. For each scenario the flood extent, water depths or water level and the flow velocity should be shown. To assess this, complete analyses of the watershed hydraulics based on one, two or even three-dimensional modeling are needed.
Traditionally, 1D models have been used to simulate river floods using Saint-Venant equations. The final results of the modeling are the average velocity and water depth in each cross-section.
Generally, 2D models are used for local surveys in places with complicated hydraulic conditions, where it is important to have detailed information in flooded areas on the spatial distribution of the speed and water depth.

In this study, a 2D hydraulic model using HEC-RAS software for river flow and floodplains modeling was applied on part of the town of Smolyan, where the Biala River flows into the Cherna River (Fig.1). According to Flood Directive 2007/60/EC this area in the phase of Preliminary Flood Risk Assessment was defined as an area with potentially significant flood risk.

In the frame of development of flood warning system under ARDAFORECAST project between Bulgaria and Greece, 1D modeling was applied for the segment of the Arda river in the region of the town Smolian.

This paper presents a comparative analysis of the performance of 1D and 2D modelling of floods in an urban area with respect to the generation of inundation for flood events with 20, 100 and 1000 – year return periods. The 1D analysis and 2D modelling are performed using the software HEC-RAS.

Fig. 1 Location of the study area (part of the town of Smolyan, Bulgaria)

Methodology

Traditionally one-dimensional (1D) approach is used for fluvial flood modeling where the river and the surrounding floodplains are represented by a set of cross-sections. The geodetic survey of cross-sections and engineering structures along rivers Cherna and Biala in the Smolyan region was used for hydraulic modeling and creation of a digital terrain model (DEM) in the scope of the ARDAFORECAST project. The simulations for the annual maximum water discharges with return periods – 20, 100, and 1000 years were performed. The water levels resulting from hydraulic modeling were used to create a water surface. In GIS were defined flooded areas. Accurately determining the extent of inundated areas is essential in the development and expansion of urban areas. Accurate flood modeling in the selected urban area was performed using HEC-RAS 2D with diffusion wave (DW) approximation (Horritt et al., 2002). The computational mesh for terrain representation has a cell size of 2.5 / 2.5 m. Detailed terrain data for mesh generation in the 2D model was provided by Drone. The upstream boundary conditions were performed by synthetic hydrographs calculated using the Socolovsky method (Соколовски, 1959). For the downstream boundary condition, normal depth was assumed. Land use data and aerial photographs from Drone were analysed in order to get reasonable Manning's n values.

1D and 2D modeling were performed for two scenarios. The first was when the high wave is on the Cherna river (A) and the second when the high wave was on the Biala river (B). Hydrological scenarios are presented in Figure 2.
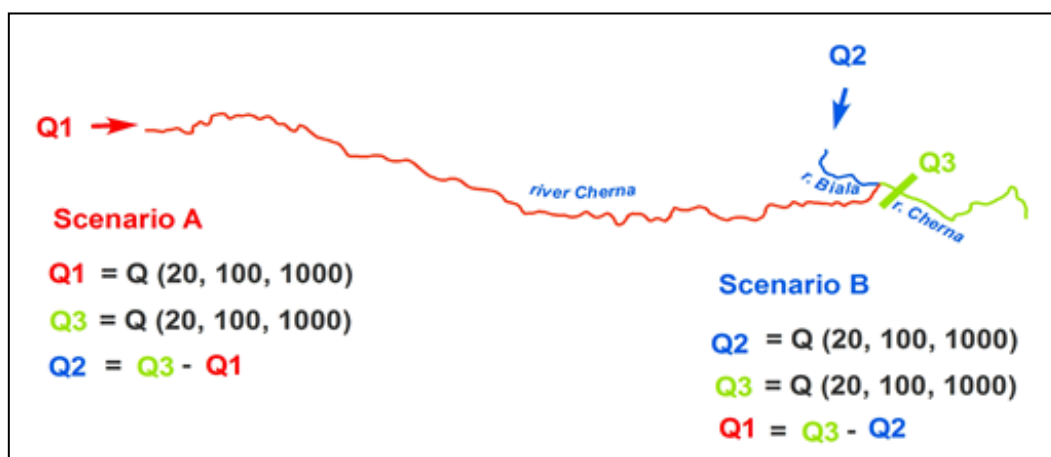
Fig. 2 Hydrological scenarios

Scenario A

PF1 – Simulation water discharges with return periods 1000 years were performed

PF3 – Simulation water discharges with return periods 100 years were performed

PF5 – Simulation water discharges with return periods 20 years were performed

Scenario B

PF2 – Simulation water discharges with return periods 1000 years were performed

PF4 – Simulation water discharges with return periods 100 years were performed

PF6 – Simulation water discharges with return periods 20 years were performed

Results

Comparison of HEC-RAS 1D and 2D model results for PF1 and PF2

Flooded area

When comparing the results of the 1D and 2D models for each of the scenarios, it was found that there is a significant difference in the extent of the flooded areas. The extent of the flood in the 2D simulation is larger and more detailed due to the more detailed terrain data and the bathymetry of the river (Fig.3 and Fig.4).
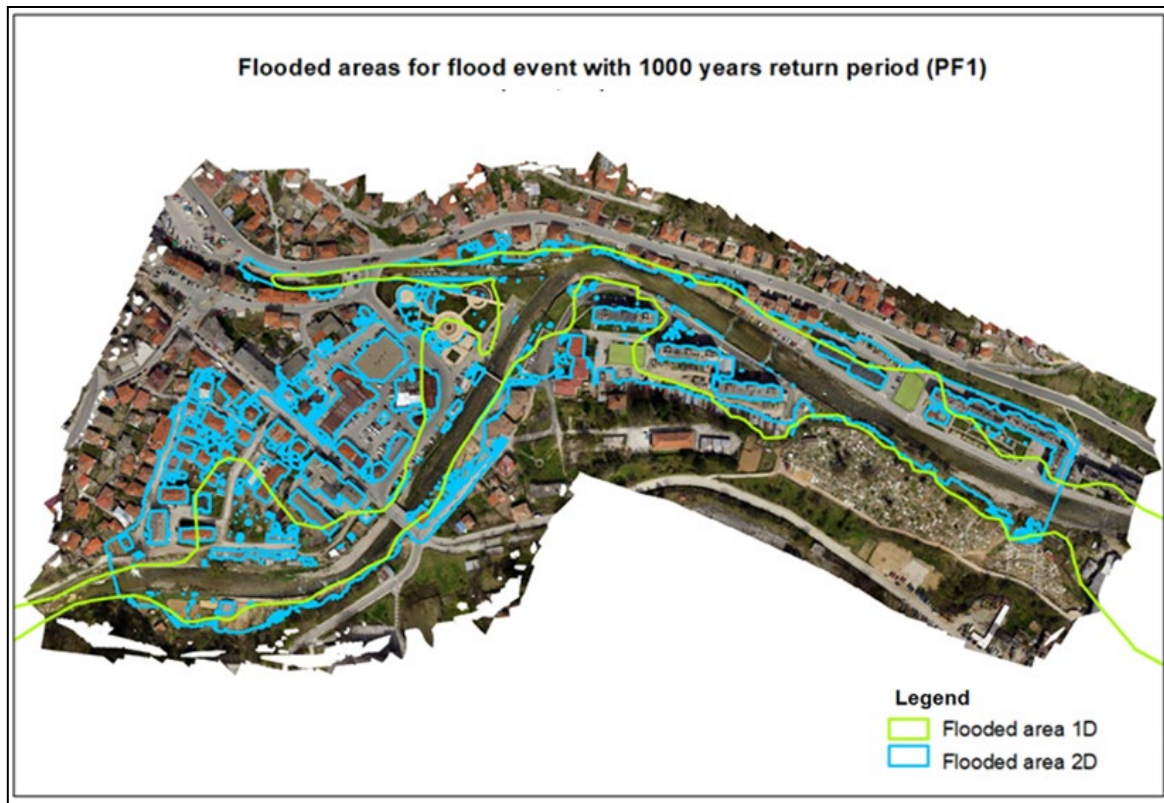
Fig. 3 Flooded areas for flood event with 1000 years return period (PF1)
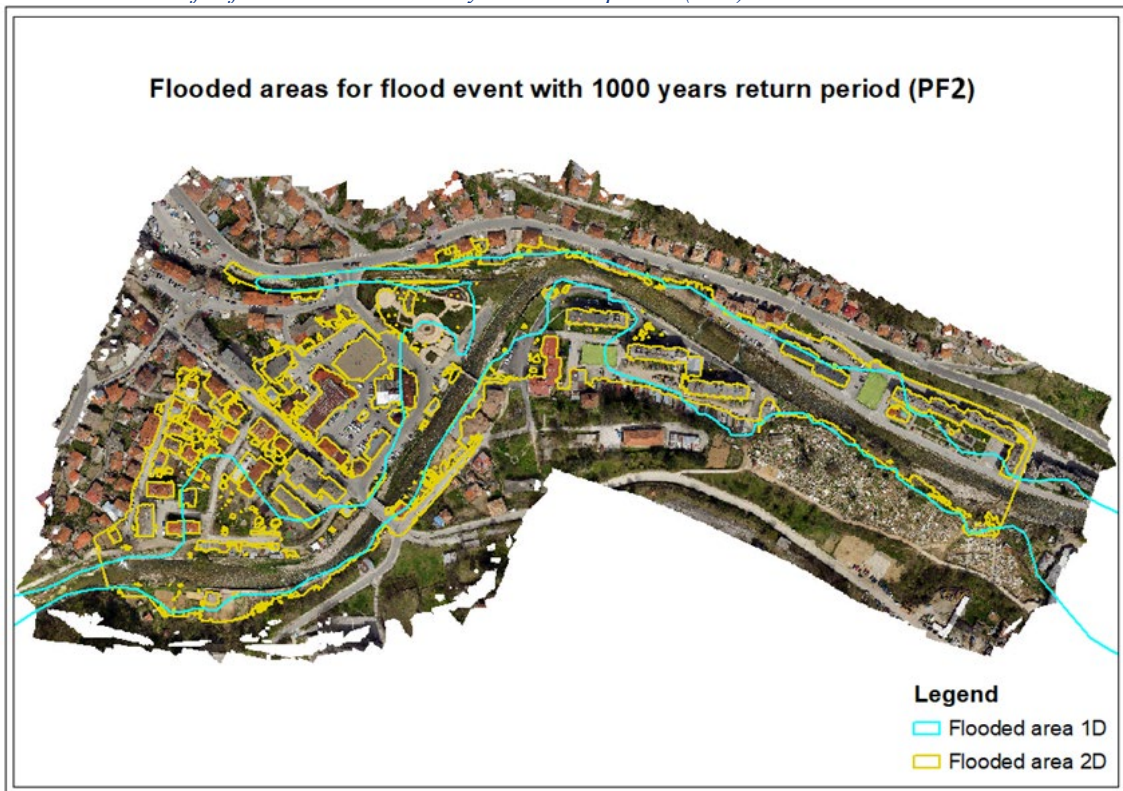
Fig. 4 Flooded areas for flood event with 1000 years return period (PF2)

Water level

The distribution of depths in 1D and 2D modeling is presented in Figure 5 and Figure 6 in the form of maps.
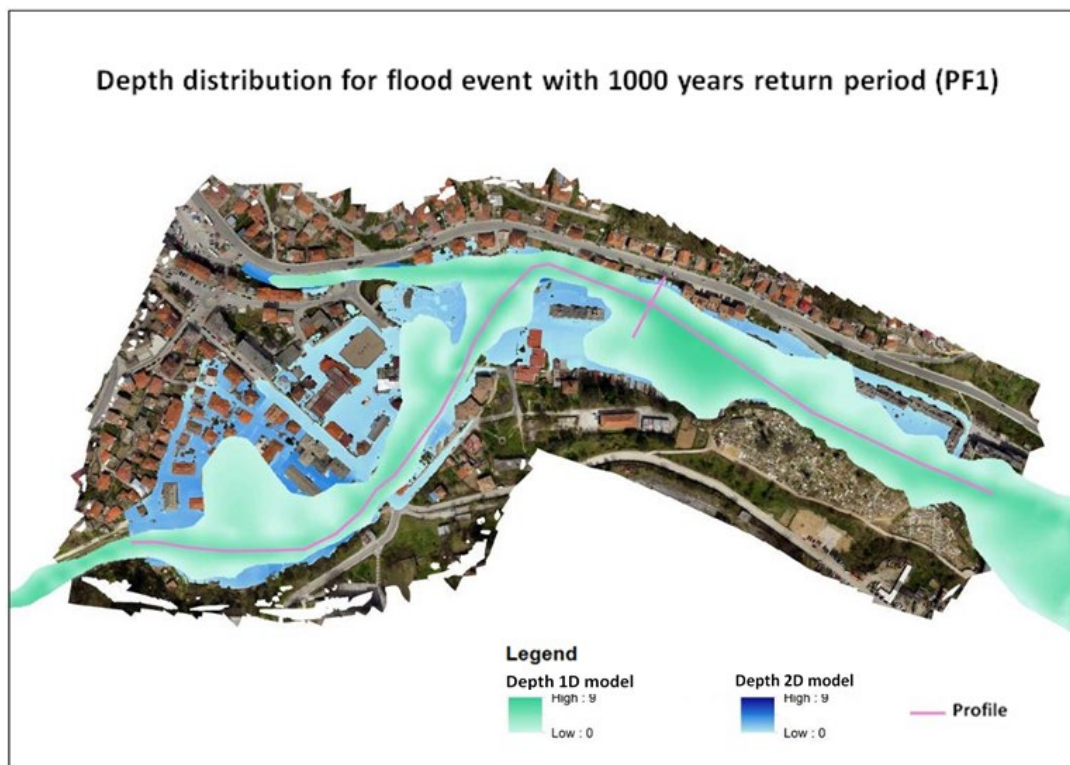
Fig. 5 Depths distribution for flood event with 1 000 years return period (PF1)
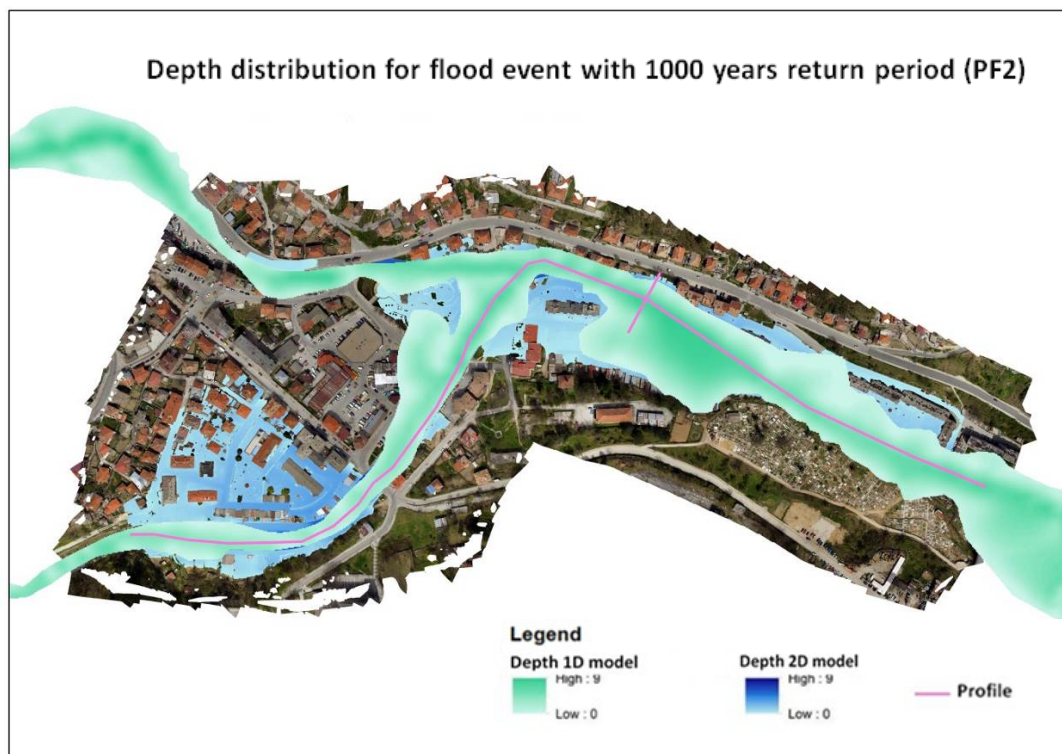
Fig. 6 Depths distribution for flood event with 1 000 years return (PF2) On Figure 5 and Figure 6 are shown comparisons of the results of 1D and 2D models in cross-section and longitudinal profile. The differences in water levels in the longitudinal profile in the different scenarios are presented in Table 1 and Table 2.

Table 1 Differences in water levels (PF1)

Profile	WSEL 1D	WSEL 2D	Variation
32	792.13	792.789	0.659
31	791.88	792.641	0.761
30	791.44	792.498	1.058
28	790.78	790.608	-0.172
27	789.63	789.991	0.361
25	789.43	789.263	-0.167
24	788.92	788.935	0.015
23	788.18	788.653	0.473
22	787.723	788.25	0.527
21	785.94	786.268	0.328
20	785.41	785.723	0.313
19	785.62	785.213	-0.407
18	785.51	784.987	-0.523
Max variation			0.527

Table 2 Differences in water levels (PF2)

Profile	WSEL 1D	WSEL 2D	Variation
32	790.93	791.916	0.986
31	789.88	791.784	1.904
30	790.07	791.685	1.615
28	789.92	789.84	-0.08
27	789.58	789.354	-0.226
25	789.14	788.919	-0.221
24	788.64	788.757	0.117
23	788.18	788.535	0.355
22	787.608	788.25	0.642
21	785.94	786.155	0.215
20	785.41	785.61	0.2
19	785.51	785.107	-0.403
18	785.51	784.871	-0.639
Max variation			0.674
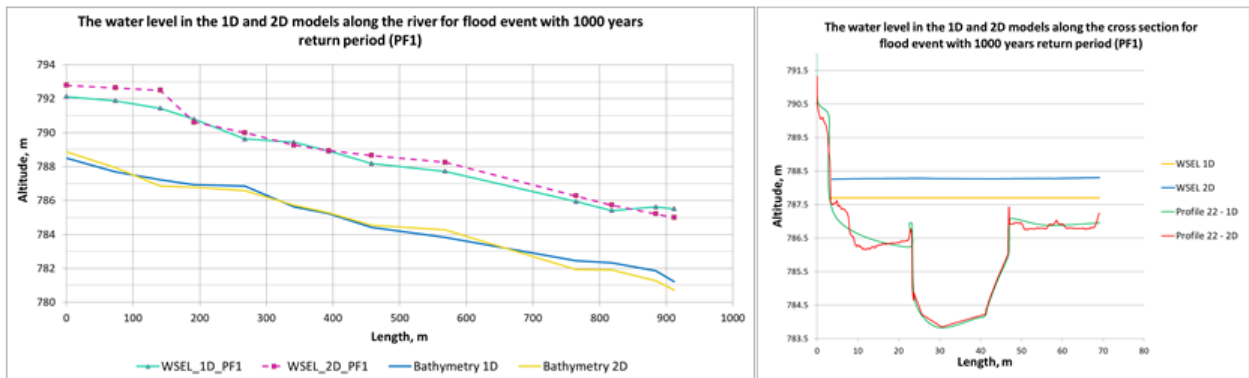
Fig. 7 Water level comparison 1D and 2D for flood event with 1000 years return period (PF1)
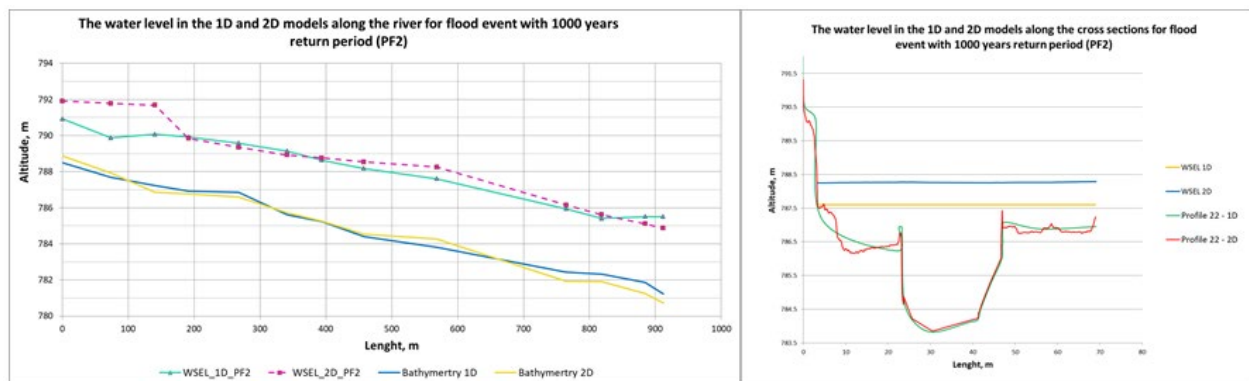
Fig. 8 Water level comparison 1D and 2D for flood event with 1000 years return period (PF2)

The results show that the differences vary from 1 cm to 67 cm and the larger differences are as a result of a more accurate description of the riverbed.

An important difference in the results of the 1D and 2D modeling can be seen at the water level in the cross-sections. The result of the 1D model for a given cross-section has one value along the whole profile, while in the 2D model the result for the water level is different for each calculation point of the cross-section, the water level in a transverse profile is variable along its length.

Conclusion

There is a similarity between the results of the two models in terms of the extent of the flooded areas. The 2D model takes into consideration variation in ground geometry because it computes all hydraulic properties at each mesh cell and computes the water surface elevation at each cell. While the 1D model just computes WSL at cross sections and between them uses the interpolation technique and does not take into consideration any changes in the characteristics of the river bed.

References

Horritt, M. S., & Bates, P. D. (2002). Evaluation of 1D and 2D numerical models for predicting river flood inundation. *Journal of hydrology*, **268** (1–4), 87–99.

Д. Соколовски, РЕЧНИЙ СТОК, Гидроме теорологическое издателство, Ленинград, 1959

Topic 2

Current status of the hydrological basis of the Danube water management (gauge network and water ecosystem)

Hydrological modelling to investigate climate change as part of transboundary river sediment management: Case study of the Thaya River Basin Czech Republic

Martin BEDNÁŘ, Vojtěch ČERNÝ, Daniel MARTON

Brno University of Technology, Faculty of Civil Engineering, email: bednar.m@fce.vutbr.cz (for author 1), email: 1782595@vutbr.cz (for author 2), email: marton.d@fce.vutbr.cz (for author 3)

Abstract

The water demand, ecology and sustainability of a river basin are very complex. As rivers form borders across many countries, cross-border cooperation is essential in their management and protection. This paper introduces a newly developed hydrological lumped water balance model on a daily time step basis and usage of climate change data constructed by the statistical downscaling tool LARS WG. The hydrological data under climate change will be represented using simulations of nine climate scenarios. The hydrology analysis of the climate change impact will be presented in the case study of the Thaya river basin in the cross-border area of Austria and the Czech Republic.

Introduction

With the growing population, the water demand, ecology and sustainability of a river basin have always been very complex, and with ongoing climate change, they are going to become increasingly significant. As rivers form borders across many countries, access to water causes stress for inhabitants; therefore, cross-border cooperation is essential for their management and protection. Consequently, international agreements and cross-border cooperation are necessary. In Europe, the Danube affects the life of human communities in 19 European countries inside and outside the European Union (EU), approximately 81 million inhabitants. Inside the EU, the cooperation is framed by the Convention on the Protection and the Use of Transboundary Watercourses and International Lakes (Council of the EU, 1995), which is based on the agreement of the cross-border commissions. Furthermore, the EU supports cross-border development via European funding.

The paper will present the interim results of the Interreg project ATCZ28 Sediments, ecosystem services and interrelation with floods and droughts in the Austrian–Czech border region (SEDECO), which is based on close bilateral cooperation and sharing of the data on the Thaya river, a tributary of the Danube. The main aim of SEDECO is to develop sustainable river sediment management in the Austrian and Czech cross-border part of the Thaya river basin. To map the river sediment balance, a new hydrological lumped water balance model of the Thaya river basin under climate change has been developed. For this paper, the control formulas of the water balance model were adapted to a different time scale. The optimal calibration setup was based on four sets of decision variables and four different methods for evaluating potential evapotranspiration. For the climate change projections, the weather generator LARS WG was used. The climate change application was based on the representative concentration pathways coupled with four global climate models implemented in the LARS WG software.

Study area
The Thaya river basin is situated in the cross-border region of Austria and the Czech Republic in Central Europe with an area of 13,419 km^2, of which 11,165 km^2 is on the Czech border side. The Thaya river has a total length of 311 km, of which 235 km is on the Czech border side. This study aims to gather information on only a part of the Thaya river basin: the part that contributes to inflows into the Nové

Mlýny reservoir. The area of interest covers 4,602 km² of the whole Thaya river catchment. The location of the study area is shown in Fig. 1.

For hydrological modelling, the area was divided into three subbasins: 1) Thaya 1 basin with an area of 1,755 km²; 2) Jevišovka basin with an area of 643 km²; and 3) Thaya 2 basin with an area of 4,602 km². In the study area, there are 19 precipitation stations (green dots in Fig. 1), 11 meteorological stations (purple dots in Fig. 1), and 8 hydrometric profiles (blue dots in Fig. 1), from which the observation data were gathered. Only the results of hydrological modelling of the Thaya 1 basin will be presented in the paper (blue area in Fig. 1). Therefore, data from only 14 measurement stations were used. Specifically, data from 2 hydrometric profiles (both on the Czech side of the subbasin) and 12 precipitation stations (of which only two were on the Czech side of the subbasin) and temperature data were used.
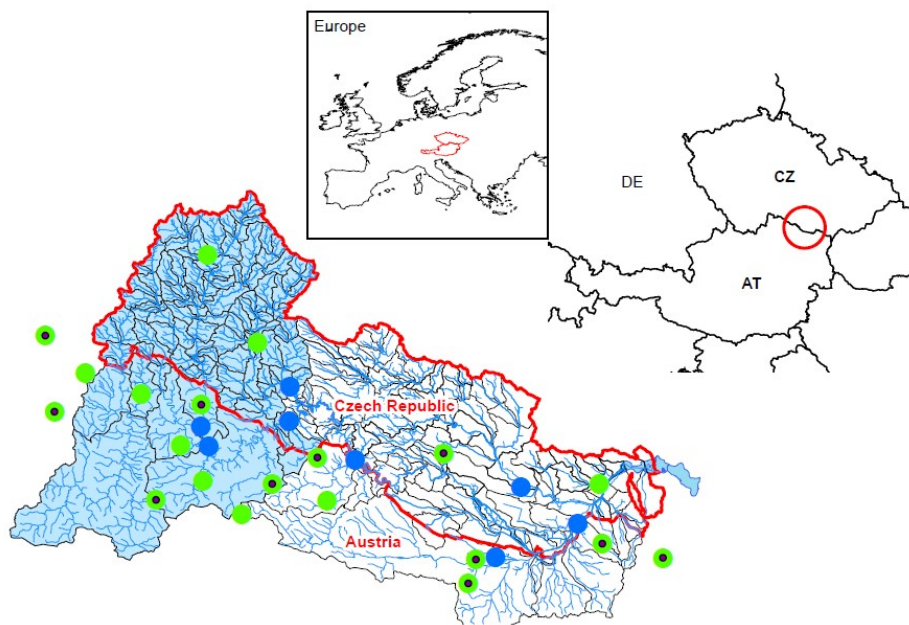
Fig. 1 General location of the part of the Thaya river basin with the marked river network, reservoirs and measurement stations; blue area – Thaya 1 basin, green dots – precipitation stations, green/purple dots – meteorological stations, blue dots – hydrometric profiles, red line area – the Czech part of the study area

From Fig. 1, it is apparent that several meteorological stations are located beyond the border of the subbasin. To determine whether they have a significant effect on the subbasin, two combinations of number of measurement stations were tested. The uniform length of hydrologic data from the relevant stations was available from 1991 to 2018. The input data for the model were provided by Austrian and Czech hydro-meteorological authorities. Meteorological data were in the form of maximum, minimum and mean daily air temperature and total daily precipitation, and hydrological data were in the form of mean daily flows.

Methods

As a hydrological modelling tool, the lumped water balance model is one of the bases of the method adopted. The water balance model is based on the control formulas, which specify the total daily flow and daily soil moisture. The control balance formulas are defined as mean daily surface flow q_s, mean daily groundwater discharge q_g, and mean daily evapotranspiration E_p. The rainfall-runoff equations were published by Wang et al. (2014) and Wang, Zhang and Yang (2016), and the conditions of the Central European hydrology and climate were adapted by Marton and Knoppová (2019). The above-mentioned approaches modelled the rainfall-runoff process in a monthly time step. This paper aims to adjust the model's computation to a daily time step. The main formulas that define the rainfall-runoff process are described as follows:

$$q_{s,i} = k_s \cdot \frac{S_{i-1}}{S_{max}} \cdot h_{s,i} \quad (1)$$

where $q_{s,i}$ is mean daily surface flow [mm], k_s is the coefficient of the surface flow [–], S_{i-1} is mean soil moisture in the $(i-1)$-th time step [mm], S_{max} is maximum soil moisture storage [mm], and $h_{s,i}$ is mean daily precipitation [mm]. Equation (2) describes the computation of the groundwater discharge $q_{g,i}$:

$$q_{g,i} = k_g \cdot S_{i-1} \qquad (2)$$

where $q_{g,i}$ is mean daily groundwater discharge [mm], k_g is the coefficient of the groundwater discharge [–], and S_{i-1} is mean soil moisture in the $(i-1)$-th time step [mm]. Furthermore, the daily mean evapotranspiration E_i is evaluated using Eq. (3):

$$E_i = k_e \cdot \frac{S_{i-1}}{S_{max}} \cdot E_{p,i} \qquad (3)$$

where E_i is mean daily evapotranspiration from the river's catchment [mm], k_e is the coefficient of the estimated evapotranspiration [–], and $E_{p,i}$ is the potential mean daily evapotranspiration [mm]. The total discharge $q_{c,i}$ from the river's catchment is estimated by the sum of the main daily surface flow $q_{s,i}$ and the mean daily groundwater discharge $q_{g,I}$.

$$q_{c,i} = q_{s,i} \cdot q_{g,i} \qquad (4)$$

Moreover, the soil moisture content S_i is estimated by Eq. (5):

$$S_i = S_{i-1} + h_{s,i} - q_{c,i} - E_i \qquad (5)$$

where S_i is soil moisture at the end of the ith day [mm], S_{i-1} is mean soil moisture in the $(i-1)$-th time step [mm], $h_{s,i}$ is mean daily precipitation [mm], $q_{c,i}$ is mean daily groundwater discharge [mm], and E_i is mean daily evapotranspiration from the river's catchment. Eqs. (1) to (5) are for $i = 1, 2, \ldots, n$, where n is the length of the data time series.

Due to the conversion to the daily time step, the rainfall-runoff process has to be investigated to determine the lag time between groundwater and surface flows. The lag time of the groundwater discharge was not integrated into the original formulas since it was averaged in the monthly time step. Therefore, the formula of the groundwater discharge was extended to cover this lag time. Therefore, Eq. (2) was replaced by Eq. (6):

$$q_{g,i} = k_g \cdot S_{i-k} \qquad (6)$$

where $q_{g,i}$ is mean daily groundwater discharge [mm], k_g is the coefficient of the groundwater discharge [–], and S_{i-k} is mean soil moisture in the $(i-k)^{th}$ time step [mm], which represents the lag time of the groundwater discharge.

Within a monthly time step, Marton and Knoppová (2019) effectively used the presented model with 37 parameters (12 coefficients of the monthly surface flow, 12 coefficients of the monthly groundwater discharge, 12 coefficient of monthly evapotranspiration, and 1 parameter of the initial surface soil moisture) as three parameters for each month in a year. The three parameters per month represent the time interval for the constant parameters within the daily time step. The number of parameters was uncertain. Therefore, four different sets of decision variables were tested:

- 82 parameters – constant parameters for every two weeks in a year + 1
- 157 parameters – constant parameters for each week in a year + 1
- 367 parameters – constant parameters for every three days in a year + 1
- 1099 parameters – each of the parameters for every day in a year + 1

Each set of decision variables consists of a fixed number of coefficients of the monthly surface flow, the monthly groundwater discharge, and the monthly evapotranspiration + 1 parameter of the initial surface soil moisture. Three different lag times were tested for each set of decision variables using Eq. (6) for $k = 1, 2, 3$ (1 – no lag time, 2 – one-day lag time, 3 – two-day lag time).

Potential evapotranspiration (PET)

For the computing process in the lumped water balance model, the mean daily evapotranspiration must be provided (Eq. [3]). The four empirical (temperature-based) methods for calculating PET were tested: the Blaney–Criddle, Hargreaves, Turc, and Thornthwaite methods.

The Blaney–Criddle method (Allen et al., 1998) is a straightforward method that uses temperature and daily sunshine duration to calculate the reference crop evapotranspiration. This method relates to mean monthly values of temperature and evapotranspiration. However, to obtain the mean monthly evapotranspiration, it is necessary to multiply the result by the number of days in each month. The developed simulation model works within a daily time step. Therefore, the result is not multiplied by the number of days within a month and the computation is in the daily time step. The Hargreaves method (Hargreaves & Samani, 1985) estimates the reference PET by considering the maximum, minimum and mean air temperature and extra-terrestrial radiation. This method can be used within both a monthly and a daily time step. Therefore, there was no need to adjust the formulas, and the evaluation of the mean daily evapotranspiration is given in daily values. The Turc method (Turc, 1961) is similar to the Hargreaves method. It also estimates PET within both a monthly and a daily time step. Moreover, the method is based on the maximum, minimum and mean air temperature; however, solar radiation is used instead of extra-terrestrial radiation. The Thornthwaite method (Thornthwaite, 1948) estimates the potential evapotranspiration for a standard month of 30 days, each day with a photoperiod of 12 hours, as a function of the monthly average temperature. For the daily time step computation, the photoperiod of a day has to be evaluated separately for each day in a year.

Optimisation method

First, the period for the calibration process had to be set. The input data were time series of the observed values for daily temperature and precipitation for the period 1991 to 2018. The percentage ratio of the calibration/validation data sets was 70/30. Therefore, the calibration data were from the period 1991 to 2009 and the validation data were from the period 2010 to 2018. The objective function for the optimisation was the Nash–Sutcliffe model efficiency coefficient (NSE, Nash & Sutcliffe, 1970), which led to a maximising optimisation problem. The NSE acquires values in the interval from $-\infty$ to 1 (inclusive). The value of NSE is calculated by Eq. (18):

$$NSE = 1 - \frac{\sum_{i=1}^{n}(Q_{o,i}-Q_{p,i})^2}{\sum_{i=1}^{n}(Q_{o,i}-\overline{Q_o})^2} \qquad (18)$$

where NSE is the Nash–Sutcliffe model efficiency coefficient [–], $Q_{o,i}$ is the observed value of daily flow [m³.s⁻¹], $Q_{p,i}$ is the predicted value of daily flow [m³.s⁻¹] for $i = 1, 2, …, n$, where n is the length of the data time series, and Q_o is the average value of the flow from the whole period observed [m³.s⁻¹].

Moriasi et al. (2007) highlighted that values between 0 and 1 are generally considered as an acceptable level of the model's performance, whereas values less than 0 indicate that the mean observed value is a better predictor than the simulated values, which denotes unacceptable performance. The authors also established general performance ratings for recommended statistics: unsatisfactory (NSE < 0.50), satisfactory (0.50 < NSE < 0.65), good (0.65 < NSE < 0.75), and very good (0.75 < NSE < 1.00). These ratings were established for a monthly time step; therefore, we considered NSE values of 0.2 and above as satisfactory.

Statistical downscaling

For the simulation of climatological data, LARS WG (version 6.0) software was used. LARS WG is a well-known statistical downscaling tool widely used for climate change projections. The software is based on the series weather generator described in Racsko et al. (1991). A detailed description of the model and downscaling procedures can be found in the user manual for LARS WG version 3.0 by Semenov and Barrow (2002).

The LARS WG downscaling method was coupled with EC EARTH, HadGEM2-ES, MIROC5 and MPI-ESM-MR as global climate models (GCMs) using 2.6, 4.5 and 8.5 representative concentration pathways (RCPs) as the boundary conditions for the future climate projections. The future climate change projections, provided by the fifth phase of the Coupled Model Intercomparison Project by the

Working Group on Coupled Modelling, are based on climate scenarios that use a time series of emissions and concentrations from the RCPs described by Moss et al. (2010). The RCP2.6, RCP4.5 and RCP8.5 scenarios were chosen for this paper. The peak-and-decline RCP2.6 is a mitigation scenario. The optimistic progression of this scenario leads to a low forcing level at the end of the 21st century (2.6 W.m^{-2}). This scenario is designed to meet the 2°C average global warming target compared to pre-industrial conditions (van Vuuren et al., 2011). The RCP4.5 scenario is a medium stabilisation scenario in which radiative forcing peaks at about 4.5 W.m^{-2} in 2100, and then a slow decrease and stabilisation at 4.2 W.m^{-2} is expected (Thomson et al., 2011). The RCP8.5 scenario assumes a high rate of emissions, leading to high radiative forcing in the 21st century. In this scenario, the value of radiative forcing reaches 8.5 W.m^{-2} in 2100 and continues to increase (Riahi et al., 2011).

Using LARS WG, baseline data and the nine climate scenarios were created based on the boundary conditions of the four above-mentioned GCMs and three RCP scenarios for two time periods: PI (2021–2040) and PII (2041–2060). The final combination of GCMs and RCPs used to obtain the nine climate scenarios is shown in Table 1.

Table 1 Combinations of GCMs and RCPs used (nine climate scenarios)

Representative Concentration Pathways	Global Climate Models			
	EC EARTH	HadGEM2-ES	MIROC5	MPI-ESM-MR
RCP2.6	–	✓	–	–
RCP4.5	✓	✓	✓	✓
RCP8.5	✓	✓	✓	✓

The outputs generated from LARS WG were daily minimum, maximum and mean air temperature and daily mean precipitation for each of the determined scenario combinations (Table 1).

Results

To find the best model setup, all the above-mentioned methods for evaluating PET were tested first. For each method, the model was calibrated and validated separately. The best method would be the one with the highest NSE value for the calibration and validation. During the calibration and validation processes, all the sets of decision variables were tested. The generalised reduced gradient algorithm (Landson et al., 1978) implemented in Microsoft Excel was applied to solve the optimisation problem. As mentioned above, the decision variables were tested for three different lag times (no lag time, one-day lag time, and two-day lag time) and for a different quantity of gauging stations (8 or 12) using the Turc, Thornthwaite, Hargreaves, and Blaney-Criddle methods for evaluating PET. The NSE values for calibration and validation were compared for each PET method and each set of decision variables. Based on the comparison, the best model setups were for the Turc and Blaney-Criddle PET methods. The best model setups are shown in Table 2.

Table 2 The best model setups chosen for the Turc and Blaney–Criddle PET methods

PET Methods	Model Setup			NSE	
	Decision variables	Groundwater delay	Number of stations	Calibration	Validation
Turc	82	1 day	8	0.443	0.221
Blaney–Criddle	157	1 day	8	0.422	0.240

Since the two best PET methods give a similar NSE, the best method was chosen subjectively based on the mean daily and monthly flow time series progressions. The monthly average flows for both model setups were compared with monthly average flows obtained from the observed data. The average values for both methods were obtained by the arithmetic average of the future data within the period 2021 to 2060. The graphical comparison of the observed and simulated data is shown in Fig. 2.
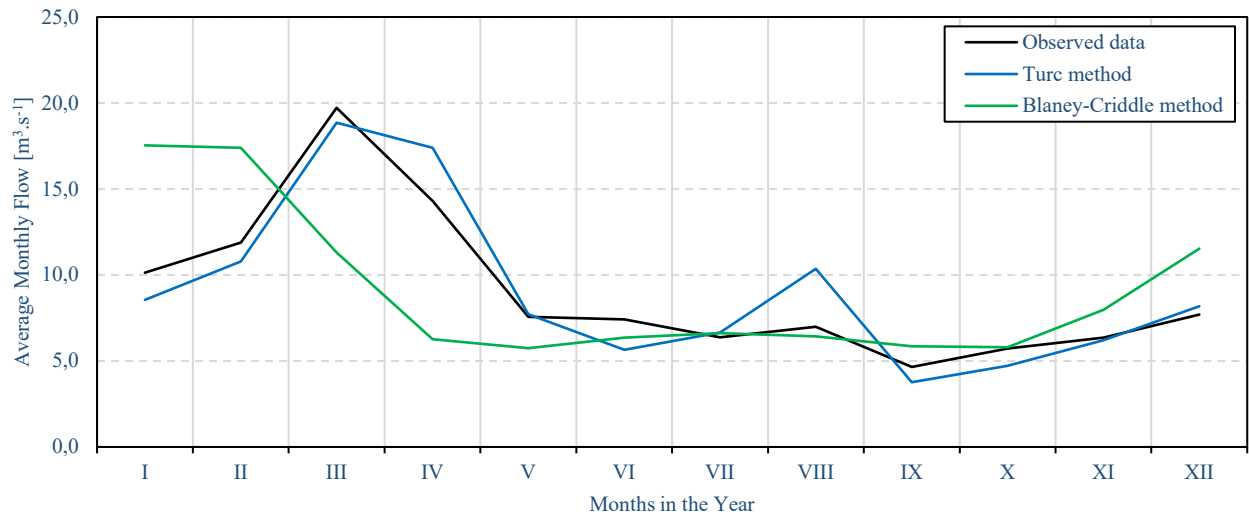
Fig. 2 Comparison of the monthly average flow values obtained from the observed data and model setups with the Turc method and Blaney–Criddle method

From Fig. 2, it is obvious that the model setup with the usage of the Turc method returns slightly better values than the observed data. Flow peaks in the time series of the monthly mean flows are situated where they were expected. Although, the Blaney-Criddle method was not very accurate in simulating mean monthly flows, it was still compared also in mean daily flows. The comparison of the time series of the mean daily flows for the observed data and both model setups is shown in Fig. 3.
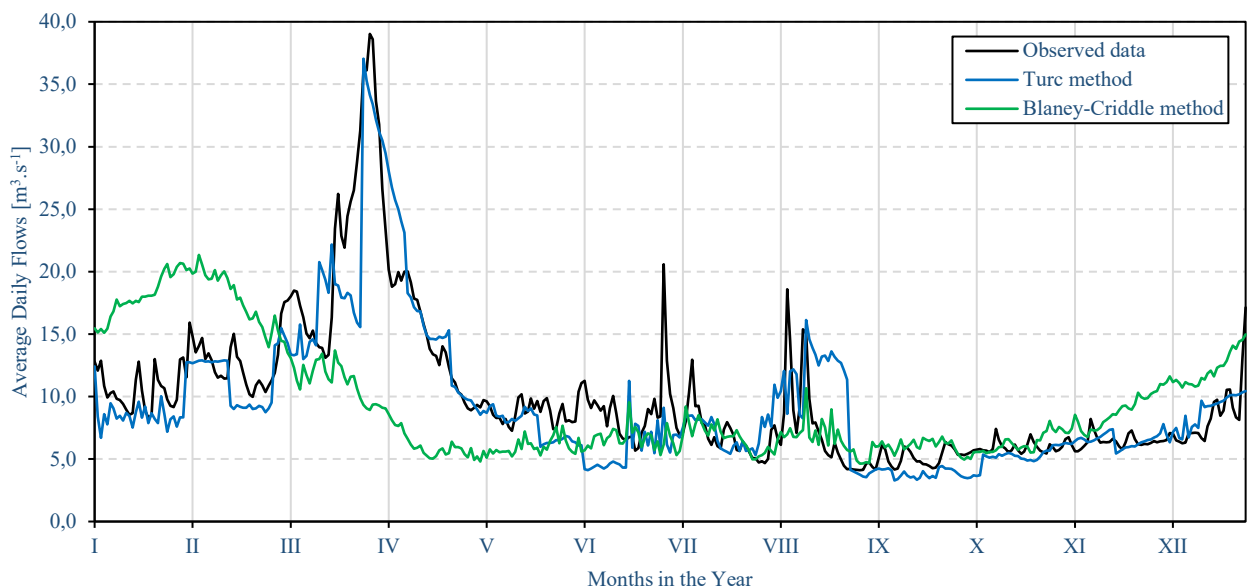
Fig. 3 Comparison of the daily average flow values obtained from the observed data and model setups with the Turc method and Blaney–Criddle method

It can be seen from Fig. 3 that the time series of the daily mean flow values simulated using the Blaney-Criddle method do not correspond to the observed data. However, although the method gave a quite satisfactory NSE, it did not simulate the peaks correctly, and at the beginning of the year, it was not even close to the observed data. Conversely, the Turc method showed good accuracy of the simulated data. Based on results presented in Fig. 3, the Blaney-Criddle method was rejected and the Turc method was chosen as the best method for the model setup. Therefore, the final model setup included 82 decision variables, 8 measurement stations counted, 1 day of groundwater discharge delay, and the usage of the Turc method for PET evaluation. This setup with NSE = 0.443 for the calibration and NSE = 0.221 for the validation was used to simulate the effect of the future climate change projections in the study area.

73

The input data for the created lumped water balance simulation model were gathered from the LARS WG software for the two time periods: PI (2021–2040) and PII (2041–2060). The data obtained were represented as daily maximum, daily minimum and daily mean air temperature and daily total precipitation. The simulation model was used with the obtained input data, and the daily average flows for the two time periods were obtained. Further work on the output data involved performing the 'bias correction'. The output daily data were linearly scaled by the ratio between the monthly average values of observed and simulated data (Lenderink et al., 2007). This linear-scaling method was used for both the temperature and precipitation data sets. The value of long-term average flow for the historical observed data was evaluated at $9.316 \, \mathrm{m^3.s^{-1}}$ for the period 1986 to 2018. The long-term average streamflow for the corrected baseline was then evaluated at $9.316 \, \mathrm{m^3.s^{-1}}$. The long-term average flow values for each combination of GCM and RCP were then compared with the baseline value. For the comparison of these values, see Table 3.

Table 3 Long-term average streamflows of the predicted climate change data with the evaluation of the relative difference to the baseline data

Combinations of GCMs and RCPs	Mean long-term streamflows of the predicted climate change data [$\mathrm{m^3.s^{-1}}$]				Relative difference to the baseline [%]		
	Baseline	2021–2040	2041–2060	2021–2060	2021–2040	2041–2060	2021–2060
EC EARTH 4.5	9.316	8.688	8.384	8.536	−6.7	−10.0	−8.4
EC EARTH 8.5	9.316	8.771	7.688	8.229	−5.9	−17.5	−11.7
HadGEM2-ES 2.6	9.316	7.216	7.352	7.284	−22.5	−21.1	−21.8
HadGEM2-ES 4.5	9.316	7.698	6.708	7.203	−17.4	−28.0	−22.7
HadGEM2-ES 8.5	9.316	7.624	6.659	7.142	−18.2	−28.5	−23.3
MIROC5 4.5	9.316	8.517	8.287	8.402	−8.6	−11.0	−9.8
MIROC5 8.5	9.316	8.224	7.756	7.990	−11.7	−16.7	−14.2
MPI-ESM-MR 4.5	9.316	8.037	7.785	7.911	−13.7	−16.4	−15.1
MPI-ESM-MR 8.5	9.316	8.109	8.445	8.277	−13.0	−9.4	−11.2

Table 3 shows that there is clearly a downward trend in the mean long-term streamflow value during both future periods. The long-term average streamflows were plotted to better display their future progression (see Fig. 4).
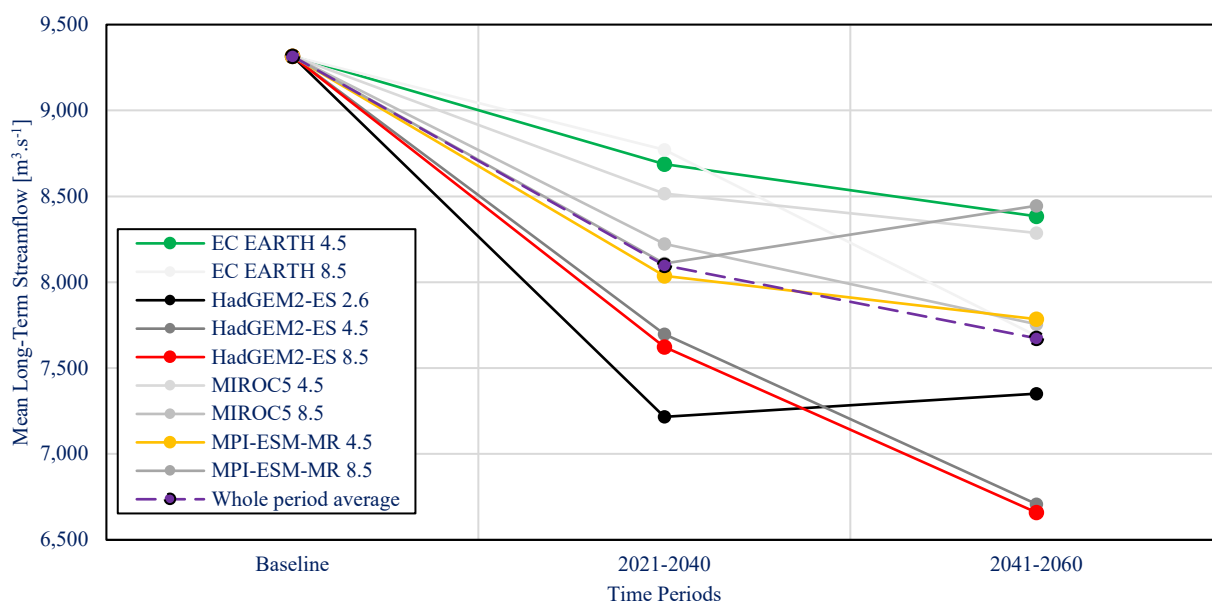
Fig. 4 Evaluation of mean long-term streamflow progression for periods PI and PII towards the baseline period

The results show that the combination of EC EARTH and RCP4.5 gave the most optimistic results for the future projection, in which the mean long-term streamflow will decrease by 6.7% until 2040 and then by another 3.3% until 2060 compared with the baseline period. However, the RCP2.6 scenario is an optimistic mitigation scenario since the results for HadGEM2-ES and RCP2.6 show the highest decrease in mean long-term streamflow until 2040. The streamflow decreased by 22.5% in the PI period,

and then the value of the mean long-term streamflow increased slightly to a decrease of 21.1% in the PII period compared with the baseline period. The whole period average of the mean long-term streamflow across all the scenario combinations was virtually identical to the combination of MPI-ESM-MR and the medium stabilisation scenario RCP4.5. This combination gave a decrease of 13.7% in the value of mean long-term streamflow in the PI period and a 16.4% decrease in the PII period compared with the baseline period. The lowest value of the mean long-term streamflow was obtained by using the combination of HadGEM2-ES and RCP8.5, which represents the pessimistic RCP scenario. Until 2040, a decrease of 18.2%, given by this combination, is not the lowest compared with the baseline period across all the results. However, in the PII period, the value of mean long-term streamflow decreased by another 10.3%, which was a total decrease of 28.5% compared with the baseline period. The analysis of the results shows that the water flow in Thaya 1 basin decreased in PI from −5.9 % to −22.5% compared with the baseline period and decreased in PII from −9.4% to −28.5% compared with the baseline period. On average, overall, the inflow will decrease by −8.4% to −23.3% compared with the baseline period until 2060. Therefore, there is a high expectation that there will be a downward trend in the values of the streamflow in the study area.

Conclusion

The developed lumped water balance simulation model proved that the methods used can be applied without any difficulties to simulate catchment outflows in the daily time step. The computational algorithm is set up in a general way and can be quickly used in other catchments. The final model setup used for the simulation works with a set of 82 decision variables, one-day lag time of the groundwater discharge, 8 gauging stations (precipitation and temperature data), and the Turc method for evaluating PET. This model setup achieved an optimisation criterion NSE = 0.443 in the calibration process and NSE = 0.221 in the validation process for the study area. The positive values of the NSE are generally considered as an acceptable level of the model performance. According to the established recommended general performance ratings, NSE values lower than 0.500 are considered unsatisfactory model performance. However, these ratings were established for a monthly time step. Therefore, we considered the NSE values obtained in the calibration and validation processes as satisfactory.

The preliminary results show a promising way to set up the lumped water balance model in the daily time step. Therefore, the model is considered as suitable for the climate in the Czech Republic. To enhance the performance and the precision of the simulated results, model improvement is needed. The investigation will be as follows: i) a different ratio of calibration/validation data sets will be used since it is known that in the period from 2015 to 2019, there was an unusual extreme drought in the river basin; ii) the lag-time in groundwater flow will be tested in a more detailed way; iii) a different method of optimisation will be used; iv) the snowmelt model extension will be implemented, which is very important in our region since water from snowmelt contributes to high participation in catchment outflows during the spring season; and v) the Horton–Thiessen method will be used for more precise evaluation of daily average precipitation in the catchment.

Furthermore, the results will be used in SEDECO for the simulation of reservoir system management, cross-border sediment balance analysis, and as part of the boundary condition of the hydraulic model of reservoir sedimentation. All this work will provide the first scientific foundation to coordinate joint cross-border river and reservoir sediment management in this area and help to improve the knowledge of cross-border river basin management on a wider scale.

Acknowledgements

References

Allen, R. G., Pereira, L. S., Raes, D., & Smith, M. (1998). *Crop evapotranspiration – Guidelines for computing crop water requirements – FAO Irrigation and drainage paper 56*. FAO – Food and Agriculture Organization of the United Nations.

Council of the European Union. (1995). Council Decision of 24 July 1995 on the conclusion, on behalf of the Community, of the Convention on the Protection and Use of Transboundary Watercourses and International Lakes (95/308/EC). Retrieved from https://eur-lex.europa.eu

Hargreaves, G. H., & Samani, Z. A. (1985). Reference crop evapotranspiration from temperature. *Applied Engineering in Agriculture, 1*(2), 96–99. https://doi.org/10.13031/2013.26773

Lasdon, L. S., Waren, A. D., Jain, A., & Ratner, M. (1978). Design and testing of a generalized reduced gradient code for nonlinear programming. *ACM Transactions on Mathematical Software, 4* (1), 34–50. https://doi.org/10.1145/355769.355773

Lenderink, G., Buishand, A., & van Deursen, W. (2007). Estimates of future discharges of the river Rhine using two scenario methodologies: Direct versus delta approach. *Hydrology and Earth System Sciences, 11* (3), 1145–1159. https://doi.org/10.5194/hess-11-1145-2007

Marton, D., & Knoppová, K. (2019). Developing hydrological and reservoir models under deep uncertainty of climate change: Robustness of water supply reservoir. *Water Supply, 19* (8), 2222–2230. https://doi.org/10.2166/ws.2019.102

Moriasi, D. N., Arnold, J. G., Van Liew, M. W., Bingner, R. L., Harmel, R. D., & Veith, T. L. (2007). Model evaluation guidelines for systematic quantification of accuracy in watershed simulations. *Transactions of the ASABE, 50*(3), 885–900. https://doi.org/10.13031/2013.23153

Moss, R. H., Edmonds, J. A., Hibbard, K. A., Manning, M. R., Rose, S. K., van Vuuren, D. P., Carter, T. R., Emori, S., Kainuma, M., Kram, T., Meehl, G. A., Mitchell, J. F. B., Nakicenovic, N., Riahi, K., Smith, S. J., Stouffer, R. J., Thomson, A. M., Weyant, J. P., & Wilbanks, T. J. (2010). The next generation of scenarios for climate change research and assessment. *Nature, 463* (7282), 747–756. https://doi.org/10.1038/nature08823

Nash, J. E., & Sutcliffe, J. V. (1970). River flow forecasting through conceptual models part I – A discussion of principles. *Journal of Hydrology, 10* (3), 282–290. https://doi.org/10.1016/0022-1694(70)90255-6

Racsko, P., Szeidl, L., & Semenov, M. (1991). A serial approach to local stochastic weather models. *Ecological Modelling*, *57* (1–2), 27–41. https://doi.org/10.1016/0304-3800(91)90053-4

Riahi, K., Rao, S., Krey, V., Cho, C., Chirkov, V., Fischer, G., Kindermann, G., Nakicenovic, N., & Rafaj, P. (2011). RCP 8.5—A scenario of comparatively high greenhouse gas emissions. *Climatic Change, 109* (1–2), 33–57. https://doi.org/10.1007/s10584-011-0149-y

Semenov, M. A., Pilkington-Bennett, S., & Calanca, P. (2013). Validation of ELPIS 1980–2010 baseline scenarios using the observed European Climate Assessment data set. *Climate Research, 57* (1), 1–9. https://doi.org/10.3354/cr01164

Thomson, A. M., Calvin, K. V., Smith, S. J., Kyle, G. P., Volke, A., Patel, P., Delgado-Arias, S., Bond-Lamberty, B., Wise, M. A., Clarke, L. E., & Edmonds, J. A. (2011). RCP4.5: A pathway for stabilization of radiative forcing by 2100. *Climatic Change, 109* (1–2), 77–94. https://doi.org/10.1007/s10584-011-0151-4

Thornthwaite, C. W. (1948). An approach toward a rational classification of climate. *Geographical Review, 38 (*1), 55–94. https://doi.org/10.2307/210739

Turc, L. (1961). Water requirements assessment of irrigation, potential evapotranspiration: Simplified and updated climatic formula. *Annales Agronomiques, 12*, 13–49.

van Vuuren, D. P., Edmonds, J., Kainuma, M., Riahi, K., Thomson, A., Hibbard, K., Hurtt, G. C., Kram, T., Krey, V., Lamarque, J.-F., Masui, T., Meinshausen, M., Nakicenovic, N., Smith, S. J., & Rose, S. K. (2011). The representative concentration pathways: An overview. *Climatic Change, 109* (1–2), 5–31. https://doi.org/10.1007/s10584-011-0148-z

Wang, G. Q., Zhang, J. Y., Jin, J. L., Liu, Y. L., He, R. M., Bao, Z. X., Liu, C. S., & Li, Y. (2014). Regional calibration of a water balance model for estimating stream flow in ungauged areas of the Yellow River Basin. *Quaternary International,* **336**, 65–72. https://doi.org/10.1016/j.quaint.2013.08.051

Wang, G., Zhang, J., & Yang, Q. (2016). Attribution of runoff change for the Xinshui river catchment on the Loess Plateau of China in a changing environment. *Water,* **8** (6). https://doi.org/10.3390/w8060267

Issues of Operational Hydrology in Ukraine in the Context of WMO Strategy and Organizational Arrangements for Hydrology and Water Resources

Viacheslav MANUKALO[1], Victoria BOIKO[2], Valeriy VODOLASKOV[3]

[1] Ukrainian Hydrometeorological Institute, e-mail: manukalo@ukr.net, [2] Ukrainian Hydrometeorological Centre,
[3] State Emergency Service of Ukraine, e-mail: vodolaskov@meteo.gov.ua

Abstract

In Ukraine almost all issues of operational hydrology, as they are indicated in WMO documents, belong to a competence of the State Hydrometeorological Service, which is the principal governmental body responsible for providing hydrometeorological information, forecasting and warnings to authorities, economic sectors and population. Over the past few years, the World Meteorological Organization (WMO) has organized a number of landmark events that addressed the development of activities in the field of hydrology and water resources at national, regional and international levels. The decisions taken at these events relate to the hydrological activity in all countries – WMO members, including Ukraine, both in a broad sense (practice, science and education ones) and in its specific area, namely, operational hydrology.

The current state and main problems of operational hydrology in Ukraine, new WMO initiatives in the field of hydrology and water resources, possible areas of participation of Ukrainian scientists and practitioners in the implementation of these initiatives are considered in the paper.

Introduction

The issue of improving a hydrological direction of activities of national hydrometeorological and / or hydrological services is a key importance for assessing quantitative and qualitative indicators of surface waters as a necessary component of effective management and protection of water resources. Therefore, this issue is given much attention by both national hydrometeorological services and the World Meteorological Organization.

The history of formation of hydrological direction in WMO activities dates back to 1946, when the Commission on hydrology was established at the International Meteorological Organization, which was the WMO predecessor. However, a path of development of the hydrological direction in the activities of WMO was not easy and it received less attention than the meteorological direction. This can be explained by objective and subjective reasons related to specifics of WMO activities. For those wishing to familiarize themselves with the history of hydrological activities of WMO, we recommend reading the publication (Lins HF, 2010).

Issues of further development of the hydrological direction of WMO activities has become especially relevant in recent years given the need to more effectively use the capabilities of national hydrometeorological and hydrological services as well as WMO itself in solving problems of management and protection of water resources. Over the past few years WMO has organized a number of landmark events that addressed the development of activities in the field of hydrology and water resources at national, regional and international levels: the WMO Global Conference on Prosperity Through Hydrological Services, 2018; the 70th Session of WMO Executive Council, 2018; the Extraordinary Session of WMO Commission for Hydrology, 2019; the 18th Session of World Meteorological Congress, 2019; the first and second sessions of Forum of Hydrological Advisers for WMO Regional Association –VI (Europe), 2020 and 2021; the WMO Data Conference, 2020. The decisions taken at these events relate to the hydrological activity in all countries – WMO members,

including Ukraine – both in a broad sense (practice, science and education ones) and in its specific area, namely, the operational hydrology.

The purpose of this publication is to consider the current state, needs and areas for the development of the operational hydrology in Ukraine in the context of WMO recent initiatives.

Methodology

The paper has been prepared jointly by the Ukrainian Hydrometeorological Institute, the Ukrainian Hydrometeorological Center and the Department of Hydrometeorology of the State Emergency Service of Ukraine. The study is based on:

- the analysis of the final materials (reports, recommendations, so on) of events (meetings, conferences, so on) carried out by WMO in the field of hydrology and water resources. One of authors of this paper (V. Manukalo) participated in a number of these events as the Hydrological Adviser to the Permanent Representative of Ukraine to WMO. Mentioned materials can be found on the official site of WMO.
- expert assessments of the current state and problems of operational hydrology in Ukraine and the possible benefits of participation of the Ukrainian Hydrometeorological Service and some others water-related institutions in recent WMO initiatives in the field of hydrology and water resources.

Results

Definition of the term "Operational Hydrology".

The term „Operational Hydrology" was first defined at the 6th Session of the World Meteorological Congress in 1971. This term included: „... measurements of basic hydrological elements from networks of meteorological and hydrological stations: collection, transmission, processing, storage, retrieval and publication of basic hydrological data; hydrological forecasting; development and improvement of relevant methods, procedures and techniques in network design; specification of instruments, standardization of instruments and methods of observation; data transmission and processing, supply of meteorological and hydrological data for design purposes and hydrological forecasting".

Taking into account the growing demands of society for a study, management and protection of water resources as well as present achievements in a development of scientific and applied hydrology, the new definition of the term „Operational Hydrology" was adopted by the 18th Session of the World Meteorological Congress in 2019. The term „Operational Hydrology" is defined in Annex 1 to the 24th Congress Resolution. The full text of this resolution is as follows: „...operational hydrology is the real-time and regular measurement, collection, processing, archiving and distribution of hydrological, hydrometeorological and cryospheric data, and the generation of analyses, models, forecasts and warnings which inform water resources management and support water-related decisions, across a spectrum of temporal and spatial scales. Operational hydrology requires capacity building and scientific and technical advancement and innovation in the areas of observation, data standards and services, modelling, prediction, hydro-informatics and decision support, communications, training, and outreach. Annotation: These data include, but are not limited to, precipitation; air temperature and humidity; water level of streams, lakes, deltas and estuaries; stream flow; snow and ice cover, depth and water equivalent; river and lake ice; glacier mass balance; reservoir storage; soil moisture; groundwater and ground frost; evaporation and evapotranspiration; water temperature; sediment dynamics; water and sediment quality and other related variables, including within the context of global change. Global change is expressed through different aspects, such as land use changes, socioeconomic dynamics, climate variability and climate change".

As we can see, the latter definition significantly expands the term „operational hydrology", which corresponds to the growing importance of scientific and practical hydrology in solving water problems of today.

Present status of operational hydrology in Ukraine

In Ukraine, the national water-related activity is regulated by legal acts: the Water Code, the Law on Hydrometeorological Activities, and a number of governmental decrees. According to the Ukrainian legislation almost all issues of operational hydrology, mentioned above, belong to the competence of the State Hydrometeorological Service, which is the principal governmental body responsible for providing hydrometeorological information, forecasting and warnings to authorities, economic sectors and population. The Hydrometeorological Service is working under the State Service of Emergencies and is the multifunctional system constructed according to the vertical principle. Different levels of organizational, methodological and technical management (e.g. state, regional, district) have created in this system. The Hydrometeorological Service manages national hydrometeorological activities via its structural units that are responsible for:

- the Ukrainian Hydrometeorological Center (located in Kyiv) and 24 regional centers on Hydrometeorology – for the operational processing of observation and data collection, operational forecasting, official dissemination of observation data, forecasts and warnings for the central and local Governments, economic sectors and population;
- the Central Geophysical Observatory (located in Kyiv) – for storage and long-term processing of hydrometeorological data, data archiving, methodological guidance of hydrometeorological observation networks;
- the Ukrainian Research Hydrometeorological Institute (located in Kyiv) for researches in the field of hydrological and meteorological observations and forecasting as well as for scientific support of practical activity of the Hydrometeorological Service.

The Hydrometeorological Service operates extensive meteorological and hydrological monitoring network which includes 187 meteorological stations and about 400 point of hydrological observation located on surface water bodies – rivers, lakes and reservoirs.

The forecasting of hydrological events in Ukraine has a long traditions. Indeed the systematic forecasting of water levels and discharges started in 1930s on the basis of long-term observations in many gauges on rivers and their transfer (mainly graphical) relationship downstream. At present during a year organizations of the Hydrometeorological Service make more than 1 500 long-term forecasts and more than 9 000 short-term forecasts. More than 3 500 forecasts concern floods. The water regime characteristics (maximum water levels and it's temporal distribution, dates of maximum water levels and discharges, runoff volume) are forecasted with different degrees of detail. The hydrological and related meteorological information, forecasts and warnings are widely used by the central and local authorities, as well as different water -depended socio- economic sectors of the national economy: agriculture, domestic drinking water supply, energy production, navigation, civil defense, recreation and environmental protection. It should be note that combining meteorological and hydrological activities into one state body facilitates the interaction of meteorologists and hydrologists, which has a positive impact on the quality of hydrometeorological products and services provided to end – users.

In addition to the Hydrometeorological Service, hydrological measurements are performed by organizations which work in systems of the State Agency of Water Resources (on water reclamation systems) and the Ministry of Education and Science (in a process of training specialists – hydrologists). These organizations use the methodology of measuring hydrological variables used by the Hydrometeorological Service.

Unfortunately, there are a number of problematic issues (logistical, technological and financial ones) in activities of the Hydrometeorological Service, some of which are systemic and long-lasting. As noted above, the Hydrometeorological Service is managed by the State Emergency Service of Ukraine, the main task of which is to prevent negative consequences of natural and man-made emergencies. The hydrometeorological activity are organized and supervised by a very small staff specialists of the State Emergency Service. This makes it difficult to manage the Hydrometeorological Service, especially when we need to make quick and correct decisions. For example, it delays works in the field of improving

documents regulated the activity of the Hydrometeorological Service, or developing the national and international investment projects for a technological development of the Service.

The density of the ground network of hydrological observation and especially points of precipitation measuring is comparatively low. This does not allow to introduce in an operational work modern models of floods forecasting, especially, flash floods in mountain river basins. Studies performed by the Ukrainian Hydrometeorological Institute show that in mountain river basins the number of water flow measuring points should be increased by 30–40%, and the number of precipitation measuring points – by 100–120%.

The technological equipment of the Hydrometeorological Service remains a systemic and long-term problem. To overcome this problem during 1997–2006 the State target program of technological re-equipment of the Hydrometeorological Service was realized in Ukraine. The program allowed to organize in Ukraine own production of hydrometeorological equipment. In particular, the production of automated hydrological stations was established. These stations also allowed to determine a temperature of air and water, and an intensity of precipitation. Prototypes of Doppler flow velocity meters have been developed and successfully field tested. The production of a large number of auxiliary hydrometric equipment was also mastered. However, the lack of needed state funding did not allow to complete the planned developments and to carry out mass purchases of already developed equipment.

That is why old technologies of hydrometric measurements are still widely used in the Hydrometeorological Service to this day. The water stages have been measured by float type of water-stage measurement with chart recorder. The water velocity has been measured on the basis of using of propeller current meters. The hydrological instruments have not been equipped with data loggers. A significant drawback is the lack of the required number of automated hydrometric stations and technical means of ultrasonic measurement of flow velocity in rivers. To improve the timeliness and accuracy of rain flood forecasting in mountain river basins, it is extremely important to create in these regions a network of small hydrometeorological radars.

We connect the next stage in the technological re-equipment of the Hydrometeorological Service with an approval by the Ukrainian Government of a new target program, the project of which was developed by the Hydrometeorological Service. Approximately 30% of the funding provided for the program implementation should be spent on re-equipping the hydrological direction of activities of the Hydrometeorological Service.

The organizational and technological measures listed above require significant financial resources. Given the real economic situation in the country, it is difficult to expect that needs of the Hydrometeorological Service can be fully met from the state budget. This forces us to look for other sources of investment both in Ukraine and abroad. In Ukraine, this can be achieved by expanding the provision of paid services to users.

Significant work is being done with international financial institutions, governments of some countries and well-known manufacturers of hydrometeorological equipment to launch a large investment project that will allow to acquire modern technologies and to improve a quality of observations and forecasting. How successfully these plans will be implemented can be said in 2–3 years.

Recent WMO initiatives

Taking into account the growing demands of society for a study, management and protection of water resources as well as present achievements in a development of scientific and applied hydrology it was decided by the 18th WMO Congress to prepare the Plan of Actions in order '...to strengthen operational National Hydrological Services and the capabilities of national service providers that will support Member states' efforts to fulfil the following long-term ambitions: a) „no one is surprised by a flood"; b) „everyone is prepared for drought"; c) „hydro-climate and meteorological data support the food security agenda"; d) „high-quality data supports science"; e) „science provides a sound basis for operational hydrology"; f) „we have a thorough knowledge of the water resources of our world"; g) „sustainable development is supported by informationcovering the full hydrological cycle"; h) „water quality is known'. The draft of the Plan of Action was prepared by the Hydrological Coordination Panel

in cooperation with other working bodies of WMO, and was circulated to the wider hydrological community for consideration and giving comments which to be send to WMO by end of May 2021.

The Plan of Actions includes five action areas completed by a group of cross-cutting activities that lead to the achievement of long-term ambitions. These activities are also coordinated by the WMO Research Board in developing the Research Strategy for Hydrology.

Activities in the frame of the action area 'floods' are supposed to achieve goals of the ambition 'no one is surprised by a flood'. It is expected that ambitions 'everyone is prepared for drought' & 'hydro-climate and meteorological data support the food security agenda' will be achieved through the implementation of the action area 'droughts and support to food security agenda'. Activities within the action area 'interfaces with science' will contribute to achieve ambitions 'high-quality data supports science' & 'science provides a sound basis for operational hydrology'. Goals of activities of the action area 'water resources assessment and information for SDG' are achieving ambitions 'we have a thorough knowledge of the water resources of our world' & 'sustainable development is supported by information covering the full hydrological cycle'. Activities in the action area 'water quality' will contribute achieving objectives of ambition 'water quality is known'. Finally, the sixth area of activity –'crossed issues' – should be noted, which, although not directly related to the achievement of any long-term ambitions, but it is very important for the development of operational hydrology in general. It aims to enhance the operation of national hydrological services, including, their financing and sustainability.

Each of the sections of the Plan devoted to a specific area of actions, structurally consists of the following sub-sections: 'outcomes', metrics', 'needs and gaps', 'outputs', 'on-going activities', 'assumptions and risks'. We consider such a structure of the Plan quite successful, as it allows not only to plan final results and to propose a mechanism for achieving them, but also offers ways of evaluating the plan effectiveness. This will allow, if necessary, to promptly make some adjustments to the Action Plan.

WMO has also identified in the Action Plan the following ongoing activities that should contribute to the achievement of long-term Ambitions: a) quality Management Framework – Hydrology and its further implementation with the aim of promoting a stronger culture of compliance and quality assurance; b) assessment of performance of flow measurement instruments and techniques: the development of software to assist Hydrological Services to assess an uncertainty of discharge measuring; c) the HydroHub: implementation of HYCOS components according to countries priorities under new WHYCOS framework; d) hydrological data operational and management: the implementation of WMO WHYCOS Phase II, in accordance with its Implementation Plan endorsed by the 71-st session of the WMO Executive Council; e) the WMO Flood Forecasting Initiatives and hydrological contributions to disasters risk management; f) the WMO Global Hydrological Status and Outlook System which is aimed to produce regular analyses of current national hydrological conditions complimented by forward looking assessment of how the water situation may change over sub-seasonal and seasonal time scales, and taking into consideration the need to link this initiative closely with other relater WMO activities; g) the WMO Strategy for Capacity Development and Water Resources Management; h) the World Water Data Initiative which is aimed to promote national strategies to improve water information.

Participation of Ukraine in WMO initiatives

The Hydrometeorological Service of Ukraine is interested to participate in all WMO hydrological initiatives mentioned above, as, on the one hand, it hopes to gain a new knowledge and a good experience from international partners, and, on the other hand, it will be able to present achievements of Ukrainian scientists in hydrological researches and equipment manufacturers in development and production of hydrological technologies. Some of these researches and technologies have gained recognition outside Ukraine.

The following issues will be considered below: a) in which areas of WMO hydrological activities Ukraine is interested to participate; b) what knowledge and practical experience the Ukrainian operational hydrology can gain from participation in these initiatives; c) what scientific and technical achievements Ukrainian scientists and manufacturers can offer to international partners; d) what

organizational measures should be taken by Ukrainian institutions in order to benefit most from participation in WMO initiatives.

Action area 'floods'. River floods and inundations caused by them are among the most common natural hazards in Ukraine, especially in mountainous regions. Therefore, the improvement of methods and technologies for hydrological observations, forecasting and warnings is the top priority of the Hydrometeorological Service. Within this area of actions, Ukraine institutions may offer to share their experience in the fields of: a) collaboration between meteorological and hydrological units of the Hydrometeorological Service during a formation and passage of floods; b) organization of interaction with end users of forecasts and warnings; c) organization of exchange of information and forecasts with national hydrometeorological services of neighboring countries; c) developing methods of hydrological forecasts and producing a number of hydrometric instruments. At present intensive works are also underway in Ukraine to implement provisions of the European Floods Directive (Directive 2007/60/EC]). We suppose that practical results of these works would be interesting for other countries. In turn, the Hydrometeorological Service has gaps and needs in some areas of its activities. We are interested in gaining knowledge and practical experience in the following areas: a) designing observation networks in flood-prone regions which are effective in practical and economic senses; b) application of remote and automated technologies for obtaining and assimilation information for flood forecasting models; c) integrating flood forecasting models in end-to- end multi-hazards warning systems, including guidance on emerging technologies and services for data acquisition and analysis; d) guidelines for harmonizing information and products that are used to communicate forecasting results and related risks; e) establishing a collaboration with private sector to support activities in flood early warnings and risk management

Action area 'droughts and support to food security agenda'. Meteorological and associated hydrological droughts are common in the southern and eastern parts of Ukraine. Scientific estimates show that the frequency and intensity of droughts will increase in the country as a result of expected regional climate changes. The sectors of water management and agriculture production suffer from these adverse natural phenomena. The Hydrometeorological Service annually provides more than 6000 information and forecasts of water inflow to reservoirs of the main rivers of Ukraine – the Dnipro, Dniester, Southern Bug, Siverskiy Donets. The current hydrological information and forecasts of water inflow to river reservoirs during the growing season are especially important as they help to plan measures of crops irrigation. Ukraine is ready to share its experience in fields of: a) an organization of interaction with the main end-users of hydrometeorological products and services; b) an elaboration and using methodologies to forecast river runoff in dry periods.

On the other hand, the Hydrometeorological Service is interested: a) to study an experience of other hydrometeorological services on using satellite data in assessing a risk of drought on crop yields; b) to obtain expanded access to satellite products; c) to participate in developing requirements to data produced at global/regional scales for using in drought assessment, modeling and prediction at national scale.

Action area 'interfaces with sciences'. The participation in this action area is extremely important for the development of operational hydrology in Ukraine, as it allows to implement the latest achievements of hydrometeorological science in practical activities. It can be argued that a level of development of scientific hydrological researches will determine a level of development of operational hydrology in general. On the other hand, the implementation of this action area will help scientists to better understand practical needs of hydrometeorological services.

There is only one scientific institution in the structure of the Hydrometeorological Service – the Ukrainian Hydrometeorological Institute, which provides scientific support of all areas of hydrological activities, from primary measurements of hydrometric and water pollution characteristics to providing end – users with products – the current information, forecasts, warnings and results of researches. Hydrological researches for needs of the Hydrometeorological Service are also performed in some educational institutions – the Odesa State Environment University, the Kyiv National Taras Shevchenko University, the Chernivtsi National University. Ukrainian hydrologists have many years of experience in participating in international scientific projects implemented under the auspices of UNESCO, the International Commission for the Protection of the Danube River, a number of other international organizations working in fields of water issues.

The contribution of Ukrainian scientists in the implementation of WMO initiatives may cover such areas of operational hydrology as: a) development of methods for hydrological forecasts of water and ice regimes of rivers and reservoirs; b) assessment of water balances of river basins and administrative territories; c) assessment of impact of climate change and economic activity on hydrological and hydrochemical regimes of water bodies; d) development of methods for integrated assessment of ecological status of water bodies.

However, there are gaps in the scientific support of operational hydrology in Ukraine. A rather acute problem is strengthening of professional level of young professionals who come to work in operational and scientific organizations. Specialists from operationsl organizations of the Hydrometeorological Service often do not have time to study the latest scientific achievements in hydrometeorology, and young researchers from scientific institutions need time to get acquainted with needs of operational hydrology. Therefore, we are very interested in the participation of Ukrainian young practitioners and scientists in the WMO capacity building activity.

Ukraine is interested in participating in such sections of the Action Plan as: 'guidelines on development of practical methods for assessment of hydrological data'; 'development of generic data production processes (schemes), metrics and internal guidelines (ISO 9001 like)'; 'training materials and e-learning on Quality Management Framework – Hydrology'; 'database of research needs from NHSs as a project topics repository for scientist'; 'implementation of research strategy for hydrology'.

Action area 'water resources assessment'. The assessment of natural water resources of river basins and administrative territories, as well as assessing the impact of climate change and economic activities on surface waters have a high priority in the activity of the Hydrometeorological Service. Data of these assessments are the basis for planning state measures for integrated management and protection of water resources.

Ukrainian practitioners and scientists would be able to participate in all sections of this action area of Plan. However, of particular interest to us are the following sections: 'provide for the development of methods for assessing water resources for different spatial and temporal scales'; 'related to issues of research on the assessment of water resources of transboundary river basins'; 'increased national capacities to collect water-related data and transform them to useful/relevant products through capacity building'.

Action area 'water quality'. Until 2018, the surface water quality monitoring in Ukraine was distributed among several agencies. The Hydrometeorological Service had the largest monitoring network located on natural water bodies (rivers, lakes) and river reservoirs. In 2018 the Resolution of the Government of Ukraine approved a new procedure for water monitoring of water (by water bodies) according to the methodology of the Water Framework Directive of the European Union, which led to a changing monitoring tasks between agencies. The task of monitoring chemical pollution of water bodies was assigned to the State Agency for Water Resources. At the same time, the Hydrometeorological Service has expanded the number of observation points and program in the area of hydrobiological monitoring. In addition, the Hydrometeorological Service was tasked with conducting hydromorphological monitoring on all Ukrainian rivers in accordance with the recommendations of the European Water Framework Directive.

The Hydrometeorological Service and the Agency for Water Resources are interested to participate in the following sections of Action Plan*: 'water quality training materials development', 'supporting building of national partnerships for water quality', 'supporting formulation of the National Water Quality Management Strategy, action plan and monitoring programs', 'review of state of operational monitoring, modelling and assessment of water quality at Members and basin level'. There is reason to believe that the participation of mentioned Ukrainian water – related agencies in activities of this section of the Plan will be mutually beneficial, as a lot of WMO members have accumulated significant positive experience in water quality monitoring.*

Action area 'cross-cutting issues'. Areas of activity under this section of the Plan can be called "key" in improving an efficiency of national hydrometeorological / hydrological services and operational hydrology at the national and global levels in general. In particular, the areas of action provided for in this section of the Plan will help to address the challenges currently facing the Hydrometeorological Service of Ukraine and some other Ukrainian agencies from water-related sectors of economy. These challenges include: a) needs to raise awareness of managers of water-dependent sectors of the economy about the importance of information and forecasts of the Hydrometeorological Service in the

development of sectors development programs as well as their skills to use these information and forecasts effectively; b) enhancing an efficiency of mobilization of expertise and financial resources for capacity building, technical assistance, training of personnel; c) the assistance of the Ukrainian operational hydrology community to access the global hydrological products and tools; d) the experience in developing marketing proposals for the provision of services to the private sector.

Therefore, the Hydrometeorological Service, is interested in participating in almost all activities of this section of the Plan. Ukrainian specialists can share their knowledge and experience in the process of implementing the following points of the plan: 'creation of communication materials for NHSs towards Governments'; 'guidance on managing the NHSs'; 'developing of unified communication standards for hydrological information based on definition of guidelines and regulatory material to ensure that communication is based on uptake requirements defined by end-users'. Ukrainian hydrologists, both scientists and practitioners, are interested in improving their knowledge and practical skills through a participation in the activity in the following areas of the plan: 'using the water and climate leaders group and the coalition to transport effective WMO messaging towards governments and ministries'; 'e-learning training course(s) for management of NHSs developed'; 'twinning projects targeted at management skills Management TED talks programme'; 'regional Associations hydrological activities (e.g. HydroConference in RAVI) and support to other technical symposia organized at regional level'; 'catalog of case studies of product and service development as well as marketing strategies for customers and development of process/check list, methodology to support strategic service planning of NMHSs including catalogue of products and services in response to customer requirements'; 'NHS providers have the tools to plan and construct hydrological networks that can grow/adapt as needs and resources changes'.

In order to get the maximum possible benefit from the participation in the Action plan, the Hydrometeorological Service of Ukraine should carry out a number of preparatory activities. These activities should be undertaken together with key users of hydrological products from public and private sectors, as well as from scientific and educational institutions where hydrological observations are conducted. The Hydrometeorological Service proposed to submit necessary activities in a form of the Task Program of Measures lasting up to 3 years. Other interested participants in this program have supported this proposal. The interdepartmental working group was formed to develop the Program. The Program will consist of the following principal large sections:

- *regulation actions*: an elaboration of regulation acts which regulate isuues of collaboration of the Hydrometeorological Service with other governmental agencies and organizations as well as with the private sector in the area of operational hydrology;
- *institutional arrangements:* organizational actions which should be undertaken by the Hydrometeorological Service to improve its activities in different areas of operational hydrology;
- *scientific and technological development*: actions which will strength a scientific support and technological level of all segments of hydrometeorological activities – from hydrometric measures up to providing end-users with products and services;
- *international collaboration:* actions which should be taken on national, regional and international levels to strength collaboration with other hydrometeorological services of Europe and with WMO in frames of implementation of join projects in the area of operational hydrology.

Conclusions

In order to meet further ever-increasing demands of water-related sectors of economy of Ukraine to a quality of products of the Hydrometeorological Service the present status of operational hydrology should be strengthen. The participation of the Hydrometeorological Service in the recent initiatives of the WMO will give them the good chance to significantly improve all areas of the operational hydrology in Ukraine through obtaining new expertise and skills from the international hydrological community. On other hand, Ukrainian professionals which are worked in the areas of operational hydrology will be able to present their scientific and practical experience to their colleagues from other countries. In order to benefit from participation in this activity, it is very important to properly organize the broad

participation of representatives from various Ukrainian institutions involved in the operational hydrology.

References

Lins HF (2010) The evolution of Operational Hydrology within WMO, WMO Bulletin, vol. 59 (1), pp. 40–45.

Flood Discharges Analysis at River Confluences – PROIL model

Aleksandra ILIĆ[1], Stevan PROHASKA[2]

[1] Faculty of Civil Engineering and Architecture of Uneversity of Niš, Aleksandra Medvedeva St. No. 14, Niš, Serbia, [2]Jaroslav Černi Institute for the Development of Water Resources, Jaroslava Černog St. No. 80, Belgrade, Serbia, email: aleksandra.ilic@gaf.ni.ac.rs, stevan.prohaska@jcerni.rs

Abstract

The theoretical background for determining the level of coincidence of flood discharges at river confluences is outlined in the paper. Considering the case of a river sector bounded by two model input cross-sections (of the recipient river and a tributary) and one output cross-section (of the recipient), with no major inflow from the intermediate basin, combinations of maximum annual discharges and corresponding discharges at other input/output cross sections are defined. The results of solving such a problem are lines of the same probabilities of occurrence and lines of exceedance of two random variables. Contingent on the level of coincidence, the paper proposes a practical application of the results for:

a) determining the input parameters (theoretical flood discharges of characteristic probabilities for generating the water level line at the confluence of two rivers) for economically optimal sizing of structural flood protection measures,

b) assessing statistical significance of flood waves of the recipient and the tributary.

The results of the proposed procedure are shown for the reach of the Danube River from the gauging station in Vienna to the gauging station in Bratislava, including the lower course of the Morava River. Such results are compared to one-dimensional frequency analysis which is standard method for design flood evaluation.

KEY WORDS: coincidence of flood discharges, lines of same probabilities of occurrence, exceedance probabilities, design flood discharges, return period of flood event

Introduction

When structural flood management measures are designed, it is common to determine the design river discharge based on the probability that a flood will exceed a pre-defined flood wave peak, which is equivalent to determining the return period of the flood. The calculation procedure involves a statistical analysis of hydrologic data on flood discharges at the nearest gauging station (GS). Practice has shown that such an approach is justifiable when there are not confluences along the considered river reach. Maximum flood wave ordinates (peaks) do not occur at the same time on the two rivers, but a flood wave on one can have a significant effect on the flow of the other (Bender et al, 2016). The complexity of the flood genesis and its assessment requires coupling marginal distributions of several variables in order to define a uniform distribution law, which describes the flood (Wang, 2007). In that manner, Marshal and Olkin (1988) pointed out that there was an interest for multiple probability distributions (two-dimensional with marginal probabilities as distribution parameters) for a long time. Ashkar and Aucoin (2011) highlighted that the two-dimensional models were unfairly overshadowed, that didn't show enough flexibility in selecting the marginal distributions of two analyzed variables, and that coupling variables that were differently distributed, was possible. According to them, the main objective is to choose the right model with such a correlation structure that will be representative for selected data sets.

As it is known to the authors of this paper, simultaneous flooding was first time considered in Linsley et al. (1975).

Bender et al. (2016) mentioned the first practical application of general approach to determine the joint probability of occurrence at ungauged rivers for road drainage structure design by The National Cooperative Highway Research program in Washington, USA. Also, it was pointed out that two

variables of interest at river confluences do not need to occur simultaneously especially at confluences of rivers with different catchment sizes and morphology.

It is of great importance for hydraulic structure designing to leave design methods based on single hydrological events and increase attention to multiple hydrological variables to select hydrological design event which is equal to return level of structure failure within the set of events that share the same nonexceedance joint probability (Volpi and Fiori, 2014).

Researches from Serbia carried out the study with this aim for the first time within the UNESCO International Hydrological Program (Prohaska et al., 1999).

This paper presents a methodology for the coincidence of two random variables determination, maximum and corresponding discharges of the recipient and tributary and the practical application of the proposed model in defining statistical significance of historical flood.

Data and Methods

Coincidence of two random variables

To determine the theoretical water levels within the zone of mutual influence of the recipient and the tributary, the probability of simultaneous occurrence of flood waves on the two rivers needs to be defined. These are random events on the recipient and the tributary (random variables X and Y), referred to as coincidence (Prohaska, 2006).

When two-dimensional random variables are normally distributed, the probability distribution function $f(x,y)$ (lines of same probabilities of occurrence of random variables X and Y) can be expressed as Prohaska et al. (1978):

$$f(x,y) = \frac{1}{2\pi \cdot \sigma_x \cdot \sigma_y \cdot \sqrt{1-\rho^2}} \cdot e^{-\frac{1}{2\cdot(1-\rho^2)}\left[\frac{(x-\mu_x)^2}{\sigma_x^2} - \frac{2\cdot\rho(x-\mu_x)(y-\mu_y)}{\sigma_x\cdot\sigma_y} + \frac{(y-\mu_y)^2}{\sigma_y^2}\right]}$$

(1)

where:

x, y – simultaneous occurrence of random variables X and Y, respectively;
μ_x, μ_y – mathematical expectations for X and Y;
σ_x, σ_y – standard deviations of X and Y;
ρ – correlation coefficient of X and Y.

To arrive at the distribution density, (JPDF) $f(x, y)$, the first step is to determine marginal probabilities $f(x,\bullet)$, $f(\bullet, y)$ and then their cumulative probabilities $F(x,\bullet)$, $F(\bullet, y)$.

The next step is to determine the probability of exceedance $\Phi(x, y)$ in bivariate probability space (Prohaska, Marjanović, Čabrić 1978):

$$\Phi(x,y) = \int_{t=x}^{t=+\infty}\int_{z=y}^{z=+\infty} f(t,z)dtdz = P[X > x \cap Y > y] = 1 - P[X < x \cup Y < y] =$$
$$= 1 - F(x,\bullet) - F(\bullet, y) + F(x,y)$$

(2)

Cumulative probability distribution (CDF) requires complex calculations in trivariate space, X, Y, ρ, and graphic-analytical analysis.

More details about the theoretical background for defining bivariate distribution functions and the associated graphical and analytical procedure (Abramowitz and Stegun, 1972) can be found in Prohaska et al. (1999), Prohaska and Ilić (2010), Prohaska and Ilić (2019), Ilić et al. (2021).

The correlation coefficient is adopted as the measure of dependency of two events, in this case flood wave peaks. The level of coincidence is determined via the standard correlation coefficient error using Eq. (3) (Yevjevich, 1972):

$$\sigma_R = \frac{1 - R^2}{\sqrt{N}} \tag{3}$$

where:

σ_R –   error of correlation coefficient R;

N –   total number of data points.

The criterion: $|R| \geq 3 \cdot \sigma_R$ is adopted in the present case study in order to determine level of statistical significance of the coincidence of two random variables.

Definition of variables

The analysis of the flood discharge coincidence of the recipient and the tributary is based on defining the two-dimensional distribution law for the combinations of variables shown in Table 1 (Prohaska et al., 1999).

Table 1 Combinations of variables in the case of simultaneous occurrence

River reach		Combination	Appellation
Cross-section 1	Cross-section 2		
Recipient before tributary	Recipient after tributary	max-cor	QINmax - QOUTcor1
		cor-max	QINcor1 - QOUTmax
Recipient before tributary	Tributary	max-cor	QINmax - QTRcor1
		cor-max	QINcor2 - QTRmax
Tributary	Recipient after tributary	max-cor	QTRcor2 - QOUTmax
		cor-max	QTRmax - QOUTcor2

The line of the same probabilities of the above combinations for the selected flood wave parameter (differential distribution law) and the line that defines the exceedance probability of the same combinations of variables are the result of the coincidence analysis:

$$P[X > x; Y_{cor} > y] = \int_{X_1}^{\infty} \int_{Y_1}^{\infty} g(X, Y_{cor}, R) dx dy \tag{4}$$

$$P[X > x; Y_{cor1} > y] = \int_{X_1}^{\infty} \int_{Y_1}^{\infty} g(X, Y_{cor1}, R) dx dy_{cor1} \tag{5}$$

$$P[X_{cor} > x; Y > y] = \int_{X_1}^{\infty} \int_{Y_1}^{\infty} g(X_{cor}, Y, R) dx_{cor} dy \tag{6}$$

where:

–   maximum annual flood wave peak of the recipient upstream from the mouth of the tributary X – corresponding flood wave peak of the recipient downstream from the tributary Y_{cor},

–   maximum annual flood wave peak of the recipient X – corresponding flood wave peak of the tributary Y_{cor1},

maximum annual flood wave peak of the tributary Y – corresponding flood wave peak of the recipient upstream from the tributary X_{cor}.

Theoretical flood discharges of characteristic probabilities of occurrence

In practice, the results of calculations of theoretical flood discharges of the recipient and the tributary within the zone of their confluence can be used to define:

1. theoretical water levels at a gauged confluence and
2. statistical assessment of historic flood.

Determining flood discharge coincidence at gauged confluences for sizing structural flood protection measures

The following information is needed to define design water levels at gauged confluences:

- – time-series of maximum annual discharges at input and output cross-sections, and
- – results of flood discharge coincidence calculations of the following combinations of variables:
  - o maximum annual discharge of the recipient and corresponding discharge of the tributary, and
  - o maximum annual discharge of the tributary and corresponding discharge of the recipient.

The model for determining design water levels in the sector that includes the confluence of the recipient and the tributary is shown in Fig. 1. The adopted level of flood protection corresponds to the selected probability of occurrence, p.
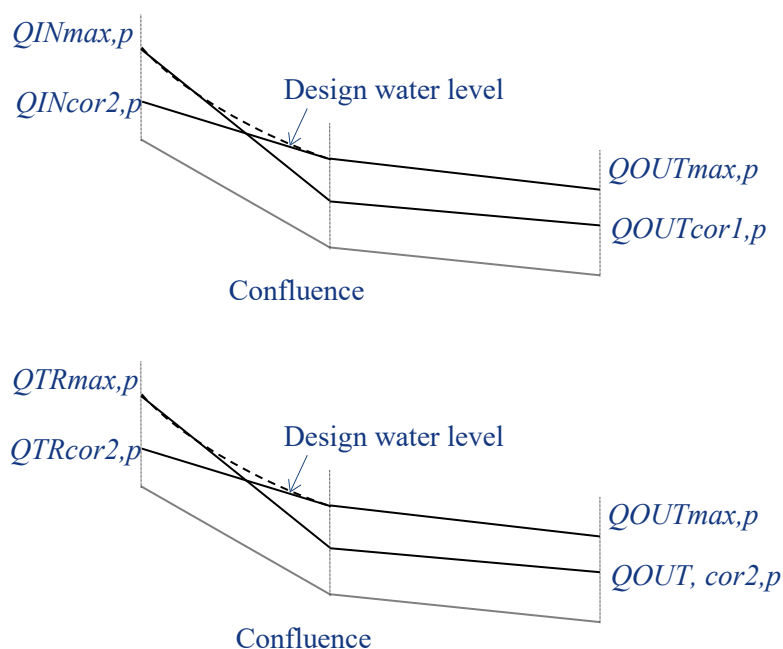
Fig.1 Schematic representation of design water level selection at a confluence

Return period assessment of flood event

Determining the return period of historical event is a measure of flood frequency (severity of flood). The procedure represents a flood assessment in multidimensional space, as a complex phenomenon. Yue and Rasmussen (2002) described in details methodology for assessing return period in the two-dimensional probability theory.

In this paper the return period of the flood in two-dimensional space is obtained like:

$T = \mu/p$, where $P[(X > x) \cap (Y > y)] = p$, and μ is a period between two adjacent members in time series.

The assessment of the return period of an event that represents a combination of two variables is determined based on the exceedance probability diagram of the corresponding combination of variables.

Results and discussion

Flood discharges of characteristic probabilities at the gauged confluence of two rivers

The sector of the Danube from input cross-sections/gauging stations at Vienna on the Danube and Moravsky Jan on the Morava, to the output cross-section/gauging station at Bratislava, is shown in Fig. 2.

Fig. 2 Extended zone of the confluence of the Danube and the Morava from GS Vienna to GS Bratislava

Structural flood management measures were designed based on theoretical discharges of various return periods at considered cross-sections, derived from the conventional procedure applied in cases of statistically significant coincidence, using time-series of maximum annual discharges from 1931 to 2006. Goodness-of-fit tests (χ^2, Kolmogorov-Smirnov and $n\omega^2$) showed that Gumbel's theoretical probability distribution function best fitted the empirical data observed at the two gauging stations on the Danube. The Log-Pearson Type 3 distribution was the best fit for the gauging station at Moravsky Jan. Table 2 shows the theoretical discharges of characteristic probabilities of occurrence.

Table 2 Theoretical maximum annual discharges of the Danube and the Morava of different probabilities of occurrence – $Q_{max, p}$ (m^3/s)

Probability (%)	The Danube		The Morava
	at Vienna	at Bratislava	at Moravsky Jan
0.1	12922	13760	2170
1	10309	10906	1541
5	8463	8890	1131

However, when defining design discharges for flood control structures design along the recipient upstream from the confluence, within the zone of mutual influence of the two rivers, values that represent derived quantities which depend on the level of coincidence of flood discharges of the Danube and the Morava need to be assessed according to Eq. (3). The optimal solution is the most probable combination of variable discharge coincidences of the Danube and the Morava, from the coincidence exceedance curve, examining the place where the flood wave rises, for the adopted return period.

In the specific case, the coincidence of flood discharges of the Danube and the Morava was estimated for the following combinations of variables:

– Maximum annual discharge at GS Vienna – corresponding discharge at GS Bratislava $\left(Q_{\max}^{Vienna}; Q_{cor1}^{Brat}\right)$

– Corresponding discharge at GS Vienna – maximum annual discharge at GS Bratislava $\left(Q_{cor1}^{Vienna}; Q_{\max}^{Brat}\right)$

– Maximum annual discharge at GS Vienna – corresponding discharge at GS Moravsky Jan $\left(Q_{\max}^{Vienna}; Q_{cor1}^{MJ}\right)$,

– Corresponding discharge at GS Vienna – maximum annual discharge at GS Moravsky Jan $\left(Q_{cor2}^{Vienna}; Q_{\max}^{MJ}\right)$,

    – Maximum annual discharge at GS Bratislava – corresponding discharge at GS Moravsky Jan $\left(Q_{\max}^{Brat}; Q_{cor2}^{MJ}\right)$,

91

– Corresponding discharge at GS Bratislava – maximum annual discharge at GS Moravsky Jan $\left(Q_{cor2}^{Brat}; Q_{max}^{MJ}\right)$.

The results of these calculations including lines of the same probabilities of occurrence (density function), izolines of exceedance probabilities (distribution function), and empirical points are graphically represented in Fig. 3.

To assess the statistical significance of the calculated variable coincidences of flood discharges of the Danube and the Morava, Table 3 shows the main indicators of the established coincidence correlations – Pearson correlation coefficient and standard error.

Table 3 Statistical significance of the considered combinations of variables

GS	Combinations of variables	R	N	σ	3σ	Statistical significance
Vienna – Bratislava	max – cor	0.92648	76	0.016247	0.04874	YES
	cor – max	0.90409	76	0.020948	0.062844	YES
Vienna – Moravsky Jan	max – cor	−0.12899	76	0.112799	0.338398	NO
	cor – max	0.20391	76	0.109938	0.329815	NO
Moravsky Jan – Bratislava	cor – max	0.02115	77	0.11391	0.341729	NO
	max –cor	0.18261	84	0.105471	0.316412	NO

The results lead to the conclusion that there is no statistically significant coincidence between the combinations of annual discharges of the tributary at GS Moravsky Jan and the corresponding discharges of the recipient at GS Vienna and GS Bratislava, but that there is statistical significance among all the combinations of discharges at the upstream (Vienna) and downstream (Bratislava) gauging stations on the recipient. None of the combinations of maximum annual discharges of the recipient (at either Vienna or Bratislava) and the corresponding discharges of the tributary is statistically significant.

The values listed in Table 3 corroborate the validity of the proposed method for calculating flood discharge coincidences in the extended area of the confluence of the Morava and the Danube.

a)   *b)*

c)

d)

e)

f)
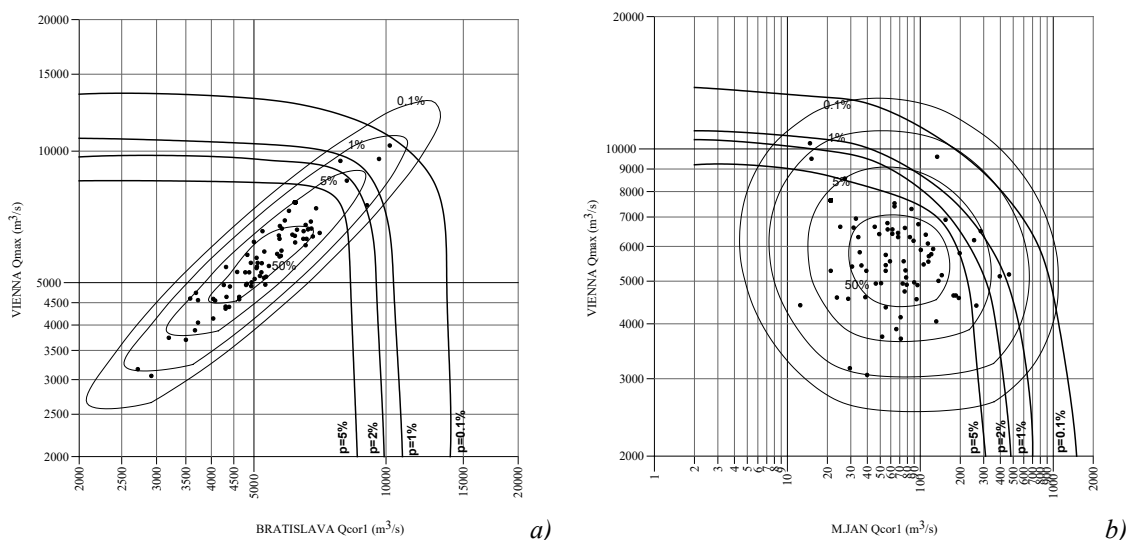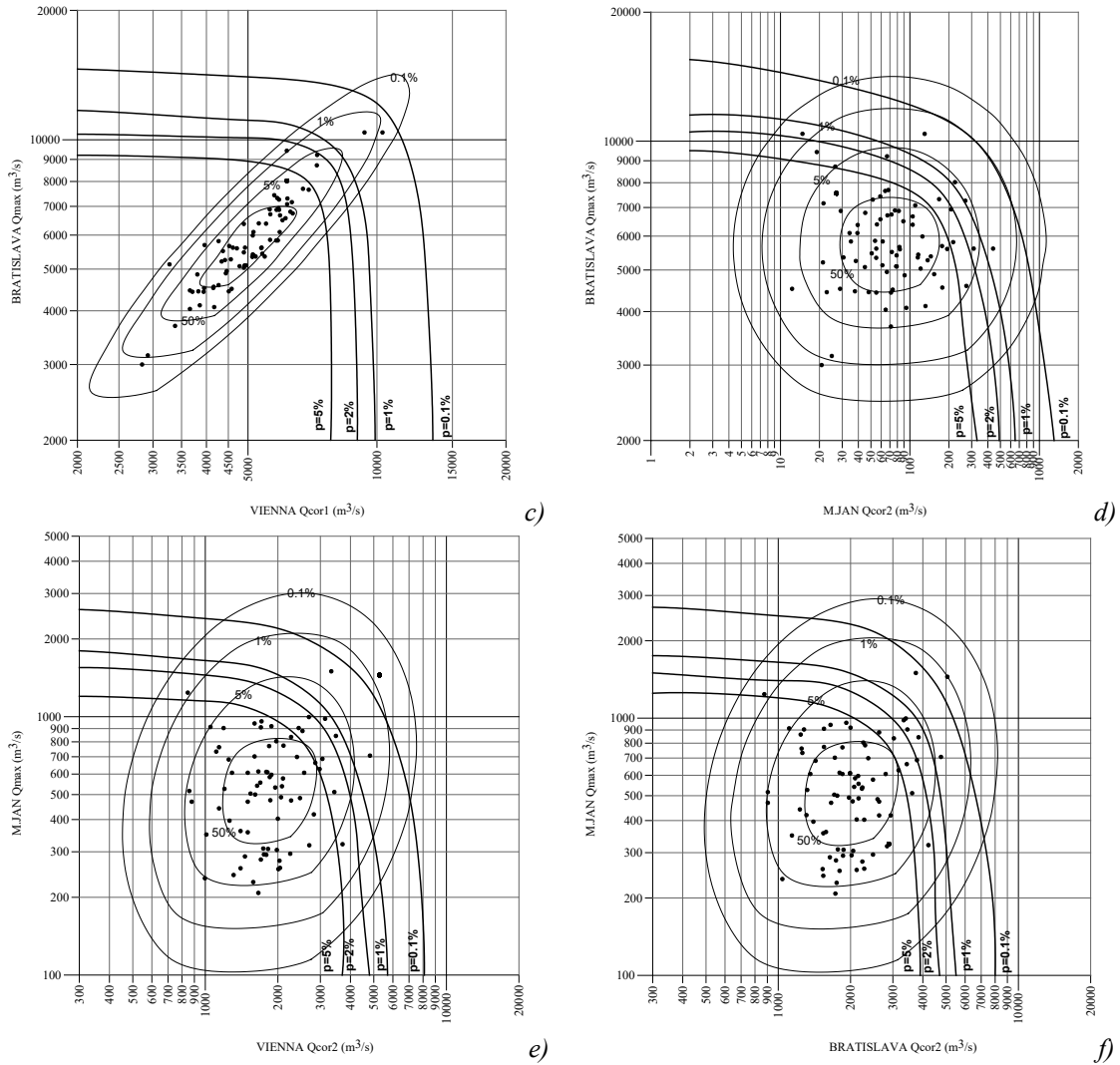
Fig. 3 Coincidence of variables in the case of simultaneous occurrence

The theoretical discharges for the different combinations of variables are shown in Table 4.

Table 4 Theoretical discharges for different flood discharge coincidence probabilities of the Danube and the Morava

p%	Danube upstream confluence			Danube downstream confluence			Morava upstream confluence		
	Q_{max}^{Vienna}	Q_{cor1}^{Brat}	Q_{cor1}^{MJ}	Q_{max}^{Brat}	Q_{cor1}^{Vienna}	Q_{cor2}^{MJ}	Q_{max}^{MJ}	Q_{cor2}^{Brat}	Q_{cor2}^{Vienna}
0.1	12922	6000	31	13760	6500	22	2170	2500	2100
1.0	10309	5800	30	10906	6100	19	1541	1800	1700
5.0	8463	5300	28	8890	5100	16	1131	1500	1250

The theoretical discharges for determining design river stages and sizing of flood protection measures along the Danube from GS Vienna to GS Bratislava, and the Morava from GS Moravsky Jan to the confluence with the Danube, are schematically represented in Figs. 4 and 5, respectively.

GS Vienna

10309m³/s

6100m³/s

Design water level

GS Bratislava

Danube/Morava confluence

10906m³/

5800m³/s
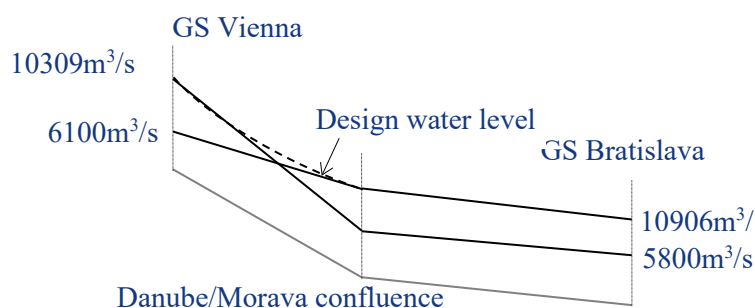
Fig. 4 Design maximum discharges for estimating 100-year water level along the considered reach of the Danube

GS Moravsky Jan

1541m³/s

19m³/s

Design water level

GS Bratislava

Danube/Morava confluence

10906m³/

1800m³/s
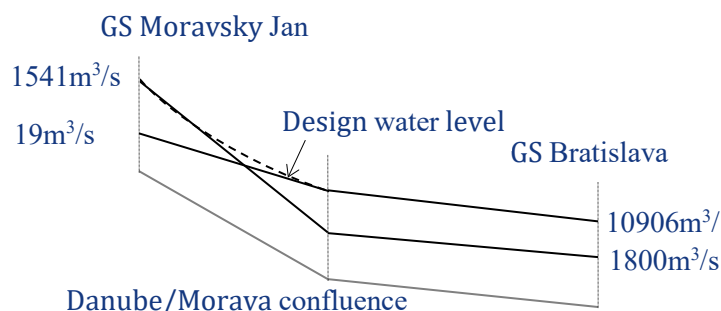
Fig. 5 Design maximum discharges for estimating 100-year water level along the Danube up to the mouth of the Morava and up the Morava to GS Moravsky Jan

For the reach of the Danube upstream from the mouth of the Morava, the 100-year water level envelope would be derived from the following combinations of discharges: $Q_{\max,1\%}^{Brat}$=10906m³/s and corresponding discharge from Fig. 5, $Q_{cor1,1\%}^{Vienna}$=6100m³/s and $Q_{\max,1\%}^{Vienna}$=10309m³/s and corresponding discharge from Fig. 4, $Q_{cor1,1\%}^{Brat}$=5800m³/s .

Assessment of statistical significance of historic floods
The return periods of the largest floods on the Danube in previous centuries occurred in September in 1899 and in July 1954 are analyzed.
The probability of exceedance of the constellation of maximum annual discharges of the Danube at Bratislava and the corresponding discharge at Vienna in 1954 is (Fig. 6):

$$P\{Q_{\max}^{Brat};Q_{cor1}^{Vienna}\} = 0.005, \text{ or } T = \frac{1}{p} = \frac{1}{0.005} = 200\text{years}$$

On the other hand, the probability of exceedance of the constellation of maximum annual discharges of the Danube at Bratislava and the corresponding discharge of the Morava at Moravsky Jan in 1954 is (Fig. 7):

$$P\{Q_{\max}^{Brat};Q_{cor2}^{MJ}\} = 0.005, \text{ or } T = \frac{1}{p} = \frac{1}{0.005} = 200\text{years}$$

It is obvious that flood in 1954 can be assessed with return period of 200 years. This flood event was assessed with return period of 80-year (Pekarova et al., 2008) by applying one-dimensional frequency analysis that is much lower than two-dimensional return period.
The probability of exceedance of the combination of maximum annual discharges of the Danube at Vienna and the corresponding discharge at Bratislava in September 1899 is (Fig. 8):

$$P\{Q_{\max}^{Vienna};Q_{cor1}^{Brat}\} = 0.003, \text{or } T = \frac{1}{p} = \frac{1}{0.003} = 300\text{years}.$$

Fig. 6 confirms that if a maximum flow at the profile in Bratislava and the corresponding discharge in Vienna occur, exceedance probability of flood is 300 years.

$$P\{Q_{\max}^{Brat}; Q_{cor1}^{Vienna}\} = 0.003, \text{ or } T = \frac{1}{p} = \frac{1}{0.003} = 300 \text{years}.$$
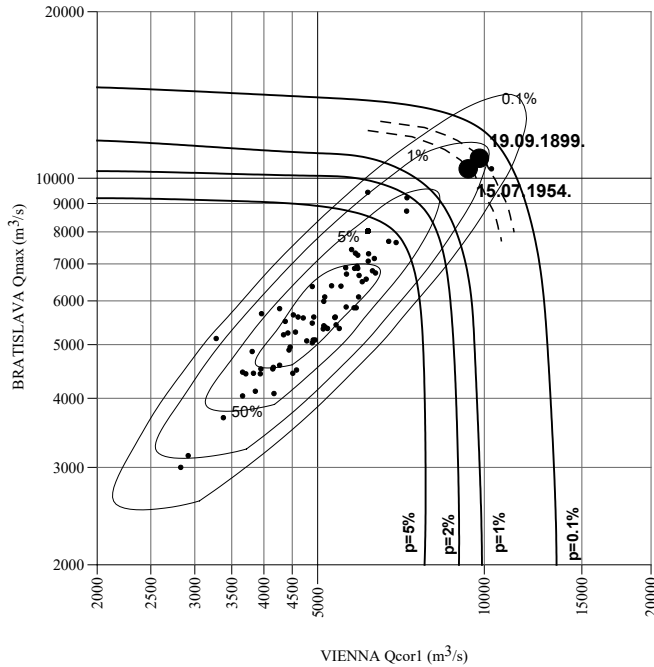

Fig. 6 Statistical significance assessment of flood events of Danube River at GS Bratislava in September 1899 and July 1954
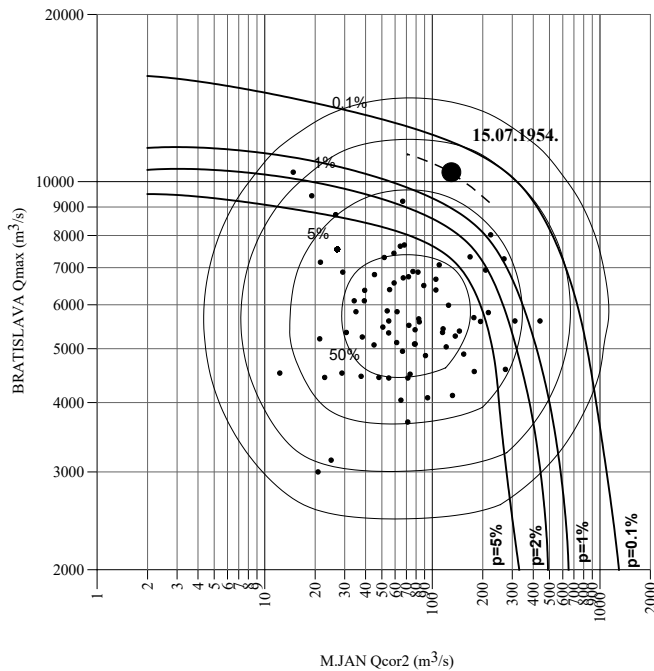

Fig. 7 Statistical significance assessment of flood event of Danube River at GS Bratislava in July 1954
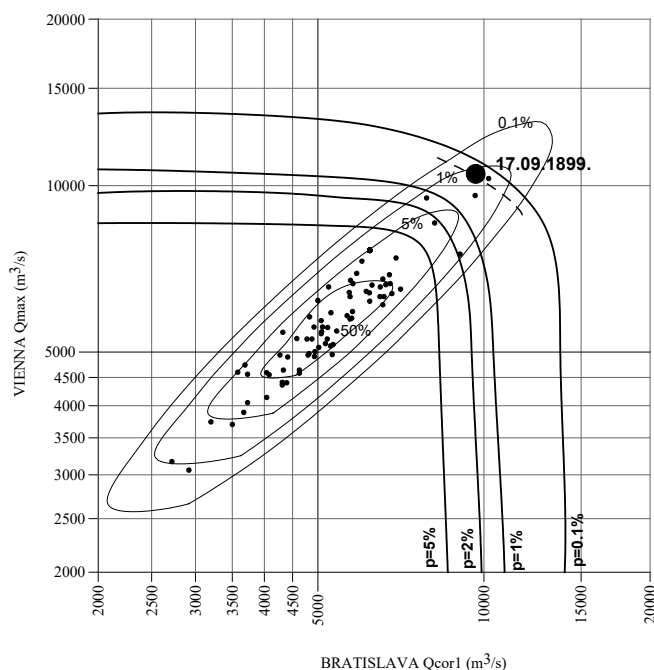
Fig. 8 Statistical significance assessment of flood event of Danube River at GS Vienna in September 1899

Conclusion

The practical significance of the coincidence analysis is that if there is no coincidence, flood control structures might be designed on the basis of design discharges that require a lower level of flood protection within the zone of mutual influence of the recipient and a tributary, relative to the conventional one-dimensional sizing procedure, while ensuring the same level of protection from a flood risk perspective. The proposed coincidence methodology provides quantitative design indicators of optimal combinations of the considered random variables, from the viewpoints of structural integrity and economics.

Since for all calculations historical data are needed, it is necessary to investigate all available sources. The authors of this paper used time-series of maximum annual discharges from 1931 to 2006 for considered stations on the Danube and Morava Rivers. The analyses will be evolved in the following period based on the recommendations from Pekarova et al. (2013).

The results of coincidence analyses can be used to assess the statistical significance of the coincidence of different flood hydrograph parameters in the extended zone of a river confluence, on both the recipient and its main tributaries.

Acknowledgment

References

Ashkar, F., Aucoin, F. (2011): A broader look at bivariate distributions applicable in Hydrology, *Journal of Hydrology*, **405** (3–4): 451–461.

Abramowitz, M., Stegun, A., I. (1972): *Handbook of Mathematical Functions with Formulas*, Graphs and Mathematical Tables, Dover Publications, INC., New York.

Bender, J., Wahl, T., Muller, A., Jensen, J. (2016): A multivariate design framework for river confluences, *Hydrological Sciences Journal*, **61**:3, 471–482.

Ilić, A., Prohaska, S., Radivojević, D., Trajković, S. (2021): Multidimensional Approaches to Calculation of Design Floods at Confluences—PROIL Model and Copulas, *Environ Model Assess*, 26, 565–579. https://doi.org/10.1007/s10666-021-09748-8.

Linsley, K., R., Kohler, A., M.,Paulhus, L., H., J. (1975): *Hydrology for Engineers*, McGrow – Hill Book Company, Inc., USA.

Pekárová, P., et al. (2008): *Hydrologic Scenarios for teh Danube River at Bratislava*, Key Publishing in cooperation with Slovak Committee for Hydrology. ISBN 978-80-87071-51-9.

Pekárová, P., Halmová, D., Mitková, V., Miklánek, P., Pekár, J., Škoda, P. (2013): Historic flood marks and flood frequency analysis of the Danube River at Bratislava, Slovakia, *Journal of Hydrology and Hydromechanics*, **61** (4), 326–333. doi:https://doi.org/10.2478/johh-2013-0041.

Prohaska, S., Marjanović, N., Čabrić, M. (1978): *Dvoparametarsko definsanje velikih voda,* Vode Vojvodine, Novi Sad.

Prohaska S., Ilić A. (2019): Coincidence of the flood flow of the Danube River and its main tributaries. In: Pekárová, P., Miklánek, P. (Eds.) Flood regime of rivers in the Danube River basin. Follow-up volume IX of the Regional Co-operation of the Danube Countries in IHP UNESCO. IH SAS, Bratislava, p. 151–174. https://doi.org/10.31577/2019.9788089139460.

Prohaska, S., Isailović, D., Srna, P., Marčetić, I. (1999): *The Danube and its Basin – A Hydrological Monograph Follow-up volume IV*, Coincidence of Flood Flow of the Danube River and its Tributaries, Regional Co-operation of the Danube Countries in the Frame of the International Hydrological Programme of UNESCO, pp 1–187, Water Research Institute Bratislava, Slovakia.

Prohaska, S., Ilic, A. (2010): *Coincidence of Flood Flow of the Danube River and Its Tributaries*, (In: Mitja Brilly (Ed.): Hydrological Processes of the Danube River Basin – Perspectives from the Danubian Countries), Publisher: Springer, ISBN 978-90-481-3422-9, Book Chapter 6, p. 175–226. DOI: 10.1007/978-90-481-3423-6_6.

Volpi, E., Fiori, A. (2014): Hydraulic structures subject to bivariate hydrological loads: Return period, design and risk assessment, *Water Resources Research*, **50**, 885–897, doi: 10.1002/2013WR014214.

Wang, C. (2007) *A joint probability approach for the confluence flood frequency analysis*. Retrospective Theses and Dissertations. 14865. https://lib.dr.iastate.edu/rtd/14865.

Yevjevich, V. (1972): *Probability and Statistics in Hydrology*; Water Resources Publications, Fort Collins, Colo. U.S.A.

Yue, S., Rasmussen P. (2002): Bivariate frequency analysis: discussion of some useful concepts in hydrological application. *Hydrological Processes*, **16**, 2881–2898, doi:10.1002/hyp.1185.

Information about authors:

Aleksandra Ilić, PhD canditate

Uneversity of Niš,PeY Faculty of Civil Engineering and Architecture, Serbia

aleksandra.ilic@gaf.ni.ac.rs

Stevan Prohaska, PhD

Institute for the Development of Water Resources „Jaroslav Černi", Belgrade, Serbia

stevan.prohaska@jcerni.rs

Dragan Radivojević, PhD

Uneversity of Niš,PeY Faculty of Civil Engineering and Architecture, Serbia

dragan.radivojevic@gaf.ni.ac.rs

Slaviša Trajković

Uneversity of Niš,PeY Faculty of Civil Engineering and Architecture, Serbia

slavisa.trajkovic@gaf.ni.ac.rs

Slaviša Trajković

Topic 3

New developments in hydrological forecasting and enabling hydrological work in the Danube catchment

Possibilities of controlling the storage function of the reservoir using a combination of dispatching graphs and a prediction model.

Matej HON [1], Tomas KOZEL[2]

[1,2] Institute of Landscape Water Management, Faculty of Civil Engineering, University of Technology, Veveří 331/95 Brno, 602 00 Czech Republic, email: Matej.Hon@vutbr.cz, email: kozel.t@fce.vutbr.cz

Abstract

The control described in the article examines the possibilities of using a combination of prediction models and the method of dispatching graphs. Based on the forecast, controlled water outflows from the reservoir are adjusted. The controlled outflows are given by individual stages of control by the method of dispatching graphs. The method itself was applied to the Vranov reservoir on the river Dyje (Czech Republic). In the application of the above mentioned procedure, better results of the selected criteria were achieved when using a combination of forecast and dispatching graphs than when using the dispatching graphs themselves.

Introduction

In the years 2016–2019, the territory of the Czech Republic was affected by a long and significant drought, which had a great impact on the water levels of the river network and the groundwater level. Flows in most of the observed specific profiles fell well below the drought limit. An exception was the profiles under the reservoirs, where the flows at the boundary of the hydrological drought were improved by the reservoirs. During the long drought the values of storage volumes were completely depleted or significantly dropped. In the case of the Vranov reservoir, extraordinary manipulation took place in the autumn of 2018, which was not ended until the spring of 2019.

In the Czech Republic, dispatching graphs are used to control the storage function of the reservoir (Broža, 1983). The dispatching graphs themselves are a very effective tool for controlling the storage function of the reservoir if there is a relatively regular hydrological cycle at the inflows to the reservoir. The second problematic aspect is that at the time of the design of the storage volumes of the tanks, it was based on significantly higher values of the long-term average flow Q_a than is stated today on the basis of recalculation by extending the real series.

The proposed procedure in the article is based on dispatching graphs taken from the Vranov reservoir handling rules (Vranov, 2013) and a deterministic prediction model based on a fuzzy learned model and bands of expected future occurrences of flows (Kozel and Starý, 2021). Based on the results of the prediction model, controlled water outflows from the tank will be adjusted.

Methods

As mentioned in the introduction, the control model is based on a combination of dispatching graphs compiled on a real series and a prediction model. The procedure itself is considered in a monthly step. Figure 1 shows a diagram of the control model.

B)

Water level ⎯⎯⎯⎯⎯⎯⎯⟶ Dispatcher graph ⎯⎯⎯⟶ Control of water level

Prediction of the future flow
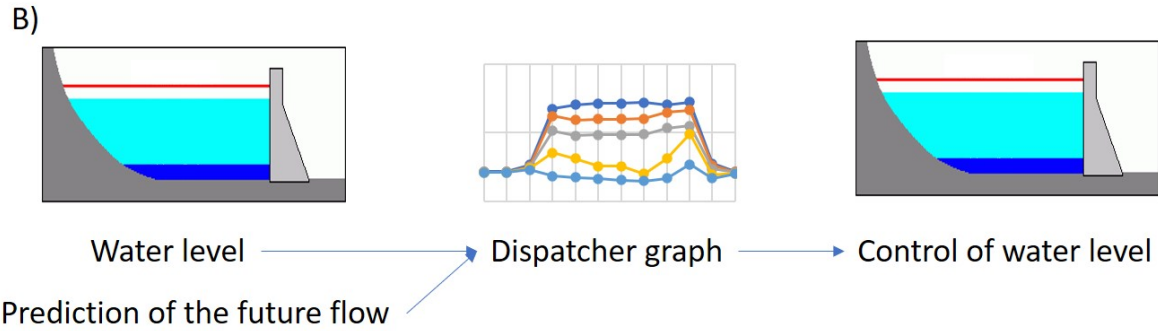
Fig. 1 Schema of proposed method.

The control module itself consists of a prediction model that provides a prediction vector $\boldsymbol{Q}$ (real inflows are replaced by predictions) and its own control algorithm. The algorithm at the beginning of each control step determines the degree (band) of the dispatching graph based on the value of the storage volume at the beginning of the step. The DG level determines the value of the controlled outflow of water from the reservoir. Subsequently, a control simulation is performed, which uses the equation of the reservoir in differential form (Equation 1) and checks whether the values of the storage volume do not deviate from the interval of the allowed occurrence of its values (V_{min}, V_{max}). At the end of the time step of simulation, the value of the storage volume is determined and the DG level is determined. If the prediction vector is longer than 1, the controlled outflows for other members are considered from the DG level determined at the beginning of the calculation step. Script an indicates the number of the current DG control level. If the DG stage is one lower, the algorithm reduces the outflow value O^1 subtracted from the current value O^1_a stage by 20% of the difference between the current outflow value O^1_a and the lower stage value O^1_{a-1}. If the DG level is reached lower by more than one degree, the outflow value is the average between the current value and the value one degree lower. If a higher stage is reached, the outflow value is increased by 20% of the difference between the value of the current stage and the stage by one higher O^1_{a+1}. If the stage at the end of the procedure is the same as at the beginning, the outflow is left unchanged. More in Table 1, which shows the rules of change.

Tab. 1 Evaluating of controled outflow.

DG current level – DG level on simulation end	Control outflow O^1
−2 a méně	$O^1 = (O^1_a + O^1_{a-1})/2$
−1	$O^1 = O_1{}^a − (O^1_a − O^1_{a-1})/5$
0	$O^1 = O^1_a$
1 a více	$O^1 = O^1_a + (O^1_{a+1} − O^1_a)/5$

When controlling the storage function of the reservoir, the values of the controlled outflows of water from the tank O^τ are unknown, where τ indicates the time step from one to N (size of the prediction vector). During the procedure itself, the value of the volume at the end of step τ must still be checked throughout the solution, because the volume of water in the tank cannot be negative. The check is performed by the reservoir equation ,

$$Q^\tau - O^\tau = \frac{V^\tau - V^{\tau-1}}{\Delta t} \quad (1)$$

where $V^{\tau-1}$ is the volume of water in the tank at the beginning of the respective time step and for the time step $\tau = 1$ the initial condition is V^0. The members of the series O^τ for $\tau = 1,2, .., N$ can take infinitely many values which depends on the filling of the tank and the method of controlling the outflow of water

from the tank. The initial volume of water in the tank V^0 is replaced by the volume obtained by measurement during control in real operation. In the simulation, V^0 for repeated calculation is replaced by V^1 from the previous calculation.

Prediction model

The prediction model itself works on the basis of a combination of a learned fuzzy model and the historical behavior of the flow series (Kozel and Stary, 2021), where the historical waveforms themselves are classified into zones based on the values of the current month. The flow zone is determined according to the last measured value. The fuzzy model itself is taught only on the data of the given zone. The inputs to the learned fuzzy model are the last two measured flow values and the output is a recurrent series of predicted flows.

Application

Fig. 2 Position of Vranov reservoir.

The Vranov reservoir was chosen for the application of the method described above. The reservoir was selected on the basis of data availability and the problems it faced during the 2016–2019 drought. The position of the reservoir is shown in Figure 2. The values of controlled outflows were taken from the handling rules of the Vranov reservoir and are given in Table 2 (Vranov, 2013). The values of targeted outflows themselves consist of the values of consumption and expected evaporation losses.

The real series of water inflows into the reservoir itself was created by the sum of average monthly flows in the profiles of Podhradí (river Dyje) and Vysočany (river Želetavka). The long-term average flow for the specific profile Podhradí is 8 m³/s and for the profile Vysočany is 0.6 m³/s. After summing the two inflows, the long-term average flow Q_a is obtained (8.6 m³/s). The average annual value of O_p is 7.12 m³/s. The storage volume of the Vranov reservoir is 78,900,000 m³.

The period 1922–2003 was chosen for the calibration of the prediction model. This period was gradually extended by the years already passed from the point of view of management in the validation period. The procedure described above is commonly used in practice, where all available data are used to achieve quality results.

The aim of the procedure is to achieve shallow and long failures (limitation of water supply for customers), which generally have a significantly smaller impact on water customers than in the case of

short and deep failures (need to stop production, stop drinking water supply to the public network, non-compliance with minimum residual outflow). With regard to the previous view of the target procedure, the criterion π was chosen to assess the success of the procedure, where the criterion itself is calculated according to the equation:

$$\pi = \sum_{i=1}^{N}(O_i - O^1{}_i)^2 \quad (2)$$

Where N is the total number of months in the evaluated period and i are the individual months.

This criterion was chosen with regard to its feature, which meets the requirements for the implementation of long and shallow failures. During the calibration of the second part of the method (changes in the prescribed outflow according to the degree of DG regulation), the period 1922–2003 was chosen. For this part of the calibration, the predictions were replaced by sections from the real series (100% forecast). The prediction model is not able to make a 100% prediction, and therefore the calibration was performed on three sets of inflows. The individual sets were represented by real inflows, real inflows reduced by 25% and real inflows overestimated by 25%. The above sets simulated a possible trend of the prediction model. The values of the achieved criteria for the different sets of inflows and the settings of the changes of the controlled outflow were then evaluated. In general, the best results were obtained for the settings listed in Table 1. Figure 3 shows that both methods (DG, DG + forecast) achieved very similar management processes.
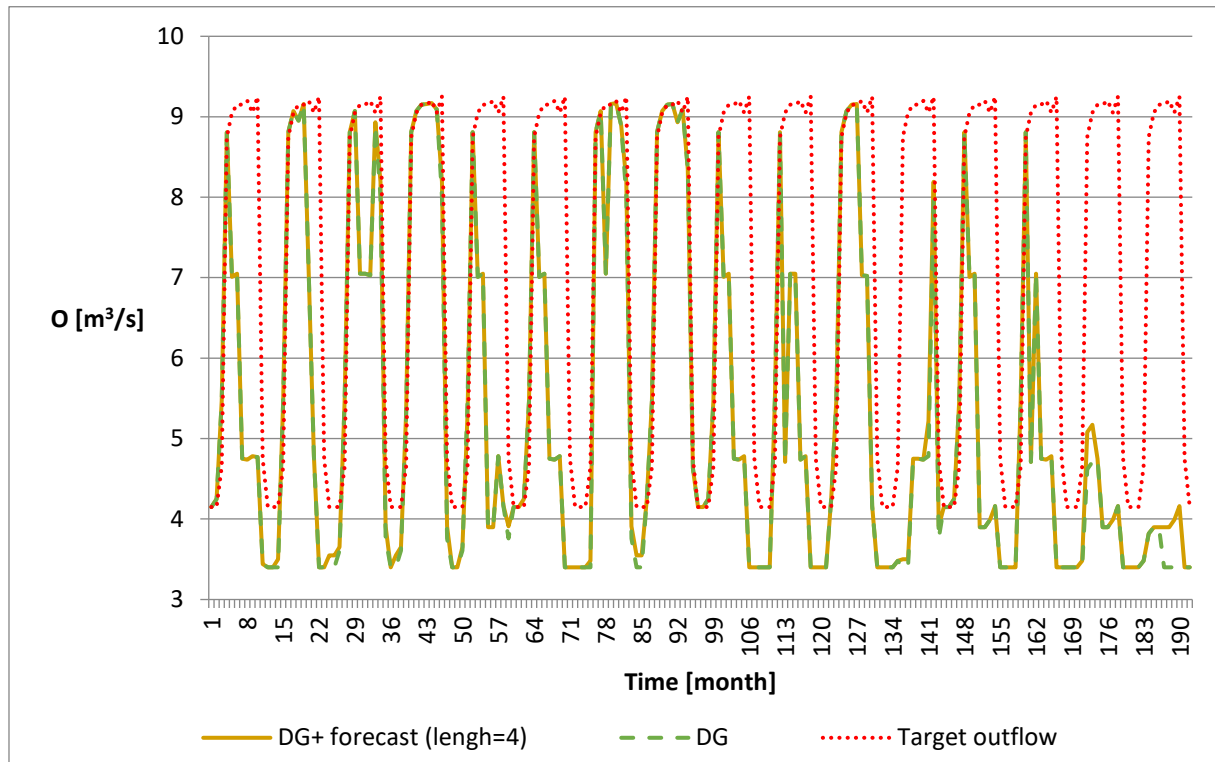
Fig. 3 Results of DG method, DG + forecast and target outflow during validation period.

The method was further tested for the validation period in the years 2004–2018. Different lengths of predictions were tested as part of the validation. Table 3 shows the achieved values of the criterion π, for individual combinations of the DG method and predictions as well as the DG method itself

Tab. 2 Results of criterion π for both methods.

Control method	π (m³s⁻²)
DG + fuzzy forecast model (length =1)	1125.95
DG + fuzzy forecast model (length =2)	1132.62

DG + fuzzy forecast model (length =3)	1129.99
DG + fuzzy forecast model (lenght = 4, the best))	1121.91
DG + fuzzy forecast model (lenght = 5)	1129.41
DG + fuzzy forecast model (lenght = 6)	1136.39
DG + fuzzy forecast model (lenght = 7)	1139.42
DG + fuzzy forecast model (lenght = 8)	1147.88
DG + fuzzy forecast model (lenght = 9)	1134.24
DG + fuzzy forecast model (lenght = 10)	1140.59
DG + fuzzy forecast model (lenght = 11)	1159.98
DG	1409.51

Results

From the above results, it is clear that the combination of a quality prediction model and the DG method is able to achieve good results. The best results of the criterion π were achieved for the length of the forecast of 4 months. On the contrary, the worst results of the criterion were achieved for the length of the forecast of 11 months. As the length of the prediction increases, so does its entropy. For this reason, the accuracy of the forecast decreases and at some point the inaccuracy of the forecast outweighs the benefit of the forecast length for controlling reservoir. In the case of a shorter forecast, the time for possibility change of controlled outflows is reduced. The results of the combination achieved better results than controlling provide with the DG method.

Thanks to the use of a prediction model, the control is able to react earlier to the occurrence of long and dry periods of implementation of the reduction of controlled outflows listed in Table 1. Conversely, information provided by the prediction model may lead to earlier termination (mitigation) of the introduced failure. The combination of the DG method and prediction can be an effective tool for controlling the storage function of reservoir for long and shallow periods. With a regular cycle of water inflows into the reservoir, the DG method has proven its qualities and, due to its simplicity, proves to be a very suitable tool for controlling the storage function of the reservoir.

Acknowledgement

Reference

Broža V., 1981: Metodické návody k vodohospodářským řešením nádrží, ČVUT v Praze, Praha, 1981

Manipulační řád pro VD Vranov, 2013, s. 1–77.

Kozel T., Stary M., 2021: Adaptive management of the storage function for a large reservoir using learned fuzzy models, Water Resources,Pleiades Publishing, Ltd. ISSN PRINT: 0097-8078, ISSN ONLINE: 1608-344X.

WEB.BM – Introducing a new tool and a new paradigm for using optimization to revise reservoir operating rules and improve real time operation

Nesa ILICH[1], Jovan DESPOTOVIC[2]

1 Optimal Solutions Ltd., Calgary, Canada, Corresponding author: nilich@optimal-solutions-ltd.com, 2 National IHP UNESCO Com., Faculty of Civil Engineering, Belgrae, Serbia, ihp.unesco.rs@grf.bg.ac.rs

Abstract

This paper introduces a new web-based modeling tool for multi-purpose multi-reservoir river basin management. The main model features include basin optimization over single or multiple time steps, flexible time step length, and optional use of reservoir and hydrologic channel routing built as LP constraints. WEB.BM includes the most common river basin management components and constraints such as reservoirs, hydro power, environmental flow targets, return flows from irrigation, diversion volume licenses, apportionment agreements between neighboring states and net-evaporation. The model is created using .NET Core technology with MS SQL database and Google Maps interface. It is accessible free of charge at www.riverbasinmanagement.com as a planning tool or a short-term operational model where runoff forecasts are available. The priority among different users is represented by a proper selection of weight factors which are user defined. So far, the model has been used in Western Canada, India and Serbia. The paper describes the process of building input data, conducting long term reservoir optimization to help revised reservoir operating rules, and inspects the implementation of these revised rules in an environment where runoff forecasts of up to 4 weeks are combined with using optimization modeling to improve the real time operation. The model is demonstrated on a small system or river Uvac in Serbia that consists of three dams and their hydro power plants.
Keywords: Real Time Reservoir Operation, Reservoir Operating Zones, Multiple Time Step Optimization

[1] Senior River Basin Modelling Consultant, Optimal Solutions Ltd., Calgary, Canada. Corresponding author. Email: nilich@optimal-solutions-ltd.com
[2] Professor (retired), University of Belgrade, Department of Civil Engineering

Introduction and Literature Review

There has probably been no other topic in water resources management that has generated more interest and more publications than river basin management modeling, or its principal component known as optimization of reservoir operation, since without reservoirs, the basin management options are severely curtailed and reduced to using water only when it is naturally available in sufficient quantities. There are literally hundreds of papers published in the last three decades related to the topic of "optimizing reservoir operation", which typically examine the performance of various heuristic search engines. A literal flood of those publications has created a deceptive image that these solution techniques are somehow better than Linear Programming (LP), while those who are familiar with mathematical optimization know that LP is the only solution technique that guarantees to find the global optimum. What helped proliferate this situation is the lack of real-world benchmark test problems which the new models should be subjected to getting a green light for publication. Without such benchmarks, the proliferation of the heuristic solvers has centered on very simple test problems that date back to 1974 (Chow and Cortes-Rivera) and 1979 (Murray and Yakowitz) that used hydro power optimization as an example, without ever calculating hydro power as part of the objective function, but rather by equating

the flows through the turbines to generated power, while also disregarding the evaporation constraints and assuming fixed turbine flow limits without relating them to the reservoir levels. These gross simplifications in assumptions are still used in numerous recent publications, thus making such model solutions practically useless. Yet, they are routinely being approved for publication in various reputable journals. As a representation of the otherwise huge sample of similar works, we include Asadieh and Afshar (2019) that applied the Charged System Search algorithm, or Ehteram et al. (2017) that used the Shark algorithm. These papers routinely test their ideas on a single reservoir problem with no more than two users, without any real-world constraints. Some of these publications are truly entertaining, like for example Samadi-Koucheksaraee et al (2019), claiming that their heuristic solvers managed to produce a solution of better quality than the LP based solution that was also included in the testing, without offering an explanation how that was possible! One cannot help but wonder how such lapses were possible with four joint authors, along with the editors and reviewers that allowed the publication of their paper. To make matters worse, this is a widespread problem when one realizes that one of the co-authors of this paper has over 100 similar publications throughout the scientific literature!

The other major source of distraction when it comes to reservoir optimization is the focus on the so-called multi-objective optimization (Reddy and Kumar, 2006), which favours the development of a multitude of solutions that are referred to as „pareto-optimal", implying some sort of equal distribution of priorities typically among only two stakeholders. This approach has a huge popularity in academia, but its application to real time reservoir operation has not yet been demonstrated. How can a multitude of solutions that are "pareto optimal" help the reservoir operator decide on how much storage to release at a given point in time? In the real world, the dams are built with specific goals in mind, where the priorities have been clearly established before the dam was built, i.e. it is either an irrigation supply dam with hydro power begin produced as a by-product of releases for irrigation, or the main function of the reservoir is to produce hydro power and all other stakeholders need to conform to the hydro power schedule, while the hydro power operators have to observe certain minimum releases related to biological or drinking water requirements.

In an environment where there are no respectable benchmark tests, everyone seems to favor their own solution techniques and make claims that those are superior to others, including the supporters of the old style simulation approach, such as Sulis and Sechi (2013). The authors of this paper have made several unsuccessful attempts to verify the claims made by Sulis and Sechi (2013) as well as the other authors that favor the use of heuristic solvers by asking that the input data and the model results be shared for further research collaboration, without ever received an answer. This shows a dismal picture of the current stated of the art in academia, although the more recent review papers by Rani and Moreira (2010) as well as Dobson et al. (2019) still seem to paint a rosy outlook. The latter also use an oversimplified test case at the end of their paper that leaves a lot to be desired when compared to the needs of the practitioners that deal with the real-world problems. One positive thing about the work of Dobson et al. (2019) is that they define the importance of developing the so-called multiple time step optimization (MTO) capabilities that are discussed in more detail in this paper.

Contrary to the efforts in academia that are focused on the heuristic solvers and multi-objective optimization, the models that have gained acceptance and popularity among practitioners are all based on LP. They include MODSIM (Colorado State University, 2021), REALM (Victoria State Government, 2021), or WEAP (Yates et al, 2005), all of which use some form of a "Network Flow Algorithm" (NFA) which is a Primal-Dual algorithm based on the theory of Linear Programming. NFAs are limited to modeling fixed bounds of the flow limits, and thus are unable to properly address dynamic constraints that may exist on reservoir outflows, return flow channels which are a function of consumptive use, or turbine flow capacities being dependent on storage. This limitation has been removed by the use of commercial LP solvers in models such as RiverWare (Zagona et al, 2001), Oasis (Randall et al, 1997) or the WEB.BM (2021) model presented in this paper. These are also the only LP based models that can handle multiple time step optimization, while the WEB.BM is the only one of them that takes the channel routing as constraints to an optimization program by using the SSARR (US Army Corps of Engineers, 2021) based channel routing procedure. Based on the above introduction, the existing situation related to the river basin optimization modeling tools could be described as follows:

  – A small number of models are widely accepted and used among practitioners, and they are almost exclusively based on LP solution techniques of some sort;
  – There are no real-world benchmark problems in the literature that could help the practitioners with model selection and comparison; and,
  – In addition to the WEB.BM, only two other models (RiverWare and OASIS) can solve multiple time step optimization problems, although they last two are unable to address the channel routing constraints properly, in spite of their steep licensing cost.

The rest of paper is structured in the following way: Section 2 explains the procedure for developing hydrologic input data; Section 3 provides an overview of the WEB.BM modeling capabilities with emphasis on the importance of combined use of multiple time step optimization and channel routing; Section 4 provides a description of the Numerical test problem on the Uvac River which is a tributary of the Drina river in Serbia, while Section 5 provides final discussion and conclusions, followed by a list of references used in the paper.

Development of Historical Natural Flows

The process of naturalizing historical flow records involves undoing the effects of regulation. This is achieved by reversing the effects of storage change and diversion from the stream by starting from the most upstream control points and by moving reach by reach in a downstream progression. For example, assuming that inflow into a reservoir comes from two streams that have their natural flows designated as Q_1 and Q_2, the natural flow at the downstream reservoir R can be calculated by using the following expression:

$$Q_R = Q_1 + Q_2 + LR \tag{1}$$

Where the term LR represents local runoff from a sub-catchment delineated by locations where natural flows Q_1 and Q_2 are known and the downstream point of interest (in this case a reservoir). The term LR is calculated by using:

$$LR = \sum_{i=1}^{m} Q_i - \sum_{j=1}^{n} Q_j + \frac{\Delta V}{\Delta t} \tag{2}$$

where:

  Q_i average outflows (i=1,m) from a sub catchment within time step t
  Q_j average inflows (i=1,m) into a sub catchment within time step t

  $\Delta V/\Delta t$ total storage change within the sub-catchment over duration of step t (Δt)

Figure 1 shows an example of calculating natural flows for reservoir sites 1 and 2, with the explicit addition of the net evaporation term (NE) which is considered to be part of the storage change in general expression (2) above.
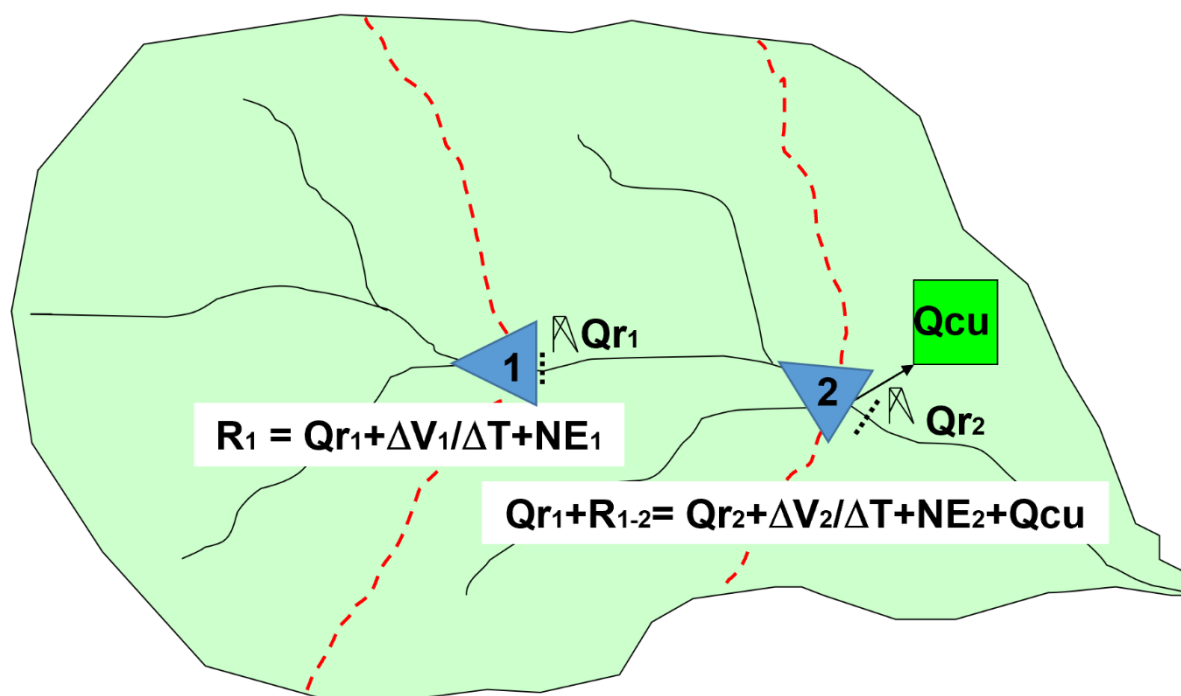
Figure 1 Example of Natural Flow Calculations

The natural flow into reservoir 1 is given by the formula for R_1 (representing runoff at the site of Reservoir 1). The total natural runoff at the site of Reservoir 2 is then sum of R_1 and R_{1-2}, where R_{1-2} represents the runoff from the intermediate catchment between the two reservoirs that can be calculated using the water balance expression associated with Reservoir 2. This approach can be applied only on gauged basins where storage change, inflows into and out of each sub-catchment areas are based on the flow records. While many river basins have sufficient information to enable this kind of assessment, the old approach to resort to rainfall-runoff modelling so as to estimate the available runoff is unfortunately still dominant. Rainfall-runoff modelling should not be used as a way to assess natural flows in gauged basins, since the simulated runoff usually shows huge discrepancies in the validation stage when compared to the historic flow records. Once the historic runoff series have been estimated properly, the initial model setup should involve the execution of the so called "verification" scenario, which should repeat the historic reservoir levels by balancing the runoff estimates with net evaporation and historically recorded outflows from the reservoir.

Section 3. WEB.BM Modeling Capabilities

WEB.BM is built around the public domain LP solver provided by the COIN-OR library (COIN-OR, 2021). The basic model properties are listed below:

– A web-based application using the Amazon Web Services with .NET Core technology;
– MS SQL relational database for storage and retrieval of data;
– User friendly upload and download based on the use of copy and paste commands;
– Ability to provide interface for remote use of its solver to other similar DSS platforms;
– Includes Google Maps interface for schematic representation;
– Graphical and statistical analyses routines of model output;
– Ability to use the model as a planning or real time operational tool;
– Three solutions modes (single time step, multiple time step, or a combined solution mode);
– Flexible time step lengths, which can be any multiple of 1 days, or fraction of a day if hourly simulations are used;
– Free access to interested users; and,
– User's Manual and instructional videos that cover all aspects of model use.

The principal concept built into the model is to provide the definition of a project as a set of inter-connected nodes and channels. Model components can be described as "nodes" (implying that they require mass balance calculation during simulation, such as for example reservoirs, junction nodes or

consumptive use nodes), and links, which define channels (river reaches, diversion canals or return flow channels from consumptive use nodes). Each of those components can have additional functions associated with them, as shown in Table 1.

WEB.BM accepts inputs in m^3/s for inflows and water demands, mm for precipitation and evaporation, and m.a.s.l. for key reservoir elevations, while the surface area and volume coordinates for storage capacities are given respectively in hectares and 1000 m^3. One project can have one or more operating scenarios that define how the system should be operated, while the post processing routines can help evaluate the differences between different scenario outputs. The length of simulated time steps can be monthly, weekly, daily, or custom, which can represent non-standard time step lengths such as 10-daily (often used in Asia) or time steps that are shorter than one day when hourly, 3-hourly, 6-hourly or 12 hourly modelling is used, in which case the length of the time step is entered by the user as the appropriate fraction of the day. If such modelling also involves hydrologic channel routing, the time intervals must have the same length throughout the simulation.

Table 1. WEB.BM components and their functions

	Component	Available Component Functions
Nodes	Consumptive Use	Evapotranspiration loss associated with irrigation or other water use
	Junction	Mass balance for all connecting flow links (channels)
	Reservoirs	Mass balance at reservoirs
		Storage change
		Net evaporation on reservoirs
Links	River Reach	Channel flow (steady state or with hydrologic routing)
		Hydro power generation
		Apportionment agreements between bordering states
		Dynamic setting of maximum reservoir outflow as a function of storage
		Environmental flow targets (minimum and/or preferred)
	Diversion Canal	Diversion flows from the stream with canal capacity limits
		Diversion license limits
		Hydro power generation
		Dynamic setting of maximum flow limits on diversion flows when used as outlets from Reservoirs or in relation to flows in another river reach or a diversion canal
	Return Flow Channels	Dynamic setting of return flows as percentage of consumptive use of the upstream consumptive use nodes. It can be unique for each time step.

An optimization problem in river basin management models is typically defied as a search for the best set of flow distribution that minimize or maximize the sum product of flows and their respective weight factors, which represent the value attached to water by river basin managers. The other way to look at the weight factors is as "parameters that define priority of allocation". The minimization form of the objective function is typically referred to as goal-programming, where the goal is to minimize te deficits defined as the difference between the required allotments and the achieved allocation. The same solutions can be obtained if the LP is formulated as a maximization problem defined in equation 3.

$$Max \sum_{t=1}^{m} \sum_{i=1}^{n} X_{i,t} P_i \qquad (3)$$

The terms used in the above expression are explained below:
$X_{i,t}$ is the allocated flow to component i in time step t
P_i is the weight factor associated with component i
n is the total number of model components
t is the time step index
m is the total number of time steps

Expression (3) defines optimization over m time steps simultaneously, which can be depicted graphically in Figure 2 by the carry over storage arc that connects the same storage through consecutive time intervals. This solution strategy is necessary when using daily calculation time step to optimize allocation in river basins where the total travel time is more than one day.
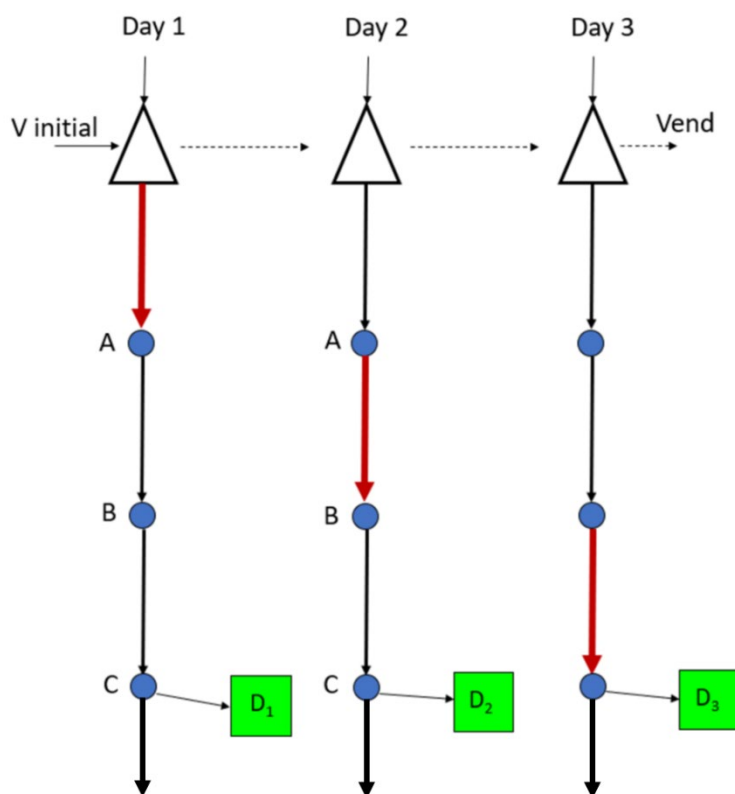
Figure 2 Graphical representation of MTO solution approach

While the MTO solution requires foreknowledge of inflows for all time steps that are included in the solution process, its advantage is that it produces the best possible solution for a given inflow sequence and starting reservoir levels at the beginning of the simulation, especially if it is combined with the equal deficit sharing constraint defined below:

$$\frac{X_{1,t+1}}{D_{1,t+1}} = \frac{X_{1,t}}{D_{1,t}} \qquad (4)$$

Where the terms D1,t and D1,t+1 refer to water demands at block D1 for two subsequent time steps. This constraint makes sure that when deficits are inevitable, they are evenly distributed throughout the

irrigation season. With this kind of constraint, the model determines both the optimal shape of the rule curve, as well as the optimal amount of demand hedging for each simulated time step, thus provided important information which can be statistically analyzed to derive better operating rules that can later be tested over assumed foreknowledge of inflows over shorter time horizons (Ilich and Basistha, 2021). It should also be noted that the above procedure should be used in real time over short-term operational horizons for which the runoff forecasts can be made available, provided that the channel routing is properly incorporated so as to account for channel storage change between the reservoir and the downstream user. Any significant change in the existing flow conditions caused by a spike in downstream water demand can be properly addressed with the joint use of the MTO solution technique that contains proper inclusion of channel routing as constraints in the optimization process. The WEB.BM manual contains two numerical examples that demonstrate the ability of the model to derive optimal solutions while taking into account proper hydrologic routing based on the SSARR routing method (US Army Corps of Engineers, 2021).

The art of selecting the weight factors P_i that will deliver a desired solution is still subject to on-going research. In the beginning, when simplistic search engines were used based on the Network Flow algorithms (Fulkerson, 1961), it was relatively easy to identify one out of infinite number of selections for factors that would result in the same flow solutions. Subsequent introduction of model constraints was making this issue more complex, as identified Israel and Lund (1999). The modelers now require careful examination of model results to ensure that the right weight factors had been selected.

The WEB.BM model can call the solver engine in three ways:
   a) To execute a Single Time Step solution (STO) which only assumes the knowledge of the runoff forecast over the duration of the current time step.
   b) To execute a Multiple Time Step (MTO) solution. This solution can be executed over individual years in sequence, or over all simulated years at once, typically by using weekly time steps.
   c) Combined STO/MTO mode, where for example an MTO solution is derived over 5 days assuming known inflow forecasts for all 5 days, but the solution is only adopted for the first day, and the next time step assumes the starting reservoir levels as the ending reservoir levels for the first day, with another MTO solution derived for the upcoming 5-day period. This solution mode can be used to test the model performance assuming historical runoff could have been predicted 5 days ahead. It also allows for the possibility of using the WE.BM optimization model as a real time reservoir operation tool.

Section 4. Uvac River Basin Case Study
The case Study includes three hydro power plants located on the River Uvac in Western Serbia. The entire process outlined in the paper is applied to demonstrate the potential improvements in generated hydro power compared to the historical operation. The operation has been tested with MTO solutions with for assumed forecasts of 1, 2, 3 and 4 weeks. The system has a short travel time of about 1 day, hence the weekly flows are not ideally suited for this study, but they were the only historical flows presently available directly from the Electrical Power Company of Serbia (the client). There is a small amount of water use from the river that has been ignored in the compilation of natural flows. Since the small withdrawals have been ignored in the development of natural flows, they can also be ignored during the model simulation. In that context, all available flows and reservoir storage are to be exclusively used for the purpose of maximizing hydro power. This can be achieved by joint maximization of flows through the turbines and well as the reservoir storage levels. While seemingly a relatively simple objective to implement, it does require both runoff forecasts and optimization capabilities, such that when incoming runoff is higher than the turbine capacities, it can be evacuated through the turbine assuming the reservoir was previously drawn down to accommodate such outflows. Note that the turbine capacities are reduced with the drop in storage levels based on the head-flow-efficiency curves provided by the client for all three hydro power plants. The Uvac River basin modelling schematic is shown in Figure 3, and the head – flow – efficiency curves are given for the turbine at reservoir Uvac in Figure 4.

Figure 3 Uvac River Basin Modeling Schematic

The first step in the process was to develop natural flows and verify them by using the Verification Scenario. In this scenario, the starting water level is equal to the historic level at the start of the simulation, which was chosen as January 1,1967. Two of the reservoirs (Bistrica and Kokin Brod) were built at that time, however the Uvac facility was added in 1979. To include the Uvac hydro power plant and reservoir storage into the Verification Scenario, the starting storage was kept at zero until 1979, implying zero storage change, and the reservoir outflows were substituted with the recorded flow station which was operated on the reservoir site before the reservoir was built. If the calculated runoff into the Uvac reservoir was correct, imposing the historic outflows should produce simulated water levels that coincide with the historic water levels for all 47 years. This is demonstrated in Figure 5.
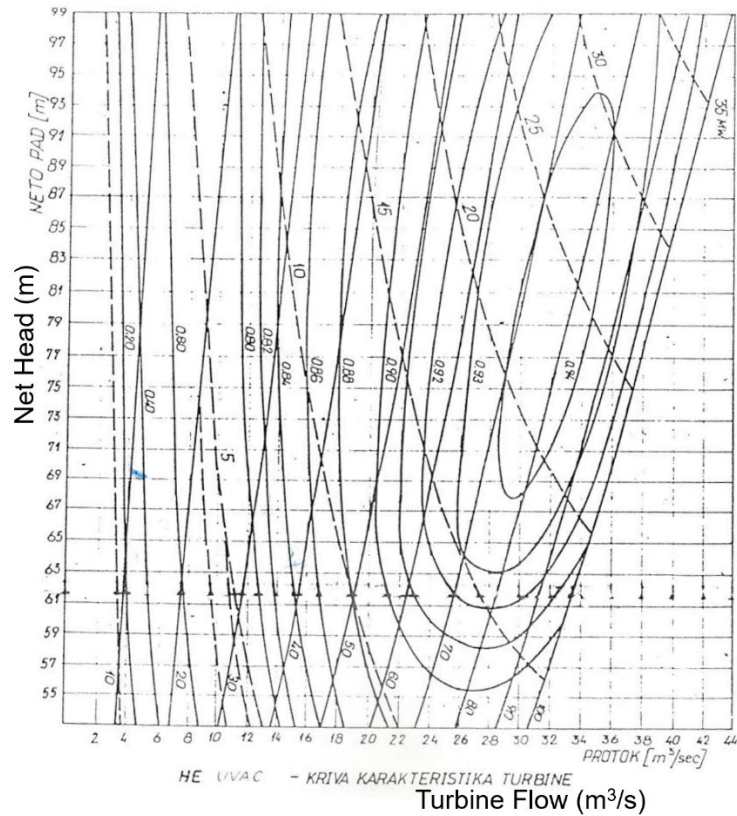
*Figure 4. Net Head – Flow – Efficiency Curve for Uvac HP*
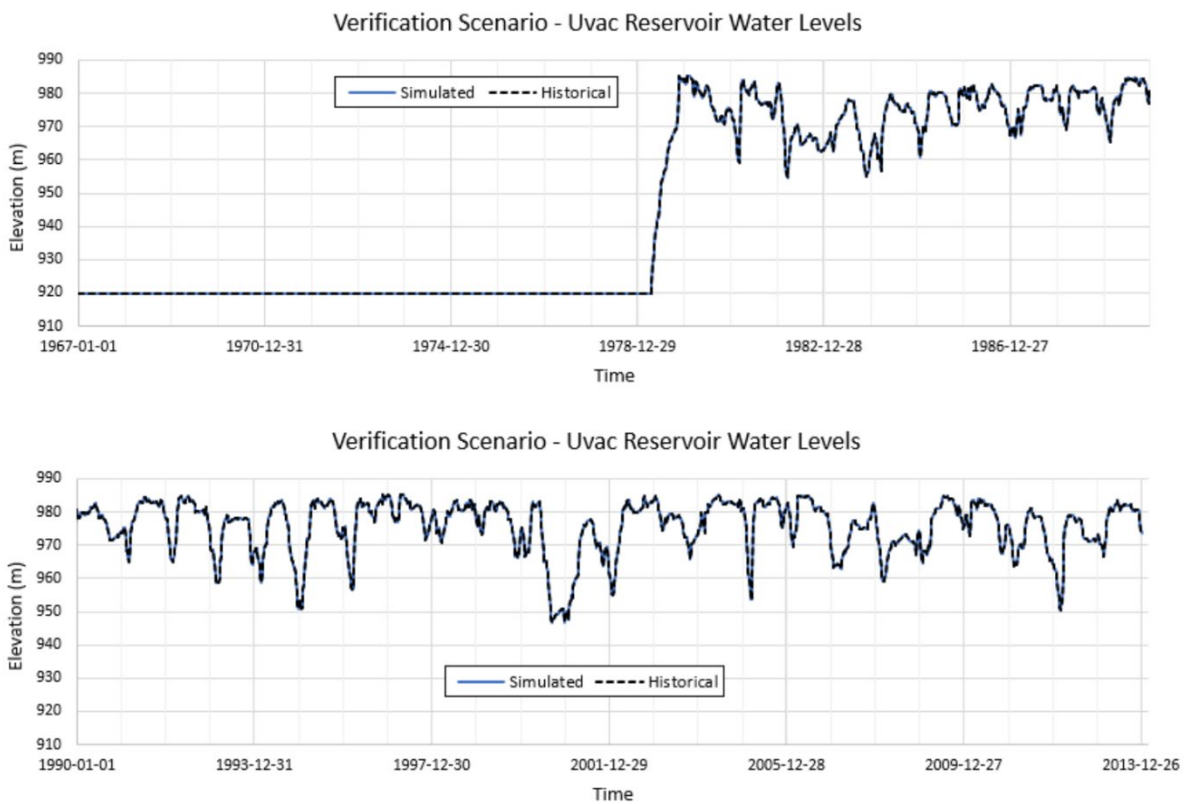
Figure 5 Simulated and historic water levels at Uvac reservoir

Similar match between the historic and simulated storage levels was also achieved for the remaining two reservoirs. The Verification Scenario also confirmed that the model produced the same hydro power

113

as the one that was recorded historically. Once the verification scenario was completed, the next step was to apply the MTO solution technique and evaluate the model outputs. The best output was obtained by setting the assumed forecast of runoff to 4 or more weeks, for which the same solutions were obtained. Reducing the length of the forecast horizon implies reduction in generated hydro power, since some spills bypassing hydro power plants become inevitable. It is interesting to compare the historic operation with the best possible model performance, which is shown for Kokin Brod reservoir in Figure 6.
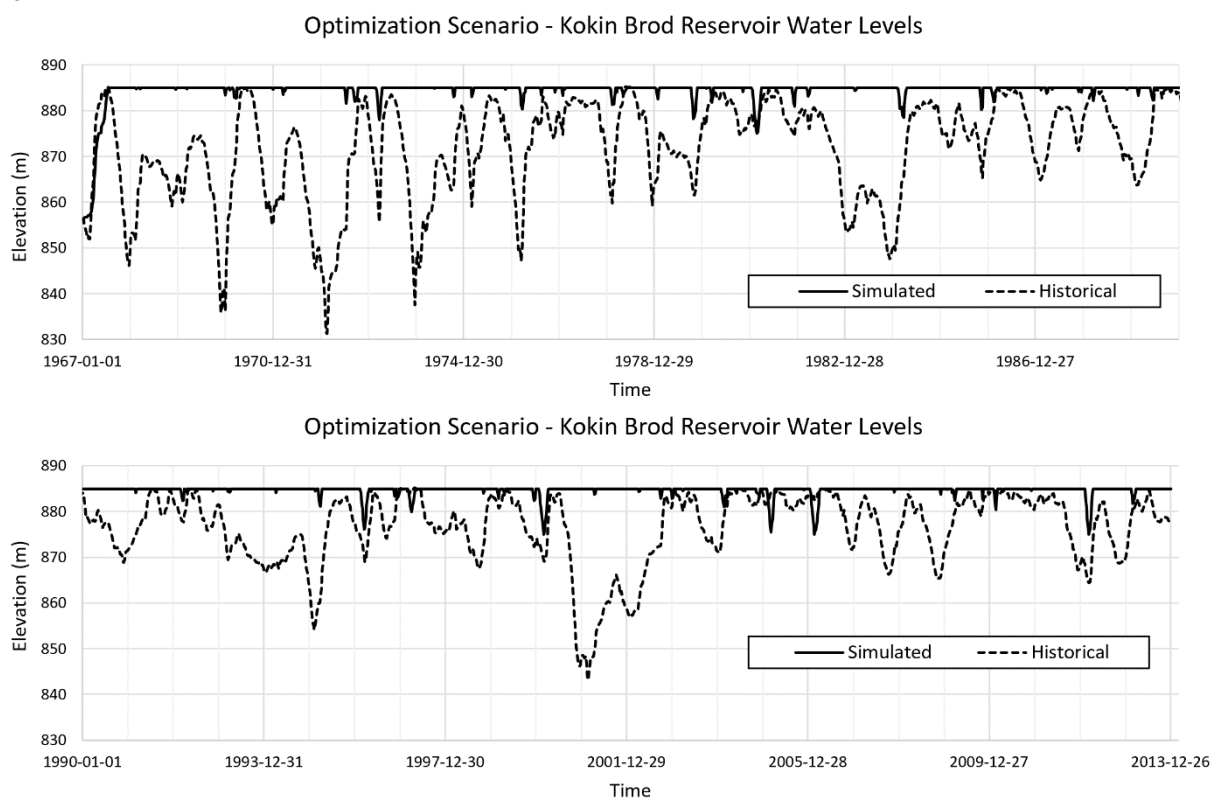
Figure 6 Historic and Optimal water levels of Kokin Brod reservoir

It is not clear why the storage at Kokin Brod reservoir was brought down historically, but the best scenario never required pre-flood drawdown of more than 10 meters, which is hardly visible on the graph (solid line) compared to the drawdowns imposed historically that go well over 40 meters. Consequently, the Kokin Brod hydro power plant shows the best possible improvement of 14% compared to the historic operation. The total generated hydro power an all three hydro power plants was assessed in terms of the length of the available forecast. The results are shown in Table 3. The production for Uvac was assessed from 1979, since that is when the hydro power plant started to operate historically, while the other two plants had their comparison on the bases of full historic flow series of 47 years (1967 – 2013).

Table 3 Mean Annual Generated Energy for all HP facilities

Hydro Power Plant	Mean Annual Generated Energy (GWh)			
	Uvac (1979–2013)	Kokin Brod (1967–2013)	Bistrica (1967–2013)	Total
Historic Generation	58.90	54.56	333.87	447.33
7 days forecast	62.89	61.15	333.05	457.09
14 days forecast	63.66	61.73	337.99	463.37
21 days forecast	64.00	61.98	342.37	468.36
>28 days forecast	64.31	62.22	352.17	478.71

Hydro Power Plant	Percent increase compared to historical operation			
	Uvac (1979–2013)	Kokin Brod (1967–2013)	Bistrica (1967–2013)	Total
Historic Generation	0.00	0.00	0.00	0.00
7 days forecast	6.79	12.07	0.00	2.18
14 days forecast	8.09	13.13	1.23	3.59
21 days forecast	8.67	13.60	2.55	4.70
>28 days forecast	9.20	14.03	5.48	7.01

Conclusions and Recommendations

This study demonstrates the use of the WEB.BM model and presents the procedure for generating and verifying the required input data. The model runs that employ optimization routines have been conducted using 1, 2, 3 and 4 weeks of the assumed forecast horizon. It is believed that more instructive results could be obtained by repeating the simulation runs with daily time steps. That would generate a more realistic relationship between the length of the forecasting time horizon and the improvements in operation. The results in Table 3 assume the use of WEB.BM as a real time operational model that would guide the reservoir operation in combination with a reliable forecasting tool. Given the results in Table 3, it is believed that future refinements of this study could demonstrate improved power output of the entire system of close to 5% compared to the average historic generation. The exact length of the required time steps cannot be ascertained without daily simulation, but is believed that it would be between 5 and 10 days. While this study demonstrates that WEB.BM can be a powerful tool for modelling hydro power generation, it also has many other options for addressing complex issues related to river basin allocation.

References

Asadieh, B. and Afshar, A., 2019. Optimization of water-supply and hydropower reservoir operation using the charged system search algorithm. *Hydrology*, **6** (1), p.5.

Chow, V. T. & Cortes-Rivera, G. (1974) Applications of DDDP in water resources planning. Water Resour. Plan. (78), Res. Rep. 78. Retrieved from http://hdl.handle.net/2142/90341.

Colorado State University. 2012. Modsim-DSS. http://modsim.engr.colostate.edu/modsim.php, last accessed April 7, 2021.

Dobson, B., T. Wagener, and F. Pianosi. 2019. An Argument-Driven Classification and Comparison of Reservoir Operation Optimization Methods. *Advances in Water Resources* **128** (October 2018): 74–86. Elsevier Ltd. doi:10.1016/j.advwatres.2019.04.012.

Ehteram, M., Karami, H., Mousavi, S.F., El-Shafie, A. and Amini, Z., 2017. Optimizing dam and reservoirs operation-based model utilizing shark algorithm approach. *Knowledge-Based Systems*, **122**, pp.26–38.

Fulkerson, D. R. (1961), An out-of-kilter method for minimal cost flow problems, *SIAM J. Appl. Math*., **9** (1), 18– 27.

Ilich N. and A. Basistha. 2021. Importance of multiple time step optimization in river basin planning and management: a case study of Damodar River basin in India. Hydrological Sciences Journal, https://doi.org/10.1080/02626667.2021.1895438.

Murray, D. M. & Yakowitz, S. J. 1979. Constrained differential dynamic programming and its application to multireservoir control. *Water Resources Research* **15** (5), 1017–1027. doi:10.1029/WR015i005p01017.

Randall, D., L. Cleland, C. S. Kuehne, G. W. Link and D. P. Sheer. (1997). Water supply planning simulation model using mixed-integer linear programming 'engine.' *Journal of Water Resources Planning and Management*, **123** (2), 116–124.

Rani D, and M. Moreira. 2010. Simulation-optimization modeling: a survey and potential application in reservoir systems operation. *Water Resources Management,* **24**:1107–1138.

Reddy, M.J. and Kumar, D.N., 2006. Optimal reservoir operation using multi-objective evolutionary algorithm. *Water Resources Management*, **20** (6), pp.861–878.

Samadi-koucheksaraee, A., Ahmadianfar, I., Bozorg-Haddad, O. and Asghari-pari, S.A., 2019. Gradient evolution optimization algorithm to optimize reservoir operation systems. *Water resources management*, **33** (2), pp.603–625.

Sulis. A and G. Sechi. 2013. Comparison of generic simulation models for water resource systems. *Environmental Modeling and Software*, Vol. **40**, p. 214–225.

Yates D, J. Sieber, D. Purkey, A. Huber-Lee. 2005. WEAP21 – A Demand-, Priority-, and Preference-Driven Water Planning Model: Part 1. *Water International,* Vol. **30** (4), 501–512.

US Army Corps of Engineers. 2021. Program Description and User Manual for SSARR – Streamflow synthesis and reservoir regulation. http://137.229.188.87/susitnadocfinder/Record/dbtw1955

Victoria State Government. 2012. Resources Allocation Model (REALM). https://www.water.vic.gov.au/water-reporting/surface-water-modelling/resource-allocation-model-realm.

WEB.BM. 2021. Web based river basin management model, www.riverbasinmanagement.com.

Zagona, E.A., T.J. Fulp, R. Shane, T. Magee and H.M. Goranflo. 2001. RiverWare: A generalized tool for complex reservoir system modeling. *Journal of the American Water Resources Association*. **37** (4), 913–929.

Comparison of simulated discharge over Ogosta river basin using ground, satellite and merged data as precipitation input for the purpose of flood forecasting

Georgy KOSHINCHANOV[1], Petko TSAREV[2]

[1] National Institute of Meteorology and Hydrology, Bulgaria, Sofia, email: georgy.koshinchanov@meteo.bg,
[2] National Institute of Meteorology and Hydrology, Bulgaria – branch Plovdiv, email: petko.tsarev@meteo.bg

Abstract

The hydrological processes are very complex and the hydrological and hydraulic models are the main components of the flood forecasting and warning systems. They identify the dominant hydrological processes, which influence water balance and result in conditions of extreme hydrological events. A variety of hydrological models (lumped, semi-distributed, distributed) exist nowadays. In this study the physically-based, fully distributed hydrological model TOPKAPI (TOPographic Kinematic APproximation and Integration) is applied. The model utilities three non-linear reservoir differential equations for the drainage in the soil, the overland flow on saturated or impervious soil, and the channel flow along the drainage network (Yordanova et.al., 2017). The model was successfully applied over two basins in Bulgaria – Ogosta river basin with attempt to include the management of big reservoir (Yordanova, Stoyanova, 2020), and Aytoska river basin with meteorological stations outside of the watershed (Yordanova, Stoyanova, 2020).
The precipitation has high spatial variability especially in convective events. The conventional methods of measuring the precipitation is using rain-gauges, which are sometimes more than 30 km from one another. Thus it is of great importance to have precipitation in denser points especially in convective events as the one, which will be presented in this study (01–03 June 2019). One possible solution for denser estimates of the precipitation is to merge conventional with satellite data.

Model description
TOPKAPI is a fully-distributed, physically based hydrological model. It represents river flows using meteorological inputs and geo-morphological characteristics of the catchment (Mazzaretti, 2018). For each pixel of the DEM unique values of the model parameters – slope, superficial soil permeability, surface and channel roughness – are assigned. The spatial patterns for the parameters values are derived from the DEM, soil map and land-use map.
The model describes the components of the hydrological cycle: sub-surface flow, overland flow, channel flow, infiltration, evapotranspiration, snow melting and accumulation, percolation and retention and redistribution of the flow in the dams (Fig.1) (Mazzaretti, 2018).
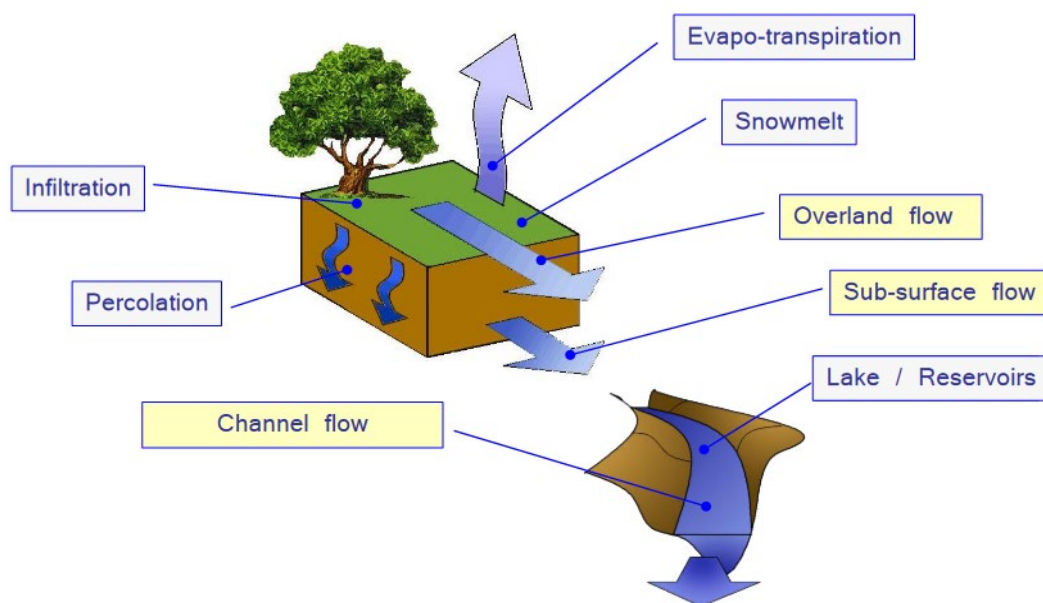
Fig. 1 Components of the TOPKAPI model.

The model is based on the following basic concepts at single cell level (Mazzaretti, 2018):

Precipitation is assumed to have single value over a single cell;

All the precipitation falling on the soil infiltrates into it, unless the soil in the cell is saturated;

The slope of the water table is assumed to coincide with the slope of the ground, unless the latter is very small (less than 0.01%); this constitutes the fundamental assumption of the Kinematic wave approximation in Saint Venant equations, and it implies the adoption of a Kinematic wave propagation model with regard to horizontal flow, or drainage, in the unsaturated area;

Local transmissivity, like local horizontal flow, depends on the total water content of the soil, i.e. it depends on the integral of the water content profile in a vertical direction (vertical lumping);

Saturated hydraulic conductivity is constant with depth in a surface soil layer but much larger than that of deeper layers; this forms the basis for the vertical aggregation of the transmissivity (constancy in space of the time variation of the water storage).

The integration in space of the kinematic wave equations results in three "structurally-similar" nonlinear reservoir equations (Fig. 2).
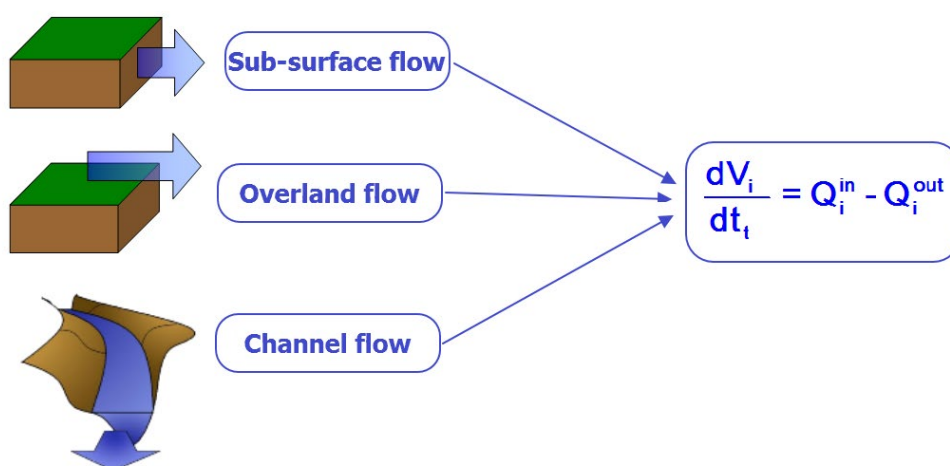

Fig. 2 Non-linear reservoir equations.

118

where: V_i – the total volume stored in the reservoir;

$\dfrac{dV_i}{dt_t}$ – the rate of change of water storage;

Q_i^{in} – the total inflow rate to the reservoir;

Q_i^{out} – the total outflow rate from the reservoir.

Background

The TOPKAPI model is applied over Ogosta river basin in the PhD thesis of Valeriya Yordanova (Yordanova, 2019). This basin is situated in the northwestern part of Bulgaria (Fig. 3). Its watershed is around 4280 km². and is one of the biggest in Bulgaria. In the upper part of the basin is situated one big damn (Ogosta damn) with capacity of 574 mln. m³. It significantly changes the river flow in the downstream part of the river. The watershed is under the influence of moderate continental climate, which is characterized with comparatively cold winter due to the arctic air masses, mild and rainy spring under the influences of air masses from the Atlantic ocean, comparatively dry and hot summer, and mild autumn. The average annual precipitation in the basin is between 650 and 900 mm. Generally the highest amount of precipitation falls in mountainous part of the basin and in the spring and beginning of summer, and the lowest amount of precipitation is in the summer and autumn and northern part of basin (the lower part of the basin). The flow regime follows the pattern of the precipitation and its formation is mainly with rainy and rainy-snow origin.
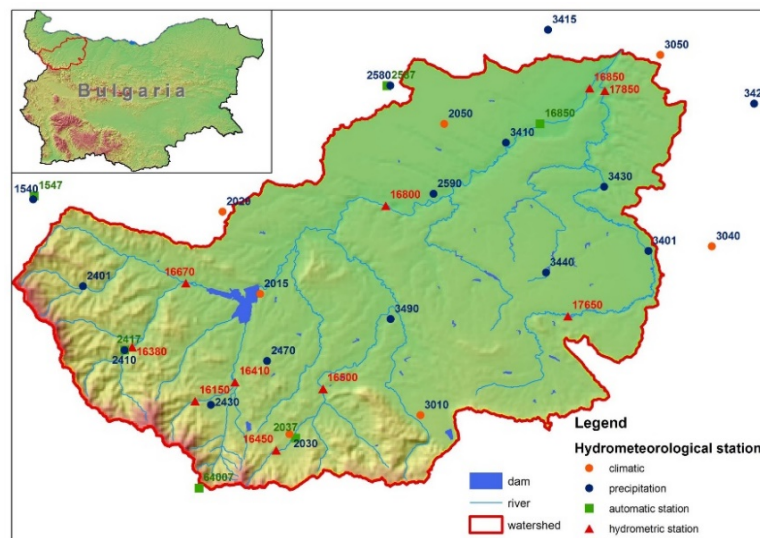
Fig. 3 Ogosta river basin, meteorological stations, hydrometric stations, DEM (digital elevation model) and the river network

The model was calibrated for the period 2012–2015 and in the process of calibration was taken into account the regime of the above mentioned reservoir. The time step of the model is 24 hours. For the calibration were used meteorological and hydrological station in and around the basin (Fig. 3). The model performance is quite good especially during high waves and flood events (Fig. 4).

Име	Висока вълна		PEAK [m³/s]	MAXQOBS	MAXQ	SHIFT	RMSE	R2	E	d
с. Говежда	22/05/2012	07/06/2012	28.6	24.71	32.37	0	1.72	0.8	0.58	0.88

a)

Име	Висока вълна		PEAK [m³/s]	MAXQOBS	MAXQ	SHIFT	RMSE	R2	E	d
с. Гаврил Геново	22/05/2012	07/06/2012	81	63.5	62.83	0	2.81	0.95	0.83	0.95

b)

c)

Име	Висока вълна		PEAK [m³/s]	MAXQOBS	MAXQ	SHIFT	RMSE	R2	E	d
с. Бутан	22/05/2012	07/06/2012	132	92.08	114.07	2	6.99	0.9	0.68	0.93
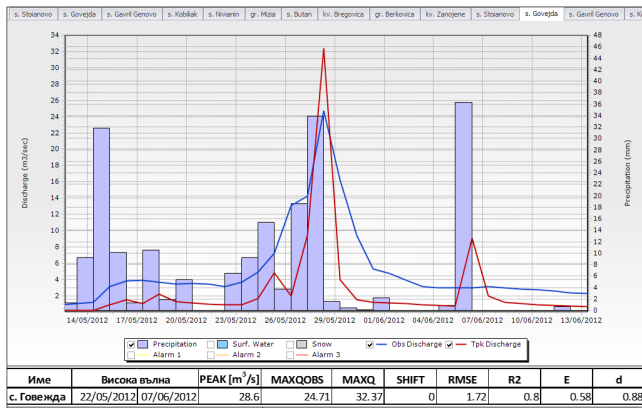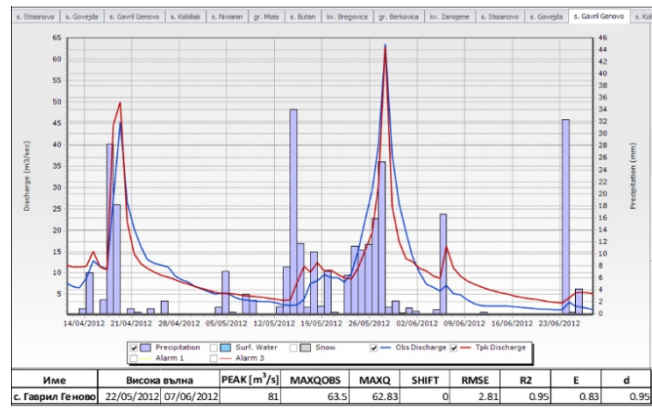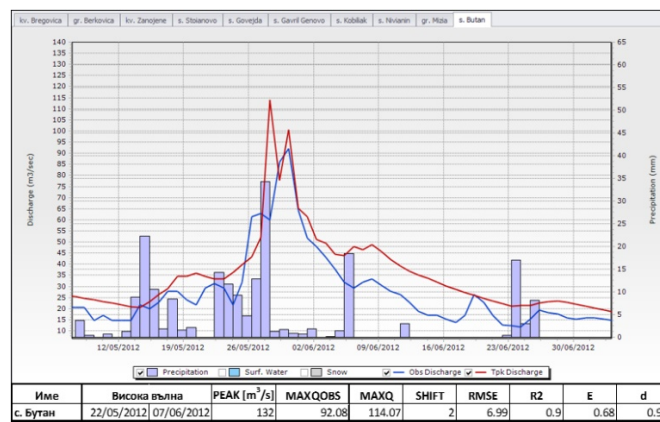
Fig. 4 Calibration results for the period (May 2012–June 2012) for station 16380 (a); 16670 (b); 16850 (c)

As it is seen from figure 4 the model performance is quite good the efficiency coefficient (Nash-Sutcliffe) is quite good for both stations above the damn and for the station below the damn. For the three stations the coefficient varies between 0.6 and 0.8. The peaks are quite good simulated in time and magnitude and the model can be used for flood forecasting purposes.

Data

For this study was taken one convective situation over Bulgaria during the period between 1st and 3rd of June 2019. This situation is characterized with intensive precipitation over the whole country and over the basin of Ogosta river. On table 1 are shown some of the precipitation sums for different periods i.e. maximum 24 hours for some of the conventional (blue) and automatic (green) stations and for the whole event (i.e. 72 hours). Another type of data, which are used in this study is data derived from satellites (in yellow) (Tabl. 1).

The reason to use satellite data is that the precipitation has high spatial variability, especially in convective situations like the one in our focus. The conventional and automatic stations can measure the amounts with sufficient accuracy for the respective period. The only constraint is that their measurements are representative only for their locations. Sometimes the distance between two adjacent sensors could reach more than 30 km (fig. 1). This is quite big gap with no information what is happening in it. For this purpose could be use remote sensing techniques – radars and satellites. Those data can significantly improve the spatial distribution of the precipitation event and respectively can improve the hydrological modelling and forecasting especially of flood events.

Tab. 1 Precipitation data over the Ogosta river basin used in the simulation for the selected period (blue – conventional stations, green – automatic stations, yellow – satellite product)

station/product	max 24 hours precipitation, [mm]	72 hours precipitation, [mm]
1540	50.3	67.3
2015	24.1	38.2
2021	21.6	26
2030	31.5	49.5
2401	36.6	60.4
2410	31.8	54.2
2430	43.2	82.2
2470	21.8	29.1
64210	48.3	76.7
2037	29.8	44.2
2417	16	24.4
64007	29.6	40.1
H05b	26	45

Methodology

In this study will be shown model simulations using the following type precipitation data:

- Data from 21 conventional stations (Fig. 3) – used in the process of calibration;
- Data from automatic stations interpolated into the 21 meteorological stations used for the model calibration;
- Data from HSAF project. H05b product is selected for this paper. This is Accumulated precipitation by merging MW images from operational sun-synchronous satellites and IR images from GEO satellites (i.e., product P-IN-SEVIRI) (hsaf.meteoam.it). The data from this product are again interpolated in the locations of the 21 meteorological stations;
- Merged data from automatic stations and H05b product, interpolated in the locations of the 21 meteorological stations using kriging method Generalized Additive Model (GAM) (Webster and Oliver, 2001).

Results

On Fig. 5 are shown the results from the different simulations at 3 of the gauging stations. Two of them – 16 380 and 16 670 are located in the upper part of basin, above the damn, and the 3rd station, 16850, is located in the lower part of the basin near the outlet of the river.
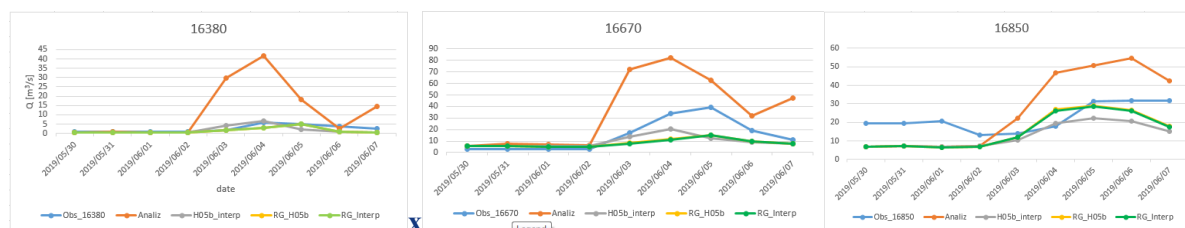

Fig. 5 Simulation results with different precipitation inputs VS observed discharge (blue): red – precipitation from conventional station; grey – interpolated data from HSAF product; green –interpolated data from automatic rain gauges; yellow line – interpolated data from automatic data and HSAF product.

The results show that the model overestimates the peak discharges, when simulations are performed with conventional ground data. It is also seen that the simulation with satellite product generally underestimates the discharge. The simulations with interpolated data from automatic stations also show better simulations in the lower part of the basin. This could be explained with the fact that in the lower part of the country there are more automatic stations than in the upper (mountainous) part, which leads to better distribution of the rainfall in the lower part of the basin. Another fact is that the model was calibrated with precipitation values in locations with raingauges and specific high waves. When we use a blended spatial interpolation /yellow line/, the new blended data is very closely to the interpolated, GAM – Krigin interpolated values /green line/. The model was calibrated using precipitation data in specific locations, not spatial interpolated data. In a new calibration of the model, from the spatial

interpolation can be generated more "extra" points, which can be used to enter more detailed precipitation in the hydrological model.

Conclusions

The results from this study show that the data from the HSAF cannot be applied alone for hydrological modelling especially in case of simulation of floods. Better results are achieved when using combination of satellite and ground data.

In this paper the simulations are performed on a 24 hours time step and the simulation results are compared with observed discharges at 8 o'clock in the morning. This is quite big step, especially when simulating and forecasting flash floods (which range is usually less than 10 hours). Our future work will be focused in decreasing the time step in order to better simulation of the time and magnitude of the flood peaks. Another focus will be the use of blended precipitation (automatic stations and satellite data) to better describe the spatial variability of the precipitation especially in convective situations.

References

hsaf.meteoam.it/Products/ProductsList?type=precipitation

Mazzetti C, (2018) TOPKAPI MODEL REFERENCE.

Yordanova VI, (2019) PhD thesis "River flow forecasting using distributed hydrological model"

Yordanova VI, Balabanova SS, & Stoyanova VT (2017). Application of the TOPKAPI model on the Ogosta river basin. In 17th Conference of the Danubian countries on Hydrological Forecasting and Hydrological bases of Water Management, Bulgaria, Electronic book with full papers (pp. 357–364).

Yordanova VI, Stoyanova, SV (2020). IMPROVED EXTREME FLOW MODELING BY RESERVOIR MANAGEMENT INPUT USING A PHYSICALLY BASED HYDROLOGICAL MODEL: A CASE STUDY OF OGOSTA RESERVOIR IN OGOSTA RIVER BASIN. International Multidisciplinary Scientific GeoConference: SGEM, 20(3.1), 185–191.

Yordanova VI, Stoyanova, VT (2020). MODELING FLOODS WITH A DISTRIBUTED HYDROLOGICAL MODEL IN A RIVER CATCHEMENT. International Multidisciplinary Scientific GeoConference: SGEM, 20(3.1), 249–255.

Webster R, Oliver MA (2001) Geostatistics for environmental scientists. Statistics in practice series Chichester: Wiley.

Possibilities of using neural networks for data preprocessing in models predicting flash floods

Tomas KOZEL[1,2], Petr JANAL[1]

[1]Czech Hydrometeorological Institute, Kroftova 43, Brno, Czech Republic, [2]Brno University of Technology, Faculty of Civil Engineering, Institute of Landscape Water Management, Veveří 331/95, Brno, Czech Republic, email: kozel.t@fce.vutbr.cz, email: janal.petr@chmi.cz

Abstract

In the article are studied possibilities of preprocessing of the radar values using methods artificial intelligence (neural network). For this study were chosen 229 meteorological stations. The data from these stations are compared with mean values of radar data. The neural networks are trained on historical episodes (2016–2019) and whole model is tested on validation period, which it was chosen year 2020. The preprocessed data and were given to model for forecasting of flash flood danger and results of both inputs were compared. Preprocessed rainfall data significantly lowered number of fake alarms, but slightly increased number of missed dangerous events. Results of neural networks model were good enough for another continuation of this applications. Where should be find some problematic issues with the neural network application as preprocessing tool for this application.

Keywords: Artificial intelligence, preprocessing, flash flood.

Introduction

In recent years, the occurrence of flash floods in the Czech Republic has been quite common. Flash floods themselves are characterized by high precipitation totals in a very short time in a small area. From the point of view of early warning systems, they are a very problematic phenomenon, because between the beginning of the causal precipitation and the culmination reaction of the basin, there is relatively little time to issue a warning and possible evacuation. For the above reason, an effort is made to predict these phenomena using different models. The fuzzy flash flood model FFF (Janal and Stary, 2012) is one of the ways to effectively predict flash floods. Models for predicting the danger of torrential rains use nowcasting, which is based on predictions based on radar observations or adjusted radar observations. The adjustment coefficients themselves are calculated retrospectively on the basis of the previous measured precipitation and are valid until the issue of new adjustment coefficients. From the point of view of nowcasting, a problem arises where the adjustment of extreme values of precipitation totals is therefore adjusted only after their measurement. From the point of view of flash floods, the above-mentioned extreme values are critical, and therefore it is necessary to create a tool for an approximate estimation of the error between radar observations and the values actually measured. The need to improve the inputs to the FFF model arose from an evaluation of the success of the FFF model (Janal and Kozel, 2019), when the FFF model reached too many false alarms for the period under review (the model issued a warning but nothing actually happened). For this purpose, the article describes a method based on the method of neural networks (Jang and Sun, 1995), where neural networks themselves are a very suitable means of finding strongly nonlinear dependencies, as has been proven by many authors (Nayak et. All, 2005; Lin et. All, 2020; Kozel and Stary 2019, Kozel et. All. 2021)

Methods

For the possibility of testing the possibilities and limit for preprocessing based on neural networks, records were selected from a total of 229 precipitation stations for the years 2016–2020. When the years 2016–2019 were used for model calibration and the year 2020 for validation. A large square (5x5) is

chosen for each station, which consists of sub-squares of the grid with a square size of 1000 x 1000 m. For next step was from each large square calculated mean for radar and measured precipitation data from each chosen station was used. Therefore mean of chosen area (radar data) and data from precipitation station were compered. The method was chosen due to the fact that radar-measured values do not always fall into the same grid square in which it is measurement performed. From the above statement it can be stated that the measured values in the station (merge) and the values obtained with the help of radar may not correspond directly in the square of the grid where the precipitation station is located, but will most likely be interdependent in the vicinity of the precipitation station. The model itself will be trained only in places of chosen rain gauge stations, where it is possible to quantify errors. Figure1 show position of chosen precipitations stations (green *), radar (black triangle) and rest precipitations station (red *).
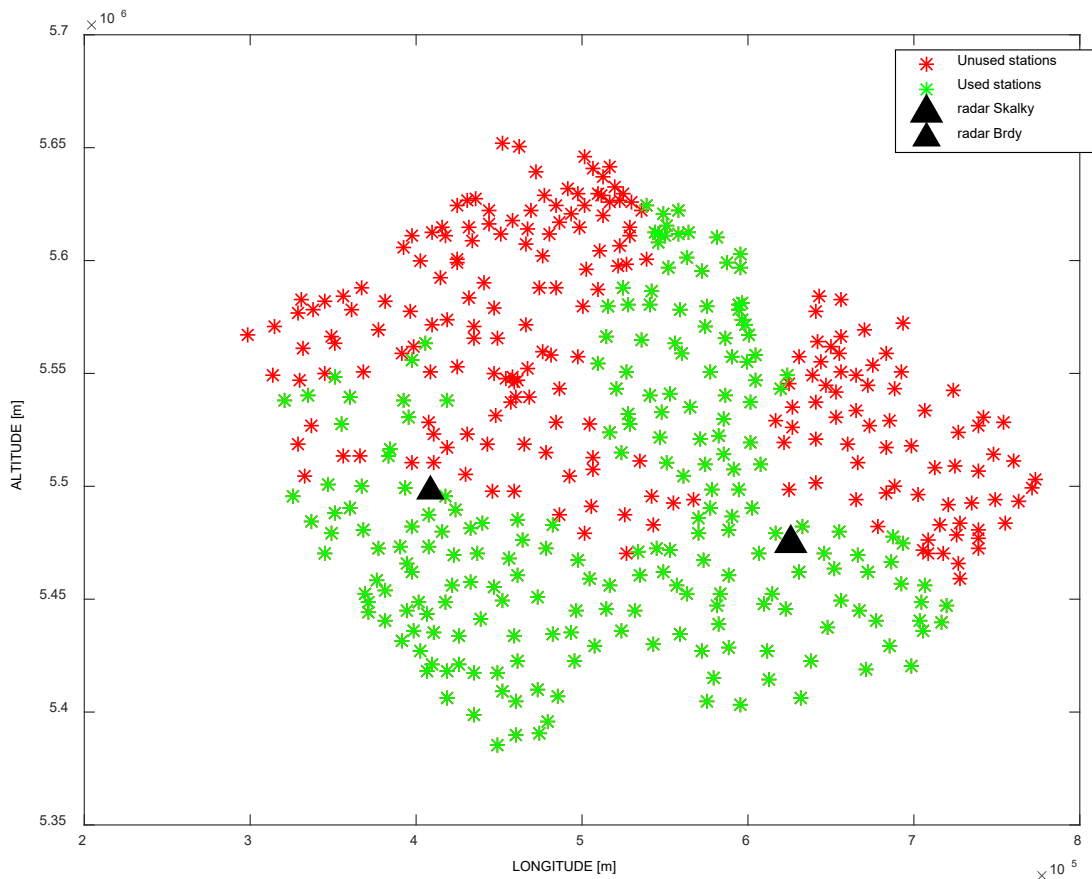
Figure 1 Position of used station.

From point of view flash flood are values of hourly sum of precipitations *hs*, which are lower than 1 mm cut off. The data were separated to five groups as is showed in table 1.

Table 1 Selecting data base on their values.

Group num.	1	2	3	4	5
hs [mm]	(0;5)	<5;10)	<10;15)	<15;25)	<25;∞)

Therefore for each station was trained neural network *NN*. As input is used mean of large square from radar data and number of group. Output is adjusted value of precipitation. This *NN* is percepton with three layers. The first layer has sigmoid transformation function and has 15 hidden neurons. The second layer has sigmoid transformation function and has 8 hidden neurons. The third layer has linear transformation function and one hidden neuron. All *NN's* was trained with backpropagation method. For NN training was used mean of large square from radar data and as target is used value of

precipitation gauged precipitation station, which timely corresponded and at least one of them was higher than 1 mm.
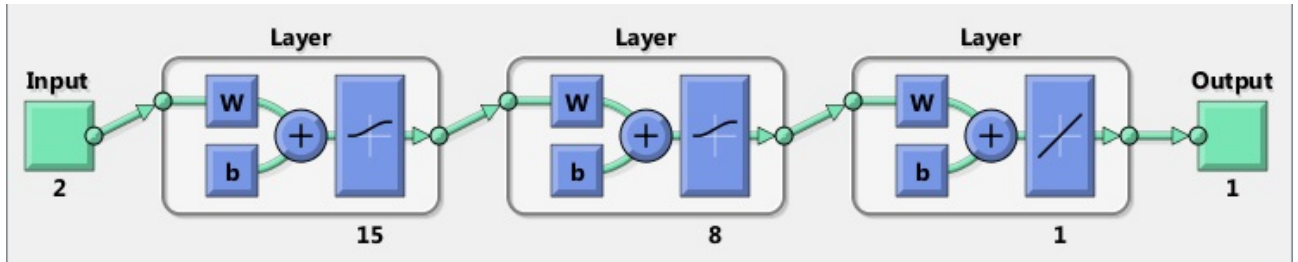

Figure 2 Schema of NN model.

The preprocessing itself will be applied to the 1st value of the sum of hourly precipitation totals. Due to the huge amount of data, a simplification will be adopted when creating a preprocessing model in the form of working with data in an hourly step. For the training itself, the hourly sums of radar measurements and the hourly sums of precipitation totals obtained by measurements at the station will be used. In real operation, the FFF model calculates the risk of the river basin in a 5-minute step (radar step). This means that the preprocessing results will be valid for the entire following hour.

As criterion was chosen RMSE :

$$RMSE = \frac{\sum_{j=1}^{m} \sqrt{\frac{\sum_{i=1}^{n}\left(Q_{sim,i,j}-Q_{real,i,j}\right)^2}{n_j}}}{m} \qquad (1)$$

,where Q_{sim} is adjusted radar value by NN's model, Q_{real} is gauged value, i is data number, j is number of station, n is total number of data for station and m is total number of stations.

During validation period was achieved around 30% improvement for criterion RMSE in total for each group. This results is good but for some stations this method caused worsening results in danger way for this application (measured values were higher than radar data for group 4 and 5, but overall tendency of NN's model was opposite)

In the last step was application of preprocessing method for rainfall data and recalculation of flash flood danger with using FFF model. For this evaluation was chosen July 2020, because in this month were many flash flood events and many fake alarms (base upon previous evaluation, Janal and Kozel, 2019) During resimulation, both preprocessed values and original values will be used by the FFF model.

During July were 1632 (100%) records in databases, which were corresponding with damage of property from flood. FFF model was able to hit 95 % these events and only have 5 % fail. This is rather good results. During tested period were around 7.8 % (averaged value from all basins) fake alarms. When adjusted values of rainfall was used the FFF was able to hit 94.8 % these events and only have 5.2 % fail. This is still good results, even if it is lower values than original data was used. During tested period were around 3.49 % (averaged value from all basins) fake alarms. Therefore number of fake alarms dropped significantly. When preprocessing was used number of fake alarm was reduced greatly, but number of miss was little higher then original FFF results.

Conclusion

The aim of the nowcasting value preprocessing application is to refine the input for models that work with flash floods. This refinement of the input lead to a reduction in the number of false alarms (expected values of precipitation totals are strongly overestimated). On the other hand the second expected impact, which should be a reduction in the occurrence of miss alarms (expected values of precipitation totals are significantly lower than the reality), was not fully achieved. The reason for this was atypical behavior some station (group 4 and 5), when gauged data were higher than radar data and thus NN model adjusted

radar values in wrong tendency. This atypical behavior should be study further and should be find a way how to predict this behavior. Also during this application were problems with exceedance of training area. This problem was approached with the simplest way. If training data were exceed unadjusted (radar value) was used as adjusted value.

If two mentioned problem will be solved or at least strongly mitigated, the preprocessing of rainfall data should be very beneficial. It is using could lead to better performance of FFF model and improve FFF's results reliability.

Acknowledgements

References

Janal, P., Stary, M., 2012. Fuzzy model used for the prediction of a state of emergency for a river basin in the case of a flash flood – PART 2. *Journal of Hydrology and Hydromechanic*, **60**, 3, 162–173.

Janal, P. and Kozel, T., 2019. Fuzzy logic based flash flood forecast, XXVIII CONFERENCE OF THE DANUBIAN COUNTRIES ON HYDROLOGICAL FORECASTING AND HYDROLOGICAL BASES OF WATER MANAGEMENT, Kyiv, Ukraine, DOI: 10.15407/uhmi.conference.01.10.

Jang, J. S. R. and Sun, C. T., 1995. "Neuro-Fuzzy Modelling and Control", Proceedings of the IEEE, vol. 83, no. 3, pp. 378–406, Mar. 1995. doi:10.1109/5.364486.

Kozel, T., Stary, M., 2019. Adaptive stochastic management of the storage function for a large open reservoir using an artificial intelligence method. *J. Hydrol. Hydromech.*, Vol. **67**, No. 4, 2019, p. 314 – 321, doi: 10.2478/johh-2019-0021.

Lin, Q., Leandro, J., Wu, W., Bhola, P. and Disse, M., 2020. Prediction of Maximum Flood Inundation Extents With Resilient Backpropagation Neural Network: Case Study of Kulmbach. Front. Earth Sci. 8:332. doi: 10.3389/feart.2020.00332.

Nayak, P., Sudheer, K., Rangan, D., and Ramasastri, K., 2005. "Short-term flood forecasting with a neurofuzzy model," *Water Resources Research*, vol. **41**, no. 4, 2005. doi:10.1029/2004WR003562.

Implementation of a Long Short-Term Memory Neural Network based hydrological model in a snow dominated Alpine basin

Karlo LESKOVAR[1], Damir BEKIĆ[2], Denis TEŽAK[1], Hrvoje MEAŠKI[1]

[1] University of Zagreb, Faculty of Geotechnical Engineering, Croatia, [2] University of Zagreb, Faculty of Civil Engineering, Croatia, email: karlo.leskovar@gfv.unizg.hr, email: damir.bekic@grad.hr, email: denis.tezak@gfv.unizg.hr, email: hrvoje.measki@gfv.unizg.hr

Abstract

Snow dominated Alpine basins are of great importance for the surrounding areas. Due to complex terrain and weather phenomena, hydrological modelling in these areas is often difficult. In this article a state-of-the-art approach based on data-driven models, in form of Recurrent Artificial Neural Networks is presented. In order to investigate the influence of different input data types three models were created. The results proved that adding more input data features can improve model prediction capabilities (R2 increased from 0.91 to 0.93 for the testing period), although fine tuning of model hyperparameters is mandatory to achieve such results. The results of this study show that Long Short-term memory neural network based hydrological models can be used in mid to high elevation snowmelt dominated basins of the Danube tributaries.

Introduction

The melting of snow and ice in high altitude region of the Alps in the past has formed several drainage basins, which are nowadays important both for the Alpine region and downstream areas. Some of the largest European rivers, such as Danube, Rhine, Sava, etc., have their origin in the Alps. The runoff regime of the Alpine mountain rivers is driven by a combination of precipitation and snow and ice melt, so in order to understand and predict runoff regime under different weather conditions it is important to obtain reliable measurements and observations of different hydrometeorological parameters. The high altitude and remote regions are usually inaccessible and a smaller density of in-situ stations has been complemented over the time with the remote sensing information. With the development of data transmission and processing techniques, the speed and accuracy of in remote sensing data have been continuously increasing. The application of remote sensing in collecting precipitation data (Duan et al., 2016; Tuo et al., 2016) and snow and ice cover data (Tekeli et al., 2005) in mountainous regions has become widely accepted. However, further validation of precipitation and other products are still recommended with the aim of a more detailed comparison and evaluation.

Runoff models can be divided into energy-based models, temperature index (degree-day) models and, data-driven models (Thapa et al., 2020). Despite the importance of the European Alps, studies on snowmelt-runoff and/or rainfall-runoff modelling based on data-driven models are rare.

This paper presents an implementation of a data-driven modelling approach based on artificial neural networks (ANN) with Long Short-Term Memory (LSTM) architecture in a mountainous basin in Tyrol, Austria (and partly Italy). The study compares the performance of Neural Network based model models trained on different datasets (runoff and precipitation, and runoff, precipitation, air temperature and snow depth). The goal of the study is to present the capabilities of data-driven models in complex situations, with limited data availability. Additionally, guidelines for hyperparameter fine-tuning are provided, which can yield further model improvements.

Methodology

Study area

The source of the Drava river is in South Tyrol, near Dobbiaco (Toblach) in Italian Alps, at an elevation of 1450 m a.s.l. The river flows eastwards, towards the city of Lienz, Austria, where it mounds with the Isel river, and after, flowing mainly south-east, through Carinthia Austria, Slovenia, and Croatia, until it mounds to the Danube near Osijek, Croatia. For this study, a part of the Drava river basin upstream of Lienz is chosen. With a drainage area of 669.35 km^2 and elevation range from 666 to 3056 m a.s.l. this basin represents a typical smaller mountain basin. Despite the high altitude and remoteness, multiple meteorological gauging stations are present in and around the basin (Figure 1.).
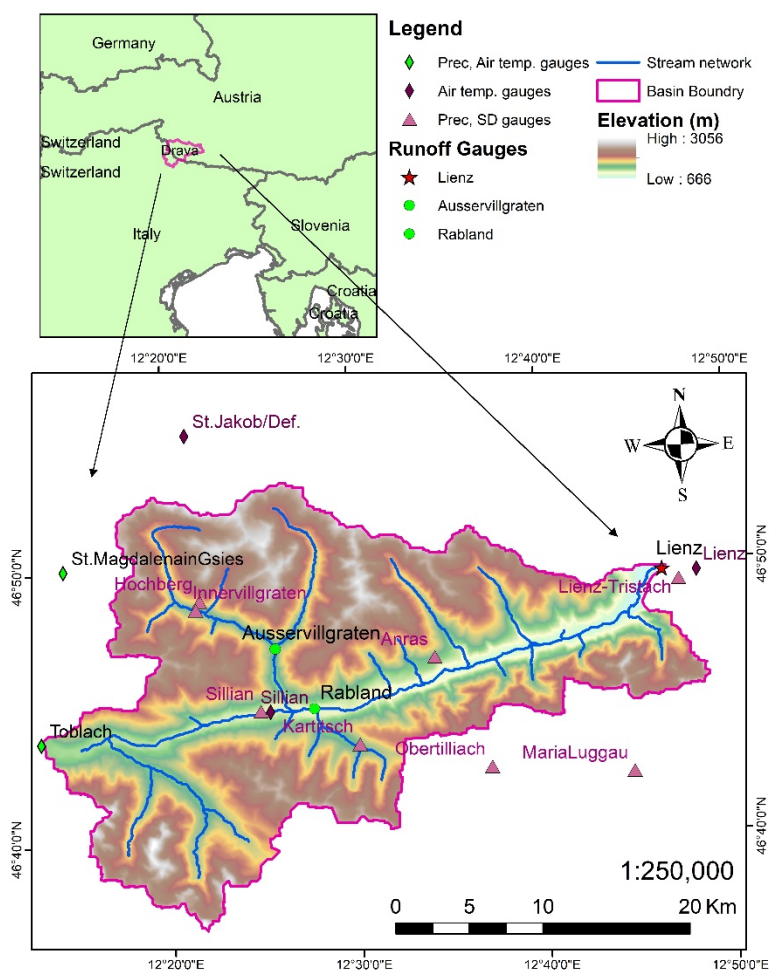

Fig. 1 Geographic location of the Drava river basin in Italy/Austria with gauging stations

Geology, hydrogeology of the study area

The drainage system of the Eastern Alps is strongly related to the evolution of the Alpine orogenic belt through time (Frisch et al., 1998). Since the recent drainage system caused by the morphology of the terrain was established in a geologically relatively short time (approx. 1 MA), the canal connection of the rivers flowing through this area and the tectonic processes taking place in the Alps is still not completely clear (Hergarten, 2007).

The drainage system of the Eastern Alps is characterized by a west-east drainage divide. It separates the Inn, Salzach and Enns catchment areas on the north, from the Drava-Mur catchment area on the south of the water divide. From the beginning of the collision of the Adriatic plate with Europe, the drainage system in the Eastern Alps has responded on changes in the uplift rate and on the lateral tectonics. Nowadays deformation is still controlled by the ongoing convergence and active tectonics, which is still evident in the pronounced seismicity caused by young uplift (Kuhlemann, 2007; Grenerczy et al., 2000; Robl et al., 2008) As both drainages systems, north and south of the Alpine water divide, are tributaries

of the Danube River, almost the entire catchment area of the Eastern Alps is discharged toward the Black Sea catchment area, as a common base drainage level.

At the southeastern border of the Eastern Alps the Drava drainage systems was ice free (Robl et al., 2008). The main channel indicates very variable values of stream power, because of the several hydropower stations that was built in this area. Due to the obvious complex morphology and the terrain and/or anthropological impacts in form of hydropower production, a data-driven modeling approach based on Artificial Neural Networks is being proposed.

Artificial Neural Networks

„An artificial neural network is a massive parallel distributed data processing system that consists of simple processing units, with a natural propensity of storing experimental knowledge and making it available for use." (Haykin, 2005) The network acquires "knowledge" by learning on the available data and stores it in the interneuron connections, so called weights (Haykin, 2005). An important aspect of neural networks is the ability to capture linear trends in the training data while resisting local perturbations (Goodfellow et al., 2016). Many studies investigating the implementation of ANN and Deep Learning (DL) frameworks in hydrological tasks have been conducted in recent years (Sit et al., 2020). Any neural network, regardless of architecture, is composed of neurons. The processes within a neuron are visualized in Figure 2. The models are trained on daily timestep, with data containing both dry and rainy years to acquire best possible results in all conditions.
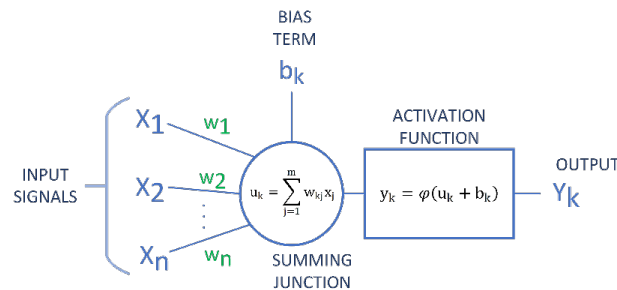

Fig. 2 Nonlinear model of a neuron (created according to: (Haykin, 2005))

Evaluation metrics

In order to quantify the performance of a hydrological model, the model outputs get compared with observed values, therefore established statistical indicators are being calculated with the goal of mutual comparisons of different models (D. N. Moriasi et al., 2007). In this paper, the mean square error (MSE) and coefficient of determination (R2) were chosen, calculated, and evaluated.

The MSE (Eq. 1) measures the average squared distance between the simulated and observed values. Basically, the closer the values of MSE to zero, the better the predictions are. Due to the square of the difference in simulated and measured data, the higher values of runoff have bigger impact on the values of the overall MSE.

$$MSE = \frac{\sum_{i=1}^{n}(Q_i - Q'_i)^2}{n} \qquad (1)$$

where: Q_i is the observed runoff at time t, and Q'_i is the simulated runoff at time t, and n is the length of the timeseries.

The coefficient of determination R2 (Eq. 2) measures the "*goodness of fit*" between simulated and observed data, and while being independent of the scale of data (Dawson & Wilby, 2001) making it very useful for comparisons with other studies.

$$R^2 = \left[\frac{\sum_{i=1}^{n}(Q_i - \bar{Q})\left(Q'_i - \bar{Q}'\right)}{\sqrt{\sum_{i=1}^{n}(Q_i - \bar{Q})^2 \sum_{i=1}^{n}\left(Q'_i - \bar{Q}'\right)^2}} \right]^2 \qquad (2)$$

where: $\bar{Q}$ is the mean observed runoff and $\bar{Q}'$ is the mean simulated runoff.

Results

In total three models (Model 1, Model 2 and Model 3) with different input data and hyperparameters were created. According to Thapa et. al. (Thapa et al., 2020), Adamax optimizer and MSE loss function were selected for all models, which were trained on the 2008–2013. period, with validation and testing on independent data from years 2013. and 2014, respectively. All three models had same architecture, two LSTM layers and one linear (densely connected) output layer.

Model 1 was trained on upstream runoff (2 gauges) and precipitation (9 gauges) only. The length of the input series was 30 days with 30 neurons in each of the 2 LSTM layers. To find an optimal training length several trial-and-error runs have been conducted, where 30 epochs were found as optimal training length. The training results are presented on Figure 3 (upper) as loss vs. epochs graph.
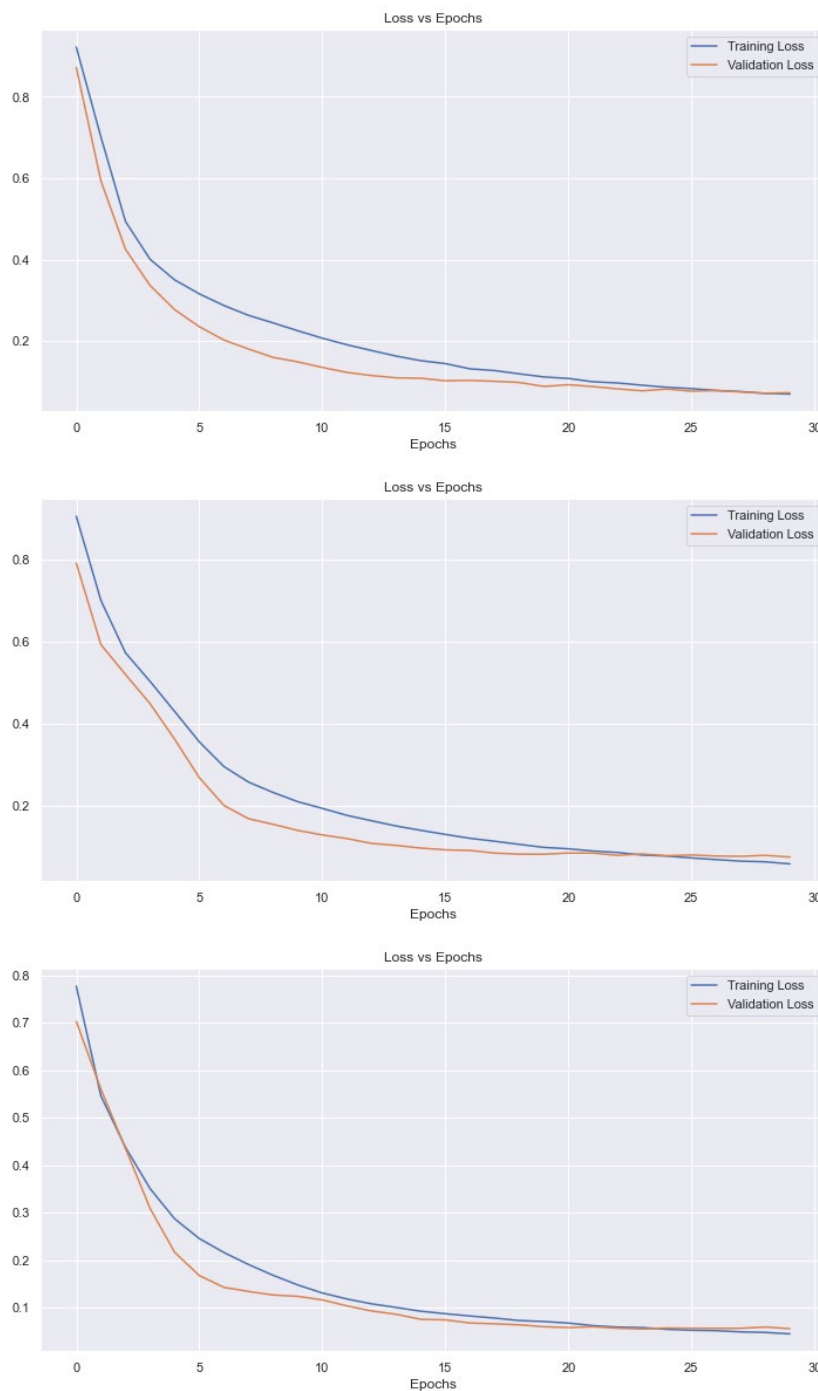

Fig. 3 Loss vs. epoch for Model 1 (upper), Model 2 (middle) and Model 3 (lower)

The resulting hydrograph for Model 1 is presented on Figure 4. Model performance during mostly dry periods (baseflow) is very satisfactory while some underestimation can be noticed during spring and early summer (May, June, July) when the snowmelt and summer rainstorms often occur. Statistically the model performance was very satisfactory, with an MSE of 5.34 and R2 of 0.94 (validation) and MSE of 8.07 and R2 of 0.91 (testing) (Table 1.).
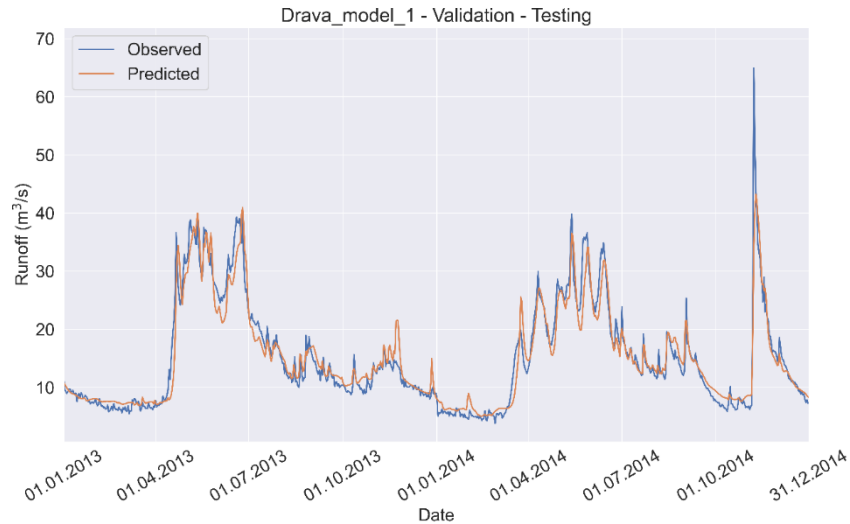
Fig. 4 Resulting hydrograph of the Model 1 – validation and testing period (2013., 2014.)

With the goal of enhancing model performance, Model 2 was created with additional input data in form of average air temperature (5 gauges) and snow depths (7 gauges). The resulting hydrograph (Figure 5.) with same hyperparameters as with Model 1 shows that some of the underestimation was corrected, but on the other hand, now some overestimation in certain periods is noticeable (November, December 2013 and May, June 2014). The slight decrease in performance is noticeable in the statistical metrics, where an increase in MSE 6.51 (validation) and 9.83 (testing) and a decrease in R2 0.93 (validation) and 0.89 (testing) was observed (Table 1.).
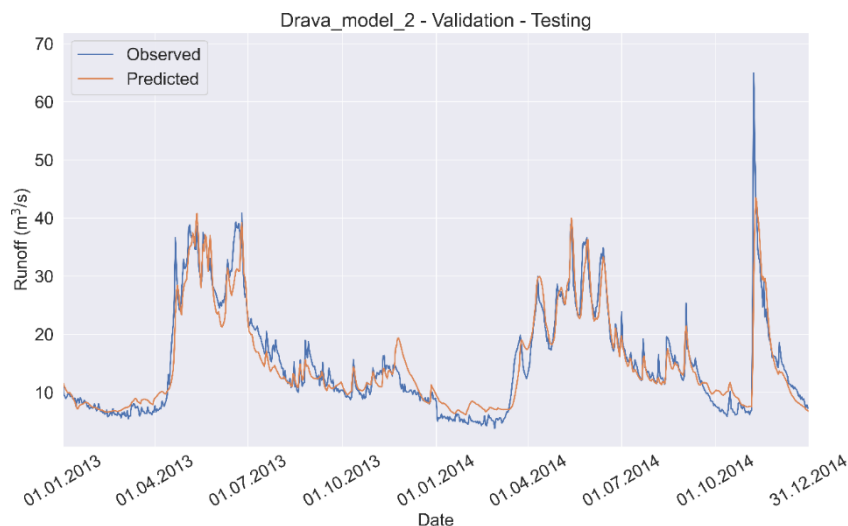
Fig.5 Resulting hydrograph of the Model 2 – validation and testing period (2013., 2014.)

A third model namely Model 3 was created with the goal of improving the performance of Model 2 by fine-tuning the model hyperparameters. Here, the length of the input sequence of data and the number of neurons in each LSTM layer is increased to 120. Also, to avoid overfitting to more feature rich

training input data, the learning rate of the model was decreased to 3.5 x 10^{-4} from the initial 1.5 x 10^{-3} and the dropout of each LSTM layer was increased from 0.15 to 0.35.
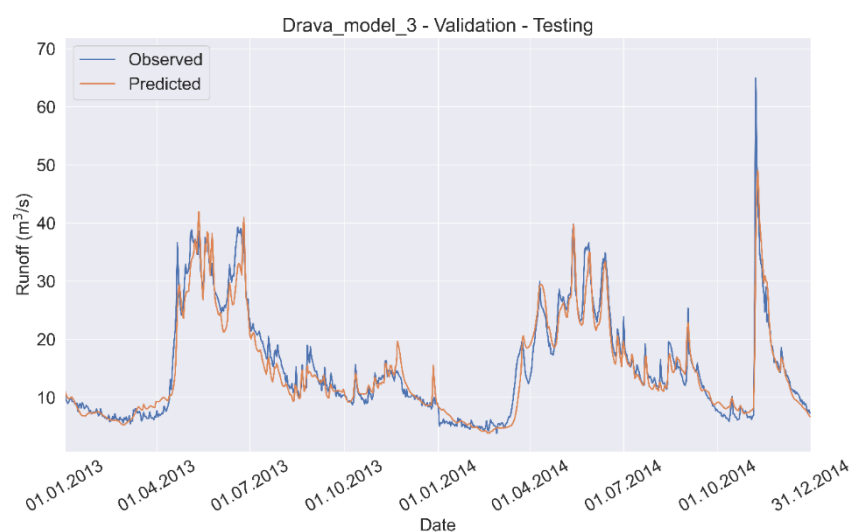
Fig. 6 Resulting hydrograph of the Model 3 – validation and testing period (2013., 2014.)

The fine-tuning improved the results visually (Figure 6) and by statistical metrics. The MSE was improved for both validation (5.29) and testing periods (6.33), same as the R2 metric which was increased to 0.94 (validation) and 0.93 (testing) (Table 1.)

Table 1 Statistical indicators of the models

MODEL	PERIOD	MSE	R2
	Train	5.385383	0.94034
Model 1	Valid	5.342877	0.937305
	Test	8.066556	0.910472
	Train	4.459333	0.948473
Model 2	Valid	6.508718	0.927374
	Test	9.834305	0.885097
	Train	3.443944	0.962228
Model 3	Valid	5.280197	0.944787
	Test	6.339774	0.929338

Additionally, the statistical indicators are presented as a bar chart in Figure 7.
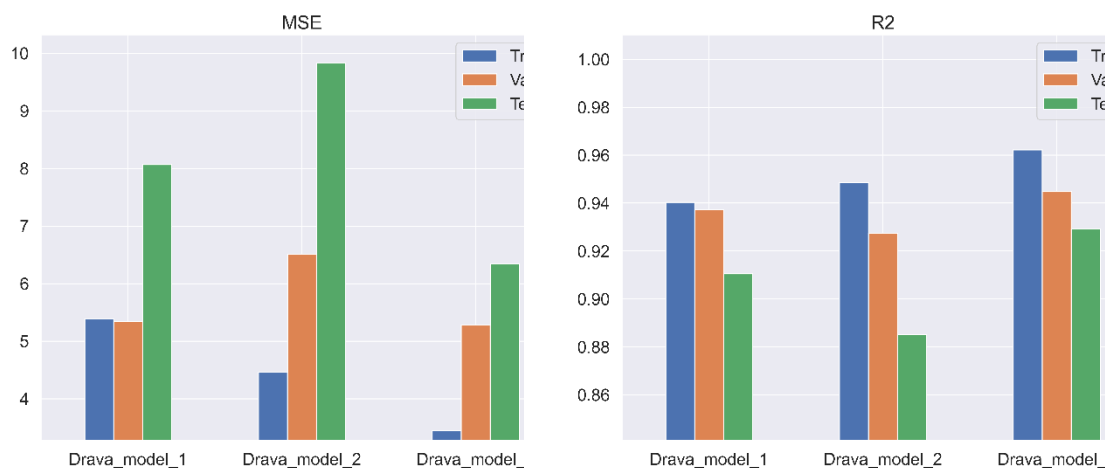
Fig. 7 Bar charts of statistical indicators of the models

Discussion

The decreased model performance observed for Model 2 can be attributed to more training data (23 vs. 11 features) and the tendency of the model to overfit to training data, which is proven by the statistical metrics (Figure 7. – left) where a slight decrease in MSE for training but a significant increase for validation and testing periods is noticeable. Similar behaviour is noticed in the coefficient of determination values (Figure 7. – right), where an increased training R2 result, but also slightly decreased validation and significantly decreased testing results are noticed.

Therefore, fine-tuning of the model (neural network) hyperparameters was done, which yields a significant decrease in MSE of the model for all three periods, followed by and slight increase in training and validation and a more pronounced increase in testing R2 metric (Model 2 vs. Model – Figure 7.).

Conclusion

The study presents an ANN based hydrological model implemented in a mountainous basin driven by snow and ice melt. The aim of the study was to present the predictive capabilities of data-driven models, even in complex terrain, geological and hydrogeological conditions.

Further improvements could be made by adapting an early stopping algorithm to the training loop, which should avoid the possibility of overfitting to training data, but this was outside the scope of this paper and therefore will be implemented in future revisions of the models. Also, adding more data, in form of remote sensed precipitation and/or snow-covered areas could enhance model performance, and will be investigated in future research regarding the topic.

References

D. N. Moriasi, J. G. Arnold, M. W. Van Liew, R. L. Bingner, R. D. Harmel & T. L. Veith (2007). Model Evaluation Guidelines for Systematic Quantification of Accuracy in Watershed Simulations. *Transactions of the ASABE*. [Online]. 50 (3). p.pp. 885–900. Available from: http://elibrary.asabe.org/abstract.asp??JID=3&AID=23153&CID=t2007&v=50&i=3&T=1.

Dawson, C.W. & Wilby, R.L. (2001). Hydrological modelling using artificial neural networks. *Progress in Physical Geography*. **25** (1). p.pp. 80–108.

Duan, Z., Liu, J., Tuo, Y., Chiogna, G. & Disse, M. (2016). Evaluation of eight high spatial resolution gridded precipitation products in Adige Basin (Italy) at multiple temporal and spatial scales. *Science of the Total Environment*. [Online]. **573** (September). p.pp. 1536–1553. Available from: http://dx.doi.org/10.1016/j.scitotenv.2016.08.213.

Frisch, W., Kuhlemann, J., Dunkl, I. & Brügel, A. (1998). Palinspastic reconstruction and topographic evolution of the Eastern Alps during late Tertiary tectonic extrusion. *Tectonophysics*. **297** (1–4). p.pp. 1–15.

Goodfellow, I., Bengio, Y. & Courville, A. (2016). *Deep Learning*. The MIT Press.

Grenerczy, G., Kenyeres, A. & Fejes, I. (2000). Present crustal movement and strain distribution in Central Europe inferred from GPS measurements. *Journal of Geophysical Research: Solid Earth*. [Online]. **105** (B9). p.pp. 21835–21846. Available from: https://agupubs.onlinelibrary.wiley.com/doi/full/10.1029/2000JB900127. [Accessed: 21 June 2021].

Haykin, S. (2005). *Neural Networks – A Comprehensive Foundation*. Hamilton, Ontario, Canada: McMaster University.

Hergarten, S. (2007). Longitudinal river profiles as tectonic archives. *Geophysical Research Abstracts*. **9**.

Kuhlemann, J. (2007). Paleogeographic and paleotopographic evolution of the Swiss and Eastern Alps since the Oligocene. *Global and Planetary Change*. **58** (1–4). p.pp. 224–236.

Robl, J., Hergarten, S. & Stüwe, K. (2008). Morphological analysis of the drainage system in the Eastern Alps. *Tectonophysics*. **460** (1–4). p.pp. 263–277.

Sit, M., Demiray, B.Z., Xiang, Z., Ewing, G.J., Sermet, Y. & Demir, I. (2020). A Comprehensive Review of Deep Learning Applications in Hydrology and Water Resources. *arXiv*.

Tekeli, A.E., Akyürek, Z., Şorman, A.A., Şensoy, A. & Şorman, A.Ü. (2005). Using MODIS snow cover maps in modeling snowmelt runoff process in the eastern part of Turkey. *Remote Sensing of Environment*. **97** (2). p.pp. 216–230.

Thapa, S., Zhao, Z., Li, B., Lu, L., Fu, D., Shi, X., Tang, B. & Qi, H. (2020). Snowmelt-Driven Streamflow Prediction Using Machine Learning Techniques (LSTM, NARX, GPR, and SVR). *Water*. [Online]. 12 (6). p.p. 1734. Available from: https://www.mdpi.com/2073-4441/12/6/1734. [Accessed: 17 December 2020].

Tuo, Y., Duan, Z., Disse, M. & Chiogna, G. (2016). Evaluation of precipitation input for SWAT modeling in Alpine catchment: A case study in the Adige river basin (Italy). *Science of the Total Environment*. **573**. p.pp. 66–82.

Improvement of the operational HEC-HMS hydrological model embedded in the Flood Forecasting and Warning System of the Sava River Basin

Mirza SARAČ[1], Maja KOPRIVŠEK[2], Oliver RAJKOVIĆ[3], Azra BABIĆ[4], Merima TRAKO[4], Saša MARIĆ[5], Adnan TOPALOVIĆ[6], Marija IVKOVIĆ[7], Srđan MARJANOVIĆ[7], Dejan PETKOVIĆ[7], Ervin KALAČ[9], Danijela BUBANJA[9]

[1]International Sava River Basin Commission, [2]Slovenian Environment Agency, Slovenia, [3]Croatian Meteorological and Hydrological Service, Croatia, [4]Federal Hydrometeorological Service, Bosnia and Herzegovina, [5]Republic Hydrometeorological Service of Republika Srpska, Bosnia and Herzegovina, [6]Sava River Watershed Agency, Bosnia and Herzegovina, [7]Republic Hydrometeorological Service of Serbia, Serbia, [8]Institute of Hydrometeorology and Seismology, Montenegro, Corresponding author: Mirza Sarač, msarac@savacommission.org

Abstract

In 2017 the HEC-HMS model for the Sava River Basin was embedded under the hydrological forecasting platform – Flood Forecasting and Warning System in the Sava River Basin (Sava FFWS) and coupled with many hydraulic models. Since the model was initially calibrated as the event-based model, a lack of accuracy has been recognized during the continuous simulations within the Sava FFWS operational use. Therefore, the Sava FFWS Users organizations: ten forecasting organizations from five Sava countries, agreed to upgrade and improve this hydrological model.

The activities on improvement of the operational Sava HEC-HMS hydrological model were performed in period January 2019 till June 2020. It was implemented by the national experts from the Sava FFWS users' organizations as a true joint action and coordinated by the Secretariat of the International Sava River Basin Commission (ISRBC). The goal of this activity was to provide a recalibrated hydrological model using the initial model version based on HEC-HMS software. The Secretariat of ISRBC made an initial improvement of the model to account for new hydrological and meteorological stations and prepared necessary technical documentation and time plan for the work of national experts: collection of historical hourly data, enhancement of the model components, calibration and validation of the model. Significant amount of observed hourly data for period from 2010 to 2018 have been collected from 199 meteorological stations and 134 hydrological stations imported and stored at the Sava FFWS Archive server for the further availability. At the end the model was significantly improved, density of meteorological data in the model was increased and the model was calibrated using continuous long term time-series.

The general approach was to provide the best calibration including validation of each tributary subbasin using the historical flow and precipitation data to identify critical events with reasonable precipitation data that specifically affect the tributary basin of interest. After the calibration and validation of the tributary and local mainstem models a combination of all models into a single model that covers the entire Sava River Basin was performed including additional two model validation processes. This paper presents the results of the Sava HEC-HMS model improvements and updated parameters, including a comparison of results of initial and improved models within the operational forecasting system. The paper also discusses the potentials of the remote sensing and radar- and satellite-based data that will be used for the future model improvements.

Introduction

The Flood Risk Management (FRM) is a complex set of actions and measures that need timely implementation in order to be successful and to protect people, infrastructure, cultural heritage and environment. The FRM in the transboundary river basins have additional specific needs and challenges.

135

The Sava River Basin is shared by five Sava countries: Slovenia (SI), Croatia (HR), Bosnia and Hercegovina (BA), Serbia (RS) and Montenegro (ME) where the objectives of transboundary FRM are regulated with the Framework Agreement on the Sava River Basin and the accompanying Protocol on Flood Protection to FASRB (Protocol). With respect to an efficient flood awareness, the Protocol has committed all Sava countries to establish a joint flood forecasting system for the entire Sava River Basin under the coordination of the Secretariat of the International Sava River Basin Commission (ISRBC).

The Flood Forecasting and Warning System in the Sava River Basin (Sava FFWS) was established in October 2018 and represents a comprehensive and versatile system that combines data and models of individual countries, as well as common models, making it a unique example of cross-border cooperation in flood forecasting even globally. The Sava FFWS consists of five hosting locations: primary and three backup server modules are installed in national institutions in the four Sava countries, while archive and web server in the Secretariat of ISRBC. The platform integrates Sava HIS – a system for collecting real-time hydrological and meteorological data from national networks, along with weather radar and satellite imagery from different sources, numerous weather predictions and hydrological and hydraulic models as well as outputs of existing national forecasting systems. One of hydrological models integrated is HEC-HMS model for the Sava River Basin (Sava HEC-HMS).

Sava HEC-HMS is recognized as backbone of the flood forecasting on the Sava River in the Sava FFWS system. The Sava HEC-HMS model was initially calibrated as event-based hydrological model on several selected periods, up to a six-month long, using rainfall and temperature from 74 meteorological stations and providing results on 140 locations. Calibration periods were mostly from the winter seasons characterized by average to high flow conditions. Dry and low flow episodes were not included in the used calibration periods. For calibration the observed inflow-outflow data and the volume curves for 20 reservoirs were used enabling a reasonable calibration in the relating submodels. In the operational mode within the Sava FFWS the lower reliability of Sava HEC-HMS was recognized during the continuous simulations. It was suspected that the way of the calibration was one of the reasons for less accurate simulations of the state of the model and forecasts. Also, given that the Sava FFWS currently collects real-time data from 209 meteorological stations through the Sava HIS, it was reasonable to expect that the improved density of the meteorological stations would result with the improved hydrological model. In general, meteorology introduces the greatest error and uncertainty to any hydrological model due to the uncertainty and randomness that is inherent to natural phenomenon, so in the Sava HEC-HMS model as well. In the reality, precipitation is highly variable spatially, temporally, and in intensity. The uncertainty associated with precipitation variability can be lessened through the use of observed meteorological stations, but never fully eliminated. Expectedly, meteorological uncertainty, both in precipitation and initial snowpack, presented the most significant challenge when performing the Sava HEC-HMS model calibration.

The initial Sava HEC-HMS model was updated without interventions on the hydrological modelling processes while the number of the measuring locations was significantly increased and the model parameters were assigned in the process of the calibration suitable for the continuous models. The process was jointly performed by the users of the Sava FFWS under coordination of the ISRBC.

The paper is organized in a way that the Flood Forecasting and Warning System for Sava River is presented in more details in Chapter 2 and the structure design of the HEC-HMS model for the whole Sava River in Chapter 3. The updated Sava HEC-HMS model is introduced in Chapter 4 together with the methodology and steps taken for the recalibration of its parameters. The results are presented in the Chapter 5 together with the conclusion remarks in Chapter 6.

Flood Forecasting and Warning System in the Sava River Basin

Sava FFWS is operating as an open shell platform for managing the data handling and forecasting processes trough the integration of the wide range of external data and models. This concept is particularly important for the cooperating countries, taking into account that the Sava River basin is shared by five countries where each country is using its own models, monitoring systems, forecasting systems, water authorities and interests.
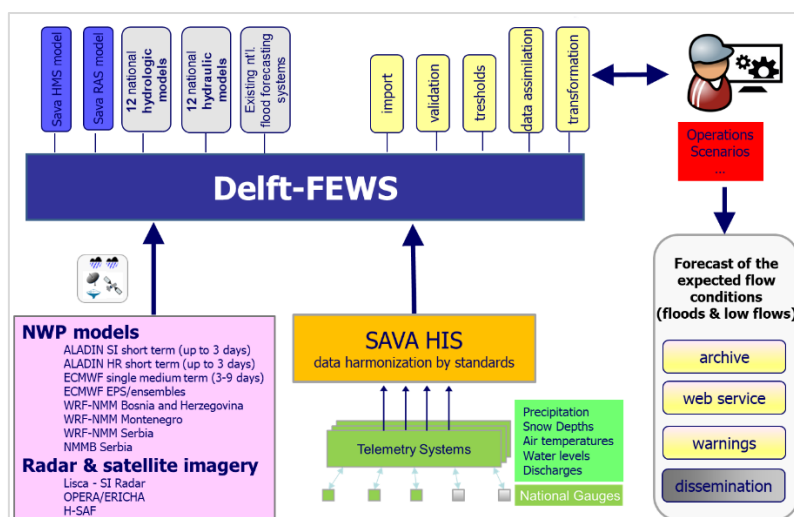
Fig. 1 Schematic overview of the Sava FFWS

Sava FFWS integrates and interconnects Hydrological Informational System for Sava River Basin (Sava HIS) – the data hub for the collection of real-time observed hydrological and meteorological data (precipitation, air temperature, snow, water levels, discharges); various Numerical Weather Prediction (NWP) models; available weather radar and satellite imagery; outputs of existing national forecasting systems and different hydrological and hydraulic models (Figure 1), including the Sava HEC-HMS model as the backbone of system.

Sava FFWS is hosted at five hosting locations: primary and three backup server modules are installed in national institutions in the four Sava countries while the archive and web server are located in the Secretariat of ISRBC. The system is in use simultaneously by several organizationally independent forecasting teams (Table 1). Given the open nature of the Sava FFWS environment, responsibilities for the output and the forecast dissemination within each country are very clearly defined in accordance with the national legislation.

Table 1 List of the Sava FFWS users and hosting organizations

Country	Institution	Note
Slovenia	Slovenian Environment Agency	Central server and User
Croatia	Croatian Meteorological and Hydrological Service	User
	Croatian Waters	3rd backup and User
Bosna and Hercegovina	Federal Hydrometeorological Service	User
	Sava River Watershed Agency	2nd backup and User
	Republika Srpska Hydro-Meteorological Service	User
	Public Institution "Vode Srpske"	User
Serbia	Republic Hydrometeorological Service of Serbia	1st backup / test system and User
	Public Water Management Company "Srbijavode"	User
Montenegro	Institute of Hydrometeorology and Seismology	User
	International Sava River Basin Commission	Archive / web server and Coordinator

An effective Sava FFWS has aim to bridge differences and supports collaboration in the field of hydrological forecasting keeping the countries own autonomy in monitoring, modelling and forecasting and remain open to developing its own models and supplementary forecasting initiatives (Figure 2). The system is assessed as added value to existing or developing systems, expecting that a common forecasting platform with well trained staff should provide better preparedness and optimized mitigation measures to significantly help reduce adverse consequences from floods, in future from droughts, ice hazards.
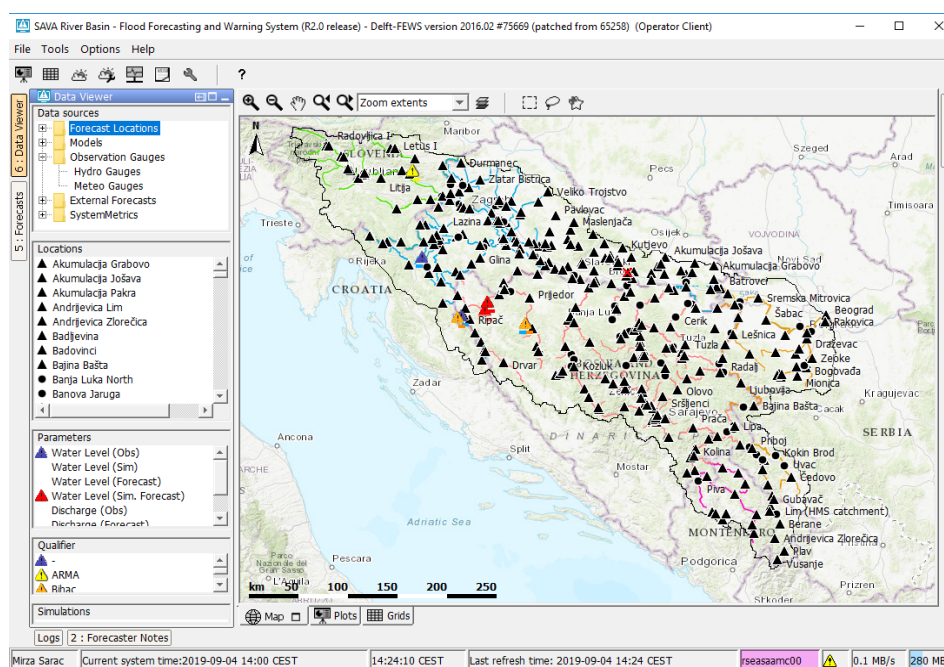
Fig. 2 Screen of the Sava FFWS operator client application (forecasting locations)

System for the collection of real-time observed hydrological and meteorological data – Sava HIS
ISRBC in cooperation with relevant national institutions from the Sava River basin, cooperating under the Framework Agreement on the Sava River Basin, in 2015 has established a joint platform Hydrological Information System for the Sava River Basin – Sava HIS, for the exchange and use of the hydrological and meteorological information and data. Sava HIS is established taking into account Policy on the Exchange of Hydrological and Meteorological Data and Information in the Sava River Basin. Sava HIS represents a tool for collecting, storing, analyzing, and reporting a sufficiently high quality hydrological and meteorological data. Sava HIS data and information are in use for decision-making system in all aspects of water resources management, in the wide range of operational applications as well as in research.

The main Sava HIS goals and objectives are to support the Sava countries, e.g. the beneficiaries in sharing and disseminating of hydrological and meteorological data, information and knowledge about the water resources in the Sava River basin and to enable an effective common channel for exchanging and viewing the hydrological and meteorological data and information in emergency situations, primarily those related to flood events (Table 2).

Table 2 Number of stations with the hourly (real-time) data exchange available in the Sava HIS / Sava FFWS

	BA	HR		ME	RS	SI	Totals
Hydrological stations	96	125		11	25	26	**283**
Meteorological stations	77	42		4	10	76	**209**

Since the Water ML 2.0 format is implemented in Sava HIS, as the WMO exchange standard via web service, the system enables storage of water observations data and spatial information, sharing by countries, in a standard format as well as supports data sharing and publication via web services for further use. Therefore ISRBC, with support of the Sava FFWS project, has started an upgrade of the Sava HIS for several new functionalities afterward Sava HIS get a very important role and become the data hub of real-time data collection in the Sava FFWS system.

It is very important to emphasize that Sava HIS is in use by countries not only for exchange of real time but also processed hydrological and meteorological data and metadata, including: spatial data (x, y coordinates of the location of the measuring stations); general data and metadata about measuring stations (organization, type, identifier); attributes of measuring data (data type, units, methods, accuracy, censoring, data quality); daily time series and statistics from historical data (Hydrological Year Books); monthly/yearly time series from discharge measurements data.

Models setup within the forecasting platform

The setup of Sava FFWS is modular where the combination of a numerical weather prediction and observations of precipitation and temperature, a hydrological model converting precipitation and temperature to discharge and, in most cases, a hydraulic model routing discharge downstream and computing water levels, define a unique forecast workflows. Due to the number of hydrological models, hydraulic models and numerical weather prediction models available for the Sava River basin, several forecast workflows are configured in the Sava FFWS. In case there was no hydrological model connected to a hydraulic model, the Sava HEC-HMS model covering entire basin is connected to deliver lateral flows.

In this moment 13 hydrological models are included in Sava FFWS where some of them are integrated models including hydraulic component. Some cover complete basin or a large area, others just small local river basins. HEC-HMS for the Sava River Basin and WFlow (BA, ME, RS) are models representing hydrological processes on the complete or the major part of the Sava basin. While Mike-NAM Sava (HR), Mike-NAM Una (BA/HR), Mike-NAM Vrbas (BA), HBV-light Bosna (BA), WFlow (ME), HEC-HMS Kolubara, HBV Kolubara and HBV Jadar (RS) are models with the local or national coverage.

Regarding hydrological modelling, the backbone of the Sava FFWS forecasting system represents the Sava HEC-HMS model, as the only hydrological model that covers the entire Sava River Basin. The model was developed by the U.S. Army Corps of Engineers, in close collaboration with ISRBC and national experts and initially calibrated as event-based model.

Development and update of the HEC-HMS model of the Sava River Basin (Sava HEC-HMS)

Initial Sava HEC-HMS model (version 1.0)

As part of the hydrological model development the Sava River basin was diverted into 20 separate basin models, including a basin model for each of the 17 major tributaries and three for the local areas along the main stem of Sava River (Figure 3). Sava HEC-HMS model consists of 235 subbasins, carefully selected to take the local hydrology into account, 174 junctions mainly located at the hydrological stations locations or locations of confluences and 158 river sections as well as 20 reservoirs.
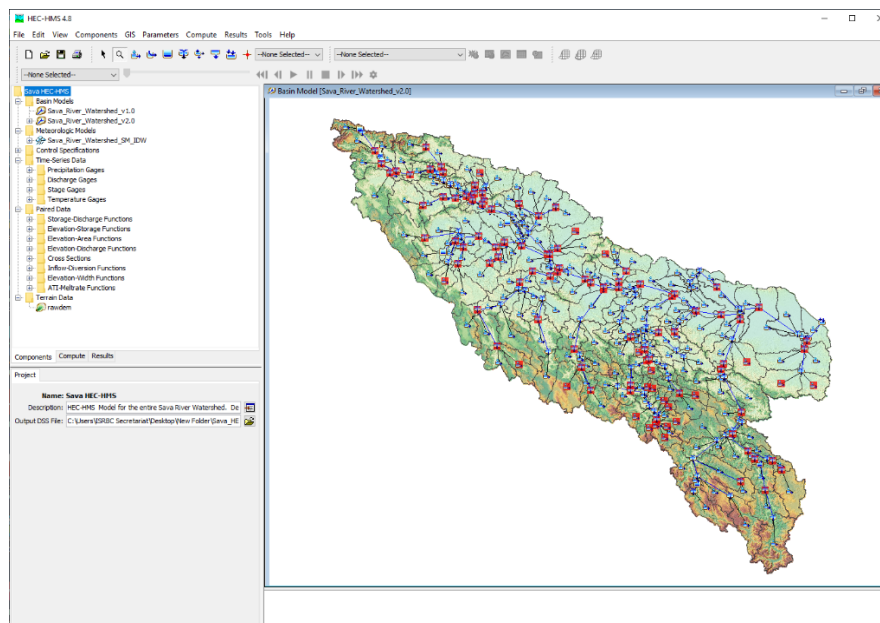

Fig. 3 HEC-HMS Sava Model structure

Sava HEC-HMS simulates hydrological processes through the meteorological and basin model working together to define the rainfall-runoff processes within the watershed.

The meteorological model provides precipitation in the form of rain or snow as input to the basin model, while the basin model uses input loss parameters to calculate precipitation lost to storage in the watershed, precipitation infiltrating into the soils, and the subsequent amount of excess runoff precipitation. Excess precipitation is routed to the subbasin outlet as overland flow using a unit hydrograph transform (Clark Unit Hydrograph) method. Precipitation infiltrating into the soil is routed to the subbasin outlet using the recession baseflow method. Overland flow and baseflow are combined at each subbasin outlet before entering the reach network. As the combined flow is routed down through the river reach network of the basin, flow is aggregated from additional subbasins and routing reaches in hydrological order.

The Sava HEC-HMS meteorological model

The meteorological model is the component of the Sava HEC-HMS model that represents the precipitation, both rainfall and snow, and is a required component for rainfall-runoff simulations. Evapotranspiration rates are also defined within the meteorological model where the Monthly Average method was utilized to represent evapotranspiration rates in the basin but also considering that the evapotranspiration is not a critical component for short-term simulations.

Hourly precipitation and temperature data at all available meteorological stations in period of the initial model development were integrated, 74 meteorological stations in total (rainfall and air temperature).

In addition to the relatively modest number of meteorological stations, within the Sava River Basin existed areas where precipitation input was very sparse. In an attempt to rectify the lack of observed precipitation in these areas, the Inverse Distance Weighting precipitation method (IDW) was applied. The IDW method calculates subbasin average precipitation by applying and inverse distance squared weighting all available precipitation gages in the user-specified search radius.

A dense coverage of stations exists in the headwaters of the Sava River Basin, mainly in Slovenia while there is a relative lack of stations in the middle and far downstream portions of the basin. Figure 4 illustrates the areas of the Sava River Basin with less meteorological station coverage showing every station with a 25 km radius buffer overlaying the basin delineation, and 50 km radius that was at the end used as a necessity. This was one of the main gaps of the initial model but a result of the real precipitation stations network coverage in the period of the model development.
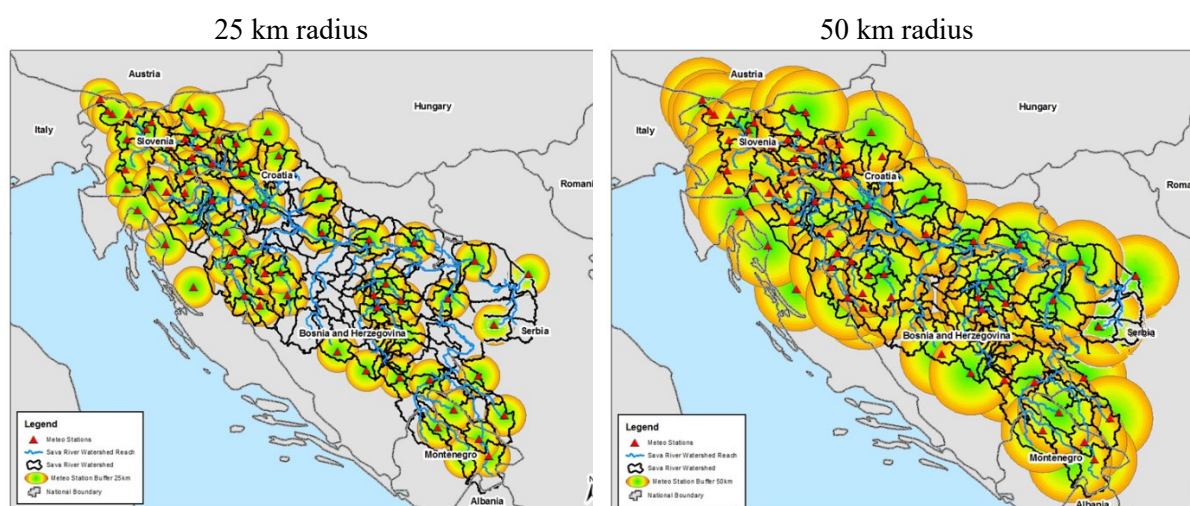
Fig. 4 Precipitation gauge coverage (Sava HEC-HMS v1.0)

In addition to precipitation in the form of rainfall, the meteorological model of the Sava HEC-HMS is configured to compute snow and snowmelt and for that purpose the temperature index method was used. The meteorological model, at every time step, whether the precipitation falling is rainfall or snowfall based on the temperature data at nearby meteorological stations. The temperature index approach considers snowmelt as a mass-balanced process. At the beginning of a simulation, the characteristics of an initial snowpack are established through the input of various parameters. When the simulation begins, precipitation falls as either rainfall or snow. Over the course of the simulation, the falling snow either builds the snowpack or warming occurs, as defined by the representative air temperature gauge, and the

snowpack melts and is converted to runoff for the specific subbasin. The temperature index method also considers the effects of rainfall on the snowpack and determines the runoff volume resulting from the melting process initiated by rain falling on the snowpack. The temperature index method uses a multitude of parameters to define the snowfall, rain on snow, and snowmelt components of the hydrological process.

Available snow-related data in the Sava River Basin are very limited, therefore the most parameters for the snowmelt method were established from the related studies and the consultation of USACE snow experts.

Initial snow-water-equivalent (SWE) values and elevation band parameters were developed through GIS processes on available data. Determining SWE is important parameter for defining the potential runoff volume of the snowpack. Daily Advanced Microwave Scanning Radiometer (AMSR-E)/Aqua Level 3 global snow water equivalent grids were compiled from the National Aeronautics and Space Administration's (NASA) National Snow and Ice Data Center (NSIDC) in Boulder, Colorado USA (Tedesco et al. 2004).

Due to the large grid size of the SWE grids, the accuracy of this method is uncertain. However, the satellite-based SWE grids were the best available data at the time of model development.

Elevation bands, which are input into the meteorological model to account for the differences in snowfall and snowpack across the range of elevations in each subbasin, were developed as the elevation-area relationships using the SRTM DEM. These elevation-area relationships were segmented at natural breakpoints in the topography to define the elevation bands for each subbasin. For each defined elevation band, initial snowpack parameters were required to define any snowpack that may be present at the beginning of the hydrological model simulation. The aforementioned AMSR-E SWE grids were used to define the initial SWE for each elevation band within each subbasin.

The Sava HEC-HMS basin model

Using GIS module of the HEC-HMS software package, a detailed subbasin delineation and river network were produced from SRTM digital elevation map with 30 meter resolution (Rodriguez et al. 2005).

The Sava HEC-HMS basin model consists of 235 analytical units carefully selected to take the local hydrology into account (Figure 5). A unique local characteristic in Sava River basin is the presence of karst which affects the subbasins boundaries and the parameterization of the subbasins. For some specific areas like karst geology, levees, and canals especially in the flatter areas of the basin SRTM DEM needed to be manually manipulated.
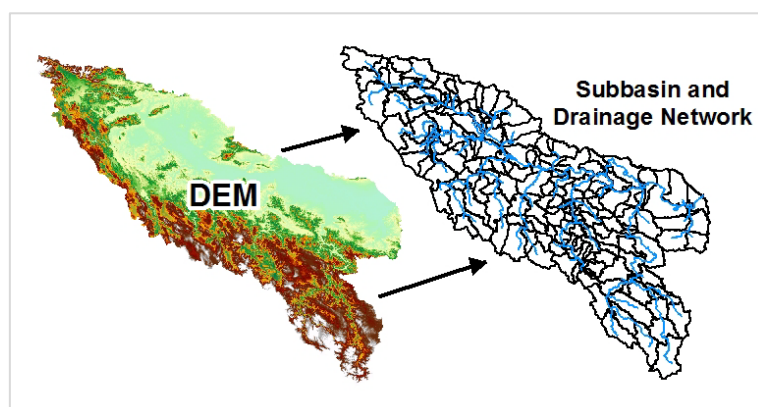
Fig. 5 Illustration of the SRTM DEM conversion to subbasin and river network

SRTM DEM and the GIS module of the HEC-HMS were also used to generate the physical parameters of the Sava River basin such as drainage area, stream lengths, basin slopes, etc. From these physical parameters, initial estimates of unit hydrograph parameters, time of concentration and storage coefficient were developed for each subbasin. Reach routing parameters, such as reach slope and length, were also extracted.

The Sava HEC-HMS implements various methods to represent the rainfall-runoff processes of the basin of interest. Various factors contributed to the decision for each of the modeling component methods Sava River Basin such as applicability of the method based on specific basin characteristics (such as terrain and urbanization) and availability of data supporting a specific method. The decision to use these methods were based on:

- Simple Canopy Method – chosen for its simplicity due to a lack of available data defining the canopy.
- Deficit-Constant Soil Loss Method – chosen based on the success of this method for large basin studies such as the Sava River Basin. The method provides the ability to simulate soil moisture characteristics throughout an event using easily derived and calibrated parameters. In addition, is the method used for most major flood forecasting models within USACE.
- Clark Unit Hydrograph Transformation Method – chosen based on its ability to be estimated using available terrain data and the successful implementation of this method across modeling studies within USACE. The parameters for this method are also fairly easy to calibrate especially in situations where discharge stations are relatively abundant such as in the Sava River Basin. In addition, this method has shown to be very effective in representing the timing and shape of flow hydrographs through varying magnitudes and volumes of floods.
- Recession Baseflow – chosen for its simplicity and its ease of application.
- Muskingum-Cunge Reach Routing Method – chosen because it primarily based on physical characteristics of the routing reaches which can be attained from the available information. This method has been widely used within USACE and provides the ability to represent the flow hydrograph translation and attenuation in situations with varying levels of floodplain storage.

The parameters used to define the hydrological model are described in more detail below and a summary of the various basin parameters is provided along with the basin modeling methods developed within the Sava HEC-HMS (Table 3). These parameters were the subject of the model calibration.

Table 3 Summary of the Sava HEC-HMS basin model parameters

Modeling Method		Parameter	Description and representative values in the model v1.0	
Canopy Storage	Canopy	Initial Storage	Initial storage in canopy	100%
		Max Storage	Maximum storage in canopy	2–50mm
Soil Losses	Deficit Constant	Initial Deficit	Initial condition for the soil layer. Amount of water required to saturate the soil layer	0–35mm
		Maximum Deficit	Maximum amount of water the soil layer can hold (30–75mm)	
		Constant Loss	Percolation rate of the soil layer	0,1–2,25mm/hr
		Percent Impervious Area	Percent of the subbasin that is covered by directly connected impenetrable surfaces such as concrete, rooftops, and urban development	0–53,8%
Hydrograph transformation	Clark Unit Hydrograph	Time of Concentration	Travel time from the most hydrologically remote point in the subbasin to the watershed outlet	0,2–50hr
		Storage Coefficient	Conceptual parameter representing basin's storage capacity	0,7–160hr
Baseflow	Recession Baseflow	Initial Baseflow	Baseflow at the beginning of the simulation	$0,001–0,621 m^3/s/km^2$
		Recession Ratio	Rate at which baseflow recedes between events	0,72–0,98
		Threshold Ratio	Flow at which the baseflow is reset.	ratio to the peak
Reach routing	Muskingum–Cunge Routing	Length	Length of reach	0,22–106,16km
		Slope	Slope of reach	0,00001–0,0196m/m
		Manning's n-Values	Roughness coefficient for the channel, left overbank, and right overbank	0,02–0,05
		Shape	Shape of the routing reach cross section	8-point or trapezoidal

The Sava HEC-HMS model was initially calibrated as event-based model on several selected periods; the periods were up to a six-month long in period 2009–2015. These calibration periods used were mostly the winter seasons and characterized by average to high flow conditions. Dry and low flow episodes were not included in the used calibration periods. For calibration the observed inflow-outflow data and the volume curves for 20 reservoirs were used and enabled a reasonable calibration in the relating sub-models.

During its development, the model was forced by 74 meteorological stations (rainfall and temperature) to provide results on 140 locations.

Updated Sava HEC-HMS (version 2.0)
Since the Sava HEC-HMS was initially calibrated as event-based model using hourly data values, the lower reliability was recognized during the continuous simulations in the operational mode within the Sava FFWS. Regularly performed simulations of the Sava HEC-HMS model coupled with NWP data in Sava FFWS shows that the model has a strong reaction to moderate amounts of rain and produce untimely and overestimated forecasts. Reasons for a such behavior of the model are the modelling methods initially selected (Table 3) e.g., soil loss method which is not capable of long-term soil moisture accounting, but also due to meteorological data availability and coverage, snow data availability as well as the reservoirs regulation at various dam.

Any intervention on the robust and complex model like Sava HEC-HMS which is in use by many experts per different institutions and countries has to be done in well organized and coordinated way. After a joint agreement of the expert team that the initial model needs to be updated with the new information, the action plan has been made to upgrade the model with new measuring locations and to perform the recalibration of the model parameters. The expected goal was that the new precipitation and air temperature data would complement the existing spatial and temporal accuracy of the meteorological component of the model.

Meteorological inputs are typically the greatest limitation in any hydrological model because meteorology is such a random and natural phenomenon. The IDW method, used to model precipitation in the Sava HEC-HMS, relies heavily on the location and density of stations because the precipitation applied at any given subbasin is computed by interpolating between measured precipitation values at these stations. If the spacing between stations is too great, a storm could pass between two stations and not be recorded at either station, which means that the Sava HEC-HMS would not register this event and apply the proper precipitation to the subbasins between the stations. In addition, if a rainfall event does not pass over enough stations to capture the shape and volume of the rainfall, the model will not accurately apply precipitation to the adjacent subbasins. These inherent limitations exist for all meteorological models relying on point stations, which is why acquiring the best available data and quality controlling this data is critical to the performance of the Sava HEC-HMS model as well. The two immediate solutions are increasing the density of stations in areas with limited or insufficient coverage and/or incorporating radar-based gridded precipitation data into the model. For a robust flood forecasting system such as Sava FFWS, incorporating both gauge- and radar-based precipitation is the best solution to create redundant data sources and to protect against one of the source data feeds failing. Radar-based precipitation has become a standard data source for hydrological models across the world because it solves the issue of spatial coverage of precipitation data that exists with readings at meteorological stations. As with any measurement, raw radar-based data possesses some level of uncertainty and must be verified and corrected to measurements made at standard single-point meteorological stations further emphasizing the need for ground stations. In spite of this uncertainty, radar-based data, when processed through proper quality controls, provides the spatial and temporal distribution of precipitation data necessary for large, complex hydrological models such as the Sava HEC-HMS. The European National Meteorological Services Network (EUMETNET), with members from the European Union and Balkans, collaborate and produce network-wide radar mosaics through the Operational Program for Exchange of Weather Radar Information (OPERA), which could provide a source of radar-based nowcasting information for the Sava River Basin. As mentioned in the Chapter 2, along with NWP data, Sava FFWS is prepared to extrapolate radar or satellite imagery in order to provide a very accurate short-term hydrological forecast (nowcasting) for several hours in advance based on measured values. Nowcasting products are currently not available within the Sava basin and the

existing radars are currently still not able to produce accurate rainfall images. Considering the importance of providing a such input and raising the awareness of experts to this type of precipitation data, the Lisca radar data (Slovenia) are implemented Sava FFWS, next to Opera radar composite images and H-SAF satellite images (Figure 6).

Lisca radar	OPERA	H-SAF

Fig. 6 Available radar and satellite images in the Sava River Basin integrated under Sava FFWS

However, considering that radar- and satellite-based images are only displayed within the system but are not connected to any of the hydrological models neither to the Sava HEC-HMS, it was decided to update the model in this stage to include the new hydrological and meteorological inputs and recalibrate Sava HEC-HMS without changing the structure of the model. Challenging work resulted with an improved Sava HEC-HMS model more suitable for continuous hydrological simulations needed for accurate process of the flood forecasting in Sava FFWS system.

Important step, beside technical interventions on the model, was managing and coordination of all activities and to apply consistent methodology since many Sava countries experts were involved in this process. The applied methodological approach consisted of the following steps: (1) preparation of the necessary technical documentation and time plan for the work of national experts; (2) inclusion of the new hydrological and meteorological stations to the model; (3) collection of historical hydrological and meteorological hourly data for the period from 2010 to 2018; (4) uploading of the collected data to Sava HIS/Sava FFWS Archive module; (5) enhance the model components; (6) calibration and validation the new model setup and (7) hindcast analysis and validation of the operability performances of the model through the Sava FFWS testing module including comparison of different model versions.

A first step of the model enhancement was related to increase of the number of precipitation and temperature data inputs at all available meteorological stations. In total 258 meteorological stations for precipitation and temperature data inputs are currently available in the Sava HEC-HMS v2.0 as well as 151 hydrological stations for the observed discharge data presentation and the purpose of comparison with the simulated runoff. From the total number of stations integrated in the model, data were collected for a part of stations that have regular and hourly measurements of precipitation, air temperature and discharge (Table 4), representing an increase of 125 meteorological and 41 hydrological stations compared to the initial setting of the model (Figure 7).

Table 4 Number of stations per countries available in Sava HEC-HMS v.2.0

Type of the station / parameter		BA	HR	ME	RS	SI	Totals
Hydrological stations	*Discharge*	96	125	11	25	26	**134**
Meteorological stations	*Precipitation*	41	49	3	10	96	**199**
	Air temperature	41	27	3	8	18	**96**

For all measuring locations (Table 4), hourly data were successfully collected for the period from 2010 to 2018 and uploaded to Sava HIS and Sava FFWS archive, which were later used for validation of the model and hindcasting.
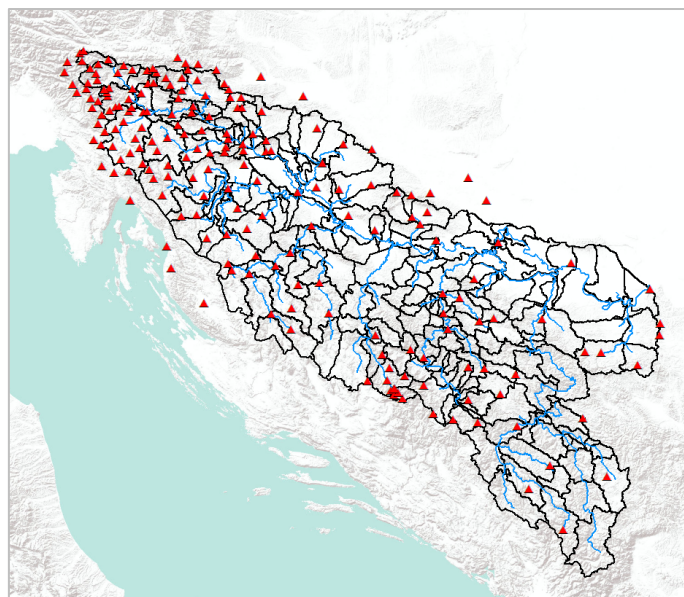
Fig. 7 Precipitation gauge coverage (Sava HEC-HMS v2.0)

The greatest number of the new meteorological stations integrated under Sava HEC-HMS v2.0 are located in the central part of the basin while the number of the stations in the upper and lower parts was not changed significantly. Following the model configuration enhancements along with integration of the new measuring locations and their historical data the model was recalibrated. Different approach to the calibration was mainly dependent on the calibration skills of the expert team members. The calibration of the parameters in the initial Sava HEC-HMS v1.0 model was performed for the six short periods related to the flood events between 2009 and 2015. The updated v2.0 model has been calibrated and primarily validated using different periods per subbasins while additional two validations of the model were performed for period 01Jan2014-31Dec2014 and 01Jan2016-31Dec2016.Work performed on calibration and validation of the Sava HEC-HMS model v2.0 was jointly agreed and distributed among the team members considering responsibility of each organization but also the model structure, capacities and expertise of individuals and a rule of equivalence as well, so activities were divided per subbasins and countries. Most of data and information used for model improvement was provided by the national organizations involved in the activity. Each organization has provided input time-series data for the stations in its responsibility despite the distribution of work related to calibration and validation of the model. A substantial amount of data was collected as part of the initial model development efforts. The period from 2010 to 2018 was divided into sub-periods where one was used for the calibration and others for the validation of the Sava HEC-HMS v2.0 model. In the end three validation procedures were performed given that the calibration and first validation were done per subbasins while additional two validations were performed for the entire model.

The model calibration was performed at 107 calibration points i.e., 32 more compared to the initial model.

For the determination of the model parameters two approaches were used: trial-and-error method and the built-in automatic calibration procedure of HEC-HMS software. The goodness of fit for each model parameter was evaluated based on the *Nash-Sutcliffe* efficiency coefficient. For both calibration approaches the hydrograph volume, peak discharge and timing of the peak were also monitored. In order to ensure the model's ability to represent these characteristics, three metrics were analyzed during the calibration simulations at various locations.

Table 5 Calibration and validation metrics used for the Sava HEC-HMS calibration process

Percent Difference in Peak Discharge (Q_P)	$Q_P = \dfrac{Q_P^{sim} - Q_P^{obs}}{Q_P^{obs}} \cdot 100\ (\%)$
Percent Difference in Runoff Volume (V_R)	$V_R = \dfrac{V_R^{sim} - V_R^{obs}}{V_R^{obs}} \cdot 100\ (\%)$

Nash-Sutcliffe Coefficient (NSE)	$NSE = 1 - \dfrac{\sum(Q_n^{sim} - Q_n^{obs})^2}{\sum\left(Q_n^{obs} - \overline{Q}^{obs}\right)^2}$
Root mean square error to Standard deviation of observations Ratio (RSR=RMSE/Std)	$RSR = \dfrac{RMSE}{Std^{obs}} = \dfrac{\left[\sqrt{\sum(Q_n^{obs} - Q_n^{sim})^2}\right]}{\left[\sqrt{\sum(Q_n^{obs} - \overline{Q}^{obs})^2}\right]}$
Coefficient of determination (R²)	$R^2 = \left[\dfrac{\sum(Q_n^{obs} - \overline{Q}^{obs})(Q_n^{sim} - \overline{Q}^{sim})}{\sqrt{\sum(Q_n^{obs} - \overline{Q}^{obs})^2}\sqrt{\sum(Q_n^{sim} - \overline{Q}^{sim})^2}}\right]^2$

where Q_P^{sim} and Q_P^{obs} are simulated and observed peak discharges, respectively; V_R^{sim} and V_R^{obs} simulated and observed total runoff through the simulation period, respectively; Q_n^{sim} and Q_n^{obs} simulated and observed discharges at time step *n*, respectively and $\overline{Q}_n^{obs}$ average observed flow. These metrics provided an overall measure of the numerical performance of the model's ability to capture all characteristics of the outflow discharge hydrographs, which incorporates peak, volume, timing, and shape.

In addition to these three metrics, calibration plots depicting the time series discharge hydrograph output versus the observed discharge hydrograph were also analyzed. The calibration plots provided an effective visual illustration of the performance of the model and were monitored using HEC-HMS, as well as the graphical user interfaces of Sava FFWS.

Results and discussion

The main improvements of the Sava HEC-HMS calibration process included: (1) improvements of the meteorological inputs with higher spatial and temporal data coverage for precipitation and air temperature; (2) some corrections of the meteorological model of snow melting; (3) increased number of calibration points; (4) increased number of calibrated sub-basins, up to 98 from initial 66; (5) longer time series of discharge observations; (6) new version of the Sava HEC-HMS model integrated under the Sava FFWS testing module.

The model skill was evaluated using NSE on the period from 2010 to 2018 and about 50% of stations score a NSE greater than 0.55 (rates: good and very good), while a higher percentage of stations score a NSE greater than 0.40 (rate: satisfactory). The higher NSE scoring was achieved in the upstream parts of the basin and along the Sava river. The new model accuracy and NSE increased in comparison to the initial model.

During the calibration process, it was noticed that the change of the model parameters would not necessarily lead to the better performance of the updated model, therefore the parameters for some computation points and accompanying subbasins have not been changed. This was the case on the parts of basin where new input data have not been changed. The changes were needed on areas where new input data were available and mainly in the module for the direct runoff transformation to decelerate and attenuate the simulated hydrographs. In the baseflow module change has been made on the recession constant that needed to be increased together with the ratio to peak parameter. In the karstic area e.g., the upstream part of the Bosna River subbasins, it was necessary to increase the soil percolation rate and initial loss. All these changes were expected having in mind a transition from the event-based to the continuous model. Statistical analysis of the performance metrics, from the initial and the updated model achieved on 87 locations, where two models were possible to compare, has been done using one and two-tailed t-test and Mann-Whitney test (Table 6). The test results are showing that there is no significant statistical difference between NSE values for the two models and that the NSE value for the updated value is greater than the initial model. In the case of root mean square error-observations standard deviation ratio (RSR=RMSE/Stdev), the p-values are indicating that statistical difference between the two models exists and that the RSR for the updated model is lower than for the initial model. R^2 is not showing a clear signal whether the updated model is better than the initial one.

Table 6 Statistics for the performed one-tailed and two-tailed t-test and Mann-Whitney test based on simulations of the two models versions

| Model performance metrics	t-test (α=0.050)		Mann-Whitney test (α=0.050)	
	one tailed	two tailed	one tailed	two tailed
NSE	0.046	0.092	0.002	0.004
RSR	0.009	0.019	0.001	0.003
R²	0.292	0.584	0.244	0.489

Following the statistics, a comparison between the initial and updated model has been performed. The Nash-Sutcliffe efficiency coefficient values, used for evaluation of the numerical model performance were greater than 0.55 for more than 50% of locations classifying the model as good and very good in the calibration period. Most of the rest of NSE values are greater than 0.4 meaning that the model is in the class of the satisfactory models.

In this paper 11 selected location (Table 7) were used for an analysis of the numerical goodness of fit for two periods. For the basin parts where, new meteorological stations have been installed the model performance has increased while the other subbasins record the same or lower values of NSE.

*Table 7 Performance metrics of the initial (v1.0) and updated (v2.0) Sava HEC-HMS model for two periods using the general performance ratings: **Very Good**; Good; Satisfactory; Unsatisfactory (Moriasi et al, 2007)*

Up to down-strem	Computation point (hydrological station)	01Jan2014 – 31Dec2014				01Jan2016 – 31Dec2016			
		Model v.1		Model v.2		Model v.1		Model v.2	
		NSE	RSR	NSE	RSR	NSE	RSR	NSE	RSR
10	J_01_08_03_Lasko	−0,03	1,01	0,57	0,65	−0.39	1.18	0.71	0.54
16	J_01_13_11_Jesenice	0,65	0,59	0,76	0,49	0.69	0.56	0.80	0.45
18	J_04_02_05_Kupljenovo	0,41	0,77	0,43	0,76	0.28	0.85	0.33	0.82
31	J_06_10_06_Farkasic	0,61	0,62	0,65	0,59	0.67	0.58	0.68	0.57
39	J_12_02_04_Kralje	0,45	0,74	0,55	0,67	0.68	0.56	0.79	0.46
48	J_14_01_02_Daljan	−1,02	1,42	−0,18	1,08	−3.38	2.09	−0.04	1.02
67	J_20_19_06_Maglaj	0,82	0,43	0,70	0,55	0.56	0.66	0.46	0.74
75	J_24_01_02_Bijelo Polje	−1,50	1,58	0,06	0,97	−0.22	1.10	0.67	0.57
82	J_27_01_04_Sr. Mitrovica	0,74	0,51	0,72	0,53	0.77	0.48	0.80	0.45
85	J_28_03_01_Beli Brod	0,59	0,64	0,59	0,64	0.28	0.85	0.15	0.92
87	J_28_03_05_Drazevac	0,03	0,98	−0,58	1,26	0.39	0.78	0.51	0.70

In addition to analysis of the numerical model performance the calibration plots, as an effective visual illustration of the model performance, depicting the simulated discharge hydrograph versus the observed discharge hydrograph, were also monitored (Figure 8). Analyzing results at the selected computation points an improvement in the matching of the simulated and observed hydrograph was obvious although parameters during the recalibration for some locations have not changed significantly (Farkašić). Also for some locations (Bijelo Polje) the initial model was not able to perform the simulated hydrograph at all, while the Sava HEC-HMS v2.0 compute it successfully. The overall hydrograph matching is also slightly better, as a result of the model inputs improvements and calibration that was carried out for a long-term period, unlike the initial model.

Sava HEC-HMS v1.0   Sava HEC-HMS v2.0
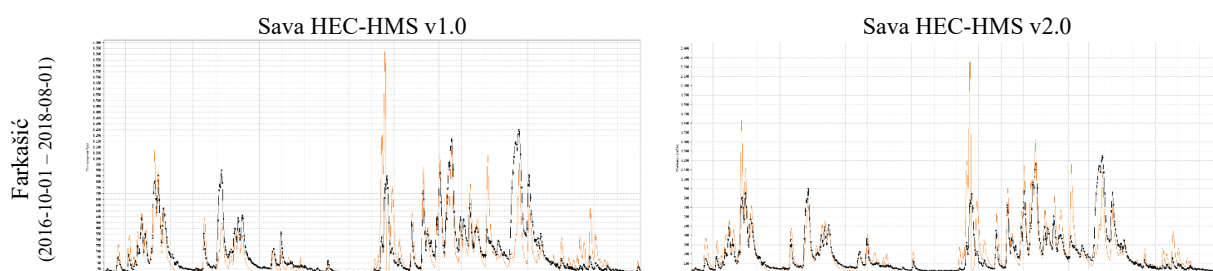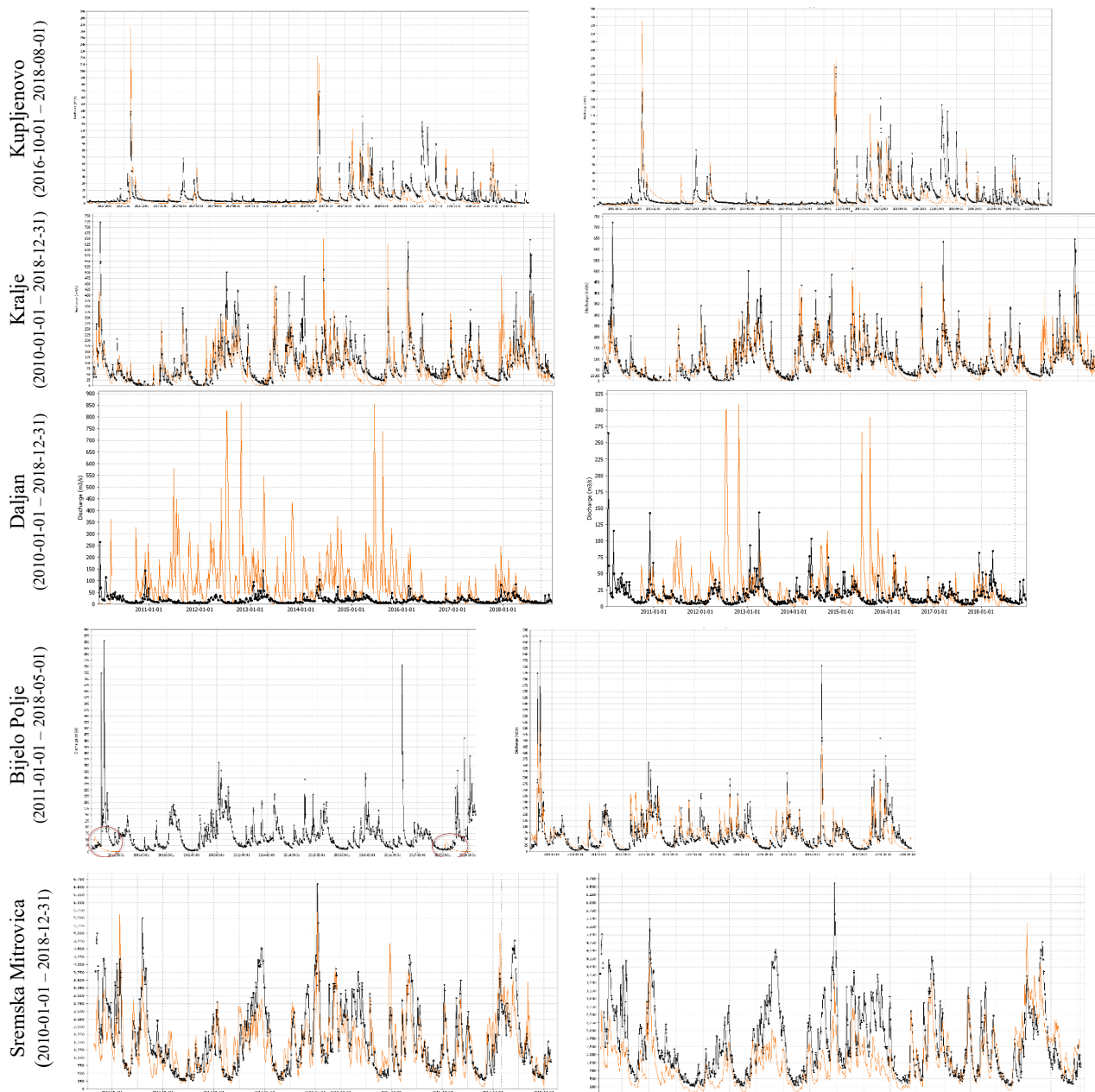
Fig. 8 Comparison of the simulated (orange) and observed (black) flow at the selected locations (source: Sava FFWS)

The added value in the updated model was recognized in the better fitting of timing of the peak and the peak value itself but also in the better fitting of low and mean flows. Good example of the peak fitting can be seen at the computation point: J_20_19_06_Maglaj (Figure 9) and where peaks are better simulated in the updated model.
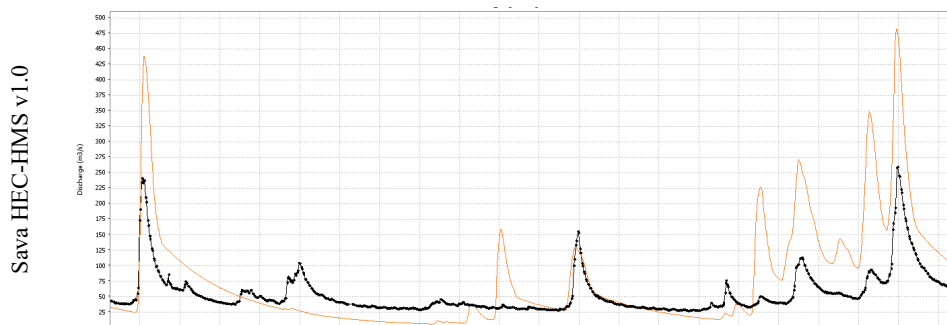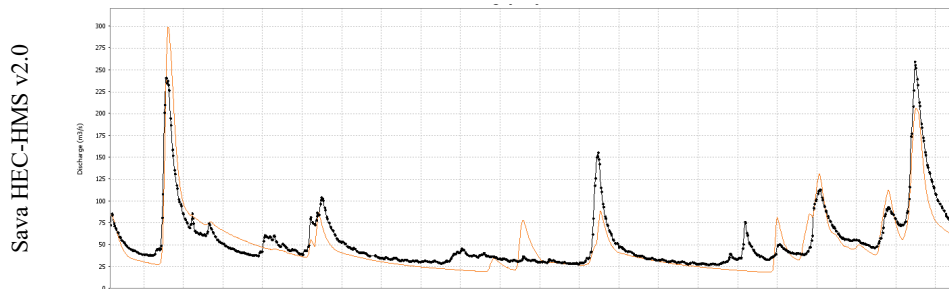
Fig. 9 Comparison of the simulated (orange) and observed (black) flow at the location Maglaj (source: Sava FFWS)

Good example of the peak but also low and mean flows fitting can be seen at the computation point: J_01_13_11_Jesenice (Figure 10) showing that data are better simulated in the updated model.
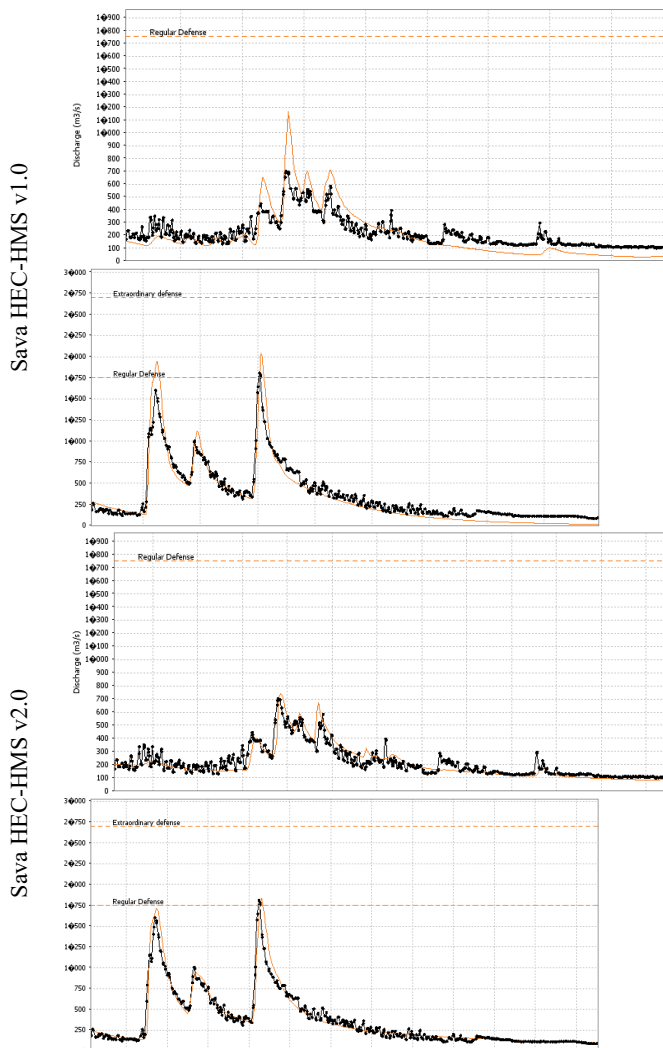

Fig. 10 Comparison of the simulated (orange) and observed (black) flow at the location Jesenice na Dolenjskem (source: Sava FFWS)

After the performed calibration of the Sava HEC-HMS model a conclusion was that the common snow model parameters are not suitable for all the tributaries subbasins since the periods where the snowmelt occurs are poorly modeled by both versions of the model. It was concluded that the snow model should be separately calibrated using the more accurate (observed) snow data. Due to the lack of in-situ measurements of stream discharges there is always a doubt whether the rating curve (discharge vs stage) of observed data is properly developed in the high flow range and the observed flow is over or underestimated and whether comparison of the simulated and observed values is reliable.

Conclusions and recommendations

The hydrological simulations were conducted for the period 2010–2018 including extreme May 2014 flood and several smaller floods, with evaluation of daily mean hydrological conditions and processes. The main findings are as follows: (i) performance and forecast accuracy of the existing Sava HEC-HMS model was significantly improved; (ii) the model was (re)calibrated for both high flows (for accuracy) and low flows (for stability and model performance); (iii) data sources for further developments were improved; (iv) a solid background for an international team of experts was established.

Considering that the Sava FFWS users have access to all data and workflows as well as managing the functioning and further developments of the system, it was very important that the national experts were fully involved in the study. Therefore, joint work and close cooperation of the national experts (duty forecasters) should be emphasized as an additional achievement, as follows: (i) experts deeply familiarized with the HEC-HMS software capabilities as well as with methods and techniques implemented into the Sava HEC-HMS model; (ii) upgraded own knowledge how to calibrate a such model; (iii) recognized all benefits of the model, its limitations and possible future applications; (iv) much more prepared for using this model under the Sava FFWS.

After performed activities and obtained results, the following recommendations are suggested: (i) development of a more complex soil loss method capable of long-term soil moisture accounting; (ii) a more detailed analysis of snowmelt within the model necessary (snow data availability); (iii) reservoir regulations at dams through the incorporation of a reservoir regulation model component (HEC-RESSIM). The future updates should utilize remote sensing data inputs for the soil moisture accounting, snow melting, reservoir regulating as well as other specific applications in the Sava HEC-HMS. For future recommendations, the incorporation of high-resolution grid-based snow water equivalent and precipitation data, as well as the placement of additional meteorological stations in areas currently lacking observed data, will serve to improve performance of the model. Application of available products of missions like Sentinel, Landsat, AVHRR (Advanced Very High Resolution Radiometer), MODIS (Moderate Resolution Imaging Spectroradiometer), AMSR-E (Advanced Microwave Scanning Radiometer-Earth Observing System), DMSP (Defense Meteorological Satellite Program) in the Sava HEC-HMS will be explored. The great potential of remote sensing data application is in general evident, both for the calibration of hydrological models and for operational hydrological forecasting, as well as for filling the data in catchments without observations or with an insufficient network of measuring stations and therefore will be used in the further Sava HEC-HMS model and Sava FFWS improvements including the related adaption of the modelling methods especially related to a rapid work of HEC and all latest developments of the software.

Acknowledgements

References

US Army Corps of Engineers, International Sava River Basin Commission (2017) Sava River Basin Flood Study: HEC-HMS Technical Documentation Report.

US Army Corps of Engineers, Hydrologic Engineering Center (2021), Hydrologic Modeling System HEC-HMS – Technical Reference Manual, web edition: https://www.hec.usace.army.mil/confluence/hmsdocs/hmstrm.

Deltares (2018) Sava Flood Forecasting and Warning System, Technical Reference Manual.

H. L. Zhang et al. (2013) The effect of watershed scale on HEC-HMS calibrated parameters, *Hydrology and Earth System Sciences*, **17**, 2735–2745.

Rodriguez, E., Morris, C. S., Belz, J. E., Chapin, E. C., Martin, J. M., Daffer, W. and Hensley, S. (2005) An assessment of the SRTM topographic products, 143 Technical Report JPL D-31639, Jet Propulsion Laboratory.

Moriasi, D.N., et al. (2007) Model Evaluation Guidelines for Systematic Quantification of Accuracy in Watershed Simulations, *Transactions of the ASABE*, **50**, 885–900.

International Sava River Basin Commission – ISRBC (2004), Framework Agreement on the Sava River Basin.

International Sava River Basin Commission – ISRBC (2010), Protocol on Flood Protection to the Framework Agreement on the Sava River Basin.

Ice monitoring and forecasting practices in the Danube River Basin

Klaudia SZABO[1], Eva KOPACIKOVA[2], Valeria WENDLOVA[3], Daniel HARABA[4], Zuzana HIKLOVÁ[5]

[1] General Directorate of Water Management, Hungary, email: szabo.klaudia@ovf.hu, [2,3] Slovak Hydrometeorological Institute, Slovakia, email: eva.kopacikova@shmu.sk, email: valeria.wendlova@shmu.sk, [4,5] Slovak Water Management Enterprise, state enterprise, Slovakia, email: daniel.haraba@svp.sk, email: zuzana.hiklova@svp.sk

Introduction

Within the framework of the DAREFFORT (Danube River Basin Enhanced Flood Forecasting Cooperation) project, an international initiative between the Danube River Basin countries came into being aiming to mitigate flood risk on the catchment level and support knowledge exchange and sharing of best practices within the Danube Basin. E-learnig materials were delivered for educational institutes, experts of national and regional authorities and non-professionals to facilitate the knowledge exchange. In the course of this activity an overview of the ice monitoring and forecasting practices in the Danube River Basin has been carried out. In this paper we'd like to present the findings of the acquired knowledge about the applied practices.

Methodology

Due to climate change, rising winter mean temperature and water temperature in Central Europe implied a considerable decrease in the number of ice cover days on the Danube river in the second half of the 20th century (Ionita et al., 2018). Beside the increase in the temperatures, the regulatory activities changed the ice regime of the Danube as well (ICPDR, 2018). However during a severe winter, when meteorological conditions favour ice formation, various forms of ice can evolve on our rivers. Monitoring and forecasting of ice phenomena is important, since in case of ice floods, ice reduces the water transport capacity of the given river section and damming increases the rate of the water level rise above the section. With an accurate forecast the risks of river ice related flooding could be reduced.

In the Danube Basin national hydrological services are responsible for monitoring the ice cover along the main flow of the Danube River and its navigable tributaries. To retrieve information on the applied practices, questionnaires were prepared during the implementation of the DAREFFORT project where, among other topics, information provided concerning ice events and availability of ice maps was also covered. Table 1 gives an overview on what kind of information on ice events is provided by the countries. It shows that almost all countries provide information on ice to some extent. Usually the percentages of surface covered by ice, the type of ice event, thickness of ice cover and duration of ice cover is granted by the consulted countries. Hungary is the only country where additionally an ice map is also provided. In Slovenia the hydrological service does not monitor river ice cover, nor prepares ice forecast. In Bulgaria the type of ice phenomenon is reported daily in case of ice events. Austria and Czech Republic indicated in the questionnaire that they do not prepare ice event reports, although they provide information on duration of ice cover.

Table 1 Information on ice events reports (DAREFFORT O.3.1, 2019)

Country	Ice events report	Information provided on ice events			
		Percentage of surface covered by ice	Thickness of ice cover	Duration of ice cover	Type of ice event
Austria (Lower Austria)	No				

Bosnia and Herzegovina	Yes	x			
Bulgaria	Yes				x
Croatia	Yes		x	x	
Czech Republic	No				
Germany	Yes			x	
Hungary	Yes	x	x	x	x
Moldova	Yes		x	x	x
Romania	Yes	x	x	x	
Serbia	Yes	x	x	x	
Slovakia	Yes	x	x		
Slovenia	No				
Ukraine	Yes	x	x	x	

In the course of the project, participating countries also carried out reports on their flood and ice forecasting methodologies. In four countries (Croatia, Hungary, Slovakia, Ukraine) more information was available on the applied methods, so river ice monitoring and forecasting practices are presented in more depth through the example of these countries (DAREFFORT O.5.4, 2020).

Croatia
Croatia does not collect ice data regularly. At hydrological stations, where an observer is available, if ice is detected the observer records ice phenomena in the daily reports. The observation is conducted without a use of an instrument. Information is stored in a databse along with the temperature data with the following classifications: ice at river bank, moving ice or complete ice cover. Croatian Waters possesses data on ice events, such as like ice cover thickness and duration of ice cover in report form which is not available online.
Croatia does not forecast ice phenomena in general. However the Croatian Meteorological and Hydrological Service (DHMZ) developed a hydrological model for navigation purposes for the Croatian section of the Danube River in the framework of the FAIRWay Danube project. In the model a 'Possible ice' warning is issued for the next 5 days for 9 hydrological stations on the Danube and for 2 stations on the Drava. The warning is issued when the predicted water temperature approaches zero. The model is available at The Agency for Inland Waterways and maintained by DHMZ.

Hungary
Observation, measurement and forecasting of ice are well organized in Hungary since the most devastating floods on the Hungarian section of the Danube were caused by ice jams (Lászlóffy, 1934). Monitoring and recording of ice phenomena of the main watercourses are carried out for decades by the Regional Directorates of Water Management under the direction of the General Directorate of Water Management.
During winter periods, typically from 15 November to 15 March (if weather conditions require it, this interval can be prolonged), the Hungarian Hydrological Forecasting Service (HHFS) receives data about river ice conditions daily from the regional directorates and other European hydrological services. They provide information about percentage of river surface covered by ice, ice cover thickness and duration of ice cover. River ice reports for Danube, Tisza, Drava Rivers and their tributaries are disseminated every morning.
Observation of ice phenomenon is carried out from the banks subjectively without the use of an instrument in the winter period during the morning water level measurement. Observation takes place within the proximity of at least 50 m of the gauging station. If there is several ice phenomena observed at the same time, the thickness of the most advanced, most dangerous phenomena in ice development is estimated. The observer's report contains a brief description of the weather and visibility conditions, the starting river section of the phenomena (upper limit according to the direction of the flow), phenomena by codes as shown in Table 2, the estimated thickness of the ice or the estimated height of the ice jam and estimated thickness of snow on the ice cover.

Table 2 Code figures of ice phenomena used by the observers

Code figure		Code figure	
00	water surface free of ice	29	floating ice covering (100%)
01	ice along banks	35	water surface frozen with breaks
07	ice cover (1/4 of the water surface)	36	water surface completely frozen over
08	ice cover (1/2 of the water surface)	37	water surface frozen over, with pile-ups
09	ice cover (3/4 of the water surface)	44	ice moving
20	floating ice covering (10%)	46	break-up (first day of movement of ice)
21	floating ice covering (20%)	50	ice jam
22	floating ice covering (30%)	53	scale and position of jam unchanged
23	floating ice covering (40%)	54	jam has frozen solid in the same place
24	floating ice covering (50%)	57	jam is weakening
25	floating ice covering (60%)	58	jam broken up by explosives or other methods
26	floating ice covering (70%)	59	jam broken
27	floating ice covering (80%)	//	missing data
28	floating ice covering (90%)		

Beside the observation of ice phenomenon the observer also performs ice thickness measurement every morning. If ice thickness is measured while standing on ice, the measurement takes place at the edge of the ice cover or in a leak cut into the ice cover. The observer can also measure the thickness from the banks in a leak cut into the edge of the ice cover, and from an icebreaker ship at the edge of the ice cover or floating ice floe in case of floating ice cover or danger. If the observer finds the conditions unsafe for the measurement, the ice thickness is estimated.

Hungary operates an icebreaker fleet, whose task is to prevent formation of ice jams that could lead to flooding and to provide safe waterway. The country suffered the largest ice flood in the spring of 1956. Following that event, a decision was made to use icebreakers to increase the effectiveness of ice destruction. The Hungarian icebreaker fleet consists of 22 ships. Most of the ships break the ice by running on the ice and break it under the weight of the ship. However, if the ice is so thick that this method does not lead to any result, then the deployment of the icebreakers with special counterweights is needed. Their rumbling movement ensures that they don't get stuck in the ice. There are 8 of these types in the fleet. Icebreakers are employed in groups for safety and efficiency. Usually 2–3 large and small icebreakers work together to help and save each other if needed (EDUVIZIG, 2019).

Beside summation of ice reports, HHFS every morning provides river ice condition forecasts for Danube and Tisza rivers for the next 6 days. The forecasting system operated by HHFS is based on two methods, the estimated energy balance method published by Liptay and Gauzer (2020) and the weighted mean temperatures method presented in detail by Liptay (2018). The energy change is calculated till the predicted water temperature reaches 0 °C, under the freezing point negative heat sum is determined. The energy change is determined with the following equation:

$$\Delta E = (1 - A) \cdot E_{sw} + E_{lw} - E_s + E_c + E_e + E_p + E_u$$

(1)

Where ΔE is the energy change per unit time, A is the albedo, E_{sw} is the total amount of shortwave radiation (direct and diffuse), E_{lw} is the atmospheric longwave radiation, E_s is the emitted longwave radiation of water surface, E_c is the direct energy exchange between air and water surface (convective heat transfer), E_e is the evaporative heat flux, E_p is the energy from precipitation and E_u is the energy exchange between riverbed and water. Under freezing point three empirical threshold values – threshold for formation of ice cover, for breakup of ice cover and for dissappearance of ice – describe the further behaviour of the ice regime (Liptay and Gauzer, 2020).

The weighted mean temperatures method is based on the assumption that all the terms of the energy balance can be neglected except the direct energy transfer between water and air. By weighting the air temperature the method establishes a relationship between air temperature and the appearance of ice,

since temperature under freezing point for a short period of time is not sufficiant for the appearance of ice (Liptay, 2018).

The Hungarian section of Danube (extended up to Bratislava) and Tisza are both divided into 4 forecast sections. The forecast model considers the most serious ice phenomena on every section. In case if both ice drift and ice cover occuring on a certain section, ice cover will be forecasted for this section if the ice cover exceeds 10% of the section length. The three main ice conditions on which the forecast is based are: free of ice, ide drift and ice cover.

Slovakia

In Slovakia river ice is monitored but not forecasted. River ice is monitored at hydrological stations by hydrological observers once a day in the morning at 6 a.m. during working days. Slovak water management enterprise, s. e. Banská Štiavnica (SWME, s. e.) as the manager of significant watercourses maintains and cleans the river channels and removes bed load, ice and other barriers and temporary islands from the watercourse, which is necessary to ensure steady runoff and flow. During the winter period, from 1st of December ice formation and ice run are monitored by SWME on a daily basis. Ice events are monitored and recorded; the river section where the ice has occurred and the conditions are also specified in the report by codes summerized in Table 3.

Table 3 Code figures of ice phenomena used in the reports

Code figure	
0	no ice
1	brash ice
2	brash ice and shore ice
3	shore ice
4	continuous ice cover on river (completely frozen)
5	ice jam (in water gauge profile)
6	ice run
7	water flowing over ice
8	ice drift and shore ice

Besides the type of ice phenomena, the ice width at the river bank is estimated by the observer using a measuring device and the observer also evaluates the intensity of the ice run. Table 4 shows the three levels that are distinguished in the assessment of the ice run.

Table 4 Code figures of ice phenomena used by the observers

Code figure	
0	no ice or brash ice does not float on the water surface
1	low ice run or run of brash ice
2	strong ice run or run of brash ice

When the ice runs, observers also estimate the average and the largest size of the ice floe. At selected stations that characterize the ice regime of the observed area, the ice thickness is measured regularly once a week on Wednesdays. Measurement is done within the proximity of 10 m of the water gauges. At severe frosts, if safe passing is ensured, the ice thickness is also measured in the middle of the watercourse. The observer drills holes into the ice and measures the ice thickness with the help of an ice rod. The collection of ice events and ice thickness data on selected water reservoirs and watercourses performed on a daily basis and the data are stored at the Branch offices. Branch offices send information related to ice events to the SWME, s. e. general directorate once a week on Fridays.

In Slovakia, flood authorities can proclaim flood alert levels also based on other circumstances stated in the law. 2nd level of flood activity is proclaimed during ice run on the higher stretches of watercourses in the river basin, when an ice dam, ice jam and threat of flooding are assumed to occur. 3rd level of flood activity is proclaimed during ice run in the watercourse or in the water reservoir, if there is a direct

risk for formation of ice dam, ice jam, or if the ice dam or ice jam has already begun to form and water start flooding the area and can cause flood damage.

Every year before winter SWME performs measures on all Branch offices to ensure winter operation. Measures are performed on water structures to check compliance with the decisions of the state water management authorities in the protection zones of water resources, compliance of the handling regulations during the winter period, including formation of retention areas depending on the water equivalent of the snow reserves, to ensure the functionality of defrosting devices and other technological equipments and also to ensure connection and to maintain access roads to water structures. Furthermore measures are taken on watercourses and canals to ensure sampling of surface water and removal of barriers from the flow profile before formation of ice cover on the water surface. Written notice is sent to object managers on watercourses (especially managers of bridges) because it is their duty to remove the captured suspended load. Finally measures are taken for ice regime monitoring, ensuring the preparedness to remove ice dam and the preparedness to ensure free flowing canals in case of snow hazard.

In case of a higher occurrence of ice on the Danube, SWME convenes a meeting of the operating group for operational management of the Gabčíkovo Water Structure in winter mode. A record is drawn up from the meeting, following which conclusions shall be subsequently taken on measures relating to the fairway. The Transport Authority of the Slovak Republic issues navigation measures on the Danube watercourse – stopping/limitation of navigation. SWME executes release or breaking of ice, release broken ice via the Čunovo Water Structure objects into the old Danube channel, manipulates the weir on the Gabčíkovo Water Structure objects and Čunovo Water Structure objects in such a way that the fairway in the territory of Slovakia is safe. The handling regulations of water structures include the handling procedures with weir constructions in case of ice sheet formation and ice release. Water structures are managed in such a way that the ice release is carried out against the flow of watercourse; it means that the ice is released into the free watercourse. At the cross-border watercourses, any ice handling must be performed only after the other party has been informed. On the Danube, in part of the approach canal and the impounding reservoir of the Gabčíkovo Water Structure, the formation of frazil ice, together with the intense ice run from the Austrian water structures and the river Morava, contributes to the faster freezing of the water surface.

Ukraine

Monitoring of ice phenomena is carried out twice a day at 8 a.m. and 8 p.m. by observers at hydrological stations. Characteristics such as the type and intensity of ice phenomena and most importantly the presence and formation of ice jam are determined. The evaluation of ice phenomena is carried out visually and the thickness of ice cover, snow on the ice are measured instrumentally every 5 days. These results are transmitted to the forecasting centers where an automatic data decoding, verification, analysis and automatic entry into database are performed. During the formation of dangerous ice phenomena, the observers also submit additional storm telegrams. Hazard criteria are set for specific water bodies: for large reservoirs, navigable rivers and rivers on which large hydraulic, water management facilities or complexes are operated.

In Ukraine forecasting of ice phenomena and processes are carried out in regional hydrometeorological centers of Ukraine for consumers in the form of background storm warnings in text form for the next 1–2 days. Both long-term and short-term forecasts are performed. Forecasting of the ice regime of the Ukrainian section of the Danube is conducted according to scientific and methodological developments of Ukrainian Hydrometeorological Institute (UHMI). The following methods are used in UHMI:

1. Forecasting of opening dates on the Ukrainian part of the Danube is issued according to the technique developed in UHMI in 1975. Determination of the opening dates is based on the accumulation time of the sum of positive average daily air temperatures.

2. Short-term forecast of ice on the Danube is made according to the technique developed in 1970 in UHMI. The method of V. Komarov and L. Shulyakovsky is based on the physical-statistical and empirical dependences of the total heat transfer required for the beginning of ice-forming processes.

3. On the Lower Danube short-term forecast of the formation of ice cover is carried out with the technique developed in 1974 in UHMI. The method is based on determining the minimum amount of negative air temperatures required to the formation of ice cover.

4. The prognostic system is a practical implementation of physical and statistical methods of short-term forecasting of ice phenomena. The model takes into account the air temperature and wind speed forecasts for 10 days. This system was developed at the Ukrainian Hydrometeorological Institute (UHMI) in the period 2003–2005 under the leadership of Anatoliy Vasyliovych Shcherbak. The parameters of physical and statistical dependences were determined on the basis of analysis and processing of long-term information on the characteristics of ice phenomena and hydrometeorological factors that influence ice processes on rivers.

5. In November, long-term forecast of ice appearance and formation on the Danube is made based on an long-term weather forecast for the territory of Ukraine. Based on the weather outlooks for the winter period a deduction can be made for the expected ice regime on the Danube River.

Results

Among the four countries, which provided detailed overviews of the applied practices, Croatia, Hungary and Slovakia disseminate their results online to the public. In Croatia a possible ice warning, in Slovakia the ice phenomenon is available through the daily hydrological reports and in Hungary along with the current ice conditions the forecasts are also published. Overview of the websites where data is accessible is shown in Table 5.

Table 5 Overview of data availability

Country	Ice data access
Croatia	https://vodniputovi.hr/en/services/ice-reports/
Hungary	https://www.hydroinfo.hu/en/jeg.html
Slovakia	http://www.shmu.sk/en/?page=1&id=ran_sprav
Hungary – Slovakia	http://www.teledan.eu/hu/hidrometeorologiai-es-jegadatok/jegadatok

On the website of the Hungarian Hydrological Forecasting Service up to date ice conditions are published between 15 November and 15 March. Ice conditions are presented in both graphical and table forms for Danube, Tisza and Drava rivers and their tributaries based on the river ice reports of the Regional Water Directorates. The tables provide information about the ice conditions, ice thickness and the thickness of snow on the ice cover. Figure 1 shows the ice conditions graph for Danube for the whole winter period based on the daily reports of the regional directorates. This graph is only available for the three larger rivers in Hungary, Danube, Tisza and Drava. OVF also disseminates daily ice regime maps, an example shown in Fig. 2. These maps show the current ice conditions on the rivers and also information from hydrological services of neighbouring countries is added. Beside observed data, ice condition forecasts for Danube and Tisza are also disseminated daily. In an ice condition forecast, present and expected ice conditions are published with the following possible states: free of ice, ice drift, ice cover and the tendency of the ice phenomena (weakening or intensifying) is indicated as well. In case of ice-free situation observed and estimated water temperatures are also published.

On the website of the Slovak Hydrometeorological Institution ice phenomenon is available for 79 hydrological stations through the daily hydrological report with verified hydrological data measured at 6:00 a.m. Ice events are also disseminated via the system of the TELEDAN project, which was a joint project of Hungary (North-Transdanubian Water Directorate) and Slovakia (Slovak Water Management Enterprise).
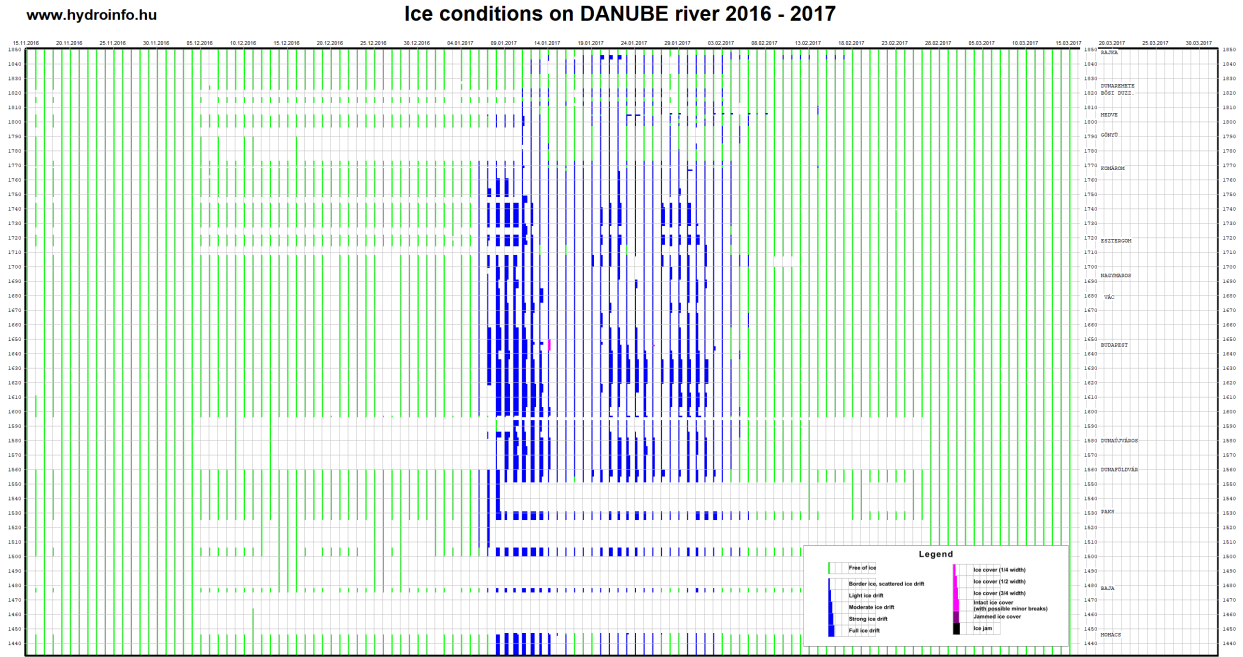
Fig. 1 Ice condition graph of the Hungarian section of Danube for 2016–2017 winter period.
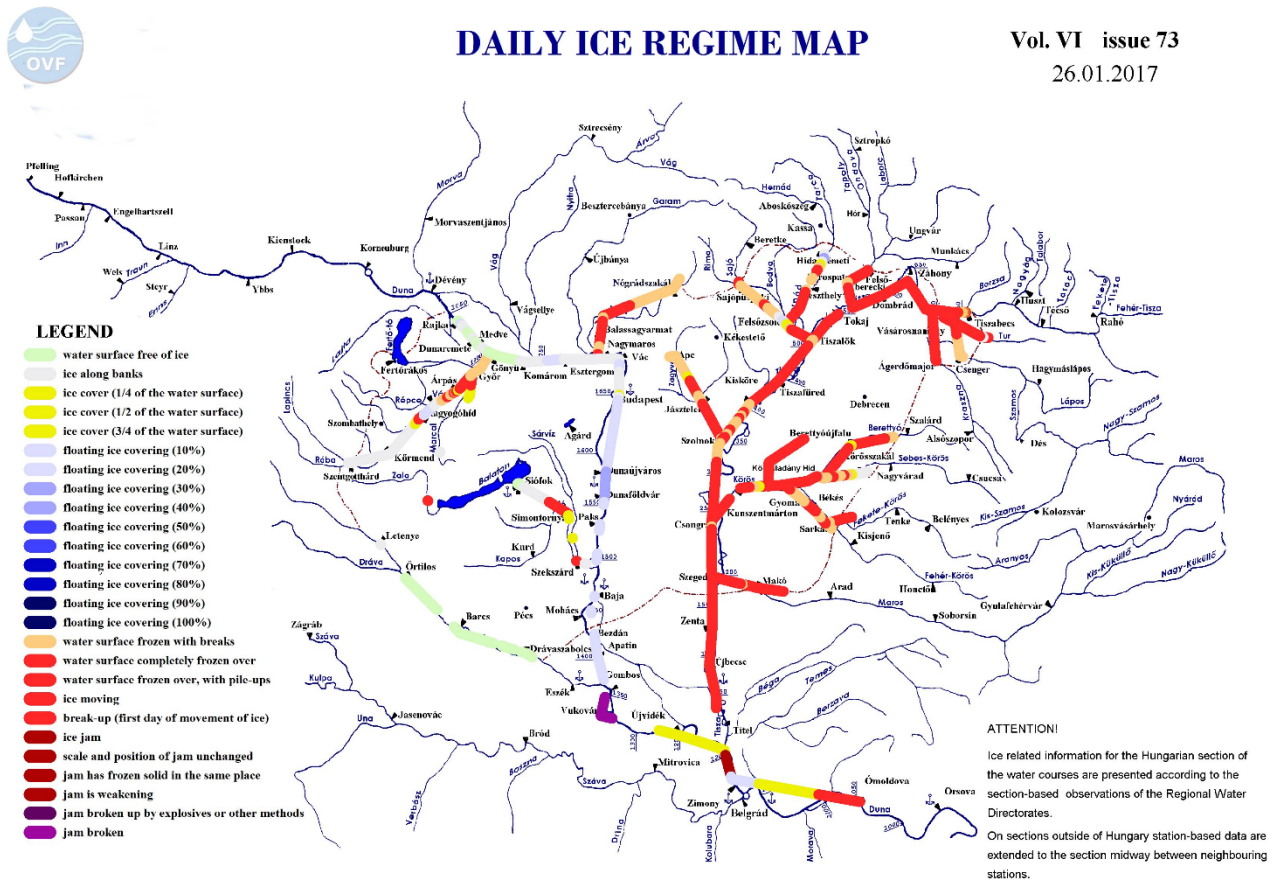

Fig. 2 Daily ice regime map disseminated by Hungary.

Conclusion

Ice monitoring and forecasting in the Danube River Basin is an important issue not only because of waterborne transport but the damage caused by river ice related flooding as well. From the information gathered in the framework of the DAREFFORT project, the following can be concluded. Almost all countries in the Danube basin give information on river ice events however ice reporting is various in light of what kind of information is provided. In the thoroughly presented four countries, monitoring of ice phenomena is based on subjective naked eye observations. Observations tipically carried out once or twice a day. Complementing these small amount of in situ observed data with satellite based observations could be beneficial. In Hungary utilazation of ice detection cameras to monitor river ice cover was researched by Keve, 2018 with good results. Country reports also show that in the Danube basin very few amount of river ice related information is available online for the public.

Acknowledgements

References

DAREFFORT O.3.1 Evaluation report on flood and ice forecasting (2019) http://www.interreg-danube.eu/approved-projects/dareffort/outputs.

DAREFFORT O.5.4 E-learning on flood and ice forecasting practices (2020) http://www.interreg-danube.eu/approved-projects/dareffort/outputs.

EDUVIZIG (2019) http://eduvizig.hu/content/k%C3%A9szen-%C3%A1ll-szezonra-magyar-j%C3%A9gt%C3%B6r%C5%91-flotta.

Liptay ZÁ (2018) Jégmegjelenés előrejelzése a súlyozott középhőmérsékletek elve alapján a Duna hazai szakaszára, *Hidrológiai Közlöny*, **98** évfolyam 1. Szám, 25–33.

Liptay ZÁ, Gauzer B (2020) Operational river ice and water temperature forecasting on the Hungarian Danube reach. FloodRisk2020 Conference Proceedings. Manuscript submitted for publication.

Ionita M, Badaluta CA, Scholz P, Chelcea S (2018) Vanishing river ice cover in the lower part of the Danube basin – signs of a changing climate, *Scientific Reports*, (2018) 8:7948, DOI: 10.1038/s41598-018-26357-w.

Keve G (2018) Folyami jégészlelés fejlesztési lehetőségei [Phd thesis, Budapesti Műszaki és Gazdaságtudományi Egyetem Építőmérnöki Kar Vízépítési és Vízgazdálkodási Tanszék].

Lászlóffy W (1934) A folyók jégviszonyai, különös tekintettel a magyar Dunára, *Vízügyi Közlemények* 1934 (16. Évfolyam), 369–435.

Mladenović MB, Gombás K, Liška I, Balatonyi L (2018) Report on the ice event 2017 in the Danube river basin, ICPDR, 72 pp.

Proposal of flood risk assessment methodology in the study time period

Mária ŠUGAREKOVÁ, Martina ZELEŇÁKOVÁ

Ústav Environmentálneho inžinierstva, Stavebná fakulta Technickej univerzity v Košiciach, Slovensko,
email: maria.sugarekova@tuke.sk, email: martina.zelenakova@tuke.sk

Introduction

Floods are a long-standing and still current problem not only in Central Europe, but all over the world. This natural event carries with it a certain risk, which can be avoided to a certain extent by appropriate preparedness, or at least partially mitigated its consequences. The most widespread method of determining flood risk worldwide is the creation of flood risk maps based on risk assessment using the generally applicable risk definition equation – risk = causality * consequence. Many foreign and domestic authors use hazard indices, vulnerability indices (Solín, 1998; V. David, 2008) as well as exposures (Mishra, Sinha, 2020) to calculate flood risk. Based on these three indices, a methodology for flood risk assessment is also proposed, which is described in this paper.

Methodology

Theoretical resources

The presented proposal of flood risk assessment methodology is based on the study of a multi-index model of flood risk assessment on the Yangtze River in China (Zhang et al., 2020). The authors in this study focused on the development of a multi-index conceptual model for the assessment of the Yangtze River in two parts – the first part deals with the preparation of the index system, the second is focused on the analysis of the proposed procedure in ArcGIS software. However, the presented paper describes the proposal of the flood risk assessment methodology based on the first part of the mentioned study, ie on the preparation and content of the index system.

The authors of the flood risk assessment study on the Yangtze River proposed a multi-index system consisting of three layers – an object layer, an index layer and an indicator layer. The object layer includes the rated Yangtze River, the index layer includes the hazard index, the vulnerability index and the exposure index. The last indicator layer contains 13 indicators that contribute to flood risk. The data contained in the indicator layer were collected and projected in a GIS environment, and subsequently, using the hierarchical AHP method, these data were assigned values according to the relative importance of each indicator. The final flood risk was calculated by the following equation:

$$YRBFR = H * w_H + V * w_V + E * w_E$$

$$(1)$$

where $YRBFR$ [–] represents the flood risk, H represents the hazard index, V represents the vulnerability index, E represents the exposure index and the w_H, w_V and w_E values are the weight values of said indices. The index layer of this methodology includes the mentioned indices of gambling (threat), vulnerability and exposure. The content of these indices are indicators, which are divided as follows: the hazard index (threat) is assigned an indicator of the cumulative average of maximum precipitation for 3 days. The vulnerability index includes indicators: data on the absolute elevation between the designated point and the sea level, data on the relative elevation, data on runoff density depending on the density of the river network in the area, surface runoff and surface coverage factor, financial returns, financial savings, levels health services and monitoring and alert system data. The exposure indicator contains 4 elements – population density, GDP per capita, degree of soil erosion and risk of soil contamination.

From the point of view of data availability and variation, it is possible to apply the multi-index conceptual model to any field of application, and it is also possible to substitute different input profitable values into individual layers. The following chapters present a proposal and a collection of data that will be used to assess flood risk in accordance with the currently valid legislation of the Slovak Republic.

Data collection

From the mentioned study of the multi-index conceptual model, a multi-index system is taken over for the proposed methodology of flood risk assessment in Slovakia, to which elements with sufficient informative value will be assigned. Since the design and application of this methodology is the research goal of the dissertation, the presented paper describes only one part, namely the part focused on the assessment of flood risk in the monitored period.

The main element of the submitted proposal is the availability of data from the Reports on the course and consequences of floods in the Slovak Republic (RoCCF-SR) since 2001. These RoCCF-SR are publicly available on the website of the Ministry of Environment of the Slovak Republic with unrestricted access. For each year, the RoCCF-SR provide detailed information on the floods that affected the territory of the Slovak Republic in the given year. The causes and consequences of floods in the Slovak Republic are mentioned at the beginning, which are divided into meteorological and hydrological causes. In the part of meteorological causes, the RoCCF-SR presents the totals of atmospheric precipitation in singular river basins for the monitored period. The hydrological situation describes the flood situations for the whole year (observed period) also in individual river basins. If a recurrent flood situation has occurred in one of the river basins, the time data are described separately for each monitored month. In the RoCCF-SR it is possible to read about the date and time when the flood occurred, which degree of flood activity was declared, what was the maximum level reached by the water level and what was the flow in the monitored stations. The section Overall assessment of the period describes summary information on flood situations in the monitored period. The final part is devoted to an overview of expenditures incurred for the implementation of flood protection and rescue work, monetary compensation and flood damage.

Results

The design of the flood risk assessment methodology is based on the above-mentioned study carried out on the Yangtze River in China (Zhang et al., 2020). The authors proposed a multi-index system, which remains in the proposed methodology. The first step is to determine the layers. These include the object, index, and indicator layers. The object layer is considered to be the investigated object, which in the methodology can be, for example, one or more river basins. The second layer consists of indices – index of risk, vulnerability and exposure. The content of the index layer is the indicator layer, which is described in the following subchapter.

Indicator layer

Hazard is a term used to describe a potential hazard that may or may not occur. It is the possibility of mobilizing danger in a certain time and space (Šimák, 2006).

In the field of study of flood risk assessment, we can identify the elements that contribute to the danger – the flood. The following indicators are therefore assigned to the design of risk indicators (Table 1): cumulative amount of precipitation, number of declarations the 3rd degree of flood activity and percentage of surface runoff in the solved area.

Tab. 1 Indicators of the hazard index

1. HAZARD		
1	Cumulative amount of the precipitation	
2	Number of declarations 3rd degree of flood activity	
3	Percentage of surface runoff in the solved area	

Vulnerability indicates a weakness that allows a threat to be applied. The following elements can be included among the vulnerability indicators (Table 2): affected inhabitants, protected landscape areas, flood protection structures.

Tab. 2 Indicators of the vulnerability index

2. VULNERABILITY		
1	Affected habitants	

2	Protected landscape areas	
3	Flood protection structures	

Exposure refers to elements exposed to danger, in this case floods. Exposure indicators include the following elements (Table 3): flooded buildings, flooded non-residential buildings, damaged utilities, affected animals, other flood damage.

Tab. 3 Indicators of the exposure index

3. EXPOSURE		
1	Flooded buildings	
2	Flooded non-residential buildings	
3	Damage utilities	
4	Affected animals	
5	Other flood damage	

The vulnerability index, together with the exposure index, contains other sub-indicators that were based on the availability of data from the RoCCF-SR. Sub-indicators in the vulnerability index fall under the indicator of "disability of the population" and includes: homeless people, evacuated and rescued persons, injured persons, evacuated and killed persons. Sub-indicators of the exposure index are described in the Table 4.

Tab. 4 Sub-indicators of exposure index

4. EXPOSURE		
1	Flooded buildings	Residential houses
		Family houses
		Other habitable buildings
2	Flooded non-residential buildings	Industrial buildings and warehouses, tanks and silos
		Farm buildings and warehouses, stables and barns
		Cultural heritage
		Hospitals, medical and social facilities
		Other non-habitable buildings
3	Damage utilities	Railways, cableways and other tracks
		Motorways, expressways, 1st class roads
		Roads 2nd and 3rd classes, sidewalks
		Local, special-purpose and forest transport communications
		Drainage channel, sewerage, culverts
		Water sources, water treatment plants, WWTPs
		Long-distance oil and gas pipelines
		Local gas distribution
		Long-distance and local water and steam distribution
		Long-distance and local electricity distribution
		Forest warehouses
		Other utilities

| 4 | Affected animals |
| 5 | Other flood damage |

Evaluation of indexes and indicators

The index layer is assigned a value of 100%. This value is divided between the indicators as follows: the risk index is 30%, the vulnerability index is 40% and the exposure index is 30%. The sum of the sub-values represents 100%. The value of each index is then divided equally between the index indicators (Table 5).

Tab. 5 Evaluation of indicators

5. HAZARD		
1	Cumulative amount of the precipitation	10
2	Number of declarations III. degree of flood activity	10
3	Percentage of surface runoff in the solved area	10
SUM		30%
6. VULNERABILITY		
1	Affected habitants	20
2	Protected landscape areas	10
3	Flood protection structures	10
SUM		40%
7. EXPOSURE		
1	Flooded buildings	6
2	Flooded non-residential buildings	6
3	Damage utilities	6
4	Affected animals	6
5	Other flood damage	6
SUM		30%

The partial weight values of the indicators will be used to quantify the values of individual indicators. Each weight is multiplied by a number that will be assigned to a specific indicator. For data whose value is known, this value will be multiplied by the corresponding weight of the individual indicator. For data that does not contain a specific number, the numerical scale will be determined based on other available data. After achieving the partial results for each indicator, the evaluation of the results for each index will follow separately, and the last step will be the final calculation of the risk level according to the partial results of the indicators.

As mentioned above, the vulnerability index and the exposure index also contain sub-indicators. Weight values are evenly assigned to this sub-indicator, which are multiplied by the input data. Thus, each sub-indicator will contain its value, and these sub-values will finally be calculated in all indicators first separately, when the total value of the indicator equals the value of the index, and finally the values of the indices are calculated to obtain the risk for a certain monitoring period.

Conclusion

The presented paper on the proposal of the flood risk assessment methodology is still in the stage of elaboration and topic, which will be gradually expanded and supplemented by the methodology of flood damage assessment based on the indicator layer in the previous methodology. Work is currently underway on a flood risk assessment methodology and a study of the available literature to plan for optimal results. The output of the proposed methodology will be the determination of flood risk from

the monitored area for a certain period, flood risk maps, which may relate to the total risk, but also to the partial risks in connection with individual indices. Another planned output is the creation of a methodology for flood damage assessment, the input data of which will also be based on the data available in the Report on the course and consequences of floods in the Slovak Republic.

Acknowledgment

Resources

David V. (2008) Metodika stanovení povodňového rizika v malých povodích. Sympozium GIS Ostrava 2008. Sborník z mezinárodního symposia konaného 27. – 30. 1. 2008 v Ostravě. VŠB Technická univerzita Ostava.

Ministerstvo životného prostredia Slovenskej republiky (dostupné 29.3.2021) Správa o priebehu a následkoch povodní na území Slovenskej Repuliky (online zdroj).

Mishra K, Sinha R. (2020) Flood risk assessment in the Kosi megafan using multi-criteria decision analysis: A hydro-geomorphic approach, In: *Geomorphology,* číslo **350**, 106861 (článok odborného časopisu).

Solín Ľ (1998) Hodnotenie povodňového rizika – súčasný stav výskumu, In: *Geologický časopis*, vol. **50**, no.1, pp 35–57 (article in a professional journal).

Šimák L. (2006) Manažment rizík, Žilinská univerzita v Žiline.

Zhang D. et al. (2020) A GIS-based spatial multi-index model for flood risk assessment in the Yangtze River Basin, China, In: *Environmental Impaxt Assessment Review,* číslo **83**. 106397 (article in a professional journal).

Combining ground data from rain gauges and satellite data for the purpose of analyses and forecasts of floods and flash floods

Petko TSAREV[1], Georgy KOSHINCHANOV[2]

[1] National Institute of Meteorology and Hydrology, Bulgaria – branch Plovdiv, email: petko.tsarev@meteo.bg,
[2] National Institute of Meteorology and Hydrology, Bulgaria, Sofia, email: georgy.koshinchanov@meteo.bg

Abstract

The availability of detailed well distributed in spatial information on precipitation is of essential importance for the hydrological modeling and forecasting. The distribution of the ground stations is quite irregular and thus distances between stations could be quite big, sometimes more than 35 km. This information is not sufficient for correct spatial distribution of precipitation. On the other hand, precipitation has high variability in space, especially in convective events. One of the possibilities to achieve high density gridded precipitation is remote sensing techniques such as using radars, products derived from satellites, etc.

One of the aims HSAF project is to produce different products for precipitation, snow and soil moisture with high resolution in order to facilitate the hydrological modelling. Bulgaria, in particular NIMH, is a partner in HSAF project since 2009 and the obligations are to validate and hydrovalidate these products.

In this paper we show how we use a GAM-Kriging interpolation of rain gauges data and this technique will be applied in two different synoptic situations in Bulgaria in the periods 30 May–05 June 2019 and 10–12 January 2021. The first one (from 2019) is characterized with convection scheme and the second one – with cloud scheme. In both situations in many places in Bulgaria there were floods and flash floods. Analyses and statistics will be made using data for both cases.

Methodology

Working area in this publication is Bulgaria. The climate in Bulgaria is moderate continental-Mediterranean. In the last few decades the tendency is towards warmer and drier climate.

Annual average rainfall is about 650 mm, more in the mountains (up to 1000 mm and more) and less on the coast (around 400–600 mm). In general, the late summer and early autumn is the driest period of the year in the country. In general there are two period with maximum precipitation – the months March till June and the months September till December. In the southern part of the country – influenced by the Mediterranean type of climate – the period with maximum precipitation is December till March. In that period and part of the country the precipitation is very often combined with intensive snowmelt which could lead to floods and flash floods. In the spring and early summer, showers, intensive precipitation and thunderstorms are common, especially in the mountains. The intensive precipitation is characterized with very small region where they fall. Very often it is impossible to be caught with conventional measurements. On the other hand according to (Spiridonov and Balabanova, 2017) in the western part of the country could be expected increase of the annual precipitation in the period (2020–2050), while in the eastern part of the country could be expected decrease in the annual precipitation. In the same study is also shown that despite the decrease of the precipitation in the eastern part of the country, the cases with intensive precipitation is expected to increase. It is obvious that the increase of cases with intensive precipitation will lead to an increase of flash floods and floods in the country. In this study we want to show one possibility to use satellite products (which have greater spatial resolution) under the cap of HSAF in combination with the conventional and automatic network of stations in NIMH.

H-SAF is project for developing products based on satellites for the "EUMETSAT Satellite Application Facility on Support to Operational Hydrology and Water Management (H-SAF)"(hsaf.meteoam.it).

The main objectives of the project are:
- to provide new products from existing and future satellites with sufficient space resolution to satisfy the needs of operational hydrology for the following products
- precipitation;
- soil moisture;
- different types of snow parameters;

In this study 3-hour sums from automatic and conventional stations are compared with HSAF's H05b product. The H05b is accumulated precipitation covering the full disk by merging MW images from operational sun-synchronous satellites and IR images from GEO satellites (i.e., product P-IN-SEVIRI) (hsaf.meteoam.it). Location of the automatic stations is shown on the fig. 1.
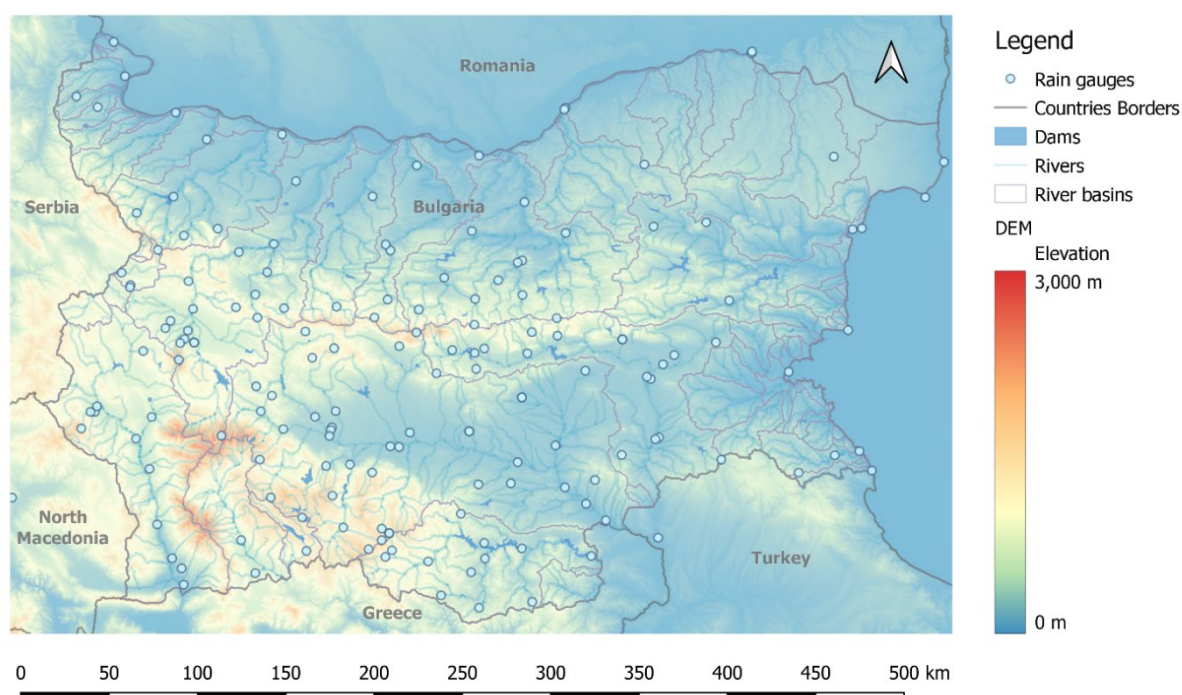

Fig. 1 Rain gauges with hour precipitation data

For the spatial calculations we use code in program language R with packages raster Geographic Data Analysis and Modeling and mgcv – Mixed GAM Computation Vehicle with Automatic Smoothness Estimation (Wood, S.N. 2017)

Kriging is one of the most widely used geostatistical method for spatial interpolation (Webster and Oliver, 2001) that predicts a value for a location with no data, based on the spatial autocorrelation of observed data. We used a kriging method Generalized additive model (GAM) with Ordinary Kriging (OK). OK is a standard kriging method based on the assumptions of stationary means and covariances (Webster and Oliver, 2001)(Hengl, 2009). On the other hand GAM is a semi-parametric extension of generalized linear models (GLM), where no parametric coefficients are estimated for predictors. GAM allows a nonlinear relationship between the response and explanatory variables.

A Generalized Additive Model (GAM) (Hastie, 1984) uses smooth functions (like SPlines) for the predictors in a regression model. These models are strictly additive, meaning we can't use interaction terms like a normal regression, but we could achieve the same thing by reparametrising as a smoother. This is not quite the case, but essentially we are moving to a model like Eq. 1:

$$y = \alpha + f(x) + \epsilon \tag{1}$$

A more formal example of a GAM, taken from (Wood, 2017) is given with Eq. 2:

$$g(\mu i) = A_i\theta + f_1(x_1) + f_2(x_{2i}) + f3(x_{3i}, x_{4i}) + \ldots \epsilon \tag{2}$$

Where:

$\mu i \equiv E(Y_i)$, the expectation of Y

$Yi \sim EF(\mu_i, \phi_i)$, is a response variable, distributed according to exponential family distribution with mean μ_i and shape parameter ϕ.

A_i is a row of the model matrix for any strictly parametric model components with θ the corresponding parameter vector.

f_i are smooth functions of the covariates, xk, where k is each function basis.

In this study we show three cases of precipitation:

Case I – Precipitation data only from H-SAF H05B product – direct visualization of 3h accumulated precipitations with extracted values over the rain gauge locations;

Case II – 3h Accumulated Precipitation data only form Rain Gauges. Interpolation using GAM Regression Kriging. With GAM formula: RR ~ 1

Case III – Mixed Precipitation data from conventional stations and H-SAF H05B, Interpolation by GAM Regression Kriging GAM formula: RR ~ H05B.RR.0, where H05B.RR.0 is the spatial data, where each pixel is divided by the maximum precipitation from the satellite grid at the time of interpolation. We use this method to add more weight to the in-situ observations.

Results

In locations with measured 3h precipitation data, the coefficient of determination (Nash, 1970) is shown in table 1.

Table 1 NSE coefficient

		2019	2021
Case I	Measured precipitation vs H05B values	0.212	0.187
Case II	Measured precipitation vs Measured Interpolated values	0.978	0.989
Case III	Measured precipitation vs Mixed Interpolated values	0.977	0.989

According to values of NSE and PBIAS (Moriasi et al., 2015) introduces the following criteria for assessing the accuracy of model data: NSE > 0.80 and PBIAS ≤ ± 5 the results are very good. In particular at 2019-06-02 18:00 h GMT the statistics between interpolated precipitation data /measured/ and mixed interpolation with H05B data are: PBIS = 3.9 and NSE = 0.973.
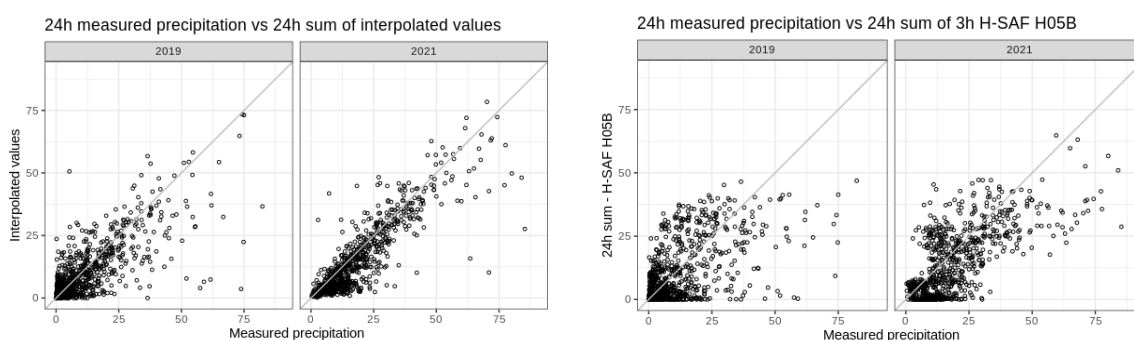

Fig. 2 Scatter plots of 24 hours sums for case III (left) and case I (right)

For result verifications we are using 24h accumulated precipitation from 204 conventional stations in Bulgaria. According to (Moriasi et. Al, 2015) values of NSE = 0.651, PBIAS= –16.9 and R^2=0.685 show satisfactory results. On 0 are shown scatter plots of 24 hours sums for case I and case III. On 0 are shown the differences between spatial interpolations /Case II – Case III at 2019-06-02 18:00/

The measured values from rain gauges are unchanged when we use GAM Regression Kriging interpolation /0b/. The red circles show the differences between measured precipitation values and spatial data. In the area under consideration there are large regions not covered by automatic rain gauges /0/. The final result with mixed data from rain gauges and H-SAF product H05b covers the area without in situ measures to make spatial interpolation of 3h accumulated precipitation /0c/
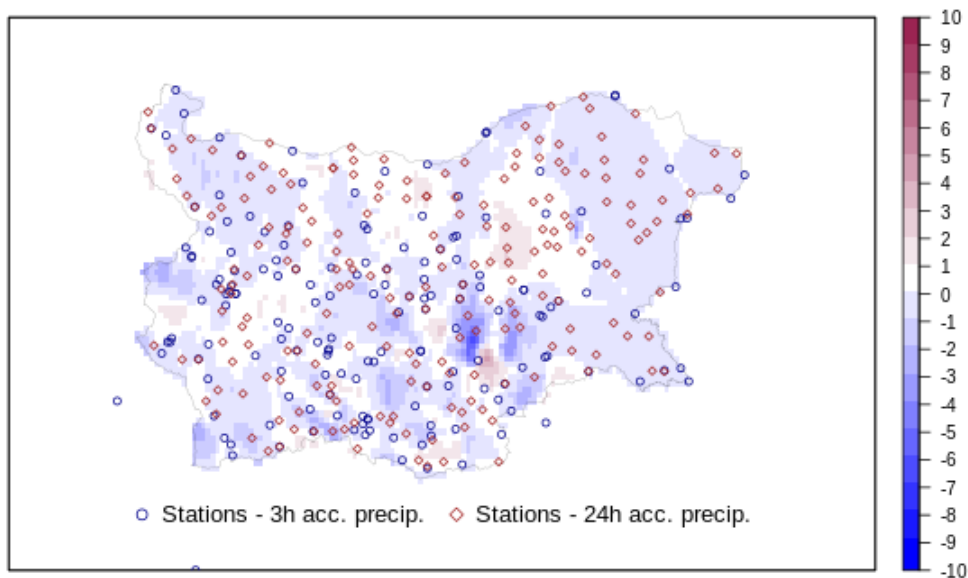

Fig. 3 Interpolated differences /Case II – Case III/ at 2019-06-02 18:00 and used meteorological stations
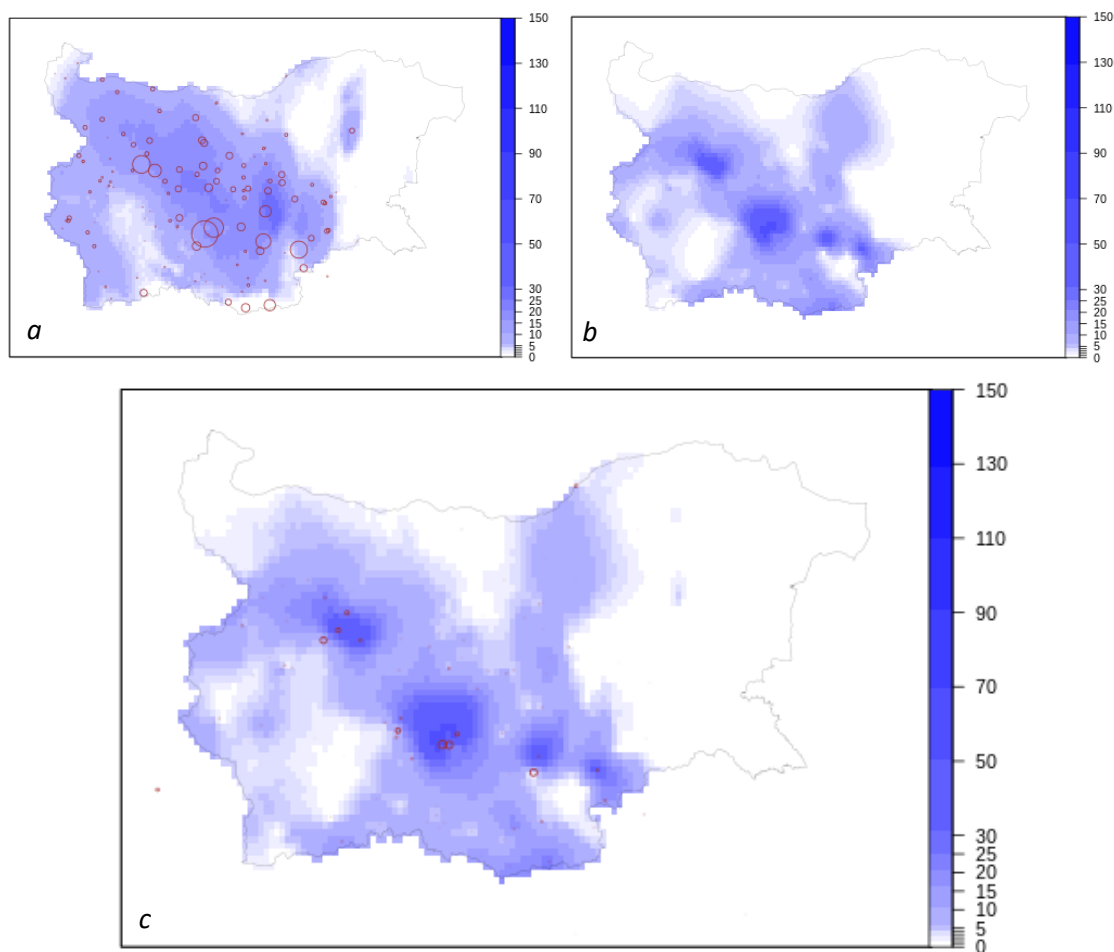
Fig. 4   a) Direct visualization of 3h acc. precipitation form H-SAF H05B product on 2019-06-02 18h GMT;
b) 3h acc. precipitation data only form Rain Gauges with GAM Regression Kriging interpolation on 2019-06-02 18h GMT;
c) 3h acc. precipitation data from Precipitation stations blended with H-SAF H05B on 2019-06-02 18h GMT;
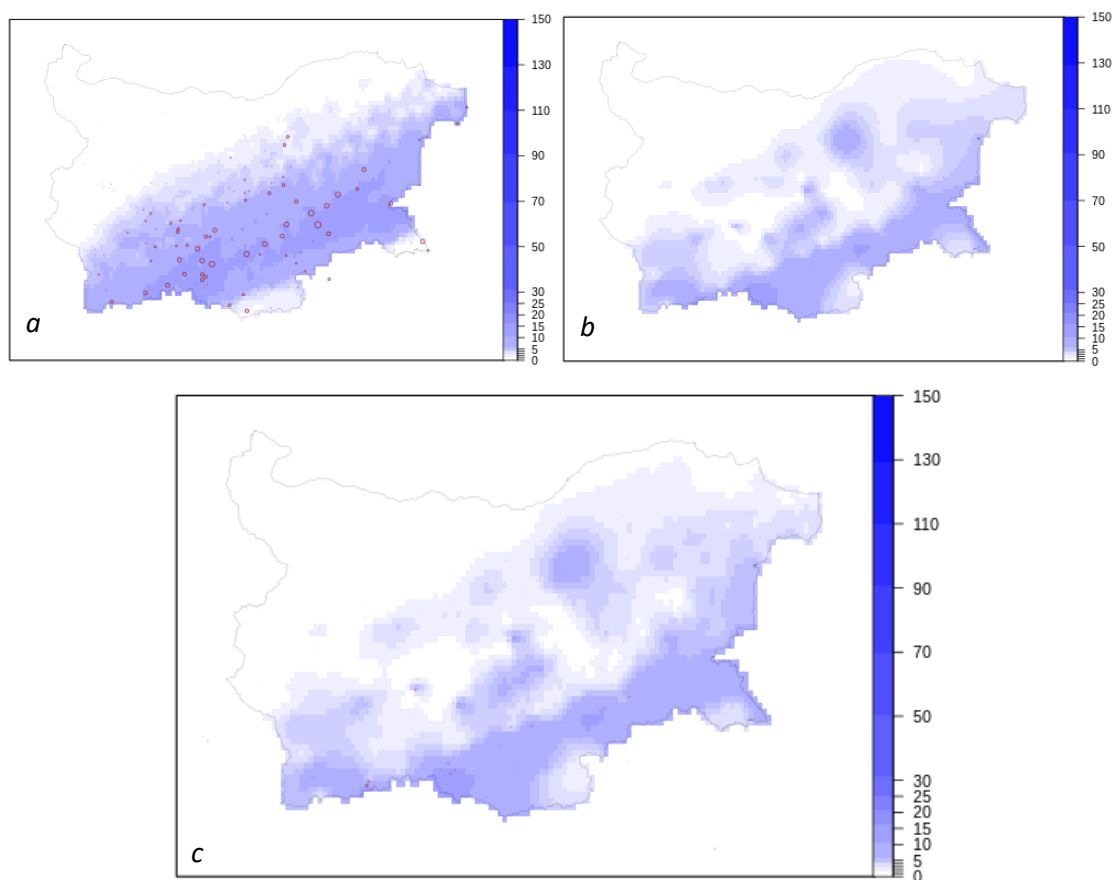

Fig. 5   a) Direct visualization of 3h acc. precipitation form H-SAF H05B product on 2021-01-11 21h GMT;
b) 3h acc. precipitation data only form Rain Gauges with GAM Regression Kriging interpolation 2021-01-11 21h GMT;
c) 3h acc. precipitation data from Precipitation stations blended with H-SAF H05B on 2021-01-11 21h GMT;

In the synoptic situation 10–12 January 2021. /0/, characterized with cloud scheme, the spatial interpolation was more different between the Case I /0a/ and Case III /0c/. The difference between H05B values and the measures precipitation /red dots on 0a/ are more than previous situation and shows more inaccurate spatial field of the precipitation on the surface.

Kriging spatial interpolation is not accurate near the borders when do not have measured data outside area. This can be improved when spatial interpolation of rain-gauges data is blended with data from other sources like H05B data.

It can be summed up that the intensive 3h accumulated precipitation values from H05b are lower than measured precipitation at ground, but the spatial field of the satellite product are very suitable for improving the ground data spatial interpolation.

Conclusions

The spatial data for precipitation from satellite product H05B can be used to improve GAM – Kriging interpolation of three-hour precipitation data from rain gauges. This improves the spatial distribution of precipitation and statistical parameters NSE, PBIAS and R^2. Still the H05B product cannot be used alone in places with no meteorological stations for now-casting of flash floods or for identification of the quantity of the precipitation in case of floods and flash floods.

The results from H05B were more accurate in periods with convective meteorology situation. This method can be used to validate and correct spatial data from satellite sensors or to fills the territory with not installed rain-gauges without or with small modifying the measured data. The programming code in R is short, fast and does not require specific computer resources. If is using multicore infrastructures with 8 or more cores, the time of calculations will be no more than 60 seconds.

References

Hengl T. (2009) A practical guide to geostatistical mapping.

http://hsaf.meteoam.it/Products/ProductsList?type=precipitation.

Nash JE; Sutcliffe JV (1970) River flow forecasting through conceptual models part I – A discussion of principles, *Journal of Hydrology*. **10** (3), 282–290.

Moriasi DN, Gitau MW, Pai N, Daggupati P. (2015) Hydrologic and Water Quality Models: Performance Measures and Evaluation Criteria // Trans. ASABE. V.58(6), 1763–1785.

Webster R, Oliver MA (2001) Geostatistics for environmental scientists. Statistics in practice series Chichester: Wiley.

Geographic Data Analysis and Modeling https://cran.r-project.org/web/packages/raster/.

Mixed GAM Computation Vehicle with Automatic Smoothness Estimation – https://cran.r-project.org/web/packages/mgcv/index.html.

Spiridonov V, Balabanova S (2017) Influence of Climate Change (by 2050) on the Intensive Rainfall on the Territory of Bulgaria. Bul. *J. Meteo&Hydro*, **22** (5), 26–37.

Wood, S.N. (2017). Generalized Additive Models: An Introduction with R, Second Edition (2nd ed.). Chapman and Hall/CRC. https://doi.org/10.1201/9781315370279.

Topic 4

Learning about hydrological extremes: then, now & in the future

Application of an indicator system for integrated space-time analysis and drought management in Northwestern Bulgaria

Yordan DIMITROV[1], Irena ILCHEVA[2]

[1] National Institute of Meteorology and Hydrology, Bulgaria, email: yordan.dimitrov14@gmail.com,
[2] National Institute of Meteorology and Hydrology, email: Irena.Ilcheva@meteo.bg

Introduction

Extreme floods and droughts have become more frequent in recent years. The river basin management planning process is the mechanism through which the available water resources and demand are balanced, thus avoiding water scarcity and drought. Adequate measures have to be included in the Programme of Measures when and where it is needed, a specific Water Scarcity and Drought Management Plan should be developed. For the implementation of Article 4.6 of the Water Framework Directive (WFD), the so-called "prolonged drought" must be adequately identified.

Hydrological drought and low flow depend on the meteorological conditions, but the severity of drought's impact depends on the vulnerability of water supply systems (WSS) and measures. Reduction of natural resources ("hydrological drought") in water sources is associated with reduced available water resources for water supply including regulating runoff ("water scarcity" or the so-called "operational" and "socio- economic" drought). Reduced water availability exerts a negative impact on people, environment and economic sectors. The severity of the "prolonged drought" is related to its duration, specificities of the river basin, reservoir management and impact. Specific indicators need to be selected and defined to identify the "prolonged drought" to prevent and mitigate its effects (Ortega-Gomes T., 2018). For each river basin, managers select the indicators that better represent the water resources offer for the different demand units existing in the basin. These indicators must reflect the resources availability in a homogeneous way and thus, these are selected among reservoir storage, piezometric levels, natural streamflows and areal precipitation (David Haro et al., 2014).

Methodology

To this end new methodological approaches, systems of criteria, indicators and drought indices have been developed in the National Institute of Meteorology and Hydrology (NIMH) (Ilcheva, I. et al., 2015; Ilcheva, I. et al., 2019a; Dimitrov, Y., 2018; Dimitrov, Y., A.Yordanova, 2017).

A methodological approach for integrated spatial-temporal analysis of drought, low flow and water scarcity in Northwest Bulgaria is applied. The aim is:

- to carry out an integrated spatial-temporal analysis of drought, low water and water scarcity, assessment of river runoff and its change in connection with the anthropogenic and natural processes;
- to identify and analyze the main factors, interactions and trends in Northwest Bulgaria in accordance with the WFD;
- to propose appropriate measures in support of the Northwest Bulgaria River Basin Management Plans in conditions of drought, low water and water scarcity.

The methodology consists of five stages:

1. Assessment of climate factors and trends. An assessment and identification of meteorological drought is performed with Standardized Precipitation Index (SPI).
2. Assessment of the water resources, trends and Hydrological drought. The stage includes:
   – Evaluation of water resources, regional dependencies and trends in water resources;

–   The Indicators of Hydrologic Alteration (IHA, Acreman, 2009), the threshold method and other methods are applied for low flow characterization;

–   An assessment and identification of Hydrological drought is performed with the Standardized Runoff Index (SRI).

3.   Hydrological, operational and socio-economic drought assessment. Water scarcity and "prolonged drought" identification. The reservoir inflows and reservoir levels are also indicators for drought and water resource availability. An assessment and identification of drought is performed with the Reservoir Inflow Index (RII), Standardized Status Index (SSI), indicators for assessing socio-economic and environmental impact, etc.

4.   Analysis of land use changes.

5.   Development and analysis of the measures for river basin management in drought conditions.

The Indicator system (including reservoir levels and inflow, some impact indicators – environmental and socio-economic) and drought indices (such as Standardized Status Index) have been developed for drought early warning and drought management needs – Table 1 (Ilcheva, I. et al., 2015; Ilcheva, I. et al., 2019a; Dimitrov, Y., 2018).

Table 1 Proposed Indicator system for drought early warning and drought management

Drought type	Evaluation Indices and Indicators	Experimentally applied
1.Meteorological Drought	**Rainfall** – SPI	SPI 1, SPI 3, SPI 6, SPI 9, SPI 12, SPI 24
2.Agrometeorological Drought	**Soil moisture –** SMI	n.a.
3.Hydrological Drought	**Runoff –** SRI	SRI 1, SRI 3, SRI 6, SRI 9, SRI 12, SRI 24
4.Hydrogeological Drought	Groundwater levels, Base Flow Index	Wells levels, springs flow, BFI
5. Operational and Socio-economic Drought and water scarcity	**Reservoir inflow** Tributaries threshold levels	Monthly and annual reservoir inflows with certain probability of exceedance – 50%, 75%, 95%. Threshold levels.
6. Operational and Socio-economic Drought and water scarcity	**Reservoir levels** Operational Indices and Dispatch Schedules. State Index. Percent from effective capacity.	*State Index (SI) and Standardised State Index (SSI)* for reservoir and river catchments
7. Operational и Socio-economic Drought and water scarcity	Water shortages in drought conditions. Indicators for assessing socio-economic and environmental impact.	Water supply reliability index. Environmental runoff vulnerability. Defining reservoir significance criteria.

As indicators for the reservoir inflow (RI) are suggested the developed by NIMH for the Ministry of Environment and Water monthly and annual inflows with certain exceedance probability (50%, 75%, 95%) Table 2 (An update of the used data for the tributaries in the reservoirs from Appendix No 1..., 2015 and 2017). The results are uploaded to the MoEW website (https://www.moew.government.bg).

Table 2 Monthly and annual inflows with certain exceedance probability PE (50%, 75%, 95%)

Reservoir	PE %	Monthly reservoir inflow with certain probability of exceedance, 10^6 m³												
		I	II	III	IV	V	VI	VII	VIII	IX	X	XI	XII	S
Ogosta	50%	16,71	20,31	35,35	49,62	45,96	26,42	11,74	7,35	6,68	7,86	10,68	17,22	255,91
	75%	11,21	11,91	15,04	28,87	23,31	11,57	7,24	5,08	3,42	4,74	6,4	9,19	137,97
	95%	0,76	0,13	0,29	0,83	2,42	0,08	0,97	0,34	0,01	0,26	0,18	0,05	6,29
Srechenska Bara	50%	2,01	5,68	3,08	8,02	9,27	7,44	4,09	2,06	1,14	1,84	2,46	2,35	49,43
	75%	1,7	2,53	2,26	6,27	6,89	4,66	2,61	1,23	0,7	1,28	1,47	1,51	33,11
	95%	0,66	0,71	1,26	2,85	2,84	2,09	1,15	0,72	0,41	0,5	0,44	0,47	14,09

The Status Index is applied for Drought Risk Assessment in Reservoir Systems and River Basins. The new Standardized Status Index is more suitable for assessing the operational drought and condition of reservoirs with seasonal flow regulation (within-year operated system) (Ortega-Gomes T. et al., 2018, David Haro et al., 2014):

$$Vi,t \geq Vmed,t \rightarrow SSI\ i,t = 1/2 * (\ 1+ ((Vi,t-Vmed,t\ )/(Vmax,t-Vmed,t)) \qquad (1)$$

$$Vi,t < Vmed,t \rightarrow SSI\ i,t = 1/2 *(Vi,t-Vmin,t\ )/(Vmed,t-Vmin,t)$$

where:

SSI i,t – the Standartised Status Index for year i and month t;

V i,t – the value of the indicator for year i and month t;

Vmed,t, Vmax,t and Vmin,t – monthly (t = 1, 2, 3, .., 12) statistics (mean, maximum, minimum).

The thresholds that define the different levels of the drought status are: Normality (green): SSI ≥0.5; Pre-alert (yellow): 0.5> SSI ≥0.3; Alert (orange): 0.3> SSI ≥0.1; Emergency (red): 0.1> SSI.

The derived Standardized Status Index at river basin level is calculated as a weighted sum (Ortega-Gomes T. et al., 2018; David Haro et al., 2014). The weight of the reservoirs takes into account their significance for the water supply and river basins, the deficiency during drought and the impact to society, ecology and economy. For this purpose the developed in NIMH for MoEW "Criteria for determination of reservoir from Appendix No 1 of the Water Law as complex and significant" are applied.

Indicators for assessment of socio-economic and environmental impact are also developed and applied: Probability of Exceeding, Reliability Index, Water Exploitation Index, etc. (Ilcheva, I. et al., 2019b).

Results

The approach is applied experimentally at three levels: in the valleys of Northwest Bulgaria, valley of Ogosta River (Petrokhan cascade and Ogosta dam supply system – Srechenska Bara) and Botunya River (Fig.1, Fig.2). A special feature of the area is the transfer of water through water intakes, dams and collecting derivations from the transboundary Nishava River basin to Ogosta River (Petrokhan cascade) and from one sub-basin to another – Fig.3. There are valuable protected territories and Natura 2000 sites in the area.
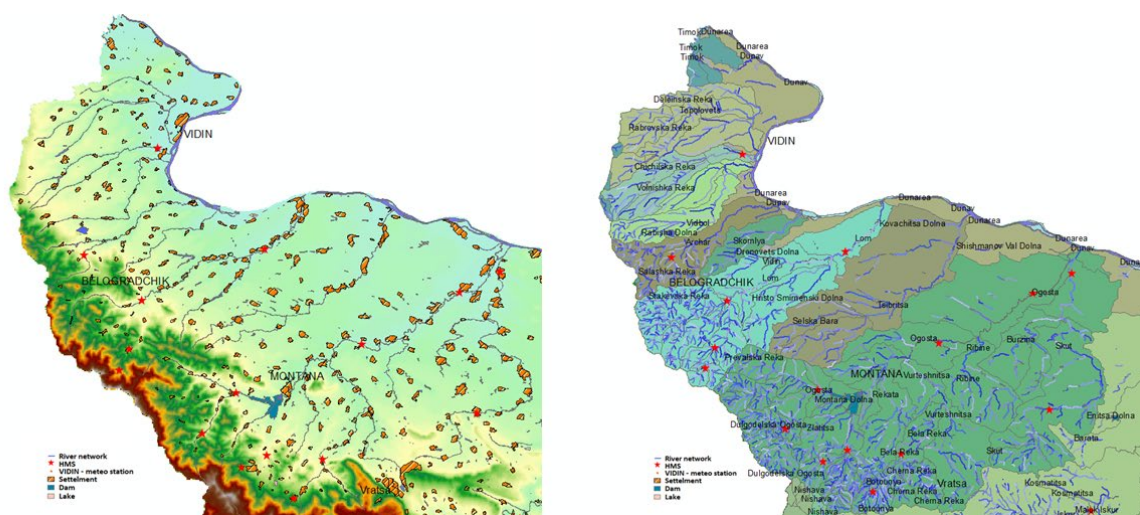

Fig. 1 Phisicogeographic map of Northwestern Bulgaria. Fig. 2 River basins in NW Bulgaria

The rivers in Northwest Bulgaria form their outflow from an area of 8 022 km², located between the West Balkan, the Timok River, the Danube River and the Iskar River. The most significant of them in the order of their influx into the Danube River are: Topolovets River, Voynishka River, Vidbol River, Archar River, Skomlya River, Lom River and Tzibritza River.
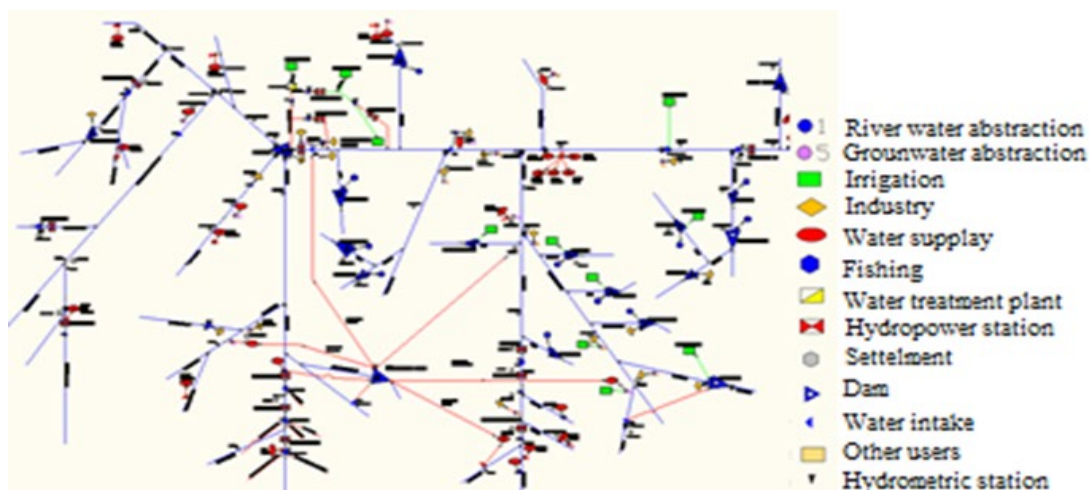
Fig. 3 Ogosta – Srechenska Bara Reservoir: updated water calculation scheme (fragment)

Ogosta is the largest river, with about 40 tributaries, the largest of which is Botunya River (69 km long, catchment area of 732 km^2) and Burzia (35 km long, catchment area of 241 km^2).

Anthropogenic and water economic activity, flow regulation and water transfer have a significant impact on the runoff, especially in the case of drought deficiency and drought. In some places, a moderate reduction in water resources (for removing and transferring water, captures, etc.) has been observed. In river stretches, such as Ogosta River in Kobilyak, the runoff decreases initially (as a result of the construction and overflow of the Ogosta River and Srechenska Bara reservoir) and increases subsequently.

The indicator system is applied for integrated space-time analysis and identification of the so-called "prolonged drought" (Ilcheva, I. et al., 2015; Ilcheva, I. et al., 2019; Dimitrov, Y., 2018). Up-to-date information from NIMH was used: precipitation and temperatures for the stations Vidin, Belogradchik, Montana, Vratsa, etc.; outflow of more than 20 HMS (Topolovets River, Voynishka River, Vidbol River, Lom River, Tzibritza River, Dalgodelska Ogosta, Berkovska River, Burzia River, Botunya River, Ogosta River, etc.; well levels; flow of springs, etc.

As a first step, with the application of SPI (SPI 1, SPI 3, SPI 6, SPI 9, SPI 12, SPI 24) periods of meteorological drought in NW Bulgaria have been identified: drought 1963–1964 (SPI3); drought 1965 (moderate); prolonged drought 1983–1994 and period 1991–1993 (extreme drought, SPI6, SPI12, SPI24); prolonged and extreme 2000–2001 (SPI6, SPI12, SPI24), 2007 and others. The comparison of the identified periods of meteorological and hydrological drought in NW Bulgaria shows synchronicity and coincidence for Lom, Ogosta and Botunya Rivers (Table 3). The Topolovets River, Voynishka and Tzibritza River watersheds show delay of hydrological drought occurrence and water storage recovery after prolonged drought, because of specific geological conditions.

Analysis by SRI (SRI 1, SRI 3, SRI 6, SRI 9, SRI 12, SRI 24) identified periods of hydrological drought in NWB: short-term drought (mainly SRI1-3) 1963, 1965; prolonged drought 1983–1995: initial period 1983–1987 (moderate to severe drought – SRI3, SRI6), final period 1991–1993 (extreme drought SRI6, SRI12, SRI24); prolonged drought 2000–2002; short-term 2007, etc.

Table 3 Relationship between SPI 1-24 (blue font) and SRI 1-24 (black font) for selected 3 meteorological and 8 hydrometric stations, situated in Northwest Bulgaria (fragment covering period – 11.1982–12.2002)
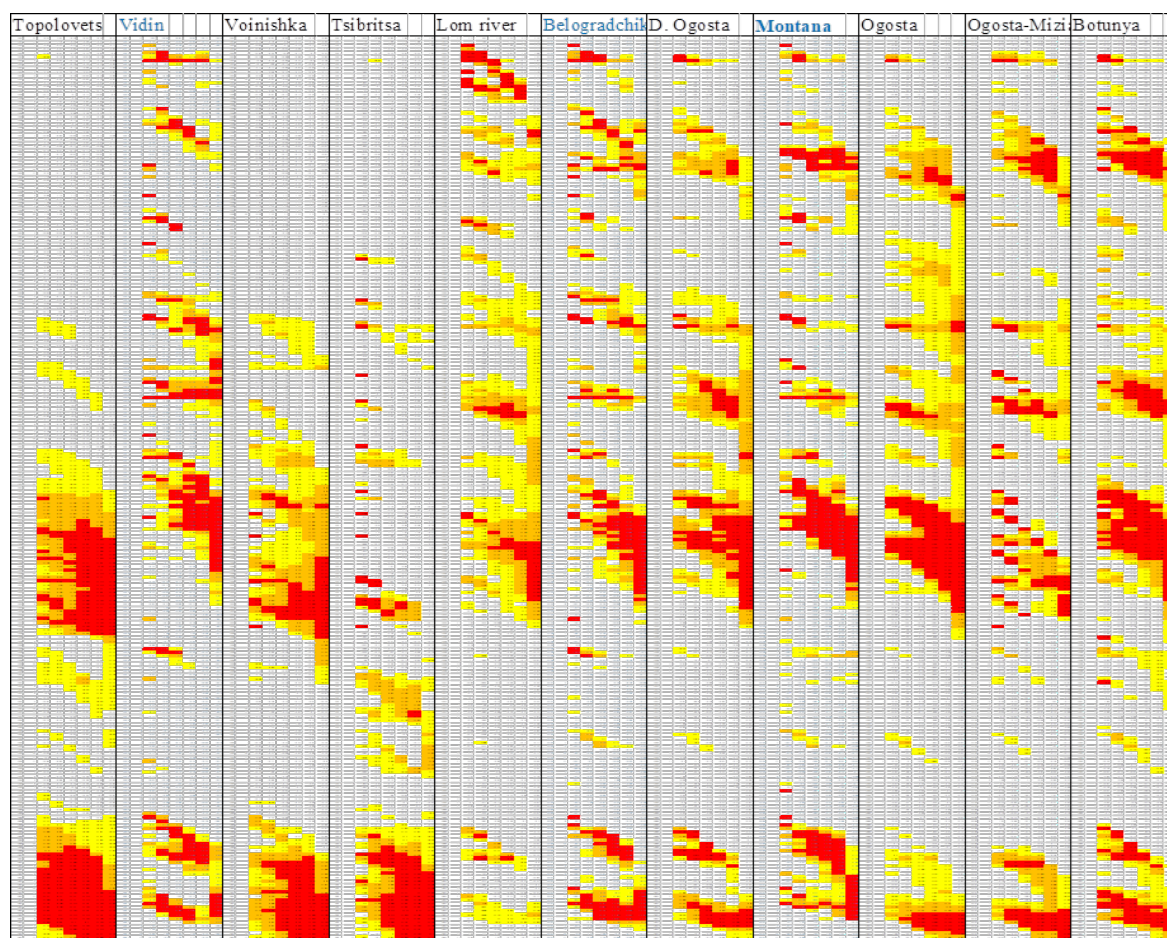
The Reservoir inflow index scale and the results for the Srechenska Bara Reservoir are given in Fig. 4 and Table 4. Representative information from the Ministry of Regional Development and Public Works was used for the inflow to Srechenska Bara Reservoir.

Monthly/ annual	Monthly reservoir inflow with certain probability of exceedance			
	>50	≤ 50%	≤ 75%	≤ 95%

Fig. 4 Reservoir inflow index scale

Table 4 The Reservoir inflow index for Srechenka Bara (volumes passed through Klisura HPP, mln.m³)

Year/month	1	2	3	4	5	6	7	8	9	10	11	12	sum
1982	1,536	5,04	1,824	8,288	9,596	7,916	4,052	1,82	0,896	2,608	3,252	2,96	**49,79**
1983	1,796	5,904	2,136	4,816	5,576	4,6	7,82	3,516	1,732	-1,32	1,648	1,504	**39,72**
1984	1,036	3,408	1,232	7,608	8,804	7,264	2,616	1,176	0,58	0,66	0,824	0,748	**35,96**
1985	0,596	1,96	0,708	4,78	5,532	4,564	1,328	0,596	0,292	1,648	2,052	1,872	**25,93**
1986	2,18	7,168	2,592	7,54	8,728	7,2	6,212	2,792	1,376	0,672	0,84	0,764	**48,06**
1987	1,176	3,868	1,4	8,088	9,36	7,72	2,312	1,04	0,512	0	0	0	**35,48**
1988	1,624	5,328	1,928	7,612	8,812	7,268	2,572	1,156	0,568	1,416	1,764	1,608	**41,66**
1989	1,056	1,056	5,7	4,548	7,08	7,38	4,92	1,8	1,26	3,708	2,952	2,58	**44,04**
1990	2,4	2,16	3,18	6,06	5,88	4,02	1,44	0,84	0,612	0,648	0,6	1,32	**29,16**
1991	0,96	0,6	3,684	6,276	9,78	7,2	5,52	3,9	1,56	1,08	3,36	2,4	**46,32**
1992	1,776	1,38	3,18	8,22	5,82	7,86	4,62	1,548	1,032	0,72	1,5	1,08	**38,74**
1993	0,66	0,516	2,852	5,58	6,62	5,02	0,712	0,708	0	0,468	0,408	0,676	**24,22**
1994	0,66	0,612	2,18	6	7,28	3,54	7,344	2,244	0,972	1,088	0,792	0,696	**33,41**
1995	1,692	2,292	4,08	7,74	9,456	6,648	3,408	2,532	2,256	1,212	0,94	3,072	**45,33**
1996	2,604	2,64	8,064	7,464	10,96	3,108	1,392	0,84	0,576	1,872	2,652	6,096	**48,26**
1997	4,896	2,184	3,3	5,784	9,168	7,392	2,328	3,12	1,08	2,4	3,768	5,016	**50,44**
1998	3	4,486	4,32	7,572	7,164	4,775	2,693	0,792	0	0	0	0,959	**35,76**
1999	2,892	1,739	4,764	9,192	7,164	3,696	3,42	2,52	2,159	1,956	2,352	3,588	**45,44**
2000	2,831	2,7	4,103	8,968	6,696	1,772	0,339	0,067	0,431	0,415	0,359	0,296	**28,98**
2001	0,489	0,66	5,256	6,792	8,392	3,605	4,077	1,103	0,64	0,077	0,243	0,059	**31,40**

The calculation scheme and balances for water management in the Ogosta River Basin (prepared in 2006, Yancheva, St. et al., 2008) have been updated. The simulation modeling with the SIMYL software (Niagolov, I., 1999) analyzes the potentiality of water resources management for the Ogosta River basin in conditions of low water and drought. This analysis shows that the water management systems have a possibility to provide runoff in periods of low flow in the area, but there are water shortages for the drinking water supply and the ecological runoff (such as the water supply from the Srechenka Bara reservoir, etc) in the periods of prolonged drought.

The new results (from 2018) show that in periods of prolonged drought and low flow there are deficits for water supply from the Srechenska Bara Reservoir, in the area of the Petrokhan Cascade and from local water sources – Table 5. The results of the experiments identify "extreme" and "prolonged drought", which is relevant for Article 4.6 of the WFD.

The results of the experimental application of the Standardized Status Index for the Srechenska Bara Reservoir are presented in Fig. 5.

The weight of the reservoirs takes into account their significance for the water supply and river basins, the deficiency during drought and the impact to society, ecology and economy. For this purpose the developed in NIMH for MoEW „Criteria for determination of reservoir from Appendix No 1 of the Water Law as complex and significant" are applied. The weights of the reservoirs are respectively 0.6 for the Srechenska Bara reservoir and 0.4 for the Ogosta reservoir – Fig. 6.

Table 5 Some results from the simulation modeling and water balance of the Ogosta River Basin, 2018

Simulation modeling Ogosta River Basin, 2018, Variant 1 – according to new permits [10³ m³/y]							
Water users	Name from 2006	Demand	Shortgs	Probability of exceedance (PE) %			Reliability Index
				By volume	By years	By months	
Chiprovtsi HPP	VECChipr	150000	14184	90.54	10.00	70.00	1.255
Water supply well and springs Berkovitsa	p5gWS	1262	19	98.49	90.00	98.33	.227
Klisura HPP	VECKlisu	500000	207239	58.55	.00	24.17	17.884
Drinking water supply from the Srechenska Bara Reservoir – Montana	p24sWS	106317	257	99.76	90.00	98.33	.006
Ecological runoff – Burzia River	Eco Barz	48000	22	99.95	90.00	99.17	.000
Drinking water supply surface water Berkovitsa	p2sWS	2934	46	98.43	70.00	97.50	.118

| Drinking water supply from the Srechenska Bara Reservoir – Vratsa, Mezdra, Krivodol	1WS	202423	2467	98.78	90.00	98.33	.149
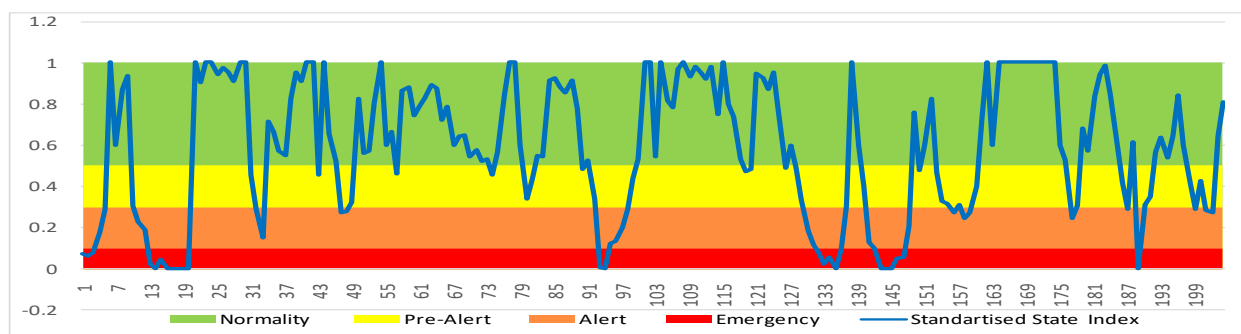
Fig. 5 Standardized Status Index – Srechenska Bara Reservoir (2001–2015)
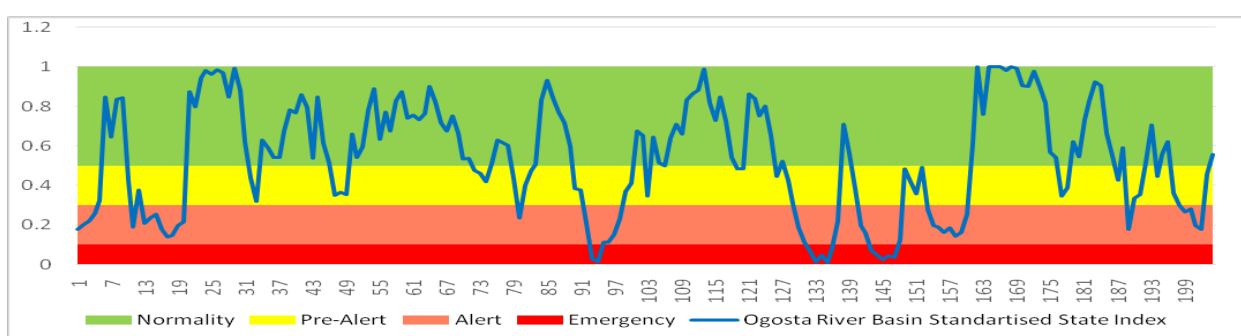

Fig. 6 The composite Standardized Status Index – Ogosta River Basin (2001–2015)

At the last stage a set of measures for prevention, adaptation and management at drought and low water level is being developed. The relationship between the drought indicator systems and the types of measures is given in Table 6.

Table 6 The relationship between the drought indicator systems and the types of measures (Monzonis, M. et al., 2015)

Status Index	Basin Drought Status	Goals	Types of measures
0,50 – 1	Normal	Planning	Strategic
0,30 – 0,50	Pre- alert	Control and information	
0,15 – 0,30	Alert	Save	Tactic
0 – 0,15	Emergency	Restrictions	Emergency

The measures are divided into two groups:
  (1) Measures directly affecting river flow management, related to planning and management of water management systems and reservoirs;
  (2) Measures, applied to catchments and related to land use.
The "Mitigating Vulnerability of Water Resources under Climate Change" catalogue (2014) with measures and good practices to support ecosystem functions through Green Infrastructure is completed. Four types of ecosystems are analyzed: forest ecosystems; wetland ecosystems; grassland ecosystems; agricultural ecosystems.

Conclusion

New methodological approaches, systems of criteria, indicators (reservoir levels and inflow, some impact indicators – environmental and socio-economic) and drought indices (such as standardized status

index) are developed in NIMH. An approach for integrated spatial-temporal analysis of drought, low flow and water scarcity is applied.

The methodology consists of five stages: assessment of climate factors and meteorological drought identification; assessment of water resources and hydrologic drought identification; simulation modeling (SIMYL simulation model), water balance – operational and socio-economic drought assessment; water scarcity and "prolonged drought" identification; mitigation measures and Drought Management Plans.

The proposed indicator system has been successfully applied for spatial-temporal analysis of the region of Northwest Bulgaria and drought identification, including the so-called "prolonged drought".

Periods of meteorological and hydrological drought in Northwest Bulgaria have been identified by SPI and SRI. The comparison of the identified periods of meteorological and hydrological drought in NW Bulgaria shows synchronicity and coincidence for Lom, Ogosta and Botunya Rivers, Topolovets River, Voynishka and Tzibritza River watersheds show delay of hydrological drought occurrence and water storage recovery after prolonged drought, because of specific geological conditions.

The new indices (reservoir levels and inflow, impact indicators – environmental and socio-economic) have been successfully applied for the Ogosta River Basin.

The Reservoir inflow index is analyzed on the basis of thresholds developed by NIMH experts, which are applied in practice by MoEW (Agreement with MoEW, 2015 and 2017, www.moew.com). Representative information from the Ministry of Regional Development and Public Works was used for the inflow to the Srechenska Bara Reservoir (which is also the basis of the derived threshold values of the indicator).

For "prolonged" droughts, we have a good match of reservoir status indices with SRI24. The SRI24 index better identifies long-term drought – there is a coincidence with the Standardized Status Index (SSI). There is a displacement, which is explained by the gradual depletion of the volumes of reservoirs and groundwater.

The experiments show the applicability of these new indicators and it is recommended to include them as part of the developed indicator systems for drought identification and management, in support of MoEW and the Basin Directorates.

The results of the balances show that in conditions of prolonged drought and low water there are deficits in the water supply from the Srechenska Bara Reservoir and local water intake catchments, in the energy production from the Petrokhan cascade, the ecological outflow of the Barzia River and others.

The application of these approaches as part of the Early Warning and Decision Support System are presented. The results, obtained from the experimental application for the specific river basins and water management systems, can be applied in practice for the purposes of MOEW.

References

An update of the used data for the tributaries in the dams from Appendix No 1 of the Law on the needs of the annual schedules for the use of their water, Agreement with the Ministry of Environment and Water, Task 21.2, 2015 and Task 3.1, 2017.

Criteria for determination of reservoir from Appendix No 1 of the Water Law as complex and significant, Agreement with the Ministry of Environment and Water, Task 21.1, 2015.

David Haro, Abel Solera, Javier Paredes, Joaquín Andreu, 2014, Methodology for Drought Risk Assessment in Within-year Regulated Reservoir Systems. Application to the Orbigo River System (Spain), Water Resour Manage (2014) 28:3801–3814, DOI 10.1007/s11269-014-0710-3.

Dimitrov, Y., 2018, Management of river water resources in Northwest Bulgaria in drought conditions, Dissertation, Abstract.

Dimitrov, Y., A. Yordanova, 2017, Trend assessment of meteorological factors, river flow and droughts in Northwest Bulgaria, Conference of the Danubian Countries 2017.

Guidebook on low flow management for drought prevention in the flood Danube River plain, Danube WATER, ...V. Alexandrov, M. Chilikova, I. Ilcheva et al., NIMH, 2015, http://danube-water.eu/wp-content/uploads/2015/07/Low-flow-Guidelines_BG.pdf.

Ilcheva, I., D. Georgieva, A. Yordanova, 2015, New methodology for joint assessment of drought risk of water supply under climate change, water stress areas identification and ecological flow provision, WFD, Ecology & Safety, ISSN 1314–7234, Volume 9, 2015, Journal of International Scientific Publications, http://www.scientific-publications.net/get/1000011/1432802839669739.pdf.

Ilcheva, I., D. Georgieva, 2018, Drought management plans for river basins, water supply and ecological runoff, *Annual of the University of Architecture*, Civil Engineering and Geodesy, UASG, SOFIA, Volume **51**, Issue 6.

Ilcheva, I., A. Yordanova, V. Rainova, 2019a, Application of Standardized Status Index for prolonged drought identification and river basin management, SocioBrains, ISSN 2367-5721, ISSUE 54.

Ilcheva, I., A. Yordanova, V. Raynova, 2019b, Water resource balance for Vitosha Nature Park and adaptive management under conditions of climate change, *European Journal of Geography*, Volume **10**, Number 3, pp 56–72.

Mitigating Vulnerability of Water Resources under Climate Change, Executive Forest Agency, Forest University, Forest Research Institute, NIMH (...*V. Spiridonov, I. Ilcheva, Kr. Nikolova, Sn. Balabanova, I. Niagolov*), 2014; http://www.iag.bg/docs/lang/1/cat/5/index.

Monzonís, M. et al., A review of water scarcity and drought indexes in water resources planning and management, *Journal of Hydrology*, 2015.

Niagolov, I., 1999. A tool for the study of water resources management systems, Jubilee Scientific Conference of the University of Architecture, Civil Engineering and Geodesy, October 6–8, Sofia.

Ortega-Gomes T., Pérez-Martín M. A., Estrela T. (2018) Improvement of the drought indicators system in the Jucar River Basin, Spain, *Science of the Total Environment*, **1**, 276–290.

Yancheva, St., A. Yordanova, M. Temelcova, 2008, Water Management Balances Assessment of a River Basin Water Resources System in Bulgaria, BALWOIS 2008.

Analysis of Low-Flow Extremes on the German Danube

Martin HELMS, Jörg Uwe BELZ

Federal Institute of Hydrology, Germany, email: helms@bafg.de, belz@bafg.de

Abstract

The sequence of low-flow events in the recent past underlines the need of a sophisticated low-flow management on the Danube river. Statistical analysis of long-term series of indices capturing various low-flow characteristics (streamflow, duration, deficit volume) may significantly contribute to this aim. Present paper describes methods of time series analysis and extreme value statistics and their exemplary application at the Danube gauge Hofkirchen taking into account suitable information expansions and hydrological reasoning in order to reduce uncertainties in the extreme low-flow range. With regard to its successful application, this methodical framework is suggested for analyses also at other Danube gauges in the scope of a joint project "Low Flows and Hydrological Drought in the Danube Basin" within the IHP-cooperation of the Danube countries.

Introduction

Like all major rivers in Central Europe, the Danube in the German section has been affected by striking low-flow events in recent years. In particular, the 2018 event significantly exceeded all previous events since around the mid-1960s. Moreover, the 2015 event was one of the most pronounced events in this period.

Hence, several questions about the hydrological evaluation of such events arise also with regard to the Danube river: which magnitude may low-flow events reach? How frequent do they occur? And did low-flow characteristics change during the last decades? Answers to these questions are of great socio-economic and ecological importance. Low flow and low water levels on the Danube federal waterway lead to restrictions on its navigability. The generation of hydroelectricity (run-of-river power plants on the Danube) is also impaired. Beside these impacts on water quantity, impacts on water quality may occur (concentration of pollutants and nutrients due to discharge of wastewater, increased water temperatures due to discharge of cooling water and periods of hot weather). Under such conditions, the hydro-ecological condition of affected water bodies frequently deteriorates. This also reduces their value as recreational area. In addition to the focus on the Danube river (or its tributaries), statements on possible hydrological conditions in the river basin are of interest, e.g. with regard to remaining groundwater supply during dry weather periods. Reduced availability of water resources in the basin may also result in adverse impacts on reservoir management and, in vulnerable regions, on drinking water supplies. For more information on the impact of drought and low flow in the German part of the Danube basin, see (LfU, 2017), (LfU, 2021) and (KLIWA, 2018).

An important contribution to answering the raised questions can be made by statistical analyses of long-term series of suitable low-flow indices at Danube gauges, including time series analysis, statistical inference and extreme value statistics with hydrologically meaningful information expansions. These analyses should take into account that low-flow events or years can have different characteristics. In addition to minimum streamflow, durations or deficit volumes below selected thresholds of streamflow during a low-flow period are of interest. These characteristics are to be captured and analyzed by different low-flow indices, depending on the aimed hydrological, water-management or hydro-ecological statement.

Against this background, extreme value statistics including the years 2015 to 2020 are developed in present study, which in turn allow the classification of the mentioned years and their low-flow events according to their occurrence probability. These analyses largely correspond to those of a Germany-wide study of the sequence of the low-flow years 2015 to 2018 (BfG, 2021), which used amongst others statistical methods recommended in a recently published new guideline for statistical analysis of low

flow (DWA, 2021). These methods are also proposed for a joint project „Low Flows and Hydrological Drought in the Danube Basin" within the IHP-cooperation of the Danube countries. In this paper, the methods are applied exemplarily to the gauge of Hofkirchen (see map in Fig. 1), which represents the German sub-basin of the Danube river upstream of the mouth of the Inn River.

The Hofkirchen gauge is located at Danube kilometer 2256.9 in a free-flowing river section (without influence by weir control during discharge measurement) and has a catchment area of 47 518 km^2. The daily streamflow series available at this gauge begins in November 1900 and has no gaps until March 2021. The catchment area is characterized in the south by the Alps and the Alpine foreland (moraines, gravel plates, Tertiary hilly landscape) and in the north and west by low mountain ranges (Black Forest and Bavarian Forest with crystalline bedrock, Mesozoic cuesta landscapes). The climate is temperate and Atlantic, but differentiated according to the orographic conditions. Average annual precipitation depth varies between 600 and 700 mm at medium altitudes and 2000 mm at higher altitudes in the Alps, with nival proportions increasing with the altitude. Corresponding to the landscape and climatological characteristics, the streamflow regime of the Hofkirchen gauge is complex with nival to pluvio-nival components. The monthly streamflow regime according to (Pardé, 1947) with the lowest long-term mean in autumn is shown in Fig. 1. Mean annual streamflow at the Hofkirchen gauge is about 640 m^3/s, the mean annual minimum flow MAM is about 315 m^3/s. Among large-scale anthropogenic influences on low flow, the Sylvenstein reservoir, which was put into operation in 1959 and has a total storage capacity of 125 million m^3 in the Isar catchment, has to be mentioned. Its function is, amongst other things, low water elevation (LfU, 2017).
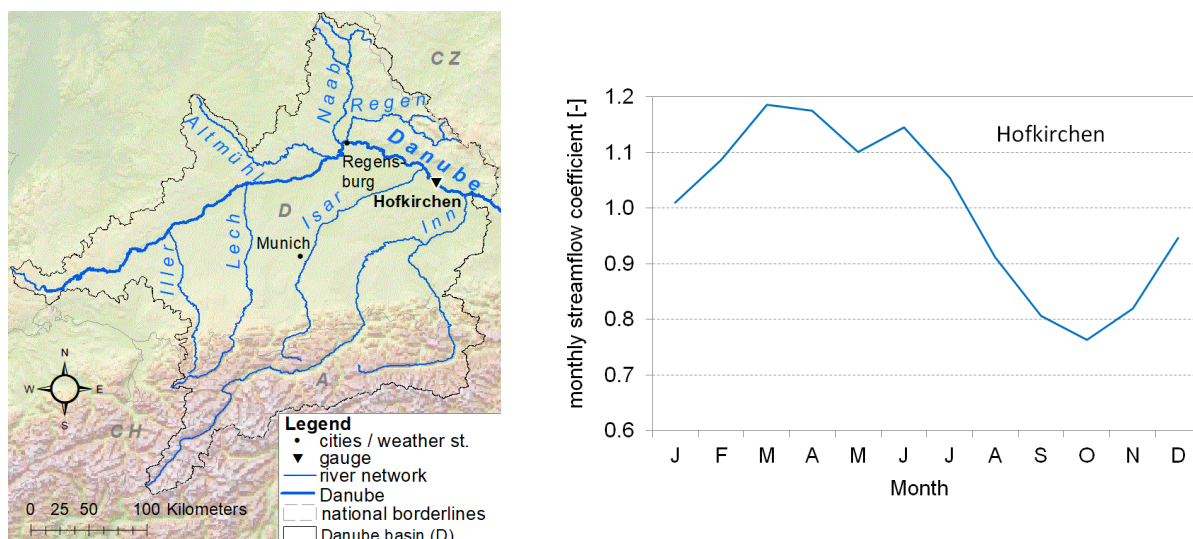

Fig. 1 Map of the upper Danube basin (German part) with positions of the Hofkirchen gauge and sites of weather stations with historical temperature data (left). Monthly streamflow regime according to Pardé of the Hofkirchen gauge (right).

Methodology

Answering the questions raised in chapter 1 requires statistical analyses of long-term series of various low-flow indices, including time series analysis, statistical inference and extreme value statistics with hydrologically meaningful information expansions. In the past decades, scientific methods in this context have been further developed and documented in literature, e.g., (Tallaksen & v. Lanen, 2004), (WMO, 2008) or (DWA, 2021). In present paper, these methods are adapted to hydrological conditions on the Danube river and applied to the Hofkirchen gauge, as it is also proposed in a broader framework of the joint project "Low Flows and Hydrological Drought in the Danube Basin" within the IHP-cooperation of the Danube countries.

The first step of the intended low-flow analysis consists in data collection, especially with daily streamflow time series of the gauge(s) to be analyzed from databases of the responsible authorities (e.g., in Germany from the Water Management Information System WISKI of the German Waterways and Shipping Administration or from the Bavarian Hydrological Service, https://www.gkd.bayern.de/). At

the river basin scale of interest here, mean daily values of streamflow are sufficiently detailed to satisfactorily capture low-flow events in their temporal dynamics and to reliably derive low-flow indices. The streamflow series should be available as uninterrupted daily time series covering the entire long-term streamflow behavior and in particular a representative number of extreme and rare low-flow events with their diverse characteristics. This requirement is closely linked to that of a (sufficiently) long observation period. A period of at least 30 years, as indicated by (WMO, 2008), is clearly exceeded at the major Danube gauges, including Hofkirchen.

However, it is also necessary that streamflow was correctly recorded during the entire observation period (data consistency) and was not subject to significantly varying (anthropogenic) impact in the watercourse of the Danube river or in its catchment (homogeneity), as inconsistent data and inhomogeneity can easily lead to false conclusions, especially in the low-flow range. Even if streamflow series have already been checked by the providing authority, their detailed examination for consistency and homogeneity against the background of intended statements (on extreme low flow) is recommended (WMO, 2008).

Hydrological methods in this respect include graphical plotting and visual inspection of daily streamflow hydrographs, if necessary in connection with reference information (e.g., hydrographs of reliable neighbor gauges), in order to detect and evaluate singular anomalies in the hydrograph. In addition, an analysis of streamflow recession curves based on, if possible, several mutually confirming, well-pronounced low-flow events originating from periods of the current hydrological state with reliable data is often revealing. Typical recession characteristics can thus be derived, which in turn can provide a reference for evaluating data in periods of presumably less reliable data. Daily streamflow series might also be evaluated using other approaches (e.g., comparison with date-related statistical streamflow parameters or with simulated streamflow values, or balancing of streamflow volumes during low-flow events among gauges in a river network), however these methods were not applied in detail in the present study. On the other hand, series of (annual) low-flow indices derived from daily streamflow series (see below) are analyzed in present study, since they focus on the relevant streamflow range in a long-term context and may hence provide indications of inconsistencies or inhomogeneities that are not readily recognizable from daily hydrographs.

Finally, information (metadata) on relevant conditions and temporal developments in the immediate environment and in the catchment of the analyzed gauge should be involved. In present study for the Hofkirchen gauge, information about low water elevation of the Sylvenstein reservoir (cf. chapter 1) and about icing conditions and resulting backwater effects in the Danube river and its tributaries during historical low-flow events (and thus temperature data during these events from the weather stations Regensburg and Munich/bot. garden) proved to be most relevant to better interpret uncertainties in the streamflow series.

Problems due to data inconsistency and inhomogeneity of streamflow series often become more pronounced the further back in time the data originate. The information gained by analyzing longer streamflow series (aiming at representativeness with regard to rare extreme events) should therefore be weighed against the possible occurrence of mentioned problems. In studies for multiple gauges, e.g. (BfG, 2021), a uniform series length should be chosen to ensure comparability.

After this preliminary analysis of daily streamflow data with regard to consistency and homogeneity, meaningful low-flow indices are extracted from daily hydrographs as annual series. To ensure independence of annual values as best as possible, the water-balance year from April 1 until March 31 of the following calendar year is chosen. Annual values are thus typically separated by groundwater recharge phases in spring and events spanning the turn of the year are avoided as best as possible. Series of the following indices are extracted with regard to minimum streamflow, duration and deficit volume of low-flow events or years (see also Fig. 2):

- AM7 [m^3/s]: annual minimum of 7-day mean streamflow rate. AM7 is preferred to the less robust annual minimum of daily mean streamflow AM which might be significantly influenced by diverse short-term and local effects during low-flow periods.

- sumD(<MAM) [days]: annual sum of days with streamflow values below the threshold of the mean annual minimum streamflow MAM. MAM is a statistical streamflow parameter and allows to compare sumD analyses across different sites, like in (BfG, 2021), rather than site

specific threshold values, which in turn might be preferred in local analyses depending on the aim of the investigation.

- sumV(<MAM) [m^3]: cumulative annual deficit volume of daily streamflow values below MAM.

sumD(<MAM) and sumV(<MAM) are censored series with relatively small sample size of real values (> 0) and correspondingly high uncertainty in their analysis. Therefore, reference series of sumD and sumV are calculated using the thresholds of quantiles of the daily streamflow series with relative exceedance frequency of 70% and 85% (Q70 and Q85). Their role in a causal information expansion to better validate probability statements for sumD(<MAM) and sumV(<MAM) in the extreme range will be discussed below.

Low-flow periods with streamflow below MAM may be distributed differently during the year. To investigate this characteristic of low-flow periods, series of the index maxD(<MAM), the longest uninterrupted duration per year with daily streamflow below MAM, are also extracted from the daily streamflow series and compared to those of sumD(<MAM). While the derivation of sumD series is straightforward, maxD series require additional considerations, mainly due to the fact that a low-flow period (streamflow below threshold) may be interrupted shortly, but not sustainably. In such a case, interrupted low-flow periods should be pooled according to a suitable rule ((Tallaksen & v. Lanen, 2004), (WMO, 2008), (Fleig et al., 2006), (DWA, 2021)). In a moving average procedure, the daily streamflow series is smoothed, e.g., using a 10-day moving average (MA10). In the resulting reference series, values during minor interruptions of the low-flow event may remain below the chosen threshold, thus indicating that the interrupted low-flow event should be pooled (Fig. 3). Alternatively, a "sequent-peak algorithm" SPA may be used. SPA is based on a balancing approach in which daily streamflow Q is interpreted as inflow quantity and the streamflow threshold QT as desired outflow quantity from an imaginary reservoir. In dry periods (Q < QT), the reservoir empties, in subsequent periods with excess streamflow (Q > QT), it is replenished. However, if excess streamflow occurs only for a short time or to a limited extent, complete replenishment of the reservoir does not occur and the interrupted low-flow periods are pooled into one period (including the intermediate period of excess streamflow). Other methods, not considered here, are based on criteria of inter-event time and inter-event excess volume, cf. (Tallaksen & v. Lanen, 2004) or (WMO, 2008) for details.
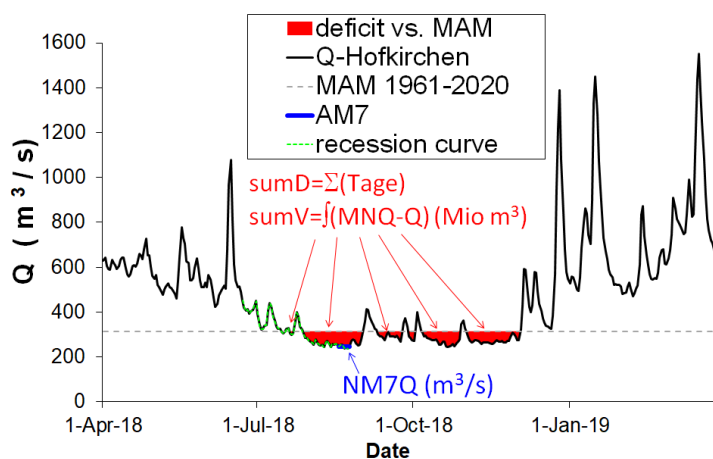

Fig. 2 Hydrograph of the Hofkirchen gauge in the water-balance year 2018 and low-flow indices and characteristics (see text).
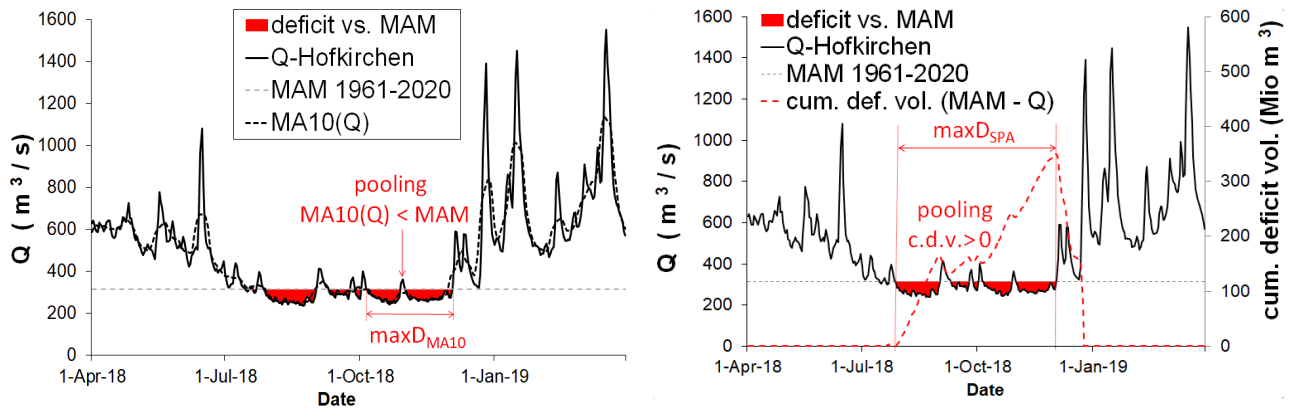
Fig. 3 Extraction of the low-flow index maxD(<MAM) from the hydrograph of the Hofkirchen gauge according to different pooling methods: MA10 (left) and SPA (right), see text

Based on available annual series of the addressed low-flow indices, information about their temporal characteristics may be derived using suitable graphical and statistical methods (among others, time series analysis, statistical inference, empirical probability plots). Due to their focus on the low-flow range (which is of interest here), these series eventually allow the identification of complex hydrological developments, changes and interrelationships in large river basins and long-term investigation periods, also beyond those to be identified by previously conducted analyses of daily streamflow series (see above) or other water-balance parameters. Beside insights about the hydrological behavior in the analyzed river basin in general, graphical and statistical analyses of mentioned series may thus also contribute to derive a representative period for the current hydrologic status in the river basin and to check prerequisites (data consistency, homogeneity, independence) with regard to extreme value statistics for the addressed low-flow indices (see below).

A first impression about temporal characteristics of the series to be analyzed (mean, variance, multi-annual grouping effects, extremes, and possibly inconsistent values or changing characteristics) can be obtained by graphical methods. These include simple time series plots (annual low-flow index vs. year) and probability plots with the empirical cumulative distribution function (cdf) of the series. In probability plots, annual index values are plotted vs. empirical non-exceedance probabilities PU or corresponding recurrence intervals T (T = 1/PU for AM7; T = 1/(1-PU) for sumD(<MAM) and sumV(<MAM)). PU is calculated here according to (Weibull, 1939) and (Makkonen, 2006) as "plotting position" from the rank m of an index value in the ascending sorted series of length n:

$$PU_m = m / (n + 1)$$

(1)

Series of different length (e.g., 1961–2020, 1971–2020, 1981–2020, ...) can be plotted together in the probability plots to detect possible long-term changes of the empirical cdf. Furthermore, comparison with extreme plotting positions of series from the beginning of systematic observation (e.g., 1901–2020 at the Hofkirchen gauge) are of particular value, as historical information about the occurrence of extreme events may be included in the consideration in this way. Even if historical anthropogenic influences usually differed from the present ones, it can be assumed that anthropogenic influence is generally strongly limited in case of extreme events due to the lack of still available water resources. Together with hydrological reasoning, including historical periods into consideration can hence be informative, at least as a reference.

After initial findings from graphical analyses (e.g., postulation of a representative period for the current status), statistical methods can be applied for further and better founded statements. In present study, autocorrelation of AM7-series and stationarity of the series all three above mentioned indices are analyzed.

Despite their reference to water-balance years (see above), annual series of low-flow indices may show persistence (stochastic dependence), e.g., between AM7 values of consecutive years ($AM7_i$ and $AM7_{i+\lambda}$), which are separated in time but show autocorrelation due to the hydrological memory in the river

185

basin or due to long-term climate variability (decadal variability). To analyze autocorrelation of AM7-series, the well-known autocorrelation coefficient according to Bravais-Pearson $r(\lambda=1)$ and the nonparametric rank-based autocorrelation coefficients $\rho(\lambda=1)$ according to Spearman are calculated. The latter corresponds to the Bravais-Pearson autocorrelations coefficient of the rank pairs of $AM7_i$ and $AM7_{i+1}$.

For the intended extreme value statistics (see below), autocorrelation results in a loss of information due to a reduced variance as compared to independent series, especially in shorter series. To assess this problem for the analyzed AM7 series, a corrected variance is calculated according to (Hansen, 1971), see (Tallaksen & van Lanen 2004), and compared to the variance of the original AM7 series.

In addition to autocorrelation in a specific series on which extreme value statistics will be based (see below), long-term development of the autocorrelation coefficient $\rho(1)$ is analyzed for an extended hydrological process understanding. For this purpose, sliding 30-year subseries are analyzed.

Another important question of fundamental interest is whether the probability distribution of the series is stationary or not (especially due to a long-term trend). Moreover, stationarity is a prerequisite for (classical) extreme value statistics. A trend or, more generally, a non-stationarity is particularly critical if it can be attributed to a known or reliably interpretable cause in the river basin (inhomogeneity, compare above). In the case of climate-induced non-stationarity, it is important to distinguish systematic changes from multi-year fluctuations. To analyze stationarity, the following methods of time series analysis and statistical inference are applied.

Stationarity of variance is analyzed for AM7 series using the Levene test (Levene, 1960), applied on subseries of equal length.

Stationarity of mean values is analyzed for all three indices (AM7, sumD(<MAM) and sumV(<MAM)) using different suitable methods.

30-year moving averages (MA30) are calculated for these series with centered reference years (e.g., 1976 for MA30 of the time window 1961–1990) and successively shortened time window at the beginning and at the end of the series (Tuszynski, 2020). As compared to linear trend analysis (see below), moving averages also reflect changeable long-term developments. They may thus contribute to an evaluation of (non-)stationarity of analyzed series, e.g., by identifying grouping effect of low-water years (decadal variability) that should receive special attention in the evaluation of a representative period for extreme value statistics.

Furthermore, linear trend analyses based on Eq. (2) are applied (with low-flow index x, year y, regression coefficients a and b and residuum r).

$$x_y = a + b \cdot y + r_y$$

(2)

Regarding the characteristics of analyzed series (non-normal distribution, autocorrelation, for sumD(<MAM) and sumV(<MAM) also truncated occurrence), adapted methods are chosen.

For AM7, the trend is calculated using the robust Theil-Sen estimator, as median of the slopes $(x_j - x_i)/(y_j - y_i)$ determined by all pairs of series values with $i < j$ ((Theil, 1950), (Sen, 1968)). Significance tests are performed as part of an iterative procedure consisting of the non-parametric Mann-Kendall test ((Mann, 1945), (Kendall, 1970), (Yue et al., 2002)) and a prewhitening which is involved to avoid erroneous trend assumptions due to autocorrelation ((Wang & Swail, 2001), (Zhang & Zwiers, 2004), (Frei, 2013)).

In the case of censored series (sumD(<MAM), sumV(<MAM)), trend estimation is performed using Tobit regression based on Eq. (2) ((Tobin, 1958), (Hirsch et al., 1993), (Henningsen, 2020)) with a lower threshold value of zero. Only if this threshold is exceeded by the latent variable calculated in the Tobit model (expected value + residuum r_y), this variable is assumed to be real. Significance of the trend is analyzed based on a t-distributed test statistic.

If prerequisites are sufficiently fulfilled in a representative period, especially in those of the current hydrological state, (classical) extreme value statistics can be developed for the series of low-flow indices. Their aim is to determine values of low-flow indices (quantiles) for any probability of

occurrence or statistical recurrence interval T. Conversely, occurrence probabilities can be calculated for index values of interest, e.g., to classify the years of the recent low-flow sequence 2015 to 2020.

For this purpose, theoretical cdf's $F(x)$ are selected and fitted to the series (with low-flow index x). These cdf's can be extrapolated and allow more robust probability statements than plotting positions, in particular in the extreme range. In present study, cdf's were fitted to series using the software EXANTO (Klein, 2010).

In case of the censored series of x = sumD(<MAM) or sumV(<MAM), this procedure is embedded in a conditional probability approach. Omitting zero values (or values below 0,5 % of the max. value of sumV(<MAM) series, cf. (Fleig et al., 2006)) results in a truncated series to which the cdf $G(x)$ is fitted. The occurrence of zero values (with relative frequency p_0) is then taken into account by the following equation:

$$F(x) = p_o + (1 - p_0) \cdot G(x)$$

(3)

For details about theoretical cdf's, corresponding quantile functions, parameter estimation methods and the conditional probability approach, see (Tallaksen & v. Lanen, 2004), (Stedinger et al., 1993) or (DWA, 2021).

Regarding manifold process characteristics in large-scale river basins, a well-founded choice of the theoretical cdf and parameter estimation method is hardly possible in advance. Therefore, various cdf's are fitted and diagnosed against empirical cdf's of the analyzed series. This diagnosis should be supported by the following information expansions.

On the one hand, extreme plotting positions related to the overall observation period at the analyzed gauge, also before the chosen representative period, might have an informative value (see above) and can be used in this case as a reference in a temporal expansion of information to support the selection of a theoretical cdf to be fitted (only) to the series of the representative period.

On the other hand, sumD and sumV series with graded thresholds (Q70 and Q85) are analyzed in a causal expansion of information. Truncated series of these indices have greater sample sizes than those for the MAM threshold and usually allow more reliable fits and extrapolations of theoretical cdf's. They may hence serve as reference for the cdf to be selected for sumD(<MAM) and sumV(<MAM). In this respect, the cdf's of indices with graded thresholds should exhibit parallel, slightly converging or slightly diverging structures up to the extrapolation range in the probability plot.

Beside the uncertainties already mentioned (unknown true cdf, possibly only approximately fulfilled prerequisites of extreme value statistics), also an uncertainty due to the limited length of the analyzed series ("sampling effect") is to be considered. Therefore, intervals with a confidence probability of 0.9 are determined for the fitted cdf's using a bootstrap resampling (Burn, 2003).

According to above mentioned aim, the chosen and fitted theoretical cdf's $F(x)$ and corresponding quantile functions $F^{-1}(PU)$ can finally be used to calculate probabilities of occurrence (or statistical recurrence intervals T) for any values of the analyzed low-flow index or, vice versa, index values (quantiles x_{PU}) of any probability of occurrence. A special case is the conditional probability model introduced with Eq. (3). Here, quantiles x_{PU} are calculated according to Eq. (4) (with symbols as in Eq. (3)):

$$x_{PU} = G^{-1}\left(\frac{PU - p_0}{1 - p_0}\right)$$

(4)

Calculated quantiles can be used, among other things, to assign the low-flow indices that occurred at the Hofkirchen gauge in the last few years (2015 to 2020) to classes of their occurrence probability (or recurrence intervals) and to present them accordingly in an overview. By this assignment of real events of the recent past, it is also intended to make low-flow statistics more tangible.

Results

In the WISKI database, the daily streamflow series from November 1900 until March 2021 is available for the Hofkirchen gauge. With 121 years of systematic observation (without gap), this series is in principle very suitable for reliable low-flow statistics. Fig. 2 shows the hydrograph of the water-balance year 2018 together with diverse low-flow indices and confirms that the daily time step is suitable to capture low-flow characteristics on the Danube sufficiently well.

To ensure reliability of the daily series also with regard to data consistency and homogeneity of hydrological conditions (in particular with regard to icing conditions and anthropogenic impact), preliminary analyses of the daily series with focus on low-flow ($< MAM = 315$ m^3/s) were carried out. Visual inspection of daily hydrographs revealed only few significant short-term anomalies in the hydrograph, all in winter and probably due to icing in the river network (see below).

Hence, multiple recession curves of low-flow periods could be well identified, in the recent past (2011, 2015, 2016, 2018), but also in the more distant past (1911, 1920, 1947, 1953, 1959). They were superimposed in time as best as possible, averaged and plotted vs. a time index (Fig. 4). The plot shows that (mean) recession curves of the recent and the more distant past are similar, however, with slightly higher values of the mean recent curve in the advanced stage of the recession. This is plausible with regard to the installation of the Sylvenstein reservoir in 1959, which is the only reservoir with a large-scale significant effect of low-flow elevation in the catchment of the Hofkirchen gauge. For example, during the low-flow event 2003 (recession disturbed by smaller streamflow events and therefore not selected for Fig. 4), the outflow of the reservoir was increased by about 10 m^3/s at the time of the lowest inflows, cf. (LfU, 2017). Hence, the (mean) recession curves confirm each other and can serve as a reference for evaluating less plausible streamflow data, such as the anomalies mentioned above.
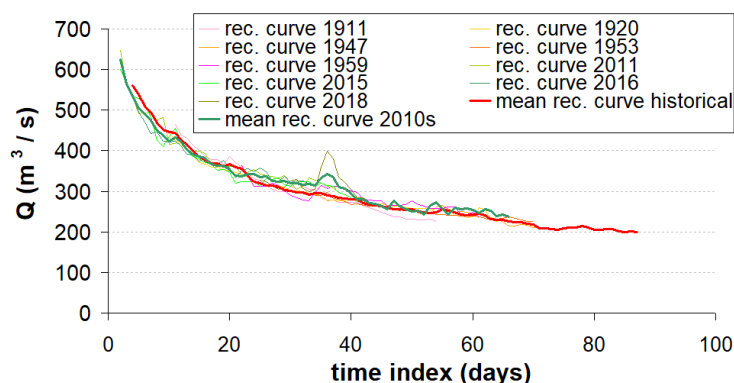

Fig. 4 Selected recession curves of the Hofkirchen gauge (individual and averaged for groups of the recent and the distant past).

Additional reference information to evaluate above mentioned anomalies include streamflow data of neighbor gauges (Pfelling/Danube upstream of the Isar confluence, Plattling/Isar), date-related streamflow indices (5%-percentile, minimum) and daily temperature data of nearby climate stations (Regensburg, Munich) with regard to possible icing in rivers. Fig. 5 shows a diagram bringing the addressed information together for the water-balance year 1928 with a severe winter 1928/29.

As compared to the mean historical recession curve and to the date-related indices, the anomaly of the observed hydrograph at the Hofkirchen gauge is obvious and can be plausibly explained by icing effects in the catchment or upstream river network with regard to the hydrographs of the reference gauges. Significant anomalies could be identified also for other water-balance years (1908, 1925, 1938, 1984), however, only the anomaly in winter 1908/09 led to a similarly strong effect in the extreme low-flow range as that of winter 1928/29. Due to complex hydrological processes associated with these situations, present study did not attempt a detailed homogenization of these anomalies, but only estimated homogenized values (without ice effect) based on the mean recession curves in order to use them in a hydrological interpretation of low-flow statistics. While statistics should be based on homogeneous data, specific effects, e.g. due to ice, should be evaluated in subsequent steps (not in present study).
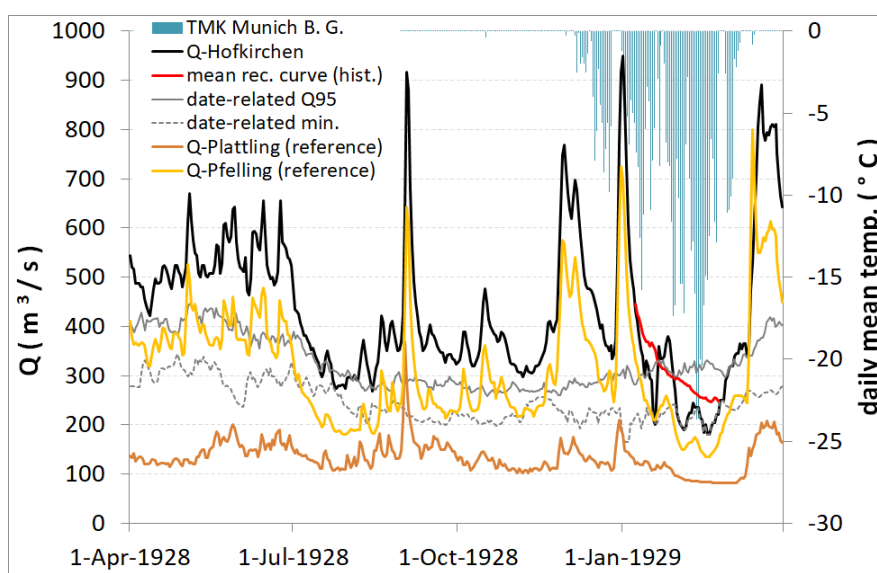
Fig. 5 Hydrograph of the Hofkirchen gauge and of the reference gauges of Pfelling (Danube) and Plattling (Isar), date-related indices (min, Q95) and mean historical recession curve of the Hofkirchen gauge, and mean daily temperature (TMK) of the station Munich botanical garden (provided by DWD) as indicator for a likely ice effect in the river network of the Danube basin.

After these preliminary analyses based on the daily streamflow series, the annual low-flow indices AM7, sumD(<MAM) and sumV(<MAM) (see Fig. 6) as well as the reference series of sumD(<Q70), sumD(<Q85), sumV(<Q70), sumV(<Q85) and maxD(<MAM) were extracted from the daily series.

Like described in chapter 2, analyses of these series focusing on the low-flow range (in particular those of AM7) may support the identification of inconsistent or inhomogeneous streamflow data and hence to derive a representative period of the current hydrological status and to check prerequisites for extreme value statistics based on series of the representative period.

Simple plots of the series vs. time (Fig. 6, containing additional information addressed below) and probability plots of these series (Fig. 7) give a first overview of the characteristics of the series.

In Fig. 7, AM7 of 1908 and 1928 clearly take the smallest values in the overall series starting from 1901, while sumD(<MAM) and sumV(<MAM) take less extreme values. Comparison of the indices of these two years with the corresponding long-term distributions thus confirms the need to interpret them correspondingly in the development of low-flow statistics, in particular for AM7. Furthermore, series of different length (overall, 1961–2020, 1971–2020, 1981–2020) are compared in Fig. 7. Up to a recurrence interval of 10 to 20 years, empirical cdf's of 1961–2020, 1971–2020 and 1981–2020 hardly differ, while they are significantly different from those of the overall series (1901–2020). Obviously, all three series starting from 1961 or later represent the current low-flow related status in the catchment of the Hofkirchen gauge and in the mentioned probability range. However, the series 1961–2020 is the only one including a rare extreme event (1962) with a magnitude comparable to that of known events in the more distant past (overall series starting in 1901, events of 1908 and 1928 estimated like described above). As shown in Fig. 7, extreme events and phases of wet and dry years are also reasonably well distributed over time during the period 1961–2020. Based on these observations and the fact that the Sylvenstein reservoir has been installed in the year 1959, the series 1961–2020 is chosen as representative period for low-flow statistics. This corresponds to the choice for other German rivers (BfG, 2021) under similar aspects and allows cross-basin comparability.

Like discussed in chapter 2, periods of low flow (<MAM) may be distributed differently during the year. To learn more about these characteristics of low-flow duration on the Danube river, series of maxD(<MAM) were derived using different pooling methods (MA10, SPA, see Fig. 3) and compared among each other and with sumD(<MAM) in scatter plots (see Fig. 8). As can be seen from Fig. 3 at the example of water-balance year 2018, the derivation of maxD can be very sensitive depending on the chosen threshold and pooling method. While $maxD_{MA10}$(<MAM, 2018) = 58 days is determined from the period of Oct. 6 until Dec. 2 (including a minor interruption from Oct. 29 until Oct. 31),

189

maxD$_{SPA}$(<MAM, 2018) = 128 days additionally includes the entire period from July 28 (with three additional minor interruptions). Like in 2018, maxD$_{MA10}$(<MAM) is often smaller than maxD$_{SPA}$(<MAM) and sumD(<MAM), in particular for pronounced low-flow years where the balance-oriented interruption criterion of the SPA is less strict than those of MA10 (see Fig. 8). For thresholds greater than MAM, this difference may even become stronger. On the other hand, the difference between sumD(<MAM) and maxD$_{SPA}$(<MAM) is often weaker and even years with greater maxD$_{SPA}$(<MAM) occur due to events spanning the turn of the year. From these comparisons, it can be concluded that streamflow thresholds and pooling methods should be defined very carefully according to the aimed statement on low-flow duration. Also more specific pooling criteria may be defined depending on hydrological conditions, relevant thresholds and aimed statements (e.g., inter-event time, cf. chapter 2). In the present, rather general oriented study, only sumD was further analyzed.
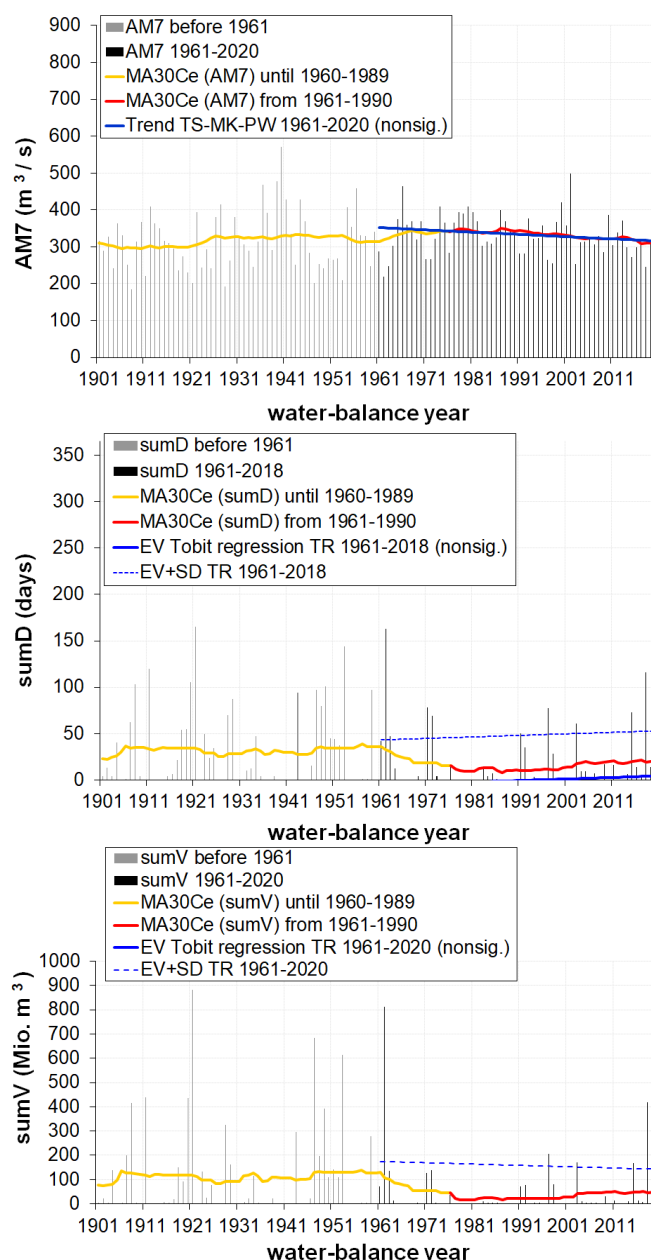

Fig. 6 Series of annual low-flow indices at the Hofkirchen gauge. In addition, 30-year moving averages with centred time reference (GM30Ce) and calculated trends for the period 1961–2020 according to different methods are included. Trends are not statistically significant. TS-MK-PW – Theil/Sen trend, trend test according to Mann-Kendall with prewhitening; TR – Tobit regression with expected value (EV) and expected value + standard deviation (EV+SD).

After initial findings from graphical analyses (e.g., suitable representative period for current status), statistical methods were applied for further and better founded statements. In present study, autocorrelation of AM7-series was investigated. Furthermore, stationarity of the series AM7, sumD(<MAM) and sumV(<MAM) was analyzed in order to detect possible long-term trends.
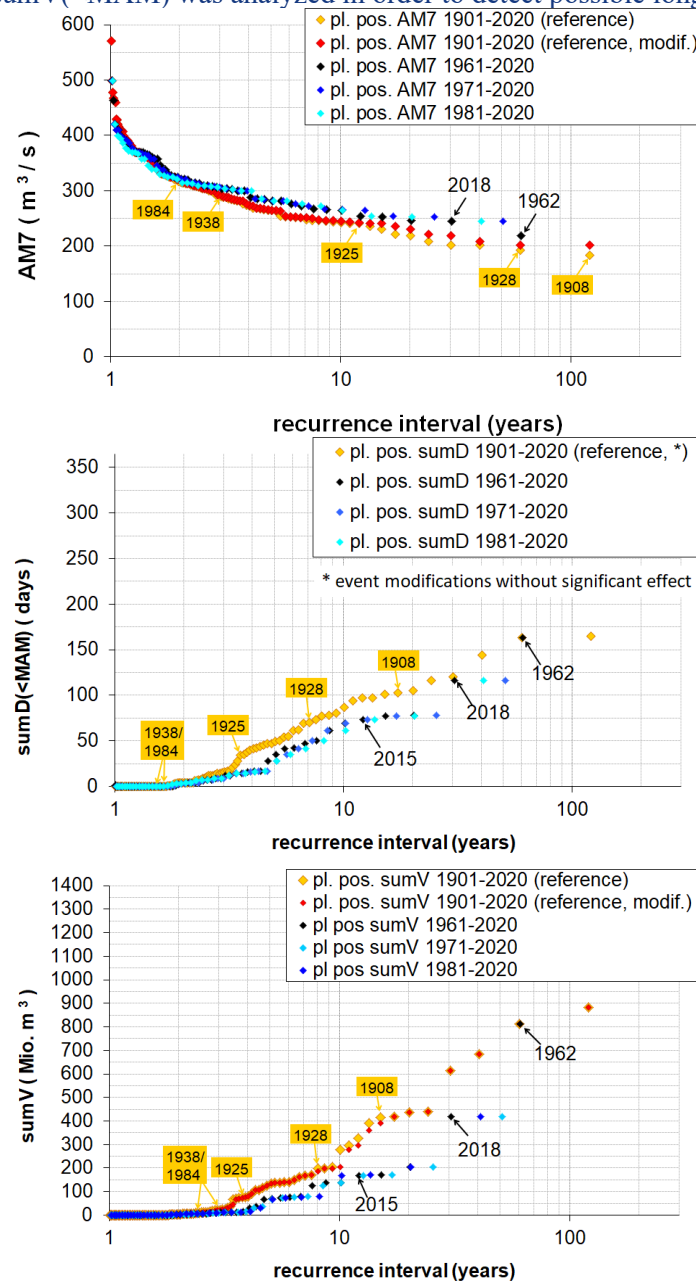

Fig. 7 Plotting positions and their empirical cdf's in probability plots for series of different low-flow indices and lengths at the Hofkirchen gauge. Overall series (1901–2020) serve as reference (partly with anomalies due to ice effects in indicated years and homogenized in modified series). Years of the series 1961–2020 are indicated if their empirical recurrence interval is >10 years.
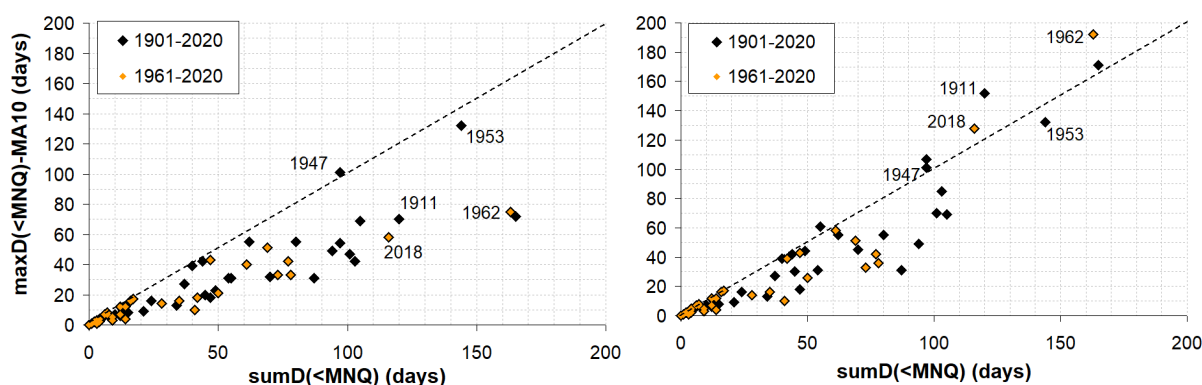
Fig. 8 Scatter plots for comparison of maxD(<MAM) and sumD(<MAM) series at the Hofkirchen gauge. maxD(<MAM) was derived using MA10-pooling (left side) and SPA-pooling (right side).

Persistence analysis of AM7 series:

Despite the reference to water-balance years, AM7 series may be persistent (autocorrelated) due to the hydrological memory in the river basin or due to long-term (decadal) climate variability. In addition to an enhanced hydrological process understanding, quantification of autocorrelation is important to evaluate the applicability of methods of trend analyses and extreme value statistics (see below). Therefore, the autocorrelation coefficient $\rho(1)$ according to Spearman was calculated with a time lag of one year. For the AM7 series 1961–2020, $\rho(1) = 0.306$ is obtained. According to an one-sided test using a t-distributed test statistic, this $\rho(1)$-value significantly deviates from zero (full independence) with a p-value of 0.009. A very similar value was obtained for the Bravais-Pearson autocorrelation coefficient $(r(1) = 0.29)$. The latter was further used to estimate the variance of the underlying independent variable according to (Hansen, 1971). Since this variance is only about 1.5 % greater than those of the original AM7 series, the loss of information due to autocorrelation at the given series length of 60 years is limited with regard to prerequisites of extreme value statistics.

Furthermore, the long-term development of autocorrelation coefficients $\rho(1)$ was analyzed. $\rho(1)$-values were calculated for sliding 30-year subseries (1901–1930 until 1991–2020) and plotted in Fig. 9 together with the one-sided significance level of $\rho(1) = 0.24$ (p-value 0.1). This analysis was expanded to additional Danube gauges (Kelheim, Pfelling, Achleiten). For all gauges, mostly significant autocorrelation is detected from the middle until the end of the 20th century, but not before and not in the recent past. This changeable development of $\rho(1)$ indicates that persistence in the AM7 series of the Danube is rather climate-induced than caused by the memory of the river basin. Autocorrelation at different Danube gauges show a changeable spatial structure over time and hence the need of more detailed investigations in tributary basins.
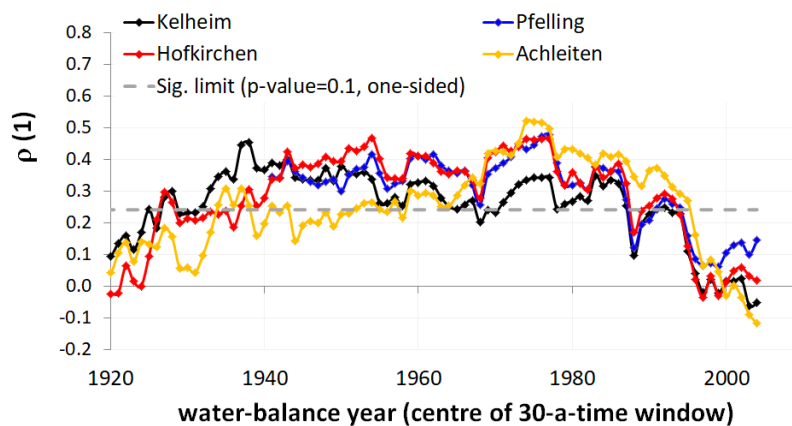

Fig. 9 Spearman autocorrelation coefficients ρ(1) at different Danube gauges with a time lag of one year for time slices of 30 years, shown with central reference points (e.g., 1976 for the time slice from 1961 to 1990).

Stationarity analysis of series of various low-flow indices (detection of possible trends):
Another important question of fundamental interest is whether the probability distribution of the series is stationary or long-term trends occur. Moreover, stationarity is a prerequisite for (classical) extreme value statistics. Therefore, stationarity analyses were carried out for means (all indices) and variances (only AM7) of the series.

To analyze stationarity of AM7 variance, the series 1961–2020 was subdivided in two sub-series (1961–1990, 1991–2020). With standard deviations of 54 and 55 m^3/s, the null hypothesis of variance homogeneity was maintained in a Levene test.

Stationarity of means of AM7, sumD(<MAM) and sumV(<MAM)) was analyzed using different methods. 30-year moving averages (MA30) indicated a long-term variability of low-flow conditions (Fig. 6). In the range of the 1980s, relatively high MA30 values were obtained for AM7 and relatively low values for sumD(<MAM) and sumV(<MAM), indicating a relatively weak low-flow characteristic in this period. On the other hand, stronger low-flow characteristics can be observed in recent years and in the 1960s. However, MA30 values of the 1960s include time windows extending beyond the chosen representative period beginning in 1961. Since similar developments were found in other German river basins (BfG, 2021), a long-term climate variability is presumably the primary cause of the described development of low-flow indices at the Hofkirchen gauge.

In addition, linear trend analyses and tests (cf. chapter 2) were performed for the series 1961–2020 of AM7, sumD(<MAM) and sumV(<MAM) (Fig. 6), but did not prove to be significant (p-values > 0.1 in one-sided tests). However, comparison with MA30 values shows that linear trends do not reflect the complete long-term dynamics of the low-flow indices. Corresponding trend analyses for tributary catchments with a comparison of northern and southern Danube tributaries might be revealing for an improved understanding of the long-term development of low-flow conditions on the Danube.

Altogether, no significant non-stationarity could be identified for the series 1961–2020 of the analyzed low-flow indices. Together with the relatively weak effect of autocorrelation (see above), the prerequisites of classical approaches for extreme values statistics are thus sufficiently fulfilled.

Extreme value statistics:
Like described in chapter 2, extreme value statistics were developed to estimate occurrence probabilities (or statistical recurrence intervals T) of given values of a low-flow index or, vice versa, quantiles of given occurrence probabilities. For this purpose, theoretical cdf's were fitted to analyzed series, for sumD(<MAM) and sumV(<MAM) embedded in a conditional probability approach. To support the selection of a suitable cdf and to reduce uncertainty in the extreme range, information expansions based on historical information and, for sumD and sumV, on graded thresholds were used.

Figure 10 shows probability plots for the Hofkirchen gauge according to the described procedure with plotting positions (PP) of the representative series 1961–2020 (for sumD and sumV also reference series with thresholds Q70 and Q85), extreme PP related to the overall observation period (only T > 30 years), selected and fitted theoretical cdf's and their confidence intervals.

For the AM7 series 1961–2018, the 2-parameter Gamma distribution, fitted using L-moments (G2 LM), agrees well with the distribution of PP's up to the extreme range. However, G2 LM takes higher values than the extreme PP of the long-term reference series (1901–2020). On the other hand, the 1908 and 1928 events are concerned by ice-related anomalies in the hydrograph (see above). After correction of these anomalies, other events are to be assigned to the extreme PP of the long-term reference series, with the autumn event 1921 (without ice influence) as smallest AM7 value. These extreme PP's are also below the fitted G2 LM. However, this difference can be explained for the PP's before 1959, at least in the order of magnitude, by the fact that the Sylvenstein reservoir was still not in operation at that time (cf. above). It should be noted that the selected G2 LM behaves more plausibly in the extreme range than the otherwise often preferred Weibull distribution (WEI, added in Fig. 10 for comparison purposes). However, this choice plays little role in the statistical classification of the AM7 values of recent years (including 2018).

For sumD(<MAM) and sumV(<MAM), the values of the water-balance year 1962, in which the low-flow event lasted until March, are significantly greater than the other values of the 1961–2018 series, resulting in corresponding uncertainties in the choice of a suitable cdf, in particular with regard to its extrapolation. Other extreme PP's of the long-term reference series show values of similar magnitude, although they extend less far into winter. Thus, for sumV(<MAM) they support the choice of a cdf with increasing values in the extrapolation range (WEI, fitted using the Max. Likelihood method ML). This choice is further supported by the cdf's of the reference series sumV(<Q15) and sumV(<Q30) with largely parallel or only slightly diverging course in the probability plot. For sumD(<MNQ), the selected cdf (Pearson-3 P3 LM) is also plausible compared to the reference series. The cdf's are embedded in the conditional probability approach according to Eq. (3).

Fitted cdf's and corresponding quantile functions could finally be used to calculate recurrence intervals T and quantiles of interest for the Hofkirchen gauge. Table 1 contains the quantiles for selected recurrence intervals (T = 2, 5, 10, 20, 25, 50, 100 and 200 years). For comparison, the values of recent years (2015–2020) are also included in the table. Based on this overview, these events or years may be assigned to classes of their probability of occurrence.

In 2015, AM7 had a return interval between 5 and 10 years. However, sumV(<MAM) and even more sumD(<MAM) had significantly higher return intervals between 10 and 20 years. Thus, the year 2015 was particularly characterized by its long-lasting duration of low flow and the resulting deficit volume. The year 2018 was even more extreme, with return intervals between 20 and 50 years for all analyzed indices. Also in this year, the duration sumD(< MAM) is to be emphasized (return interval about 40 years). In 2020, AM7 again reached a similar value as in 2015, but the return interval between 5 and 10 years also applies to the other two indices. Thus, the year as a whole was less extreme than 2015. Finally, in 2016, 2017, and 2019, above-average low-flow events also occurred, but with much smaller recurrence intervals between 2 and 5 years (around 3 years across the three indices).
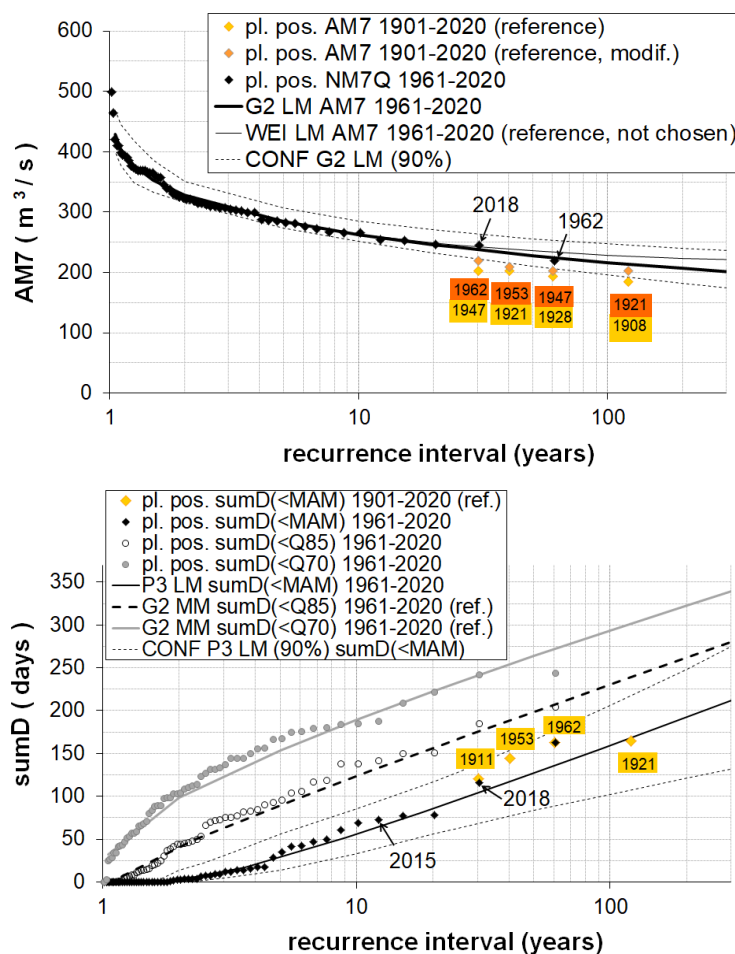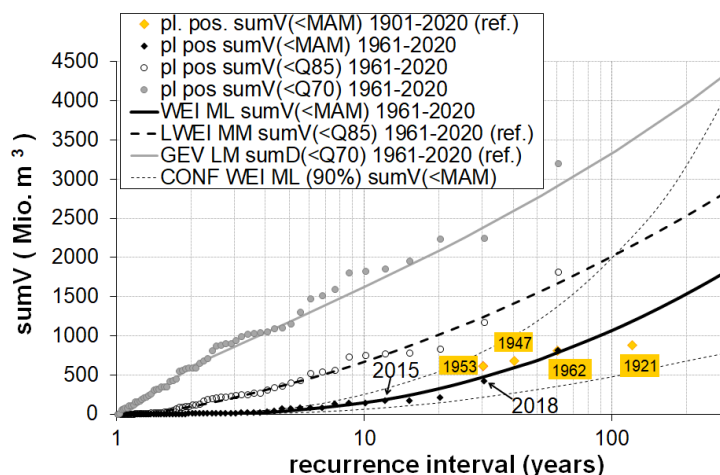
Fig. 10 Probability plots for series of different low-flow indices (see chapter 2) 1961–2020 at the Hofkirchen gauge. Years with empirical recurrence interval > 10 years are indicated. Beside plotting positions for the series 1961–2020, also those of long reference series are shown with indication of the year (only for empirical recurrence intervals > 30 years). Theoretical cdf's are fitted to these series (partly shown with confidence intervals CONF) using different methods of parameter estimation. Cdf's: G2 (2-param. Gamma), P3 (Pearson-3), WEI (Weibull), LWEI (log. Weibull), GEV (generalized extreme value distribution). Parameter estimation: MM – method of moments, LM – method of L-moments, ML – Max. Likelihood method).

Conclusions and perspectives

The low-flow sequence of the past years underlines the need for a comprehensive analysis of the low-flow situation on the Danube in order to answer questions about possible magnitudes and frequencies of extreme events or years and about the long-term development of the low-flow situation.

The methods described and applied in present paper can contribute significantly to this aim by deriving and providing meaningful hydrological information within an interdisciplinary framework on river basin level. Such a contribution by BfG is planned within the IHP project "Low Flows and Hydrological Drought in the Danube Basin". In order to demonstrate the applicability of the methods proposed for this project and to gain first insights in the German section of the Danube, different methods for inspection and preparation of hydrological data (daily streamflow series), time series analysis, statistical inference and extreme value statistics were applied to the Hofkirchen gauge. These methods were used in connection with information expansion and hydrological reasoning in order to better validate and understand the results, especially with regard to uncertain extremes. The following methodological and Danube-related findings can be emphasized.

Table 1 Quantiles of selected recurrence intervals T for different low-flow indices at the Hofkirchen gauge. For comparison and classification, also values of the years 2015–2020 are included in the table. For symbols and abbreviations, see chapter 2 and Fig. 10.

	AM7 (m³/s)	sumD(<MAM) (days)	sumV(<MAM) (Mio m³)
cdf	G2 LM	P3 LM	WEI ML
p0	–	0,45	0.55
T=2 y.	328	1	→ 0
T=5 y.	284	28	41
T=10 y.	263	56	144
T=20 y.	246	86	325
T=25 y.	241	96	400
T=50 y.	228	127	689
T=100 y.	217	159	1067
T=200 y.	206	192	1535
2015	272	73	169

2016	300	14	14
2017	307	4	7
2018	245	116	419
2019	309	14	13
2020	276	41	68

A basic inspection of streamflow data focusing on the low-flow range is recommended for low-flow studies, even if these data are already officially checked. In the best case, remaining uncertainties can be eliminated. At least, however, an (improved) knowledge of uncertainties can be achieved in order to be able to take them into account in the interpretation of analysis results based on these data.

Present study confirmed that low-flow events and years (on the Danube as well as on other rivers) can have diverse and different characteristics, especially in the extreme range. This concerns mainly the intensity (minimum streamflow), duration and deficit volume of the events and has to be captured by suitable low-flow indices. In addition to the intended hydrological or interdisciplinary statement, various aspects have to be considered very carefully when defining the indices, in particular with regard to low-flow duration and deficit volume. These aspects concern streamflow threshold values, to which duration and deficit volume refer, and the handling of short-term interruptions of non-exceedance periods (pooling with respect to maxD and maxV). For analyses across different gauges or river basins, robust or unambiguously defined parameters (sumD, sumV) show a better comparability.

Graphical methods for analyzing series of low-flow indices, especially probability plots, proved to be very useful. They can support data inspection and provide initial insights into the characteristics of the series, among other things with regard to a representative period for statistical analyses. Furthermore, probability plots are suitable for the diagnosis of extreme value statistics, since they allow to combine different information (empirical and theoretical cdf's, indices with graded thresholds, different reference periods) and to assess them in an overall picture (information expansion, cf. below).

The application of time series analysis methods provided insights into the long-term behavior of the series. A long-term variable persistence between low-flow values (AM7) of successive years (short-term autocorrelation) was detected. AM7-autocorrelation was significant during the 2nd half of the 20th century, but no longer in the last decades. The temporal variability suggests that this persistence had mainly climatic causes. Moreover, the investigated low-flow indices (themselves) show long-term dynamics with more or less affected (wetter and drier) phases. There is a need for further investigations on these topics (e.g., with regard to a spatial, possibly also scale-dependent variability in the Danube basin). However, at the Hofkirchen gauge, no significant (linear) trend can be detected for the investigated low-flow indices in the last decades. Altogether, the time series analysis showed, in addition to the basic findings, that the prerequisites for classical extreme value statistics at the Hofkirchen gauge are sufficiently fulfilled.

For extreme value statistics, information expansions proved to be very useful to better validate statements in the extreme and especially in the extrapolation range of fitted cdf's. This includes temporal expansions with the inclusion of historical information as well as for sumD(<MAM) and sumV(<MAM) causal expansions with reference series of graded threshold values aiming at plausible overall characteristics of the statistics.

Based on these analyses, answers to the question raised at the beginning could be given. Low-flow index values can be calculated for given recurrence intervals and, conversely, certain index values (e.g., from the years 2015–2020) can be statistically classified. This also allows a comparison with results from corresponding analyses for other river basins in Germany (BfG, 2021). According to this, the German Danube was affected by extreme low flow in the past years at least to a comparable relative magnitude as the Rhine, but less than the river basins further north or northeast (Weser, Elbe, Oder, see (BfG, 2021) for details). However, despite the sequence of low-flow years from 2015 until 2020, no statistically significant change of the long-term low-flow situation was detected on the German Danube (Hofkirchen gauge) so far.

The methods and results of present paper may serve as a starting point for the development of corresponding low-flow statistics for the entire Danube river and be further developed in the course of this. The spatial expansion and the occurrence of future extreme events may lead to further hydrological

challenges (among others, non-stationary extreme value statistics, differentiated treatment of different low-flow types by event classification, analysis of simulated future projections in the context of statistics derived from past observations). With regard to this, above-mentioned publications of (BfG, 2021) and (DWA, 2021) provide further results and technical information that could be taken up and further developed in an interdisciplinary and international cooperation in the Danube basin in order to serve as a basis for a river basin related low-flow management. A first step on this way is the common project "Low Flows and Hydrological Drought in the Danube Basin" within the IHP-cooperation of the Danube countries under the project lead of CHMI.

References

BfG – Bundesanstalt für Gewässerkunde (2021): Die Niedrigwassersequenz der Jahre 2015 bis 2018 in Deutschland. BfG-Mitteilung Nr. 35. Koblenz.

Burn, D. H. (2003): The use of resampling for estimating confidence intervals for single site and pooled frequency analysis. *Hydrological Sciences Journal.* **48** (1), S. 25–38.

DWA – Deutsche Vereinigung für Wasserwirtschaft, Abwasser und Abfall e.V. (2021): Merkblatt DWA-M 541 – Statistische Analyse von Niedrigwasserkenngrößen. DWA. Hennef.

Fleig, A.K., Tallaksen, L.M., Hisdal, H., Demuth, S. (2006): A global evaluation of streamflow drought characteristics. *Hydrol. Earth Syst. Sci*, **10**: 535–552.

Frei, Ch. (2013): R package 'trend 1.5.1' (Functions for trend estimation and testing).

Hansen, E. (1971): Analyse af hydrologiske tidsserier. Lab. for Hydraulik, Danmarks Tek. Hoyskole, Polytek. Forl. Lyngby.

Henningsen, A. (2020): Estimating Censored Regression Models in R using censReg Package. Univ. of Copenhagen.

Hirsch, R.M., Helsel, D.R., Cohn, T.A., Gilroy, E.J. (1993): Statistical analysis of hydrologic data. Maidment, D.R. (ed.): Handbook of Hydrology. 17.1 bis 17.55.

Kendall, M.G. (1970): Rank correlation methods, 4th edition. London.

Klein, B. (2010): EXANTO – Extreme Value Analysis Tool. Software Dokumentation. Ruhr-Universität Bochum.

Levene, H. (1960): Robust tests for equality of variances. In: Ingram Olkin, Harold Hotelling et al (Hrsg.): Contributions to Probability and Statistics: Essays in Honor of Harold Hotelling. Stanford University Press: 278–292.

KLIWA (2018): Niedrigwasser in Süddeutschland. Analysen, Szenarien, Handlungsempfehlungen. KLIWA-Bericht, Heft 23.

LfU (2021): Niedrigwasser 2018 und 2019 – Analysen u. Auswertungen für Bayern. Bericht Bayer. Landesamt für Umwelt.

LfU (2017): Niedrigwasser in Bayern – Grundl., Veränd. u. Auswirkungen. Ber. Bayer. Landesamt f. Umwelt. Augsburg.

Makkonen, L. (2006): Plotting Positions in Extreme Value Analysis. *J. of Appl. Meteorol. and Climatol*., **45**, 334–340.

Mann, H.B. (1945): Nonparametric tests against trend. *Econometrica*, **13**: 245–259.

Pardé, M. (1947): Fleuves et Riviéres. Armand Colin. Paris.

Sen, P.K. (1968): Estimates of the regression coefficient based on Kendall's tau. *J. Americ. Statist. Assoc.,* **63**, p. 1379–1389.

Stedinger, J.R., Vogel, R.M., Fourfoula-Georgiou, E. (1993): Frequency analysis of extreme events. Maidment, D.R. (ed.): Handbook of Hydrology.

Tallaksen, L.M., van Lanen, H.A.J. (2004): Hydrological drought.. Elsevier.

Theil, H. (1950): A rank-invariant method of linear and polynomial regression analysis. Parts 1–3. *Nederlands Akad. Wetensch. Proc*. **53**, S. 386–392, 521–525, 1397–1412.

Tobin, J. (1958): Estimation of Relationships for Limited Dependent Variables. *Econometrica* **26**, p. 24–36.

Tuszynski, J. (2014): R package 'caTools 1.17' (Tools: moving window statistics, GIF, Base64, ROC AUC, etc.).

Wang, X. L., Swail, V. R. (2001): Changes of extreme wave heights in northern hemisphere oceans and related atmospheric circulation regimes. *Journal of Climate*. Vol. **14**, S. 2204–2221.

Weibull (1939): Weibull, W., 1939: A statistical theory of strength of materials. Ing. Vetensk. Akad. Handl, 151.

WMO – World Met. Org. (2008): Manual on low flow estimation and prediction. *Op. Hydrology Rep.* No. **5**, WMO-No. 102.

Yue, S., Pilon, P., Cavadias, G. (2002a): Power of the Mann-Kendall and Spearman's rho tests for detecting monotonic trends in hydrologic series. *Journal of Hydrology*, **259**, S. 254–271.

Zhang, X. und Zwiers, F. W. (2004): Comment on ''Applicability of prewhitening to eliminate the influence of serial correlation on the Mann-Kendall test. *Water Resources Research*, Vol. **40**.

SWICCA data in climate change impact study on 100-year floods

Eva Kopáčiková, Hana Hlaváčiková, Kateřina Hrušková, Danica Lešková

Slovak Hydrometeorological Institute, Jeséniova 17, 833 15 Bratislava, Slovakia, email:
eva.kopacikova@shmu.sk, hana.hlavacikova@shmu.sk, katerina.hruskova@shmu.sk, danica.leskova@shmu.sk

Abstract

During the ongoing climate change, this work provides an analysis of the modelled expected change in floods (100-year) for 11 Slovak river basins. It also analyses the possibilities of using data from the latest climate projections of global and regional models from the EURO-CORDEX initiative, as well as outputs from two hydrological models from the SWICCA database (Service for Water Indicators in Climate Change Adaptation) within the Copernicus service, for regional conditions in Slovakia. To estimate the 100-year flood, a frequency analysis was applied to each member of the climate and hydrological model output ensemble. The statistical distribution of generalized extreme values (GEV) was used. In case the data showed a significant trend, the non-stationarity of the environment was also taken into account. The bias of hydrological models outputs were corrected by the variance scaling method. The results indicate an increase in Q_{100} for seven gauges, a decrease for three gauges and for one station no change in Q_{100} (change more than $\pm\ 5\%$). Based on the results, we recommend applying hydrological data from the SWICCA database, preferably for large to medium-sized river basins.

Introduction

It is not easy to estimate the impact of climate change in water management, but also in other areas. Climate change is manifested differently in different geographical areas, great variability of natural processes, not to mention anthropogenic influences, are a natural part of the climate. The expected climate change raises a number of technical issues and uncertainties that are the subject of studies and discussions. It is mainly an increase in the extremity of hydrological phenomena (increase in extreme values, but also the frequency of their occurrence) in the form of drought or floods, but also a change in the hydrological regime of watercourses themselves and the impact of these phenomena on society. It is not entirely clear how the period with the highest or the lowest expected water levels in the year, their frequency, but also the values of absolute maximum and minimum discharges, the time shift of snow accumulation and melting and the total water balance in river basins will be changed.

The aim of this work was to analyze the change in high flows, in this case hundred-year flows (Q_{100}), due to the expected climate change. In the long run, such estimates are very important. They are essential for planning water management strategies and taking early adaptation measures to mitigate climate change.

This work provides an analysis of the modelled expected change in Q_{100} for 11 Slovak river water gauging stations. It also analyses the possibilities of using data from the climate projections of global and regional climate models from the EURO-CORDEX initiative, as well as outputs from two hydrological models (HYPE and LISFLOOD) from the SWICCA database within the Copernicus service, for regional conditions in Slovakia. The SWICCA portal (Service for Water Indicators in Climate Change Adaptation, http://swicca.climate.copernicus.eu/, as of 15.5.2019) is the result of the work of the Swedish Meteorological and Hydrological Institute (SMHI) and was operational under the auspices of Copernicus. Copernicus climate data for impact studies in water sector contain modelled impact indicators such as water runoff and wetness, river flow, snow water equivalent, soil water content and other water related quantities for the European region. They were produced with the aim to speed up the workflow in impact assessments and to simplify climate change adaptation of water management practices across Europe. These quantities were modelled using the Swedish Meteorological and Hydrological Institute E-HYPE, the Wageningen University VIC and the Joint Research Centre LISFLOOD models.

The methodology of estimating Q_{100} based on the outputs of climate and hydrological models from the SWICCA database was for the first time used in Slovakia in the project C3S_441_Lot1_SMHI. Local case study "Flood warnings in a changing climate" were published in Gaál et al. (2017) for the Bratislava (Danube) water gauging station. Therefore, our goal was to test the database and methodology for more river basins in Slovakia, results of which are provided in this paper.

Methodology

The SWICCA portal and database

The aim of the SWICCA portal was to provide users with the necessary data to assess climate change and its impact in various areas of water management (for case studies) across Europe in order to subsequently quantify the impact of projected climate change in the field of water resources. The interconnection of information between experts from different fields (climatologists, water managers, hydrologists, numerical mathematicians), but also competent decision-makers should serve this goal. One of the main outcomes of the SWICCA project were case studies which were meant to serve as basis for the design of adaptation plans. SWICCA data is currently available through the Climate Data Store (https://cds.climate.copernicus.eu/cdsapp#!/dataset/sis-water-quantity-swicca?tab=overview, available 13.4.2021) within the portal Copernicus Climate Change Service (C3S). The portal offers free access to various simulated impact indicators, e.g. data on water quantity and quality, air temperature, precipitation, cloud cover, air humidity and many others, on which it is possible to analyze the impact of climate change in terms of trends and variability of a particular indicator.

For the purpose of this impact study, two types of time series of average daily flows were downloaded from the SWICCA portal as outputs of eleven mutual combinations of four global circulation models (GCM), four regional climate models (RCM), three climate scenarios (RCP) and two hydrological models: 1 / hydrological model E-HYPE and 2 / hydrological model LISFLOOD (Table 1). Table 1 lists the names of GCM and RCM, along with the name of the institute that develops these models.

*Table 1 Summary of climate model runs used in SWICCA database. RCP – indicates the representative concentration pathway and its development direction, GCM – global circulation model, RCM – regional circulation model. *missing data in years 2095 – 2100. The period 1.1.1971 – 31.12.2000 was taken as the reference period and 1.1.2011 – 31.12.2100 was considered as future.*

No.	RCP	GCM	RCM	Time period	Institute
1	2.6	EC-EARTH	RCA4	1970–2100	SMHI
2		MPI-ESM-LR	REMO2009	1970–2100	CSC
3	4.5	EC-EARTH	RCA4	1970–2100	SMHI
4		EC-EARTH	RACMO22E	1970–2100	KNMI
5		HadGEM2-ES	RCA4	1970–2098	SMHI
6		MPI-ESM-LR	REMO2009	1970–2100	CSC
7*		CM5A	WRF33	1970–2100*	IPSL
8	8.5	EC-EARTH	RCA4	1970–2100	SMHI
9		EC-EARTH	RACMO22E	1970–2100	KNMI
10		HadGEM2-ES	RCA4	1970–2098	SMHI
11		MPI-ESM-LR	REMO2009	1970–2100	CSC

Representative concentration pathway (Emission scenarios)

The different used climate datasets originate from different climate models, as well as three different emission scenarios, which represent the scenarios of climate development. The Intergovernmental Panel on Climate Change (IPCC) lists them in a recent report in the form of representative concentration pathways (RCPs) (van Vuuren et al., 2012). SWICCA works with three basic scenarios, defining them as follows: 1/ RCP2.6 assumes that CO_2 emissions will be constant at the beginning of the century, then start to decrease and reach negative values at the end of the century, 2/ RCP4.5 assumes that CO_2

emissions will increase by the middle of the century and then begin to decline, 3/ RCP8.5 assumes that CO_2 emissions will triple by the end of the century and methane emissions as well as the use of energy and fossil fuels will also increase. The most pessimistic scenario further assumes that understanding the concept of renewables will be very limited and the implementation of the climate strategy will be missing. Figure 1 shows the effect of different gas emission concentrations (expressed by RCPs) and predicted impact on the global surface temperature.
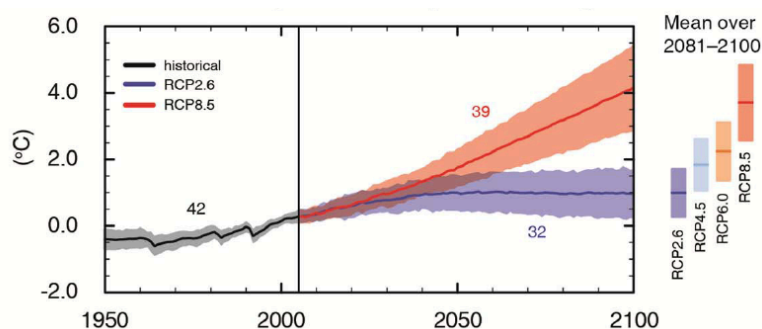

Fig. 1 The effect of different gas emission concentrations (expressed by RCPs) and predicted impact on the global surface temperature (source: IPCC AR5 WGI Global average surface temperature change).

A scheme displaying the sequence of data generation for climate change impact purposes is shown in Figure 2. First, the RCPs are being prepared and inserted to the global climate models. The results are next downscaled by regional climate models, the outputs of which are bias corrected and used in impact models (hydrological models to provide discharge).
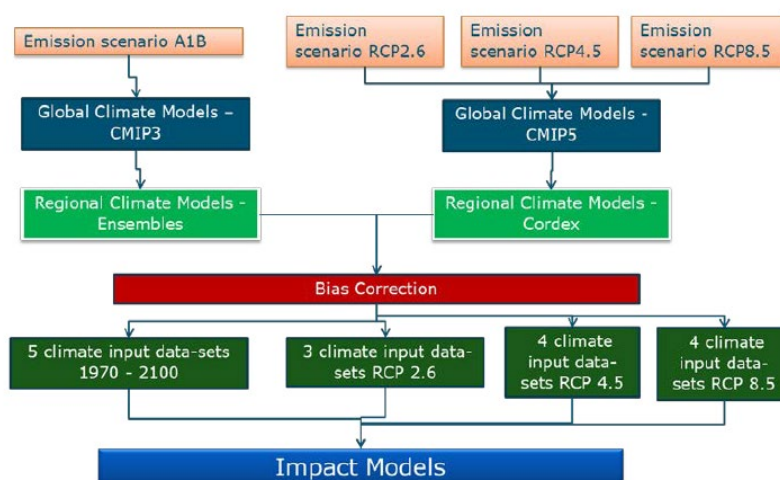

Fig. 2 Climate data flow diagram, used to generate data for impact studies. (Source: http://impact2c.hzg.de/imperia/md/content/csc/projekte/impact2c_d5.1_fin.pdf, available 5.2.2019)

Estimation of the 100-year flood

An interesting way to quantify climate change in water management is to estimate the 100-year flow based on outputs from climate models. In contrast to the analysis of long-term historical data and the assumption that conditions remain unchanged, the Copernicus Climate Change Service makes it possible to obtain predicted time series of climate characteristics from the future for 89 years and perform a frequency analysis on a relatively large sample of data.

The following procedure was chosen for estimating Q_{100}:

1/ download time series of average daily flows from all available climatic outputs and from two hydrological models HYPE and LISFLOOD from the SWICCA portal for selected gauges in Slovakia, 2/ data check and bias-correction for the reference period 1971–2000, 3/ selection of annual maxima, 4/

conversion of annual maxima of average daily flows into annual peak flows according to the methodology of Hlaváčiková et al. (2019), 5/ trend analysis by non-parametric Mann-Kendall test, 6/ frequency analysis (stationary or non-stationary).

Due to the low quality of raw data for the stations Banská Bystrica (Hron), Liptovský Mikuláš (Váh), Janík (Bodva) and Spišské Vlachy (Hornád) found by data check at the reference period, flow outputs from the SWICCA database (from hydrological models LISFLOOD and HYPE) were not used in this case. Instead, the following procedure was adopted: 1/ download of time series of precipitation and temperatures from all available climatic outputs from the SWICCA portal, 2/ calibration of hydrological model HBV for daily step, 3/ model run for different sets of input data from climate models. The next procedure was the same as in the previous one starting at point 2.

Hydrological models used for climate change impact modelling

All hydrological models, the outputs of which were used in this work, are conceptual rainfall-runoff models. The HYPE model (E-HYPE v. 3.1.2) is a semi-distributed successfully used model in the short-term and seasonal forecasting, as well as in the hydrological warning operational service at the SMHI. The model was calibrated and validated in a daily time step for more than 35,000 sub-basins in Europe with an average river basin size of 215 km^2. For these sub-basins, the suitability for application in climate change analyses has also been assessed (Hundecha et al., 2016).

The LISFLOOD hydrological model was developed as part of the Natural Hazard Project by the Joint Research Centre (JRC) of the European Commission. LISFLOOD is used for daily forecasts within the EFAS and GLOFAS operational alert systems. More information about the model can be found in the report by Burek et al. (2013).

Application of these models for climate change studies was also tested on 46 big European basins (Greuell et al., 2015). Spatial resolution of hydrological models from the SWICCA database is following: 0,5 x 0,5 degrees (ca 50 x 50 km) for the LISFLOOD model and irregular polygons of basins with the median area of 215 km^2 for the model E-HYPE v. 3.1.2.

The HBV model (IHMS 6.4) is used daily for approximately 60 Slovak river basins in the Department of Hydrological Forecasts and Warnings of the SHMÚ. It is also commonly used worldwide in a modified form such as HBV-Light. For the purpose of this analysis, the model was calibrated in a daily time step for four Slovak river basins.

Bias correction of hydrological data

Hydrological simulations of future will mostly improve if their inputs are bias corrected (Hakala et al., 2019). The parameters of the hydrological models, which were calibrated on the current climate conditions, are then used for simulations of the period of the assumed changed climate with the bias corrected forecasted meteorological data. Despite great efforts to adjust the outputs of RCM models by bias correction and downscaling, several meteorological variables from RCM models are still not suitable for their use in hydrological impact studies (Teutschbein and Seibert, 2012, Dakhlaoui et al., 2019, Gao et al., 2020). This can be resolved using e.g. a multi-ensemble approach. This approach uses an ensemble of climatic outputs from RCM models (precipitation and temperatures), downscaled so that when used in the hydrological model they correspond to the measured hydrological data as much as possible (usually comparing average monthly flows or peak flow exceedance curves according to the type of analysis) (Teutschbein and Seibert, 2010, Hakala et al., 2019, Gao et al., 2020). Another solution is to use an ensemble of climate and hydrological models (Donnelly et al., 2017, Hakala et al., 2019) without further correction of previously corrected climate data (IMPACT2C, 2015). Some authors also performed the bias correction directly on hydrological data (Gonzáles-Zeas et al., 2012, Gaál et al., 2017).

In this work, the bias correction was performed directly on hydrological data. The statistical characteristics of hydrological simulations from the SWICCA database sometimes showed a greater or lesser deviation compared to the characteristics of the measured average daily flows. For a more detailed description of bias correction applied in this analysis, please see Kopáčiková et al. (2020).

Frequency analysis and non-stationarity

The 100-year flow is generally estimated by the method of frequency analysis. In this study, we fitted the generalized extreme values (GEV) distribution function as it has a theoretical basis for application to the data of block maxima characterizing floods (Gilleland and Katz, 2016). For more details see Kopáčiková et al. (2020).

In analyses of the future, it is necessary to take into account the non-stationarity of the environment and to consider the possibility that probabilities of the occurrence of extreme phenomena in hydrology will shift (Milly et al., 2008). The change in extreme events over time can be characterized by expressing one or more parameters of the distribution function as time-dependent. In order to take into account the non-stationarity in the frequency analysis of the maximum annual flows, it is first necessary to determine the trajectory and the significance of the change in the time series. For annual maxima series, a linear trend is being used most frequently in the literature. In this analysis, a non-parametric Mann-Kendall test was applied for identification of a significant trend. Subsequently, it is decided whether and to which parameter of the distribution function, the non-stationarity will be taken into account. The choice of model should be as simple as possible and at the same time it should be able to take into account variations of the dataset as much as possible. The model of non-stationarity is applied to describe the process of data creation, not the data itself, so if the trend is not particularly significant, a simpler model should be chosen (Coles, 2001).

Expression of climate change impact for the estimation of Q_{100}

The climate change impact for Q_{100} (CCQ_{100}) was expressed as the percentage change in Q_{100} in the future compared to the present as follows:

$$CCQ_{100} = 100 * (Q_{100, fut} - Q_{100}) / Q_{100} \ (\%)$$

$$(1)$$

where $Q_{100, fut}$ – the estimated 100-year flood for the period 2011–2100, Q_{100} – the current 100-year flood at the relevant water gauging station.

The final average values of future Q_{100} were obtained from the whole ensemble of climatic and hydrological models available for a given station (i.e. for 11 outputs from climate models and 2 outputs from two hydrological models, i.e. 22 members of the ensemble). Uncertainties in estimating the change in Q_{100} were quantified from the interquartile range of average climatic impact factors of the entire CCQ_{100} ensemble for a particular station. This method expresses uncertainty by giving the range where 50% of the average CCQ_{100} values for a given station were estimated.

Uncertainties in estimation of Q_{100}

Several uncertainties need to be considered in climate change impact studies. These uncertainties cover all aspects of the lack of knowledge of the future climate (IMPACT2C, 2014). The main sources of uncertainty can be divided into several groups, with regard to:

1/ the selection of used climate models (global or regional) and their parameterization and conceptualization (i.e. by way of mathematical description of physical processes in the atmosphere), 2/ the selection of climate scenario, but also with the way these scenarios are determined (scenario uncertainty), 3/ the correction of outputs from climate models using downscaling techniques and bias correction.

In the case of impact studies in the field of water management, it is necessary to take into account the uncertainties arising from the selection of hydrological models and, similarly to climate models, their parameterization and conceptualization.

Models always represent a simplified version of natural processes. All climatic models are based on more or less the same physical principles, but differ in their mathematical expression. Model uncertainties arise from incomplete knowledge of the climate system and from the unlikelihood to include all processes and characteristics of the climate system in models. The same applies to hydrological models, reflecting hydrological processes in river basins. To reduce the degree of

uncertainty, climatologists use multi-model ensemble simulations. Different combinations of GCM and RCM are used in regional climate projections resulting in a multi-global/regional-model-ensemble dataset. An example for Europe is the results of the EURO-CORDEX project. Ensemble experiments are a common method of assessing the uncertainties arising from climate change projections (Knutti and Sedlacek, 2013).

We have tried to eliminate uncertainties related to the choice of hydrological models in several ways: First of all, we have tried to use hydrological models that have been and are tested on many river basins in Europe and provide good results. The second method of eliminating the uncertainties was a comparison of statistical characteristics of time series from HYPE and LISFLOOD models for selected Slovak water gauging stations with characteristics from measured time series on an overlapping (reference) period of 30 years and bias correction of model outputs by variance scaling method. If the results were not satisfactory even after the application of the bias correction, we excluded the models and stations from further analysis, or replaced them with the results from our own calibrated HBV model, if these were satisfactory for the reference period.

Other uncertainties may be related to the appropriate choice of the distribution function for the frequency analysis and to the uncertainties of the estimation of the peak flows from the average daily flows (Hlaváčiková et al., 2019).

Results

Our first contact with the SWICCA database was in 2017 when we participated on a case study analysis studying the impact of climate change in the Bratislava station (Danube basin). Since then, we wanted to test the database for its use on the entire Slovak territory. Following this intention, we initially downloaded the data for 26 stations and investigated their suitability over the reference period. Finally, we chose 11 stations covering all Slovak basins. They all belong to the Danube basin – Black Sea drainage area (with sub-basin sized from 378 to 131331 km^2) and one basin Poprad (Chmeľnica station) is a sub-basin of Visla river – Baltic Sea drainage area (with sub-basin size of 1262 km^2).

The final selection of river basins with the results of the climate change impact on Q_{100}, expressed by the climate change impact CCQ_{100}, which is the percentage change of Q_{100} in the future compared to the present, is shown in Table 2. The results show an increase in Q_{100} for seven stations: Bratislava (Danube), Moravský Sv. Ján (Morava), Liptovský Mikuláš (Váh), Vlkyňa (Slaná), Ipeľský Sokolec (Ipeľ), Streda n. Bodrogom (Bodrog) and Veľké Kapušany (Latorica), in the range of values 5.48–34.12%. A decrease in Q_{100} is indicated for stations Chmeľnica (Poprad), Banská Bystrica (Hron) and Janík (Ida, Bodva river basin) in the range of –17.99 to –47.03%. No significant change in Q_{100} (change of more than $\pm$ 5%) was found for the Spišské Vlachy (Hornád) station. The most significant increase is indicated for the Liptovský Mikuláš station, where the average impact of climate change CCQ_{100} is + 34%, half of the values are in the range of 17–53% (Fig. 3). On the contrary, the most significant decrease is expected in the Bodva river basin (Janík – Ida station), where the impact of climate change CCQ_{100} ranged from – 67 to –23% with an average value of –47%.

Uncertainties in estimating the change in Q_{100} can be seen from the interquartile range of average climate change impact factors of the entire CCQ_{100} ensemble for a particular station (Fig. 3). Figure 3 shows a relatively wide interquartile range of CCQ_{100} for the stations Veľké Kapušany, Ipeľský Sokolec and Chmeľnica, which indicates a greater uncertainty in the estimation of the future Q_{100}. Based on the CCQ_{100} interquartile range (range of values from the 25th to the 75th percentile), it is possible to divide stations into three categories: stations with the least estimation uncertainty in the range of 18–25% (Bratislava, Moravský Sv. Ján, Banská Bystrica, Vlkyňa, Janík), stations with a medium estimation uncertainty in the range of 34–39% (Streda n. Bodrogom, Liptovský Mikuláš, Spišské Vlachy) and stations with the highest estimation uncertainty in the range of 59–91% (Chmeľnica, Ipeľský Sokolec, Veľké Kapušany).

Table 2 Data on gauging stations, current and estimated Q_{100} along with the change in Q_{100} expressed by the average climate change impact for Q_{100} (CCQ_{100}). The applied hydrological model for the respective gauge is given in parentheses; the HYPE and LISFLOOD model were used in the other stations.

| Gauging station	River	Catchment	Catchment area (km²)	Q_{100} current (m³/s)	Q_{100} future (m³/s)	CCQ_{100} (%)
Bratislava	Dunaj	Dunaj	131331	11000	13290	⬆ 20.32
Moravský Sv. Ján	Morava	Morava	24129	1600	1690	⬆ 5.48
Streda n. Bodrogom	Bodrog	Bodrog	11474	1400	1570	⬆ 12.07
Ipeľský Sokolec	Ipeľ	Ipeľ	4838	670	710	⬆ 6.02
Veľké Kapušany	Latorica	Bodrog	2915	736	880	⬆ 19.32
Banská Bystrica (HBV)	Hron	Hron	1766	540	440	⬇ -18.00
Vlkyňa (Lisflood)	Rimava	Slaná	1377	190	220	⬆ 15.58
Chmeľnica	Poprad	Poprad	1262	820	640	⬇ -22.36
Liptovský Mikuláš (HBV)	Váh	Váh	1107	500	670	⬆ 34.12
Spišské Vlachy (HBV)	Hornád	Hornád	775	400	390	➡ -2.34
Janík (HBV)	Ida	Bodva	378	95	50	⬇ -47.03
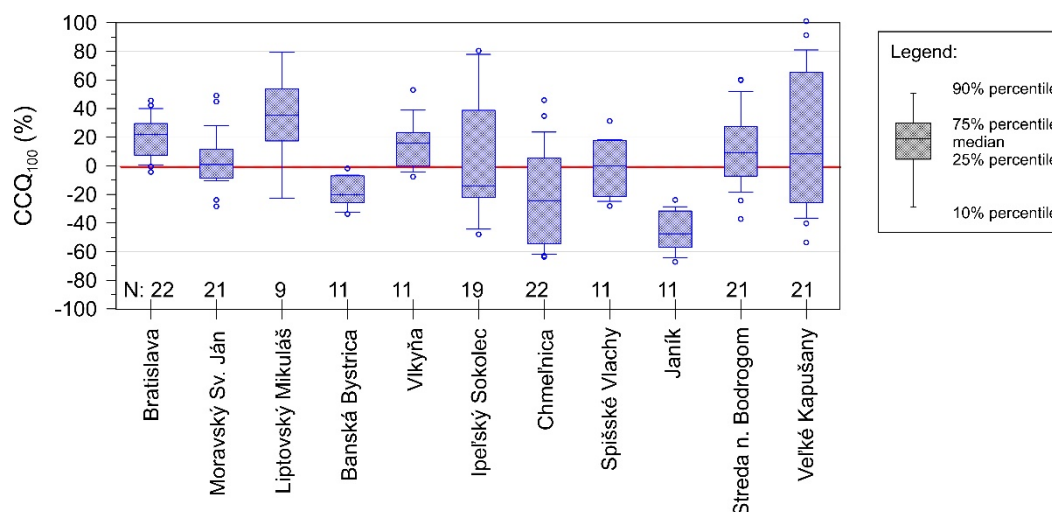
Fig. 3 Box plots showing the variability and extent of the climate change impact on Q_{100} (CCQ_{100}) obtained from ensemble of climate and hydrological models. N is the number of ensemble members used for analysis. Circles are extreme values outside the 10th to 90th percentiles.

Peak flows and their development over time represent important information for changes in high flows. Based on trends, possible future changes in Q_{100} can be expected. It was possible to identify several significant trends in future peak flows from model analyses, an example of which is shown in Figure 4 for station Moravský Sv. Ján. The dots represent the predicted annual maximum flows and the red line represents the slope of the expected linear trend of the time series.
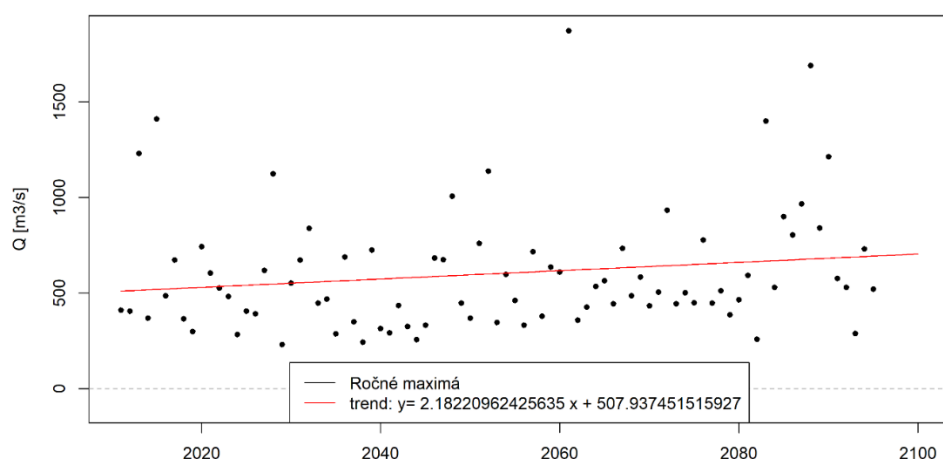
Fig. 4 Annual maxima series for the station Moravský Sv. Ján (from LISFLOOD and IPSL_WRF33_CM5A_rcp 4.5 climatic model) for the period 2011–2100 with delineated significant linear trend in red.

The list of all time series where a significant trend was identified throughout this analysis is given in the Table 3. An upward trend was identified for one model at Bratislava station, and 3 (4) models at Moravský Sv. Ján and Ipeľský Sokolec, respectively, whereby the climate model from the IPSL institute indicated an increase for both hydrological models. No significant trends were identified for the Vlkyňa and Liptovský Mikuláš stations. One or two upward trends were identified at other stations. For Janík and Banská Bystrica stations, upward trends were identified despite the fact that the estimate of the future Q_{100} was lower than the current value. These model outputs suggest that although the peak flows at these stations should be lower in the future, it is possible to expect their increasing trend. Only four downward trends were identified among the ensembles (at the stations Moravský Sv. Ján, Ipeľský Sokolec, Streda n. Bodrogom and Spišské Vlachy). Although several significant trends have been identified, their number within the whole ensemble for a particular station was relatively small.

Table 3 Identified significant increasing or decreasing trends of annual maxima series for the period 2011–2100.

gauging station	GCM-RCM-RCP - institute		hydrological model	trend
Bratislava	CM5A-WRF33-4,5	IPSL	HYPE	⬆
Moravský sv. Ján	CM5A-WRF33-4,5	IPSL	HYPE	⬆
	EC-EARTH-RACMO22E-8,5	KNMI	HYPE	⬆
	CM5A-WRF33-4,5	IPSL	LISFLOOD	⬆
	EC-EARTH-RCA4-8,5	SMHI	HYPE	⬇
Banská Bystrica	EC-EARTH-RCA4-8,5	SMHI	HBV	⬆
Ipeľský Sokolec	CM5A-WRF33-4,5	IPSL	HYPE	⬆
	EC-EARTH-RACMO22E-8,5	KNMI	HYPE	⬆
	CM5A-WRF33-4,5	IPSL	LISFLOOD	⬆
	EC-EARTH-RCA4-8,5	SMHI	LISFLOOD	⬆
	HadGEM2-ES-RCA4-8,5	SMHI	HYPE	⬇
Chmeľnica	EC-EARTH-RACMO22E-8,5	KNMI	LISFLOOD	⬆
Spišské Vlachy	EC-EARTH-RACMO22E-8,5	KNMI	HBV	⬆
	MPI-ESM-LR-REMO2009-2,6	CSC	HBV	⬇
Janík	CM5A-WRF33-4,5	IPSL	HBV	⬆
	EC-EARTH-RACMO22E-8,5	KNMI	HBV	⬆
Streda nad Bodrogom	MPI-ESM-LR-REMO2009-8,5	CSC	HYPE	⬆
	EC-EARTH-RACMO22E-4,5	KNMI	LISFLOOD	⬇
Veľké Kapušany	MPI-ESM-LR-REMO2009-8,5	CSC	HYPE	⬆
	HadGEM2-ES-RCA4-4,5	SMHI	HYPE	⬆

Finally, the estimation of Q_{100} was executed by frequency analysis, whereby for the time series showing a significant trend, the non-stationary frequency analysis was applied. The Figure 5 shows an example of diagnostic graphs that depict the goodness of fit of the applied GEV function to the particular dataset along with a return level graph for the station Banská Bystrica and simulation from the HBV model using climate predictions from the model SMHI_EC-EARTH_RC4_RCP8.5. The two upper plots show the quantile-quantile plots, where the quantiles from the analyzed dataset are compared to the theoretical ones of the GEV function. The lower left plot compares the density function of the theoretical (dashed blue line) and empirical (black line) functions. Finally, the bottom right plot represents the return level plot which shows how the estimate of the Q_{100} (red line) will evolve in time. The value of the discharge having a probability to occur equal to 0.01 is expected to change every year following a linear trend.
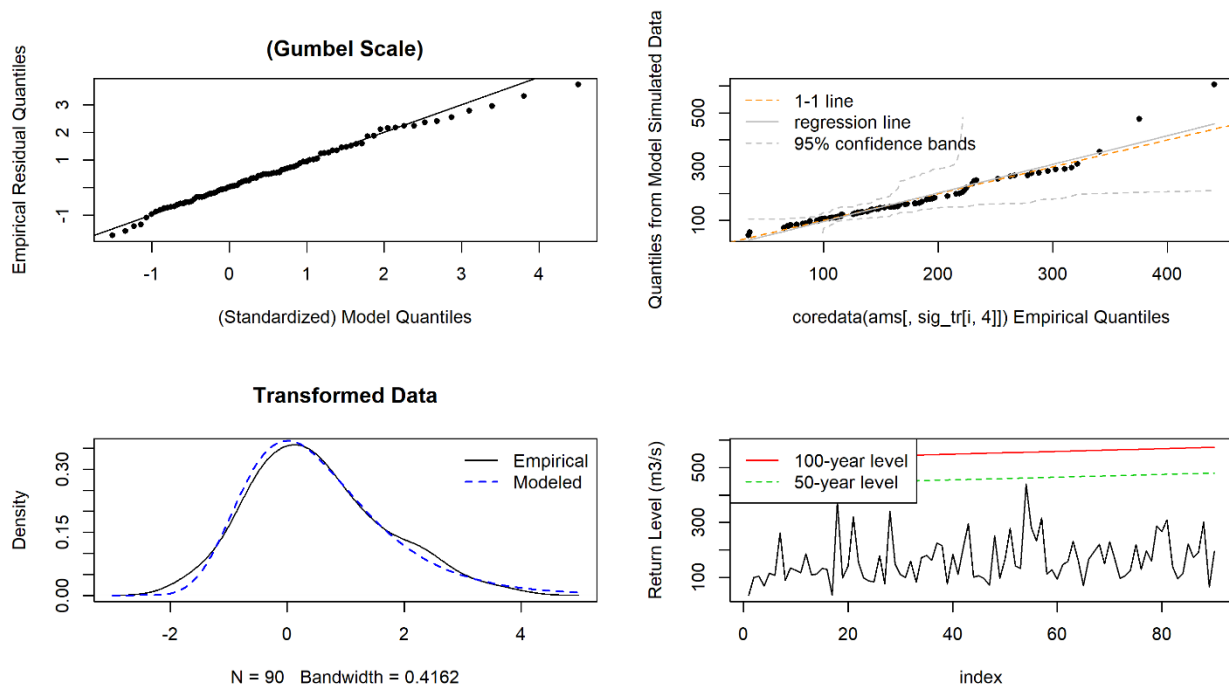
Fig. 5 Diagnostic graphs of the non-stationary fit of the GEV function for station Banská Bystrica. Data were simulated by HBV model forced by inputs from SMHI_EC-EARTH_RC4_RCP8.5. The return level graph is situated in the bottom right corner.

An overall look at the final results of the Q_{100} estimation for a selected station – Bratislava is shown in Figure 6. The mean Q_{100} estimates for individual climate models on the x axis are indicated by bigger circles, smaller dots show extremities of the 10% confidence interval. The climate models are aligned according to the RCP from the most optimistic to the most pessimistic scenario, whereby the RCP 2.6 scenario is displayed in pink, the RCP 4.5 in orange and finally the RCP 8.5 in the red color. For reference, the dashed line designates the currently used Q_{100} estimate. Based on the figures, for both hydrological models (HYPE-upper graphic, LISFLOOD – lower graphic), one can see that almost all mean values of future Q_{100} estimates are higher than the currently used one which can indicate an increase of Q_{100} in the future. Furthermore, the width of the confidence interval varies for each model and RCPs. In contrast to expectations, the application of the different RCP scenarios does not seem to have any impact on the results. The Figure 7 shows results for the station Banská Bystrica, where the analysis was performed on data simulated by the hydrological model HBV. In contrast to the Bratislava station, all the estimates are lower than the currently used value which indicates a decrease in the future value of Q_{100}.
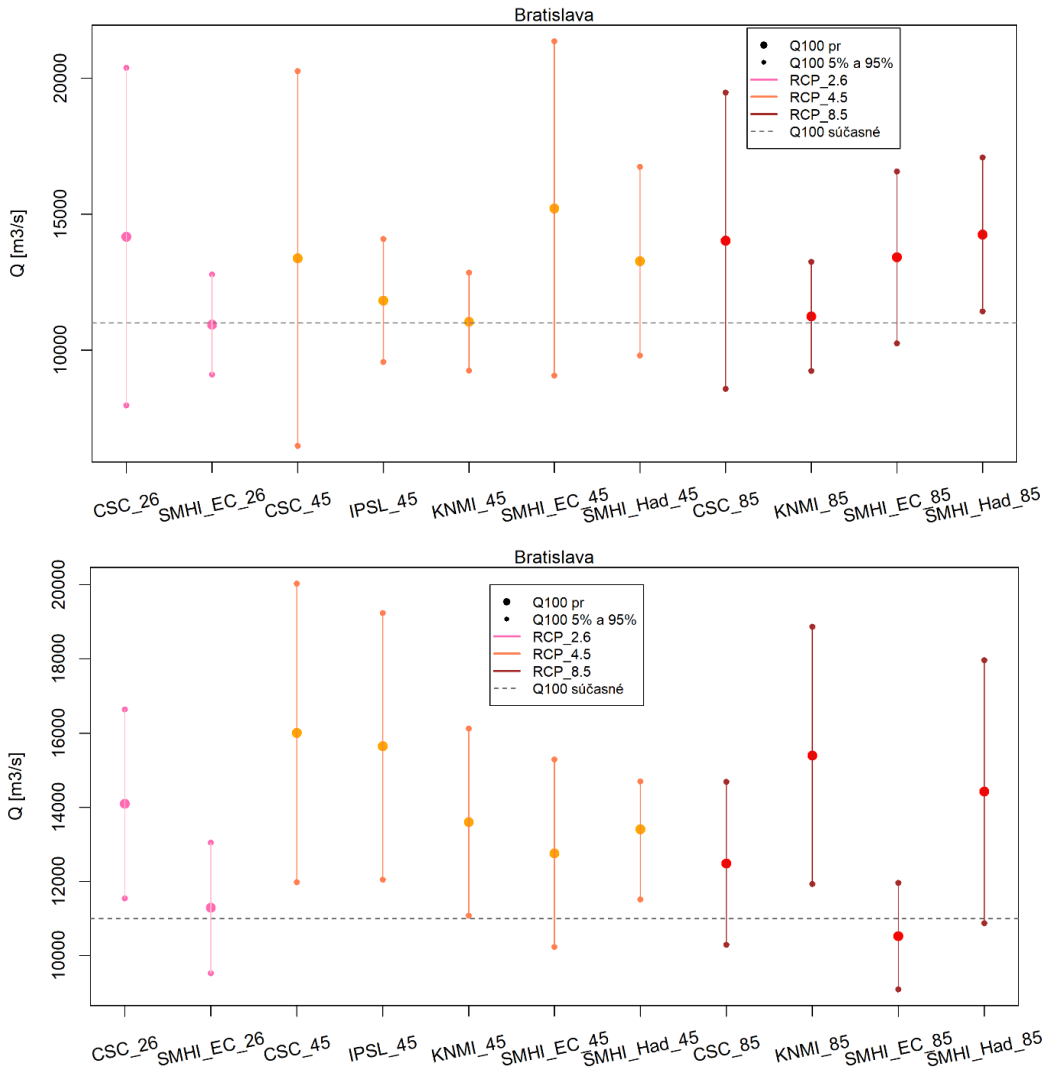
Fig. 6 The Q_{100} estimates for the Bratislava station based on simulations from the hydrological model HYPE (upper fig.) and LISFLOOD (lower fig.) that has been run for a combination of inputs from different climate models.
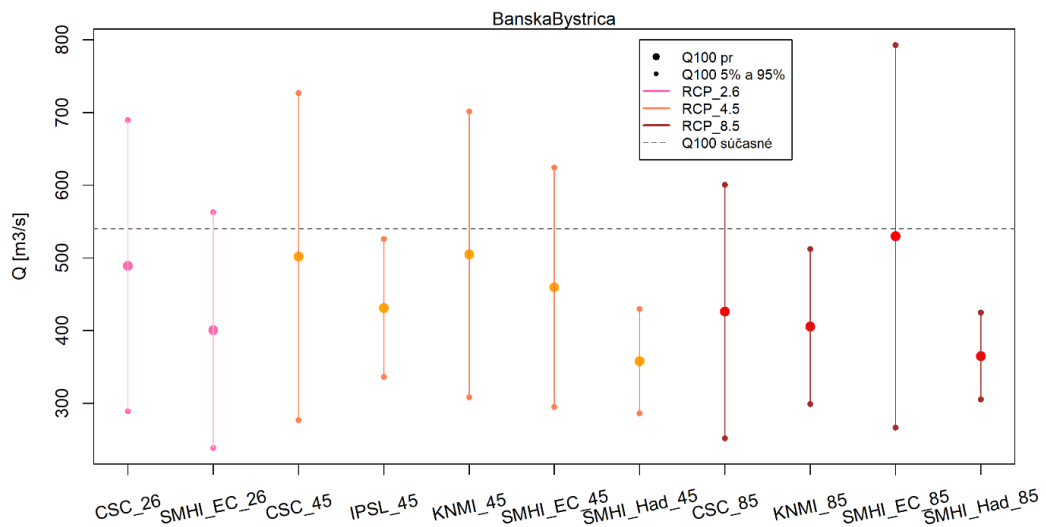

Fig. 7 The Q_{100} estimates for the Banská Bystrica station based on simulations from the hydrological model HBV that has been run for a combination of inputs from different climate models.

Discussion

With increasing global atmospheric temperature, intense precipitation is expected to strengthen due to the greater capacity of the warmer atmosphere to absorb water vapor. This fact is a common argument used for the automatic assumption that the incidence of floods and high flows will globally increase. Recent European studies suggest that the occurrence of floods and changes in their periodicity and magnitude depend primarily on the geographical location, the size of the river basin and the conditions under which floods occur (Blöschl et al., 2019). In small river basins, short-term convective precipitation with high intensities is especially important for flood generation. Conversely, in medium-sized and large river basins, longer-lasting synoptic frontal precipitation covering a larger area is crucial. From this point of view, the size of the river basin is a vital information. Also important are changes in water reserves in the snow cover and the period of snow melting, which is, in combination with liquid precipitation in the spring period, in many river basins a major factor for the occurrence of floods.

This work showed increases in Q_{100} at most stations. Decreases are estimated only at Chmeľnica, Banská Bystrica and Janík stations. The Danube basin (to the gauge in Bratislava) and the Morava river basin (to the gauge Moravský Sv. Ján) are the largest river basins in this study. An increase in Q_{100} is indicated in both stations, although in Moravský Sv. Ján only mild. The estimates of Q_{100} from the members of the ensembles are relatively consistent for both stations, i.e. the variability of the average Q_{100} is satisfactory and the hydrological models give comparable outputs for individual climatic ensembles in terms of the number of increases or decreases. The third largest catchment is the Bodrog catchment (to the gauge Streda n. Bodrogom), where an increase in Q_{100} is also indicated, but data from hydrological models are not completely consistent (HYPE model estimates increases from all 11 members of the ensemble, LISFLOOD model indicates 6 decreases out of 11).

A decrease in Q_{100} was indicated at Banská Bystrica (Hron), Janík (Bodva) and Chmeľnica (Poprad) stations. The uncertainty of the Q_{100} estimation for the Banská Bystrica and Janík stations may be higher due to the fact that only one hydrological model was available for these stations.

Stations with high uncertainty of Q_{100} estimation according to the CCQ_{100} interquartile range 59–91% are Veľké Kapušany (Latorica), Ipeľský Sokolec (Ipeľ) and Chmeľnica (Poprad). A closer analysis of the results from these stations shows that this uncertainty results from the inconsistency of outputs from hydrological models. At the Veľké Kapušany and Ipeľský Sokolec stations, the HYPE model indicates more increases, while LISFLOOD indicates decreases. At the Chmeľnica station, the situation is the opposite, with declines from the HYPE model and increases from the LISFLOOD model prevailing. The choice of hydrological model and the uncertainty associated with it is probably higher in this case than the uncertainty arising from climate models.

Furthermore, another uncertainty in the Q_{100} estimation may be the narrowed ensemble of hydrological models at some stations (Banská Bystrica, Janík, Liptovský Mikuláš, Spišské Vlachy and Vlkyňa). As the outputs from the SWICCA database of hydrological models for the mentioned stations did not meet the required criteria for the reference period, it was necessary to look for an alternative solution in form of the HBV hydrological model. Here arises a need to verify the estimated Q_{100} by other hydrological models in terms of the ensemble predictions philosophy as it is commonly used in climate models or by another suitable method, e.g. by correcting climatic ensemble data for hydrological data (Hakala et al., 2019).

The catchments with the smallest area are Spišské Vlachy (Hornád) and Janík (Ida, Bodva basin). Depending on the size of the river basin, it would seem that these river basins should provide data with the highest degree of uncertainty. It is true that hydrological data from the SWICCA database (outputs from the LISFLOOD and HYPE models) were not applicable for these river basins, probably also due to the coarse resolution of hydrological models to a small area of these river basins (775 and 378 km²). However, the calibrated HBV model provided relatively consistent results for the individual climatic ensembles, and according to the CCQ_{100} interquartile range, these two stations are among the stations with the least and medium uncertainty of the Q_{100} estimate.

No significant differences between individual climate scenarios (RCPs) were identified in this work. Probably these were masked by uncertainties related to climatic and hydrological models. This may also

be due to the fact that the data period was analyzed as a whole (2011–2100) for the purposes of the Q_{100} estimation as opposed to the more typical 30 years sections.

Conclusion

This impact study provides the results of estimating the impact of climate change on Q_{100} for 11 gauging stations covering all major river basins in Slovakia. In the first phase of the work, at least 572 time series of average daily flows for 26 stations were analyzed. Relationships between peak and maximum average daily flows were derived. For 242 time series, trends were analyzed and frequency analysis was performed fitting the GEV distribution function. Data from climate projections as well as from hydrological models available in the SWICCA database were used to analyze the impact of climate change. Such an extensive analysis of data from the C3S database has probably not yet been implemented in Slovakia, despite the fact that some reputable organizations, such as the International Association of Hydrological Sciences (IAHS) recommended it. The results of this work can lead to a discussion regarding the usability of climate data from the C3S database for Slovak river basins, their limits, but also other perspectives.

The results of the whole work can be summarized in several points:

1/ The results indicate an increase in Q_{100} for seven gauging stations: Bratislava (Dunaj), Moravský Sv. Ján (Morava), Liptovský Mikuláš (Váh), Vlkyňa (Slaná), Ipeľský Sokolec (Ipeľ), Streda n. Bodrogom (Bodrog), Veľké Kapušany (Latorica), with percentage change of Q_{100} (CCQ_{100}) 5.48–34.12%. A decrease in Q_{100} is indicated for stations Chmeľnica (Poprad), Banská Bystrica (Hron) and Janík (Ida, Bodva river basin) in the range of –17.99 to –47.03%. For the station Spišské Vlachy (Hornád) no significant change in Q_{100} was indicated (change more than ± 5%).

2/ The largest river basins in the analysis (Danube up to the Bratislava station and Morava up to Moravský Sv. Ján) provided results that fell into the group with the least degree of uncertainty in terms of CCQ_{100} impact variability and had the most consistent results for the two hydrological models used.

3/ The higher estimate uncertainty at stations Veľké Kapušany (Latorica), Ipeľský Sokolec (Ipeľ) and Chmeľnica (Poprad) resulted from conflicting outputs of hydrological models HYPE and LISFLOOD. Here, the use of a larger ensemble of hydrological models should be considered.

4/ The impact of climate change on the smallest river basins Janík (Bodva) and Spišské Vlachy (Hornád) could not be satisfactorily estimated with the hydrological outputs from the SWICCA database probably due to the rough resolution of models in relation to these river basins. The impact of climate change for these river basins was modelled by a calibrated HBV model using climate inputs from the SWICCA database. The impact of climate change for the Hron (Banská Bystrica) and Váh (Liptovský Mikuláš) river basins was estimated in a similar way. We assume that the complex orography and runoff formation in these river basins needs a finer resolution of climatic and hydrological models.

5/ In this work, it was not possible to clearly identify significant differences between individual climate scenarios (RCP) and their impact on Q_{100}. We assume that these were masked by uncertainties carried by climatic and hydrological models themselves.

The advantage of the SWICCA database is the availability of a large number of climatic and hydrological model outputs for a number of European river basins, as well as the latest knowledge on the state of the climate and modelled estimates of its development in one place. Not every user of a hydrological model has all the relevant meteorological data needed to calibrate the hydrological model and climatic data on the future climate. Another advantage is the time saved having ready to use calibrated data from the hydrological model that has been run for individual climatic inputs. The SWICCA database is constantly evolving and supplemented by necessary data. Its ambition is to provide users with a finer resolution of the outputs from the RCM models and to extend the reference period from 30 years to the longest possible period in the past. To achieve this, the necessary climatic and hydrological data in a sufficiently dense network of measurements provided by individual European countries are indispensable.

The climate change is ongoing and its impacts are visible already. Therefore, an effort is made to best understand the ongoing processes and to use different methods to estimate the final impact of these changes in the field of water management. From this point of view, this work offers possibilities for a promising way in which it is possible to estimate the impact of climate change on extreme flows on the basis of currently available data. There is a strong presumption that the future will require more frequent and in-depth analyses of the impacts of climate change on design high flows, which will need to be taken into account in individual EU countries. That is why we consider this work to be an initial step towards solving this urgent and serious task in Slovakia.

The EU Working Group on Floods (WGF) is currently calling on the professional institutions of all Member States to be involved in addressing the effects of climate change on the occurrence of floods. Interdepartmental, interdisciplinary communication and data exchange is an essential part of mastering this task at both domestic and international levels.

Acknowledgements

References

Burek P, van der Knojff J, de Roo A (2013) LISFLOOD, Distributed Water Balance Simulation Model. JRC technical report JRC78917, EUR 26162 EN, Revised User Manual, Luxembourg, 150 pp.

Blöschl G et al (2019) Changing climate both increases and decreases European river floods, *Nature*, **573**, 108–111.

Coles, S. (2001): An introduction to statistical modeling of extreme values. Springer London, 209 pp.

Dakhlaoui H, Seibert J, Hakala K (2019) Hydrological Impacts of Climate Change in Northern Tunisia, Advances in Sustainable and Environmental Hydrology, Hydrogeology, *Hydrochemistry and Water Resources*, Springer, 301–303.

Donnelly C, Greuell W, Andersson J, Gerten D, Pisacane G, Roudier P, Ludwig F (2017) Impacts of climate change on European hydrology at 1.5, 2 and 3 degrees mean global warming above pre industrial level, *Climatic Change*, **143**, 13–26.

Gaál L, Lešková D, Kopáčiková E (2017) Changes in the 100-year flood at the Danube River in Bratislava due to the expected climate change. Acta Hydrologica Slovaca, 18(2), 154–164 (Slovak with English abstract and resume).

Gao C, Booij MJ, Xu YP (2020) Assessment of extreme flows and uncertainty under climate change: disentangling the contribution of RCPs, GCMs and internal climate variability, *Hydrology and Earth System Sciences*, **24** (6), 3251–3269.

Gilleland E, Katz RW (2016) extRemes 2.0: An Extreme Value Analysis Package in R. *Journal of Statistical Software*, **72** (8), 1–3.

Gonzáles-Zeas D, Garrote L, Iglesias A, Sordo-Ward A (2012) Improving runoff estimates from regional climate models: a performance analysis in Spain, *Hydrology and Earth System Sciences*, **16** (6), 1709–1723.

Greuell JW, Andersson J, Donnelly C, Feyen L; Gerten D; Ludwig F; Pisacane G; Roudier P; Schaphoff S (2015) Evaluation of five hydrological models across Europe. *Hydrology and Earth System Sciences*, **12**, 10 289–10 330.

Hakala K, Addor N, Teutschbein C, Vis M, Dakhlaoui H, Seibert J (2019) Hydrological modeling of Climate Change Impacts. Encyclopedia of Water Science, Technology, and Society, Wiley & Sons.

Hlaváčiková H, Bírová M, Kopáčiková E (2019) Estimation of instantaneous peak flows from mean daily flows. *Acta Hydrologica Slovaca*, **20** (1), 3–9 (Slovak with English abstract and resume).

Hundecha Y, Arheimer B, Donnelly C, Pechlivanidis I (2016) A regional parameter estimation scheme for a pan-European multi-basin model. *Journal of Hydrology: Regional Studies*, **6**, 90–111.

IMPACT2C (2014) Quantifying projected impacts under 2°C warming, Deliverable D4.1, Report on requested meteorological data and climate change indicators, KNMI, 59 pp.

IMPACT2C (2015) Quantifying projected impacts under 2°C warming, D6.1 Maps showing the climate change impacts, at 1.5 and 2°C For the Water, Energy, and Tourism each sector and for coastal impacts, Wageningen University, 60 pp.

Knutti R, Sedlacek J (2013) Robustness and uncertainties in the new CMIP5 coordinated climate model projections. *Nature Climate Change*, „, 369–373.

Kopáčiková E, Hlaváčiková H, Lešková D (2020) Climate change impact study on 100-year floods of selected Slovak catchments. *Acta Hydrologica Slovaca*, **21** (2), 160–171.

Milly PCD, Betancourt J, Falkenmark M, Hirsch RM, Kundzewicz ZW, Lettenmaier DP (2008) Stationarity is dead: Whither water management? *Science*, **319** (5863), 573–574.

Teutschbein C, Seibert J (2012) Bias correction of regional climate model simulations for hydrological climate-change impact studies: Review and evaluation of different methods. *Journal of Hydrology*, 456–457, 12–29.

Teutschbein C, Seibert J (2010) Regional Climate Models for Hydrological Impact Studies at the Catchment Scale: A Review of Recent Modeling Strategies. *Geography Compass*, **4**, 834–860.

van Vuuren DP, Riahi K, Moss R, Edmonds J, Thomson A, Nakicenovic N, Kram T, Berkhout F, Swart R, Janetos A, Rose SK, Arnell N (2012) A proposal for a new scenario framework to support research and assessment in different climate research communities. *Global Environmental Change*, **22** (1), 21–35.

Spatial analysis of precipitation distribution that formed floods on the rivers of the Prut and Siret basins (within Ukraine) in June 2020

Viktoriia KORNIIENKO, Illia PEREVOZCHYKOV, Victoria BOYKO

Ukrainian Hydrometeorological Center (UHMC), Ukraine, Viktoriya.22.Kor@ukr.net, elijahmp@ukr.net, hydro@meteo.gov.ua

Introduction

The river runoff formation in the Prut and Siret basins is part of a potentially flood-hazardous area of Ukraine, where regular rain and snow melts-rain floods are recorded, some of which become catastrophic and are accompanied by negative consequences. The probability of flooding on the rivers of the basin increases with the fall of 20 mm of precipitation per day, and with the fall of more than 100 mm floods are becoming catastrophic (Kosteniuk, 2009). As a result of heavy and extreme torrential rains on June 20–25, 2020, a high rain flash flood was formed on the rivers of the Prut and Siret basins against the background of high water levels.

Maximum of flood levels in small streams was formed very quickly – by the end of the day on June 21; on the other rivers they took place mainly on June 22–24. Due to the formation of high floods, the total water content of rivers in June increased significantly; average water amount in June reached 3–4 average month long-term values.

The amplitude of the increase in levels was 2.0–2.5 m on the tributaries of the Prut and 4.5–5.5 m above the pre-flood levels on the Prut in Chernivtsi station.

Water discharge in the posts for a short period of time increased 3–17 times, in some areas on the rivers of the Prut basin – 24–34 times.

The maximum levels of floods in June 2020 on the rivers of the Prut and Siret basins were higher than the average of the maximum values for many years by 0.5–2.8 m, but 0.5–4.5 m lower than historical. Exceedance (achievement) of historical maximum levels was observed only in a few stations: the historical maximum of 1996 was exceeded on the river Iltsia in the Iltsia station (a tributary of the Prut) by 0.9 m.

Hydrometeorological conditions in the Carpathian river basins at the end of the second decade of June were favorable for the further formation of rainwater runoff with high coefficients. But the main reason for the formation of high and extremely high floods in the third decade of June was the amount and mode of rainfall.

Analysis of the synoptic situation on June 20–25, 2020

On June 20–25, 2020, the synoptic situation was associated with a series of sedentary cold atmospheric fronts, which were pressed to the Carpathians by eastern flows and due to convection and the formation of a single-center high-altitude cyclone (with very slow filling), caused very heavy and prolonged rains in western regions of Ukraine, which caused the formation of high floods on the rivers of the region with catastrophic consequences.

On June 21, the cold polar atmospheric front passed from the Baltics through Poland to the Carpathians. Cold atmospheric fronts, remaining sedentary, easterly streams pressed against the Carpathians.

During June 22–24, instead of a depression, a one-center high cyclone was observed, the center of which moved from the south of Ukraine to Bulgaria, then to the Aegean Sea, filling up very slowly. All this time it influenced the weather in the Carpathians. The process was intensified due to the fact that the basin from the latitudinal position acquired a meridional direction, narrowed in area and intensified. This activation occurred not only due to the dynamic factor, but also supplemented by thermal. From the North Sea to Germany, Austria, to the rear of our cyclone, came a new portion of cold with a minimum temperature of 6–8 °.

On June 23–24, the atmospheric pressure gradually increased, and anticyclone protrusions pressed from the north and west. The fronts were converging, the sector was occluded. Heavy rains in the Carpathian region gradually stopped.

Total flood-forming precipitation

Precipitation, which caused high floods on the rivers of the western region of Ukraine in the third decade of June, was observed for 6 days – June 20–25, 2020. They fell daily, there were heavy, extreme and prolonged rains, but especially intense rains were observed on June 22–23, when the amount of precipitation reached the criteria of danger (orange color).

Analysis of the amount and distribution of precipitation in the Prut and Siret river basins was performed according to the observations of 5 meteorological and 11 hydrological stations.

Rainfall in the catchment area was very uneven and intermittent, which is typical for the flood-danger Carpathian region.

According to the observations of meteorological and hydrological stations taken by us for analysis, at 35 stations the amount of precipitation for June 20–25 (6 days) was less than 50 mm, at 36 stations – within 51–100 mm, at 17 stations – 101–150 mm, at 7 stations –151–200 mm, at 5 stations – more than 200 mm (Fig. 1).
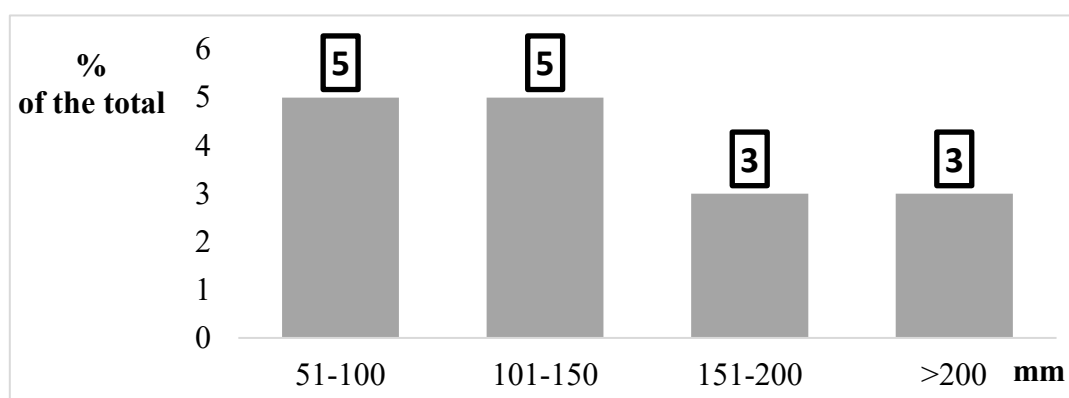

Figure 1 The number of observation points (hydrological and meteorological stations within the Prut and Siret basins) in the interval distribution by the amount of precipitation in the period 20–25 June 2020.

The largest daily amounts of precipitation at most observation points were recorded on June 22–23, 2020. The maximum values were observed at Yaremche meteorological station with the amount of precipitation per day – 124 mm. These values are 75% of the maximum daily precipitation values for the entire observation period.

At some observation stations, the amount of precipitation in 6 hours reached 20–40 mm (Kolomyia, Chernivtsi); on Iaremche station 95 mm were recorded for 6 hours on June 23, 2020 (in the period from 9 to 15 o'clock), which is 54% of the daily maximum for the entire observation period.

The highest amount of precipitation per rain was recorded by meteorological stations in Chernivtsi and Ivano-Frankivsk regions:

• June 21 Seliatyn (Chernivtsi region, Siret Basin) heavy rain 43 mm for 10 hours;

• June 23 Yaremche (Ivano-Frankivsk region, Prut Basin), extraordinary rain 106 mm / 12 hours;

• June 24 Pozhezhevska (Ivano-Frankivsk region, Prut basin) heavy rain, 33 mm / 4 hours.

The amount of precipitation on June 20–25 at the meteorological stations of Iaremche, Kolomyia, hydrological stations on the tributaries of the Prut in Ivano-Frankivsk region exceeded the climatic monthly norm of June by 1.1–1.6 times (Fig. 2, Table 1).

The largest total amount of precipitation for this period (according to operational data) was recorded (in mm):

• at meteorological stations Iaremche 242, Pozhezhevska 192, Seliatyn and Kolomyia 124–127;

• at the hydrological stations Tatariv 228, Vorokhta 201, Usteriky 187.
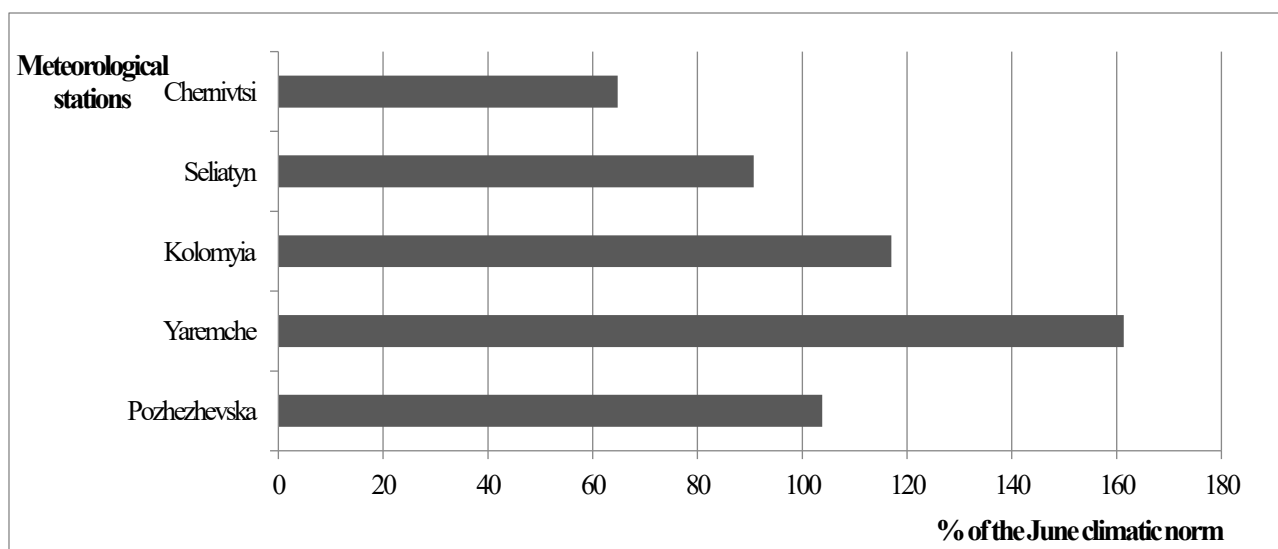
Figure 2 Total precipitation for the period 20–25 June 2020 according to meteorological stations in relation to the climatic norm of June (%)

Table 1. Characteristics of precipitation (mm), which formed a flood in June 2020, according to meteorological stations within the catchment area of the Prut and Siret rivers

Meteorological station	The June norm	The amount of precipitation for 20–25.06	Percentage to the June norm
Pozhezhevska	185	192	104
Yaremche	150	242	161
Kolomyia	106	124	117
Seliatyn	140	127	91
Chernivtsi	105	68	65

The total amount of precipitation for the period 20–25 June 2020 according to hydrological and meteorological stations within the zones of formation of runoff of rivers of Transcarpathia, rivers of the Dniester, Prut and Siret basins is shown in Fig.3.
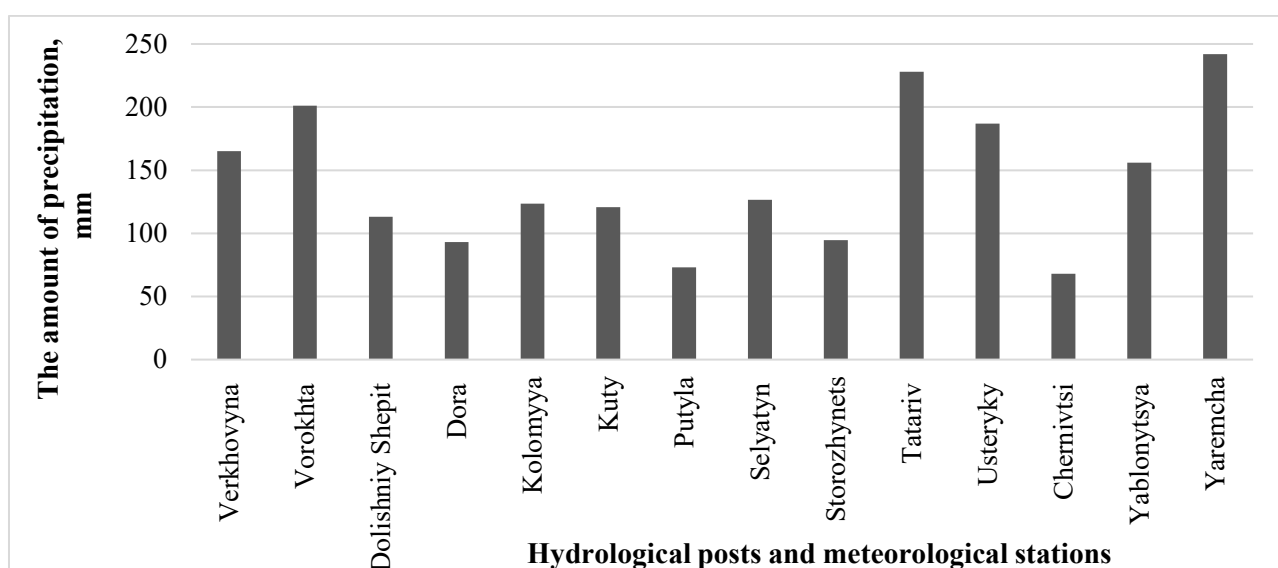

Figure.3 The total amount of precipitation for June 20–25, 2020 according to meteorological and hydrological stations within the Prut and Siret basins

Precipitation mapping.

According to the measurement of precipitation at meteorological and hydrological stations within the Prut and Siret basins, a map of isolines of distribution of the total amount of precipitation for the period of June 20–25, 2020, which formed an intense flood runoff, was built. The map is built in the ArcGis 10.1 system at a scale of 1: 1 000 000 (Fig. 4).
Data from meteorological stations in neighboring countries within the transboundary river basins (Romania, Hungary and the Slovak Republic) were also used for its construction.
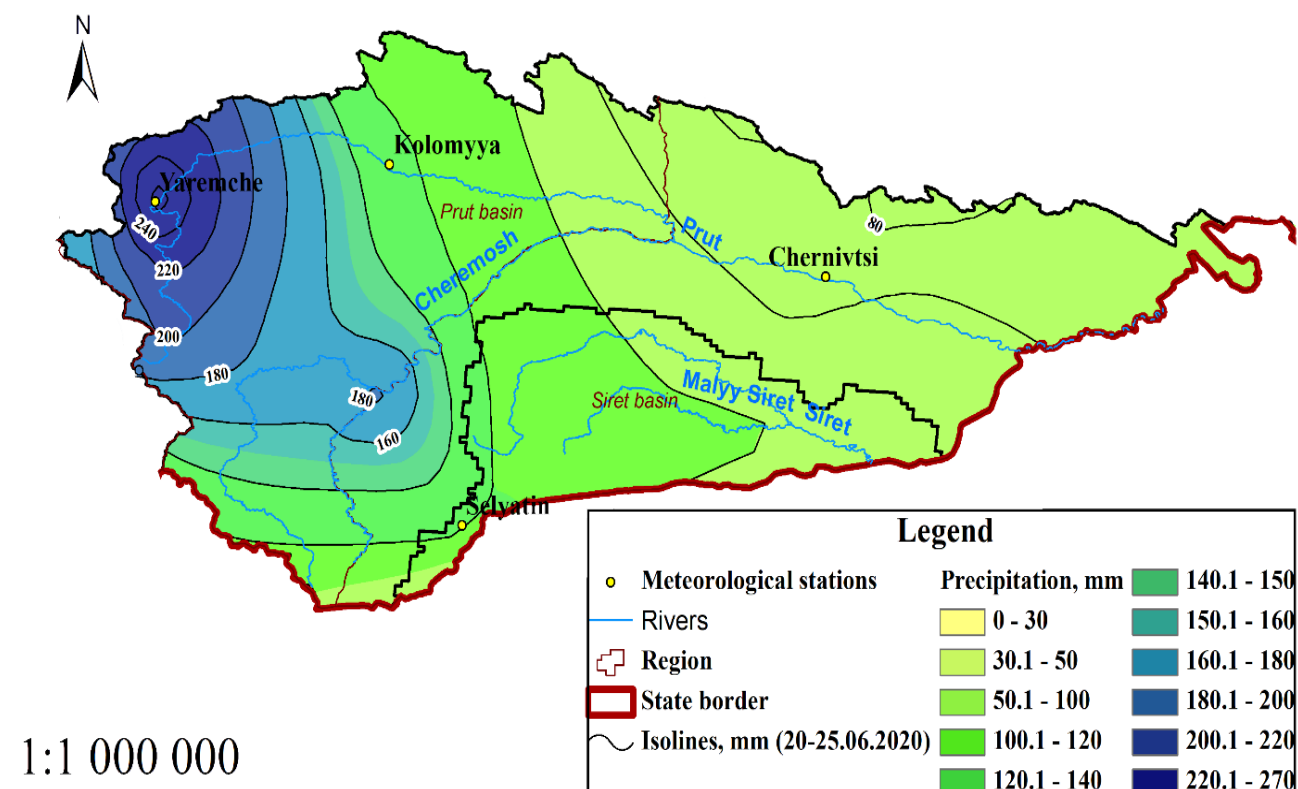
Figure 4 Total precipitation for June 20–25, 2020 according to meteorological stations and hydrological stations within the Prut and Siret basins (within Ukraine)

Based on the analysis of the constructed map and the actual data of observation points, the quantitative and spatial distribution of the total precipitation within the Prut and Siret basins was performed.
The strongest and most intense precipitation was in the zone of river runoff formation in the Prut basins within the Ivano-Frankivsk region.
The highest amount of precipitation for the period 20–25 June 2020 was observed in the basins of the Prut and Siret rivers, and the epicenter of their concentration fell on the upper reaches of the Prut (Vorokhta – Yaremche section), where the total precipitation according to precipitation stations was 200–240 mm, which is 1.6 average month long-term values.
In the upper reaches of the Bilyy Cheremosh and Chornyy Cheremosh rivers and at the confluence of the rivers, the total rainfall was 150–190 mm.
On the Prut River near the Kolomyia meteorological station, on the Cheremosh River near the Kuty hydrological station and in the Siret River basin, precipitation was distributed in the range of 90–130 mm.
In the Prut area near the Chernivtsi meteorological station, the total amount of precipitation was 56 mm.

Comparison of the temporal-spatial distribution of precipitation

The maximum water levels/discharges of the June 2020 floods were also compared with the last high floods.

In the upper reaches of the Prut river, they approached the maximums of extreme flooding in July 2008. At other posts in the region, the maximum levels of flooding in 2020 were lower than the maximum marks of the July floods of 2008.

Compared to the high floods in June 2010, the maximum water levels of the flood in June 2020. According to 7 stations of the Prut basin, were higher than in 2010 by 0.1–1.3 m.

The maximum flood discharges in a number of Prut and most of its tributaries exceeded their average of the maximum values for many years by 2–4 times, and in the two posts on the tributaries of the Prut (Chorniava-Liubkivtsi and Iltsia-Iltsi) – 6,5–8 times.

In the area of the Iltsi station on the Iltsia river, the maximum flow of the June flood in 2020 was observed at 276 m^3/s and almost 1.5 times higher than the historical maximum of 192 m^3/s in 1969 and 1996 (Table 2).

Table 2 Maximum water discharge of June floods in comparison with average long-term values

№	River	Station	Maximum water discharges, m^3/s		
			June 2020	long-term average of the maximum	historical maximum
1	Prut	Tatariv	257	119	517
2	Prut	Yaremcha	689	306	1530
3	Prut	Chernivtsi	2160	1280	5200
4	Chorniava	Liubkivtsi	101	12,5	119
5	Cheremosh	Usteriky	1165	394	1500
6	Bilyy Cheremosh	Iablunytsya	127	159	750
7	Chornyy Cheremosh	Verkhovyna	487	161	857
8	**Iltsia**	**Iltsi**	**276**	**42,4**	**192**
9	Putyla	Putyla	149	66,2	274

*Comment – the value of the historical maximum is exceeded

The formation of high floods was accompanied by flooding of river floodplains, reaching and exceeding the levels of flooding (partial flooding) of river areas, parts of settlements, damage and destruction of facilities, infrastructure, complicating the lives of the population.

Conclusion

The formation of floods with dangerous consequences was caused by heavy and prolonged rains in western Ukraine on June 20–25, 2020.

The total amount of precipitation that formed floods on the rivers of the Prut and Siret basins: in the upper reaches of the Prut 200–240 mm, amounted to 1.6 monthly norm. The rest of the region received 80–180 mm of precipitation (monthly norm 0.6–1). The main reason for such precipitation was a series of settled cold atmospheric fronts pressed against the Carpathians by the eastern currents and due to convection and the formation of a single-center high-altitude cyclone (with a very slow filling).

As a result of the flood, significant damage was inflicted on settlements and infrastructure in Chernivtsi and Ivano-Frankivsk regions.

References

Kulbida M., Boyko V., Petrenko L., Savchenko L. (2009). The analysis of time and spatial distribution of the precipitations which have generated floods on the rivers of Carpathian Mountains in July, 2008, *Hydrologist, hydrochemistry and hydroecologist.,* Issue **16**, pp. 92–98.

Kosteniuk L.(2009). The catastrophic floods in a pool of the river Prut, Scientific notes [Vinnytsia State Pedagogical University named after Mykhailo Kotsyubynsky]. Series: *Geography*. 2009. Vip. **19**. P. 43–49.

Klimatolohichni standartni normy (1960–1990 rr.). Dovidnyk. – K.:Arkhiv Tsentral′noyi heofizychnoyi observatoriyi, 2002 – 446 s.

Klimat Ukrayiny. Za red. Lipins′koho V.M., Dyachuka V.A., Babichenko V.M. – K.: Vyd-vo Rayevs′koho, 2003 – 343s.

Rainfall thresholds related to pluvial flooding in urban areas – case study in the city of Zagreb, Croatia

Tena KOVAČIĆ[1], Kristina POTOČKI[2], Martina KOVAČEVIĆ[3]

[1] Kratka ulica 14,Vinogradi Ludbreški,42230 Ludbreg, Croatia, [2,3] University of Zagreb Faculty of Civil Engineering , Department of Hydroscience and Engineering, Croatia, email: tena31@gmail.com (for author 1), email: kristina.potocki@grad.unizg.hr (for author 2), email: martina.kovacevic@grad.unizg.hr (for author 3), Corresponding author: kristina.potocki@grad.unizg.hr

Abstract

The frequency of urban pluvial flood risk has increased in recent years due to changes in the hydrological cycle and more frequent extreme rainfall events. Therefore, the analysis of rainfall tresholds trelated to pluvial urban flooding could be of great help to improve early warning systems and enable public services to plan and implement appropriate protection and rescue measures in a timely manner. The aim of this paper is to identify preliminary rainfall thresholds for different durations up to 24 hours that are related to urban floods in the city of Zagreb, Maksimir area, in the period 2007–2017. Reports from civil protection and public fire brigades of the city of Zagreb were analyzed, i.e. technical interventions for pumping water from facilities and open urban spaces during extreme hydrometeorological conditions were considered and used as impact parameters of pluvial floods. A spatial analysis was performed and a relationship was established between urban land use and the number of interventions as an indicator of flood occurrence. Total precipitation measured at Maksimir meteorological station was analyzed and maximum values for 1, 2, 3, 6, 12 and 24 hours durations were determined, and were used as flood hazard indicator. Rainfall events were analyzed using an empirical approach and extended with a statistical approach to develop rainfall thresholds, and the performance of both approaches was evaluated. The results showed that most interventions occurred during the warm season (especially in May and August). Both thresholds obtained, the empirical and the statistical, could be used for practical purposes. However, the upper statistical threshold (75% percentile) has sufficient overall correctness with more correct flood predictions and higher false alarm rates than the upper empirical threshold, while the lower statistical threshold (25% percentile) has slightly better correctness than the lower empirical threshold.

Introduction

Climate change is reflected in, among other things, intensification of the hydrological cycle and changes in precipitation extremes (Jha et al., 2012). This results in more frequent and intense pluvial urban flooding in cities around the world, causing significant material damage, including in Croatia (Potočki et al., 2018, Jelić et al., 2020). Flash floods can occur anywhere, with low-lying areas with poor drainage being particularly vulnerable to waterlogging, and this is characteristic of many urban areas. The shorter the duration, the greater the likelihood of waterlogging disasters (Ma et al., 2020). Urban flooding cannot be prevented, but effective preventive and operational measures can significantly mitigate its harmful consequences. The development and improvement of forecasting and early warning systems as part of natural hazard risk management is considered one of the most effective ways to mitigate the impact of flash floods in cities (Zanchetta and Coulibaly, 2020). The most common approach is to compare the latest precipitation forecasts from numerical weather predictions with reference thresholds, often derived through statistical analysis of long-term records of point measurements (Alfieri et al., 2012). Thresholds for rainfall intensity and duration are developed for the occurrence of debris flows, landslides and floods (Cannon et al., 2008, Guzzetti et al., 2008, Diakakis, 2012, Papagiannaki et al., 2015). Research on the temporal and spatial characteristics of short-term heavy rainfall events in Croatia has not been systematically conducted (Jurković et al., 2019). The RAINMAN project focused on the

development of practical new tools and innovative methods to reduce losses caused by heavy rainfall in the natural and built environment and presented a preliminary assessmentof urban flood hazard in the city of Zagreb (RAINMAN project, 2019). Certain attempts to determine thresholds for critical precipitation in relation to the occurrence of floods in the city of Zagreb were made by Hrastovski (2016), who analyzed only precipitation durations that exceeded 24 hours, so shorter precipitation durations that trigger urban flooding should be investigated. The preliminary thresholds for rainfall intensity and durations up to 24 hours were derived for the city of Zagreb, specifically for the Maksimir sub-area for the period 2007–2017, and their performance for urban flood warning is evaluated. Reports from civil protection and public fire brigades of the city of Zagreb were analyzed, i.e. technical interventions for pumping water from facilities and open urban spaces during extreme hydrometeorological conditions were considered and used as impact parameters of pluvial floods. A spatial analysis was performed and a relationship was established between urban land use and the number of interventions as an indicator of flood occurrence. Total precipitation measured at Maksimir meteorological station was analyzed for durations up to 24 hours and used flood hazard indicator. Rainfall thresholds were analyzed using an empirical approach that was extended with a statistical approach. The defined thresholds for peak storm intensities of different durations provide us with an approach to predict potential urban flood occurrences, allowing timely responses and preventing potential damage.

Study area and data

Study area

The study was conducted in the urban area of Zagreb, the capital and largest city of the Republic of Croatia, located in the northwest part of the country (Fig. 1). The city of Zagreb covers an area of 641,355 [km^2] with a population of 790,017 according to the 2011 census (Croatian Bureau of Statistics, 2021). It is located at the foot of the Medvednica massif and on the Sava River, and its location has posed a latent threat of flooding to the urban area throughout history. Considering the threat of flooding from the Sava River and torrential flooding from the Medvednica creeks, a flood protection system in the form of river embankments and retention areas has been constructed and is very effective. However, the city is still vulnerable to pluvial urban floods caused by heavy rainfalls of short durations. A more detailed analysis was carried out in this study in the eastern part of the city of Zagreb for the Maksimir area, near the meteorological station (MS) Maksimir (45°49'16" N, 16°2'1" E) (Fig. 1, small map).
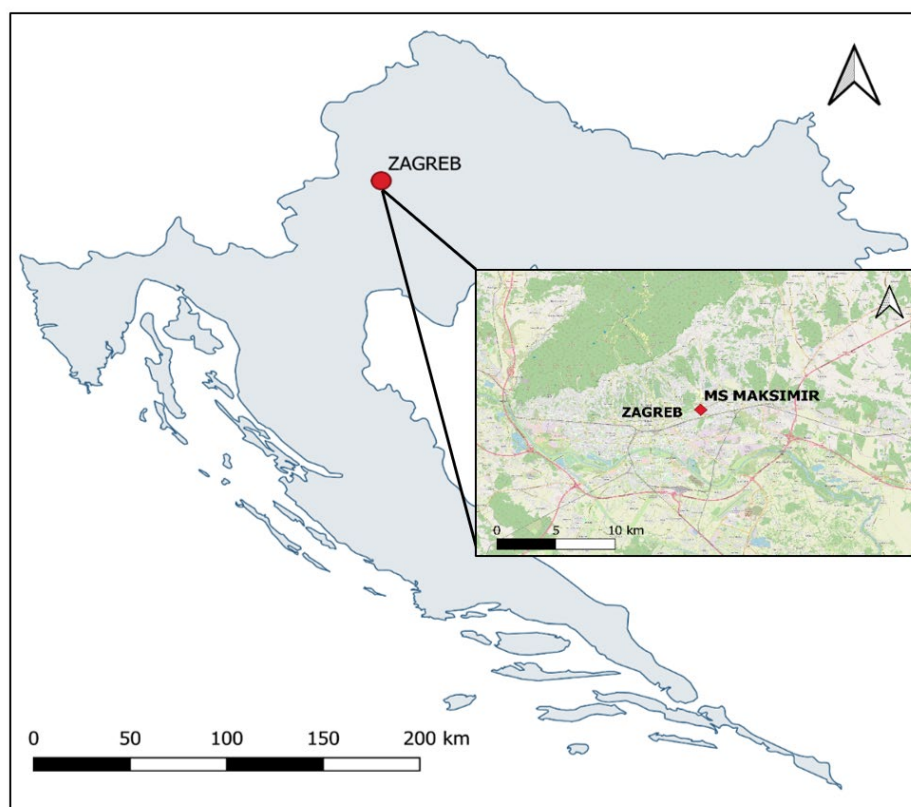
Fig. 1 Map of Croatia showing the city of Zagreb with a red marker (large map) and topographic map of the city of Zagreb area with location of meteorological station (MS) Maksimir marked in red (small map)

The city of Zagreb is characterized by continental climate with an average annual air temperature of 13.3 [C°] and annual precipitation of 908.7 [mm] for the period 2007–2017. The average monthly and annual air temperature values in Zagreb for the period 2007–2017, in contrast to 1961–1990, show the general increase in average air temperature with minor exceptions, while the monthly and annual precipitation values for the same periods show the largest monthly deviation for the month September and the annual deviation of 3% from the monthly and annual precipitation values for the period 1961–1990 (Tab. 1).

Table 1 Average monthly and annual air temperature, T [C°] and precipitation, P [mm] for the period 1961–1990 and 2007–2017 in the city of Zagreb, MS Maksimir

Average monthly and annual air temperature, T [C°] and precipitation, P [mm]													
Meteo. variable	Time period	Jan	Feb	Mar	Apr	May	Jun	Jul	Aug	Sep	Oct	Nov	Dec	Year
T [C°]	1961–1990	0.5	3.1	7.3	11.8	16.3	19.4	21.3	20.6	17.0	11.9	6.4	2.0	11.5
	2007–2017	2.9	4.7	9.3	14.0	16.8	21.7	23.9	23.2	17.8	12.6	8.4	3.6	13.3
P [mm]	1961–1990	53.0	47.0	58.0	65.0	83.0	101.0	87.0	91.0	81.0	70.0	85.0	62.0	883.0
	2007–2017	57.0	61.8	50.8	45.3	78.8	102.0	71.1	74.5	119.9	88.4	87.6	57.4	908.7

Data description

The analyzed data are intervention reports collected by the Public Fire Department of Zagreb and the National Protection and Rescue Directorate that is used as flood hazard indicator, precipitation data from the Maksimir meteorological station (MS) that is used as flood hazard indicator, and land use data for the city of Zagreb for spatial analysis, all for the period 2007–2017.

The intervention reports of water pumping during urban flash floods with various causes for the period 2007–2017 were collected from the Public Fire Department of Zagreb and the National Protection and Rescue Directorate. Technical interventions for pumping water from facilities and open urban spaces during extreme hydrometeorological conditions were filtered out from the database and used as impact parameters of pluvial floods. Unnecessary data was removed, remaining data was processed to draw conclusions about the connection between the rainfall intensity thresholds and flash floods in Zagreb, and was additionally cross-referenced with newspaper articles. Hourly precipitation data were collected from the Croatian Meteorological and Hydrological Service for MS Maksimir, and the maximum accumulated rainfall was calculated for the 1, 2, 3-, 6-, 12-, and 24-hour periods to match rainfall events with flood indicators. City Office for Strategic Planning and City Development provided data on the degree of urbanization and land use in the affected floodplains. The land use analysis around the Maksimir meteorological station shows that most of the land is built-up and only 37% of the 54 km^2 is undeveloped. Most undeveloped land is used for agriculture (21%) and is forested (7%). Of the built-up land, the largest proportion is residential (34%), commercial (13%) and transport (8%).

Methodology

Specification of study sub-area and spatial analysis of land-use

Since microclimatic phenomena have an increased impact on precipitation characteristics in the Zagreb urban area (Medvednica mountain with a peak of 1 033 m a.s.l. and River Sava with 112,260 m a.s.l., see Fig 2), the analysis was performed for a smaller sub-area around MS Maksimir, located in the watershed with an area of 142.8 km^2. The majority of interventions occurred within a radius of 4.2 km around the meteorological station. Therefore, a detailed analysis was performed for the area of Maksimir within a radius of 4.2 km^2 around the meteorological station to obtain more spatially reliable results. This radius was chosen to fit the scale of the given watershed (Fig. 2). A land use analysis was conducted for the mentioned area to determine the relationship between urbanization and surface permeability with surface runoff and flooding. A mapped database of emergency service interventions along with spatial analyzes was created based on reports of calls for service, dates, and addresses of calls for service to pump water from facilities and open spaces received from fire departments. From 331 interventions that were detected within the watershed, 273 (82%) were found within the circle around the meteorological station that presents analyzed sub-area with an area of 55.42 m^2(0).
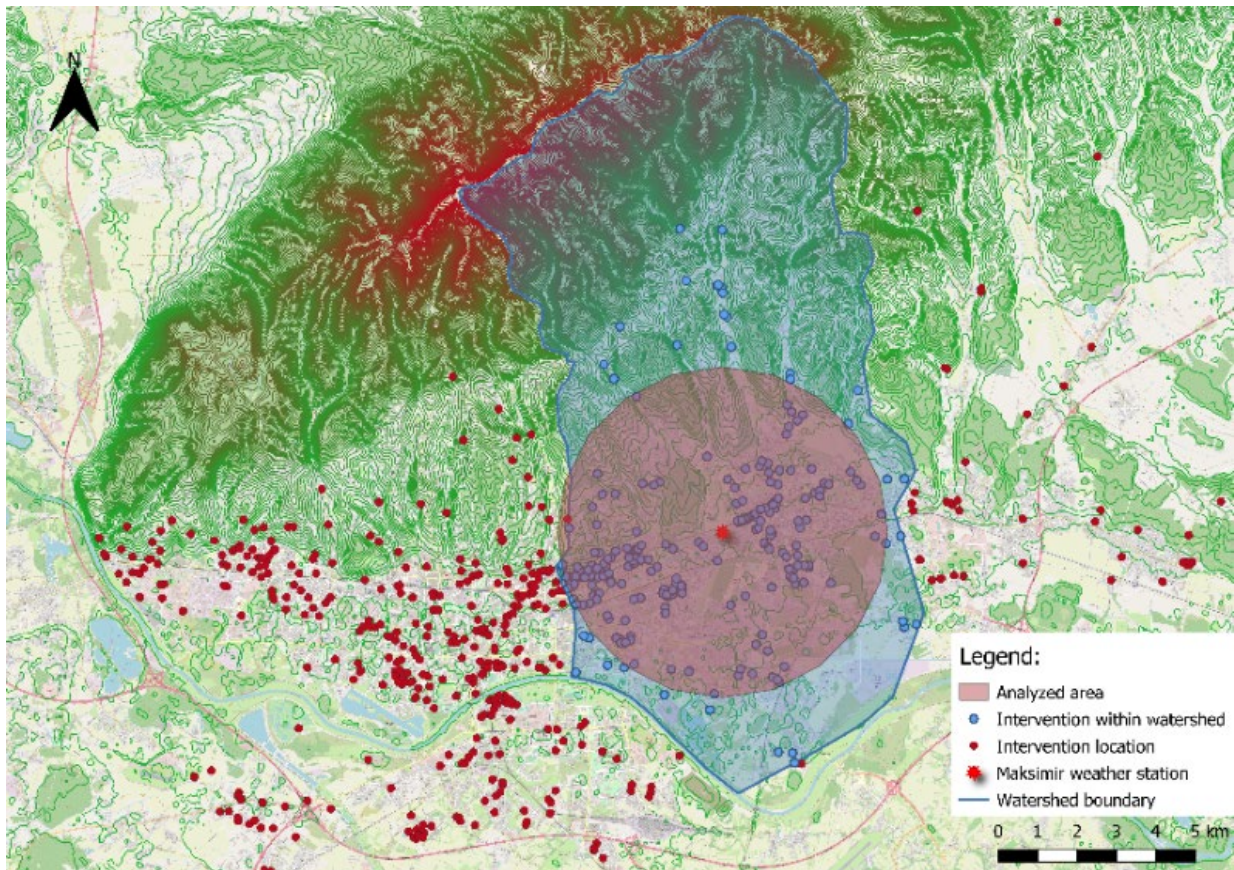
Fig. 2 Interventions recorded by the Public fire department of Zagreb from 2007 to 2017 related to rainfall events and analysed sub-area within the watershed boundary.

Maps of land use, land development and urbanization, were provided by the Zagreb City Office for Strategic Planning and City Development, and were analyzed within the sub-area. Spatial analysis revealed that most interventions occurred on developed land (96%) with development status determined by the City Office (0). In terms of land use, most interventions were recorded on residential (57 %), agricultural (2 %) , commercial (2 %) and traffic areas (28 %) accounting for 89% of all interventions (0).
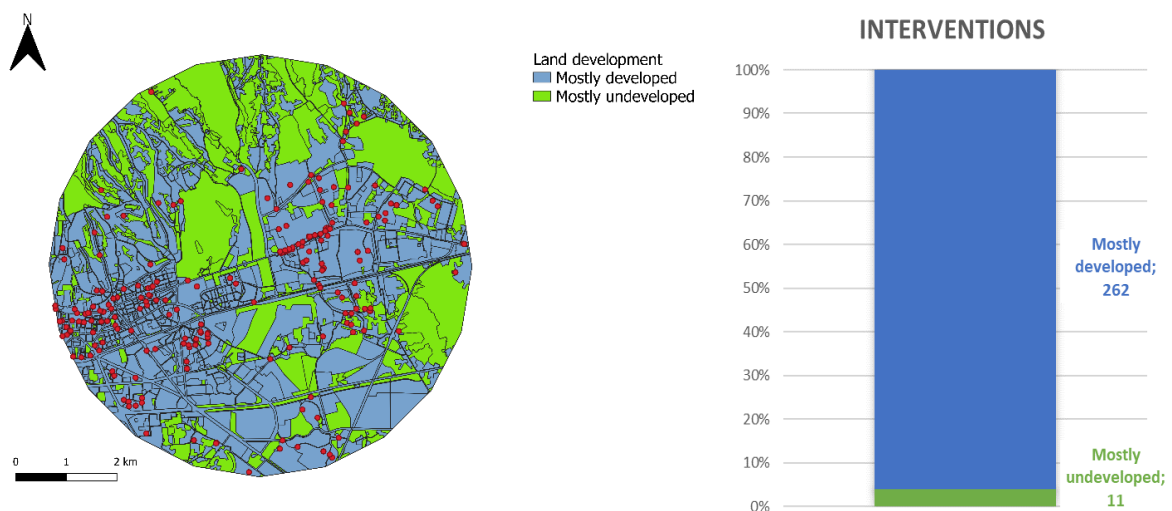
Fig. 3 Distribution of interventions (right) recorded by the Public fire department of Zagreb from 2007 to 2017 related to land development map (red dots on the map on the left).
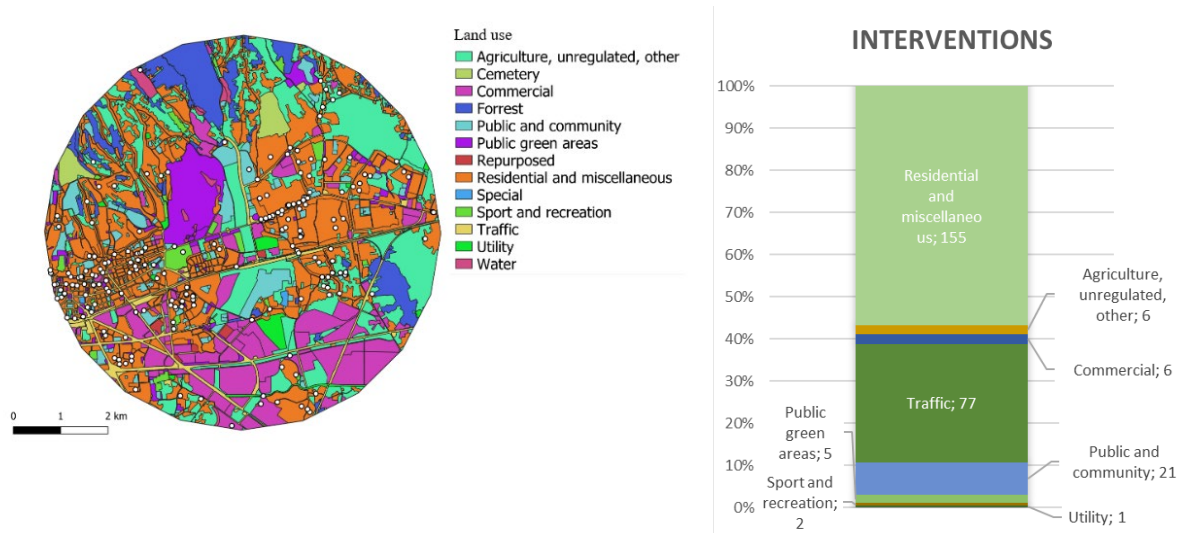
Fig. 4 Distributions of the interventions (right) recorded by the Public fire department of Zagreb from 2007 to 2017 related to the different land use (light blue dots on the map on the left).

Characterization of rainfall thresholds and evaluation criteria

Pluvial urban flood events are caused by rainfall events of different duration and intensity. Various definitions of what constitutes as a rainfall event can be found in the literature. Since this paper is partly based on the work of Papagiannaki et al. (2015), the same approach of defining a rainfall event was taken, where a rainfall event was considered any rainfall enclosed by two dry periods of 24 hours without any rain. Since the data from MS Makismir were given as hourly precipitation records, the maximum accumulated rainfall was calculated for the periods of 1-, 2-, 3-, 6-, 12-, and 24-hour periods as a moving average for related durations. Rainfall events database is formed with start date, duration and end date, accumulated rainfall in mm and related rainfall intensities in mm/h.

The methodology for determining the critical rainfall threshold is based on comparing and linking flood impact indicators with flood hazard parameters based on the date, time and address of interventions. Out of 764 rainfall events, hourly precipitation data was analyzed, and the maximum accumulated rain was calculated for durations of 1-, 2-, 3-, 6-, 12- and 24 - hours. Rainfall events were separated into two groups: related and non-related with flood indicators. Rainfall intensity-duration thresholds for the occurrence of pluvial floods were determined by plotting peak rainfall intensities of various time intervals vs. their respective durations for two groups of rainfall events. Two approaches were explored to determine a rainfall threshold that are related to the pluvial urban flood risk. The first was an empirical approach by Papagiannaki et al. (2015) defined by lowest rainfall intensities that pose no risk of flood events, and by highest rainfall intensities that cause flood events. The second approach is based on a statistical analysis of the data, examining the 25th and 75th percentiles of the precipitation data as the lower and upper thresholds. The performance of both approaches is analyzed by determining the overall correctness, hit rate, and false alarm rate of presented rainfall (Eq. 1–3):

$$Hit\ rate = \frac{h}{m+h},$$

(1)

$$False\ alarm\ rate = \frac{f}{c+f},$$

(2)

$$Overall\ correctness = \frac{h+c}{h+m+f+c}.$$

(3)

where: h – number of interventions above threshold line [–], m – number of interventions bellow threshold line [–], f – rainfall events (without intervention) above threshold line [–] and c – rainfall events (without intervention) bellow threshold line [–]. To obtain the best overall correctness, the hit

rate should be kept as high as possible while simultaneously, the false alarm rate should be kept as low as possible (Jang, 2015).

Results

Analysis of the relation between flood data and precipitation data

Frequency analysis of rainfall events and interventions was conducted by month and season, with 73% (233) of interventions reported in the warm season from April to September and 53% (407) of rainfall events recorded in this season. Therefore urban pluvial floods are more likely to occur during this period (0). The number of rainfall events during the colder periods (357) is similar, but the records of interventions (84) are considerably lower (0). This result is to be expected given the conditions of the continental climate in the Zagreb urban area.
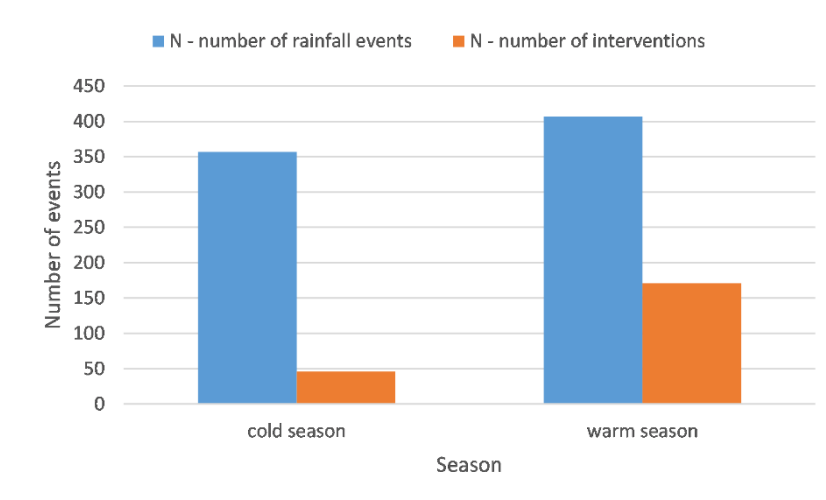
Fig. 5 Rainfall events and interventions related to urban floods during the cold and warm season
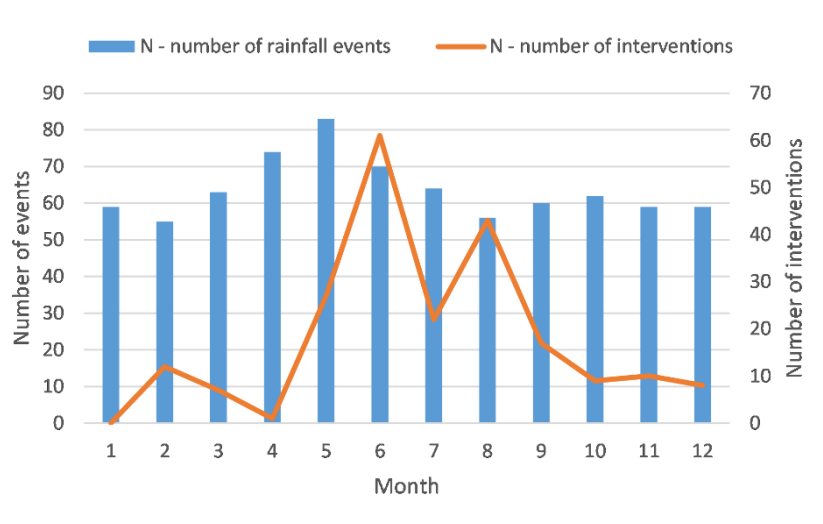

Fig. 6 Number of rainfall events and interventions related to urban floods over the months for the period 2007–2017

A number of rainfall events and interventions related to urban floods over the months for the period 2007–2017 was analyzed and, although most of the rainfall events were recorded in May, most interventions related to the urban floods were in June (61) and August (43) as can be seen in Fig. 6.
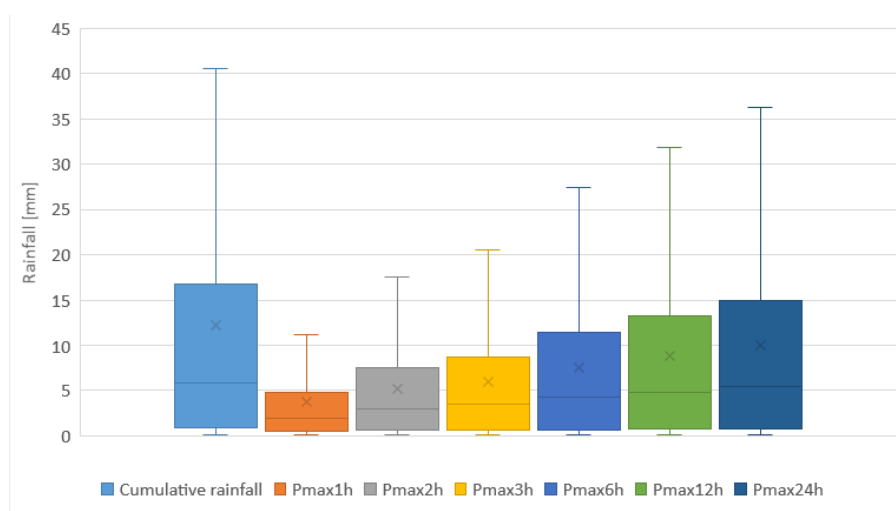
Fig. 7 Statistical characteristics of rainfall events (accumulated rainfall in [mm]) data for durations up to 24 hours.

A statistical analysis of rainfall events for defined rainfall durations up to 24 hours was conducted and results are presented in Fig 7. Numeric values of statistical characteristics of rainfall events represented in 0 are also given in 0. but expressed for the corresponding rainfall intensities in mm/h. Also, the percentile graph of rainfall data is presented in Fig 8. with the maximal accumulated rainfall during 1-, 2-, 3-, 12- and 24-hours. Except for the cumulative rainfall or the entire rainfall event, other events recorded accumulated rainfall less than 100 mm.

Table 2 Statistical characteristics of rainfall events data for durations up to 24 hours(0) converted to rainfall intensity [mm/h]

|		Pmax1h	Pmax2h	Pmax3h	Pmax6h	Pmax12h	Pmax24h
MIN		0.10	0.05	0.033	0.017	0.008	0.004
MAX		44.60	22.95	15.30	7.65	4.33	3.43
STD		5.10	3.16	2.35	1.44	0.84	0.50
MEAN		2.00	1.50	1.17	0.72	0.40	0.23
Percentile	0.25	0.50	0.30	0.23	0.12	0.07	0.04
	0.5	2.00	1.50	1.17	0.72	0.40	0.23
	0.75	4.80	3.71	2.90	1.90	1.10	0.63
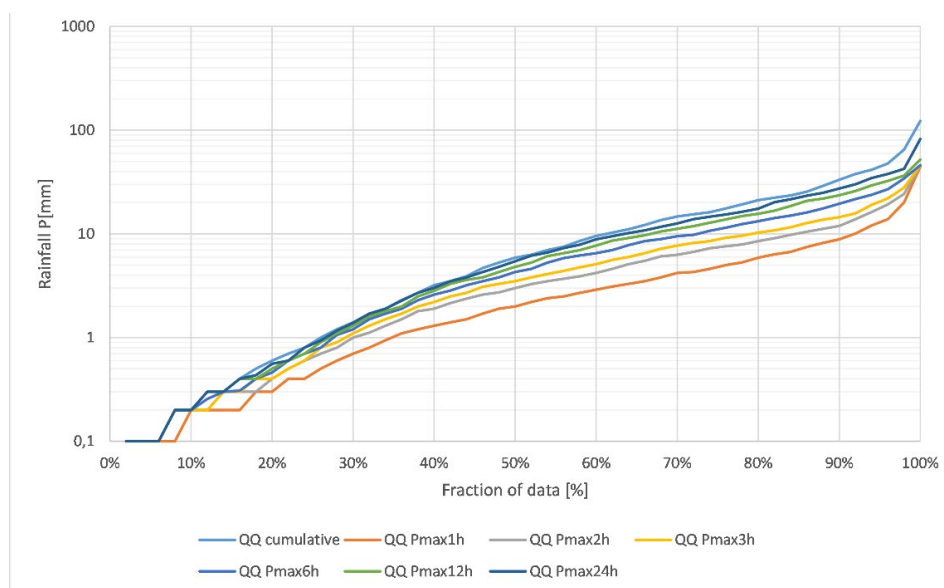
Fig. 8 Percentile graph of rainfall events data data for durations up to 24 hours

The relationship between flood impact indicators and flood hazard indicators is established by calculating Spearman correlation factors between maximal accumulated rainfall data and interventions, as shown in Tab. 3. The best correlation of ρ is around 0.6, indicating a fairly good correlation between the accumulated rainfall for the shorter duration and the number of interventions. With a more extended rainfall period, the correlation factor decreases, indicating that flash floods with more rain in shorter periods are most relevant for the prediction of flood events..

Table 3 Correlation by Spearman's rank order between flood impact indicators and flood hazard indicators for different rainfall events durations (Pmax)

Pmax	1h	2h	3h	6h	12h	24h
ρ	0,6061	0,5709	0,5419	0,5020	0,4726	0,4620

Rainfall intensity thresholds related to urban flooding

The intensity of the rainfall event is given by dividing the maximal accumulated rainfall intensities by the corresponding duration. The representation of peak storm intensity for different durations is shown in 0. Rainfall events related to floods are highlighted in orange, while events not related to the floods are highlighted in blue. Events that caused flooding are situated on top of the graph, while ones that did not are concentrated in thelower part of the graph. There is no visible border between the orange and blue marks signifying that the threshold cannot be estimated by simple graph observation. Authors Papagiannaki et al. (2015) suggested that an upper threshold should be determined as the maximum rainfall intensities that did not relate to interventions and the minimum rainfall intensities related to intervention as the lower threshold. Obtained thresholds intensity by this approach are defined here as empirical thresholds for which a linear regression equation is determined for different durations (Fig. 9). The empirical upper (Eq. 4) and lower (Eq. 5) threshold are given as:

$$I = 23.189 \, D^{-0.701}$$

(4)

$$I = 0.253 \, D^{-0.938}$$

(5)

where *I* is intensity of rainfall event [mm/h] and *D* is duration of rainfall event [h]. Based on correlation by Spearman's rank (0) for maximal accumulated rainfall of 1h period has been determined as most applicable for evaluation of urban flood hazard thresholds.

A lower empirical threshold in this paper is much lower compared to the empirical thresholds used by other authors, indicating that in database there may be rainfall events not related to flood events and therefore should be omitted. Therefore, additional threshold levels are explored, similar to the work of authors Hong, Kim and Jeong (2018) that are based on a statistical analysis of rainfall events with threshold rainfall quantities for fixed probability ranges. Here, the intensity of rainfall events for different durations was evaluated according to fixed percentile data and are referred here as statistical thresholds (0). In this case, the statistical thresholds are again determined as a linear regression equation for different durations (Fig. 10), where the statistical upper (Eq. 6) and lower (Eq. 7) threshold are given as:

$$I = 5.518 \, D^{-0.653}$$

$$\tag{6}$$

$$I = 0.531 \, D^{-0.835}$$

$$\tag{7}$$

where I is intensity of rainfall event [mm/h] and D is duration of rainfall event [h].
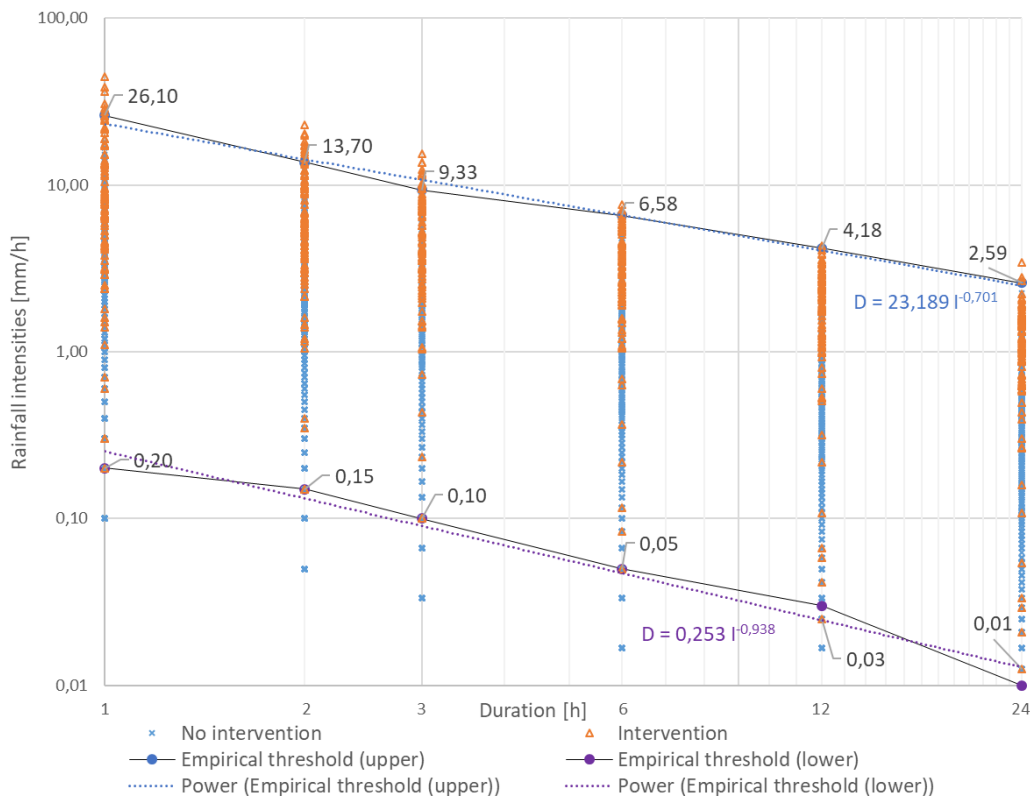

Fig. 9 Empirical critical thresholds for rainfall intensity and different duration related to pluvial urban floods

Table 4 Max accumulated rainfall [mm] for given percentile of rainfall data

| Percentile	Pmax1h	Pmax2h	Pmax3h	Pmax6h	Pmax12h	Pmax24h
0.25	0.9	0.5	0.6	0.7	0.7	0.8
0.5	5.9	2	3	3.5	4.3	4.8
0.75	16.8	4.8	7.425	8.7	11.4	13.225
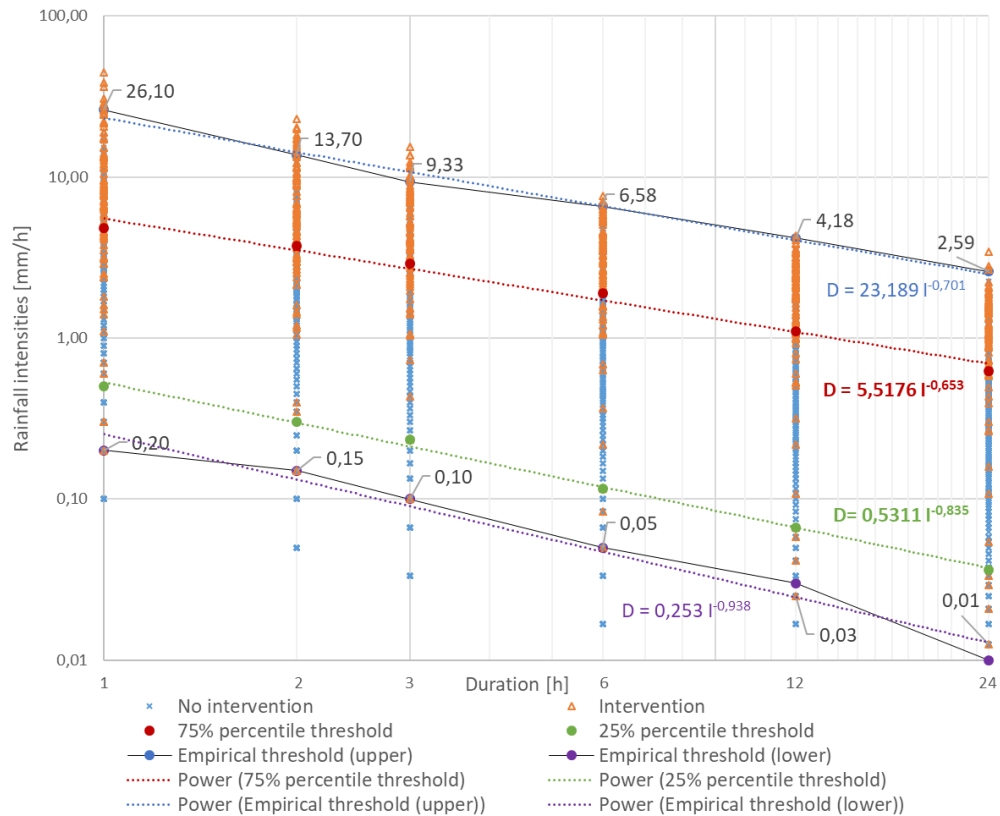
Fig. 10 Empirical and statistical (percentile based) critical thresholds for rainfall intensity and different duration related to pluvial urban floods

Evaluation of results

Performed land use analysis of subbasin area established the relationship between urbanization and surface permeability with surface runoff and flooding. Based on the obtained reports from fire brigades about interventions, dates and addresses of water pumping interventions from facilities and open spaces, a cartographic database of interventions together with spatial land use analyzes was made, the result of which showed that most of the intervention operations were related to residential (57%) and traffic areas (28%). On the other hand, the impact intensity, measured as the average number of intervention operations per event, is highest for precipitation in the range of 35–40 mm/h, with 15.5 interventions per event. 764 rainfall events were analyzed (h+m+f+c). Of these, 88 rainfall events were associated with interventions (h+m), while 676 were not associated with interventions (f+c) (Eq. 1–3).

To determine the validity of the proposed thresholds, the overall correctness rates were calculated (Tables 5–8) . It can be concluded that the upper empirical threshold gives a low false alarm rate, but the hit rate of correct flood prediction is very low, less than 13%. The lower empirical threshold gives better flood predictions but with increased false alarm rates, above 80% (00). Empirical thresholds predict only one aspect of the overall correctness value, namely that the upper threshold adequately eliminates false alarms (0), while the lower threshold adequately predicts flood events (0). To find a balance between these two extremes, the suitability of statistical thresholds was evaluated. It can be concluded that the upper statistical threshold has a decent hit rate of correctly predicted floods while also maintaining a relatively low false alarm rate. The overall correctness is around 80% (0). The lower statistical threshold values give very good flood predictions but have a high false alarm rate. It still shows better results with around 35% overall correctness than the lower empirical threshold (0). Considering these results, it can be concluded that a statistical approach could be more appropriate for predicting threshold values.

Table 5 Correctness of upper empirical threshold values

Pmax	1h	2h	3h	6h	12h	24h
Empirical threshold upper [mm]	23,189	28,529	32,206	39,623	48,748	59,974
h	11	11	9	5	2	3
m	77	77	79	83	86	85
f	1	0	0	0	1	1
c	675	676	676	676	675	675
hit rate	12,5%	12,5%	10,2%	5,7%	2,3%	3,4%
false alarm rate	0,1%	0,0%	0,0%	0,0%	0,1%	0,1%
overall correctness	89,8%	89,9%	89,7%	89,1%	88,6%	88,7%

Correctness of lower empirical threshold values

Pmax	1h	2h	3h	6h	12h	24h
Empirical threshold lower [mm]	0,253	0,264	0,271	0,283	0,295	0,308
h	87	88	88	88	88	87
m	1	0	0	0	0	1
f	551	576	579	584	585	561
c	125	100	97	92	91	115
hit rate	98,9%	100,0%	100,0%	100,0%	100,0%	98,9%
false alarm rate	81,5%	85,2%	85,7%	86,4%	86,5%	83,0%
overall correctness	27,7%	24,6%	24,2%	23,6%	23,4%	26,4%

Correctness of upper statistical threshold values (75% percentile)

Pmax	1h	2h	3h	6h	12h	24h
Percentile (75%) [mm]	5,518	7,018	8,078	10,275	13,069	16,622
h	58	64	67	69	69	64
m	30	24	21	19	19	24
f	107	138	151	137	126	97
c	569	538	525	539	550	579
hit rate	65,9%	72,7%	76,1%	78,4%	78,4%	72,7%
false alarm rate	15,8%	20,4%	22,3%	20,3%	18,6%	14,3%
overall correctness	82,1%	78,8%	77,5%	79,6%	81,0%	84,2%

Correctness of lower statistical threshold values (25% percentile)

Pmax	1h	2h	3h	6h	12h	24h
Percentile (25%) [mm]	0,531	0,595	0,637	0,714	0,800	0,897
h	85	85	85	84	84	84
m	3	3	3	4	4	4
f	476	500	493	487	485	489
c	200	176	183	189	191	187
hit rate	96,6%	96,6%	96,6%	95,5%	95,5%	95,5%
false alarm rate	70,4%	74,0%	72,9%	72,0%	71,7%	72,3%
overall correctness	37,3%	34,2%	35,1%	35,7%	36,0%	35,5%

Conclusion

Preliminary rainfall intensity thresholds for different rainfall durations based on an empirical and statistical approach that could be related to urban floods in the city of Zagreb, Maksimir area, in the period 2007–2017 are determined in this paper. Reports from the civil protection and public fire brigades of the city of Zagreb were analyzed, i.e. technical interventions for pumping water from facilities and open urban spaces during extreme hydrometeorological conditions were considered and used as impact parameters of pluvial floods. A spatial analysis was conducted and a relationship was established between urban land use and the number of interventions as an indicator of flood occurrence.The results showed that both obtained thresholds, the empirical and the statistical, could be used for practical purposes. However, evaluation of the thresholds based on hit rate, false alarm rate and overall correctness showed that the upper statistical threshold (75% percentile) has sufficient overall correctness with more correct flood predictions and higher false alarm rates than the upper empirical threshold. In comparison, the lower statistical threshold (25% percentile) has slightly better correctness than the lower empirical threshold. The analysis of urban flood indicators showed that 73% of the interventions occurred in the warm season, especially in May and August, and the spatial analysis showed that most of the interventions were related to residential (57%) and traffic areas (28%). Impact intensity is determined as the average number of interventions per event, and is highest for rainfall intensity in the range of 35–40 mm/h, with 15.5 interventions per event.

The critical thresholds for rainfall intensity with durations up to 24 hours related to pluvial urban floods, developed for this case study, could be of great assistance to public services to ensure that appropriate protection and rescue measures can be planned and implemented in a timely manner by local and national authorities. In addition, it should be noted that in future studies in the city of Zagreb, a more detailed spatial analysis of flood impacts and flood hazard indicators from other meteorological stations in Zagreb urban area should be carried, and rainfall durations shorter than one hour should be considered. Precipitation extremes should be taken into account in the developing future professional recommendations and standards, especially for the design and development of new urban infrastructure, to reduce future pluvial urban flood risk.

Acknowledgements

References

Alfieri L, Salamon P, Pappenberger F, Wetterhall F, Thielen J (2012). Operational early warning systems for water-related hazards in Europe. *Environmental Science & Policy*, **21**, 35–49.

Cannon SH, Gartner, JE, Wilson, RC, Bowers, JC, Laber, JL (2008). Storm rainfall conditions for floods and debris flows from recently burned areas in southwestern Colorado and southern California. *Geomorphology*, **96** (3–4), 250–269.

Croatian Bureau of Statistics. Available online: https://www.dzs.hr/ (accessed on 30.7.2021.)

Diakakis M (2012). Rainfall thresholds for flood triggering. The case of Marathonas in Greece. *Natural Hazards*, **60** (3), 789–800.

Guzzetti F, Peruccacci S, Rossi M, Stark CP (2008). The rainfall intensity–duration control of shallow landslides and debris flows: an update. *Landslides*, **5** (1), 3–17.

Climatology of the extreme heavy precipitation events in Slovakia in the 1951–2020 period

Ladislav MARKOVIČ, Pavel FAŠKO, Jozef PECHO

Slovak Hydrometeorological Institute, Slovakia, email: ladislav.markovic@shmu.sk, email: pavol.fasko@shmu.sk, email: jozef.pecho@shmu.sk

Abstract

In this study, we investigate extreme heavy precipitation events in the Slovak Republic in the period 1951–2020 in terms of their spatial and temporal distribution with goal to create dynamic-climatological analysis of those patterns of the atmospheric circulation, that can eventually lead to the occurrence of the extreme multi-day precipitation events. Heavy precipitation is defined as maximum precipitation total over five consecutive days (Rx5D) where a non-zero daily precipitation total must be recorded every day of selected 5-day period.

Spatial and temporal distribution of multiday precipitation totals is affected by many factors, mainly by the processes taking place in the troposphere eventually represented by the synoptic scale atmospheric circulation and by the orographic diversity of the area, which together significantly affects distribution of precipitation in the selected area. Our study is therefore constructed as an analysis of relationships between localized tropospheric circulation defined by the Czechoslovak catalogue of the typified synoptic situations (Brádka, 1968), the predominant wind patterns and the spatiotemporal distribution of Rx5D.

Introduction

Current changes in the global climate system, that are strongly correlated to the ongoing human-caused climate change, have an undeniable impact on the mean state of the climate. Long-term increase of the global temperature, particularly well expressed in the Arctic and Polar regions of the oceans in the Northern hemisphere can be directly linked to the continually diminishing sea ice areas (Bintanja et al., 2013; Vihma, 2014). It is very likely, that the rise in the ocean surface temperature in the North Atlantic Ocean and the Arctic Ocean affects the dynamics of atmospheric flows and consequently, the processes of genesis, vertical and horizontal dimensions, stability, and patterns of movement of low- and high-pressure areas. Warner (2018) proposes that there is a strong positive correlation between the October sea ice ecxtent and the DJF (December – January – February) values of the NAO index (North Atlantic index). This can, via presupossed stratospheric path, impact the strength of the polar stratospheric vortex, specifically to cause its weakening, which is subsequently manifested in the troposphere by weakening of zonal winds and more pronounced meandering the jet stream. This modifications in the synoptic scale atmospheric circulation might lead to a change in the distribution of precipitation during the year in Slovakia, displaying as an increase in the share of convective based stormy downpours in the total precipitation sums (Faško et al., 2015; Markovič et al., 2016) and the increasing extremity of precipitation events. Better understanding of the established circulation patterns associated with the extreme heavy multiday precipitation events can help us correctly and more precisely access and model trends and risks linked to human-caused climate change.

In Slovakia, general studies have been previously published that dealt with multi-day precipitation totals (Lapin, at al. 2004; Stehlová, et al., 2001; Jurčová et al., 2002; Gaál et al., 2002) however, these studies using shorter time series of daily precipitation were mostly very localized and due to the limited number of precipitation stations with processed maximum multi-day precipitation totals and time-consuming process of obtaining this data, only limited set of precipitation stations with authentic data has been used in the analysis. Dynamic-climatological analysis of extreme precipitation events was previously published only for maximum 2-day precipitation totals (Markovič, 2019). Our study uses new authentic data set of maximum 5-day precipitation totals (Rx5D) from 486 precipitation stations owned and

operated by Slovak Hydrometeorological Institute (SHMÚ), with available, complete, and consistent time series of daily precipitation from the period 1951–2020. Our spatio-temporal climatological analysis of the extreme heavy precipitation events in Slovakia is constructed as a causal analysis of relationships between spatially localized tropospheric circulation, defined by the Czechoslovak catalogue of the typified synoptic situations (Brádka, 1968), the predominant atmospheric flow and the spatial and temporal distribution of maximum 5-day precipitation totals.

Data and study area

Dataset of maximum 5-day precipitation totals

For needs of our analysis it was essential to create new Rx5D data set obtained from the network of precipitation stations operated by the SHMÚ performing precipitation observations during the 1951–2020 period (Fig. 1). Eventually, 486 stations with mean elevation 375 meters a.s.l. were selected, excluding those, which could not be incorporated due to the data inconsistency or due to short, incomplete, or unreliable time series of observations. Small portion of time series selected for the analysis still contained brief interruptions. Missing data, however, did not in any case exceed 5% of the total number of Rx5D for each station, and therefore could be fixed or calculated by using an expert approach based on the regression analysis and analogy between data measured at geographically related stations. From selected precipitation stations were prepared Rx5D maps. Spatial and vertical distribution of precipitation stations has proven to be inadequate for used interpolation tool. To improve the vertical distribution calculated for selected set of stations, resulting in a more realistic spatial distribution of Rx5D within the territory of Slovakia, there were (only in the process of creating maps) used 60 supplementary (virtual) points. (Fig. 1) These points were located in the mountain areas, at elevations over 500 meters above the sea level with mean elevation 1049 meters a.s.l. 31 additional points were placed in positions located at the elevation between 500–1 000 meters. Remaining 29 points were placed in the elevations between 1 000–2 000 meters. Exact placements of supplementary points were identified using method based on expert spatial analysis of the existing field of precipitation stations conducted by Dr. Pavel Faško.
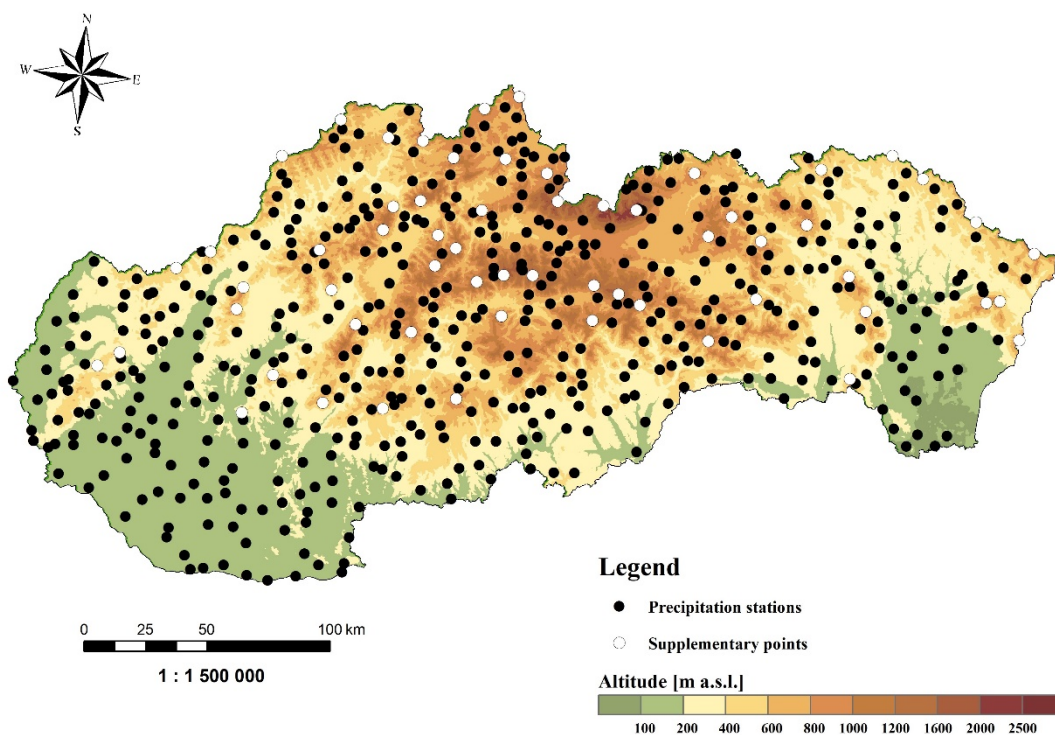

Fig. 1 Selected precipitation stations and supplementary points within the territory of Slovakia.

233

Maximum multiday precipitation totals

The sums of multi-day atmospheric precipitation totals can be calculated by two slightly different methods – the standard and the modified method (Lapin et al., 2004). Standard processing method of multi-day precipitation totals represents situations where a non-zero daily precipitation total must be recorded every day of selected n-day period. Possible occurrence of day (or days) during which the precipitation was not registered, or its amount was not measurable (0.0 mm) means, that the total precipitation amount for the considered period is excluded from the analysis. Such a relatively strict view of multi-day continuous precipitation totals is particularly preferred in hydrological treatments. In climatology, on the other hand, it is also interesting and helpful to include precipitation periods incorporating one day without registered precipitation, but which could not be the first or last day of this selected n-day period, because in that case we would be only dealing with shortened n-1 day period. This correction, of course, does not apply to 2-day totals. The monthly maximum sum of Rx5D therefore represents the highest value of all 5-day sums calculated from five successive days with the observed non-zero precipitation totals over the period of one month. Sums of Rx5D measured at the turn of months was assigned to the month with higher share on total precipitation sum. This approach was also applied to maximum totals that occurred at the turn of years meaning, that there was the possibility that they could, in some cases, be also comprised of data outside of selected 1951–2020 period – data measured in December 1950 and January 2021, which were therefore subsequently included in our study.

Methodology

Our paper deals with a climatology of the extreme heavy precipitation events in within the network of precipitation stations operated by the SHMÚ. Presented methodology has been chosen to provide a more comprehensive view of the issue by not only identifying situations with recorded highest Rx5D, but also directly incorporating the necessary condition of sufficiently large area of their distribution presented as a mean spatial value of the monthly Rx5D.

Selection of the significant maximum 2-day precipitation totals

The method used in the process of selecting significant multi-day precipitation events was based on the analysis of mean monthly values of the maximum multi-day totals earned in a given month for each year of analysis as simple average of all station values. If, in any given year, the station did not record 5-day total and hence also the Rx5D, zero value was assigned to this station for the sake of preserving constant number of station values included in each step the analysis. After calculating the average monthly maximum values for the complete set of stations for all years in the 1951–2020 period, we defined the 5 highest values in each month of the calendar year and, together with the year of occurrence, there were selected for a subsequent synoptic analysis. This selection method eventually aggregated 60 different cases available for the consequent annual and half year occurrence analysis of significant weather conditions assigned to the surveyed Rx5Ds.

Identification of the period of occurrence

Occurrence of the extreme heavy precipitation events have been identified within the selected 5 years with the highest average sums. Previously calculated Rx5D were station-wide assigned to corresponding dates, based on regional analysis conducted using precipitation reports and databased datasets from selected profile stations in each river basin determined by station's designators. The final extent of each selected heavy precipitation event has thus been set within 5 to 8-day period.

Assignment of typified synoptic situation

Process of defining the days, from which was each selected multi-day situation constituted, was followed by assignment to the corresponding typified synoptic situation. Data sources selected for identification process were represented by specialized calendars of analyzed synoptic situations containing analysis on day-to-day basis. For the period 1951–1990 a calendar elaborated for the territory of former Czechoslovakia (CHMI, 2017) was used, and since 1991 a calendar of situations identified exclusively for the territory of Slovakia (SHMÚ, 2021) was applied. Publication of each annual calendar is necessarily preceded by mutual communication between the Czech Hydrometeorological Institute and

the SHMÚ. In these analyzes, however, are for technical reasons, not identified divisions among the synoptic situations of the same circulating type following directly one after another. The general large scale circulation typification used for the territory of Czechoslovakia and later of independent Slovakia is already from the process of its creation hampered by inaccuracies and the larger the territory we try to include under a narrowly defined typified situation, the greater are the potential detection inaccuracies. We have tried to minimize this impending identification errors with a detailed study of daily totals within multi-day precipitation situation, to ascertain given significant weather situation because, in most cases these large-scale circulating units are not stationary. Great diversity and dynamics of atmospheric processes often results in the extended stay period of selected 5-day precipitation situations over the territory of Slovakia and thus, in many cases, subsequently leads to detection of two, exceptionally, up to three influencing typified situations. In the final process of assessing the occurrence of typified conditions, there have been, after analyzing daily totals, selected one, if necessary two or three influencing situations. This approach allowed us to create the input set containing 99 influencing typified synoptic situations assigned to the set of 60 cases consisting of the five heavy precipitation events with the highest spatial means. This dataset was subsequently used in the impact analysis between typified synoptic situations and the spatial distribution of the maximum sums of Rx5Ds. More accurate identification of atmospheric circulation was achieved by the archived reanalyzed large-scale maps of geopotential levels 850 hPa and 500 hPa created by the US Global Circular Model – GFS or by the US Office for Ocean and Atmosphere (NOAA).

Results

Maximum sums of the 5RxDs

The highest values of Rx5d exceeded 250 millimeters and were measured at precipitation stations located in the mountainous areas in the northern part of Slovakia at elevation over 600 meters amsl. Absolute maximum value of Rx5d, accounted for 274,7 mm, was measured in May 2014 in Tatranská Javorina on the northern slopes of the Belianske Tatry mountain range. Rx5Ds over 200 millimeters were detected only on 33 stations (7%) in the January–December period with only 4 station exceeding this Rx5D value in the cold half-year (October–March). Furthermore, it can be said, that the Rx5Ds greater than 100 millimeters was at least once recorded at 466 stations, representing almost 96% of the whole set.

Spatiotemporal analysis of annual and seasonal maximum Rx5d (Fig. 2) points to the fact, that higher values of Rx5D were in the period 1951–2020 generally achieved in the warm half-year (April–September) (Fig. 3) with significantly pronounced orographic – windward and leeward effects during the cold half-year (October–March) (Fig. 4). The highest values of Rx5d exceeded 250 millimeters and were measured at precipitation stations located in the mountainous areas in the northern part of Slovakia at elevation over 600 meters above mean sea level. Absolute maximum value of Rx5d, accounted for 274,7 mm, was measured in May 2014 in Tatranská Javorina on the northern slopes of the Belianske Tatry mountain range. Domains with high total values – over 180 millimeters are concentrated mostly in the mountainous northern parts, in the Vysoké Tatry and Západné Tatry mountain ranges, in the north parts of Orava and Kysuce regions and in the southwestern Slovakia in the Malé Karpaty mountain range. However, a relatively large region with high anuall Rx5D values is localized also in the northeastern part of the republic. Most of the area of Slovakia is contained in a value range from 110 to 160 millimeters. Isolated areas of the lowest calculated values – under 100 millimeters, are situated mostly in the west on the Podunajská nížina lowland. Spatial distribution of Rx5Ds during warm half year (Fig. 3) resembles overall annual distribution. During the cold half-year are generally observed lower absolute values (Fig. 4), Areas of the highest achieved values – above 140 mm – are in the cold half-year, unlike in the previous cases, located mainly in the central part of the territory, namely in the region containing western parts of Nízke Tatry mountain range and Veľká Fatra mountain range. Areas with high values are also situated in its west and southeast neighborhoods. Relatively extensive area with sums below 80 millimeters is located in the southeast part of the territory in the Východoslovenská nížina lowland.
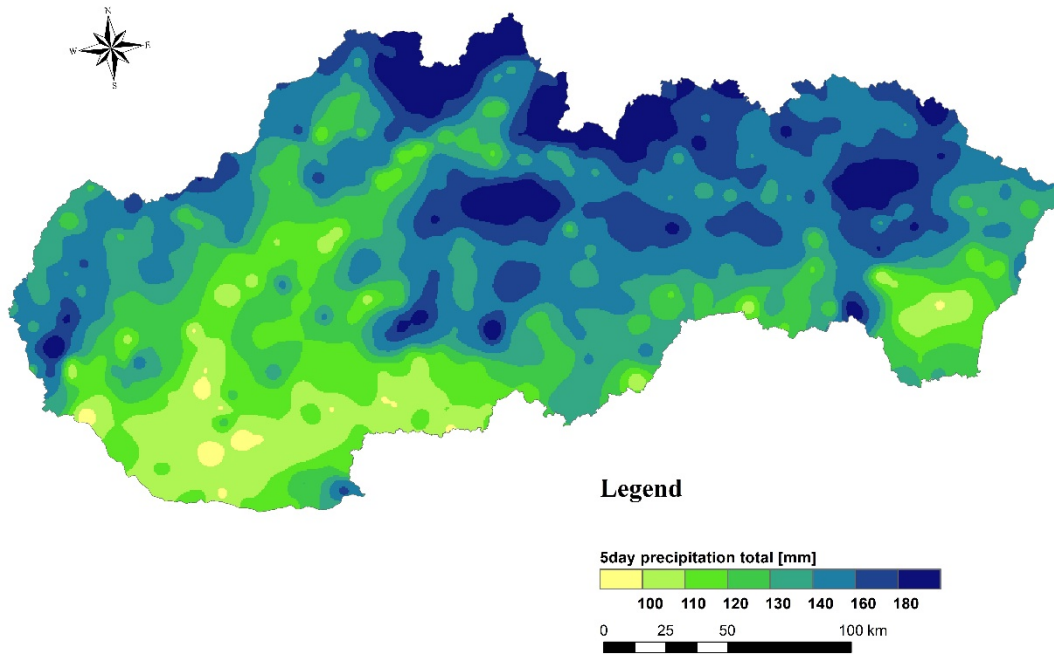
Fig. 2 Maximum 5-day precipitation totals in Slovakia in the 1951–2020 period.
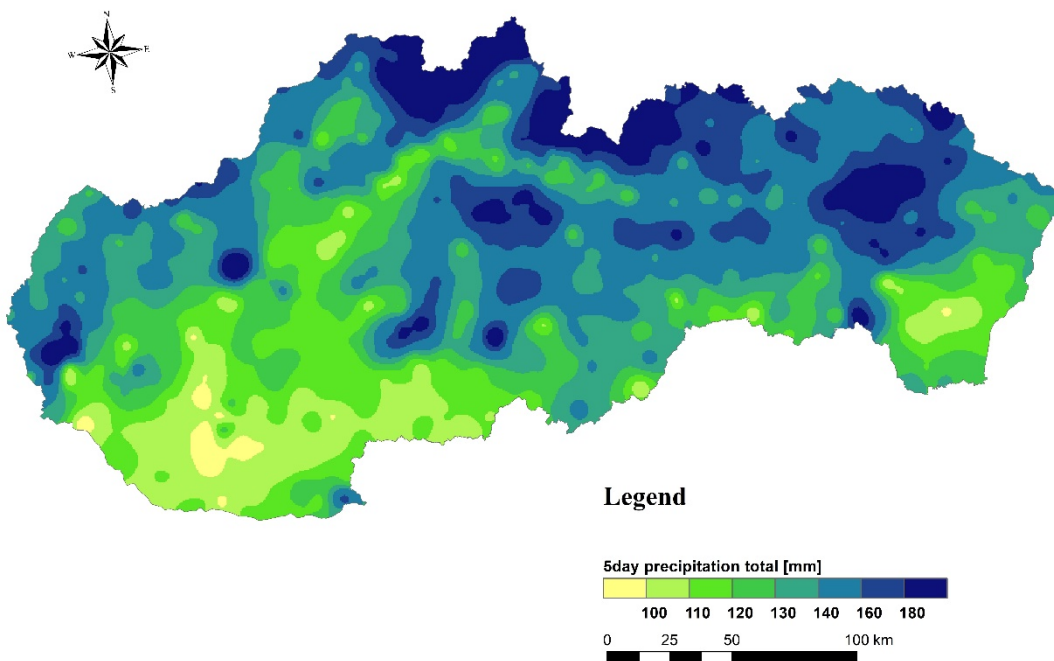

Fig. 3 Maximum 5-day precipitation totals during the warm half-year in Slovakia in the 1951–2020 period
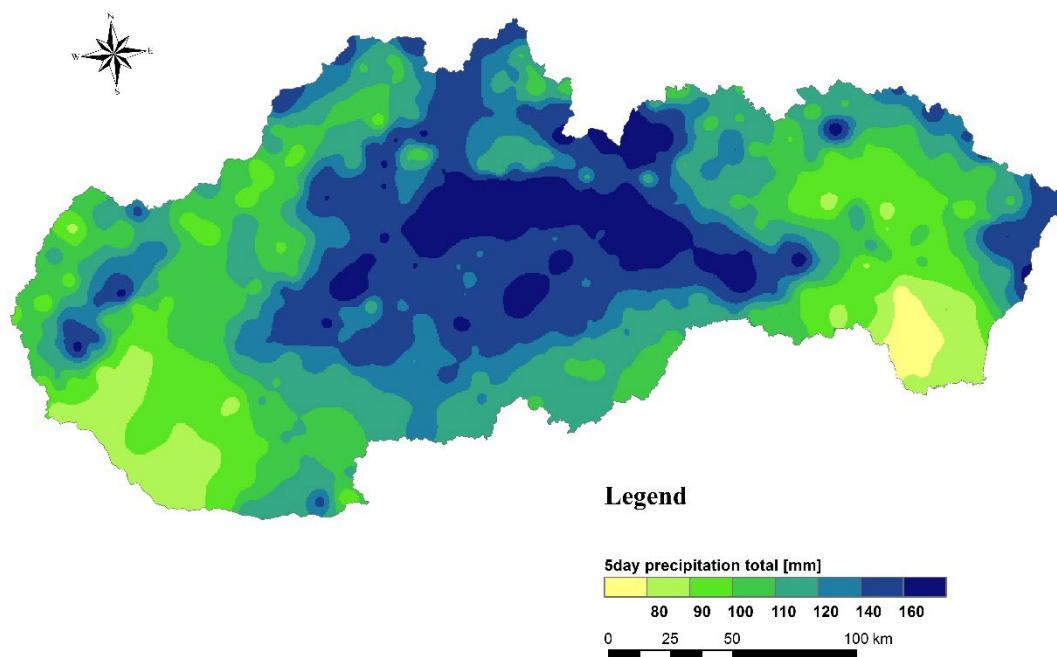
Fig. 4 Maximum 5-day precipitation totals during the cold half-year in Slovakia in the 1951–2020 period.

Maximum mean values

The analysis of the highest values of the Rx5Ds can provide a good point of view on the distribution of extreme values, but it is not necessarily suitable for a large-scale study dealing with the effects of the significant typified synoptic situations on the spatio-temporal distribution of the extreme heavy precipitation events. Use of mean values calculated for a complete set of 486 precipitation stations represents a relatively simple and accurate means for determining precipitation events with greater spatial impact. Calculated mean value and accuracy of the detection of the real extreme precipitation event is greatly dependent on the number of stations reaching Rx5D simultaneously. Mean value of the maximum precipitation totals from the complete set of 486 precipitation stations used as a measure to detect the occurrence of the spatially significant precipitation events reached its highest values within the May – October period. The highest mean value and at same time, the only total with value in the 90-millimeter range, was recorded only recently in October 2020 with mean Rx5d value 90,0 millimeters. The second (80.7 mm) and third (78,3 mm) highest values were calculated for July 16 to July 21, 197 and July 16 to July 22, 2001 respectively. (Table 1) Within the entire set comprised of 720 values of mean monthly Rx5Ds, values greater than 50 millimeters were achieved only 18 times, of which 6 in July and 5 in October. Values greater than 50 millimeters were never, within this data set, recorded in the period from January to April.

Table 1 Ranking of the 10 highest mean monthly values of the Rx5D in Slovakia in the 1951–2020 period.

Rank	Mean [mm]	Year	Month	Date	Situation	Max [mm]
1	90.0	2020	October	10. – 17.	NWc-C	174.3
2	80.7	1997	July	16. – 21.	C-NEc	253.6
3	78.3	2001	July	16. – 22.	B-Bp	274.0
4	77.2	1984	September	21. – 25.	B	219.7
5	74.5	1980	October	08. – 12.	B-Bp	268.8
6	72.2	2010	May	13. – 18.	B-NEc	219.7
7	65.5	2007	September	04. – 08.	Ec	215.8
8	62.4	2011	July	18. – 22.	B-C	155.2
9	61.3	1960	July	23. – 27.	C	229.6
10	59.8	1964	October	09. – 15.	B-C	211.6

Dynamical-climatological analysis of maximum average values

Form of a cluster analysis was selected to maintain the transparency and informative value of obtained results. Clusters were based on the relative geographic position of the typified synoptic situation in relation to the territory of Slovakia. Using this approach, 25 typified synoptic situations were clustered to the 9 main groups (clusters). These clusters consisted of one, two or three typified situations. We subsequently obtained 7 clusters for cyclonic types – 1. trough of low pressure over the central Europe and trough moving over the central Europe (B/Bp), 2. cyclone over the central Europe (C), 3. the upper-level cyclone (Cv), 4. eastern cyclonic situation (Ec), 5. northern cyclonic situations (Nc/NEc/NWc), 6. southern cyclonic situations (SEc/SWc) and 7. western cyclonic situations (Wc/Wcs). Anticyclonic and transient situations were thus each assigned into its own one cluster – 8. entrance to the frontal zone (Vfz) and 9. anticyclonic situations. In section of our analysis, we worked with the collection of 60 cases consisting of five Rx5D events with the highest spatial mean values for each month of year. Considering, that the extent of each selected extreme heavy event has been previously set within 5 to 8-day period each event could be represented by up to three typified situations. The final analyzed input set consisted of 98 individual typified synoptic situations – 21 one-situation events, 37 two-situation events and 1 three-situation event.
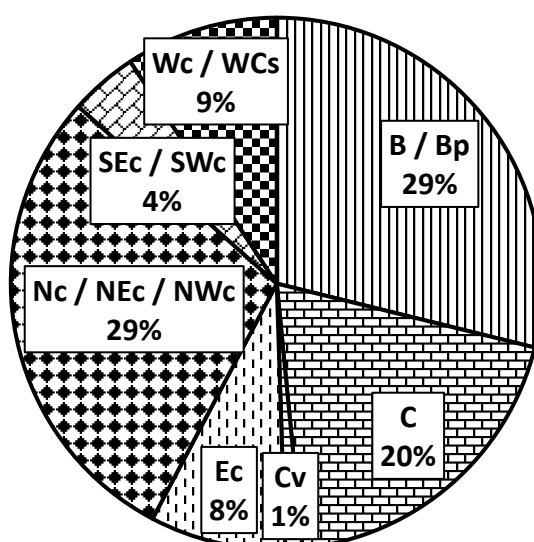

Fig. 5 Relative representation of typified synoptic situation on occurrence of highest average Rx5D [%] from January to December in Slovakia in the 1951–2020 period.

Relative dominance of the B/Bp and Nc/NEc/NWc clusters with exactly the same relative occurence (29 %) was observed when analyzing relative occurrence of significant synoptic types during events with the highest calculated mean values, regardless of the month of their occurrence (Fig. 5). Significant relative representation was also observed in case of cyclonic circulation types with central position C (20 %). No other cluster managed to reach at least 10% relative occurrence. The highest spatial mean value 90,0 milimeters measured during heavy precipitation event form 10. to 17. October 2020 occured during NWc situation transitioning into C situation.
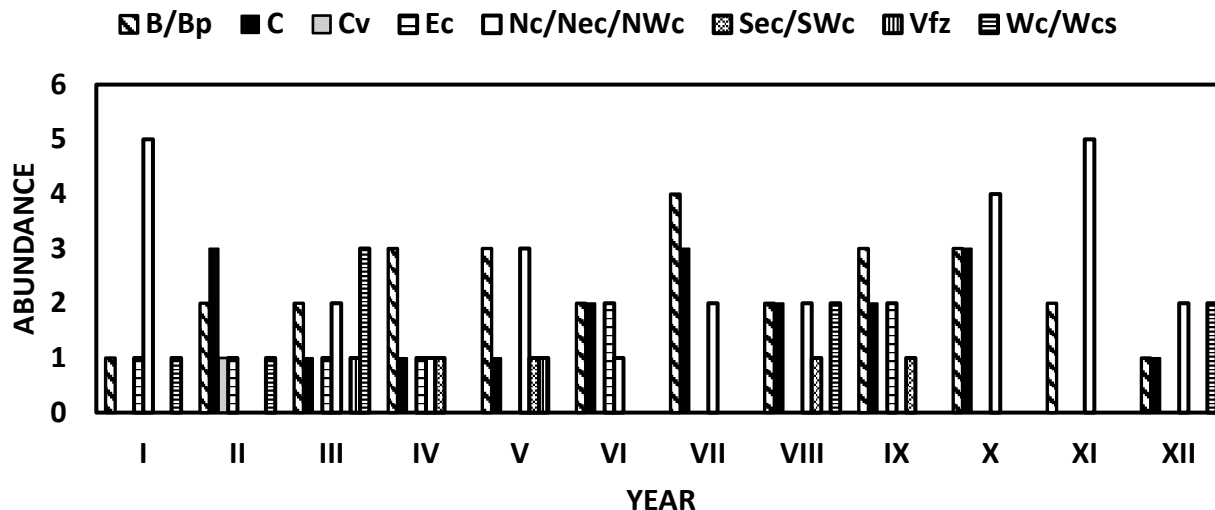
Fig. 6 Relative representation of typified synoptic situation on occurrence of highest average Rx5D [%] from January to December in Slovakia in the 1951–2020 period.

The cluster-based analysis of the absolute frequency of occurrences of the typified synoptic situations during the months of calendar year (Fig. 6) provides more detailed look on their temporal distribution. From 2 to 6 detected influencing clusters were identified for each month of the year, the most (6) in March. February, April, May, and August recorded 5 clusters, and the least (2) were recorded in November, which also saw considerable prevalence of a Nc/NEc/NWc cluster.

A better view on distribution, and the possible change in the impact of selected clustered circulating types during year can be achieved by a separate analysis using, in climatology common division into the warm half-year (April–September) (Fig. 7) and the cold half-year (October–March) (Fig. 9).

In the warm half-year was detected a significant decrease in the relative occurence of cyclonic situations with northern orientation (Nc/NWc/NEc) (10% decrease) (in comparison to the year-round relative distribution). Cluster B/Bp maintained its most influential positon with 6% increase in the relative occurence. Cyclonic situation with a central orientation (C) increased its occurence and become the second most prevalent circulation type (10% increase). Increse in the relative occurence was detected for circiulation clusters Ec (3% increase) and SEc/SWc (4% increase) while western cyclonic situations occurence decreased by 5%. It can be also further noted, that, during this period, Cv circulation type didn't even participate in the genesis of situations with highest maximum precipitation totals.
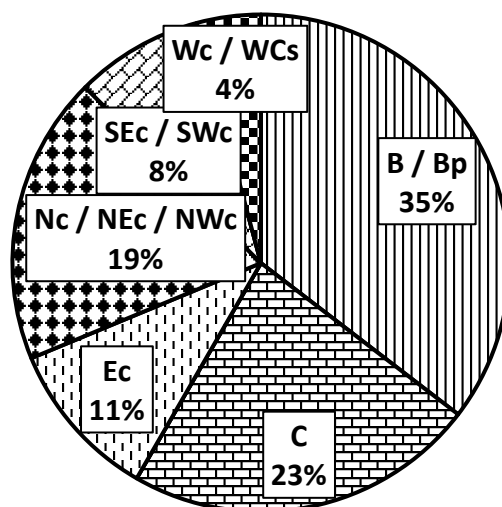

Fig. 7 Relative representation of the typified synoptic situations on occurrence of the highest average Rx5D [%] in the warm half-year in Slovakia in the 1951–2020 period.

Summer months of July and August can be presented as a typical period, during which can be observed large-scale atmospheric circulation necessary for occurrence of the extreme precipitation events with a good spatial distribution. Summer months are usually characterized by high percentage of the convective precipitation, but warm and humid atmosphere can during favorable atmospheric circulation provide ideal condition for heavy precipitation events influencing even lowland areas. Spatial distribution of stations with the highest values of the Rx5Ds calculated for five situations with the highest mean values is displayed in the Figure 8. Most stations are in the mountain areas in the central part of the territory with a patch of stations located in the eastern part of Slovakia, even in the Východoslovenská nížina lowland. This heavy precipitation event occurred during situation Bp transitioning into NEc situation in 2004. Heavy precipitation event in 1997 (C-NEc), significantly impacted even areas in the west of Slovakia in the Malé Karpaty mountain range, Biele Karpaty mountain range and Javorníky mountain range.
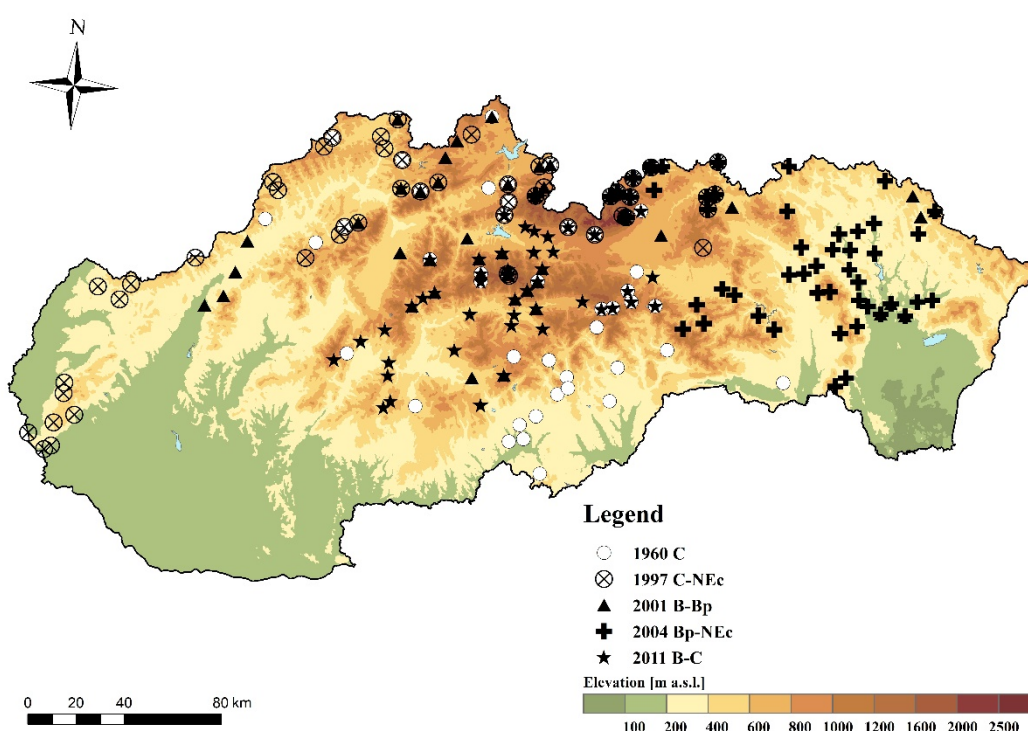

Fig. 8 Placement of 50 stations with the highest Rx5D measured during occurrence of typified synoptic situations with the highest calculated mean values in Slovakia in July in the 1951–2020 period.

In the cold half-year can be observed a significantly different relative distribution of clusters detected during heavy precipitation events (Fig. 9). Unlike in the warmer half-year, in this part of year there was recorded (in comparison to the year-round relative distribution) a significant increase in the relative representation of Nc/NEc/NWc cluster (10% increase), wich ment, that this cluster become the most prevalent with relative ocurence of 39%. Decrease in the relative curence was detected for cluster B/Bp (6% decrease) and C (4% decrease) (but during the month of January February and March, even the highest average values during these circulation types. Cyclonic circulation cluster with the southern orientation SEc/SWc didn't even participate in the genesis of the extreme heavy precipitatio.
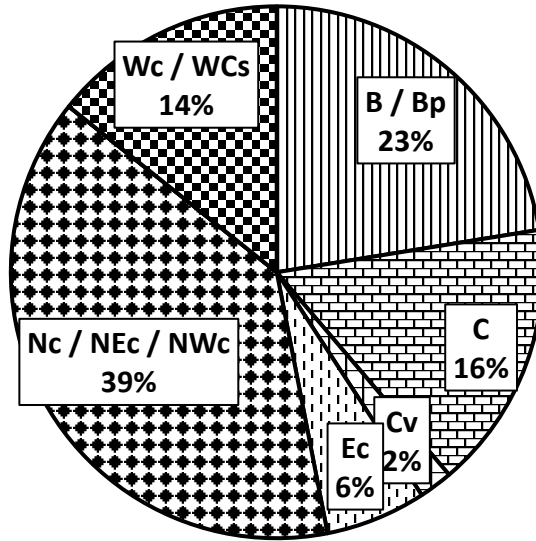
*Fig. 9 Relative representation of typified synoptic situations on occurrence of the highest average Rx5D [%] in Slovakia in the cold half-year of the 1951–2020 period.*
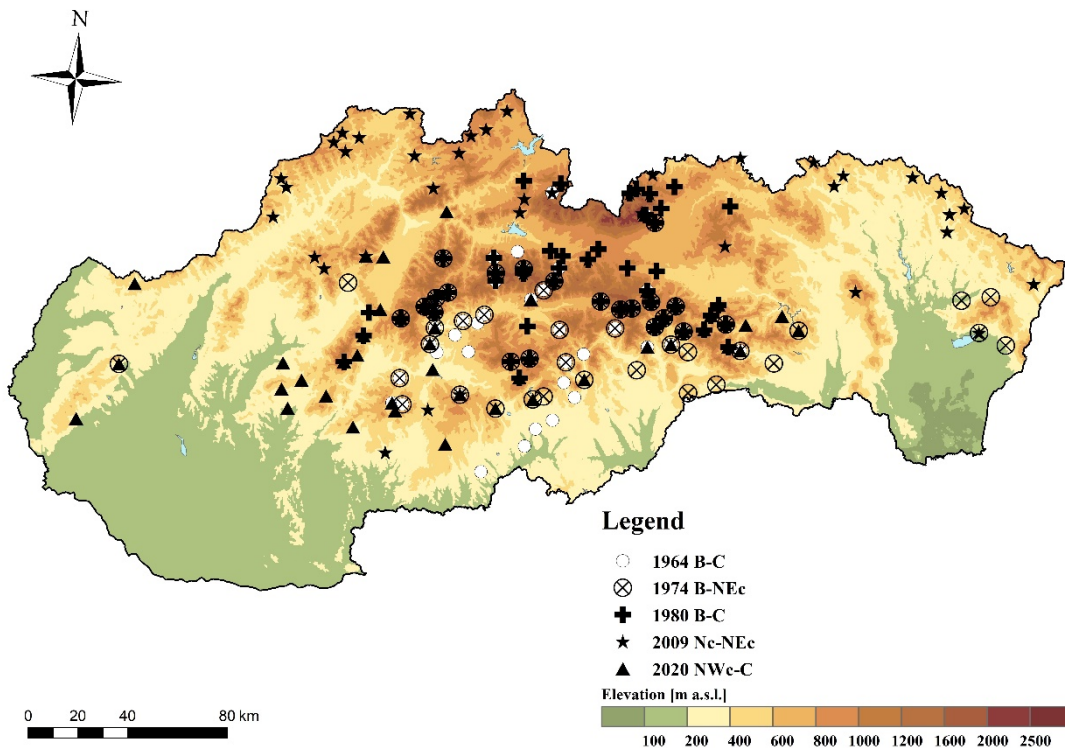

Fig. 10 Placement of 50 stations with the highest Rx5D measured during occurrence of typified synoptic situations with the highest calculated mean values in Slovakia in October in the 1951–2020 period.

The spatial distribution of the maximum values calculated for 5 events with highest mean maximum precipitation totals displayed for December (Fig. 10) represents a typical placement on the southern westward slopes in the mountanious regions in the central part of Slovakia during wide range of synoptic situations. The absolutely highest mean value calculated for the whole Rx5D data set was set during NWc-C extreme heavy precipitation event in October 2020.

Conclusion

Spatiotemporal analysis of annual and seasonal maximum Rx5d points to the fact, that higher values in the period 1951–2020 of Rx5d were generally achieved in the warm half-year (April–September) with significantly pronounced orographic – windward and leeward effects during the cold half-year (October–March). Mean value of the maximum precipitation totals from the complete set of 486 precipitation stations used as a measure to detect the occurrence of the spatially significant precipitation events reached its highest values within the May – October period. The highest mean value was recorded during heavy precipitation event in October 2020 with mean Rx5d value 90,0 millimeters. The maximum mean values, independent of the month of occurrence, were recorded during the presence of the typified synoptic situations characterized as low-pressure trough (B/Bp) and the cyclonic situations with northern orientation (Nc/NWc/NEc). Changes in the spatial distribution of Rx5d during the year were clearly identified in the separate warm half-year (April–September) and cold half-year (October–March) analyzes. Spatially significant precipitations events recorded in the warm half-year were, in more than 1/2 of the identified events, caused by the cyclonic situations with central position (C) and and by the low-pressure trough (B/Bp). Cold half-year is, on the other hand, defined by a dominant influence of the cyclonic situations with northern orientation (Nc/NWc/NEc) complemented by the low-pressure troughs (B/Bp).

Our analysis highlights the fact, that regional Czechoslovak typification of significant synoptic situations can, despite its often-present subjectivity, provide very good results that correlate with the long-term climatological knowledge of atmospheric circulation over the territory of Slovakia. It also provides god basis for the future objective dynamic-climatological analysis.

Acknowledgements

References

Bintanja R, Van Oldenborgh, GJ, Drijfhout SS, Wouters B, Katsman CA (2013) Important role for ocean warming and increased iceshelf melt in Antarcticsea-iceexpansion, *Nature Geoscience* **6**, 376–379.

Brádka J, and HMI collective (1968) Typizace v meteorologii, Meteorologické Zprávy, Český hydrometeorologický ústav, Praha.

ČHMÚ, (2017) Typizace povětrnostních situací pro území České republiky, Kalendář pro jednotlivé roky, Praha, dostupné online: http://portal.chmi.cz/historicka-data/pocasi/typizace-povetrnostnich-situaci.

Faško P, Šťastný P, Švec M, Kajaba P (2015) Výskyt a priestorové rozloženie vysokých denných a viacdenných úhrnov zrážok na Slovensku, Manažment povodí a povodňových rizík 2015 a Hydrologické dni 2015, ÚH SAV, Bratislava.

Gaál L, Lapin M (2002) Extreme several day precipitation totals at the Hurbanovo observatory (Slovakia) during the 20th century. *Contributions to Geophysics and Geodesy*, vol. **32** no. 3, 197–213.

Jurčová S, Kohnová S, Szolgay J, Gaál L (2002) K výberu vhodnej distribučnej funkcie maximálnych 5-denných úhrnov zrážok, Acta Hydrologica Slovaca, ÚH SAV, Bratislava.

Lapin M, Gaál L, Faško P (2004) Maximálne viacdenné úhrny zrážok na Slovensku, Seminár „Extrémy počasí a podnebí ", Brno, 2004, ISBN 80-86690-12-1.

Markovič L, Faško P, Bochníček O (2016) Zmeny dlhodobých priemerných mesačných a ročných úhrnov atmosférických zrážok na Slovensku. *Acta Hydrologica Slovaca*, č. **2**, 2016, ÚH SAV, Bratislava, 235–242.

Markovič L, (2019) Dynamic-climatological analysis of the maximum 2-day precipitation totals in Slovakia. Meteorologický časopis. Bratislava: *Slovenský hydrometeorologický ústav*, **22** (1), 31–38. ISSN 1335-339X.

Stehlová K, Kohnová S, Szolgay J (2001) Analýza dvojdňových úhrnov zrážok v oblasti horného Hrona, *Acta Hydrologica Slovaca*, 2001, vol. **2**, no. 1, 167–174.

SHMÚ (2021) Typy poveternostných situácií, Slovenský hydrometeorologický ústav, Bratislava, dostupné online: http://www.shmu.sk/sk/?page=8.

Vihma T, (2014) Effects of Arctic Sea Ice Decline on Weather and Climate: A Review, Surveys in Geophysics, Volume 35, Issue 5, 1175–1214.

Wetterzentrale (2021) NOAA 20th century, online:
https://www.wetterzentrale.de/en/reanalysis.php?model=noaa.

Stehlová K, Kohnová S, Szolgay J (2001) Analýza dvojdňových úhrnov zrážok v oblasti horného Hrona, *Acta Hydrologica Slovaca*, 2001, vol. **2**, no. 1, 167–174.

Hydrological Modelling for Water Balance Components Assessment

Silviya STOYANOVA

MSc, Bulgaria, email: silviya.stoyanova@meteo.bg

Introduction

Applying the law of conservation of mass to the hydrologic cycle is what water balance stands for. This states that, for any arbitrary volume and during any period of time, the difference between total input and output will be balanced by the change of water storage (UNESCO, 1971). A simple expression of the water balance equation reads: Inflow (precipitation) = Outflow (runoff, ET, groundwater) + Change in storage.

Present-day environmental challenges are much related to the hydrologic cycle hence a better understanding of water balance is needed for meeting them.

Water balance is a well acknowledged technique for analyzing the hydrology of a watershed. Quantifying the parameters of the hydrological cycle is the first step for estimating water resources and water balance. Due to the complex character of hydrological processes the usage of hydrological models is widely recognized as an effective tool for understanding and representing the relationship between different processes and water balance parameters (Koshinchanov et al., 2014). Hydrological models identify the dominant hydrological processes which influence water balance (Yordanova et al., 2020). Hydrological models delineate the partition of water input to a watershed (mainly rainfall) into hydrological processes – surface run-off, base flow, ET and storage changes. The water balance components that are commonly interpolated for WRA purposes are the characteristics of precipitation and runoff (WMO, 1992a).

In this study SWAT (Soil Water Assessment Tool) hydrological model was applied to Vit river basin to estimate the water balance components of the catchment – surface run off, lateral flow, evapotranspiration, etc.

Methodology

Study area

The study area (Vit river watershed) is located in northern Bulgaria and is part of the Danube river basin (Fig. 1). Vit river catchment is elongated with an area of 3225 km^2. The river begins after the confluence of the Beli Vit and Cherni Vit rivers, both springing from the Balkan Mountain. The slope of the river in the mountainous part of the watershed reaches up to 200 ‰. The mainstream goes on directly northward through large valley with lower slope to the Danube river. The average slope of Vit river is 9.6 ‰. The density of the river network is very small – 0.5 km/km^2. The average altitude of the watershed is about 400 m. There are five monitoring hydrometric stations and nine monitoring meteorological stations in the watershed.

The maim channel and its tributaries are of great importance for the development of the cities and villages located in the catchment area. Bankfiltration is the major source of drinking water supply for the inhabited areas. Along the middle and downstream part of the watershed some of the water is used for irrigation.

The distribution of annual runoff in Vit river basin is dominated by the seasonal characteristics of the moderate continental climatic conditions. Typically winter months come along with a snow cover in the mountainous areas. Precipitation occurs during spring, early summer and autumn. In summer however the rain events are of short duration and high intensity. The maximum discharge of the river can be observed during spring (March to June) (DBMC, 2005, Stefanova, 2011).
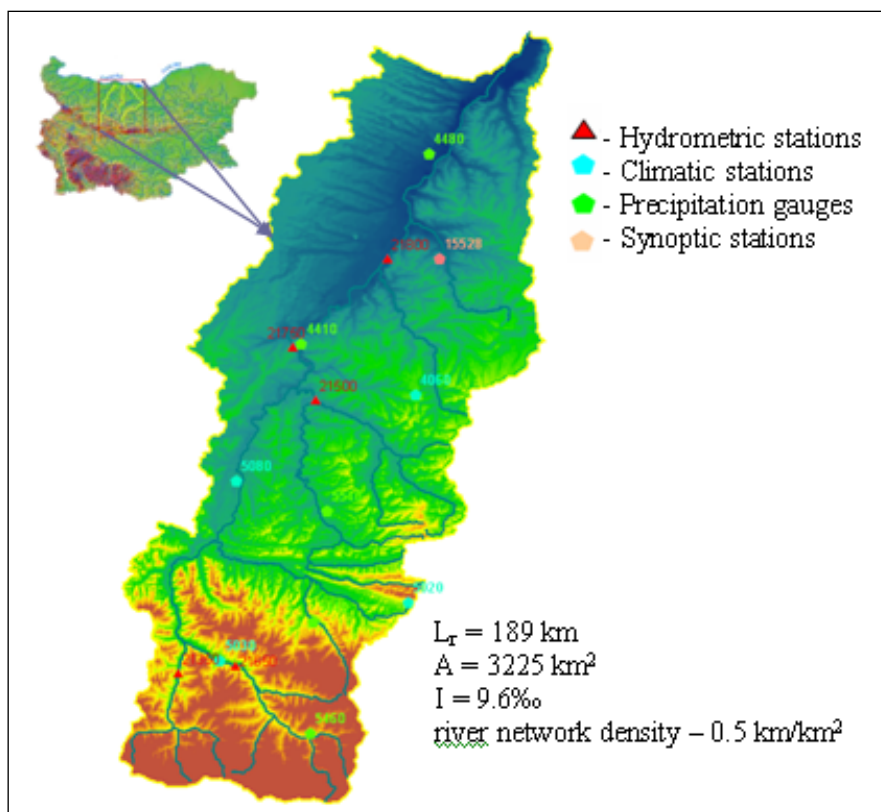
Fig.1 Vit river watershed

Methods and materials

In this study the Soil and Water Assessment Tool was used (Arnold et al., 2012). SWAT is an open source watershed scale, semi-distributed hydrological model. Water balance is the main driving force behind every process in the SWAT model as a result of its effects on plant development and the movement of sediments, nutrients, pesticides, and pathogen within the watershed region (Arnold et al., 2011). It uses physically-based input such as topography, soil properties, land cover and weather data to evaluate temporal and spatial variability of water cycle parameters. For modelling the spatial variability of the watershed SWAT divides it into subwatersheds, each of them further subdivided into hydrologic response units (HRUs) by overlaying the slope map, generated from the DEM with the soil and land use maps. The major components, such as soil water content, surface runoff, streamflow and etc. are calculated for each HRU before being aggregated by a weighted average for every subbasin (Gassman et al., 2008). For setting up the model spatial data set was processed including a digital elevation map (DEM), landuse and soil maps. Meteorological data* i.e. daily precipitation, maximum and minimum daily temperature, daily relative humidity and daily wind speed from nine rainfall gauges and four meteorological stations was also collected and processed. *Hydrometeorological data sets for the period 2000–2010 were provided by the National Institute of Meteorology and Hydrology in Bulgaria.

Each subbasin in SWAT model is assigned the precipitation station closest to its centroid. This assumption may lead to under- or overestimations of the amount of precipitation in subwatersheds with no direct observations. That is why additional GIS-based interpolation (Thiessen Polygons) between the available rainfall stations was performed thus both filling missing records and attributing precipitation data to ungauged subbasins.

A sensitivity analysis towards daily discharge records from three flow gauges was performed prior to model calibration and validation. The sensitivity analysis was performed towards simulated versus observed data using the automated tool in SWAT. The LH-OAT method (Van Griensven et al., 2006) and the SSQ (Sum of the squares of the residuals) objective function were applied.

Two quantitative statistics were used to evaluate the goodness of calibration – the Nash-Sutcliffe efficiency (NSE) and the coefficient of determination (R2).

Results

After the initial simulations a sensitivity analysis was performed. Further adjustment of selected sensitive parameters was performed for model calibration.

Based on the results of both the initial simulation results and the sensitivity analysis the following SWAT parameters were chosen to be further adjusted: Cn2, Alpha_Bf, CH_K2 and Gwqmn. Cn2 (Initial SCS CN II value) parameter is related to surface flow representation. Parameters Alpha_Bf (Baseflow alpha factor) and Gwqmn (Threshold water depth in the shallow aquifer for flow) are related to groundflow representation. CH_K2 (effective hydraulic conductivity in main channel alluvium) is related to flow routing (Arnold et al., 2000).

The accuracy of the calibrated model results was evaluated at three control gauges of the watershed – 21650 and 21350 upstream and 21800 at downstream Vit river. The Nash-Sutcliffe efficiency (NSE) and the coefficient of determination (R2) statistical indicators were used to assess the overall model performance. On figures 2 and 3 the initial simulation results and the calibrated streamflow for station №21650 are shown. As seen from the graphs presented the calibrated SWAT model showed a good temporal streamflow representation (Fig.3), Nash-Sutcliffe coefficient (NSE) was 0.74 and the correlation coefficient (R2) was 0.76 (table 1). Also in table 1 the statistical estimates at the other two control hydrometric stations are presented. The overall estimated daily discharges ranged from satisfactory (downstream Vit river basin at station 21800) to good and very good for upstream Vit river basin.
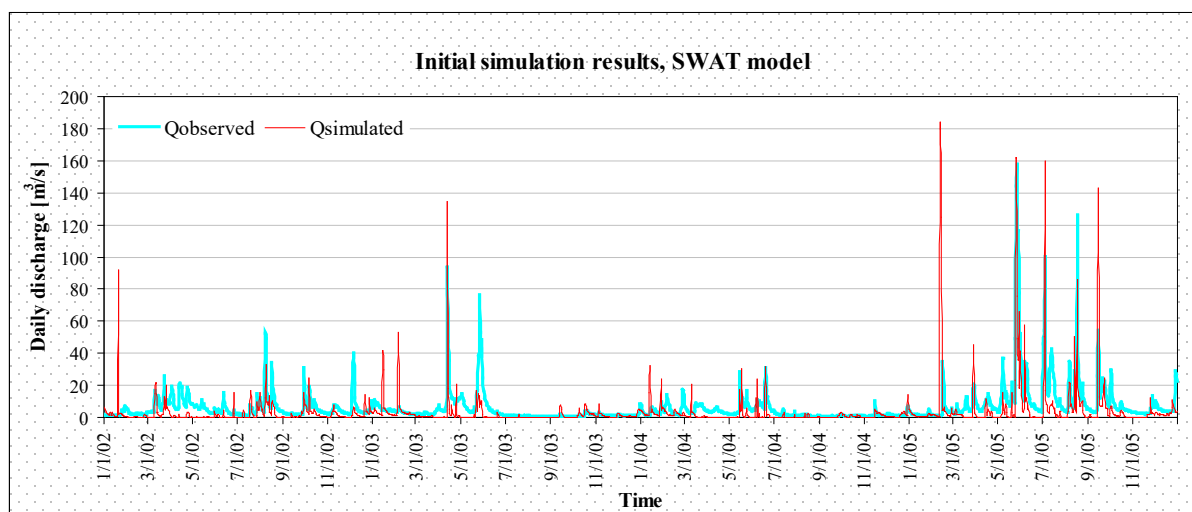

*Fig.2 Initial simulation results at station 21650 (upstream Vit river)*
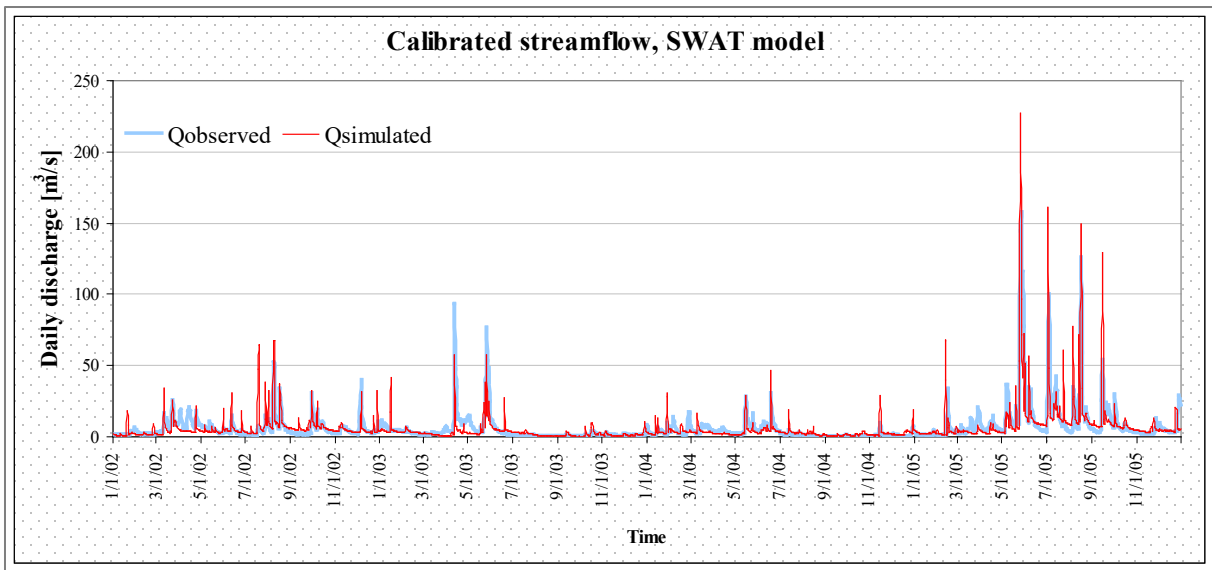
Fig.3 Calibrated streamflow for station 21650 (upstream Vit river)

Table 1 Streamflow results at the three control gauges:

|	21350	21650	21800
average daily Q simulated, m3/s	2.84	6.13	13.08
average daily Q observed, m3/s	3.59	6.40	15.96
NSE	0.62	0.74	0.52
R2	0.65	0.76	0.58
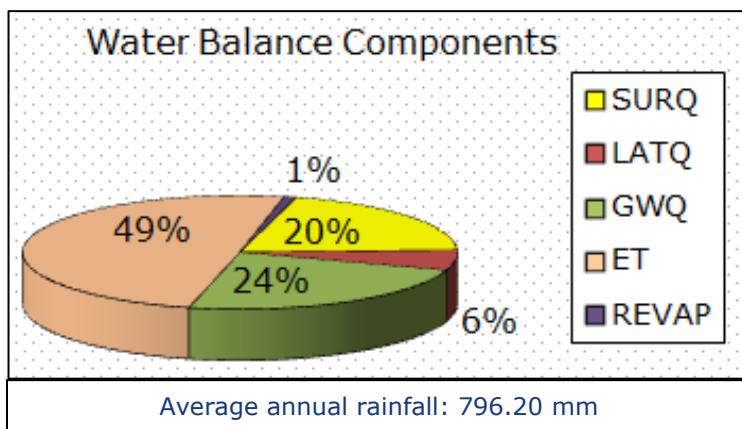
Fig.4 Vit river basin water balance components ratio

Table 2 Water balance components for Vit river basin:

Water Balance Components	AMOUNT, [mm]	
Precipitation	796.20	
Surface runoff		157.50
Groundwater flow		183.92
Lateral flow		44.81
Revap		7.16
Recharge of deep Aquifer		10.12
Evapotranspiration		385.30
TOTAL	796.20	788.81

The average annual water balance components for the entire Vit Basin (Fig. 4, Table 2) were obtained after running the calibrated model (simulation period 2000–2010).

SWAT-based water balance component calculations (Fig.2) showed that ET has the highest share of the water balance with a value of 49%. Revap (1%) and lateral flow (6%) have the lowest percentage of all. In table 2 Vit river basin water components are presented: the watershed receives 796.20 mm precipitation per year (83.90 mm of which is snowfall). Evapotranspiration is 385.30 mm, surface runoff is 157.50 mm and subsurface flow is only 6% (44.81 mm) of the total precipitation. Groundwater contribution to the stream is significant- 183.92 mm (24%). The amount of water passing from the shallow aquifer and recharging the deep aquifer is 10.12 mm (about 1%). The sum of the simulated hydrological components is only 7.40 mm less than the total precipitation received by the catchment.

Conclusion

This study provides an insight into the hydrology of Vit river basin through the use of monthly water balance.

An in-depth understanding of the hydrological processes as well as model parameters is needed for setting-up a reliable hydrological model. Applying precise parameterization for SWAT model greatly improves model simulation results.

Spatial and temporal characteristics of the observed daily discharge data were properly represented by SWAT. The high values of the statistical estimates R2 and NSE for calibration period imply SWAT model is useful in studying hydrology and estimating water balance components in the study watershed.

SWAT-based water balance component calculations show that the model succeeded in preserving the water balance equation for the Vit river watershed.

The results of the water balance study presented in this paper indicate that surface water availability is considerable.

Simulation results however are subject to further validation and further improvements in model performance should be sought.

Additional land cover analysis is required during the available period of rainfall-run-off record to establish a statistically valid link between changes in land cover and hydrological response (Baker et al, 2012).

The calibrated model could be used to study the effects of future land-use change on water quantity.

References

Arnold, J. G., Kiniry, J. R., Srinivasan, R., Williams, J. R., Haney, E. B., and Neitsch, S. L. (2011). Soil and Water Assessment Tool Input-Output File Documentation.

Arnold, J. G., Moriasi, D. N., Gassman, P. W., Abbaspour, K. C., White, M. J., Srinivasan, R., et al. (2012). SWAT: model use, calibration, and validation. Trans. ASABE 55, 1491–1508 pp.

Arnold J. G., R. S. Muttiah, R. Srinivasan, T. S. Ramanarayanan and P.M. Allen, Wtaer Regional estimation of base flow and groundwater recharge in the upper Mississippi basin, *Journal of Hydrology*, pp 227 (1–4): 21–40, 2000.

Anastassi Stefanova The use of remotely sensed data for validating a SWAT model: Application on the Vit River Basin, Bulgaria, Master Thesis, 2011.

Baker, Tracy, Miller, Scott. (2013), Using the Soil and Water Assessment Tool (SWAT) to assess land use impact on water resources in an East African watershed, *Journal of Hydrology* **486**, 100–111 pp.

Frederick Ayivi, Manoj K.Jha (2018) Estimation of water balance and water yield in the Reedy Fork-Buffalo Creek Watershed in North Carolina using SWAT, *International Soil and Water Conservation Research*, Volume **6**, Issue 3, 203–213 pp.

G. Koshinchanov, Sn. Balabanova, E. Artinyan (2014), Validation activities on some of the elements of hydrological cycle in the framework of HSAF project, INHGA – Scientific Conference, Romania, ISBN 978-973-0-18825-7.

Philip W. Gassman, Manuel R. Reyes, Colleen H. Green and Jeffrey G. Arnold (2008), The Soil and Water Assessment Tool: Historical Development, Applications and Future Research Directions, Special Publication No 4 by The World Association of Soil and Water Conservation, 25–93 pp.

UNESCO (1971) Scientific framework of world water balance. *Technical papers in hydrology*, no. **7**, Paris, 27 p.

Van Griensven A., T. Meixner, S. Grundwald, T. Bishop, M. Diluzio and R. Srinivasan, A global sensitivity analysis tool for the parameters of multi-variable catchment models, *Journal of Hydrology*, pp 324 (1–4):10–23, 2006.

World Meteorological Organization (1997), Water Resources Assessment Handbook For Review Of National Capabilities.

Yordanova, V., Stoyanova, V. (2020), Modeling floods with a distributed hydrological model in a river catchment, International Multidisciplinary Scientific GeoConference Surveying Geology and Mining Ecology Management, 249–255 pp.

Public awareness about floods – High water marks

Florjana ULAGA, MSc [1]**, Peter FRANTAR, PhD** [2]**, BRICELJ Mitja, PhD** [3]

[1] Slovenian Environment Agency, Slovenia, florjana.ulaga@gov.si, [2] Slovenian Environment Agency, Slovenia, peter.frantar@gov.si, [3] Ministry of Environment and Spatial Planning, mitja.bricelj@gov.si

Abstract

Slovenian Environment Agency (ARSO), Ministry of the Environment and Spatial Planning (MOP) and Association of Slovenian Geographers (ZGS) initiated the placement of high water marks on rivers, lakes and sea. The aim of the action is to educate and inform the local population of the natural phenomenon of high waters which more or less frequently, needs its natural extended space. The action is set as a typical bottom-up approach in order to include as many local stakeholders as possible. In the past 7 years over 60 standardized high water marks on 16 on-site events were placed.

Key words: hydrogeography, hydrology, high water marks, flood, education, awareness raising

Introduction

In the year 2014 Slovenian Environment Agency (ARSO) and Ministry of the Environment and Spatial Planning (MOP) together with Association of Slovenian Geographers (ZGS) initiated the placement of high water marks on rivers, lakes and sea. The aim of the action is to inform the inhabitants of the natural phenomenon of high waters, improve their knowledge of the regular impoundments of karstic poljes, flood prone areas near rivers and raise awareness that, more or less frequently, the water needs its natural extended space (ie. floodplains). Besides the official institutions, local stakeholders are crucial (local population, schools, local government, real estate owners of buildings with the installed high water marks) and are also included in the action.

The main purpose of the action is to encourage critical judgment of one's own and others' actions, while raising the individual's sense of responsibility in case of floods. Purposes such

- ▪ informing of high waters
- ▪ education about floodplain
- ▪ raising public awareness – to remind of the fact that water more or less often requires space, land for itself,

are of great importance for preparation of long-term and sustainable River basin management plans and also for Spatial plans on a regional level.

Purpose, objectives and presentation of the high water marking action

The marking of high water levels in physical space is based on "historical" sources on the occurrence of past high waters. These are different forms of recording the highest floodwaters, usually with the help of various markings, plates, lines drawn in stone or facades of excavated markings with the date or year of the flood event on public (various buildings, bridges, walls, flood embankments, etc.) or private buildings (residential houses, apartment blocks). High water marking has been taking place in different countries, regions, and local environments for various past events, but mostly incoherently, without central management, organization, and management by a designated organization. In some developed countries, the high water marking system is more established (Fig. 1), but for the most part, it does not follow a uniform concept and in conjunction with umbrella state or non-governmental institutions.

Fig. 1 Example of high water markings in Passau (Germany) on the German-Austrian border. The city is located at the confluence of the Danube and Inn river's.

In Slovenia, high water markings were installed by ARSO at gauging stations and also on some other locations. The disorganization and non-transparency of the high water markings and the inappropriate use of space on floodplains and elsewhere in the river basin, led to the initiative and establishment of the ARSO and ZGS High water markings action, which also aimed to visibly unify markings throughout the country (Fig. 2).

Fig. 2 High water mark

The main purpose of the action is to raise awareness and educate the public about the sustainable use of space in river basins, taking into account high waters. The key objectives of the action are:

– informing the population about high waters as a natural phenomenon in a specific area, which must be increasingly aware of in the context of climate change;

– education on floodplains of surface running waters (rivers, streams, torrents), sea and karstic floods (karstic poljes, floods associated with reduced sink capacity);

– awareness and reminders of the fact that water more or less often needs land for itself.

251

Visible and uniform high water markings in the field should raise awareness of the locals, visitors, and land use planners and remind them of the phenomenon of high waters, which must be taken into account when planning the use of space. Physical markings are a lasting reminder in space and are only a part of the process of raising awareness and educating about high waters.

The campaign is linked to the guidelines of the Water (Water Framework Directive, 2000) and the Floods Directive (Directive, 2007). Both directives are based on the principles of sustainable development and thus the sustainable use of space and water. This is very important in the river basins where floods cannot be completely avoided, but can be adapted to them. The adjustment will also be necessary due to the impact of the climate changes on the frequency of high waters in the future, as increased atmospheric energy is already showing changes in the geographical distribution of precipitation patterns, changes in precipitation regimes, and also increasing frequency of extreme precipitation events and related hydrological extremes on one hand and floods on the other; even though the trends of increasing frequency of high water extremes in recent decades are not statistically significant everywhere (Armstrong, Collins and Snyder, 2012; Šraj et al, 2016).

Methodology

The methodology or process of marking high waters and placing marks in the physical environment is not completely uniform (Frantar et al., 2016; Ulaga, 2019a). The basic principle of operation is procedurally seen "from the bottom up", where the local population is on the lower side, and national and international institutions on the upper side (Rutar-Ilc, 2008; Semeraro et al., 2020). The bottom-up process means targeted action from local stakeholders to official institutions. With this mode of operation, we ensure that the local population is actively involved in the action, which wants to maintain knowledge about high waters, floods, and in general about historical and contemporary events in their home geographical environment.

The bottom-up process is a procedural framework, as various factors in the design, planning, and implementation of individual events require more or less adjustment of the process or methodology. The high water marks action differs from similar regulated actions led by certain institutions, by the fact that it is entirely based on volunteering and the principle of participation, involvement. Stakeholders are involved in all parts of the action, which contributes to the satisfaction of all involved in the successful implementation of the action and the final event by placing a high water mark – also because they recognize their own contribution and role within the event. Due to their knowledge of the local physical- and socio-geographical characteristics of the home region, local stakeholders are the key in setting up markings, using local knowledge about flood events, and consequently including this knowledge in relevant documents, reports and more.

The action needs high level of organizational skills and is time-consuming. The selection of locations and the installation of markings take place individually, in an agreement between the members of ZGS, ARSO and other stakeholders. The process (Fig.3) starts with the initiative of local residents or other stakeholders to put up a marking. In cooperation between ARSO, ZGS, and MOP, the initiative is examined, and the basic conditions necessary for a successfully implemented action are agreed upon with local stakeholders. One of the key stakeholders in the action is educational institutions (Lipovšek, 2016; Lipovšek, 2018; V Izoli…, 2020). This is followed by the preparation of the installation facility, the determination of the exact location, and the agreement on the date of the event. The event is a key and at the same time the final part of the action, where a marking is placed in the presence of local, professional, state, and other interested stakeholders. The event is announced and covered by various media at the local and national level. It is of great importance to disseminate it by various social networks, in case of involving schools and information between teachers on a personal level. Information on a high water marking event that has just taken place may thus make other interested local stakeholders to take the initiative to organize a new event.
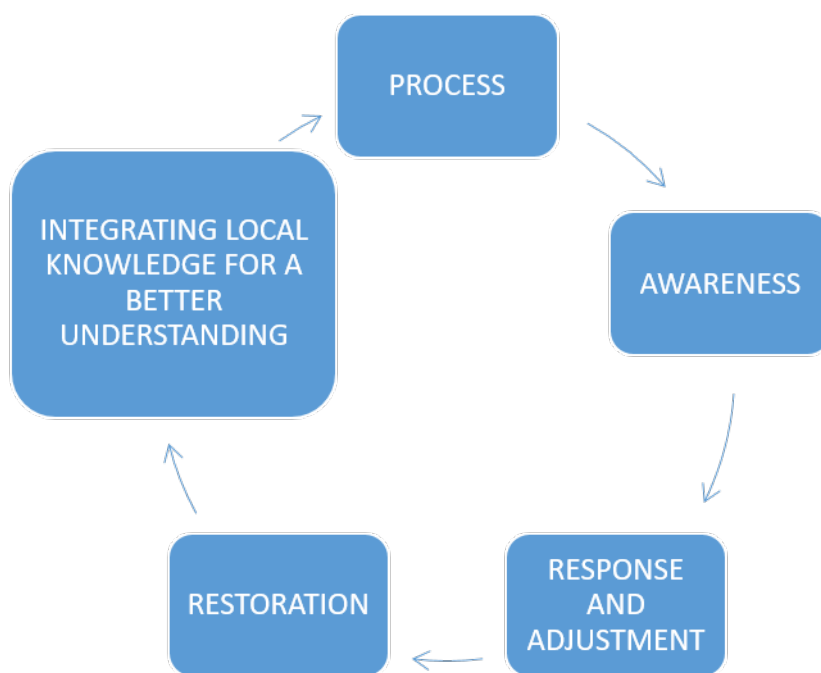
Fig. 3 The basic process of high water marking action.

For placement of each high water marking it is necessary to follow these general points (Ulaga, 2019a; 2019b):

1. To determine when and to what height the floodwater reached at a certain high water event; discuss this with the local population, schools, associations, municipalities…

2. To find the right building or physical object to place the mark that is exposed and publically accessible, visible and frequently visited.

3. To get permission from the real estate owner of the building or physical object to place the mark.

4. To coordinate the installation of the marking with the local stakeholders and prepare the public event with media coverage.

All installed high water marks are entered in the database and displayed online (Atlas, 2021) http://gis.arso.gov.si/atlasokolja/profile.aspx?id=Atlas_Okolja_AXL@Arso
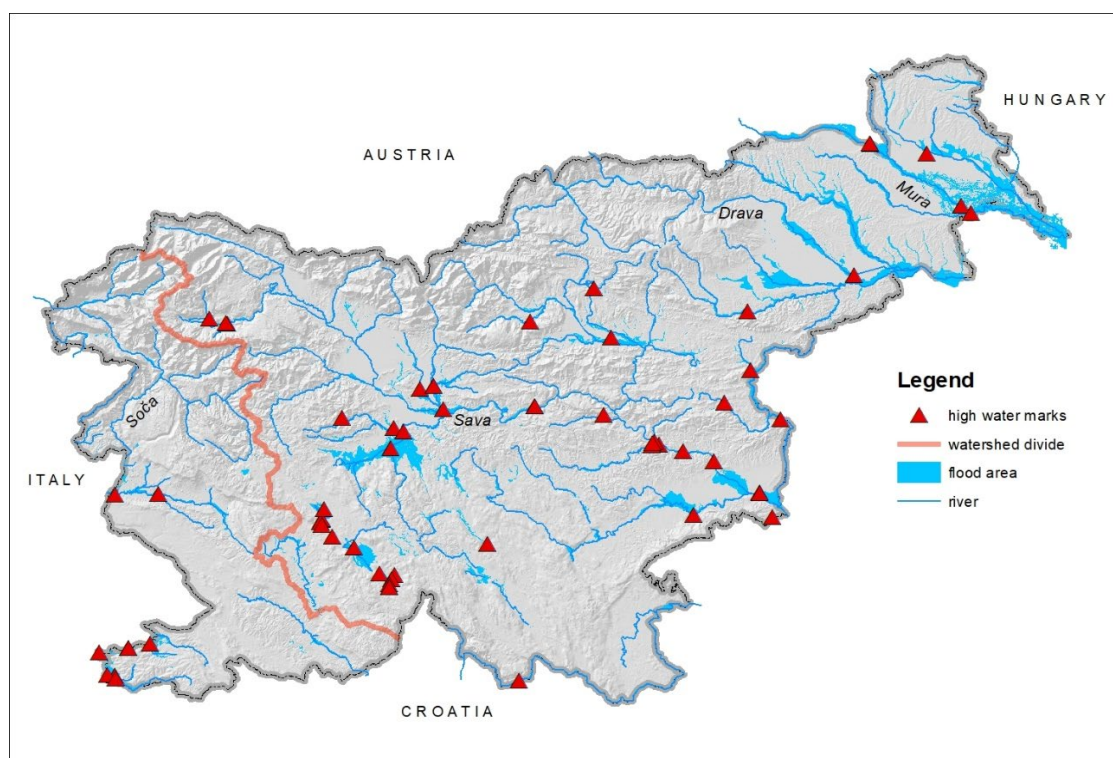
Fig. 4 Locations of installed high water marks in Slovenia.

When pupils and students are involved in setting the markings, teachers place their participation in the context within the regular educating programme. They relate to the objectives of the curriculum and prepare in-field activities. Due to the practicality and feasibility and placement of activities in the schedule, field work is limited to two school hours (Fig. 5). In the preparation process for the event, pupils and students perform various activities, e.g. they collect and analyze data on the flood event, perform field measurements and compare the situation with the highest, attach the findings to the cause-and-effect framework and present them at the event. The presentation is an important part, as students acquire the skills of public speaking in front of a non-school audience and in the public. At the same time, they are not only inactive attendants of the event, but they take an active part in its creation, and carefully prepare for it in terms of content. This is very important in developing active citizenship competencies. The high water mark can be later included in achieving the educational goals of various school topics. The described framework of the event with the involvement of schools is flexible and adjustable, and the success depends on several factors; mainly from the commitment of the stakeholders involved and from the support of local communities. Dissemination of information about the actions takes place through the public media, where news is published at events. At ARSO and ZGS, the news is published on social networks (twitter and facebook). Local newspapers, radio and television are usually covered by local stakeholders. In addition, actions and individual events are also presented on the website of the Commission for hydrogeography ZGS (Komisija za…, 2021).

Fig. 5 Cooperation with pupils and students.

Realised events and further steps

The action started in year 2014 and it is an ongoing activity. It represents good practice of cooperation between government institutions, regional and local institutions, universities and schools as well as local communities (Ulaga, 2018). In the last seven years over 60 high water marks (Fig.4) were placed, and 16 events has been organised. More than 60 different institutions were involved and over 700 people working in the fields of education, research and management, both at the local and national level, were present at the events (Table 1).

Table 1. Participants in the action of installing high water marks

Institution	School
Slovenian Environment Agency	Primary school Planina
Commission for Hydrogeography, Geographical Association of Slovenia	Primary school Miren
Ministry of environment and spatial planning	Primary school Livada
University of Ljubljana, Faculty of Arts	Primary school Sevnica

University of Primorska, Faculty of Humanities	Primary school Dornberk
University of Maribor, Faculty of Arts	Primary school Bohinjska Bistrica
Geography Teachers Association of Slovenia	Primary school Lesično
National Education Institute Slovenia	Primary school Livade
Karst Research InstituteZRC SAZU	Primary school Cirila Kosmača Piran
ICRO – Inštitut za celostni razvoj in okolje Domžale	Primary school Jurija Dalmatina Krško
Kozjansko regional park	Primary school Koper
Kmetijska zadruga Šmarje	Primary school Polhov Gradec
International Commission for the Protection of the Danube River (ICPDR)	High school Piran
International Sava River Basin Commission (ISRBC)	High school Koper
National museum of Slovenia	High school Brežice
Global water partnership	High school Izola
Aquarium Piran	High school Domžale
Regional park Sečoveljske soline	**Others**
Regional park Ljubljansko barje	Voluntary fire department Planina
City museum Krško	Voluntary fire department Polhov Gradec
Administration of the Republic of Slovenia for Civil Protection and Disaster Relief	Brodarsko turistično društvo Mostec
Civil protection Izola	Galerija Rex Izola
Harbour Master's Office Koper	fishermen, boatmen , various services
Komunala Izola d.o.o.	local and voluntary stakeholders
Municipality	
Minicipality of Postojna	
Minicipality of Miren Kostanjevica	
Minicipality of Lož	
Minicipality of Sevnica	
Minicipality of Domžale	
Minicipality of Brežice	
Minicipality of Nova Gorica	
Minicipality of Velenje	
Minicipality of Bohinj	
Minicipality of Poljčane	
Minicipality of Kozje	
Minicipality of Izola	
Minicipality of Krško	
Minicipality of Piran	
Minicipality of Podčetrtek	

| Minicipality of Bistrica ob Sotli |
| Minicipality of Ljubljana |
| Minicipality of Koper |
| Minicipality of Dobrova – Polhov Gradec |

The action has international recognition. It is recognized by the European Union Strategy for the Adriatic-Ionian Regional Strategy EUSAIR, International Commission for the Protection of the Danube River (ICPDR), and the International Sava River Commission (ISRBC).

Due to good practice and excellent experience in last years we proposed to extend the action also in other countries. In cooperation with ISRBC and Institutions of countries in Sava River basin, we prepared common celebration of Sava Day, 1. June 2021. The event was jointly made by Slovenia along with Croatia (National hydrometeorological office), Bosnia and Hercegovina (Hydrometeorological offices of Republika Srpska and Federal hydrometeorological office), and Serbia (Hydrometeorological office of the Republic of Srbije) (Fig. 6). On Sava Day all involved countries prepared an event at various locations in Sava watershed and marked the high water level of the river Sava or its tributary. The events were also live streamed, so countries were really connected and all participants as well. Part of the event was intended also for celebrating of Danube Day (29. June), as for Sava River basin is part of Danube basin Important role in this common event played pupils, schoolers and students. In each country they prepared presentations or flood related exercises, posters or poems, even cultural program about water and its importance for life on Earth. In Slovenia, in the country with the spring of the Sava River, pupils even made small paper boats and launched them to their colleagues downstream. The question for downstream countries was: how long will boats float to reach their locations and finally the Danube River? (Fig. 7).

Fig. 6 High water marks of countries of Sava River Basin involved in the action – Sava Day 2021

Fig. 7 Pupils from Slovenj Gradec in Slovenia are launching boats to their colleagues downstream all the way to Danube River.

Results and conclusions

The Action of placement of high water marks is all about linking the "fragmented" activities of public institutions, the economy, the societies and local communities to manage water resources responsibly and improve high water safety. It is about intergenerational integration, connecting sectors with the educational system and local communities and civil protection for the responsible management of water resources in the local environment. It is an innovative, direct field approach to raise public awareness for responsible management and adaptation to the changed dynamics of fresh water and the sea. Common marks were already placed along the Mura River in cooperation with Austria, on Sotla River (Fig. 8) in cooperation with Croatia and ICPDR, and on rivers in whole Sava River Basin.

Fig. 8 Placement of the high water mark on the Sotla River

The methodology or process of the action of installing high water marks is based on bottom-up operation, but in the actual implementation of the installation of marks and events, we find that from time to time a "top-down" incentive is also needed. We believe that the methodological concept will have to be adapted to the situation in the future and at the same time work in both directions of the process – "from top to bottom" and "from bottom to top". With the support of state and other institutions, the action can be provided with greater professional and organizational quality, and a bottom-up approach is necessary for the success of the action at the local level and for the sustainability of the activity itself.

References

Armstrong, W. H., Collins, M. J., Snyder, N. P. (2012). Increased Frequency of Low-Magnitude Floods in New England. Journal of the American Water Resources Association 48-2. https://doi.org/10.1111/j.1752-1688.2011.00613.x.

Atlas okolja (2021). Agencija za okolje Republike Slovenije. Ljubljana. http://gis.arso.gov.si/atlasokolja/profile.aspx?id=Atlas_Okolja_AXL@Arso (10. 6. 2021).

Directive 2007/60/EC of the European Parliament and of the Council of 23 October 2007 on the assessment and management of flood risks.

Frantar P., Ulaga F., Bat M., Jarnjak M. (2016). Akcija postavljanja oznak visokih voda v Sloveniji, Ujma, 30, 166–170.

Komisija za hidrogeografijo (2021). http://zgs.zrc-sazu.si/sl-si/zveza/organizveze/ komisijazahidrogeografijo#akcije (10. 6. 2021).

Šraj, M., Viglione, A., Parajka, J., Blöschl, G. (2016). The influence of non-stationarity in extreme hydrological events on flood frequency estimation. Journal of Hydrology and Hydromechanics 64-4. https://doi.org/10.1515/johh-2016-0032.

Lipovšek, I. (2016). Projekt ATS in geografsko raziskovanje vode v Sevnici. https://novice.sio.si/2016/09/18/projekt-ats-in-geografsko-raziskovanje-vode-v-sevnici/ (10.6.2021).

Lipovšek, I. (2018). Geografski pouk o(b) vodi. Geografija v šoli 26-1.

Rutar-Ilc, Z. (2008). Iskanje ravnovesja med pristopom "od zgoraj navzdol" in "od spodaj navzgor" – Študija primera. Vzgoja in izobraževanje: revija za teoretična in praktična vprašanja vzgojno izobraževalnega dela 39-3.

Semeraro, T., Zaccarelli, N., Lara, A., Cucinelli, F. S., Aretano, R. (2020). A Bottom-Up and Top-Down Participatory Approach to Planning and Designing Local Urban Development: Evidence from an Urban University Center. Land 9-4. https://doi.org/10.3390/land9040098.

Šraj, M., Viglione, A., Parajka, J., Blöschl, G. (2016). The influence of non-stationarity in extreme hydrological events on flood frequency estimation. Journal of Hydrology and Hydromechanics 64-4. https://doi.org/10.1515/johh-2016-0032.

Ulaga, F., Jarnjak, M., Frantar, P., Bat, M., Draksler, A. (2018). Akcija postavljanja oznak visokih voda v Sloveniji 2014–2018. Mišičev vodarski dan. Maribor.

Ulaga, F. (2019a). Ozaveščanje javnosti o poplavah – Oznake visokih voda. http://zgs.zrc-sazu.si/Portals/8/hidrogeografija/Oznake_2019.pdf (1. 3. 2021).

Ulaga, F. (2019b). Ozaveščanje javnosti o poplavah. Napovedovanje poplav, opozarjanje in sodelovanje pri ukrepanju ob poplavah. Interreg projekt DAREFFORT – Diseminacijski dogodek in nacionalna delavnica, Ljubljana, 10. 9. 2019. http://ksh.fgg.uni-lj.si/ksh/razisk_dej/Dareffort_delavnica.html (1. 3. 2021).

V Izoli označili najvišjo raven vode ob lanskoletnih poplavah. (2020). https://izola.si/medijsko-sredisce/novice/v-izoli-oznacili-najvisjo-raven-vode-ob-lanskoletnih-poplavah/ (1. 3. 2021).

Water Framework Directive (WFD), Directive 2000/60/EC of the European Parliament and of the Council establishing a framework for the Community action in the field of water policy.